



Earth Resources
A Continuing
Bibliography
with Indexes

NASA SP-7041 (58)
August 1988

National Aeronautics and
Space Administration

es Earth Resources
s Earth Resources
E
th Resources Ear
Resources Earth
Resources Earth F
sources Earth Re

(NASA-SP-7041 (58)) EARTH RESOURCES: A
CONTINUING BIBLIOGRAPHY WITH INDEXES (ISSUE
58) (NASA) 139 p CSCI 08B

N89-10398

Unclas
00/43 0168478

This bibliography was prepared by the NASA Scientific and Technical Information Facility operated for the National Aeronautics and Space Administration by RMS Associates.

INTRODUCTION

The technical literature described in this continuing bibliography may be helpful to researchers in numerous disciplines such as agriculture and forestry, geography and cartography, geology and mining, oceanography and fishing, environmental control, and many others. Until recently it was impossible for anyone to examine more than a minute fraction of the Earth's surface continuously. Now vast areas can be observed synoptically, and changes noted in both the Earth's lands and waters, by sensing instrumentation on orbiting spacecraft or on aircraft.

This literature survey lists 500 reports, articles, and other documents announced between April 1 and June 30, 1988 in *Scientific and Technical Aerospace Reports (STAR)*, and *International Aerospace Abstracts (IAA)*.

The coverage includes documents related to the identification and evaluation by means of sensors in spacecraft and aircraft of vegetation, minerals, and other natural resources, and the techniques and potentialities of surveying and keeping up-to-date inventories of such riches. It encompasses studies of such natural phenomena as earthquakes, volcanoes, ocean currents, and magnetic fields; and such cultural phenomena as cities, transportation networks, and irrigation systems. Descriptions of the components and use of remote sensing and geophysical instrumentation, their subsystems, observational procedures, signature and analyses and interpretive techniques for gathering data are also included. All reports generated under NASA's Earth Resources Survey Program for the time period covered in this bibliography are also included. The bibliography does not contain citations to documents dealing mainly with satellites or satellite equipment used in navigation or communication systems, nor with instrumentation not used aboard aerospace vehicles.

The selected items are grouped in nine categories. These are listed in the Table of Contents with notes regarding the scope of each category. These categories were especially chosen for this publication, and differ from those found in *STAR* and *IAA*.

Each entry consists of a standard bibliographic citation accompanied by an abstract. The citations include the original accession numbers from the respective announcement journals.

Under each of the nine categories, the entries are presented in one of two groups that appear in the following order:

- IAA* entries identified by accession number series A88-10,000 in ascending accession number order;

- STAR* entries identified by accession number series N88-10,000 in ascending accession number order.

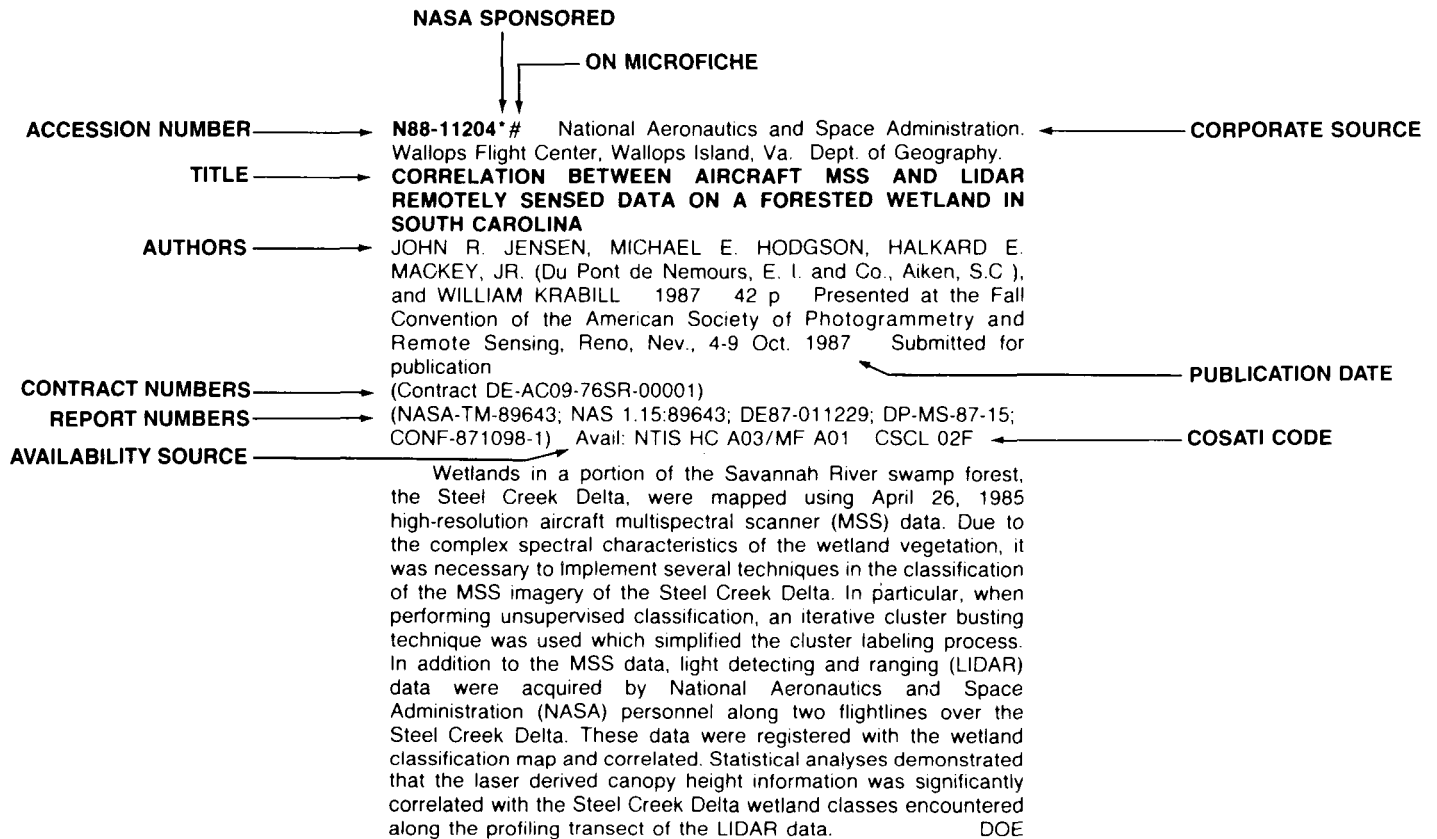
After the abstract section, there are seven indexes:

- subject, personal author, corporate source, foreign technology, contract number, report/ accession number, and accession number.

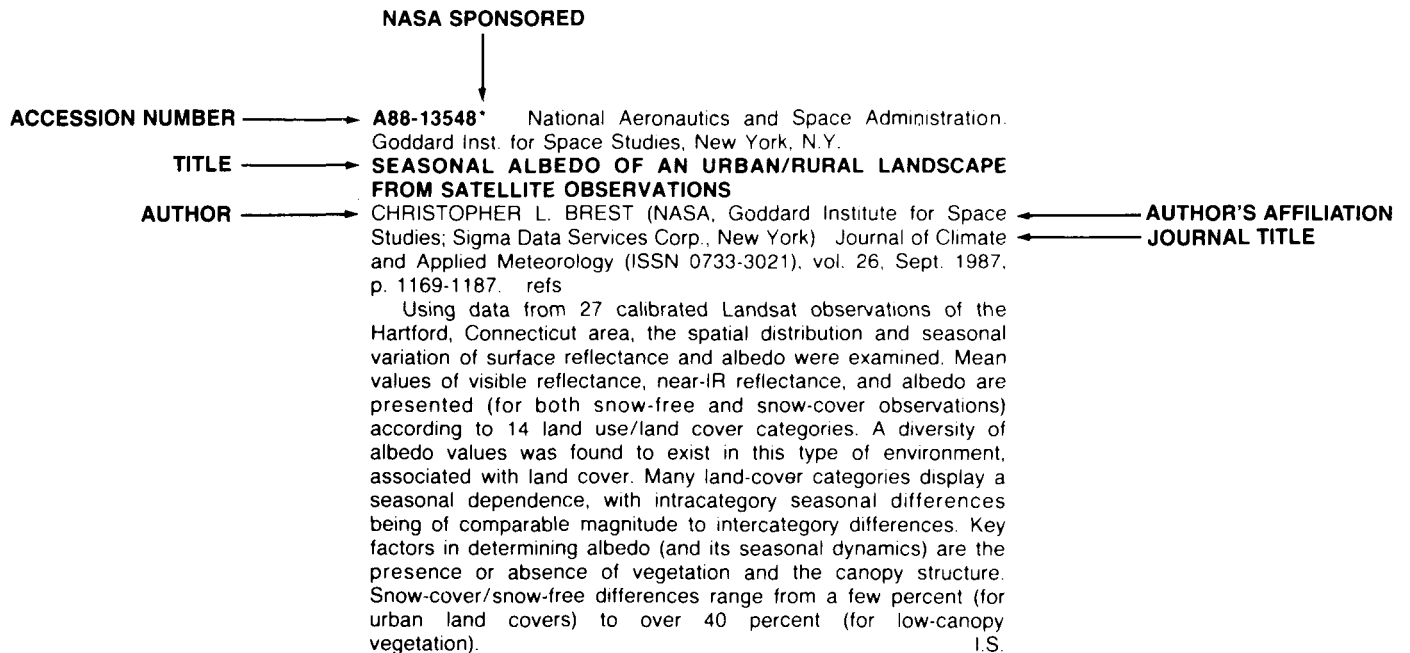
TABLE OF CONTENTS

	Page
Category 01 Agriculture and Forestry	1
Includes crop forecasts, crop signature analysis, soil identification, disease detection, harvest estimates, range resources, timber inventory, forest fire detection, and wildlife migration patterns.	
Category 02 Environmental Changes and Cultural Resources	17
Includes land use analysis, urban and metropolitan studies, environmental impact, air and water pollution, geographic information systems, and geographic analysis.	
Category 03 Geodesy and Cartography	20
Includes mapping and topography.	
Category 04 Geology and Mineral Resources	24
Includes mineral deposits, petroleum deposits, spectral properties of rocks, geological exploration, and lithology.	
Category 05 Oceanography and Marine Resources	30
Includes sea-surface temperature, ocean bottom surveying imagery, drift rates, sea ice and icebergs, sea state, fish location.	
Category 06 Hydrology and Water Management	50
Includes snow cover and water runoff in rivers and glaciers, saline intrusion, drainage analysis, geomorphology of river basins, land uses, and estuarine studies.	
Category 07 Data Processing and Distribution Systems	54
Includes film processing, computer technology, satellite and aircraft hardware, and imagery.	
Category 08 Instrumentation and Sensors	64
Includes data acquisition and camera systems and remote sensors.	
Category 09 General	72
Includes economic analysis.	
Subject Index	A-1
Personal Author Index	B-1
Corporate Source Index	C-1
Foreign Technology Index	D-1
Contract Number Index	E-1
Report Number Index	F-1
Accession Number Index	G-1

TYPICAL REPORT CITATION AND ABSTRACT



TYPICAL JOURNAL ARTICLE CITATION AND ABSTRACT



EARTH RESOURCES

A Continuing Bibliography (Issue 58)

AUGUST 1988

01

AGRICULTURE AND FORESTRY

Includes crop forecasts, crop signature analysis, soil identification, disease detection, harvest estimates, range resources, timber inventory, forest fire detection, and wildlife migration patterns.

A88-21013

AN EVALUATION OF THE USE OF TM DIGITAL DATA FOR UPDATING THE LAND COVER COMPONENT OF THE SCS 1987 MULTIRESOURCE INVENTORY OF NEW JERSEY

JOANNE VOGEL (USDA, Soil Conservation Service, Somerset, NJ) and TEUVO M. AIROLA (Rutgers University, New Brunswick, NJ) IN: American Society for Photogrammetry and Remote Sensing and ACSM, Annual Convention, Baltimore, MD, Mar. 29-Apr. 3, 1987, Technical Papers. Volume 1. Falls Church, VA, American Society for Photogrammetry and Remote Sensing and ACSM, 1987, p. 113-120. refs

The New Jersey USDA Soil Conservation Service (SCS) and the Cook College Remote Sensing Center have been jointly involved in an evaluation of the use of remote sensing data to acquire land cover information for the National Resource Inventory (NRI) update in 1987. NRI data was first collected in 1982 through intensive field survey of primary sampling units (PSUs). At that time, the PSU locations were recorded on county soil survey atlas sheets. The process of relocating selected PSUs from these maps and acquiring field data in 1987 using traditional techniques promises to be extremely time consuming and expensive. This paper provides an overview of: (1) the derivation of land cover information from TM digital data for a study area in New Jersey, and (2) the process used to determine the UTM coordinates of the PSUs used in the 1982 NRI, and (3) an evaluation of the accuracy of the classification map produced and a comparison of the results with land cover information collected by the SCS in the 1982 NRI. Author

A88-21015

MULTISPECTRAL VIDEO SURVEY OF A NORTHERN ONTARIO FOREST

X. YUAN, D. KING, F. CADEAU, and J. VLCEK (Toronto, University, Canada) IN: American Society for Photogrammetry and Remote Sensing and ACSM, Annual Convention, Baltimore, MD, Mar. 29-Apr. 3, 1987, Technical Papers. Volume 1. Falls Church, VA, American Society for Photogrammetry and Remote Sensing and ACSM, 1987, p. 140-147. Research supported by the Department of Energy, Mines and Resources and NSERC. refs

Multispectral video imaging can provide quick and low cost means for forest surveys. This paper describes the initial use of multispectral aerial video data in a forest survey in Northern Ontario. Field reconnaissance and preliminary visual and digital image analysis indicate that multispectral video, at low altitudes, is capable of discriminating major tree species, assessing forest regeneration, site wetness and detecting forest changes. The potential value of video imaging exists in the updating of data bases such as, forest inventory maps and GIS data bases, which could provide timely information on forest resources to assist decision making. Limitations of the video system are also presented. Author

A88-21016

MID-INFRARED (1.45 TO 2.0 MICRONS) VIDEO - A POTENTIAL AID IN WILDFIRE MOP-UP OPERATIONS

J. H. EVERITT, P. R. NIXON, D. E. ESCOBAR, and M. R. DAVIS (USDA, Agricultural Research Service, Weslaco, TX) IN: American Society for Photogrammetry and Remote Sensing and ACSM, Annual Convention, Baltimore, MD, Mar. 29-Apr. 3, 1987, Technical Papers. Volume 1. Falls Church, VA, American Society for Photogrammetry and Remote Sensing and ACSM, 1987, p. 148-154. refs

This paper demonstrates the applicability of a black-and-white visible-infrared sensitive video camera, filtered to record radiation in the 1.45 to 2.0 micron midinfrared spectral region, to detect hot spots within the perimeter of a wildfire. Imagery of a burned rangeland area obtained at an altitude of 900 m showed that hot spots (smoldering logs) could be clearly delineated from other landscape features. Midinfrared video imagery should be useful to detect hot spots at temperatures as low as 900 K. Real-time 'live' imagery can be viewed on a monitor in an aircraft allowing hot spots to be immediately detected. Author

A88-21017

DIFFICULTIES AND RECOMMENDATIONS FOR OBTAINING VERY LARGE SCALE 70 MM AERIAL PHOTOGRAPHY FOR RANGELAND MONITORING

LEE F. WERTH (U.S. Bureau of Land and Management, Branch of Remote Sensing, Lakewood, CA) IN: American Society for Photogrammetry and Remote Sensing and ACSM, Annual Convention, Baltimore, MD, Mar. 29-Apr. 3, 1987, Technical Papers. Volume 1. Falls Church, VA, American Society for Photogrammetry and Remote Sensing and ACSM, 1987, p. 155-159. refs

Very large scale (larger than 1:1000 scale) 70 mm aerial photography has been used for rangeland inventory. A combination of a skilled pilot, photographer, and special 70 mm camera is required, however, to obtain good stereoscopic coverage. An unsuccessful attempt was made in acquiring very large scale stereoscopic color and color infrared photography for rangeland monitoring plots in northeastern Oregon. A fixed-wing aircraft was the platform for rapid recycling 70 mm Mauer cameras. This paper will discuss the problems encountered and recommendations for operationally obtaining very large scale 70 mm aerial photography. Author

A88-21020* National Aeronautics and Space Administration. Goddard Space Flight Center, Greenbelt, Md.

VALIDATING REGIONAL DIFFERENCES IN MODELLED SATELLITE MICROWAVE SIGNATURES

MANFRED OWE (NASA, Goddard Space Flight Center, Greenbelt, MD) IN: American Society for Photogrammetry and Remote Sensing and ACSM, Annual Convention, Baltimore, MD, Mar. 29-Apr. 3, 1987, Technical Papers. Volume 1. Falls Church, VA, American Society for Photogrammetry and Remote Sensing and ACSM, 1987, p. 176-184. refs

A three-part microwave T(B) brightness temperature model was tested for applicability in regions of differing climatic and vegetation regime. Model parameters were limited to vegetation in the form of the normalized vegetation index (NDVI) and climatically modeled soil moisture. The T(B) model was calibrated for two climatically contrasting areas and subsequently validated on different test sites of similar climatic character. Vegetative characteristics in the form

01 AGRICULTURE AND FORESTRY

of the mean NDVI was used to partition and lump data from different test sites. Good agreement was realized between estimated T(B) and Nimbus-7 SMMR T(B) at the 6.6 GHz horizontal channel. Author

A88-21028* Illinois Natural History Survey, Champaign.
ESTIMATING FOREST PRODUCTIVITY IN SOUTHERN ILLINOIS USING LANDSAT THEMATIC MAPPER DATA AND GEOGRAPHIC INFORMATION SYSTEM ANALYSIS TECHNIQUES

ELIZABETH A. COOK, LOUIS R. IVERSON (Illinois Natural History Survey, Champaign), and ROBIN LAMBERT GRAHAM (Oak Ridge National Laboratory, TN) IN: American Society for Photogrammetry and Remote Sensing and ACSM, Annual Convention, Baltimore, MD, Mar. 29-Apr. 3, 1987, Technical Papers. Volume 1. Falls Church, VA, American Society for Photogrammetry and Remote Sensing and ACSM, 1987, p. 255-265. refs
(Contract NAS5-28781)

A88-21029
THE USE OF DIGITAL LANDSAT DATA FOR WILDLIFE MANAGEMENT ON THE WARM SPRINGS INDIAN RESERVATION OF OREGON

WILLIAM J. RIPPLE (Oregon State University, Corvallis) and TERRY LUTHER (Warm Springs, Confederated Tribes, OR) IN: American Society for Photogrammetry and Remote Sensing and ACSM, Annual Convention, Baltimore, MD, Mar. 29-Apr. 3, 1987, Technical Papers. Volume 1. Falls Church, VA, American Society for Photogrammetry and Remote Sensing and ACSM, 1987, p. 266-274. refs

A88-21031
DEFINITION OF FOREST STAND CHARACTERISTICS BASED ON MULTI-INCIDENCE ANGLE SIR-B DATA

R. M. HOFFER and D. F. LOZANO-GARCIA (Purdue University, West Lafayette, IN) IN: American Society for Photogrammetry and Remote Sensing and ACSM, Annual Convention, Baltimore, MD, Mar. 29-Apr. 3, 1987, Technical Papers. Volume 1. Falls Church, VA, American Society for Photogrammetry and Remote Sensing and ACSM, 1987, p. 296-304.

Digital L-band HH-polarized SIR-B data obtained at multiple incidence angles on test sites throughout the world during the Shuttle Mission 41-G in October 1984 were analyzed in relation to reference data obtained for individual forest stands. It is shown that the SIR-B data can be correlated with several of the forest stand characteristics including age, cords per acre, and biomass. Incidence angle controlled to a large extent the characteristics of the data and the type of information that could be obtained. In some instances, statistically significant relationships were obtained between the relative radar backscatter and forest stand characteristics, particularly age. Computer classification of the SIR-B data, using per-point and contextual classification algorithms, yielded overall classification accuracy of 56 percent and 78 percent, respectively. I.S.

A88-21032* Jet Propulsion Lab., California Inst. of Tech., Pasadena.

CHARACTERIZATION OF VEGETATION WITH COMBINED THEMATIC MAPPER (TM) AND SHUTTLE IMAGING RADAR (SIR-B) IMAGE DATA

JACK F. PARIS and HELENANN H. KWONG (California Institute of Technology, Jet Propulsion Laboratory, Pasadena) IN: American Society for Photogrammetry and Remote Sensing and ACSM, Annual Convention, Baltimore, MD, Mar. 29-Apr. 3, 1987, Technical Papers. Volume 1. Falls Church, VA, American Society for Photogrammetry and Remote Sensing and ACSM, 1987, p. 305-319. refs

A88-21033* National Aeronautics and Space Administration. Earth Resources Lab., Bay St. Louis, Miss.
PARAMETRIC ANALYSIS OF SYNTHETIC APERTURE RADAR DATA FOR CHARACTERIZATION OF DECIDUOUS FOREST STANDS

SHIH-TSENG WU (NASA, Earth Resources Laboratory, Bay Saint Louis, MS) IN: American Society for Photogrammetry and Remote Sensing and ACSM, Annual Convention, Baltimore, MD, Mar. 29-Apr. 3, 1987, Technical Papers. Volume 1. Falls Church, VA, American Society for Photogrammetry and Remote Sensing and ACSM, 1987, p. 320-328. refs

The SAR sensor parameters that affect the estimation of deciduous forest stand characteristics were examined using data sets for the Gulf Coastal Plain region, acquired by the NASA/JPL multipolarization airborne SAR. In the regression analysis, the mean digital-number values of the three polarization data are used as the independent variables to estimate the average tree height (HT), basal area (BA), and total-tree biomass (TBM). The following results were obtained: (1) in the case of simple regression and using 28 plots, vertical-vertical (VV) polarization yielded the largest correlation coefficients (r) in estimating HT, BA, and TBM; (2) in the case of multiple regression, the horizontal-horizontal (HH) and VV polarization combination yielded the largest r value in estimating HT, while the VH and HH polarization combination yielded the largest r values in estimating BA and TBM. With the addition of a third polarization, the increase in r values is insignificant. I.S.

A88-21035
RADAR FLOOD INUNDATION MAPPING OF UPPER BENUE TROUGH, NIGERIA

SOLOMON A. ISIORHO (Case Western Reserve University, Cleveland, OH) IN: American Society for Photogrammetry and Remote Sensing and ACSM, Annual Convention, Baltimore, MD, Mar. 29-Apr. 3, 1987, Technical Papers. Volume 1. Falls Church, VA, American Society for Photogrammetry and Remote Sensing and ACSM, 1987, p. 339-347. Research supported by the University of Port Harcourt and Nigerian Geological Survey. refs

A88-21040
EVALUATION OF THEMATIC MAPPER DATA FOR MAPPING TIDAL WETLANDS IN SOUTH CAROLINA

RICHARD B. LACY (South Carolina Land Resources Commission, Columbia) and JOHN R. JENSEN (South Carolina, University, Columbia) IN: American Society for Photogrammetry and Remote Sensing and ACSM, Annual Convention, Baltimore, MD, Mar. 29-Apr. 3, 1987, Technical Papers. Volume 1. Falls Church, VA, American Society for Photogrammetry and Remote Sensing and ACSM, 1987, p. 393-401. refs

The utility of Landsat Thematic Mapper data analysis as a technique for preparing a vegetation map and inventory is evaluated by testing its capability to discriminate tidal plant associations on the Santee Delta, South Carolina. The methodology used is discussed, as it is shown that the repeatable and reliable nature of Thematic Mapper image processing offers an alternative to conventional methods of tidal wetland mapping. V.L.

A88-21046
AMERICAN SOCIETY FOR PHOTOGRAMMETRY AND REMOTE SENSING AND ACSM, ANNUAL CONVENTION, BALTIMORE, MD, MAR. 29-APR. 3, 1987, TECHNICAL PAPERS. VOLUME 2 - PHOTOGRAMMETRY

Convention sponsored by the American Society for Photogrammetry and Remote Sensing and ACSM. Falls Church, VA, American Society for Photogrammetry and Remote Sensing and ACSM, 1987, 394 p. For individual items see A88-21047 to A88-21053.

The conference presents papers on practical photogrammetric procedures for large-scale forest inventories, a satellite image mosaic of Illinois, computer-assisted color generation for thematic mapping, and a comparison of the gridded finite element and the polynomial interpolations for geometric rectification and mosaicking of Landsat data. Other topics include spatial accuracy specification for large-scale topographic maps, geographical position plotting by photointerpreters from Space Shuttle large format camera photography, parallax bar heighting accuracy of large format camera photography, and terrain analyst work station demonstrations. Consideration is also given to a numerical photogrammetric model for software applications, classification

quality assessment for object identification systems, and an expert system for the computer-assisted analysis of radar imagery. K.K.

A88-21065

DETECTING SUBPIXEL WOODY FEATURES USING SIMULATED MULTISPECTRAL AND PANCHROMATIC SPOT IMAGERY

PATRICIA G. FOSCHI (Oxford University, England) IN: American Society for Photogrammetry and Remote Sensing and ACSM, Annual Convention, Baltimore, MD, Mar. 29-Apr. 3, 1987, Technical Papers. Volume 6. Falls Church, VA, American Society for Photogrammetry and Remote Sensing and ACSM, 1987, p. 15-22. refs

A method for detecting small woody features in digital imagery was developed and automated. Simulated SPOT imagery of an agricultural area, containing numerous linear woody features, was used to test the method. The results indicate that the method found significantly more woody vegetation than a standard multispectral classification found. Interference from subpixel nonwoody features and from soil moisture decreased classification accuracy. Further testing is necessary to determine an optimal set of computation parameters. Author

A88-21351

REMOTE SENSING SCIENCE APPLICATIONS IN ARID ENVIRONMENTS

PAUL T. TUELLER (Nevada, University, Reno) Remote Sensing of Environment (ISSN 0034-4257), vol. 23, Nov. 1987, p. 143-154. refs

Remote sensing in aridland/rangeland regions has developed to meet the need for low cost management information over large expanses of land. Applications include rangeland management, watershed analysis, antidesertification, wildlife habitat management, mine waste reclamation, management of the arid land-irrigated agriculture interface, and outdoor recreation. Unique remote sensing problems in arid regions are related to sparse vegetation, multiple species, and considerable bare ground. Thus spectral interpretations must consider: multiple intermingled green and senescent species; considerable bare ground which includes cryptogamic soil crusts and powdery, enduring, or salinized surfaces; standing dead vegetation; litter; and shadows. Pixel modeling will be required in these heterogeneous environments. In particular, the lack of greenness tends to preclude the application of vegetation indices based on infrared/red ratios. New interpretation approaches to scene understanding, such as those included in this issue, should lead to useful procedures for aridlands. Author

A88-21352

SPECTRAL CHARACTERISTICS OF SELECTED SOILS AND VEGETATION IN NORTHERN NEVADA AND THEIR DISCRIMINATION USING BAND RATIO TECHNIQUES

MELVIN B. SATTERWHITE and J. PONDER HENLEY (U.S. Army, Engineer Topographic Laboratories, Fort Belvoir, VA) Remote Sensing of Environment (ISSN 0034-4257), vol. 23, Nov. 1987, p. 155-175. refs

A88-21353

AERIAL AND GROUND SPECTRAL CHARACTERISTICS OF RANGELAND PLANT COMMUNITIES IN NEVADA

RICHARD O. WILSON and PAUL T. TUELLER (Nevada, University, Reno) Remote Sensing of Environment (ISSN 0034-4257), vol. 23, Nov. 1987, p. 177-191. refs

Visible and near infrared spectral reflectance values were recorded from Nevada rangeland plant communities using both low flying aircraft and ground measurement approaches. The individual spectrum values, four-band signatures and infrared:red scatterplots were used to compare 5 x 5 m aerial pixels with data from various ground components. Results show that vegetation and soil do not account for the integrated aerial spectra. The composite ground signatures indicate that spectrally dark components exist in rangeland plant communities which decrease the brightness of a scene measured from the air. Shadow and

litter are presumed to be the primary sources of spectral darkening. An estimate of the overall signature of the shadow/litter component was calculated. Author

A88-21354*

National Aeronautics and Space Administration. Goddard Space Flight Center, Greenbelt, Md.

SURFACE ANISOTROPY AND HEMISPHERIC REFLECTANCE FOR A SEMIARID ECOSYSTEM

ELIZABETH M. MIDDLETON, DONALD W. DEERING (NASA, Goddard Space Flight Center, Greenbelt, MD), and SURAIYA P. AHMAD (Science Applications Research, Lanham, MD) Remote Sensing of Environment (ISSN 0034-4257), vol. 23, Nov. 1987, p. 193-212. NASA-supported research. refs

A88-21355

SUITABILITY OF SPECTRAL INDICES FOR EVALUATING VEGETATION CHARACTERISTICS ON ARID RANGELANDS

A. R. HUETE (Arizona, University, Tucson) and R. D. JACKSON (USDA, Water Conservation Laboratory, Phoenix, AZ) Remote Sensing of Environment (ISSN 0034-4257), vol. 23, Nov. 1987, p. 213-232. refs

A88-21356*

National Aeronautics and Space Administration. Goddard Space Flight Center, Greenbelt, Md.

SATELLITE OBSERVED SEASONAL AND INTER-ANNUAL VARIATION OF VEGETATION OVER THE KALAHARI, THE GREAT VICTORIA DESERT, AND THE GREAT SANDY DESERT - 1979-1984

B. J. CHOUDHURY and C. J. TUCKER (NASA, Goddard Space Flight Center, Greenbelt, MD) Remote Sensing of Environment (ISSN 0034-4257), vol. 23, Nov. 1987, p. 233-241. refs

Time-series observations by two spaceborne sensors over three desert regions, the Kalahari (in southern Africa) and the Great Victoria Desert and the Great Sandy Desert (in western Australia), are presented. The observations are by the Advanced Very High Resolution Radiometer on board the NOAA-7 satellite from April 1982 to December 1984, and by the Scanning Multichannel Microwave Radiometer on board the Nimbus-7 satellite from January 1979 to February 1985. The objective was to compare and contrast seasonal and interannual variation of vegetation over these three deserts using the normalized difference vegetation index and the 37 GHz brightness temperature. The seasonal variation from both sensors was found to be most pronounced over the Kalahari, followed by the Great Sandy Desert and the Great Victoria Desert. The normalized difference vegetation index was roughly identical over the two Australian deserts and was significantly higher for the Kalahari. There was no consistent change from both sensors over the two Australian deserts, but a consistent decrease from 1979 to 1984 over the Kalahari was found in the 37 GHz microwave data. Author

A88-21357*

National Aeronautics and Space Administration. Goddard Space Flight Center, Greenbelt, Md.

SATELLITE REMOTE SENSING OF DROUGHT CONDITIONS

COMPTON J. TUCKER and BHASKAR J. CHOUDHURY (NASA, Goddard Space Flight Center, Greenbelt, MD) Remote Sensing of Environment (ISSN 0034-4257), vol. 23, Nov. 1987, p. 243-251. refs

Multitemporal satellite data have application in the detection and quantification of drought through the ability of these data to estimate the photosynthetic capacity of the terrestrial surface and record microwave surface brightness at the 37 GHz frequency. With proper calibration and registration, comparisons can be made between and among years for specific months using the photosynthetic capacity and the 37 GHz microwave surface brightness for selected time periods or growing seasons. This technology has application in identifying and quantifying areas experiencing drought. Author

A88-21358

Pennsylvania State Univ., University Park.

AIRCRAFT AND SATELLITE REMOTE SENSING OF DESERT SOILS AND LANDSCAPES

G. W. PETERSEN, K. F. CONNORS, D. A. MILLER, R. L. DAY,

01 AGRICULTURE AND FORESTRY

and T. W. GARDNER (Pennsylvania State University, University Park) Remote Sensing of Environment (ISSN 0034-4257), vol. 23, Nov. 1987, p. 253-271. DOE-NASA-supported research. refs

Remote sensing data on desert soils and landscapes, obtained by the Landsat TM, Heat Capacity Mapping Mission (HCMM), Simulated SPOT, and Thermal IR Multispectral Scanner (TIMS) aboard an aircraft, are discussed together with the analytical techniques used in the studies. The TM data for southwestern Nevada were used to discriminate among the alluvial fan deposits with different degrees of desert pavement and varnish, and different vegetation cover. Thermal-IR data acquired from the HCMM satellite were used to map the spatial distribution of diurnal surface temperatures and to estimate mean annual soil temperatures in central Utah. Simulated SPOT data for northwestern New Mexico identified geomorphic features, such as differences in eolian sand cover and fluvial incision, while the TIMS data depicted surface geologic features of the Saline Valley in California. I.S.

A88-21359* California Univ., Berkeley.

DISCRIMINATING SEMIARID VEGETATION USING AIRBORNE IMAGING SPECTROMETER DATA - A PRELIMINARY ASSESSMENT

RANDALL W. THOMAS (California, University, Berkeley) and SUSAN L. USTIN (California, University, Berkeley and Davis) Remote Sensing of Environment (ISSN 0034-4257), vol. 23, Nov. 1987, p. 273-290. refs
(Contract NAS7-918)

A preliminary assessment was made of Airborne Imaging Spectrometer (AIS) data for discriminating and characterizing vegetation in a semiarid environment. May and October AIS data sets were acquired over a large alluvial fan in eastern California, on which were found Great Basin desert shrub communities. Maximum likelihood classification of a principal components representation of the May AIS data enabled discrimination of subtle spatial detail in images relating to vegetation and soil characteristics. The spatial patterns in the May AIS classification were, however, too detailed for complete interpretation with existing ground data. A similar analysis of the October AIS data yielded poor results. Comparison of AIS results with a similar analysis of May Landsat Thematic Mapper data showed that the May AIS data contained approximately three to four times as much spectrally coherent information. When only two shortwave infrared TM bands were used, results were similar to those from AIS data acquired in October. Author

A88-21360

NEAR-REAL-TIME VIDEO SYSTEMS FOR RANGELAND ASSESSMENT

J. H. EVERITT, D. E. ESCOBAR, and P. R. NIXON (USDA, Agricultural Research Service, Weslaco, TX) Remote Sensing of Environment (ISSN 0034-4257), vol. 23, Nov. 1987, p. 291-311. refs

This paper reviews the current capability of video imagery for rangeland management assessment. Three video systems are described and evaluated: (1) a black-and-white four-band system with visible/near-infrared (0.4-1.1 microns) sensitivity, (2) a selectable three-band color system, and (3) a black-and-white monoband system with midinfrared (1.45-2.0 microns) sensitivity. These systems have provided near-real-time imagery that could be useful to detect differences among many variables such as plant species, phytomass levels, fertilized and drought-stressed grass, heavy grazing, and burned areas. The computer compatibility of video imagery also has been demonstrated. Finally, results have shown that video systems may have considerable application to integrate the above-listed variables for rangeland resource management assessment. Author

A88-21361

SATELLITE REMOTE SENSING OF AUSTRALIAN RANGELANDS

R. D. GRAETZ (CSIRO, Div. of Wildlife and Rangelands Research, Lyneham, Australia) Remote Sensing of Environment (ISSN 0034-4257), vol. 23, Nov. 1987, p. 313-331. refs

The nature of the soil and vegetation of the Australian landscape and the pattern and dynamics of pastoral land use are discussed along with the application of Landsat MSS and NOAA AVHRR data for the assessment and monitoring of these characteristics. Most current applications are directed towards obtaining quantitative, rather than qualitative, assessment and monitoring of rangelands; information related to land degradation is of greatest interest. A key to the successful application of either of the two satellite systems depends on the models developed to relate the spectral data to the ecological variables or parameters of interest. It is noted that the NOAA AVHRR data can replace Landsat MSS data in providing cost-effective information concerning pasture productivity but not land degradation, where the higher spatial resolution of the Landsat MSS is required. I.S.

A88-21362

DETECTION OF YEARLY COVER CHANGE WITH LANDSAT MSS ON PASTORAL LANDSCAPES IN CENTRAL AUSTRALIA

B. D. FORAN (CSIRO, Div. of Wildlife and Rangelands Research, Alice Springs, Australia) Remote Sensing of Environment (ISSN 0034-4257), vol. 23, Nov. 1987, p. 333-350. refs

This paper outlines the use of Landsat MSS for cover monitoring on sparsely vegetated landscapes grazed by cattle in central Australia. For important pastoral landscapes, a 5/7 ratio based on absolute reflectance was found to be linearly related to total plant cover, with correlation coefficients varying from -0.90 to -0.98. The strength of this relationship was notable in that the predictive regressions used data from Landsats 2, 3, and 4 and had sun angles varying from 32 to 46 deg. Prediction of cover change on some landscapes was difficult because response to rainfall was confined in limited locations, or occurred at a subpixel level. Yearly or twice yearly cover measurement at a regional level is now feasible, but implementation depends on successfully blending the technology in the decision making processes of government agencies and pastoral managers. This blending will determine whether the coarser scale NOAA imagery will be more cost-effective than Landsat MSS, considering the scale at which decisions are taken. Author

A88-21363

THE USE OF SPECTRAL AND SPATIAL VARIABILITY TO MONITOR COVER CHANGE ON INERT LANDSCAPES

G. PICKUP and B. D. FORAN (CSIRO, Div. of Wildlife and Rangelands Research, Alice Springs, Australia) Remote Sensing of Environment (ISSN 0034-4257), vol. 23, Nov. 1987, p. 351-363. refs

In a study aimed at developing methods of monitoring arid landscapes used for pastoralism in central Australia, a group of sites were identified that showed little change on Landsat MSS during 1980-1984, despite total summer rainfalls of 30-220 mm, which produced visible plant response at ground level. This seems due to growth responses being hidden at a subpixel level or confined to discrete bands in the landscape. A series of methods to detect changes in spectral and spatial variability were analyzed. The spatial autocorrelation function (ACF) and mean-variance plots of the Band 5/Band 7 ratio were found to be successful in separating cover responses typical of good, medium, and poor rainfall years. When the ACF was plotted, the years with the greatest plant cover had the highest ACF values and the decrease in autocorrelation with increasing spatial lag was slow compared with the ACFs for low cover and drought conditions. Both the visual form of this plot and its slope were found to be good general indicators of seasonal conditions and could also be used on landscapes which were structurally simpler. The mean-variance plots were another method which allowed seasonal conditions to be inferred from the position of a site in relation to its trajectory over a series of years during which plant response was known. The relative success of this work may provide a basis for plant response modeling at the landscape level. Author

A88-21364

REFLECTANCE MODELING OF SEMIARID WOODLANDS

R. P. PECH (CSIRO, Div. of Wildlife and Rangelands Research,

Lyneham, Australia) and A. W. DAVIS (CSIRO, Div. of Mathematics and Statistics, Glen Osmond, Australia) *Remote Sensing of Environment* (ISSN 0034-4257), vol. 23, Nov. 1987, p. 365-377. refs

Semiarid woodlands present a complex problem for quantitative assessment with remotely sensed data. Vegetation is sparse and unevenly distributed, with trees obscuring and shadowing both understory and bare soil. Reflectance modeling and calibration were tested using low-level aerial radiometry and photography. Modified forms of two proposed models were fitted to the data and estimates of the cover of each landscape component were calculated using two multivariate calibration methods. Author

A88-21365

SPECTRAL ASSESSMENT OF INDICATORS OF RANGE DEGRADATION IN THE BOTSWANA HARDVELD ENVIRONMENT

SUSAN RINGROSE (University of Botswana, Gaborone) and WILMA MATHESON (Gaborone Secondary School, Botswana) *Remote Sensing of Environment* (ISSN 0034-4257), vol. 23, Nov. 1987, p. 379-396. Research supported by the University of Botswana and Canadian International Development Agency. refs

The literature suggests that two different approaches have been applied to problems of rangeland monitoring using MSS data. These are referred to as the near infrared over red ratio which has been successfully applied to areas of relatively dense vegetation in the humid zone, and the darkening effect which is applicable in the sparsely vegetated semiarid zone. Data from Botswana suggests that neither of these is singularly appropriate in the savanna woodland zone of southern Africa. In the Botswana hardveld, the measured vegetation cover consists of green vegetation which generally occupies less than 60 percent of the cover in a given area. The soil component is dominant. This, in addition to other vegetation components which produce a darkening effect, results in high reflectance values in the red and infrared parts of the spectrum for areas with a low vegetation cover, and low reflectance values in both wavebands for areas with a high vegetation cover. In savanna woodland environments, which contains elements of both the near infrared to red ratio and the darkening approach, the most suitable indicators of range condition and degrees of desertification can be obtained by directly applying spectral ranges from the red band. The range of values used is heavily ecosystem, therefore soil-type-dependent, and is referred to as the savanna woodland model. Author

A88-21501

MODELLING RADAR BACKSCATTER FROM VEGETATION

JACQUELINE M. DEANE (GEC Research, Ltd., Marconi Research Centre, Chelmsford, England) *GEC Journal of Research* (ISSN 0264-9187), vol. 5, no. 3, 1987, p. 182-188. refs

Two types of model which relate radar backscatter from vegetated areas to system and target parameters have been studied. This paper contains the results of that analysis presented in a form suitable for comparison with measured backscatter and plant data. Author

A88-22617

PRELIMINARY SPOT RESULTS IN LORRAINE RELATED TO PERMANENT GRASSLANDS (PREMIERS RESULTATS SPOT EN LORRAINE RELATIFS AUX PRAIRIES PERMANENTES)

COLETTE M. GIRARD (Paris-Grignon, Institut National Agronomique, Paris, France) *Societe Francaise de Photogrammetrie et de Teledetection, Bulletin* (ISSN 0244-6014), no. 106, 1987, p. 33-40. In French. refs

Three SPOT scenes have been obtained in the southwest part of the Lorraine region in 1986. Nearly simultaneous observations and measurements from 38 test areas have made possible the characterization of seasonal spectral behavior for different grasslands. Comparison of this data with radiance data from various SPOT channels has led to the classification of eight grassland types corresponding to specific ecological conditions and agricultural types. This classification is used to produce grassland

maps. It is noted that satellite data can also be used to evaluate the instantaneous airborne chlorophyll phytomass. R.R.

A88-23253

GEOGRAPHIC INFORMATION SYSTEMS FOR RESOURCE MANAGEMENT: A COMPENDIUM

WILLIAM J. RIPPLE, ED. (Oregon State University, Corvallis) Falls Church, VA, American Society for Photogrammetry and Remote Sensing and American Congress on Surveying and Mapping, 1987, 293 p. No individual items are abstracted in this volume.

An introduction is given to the techniques and functional capabilities of geographic information systems. Recent information on the use of geographic information systems for a variety of resource management applications is compiled. An overview is provided on the nature of geographic information systems. A detailed description of the techniques required to create a computerized spatial database is presented. The capabilities of computer-based geographic information systems are reviewed on a function-by-function basis. The applications of geographic information systems in the management of water, soil, and vegetation resources and in land suitability studies, urban studies, and global studies are considered. C.D.

A88-23548

MULTIBAND-SCATTEROMETER DATA ANALYSIS OF FORESTS

DIRK H. HOEKMAN (Landbouwhogeschool, Wageningen, Netherlands) *International Journal of Remote Sensing* (ISSN 0143-1161), vol. 8, Nov. 1987, p. 1695-1707. Research supported by the Netherlands Remote Sensing Board. refs

The airborne multiband scatterometer DUTSCAT promises to become a useful tool for research in the field of active microwave remote sensing. The system can measure accurate σ_0 values in six frequency bands simultaneously at a selected incidence angle and polarization. An evaluation of the use of this system for research in forestry, in particular the problems related to probing thick vegetation canopies, is given. The system can acquire information on the vertical distribution of backscattering. Through inversion of a multilevel model, σ_0 of forests can be divided in contributions from a number of arbitrarily chosen layers (three or four). A simple and accurate new approach for the computation of σ_0 values for forests (or other thick vegetation covers) from scatterometer data is given and compared with the less accurate 'standard' way of processing used for other types of targets. Author

A88-23549

THE DUT AIRBORNE SCATTEROMETER

PAUL SNOEIJ and PETER J. F. SWART (Delft, Technische Hogeschool, Netherlands) *International Journal of Remote Sensing* (ISSN 0143-1161), vol. 8, Nov. 1987, p. 1709-1716. Research supported by the Netherlands Remote Sensing Board. refs

An airborne scatterometer system operating at six frequencies simultaneously between 1 and 18 GHz has been developed for the measurement of the microwave scattering of vegetation, forests, sea, and other targets. After a description of the instrument, some C- and L-band results are presented. Author

A88-23764

CANOPY REFLECTANCE OF SEVEN RANGELAND PLANT SPECIES WITH VARIABLE LEAF PUBESCENCE

J. H. EVERITT and A. J. RICHARDSON (USDA, Agricultural Research Service, Weslaco, TX) *Photogrammetric Engineering and Remote Sensing* (ISSN 0099-1112), vol. 53, Nov. 1987, p. 1571-1575. refs

Spectroradiometric canopy light reflectance measurements were used to distinguish among seven rangeland weed species with various amounts of leaf pubescence. The results showed that increased reflectance in the visible wavelengths distinguished dense from sparse and nonpubescent species. Water content and plant height were the most important field variable effects for distinguishing nonpubescent from sparsely and densely pubescent

01 AGRICULTURE AND FORESTRY

species. This information should be significant in the use of remote sensing imagery for mapping plant communities and identifying plant species in rangeland environments. C.D.

A88-23765* Delaware Univ., Newark.

QUANTIFICATION OF BIOMASS OF THE MARSH GRASS SPARTINA ALTERNIFLORA LOISEL USING LANDSAT THEMATIC MAPPER IMAGERY

M. F. GROSS, V. KLEMAS (Delaware University, Newark), M. A. HARDISKY (Scranton, University, PA), and P. L. WOLF (Lebanon Valley College, Annville, PA) Photogrammetric Engineering and Remote Sensing (ISSN 0099-1112), vol. 53, Nov. 1987, p. 1577-1583. Research supported by the University of Delaware. refs

(Contract NAGW-374; NOAA-NA-85AADSG033; NSF DAR-80-17836)

A88-23766* Purdue Univ., West Lafayette, Ind.

INTEGRATING SPHERE TRANSMISSOMETER FOR FIELD MEASUREMENT OF LEAF TRANSMITTANCE

V. C. VANDERBILT, D. P. DEWITT, and B. F. ROBINSON (Purdue University, West Lafayette, IN) Optical Engineering (ISSN 0091-3286), vol. 26, Dec. 1987, p. 1191-1196. refs (Contract NAS9-14016)

A simple field-rated transmissometer is described for rapidly determining the normal hemispherical transmittance $T(0 \text{ deg}, 2 \pi)$ of leaves measured in situ in the four Landsat wavelength bands. The transmissometer requires direct solar illumination of the leaf sample. It collects the transmitted light with an integrating sphere and measures the collected light using a commercially available radiometer. The transmittances determined by the transmissometer are comparable with those measured by a laboratory spectrophotometer with an integrating sphere attachment.

Author

A88-24510

AN APPLICATION OF DIVERGENCE MEASUREMENT USING TRANSFORMED VIDEO DATA

PAUL MAUSEL and WILLIAM KRAMBER (Indiana State University, Terre Haute) Geocarto International (ISSN 1010-6049), vol. 2, Dec. 1987, p. 3-10. refs

Multispectral aerial video data (0.42-0.43 microns, 0.52-0.55 microns, 0.64-0.67 microns, and 0.85-0.89 microns) with 0.13 meter resolution were collected over test plots of cotton, sorghum, cantaloupe, soil, pigweed, and johnson-grass on May 31 and July 24, 1983, near Weslaco, Texas. These data were transformed into four principal component (PC) bands for each date and used to classify the six features. The classification accuracy of individual features and associated omission/commission errors were determined. Classification accuracy characteristics associated with different numbers of PC bands were analyzed using divergence measurements derived from class training statistics. Evaluation of PC transformed data divergence indicated that: (1) divergence identified the same number and type of PC bands needed for successful feature discrimination as was determined through classification, (2) correlations between omission/commission misclassification errors and divergence values averaged -0.92 for all classifications conducted, and (3) correlations between classification accuracy and divergence averaged 0.85 for all classifications conducted. Divergence measurements derived from transformed data are potentially valuable as a guide for feature selection in classification.

Author

A88-24513* South Carolina Univ., Columbia.

CORRELATION BETWEEN AIRCRAFT MSS AND LIDAR REMOTELY SENSED DATA ON A FORESTED WETLAND

JOHN R. JENSEN (South Carolina University, Columbia), MICHAEL E. HODGSON (Colorado, University, Boulder), HALKARD E. MACKEY, JR. (Savannah River Laboratory, Aiken, SC), and WILLIAM KRABILL (NASA, Wallops Flight Center, Wallops Island, VA) Geocarto International (ISSN 1010-6049), vol. 2, Dec. 1987, p. 39-54. refs

(Contract DE-AC09-76SR-00001)

Inland wetland in a portion of the Savannah River swamp forest were mapped with an overall accuracy of 88.5 percent on April 26, 1985 using high resolution aircraft Daedalus AADS-1268 MSS data. In addition, data were acquired using a NASA sensor system flown along two flight lines over the Steel Creek Delta. The data were significantly correlated with in situ tree height measurements. The data were registered to the wetland classification map and correlated. Statistical analyses demonstrated that the laser derived canopy height information was significantly associated with the Steel Creek Delta wetland classes encountered along the transect (an F-value of 58.46 at the 0.0001 level of confidence). The relationship between vegetation height and vegetation type was then used to produce a three-dimensional model of the landscape which can be of value when computing biomass or canopy density in this forested wetland environment. Author

A88-24514

REMOTE SENSING OF FOREST COVER DISTRIBUTION IN THE PHU WIANG WATERSHED AREA OF KHON KAEN PROVINCE, NORTHEAST OF THAILAND

K. R. ISLAM (Chittagong, University, Bangladesh), M. M. DEY, D. AHMAD (Ministry of Agriculture and Lands, Kuala Lumpur, Malaysia), and ALAI CHANTARAPANICH (Buriram Teacher's College, Muang, Thailand) Geocarto International (ISSN 1010-6049), vol. 2, Dec. 1987, p. 55-59.

Landsat 4 MSS data were analyzed in conjunction with an amount of ancillary data to identify forest cover types. Computer analysis of data, as complemented by ground truths, evince that the study area is covered by evergreen forest (hill evergreen), mixed deciduous forest, mixed deciduous/evergreen forest, dry dipterocarp forest, scrub forest and fallow agricultural land, respectively. Higher spectral reflectance (78 percent) was observed for evergreen forest as compared to only 65 percent for dry dipterocarp forest in the infrared wavelength (MSS band 7). Landsat MSS band 7 was found excellent for discrimination of different types of forest cover in the study area. Total forest coverage was obtained 63 percent (188 sq km) as compared to 68.3 percent in 1982. The classification accuracy of the Landsat MSS data was found to be 82 percent, with less than 20 percent omission and commission errors. Author

A88-24932* National Aeronautics and Space Administration. Ames Research Center, Moffett Field, Calif.

SPECTRAL CHANGES IN CONIFERS SUBJECTED TO AIR POLLUTION AND WATER STRESS: EXPERIMENTAL STUDIES

WALTER E. WESTMAN (NASA, Ames Research Center, Moffett Field; California, University, Berkeley) and CURTIS V. PRICE (USGS, Water Resources Div., Trenton, NJ) IEEE Transactions on Geoscience and Remote Sensing (ISSN 0196-2892), vol. 26, Jan. 1988, p. 11-21. refs

The roles of leaf anatomy, moisture and pigment content, and number of leaf layers on spectral reflectance in healthy, pollution-stressed, and water-stressed conifer needles were examined experimentally. Jeffrey pine (*Pinus jeffreyi*) and giant sequoia (*Sequoiadendron gigantea*) were exposed to ozone and acid mist treatments in fumigation chambers; red pine (*Pinus resinosa*) needles were artificially dried. Infrared reflectance from stacked needles rose with free water loss. In an air-drying experiment, cell volume reductions induced by loss of turgor caused near-infrared reflectance (TM band 4) to drop after most free water was lost. Under acid mist fumigation, stunting of tissue development similarly reduced band 4 reflectance. Both artificial drying and pollutant fumigation caused a blue shift of the red edge of spectral reflectance curves in conifers, attributable to chlorophyll denaturation. Thematic mapper band ratio 4/3 fell and 5/4 rose with increasing pollution stress on artificial drying. Loss of water by air-drying, freeze-drying, or oven-drying enhanced spectral features, due in part to greater scattering and reduced water absorption. Grinding of the leaf tissue further enhanced the spectral features by increasing reflecting surfaces and path length. In a leaf-stacking experiment, an asymptote in visible and infrared reflectance was reached at 7-8 needle layers of red pine. I.E.

A88-25444

MEASUREMENTS OF THE BACKSCATTER AND ATTENUATION PROPERTIES OF FOREST STANDS AT X-, C- AND L-BAND

D. H. HOEKMAN (Landbouwhogeschool, Wageningen, Netherlands) Remote Sensing of Environment (ISSN 0034-4257), vol. 23, Dec. 1987, p. 397-416. Research supported by the Netherlands Remote Sensing Board. refs

The new airborne multiband scatterometer (DUTSCAT) promises to be a useful tool for research in the field of active microwave remote sensing. An evaluation of the use of this system for research in forestry is given. Besides accurate values of the differential scattering coefficient (DSC), the system can acquire information on the vertical distribution of backscattering. Through inversion of the multilevel model, DSC can be divided into contributions from a number of layers (three or four). An experiment with large corner reflectors placed on the forest floor was conducted in an effort to gain more insight into the attenuating properties of the forest canopy. The measurements of attenuation properties together with the division of the DSC into contributions from several layers simplify the model-construction effort considerably. Author

A88-25446

DIFFERENCES IN VEGETATION INDICES FOR SIMULATED LANDSAT-5 MSS AND TM, NOAA-9 AVHRR, AND SPOT-1 SENSOR SYSTEMS

K. P. GALLO (NOAA, Office of Research and Applications, Washington, DC) and C. S. T. DAUGHTRY (USDA, Remote Sensing Research Laboratory, Beltsville, MD) Remote Sensing of Environment (ISSN 0034-4257), vol. 23, Dec. 1987, p. 439-452. refs

The effects of the different wavelength bands of the Landsat-5 MSS and TM, NOAA-9 AVHRR, and SPOT-1 sensors on two vegetation indices (the normalized difference, and the near IR to red ratio) are evaluated. It is shown how NOAA-9 AVHRR data can be used to estimate vegetation indices for the Landsat-5 MSS and TM, and SPOT-1 systems. Agronomic and spectral reflectance measurements of corn canopies were acquired and the reflectance factor data were averaged into 10-nm bands over the 400-2400 nm wavelength interval. Variability in the near IR to red ratio between the four sensor systems was greatest during midseason when maximum amounts of green vegetation were present. K.K.

A88-25447* National Aeronautics and Space Administration. Goddard Space Flight Center, Greenbelt, Md.

A CANOPY REFLECTANCE MODEL BASED ON AN ANALYTICAL SOLUTION TO THE MULTIPLE SCATTERING EQUATION

PETER CAMILLO (NASA, Goddard Space Flight Center, Greenbelt, MD) Remote Sensing of Environment (ISSN 0034-4257), vol. 23, Dec. 1987, p. 453-477. refs

An approximation to the radiative transfer equation for solar radiation in relatively full, homogeneous plant canopies is presented and solved analytically for solar zenith angles less than 60 deg. The model predicts reflectance at any depth in the canopy and in any direction and may be inverted with bidirectional reflectance measurements. The model was fit to data at two sun angles and two wavebands (visible and NIR) to within the assumed errors on the reflectance data. The calculated albedos are insensitive to achievable measurement errors. Some of the parameter values themselves found by the inversion agree reasonably well with independent measurements, but the uncertainties introduced by the data noise are rather large. However, the agreement is good enough to demonstrate that the model is physically realistic. Author

A88-26335

OPERATIONAL INTERPRETATION OF AVHRR VEGETATION INDICES FOR WORLD CROP INFORMATION

WARREN R. PHILIPSON (USDA, Agricultural Research Service, Beltsville, MD) and WILLIAM L. TENG (USDA, Foreign Agricultural

Service, Washington, DC) Photogrammetric Engineering and Remote Sensing (ISSN 0099-1112), vol. 54, Jan. 1988, p. 55-59. refs

The Foreign Crop Condition Assessment Division of the U.S. Department of Agriculture analyzes satellite images and supporting information to monitor and assess crop condition in selected countries. Available to the analysts is a potentially useful database, containing a continually supplemented archive of vegetation index numbers (VINs) derived from the AVHRR satellite data. Each VIN is calculated as the average vegetation index of a geographically referenced cell of AVHRR pixels. This study has found that, despite the preponderance of mixed pixels, useful crop information can be reliably and efficiently derived from the database, and that its operational use will improve crop assessment. Author

A88-26336

ASSESSMENT OF THEMATIC MAPPER IMAGERY FOR FORESTRY APPLICATIONS UNDER LAKE STATES CONDITIONS

PAUL F. HOPKINS, ANN L. MACLEAN, and THOMAS M. LILLESAND (Wisconsin, University, Madison) Photogrammetric Engineering and Remote Sensing (ISSN 0099-1112), vol. 54, Jan. 1988, p. 61-68. Research supported by the University of Wisconsin. refs

The utility of Landsat TM data for forestry applications under Lake States conditions is assessed. Two study sites in Wisconsin with distinctly different forest character were analyzed via visual and computer-assisted interpretation techniques. Highly accurate hardwood versus softwood and upland versus lowland forest type separations were made, and further specification was shown to be possible. The results suggest that TM data can provide better forest type mapping and condition assessment information than MSS data and may, in effect, be more widely used in forestry applications. K.K.

A88-26624* Purdue Univ., West Lafayette, Ind.

POLARIZED AND NON-POLARIZED LEAF REFLECTANCES OF COLEUS BLUMEI

LOIS GRANT, C. S. T. DAUGHTRY (Purdue University, West Lafayette, IN), and V. C. VANDERBILT (NASA, Ames Research Center, Moffett Field, CA; Purdue University, West Lafayette, IN) Environmental and Experimental Botany (ISSN 0098-8472), vol. 27, no. 2, 1987, p. 139-145. refs
(Contract NAG5-269)

A polarization photometer has been used to measure the reflectance of three variegated portions of *Coleus blumei*, Benth. in five wavelength bands of the visible and near-infrared spectrum. The polarized component of the reflectance factor was found to be independent of wavelength, indicating that the polarized reflectance arises from the leaf surface. It is suggested that differences in the polarized component result from variations in surface features. The nonpolarized component of the reflectance factor is shown to be related to the internal leaf structure. The variation of the degree of polarization with wavelength was found to be greatest in the regions of the spectrum where absorption occurs. R.R.

A88-27207

USE OF MICROWAVE RADIOMETRY FOR MEASURING THE BIOMETRIC CHARACTERISTICS OF VEGETATION COVER [PRIMENENIE SVCH-RADIOMETRICHESKOGO METODA DLIA OPREDELENIYA BIOMETRICHESKIKH KHAARAKTERISTIK RASTITEL'NYKH POKROVOV]

A. A. CHUKHLANTSEV and A. M. SHUTKO (AN SSSR, Institut Radiotekhniki i Elektroniki, Moscow, USSR) Issledovanie Zemli iz Kosmosa (ISSN 0205-9614), Sept.-Oct. 1987, p. 42-48. In Russian. refs

This paper examines the possibilities of using microwave radiometry for determining biometric characteristics of vegetation from spectra of water surfaces and water-logged soils. The attenuation characteristics of microwave radiation due to vegetation are analyzed together with the accuracy of measurements. The

01 AGRICULTURE AND FORESTRY

method is applied to determine the values of above-water phytomass for rice and reed from data obtained by an airborne microwave radiometer. I.S.

A88-27208

THE EMISSIVITY OF THE VEGETATION-SOIL SYSTEM [KOEFFITSIENT IZLUCHENIIA SISTEMY POCHVA-RASTITEL'NOST']

IA. A. ANTON and IU. K. ROSS (AN ESSR, Institut Astrofiziki i Fiziki Atmosfery, Tartu, Estonian SSR) Issledovanie Zemli iz Kosmosa (ISSN 0205-9614), Sept.-Oct. 1987, p. 49-55. In Russian. refs

The relationships between physical parameters of the vegetation-soil system and its IR emissivity are investigated, and the factors which determine the difference between the true and the apparent temperature of the vegetation-soil system are considered. Using an opaque-medium model, the changes of emissivity were determined as a function of the viewing angle, the leaf-area index, and the leaf-surface orientation. In connection with the difference between the true and the apparent temperature of the vegetation-soil system, it is concluded that complicated canopy structure and the scattered radiation of the atmosphere usually make the difference equal to 1 K or less provided the percent coverage is over 60 percent. I.S.

A88-27252* Simpson Weather Associates, Inc., Charlottesville, Va.

STRUCTURE AND GROWTH OF THE MIXING LAYER OVER THE AMAZONIAN RAIN FOREST

CHARLES L. MARTIN (Simpson Weather Associates, Inc., Charlottesville, VA), DAVID FITZJARRALD (New York, State University, Albany), MICHAEL GARSTANG, STEVE GRECO (Virginia, University, Charlottesville), AMAURI P. OLIVEIRA (Sao Paulo, Universidade, Brazil), and EDWARD BROWELL (NASA, Langley Research Center, Hampton, VA) Journal of Geophysical Research (ISSN 0148-0227), vol. 93, Feb. 20, 1988, p. 1361-1375. NASA-supported research. refs

The structure and growth of the atmospheric mixed layer over the Amazonian rain forest were examined using measurements obtained during the NASA Amazon Boundary Layer Experiment. Measurements of temperature, moisture, and horizontal wind were carried out in and above the mixed layer by means of a tethered balloon, rawinsonde, and aircraft; fluxes of sensible and latent heat were measured at the top of the canopy. It was found that the mixing layer grows rapidly, at 5-8 cm/sec, soon after sunrise to a mean maximum height of 1200 m by 1300 LT; during undisturbed conditions, mixed layer heights of 1000 are common between 1000 and 1600 LT. No horizontal inhomogeneities in the mixed layer structure or depth were found over large distances. A simple mixed layer model was applied to show how fluxes of species might be estimated using only quantities measured at the surface and prescribing an initial condition and boundary condition for the mixed layer. I.S.

A88-27802* Maryland Univ., College Park.

RELATIONS BETWEEN CANOPY REFLECTANCE, PHOTOSYNTHESIS AND TRANSPIRATION - LINKS BETWEEN OPTICS, BIOPHYSICS AND CANOPY ARCHITECTURE

P. J. SELLERS (Maryland, University, College Park) (COSPAR, WMO, URSI, et al., Plenary Meeting, 26th, Symposium 3, Workshop V, and Topical Meeting A2 on Remote Sensing from Space, Toulouse, France, June 30-July 11, 1986) Advances in Space Research (ISSN 0273-1177), vol. 7, no. 11, 1987, p. 27-44. refs (Contract NAG5-492)

A88-27804

REMOTE SENSING SURVEYS DESIGN IN REGIONAL AGRICULTURAL INVENTORIES

G. G. ANDREEV, N. V. SAZANOV (Vsesoiuznyi Nauchno-Issledovatel'skii Tsentr Agrosursy, Moscow, USSR), IU. A. DZHEMARDIAN, and V. V. EZKOV (Gosudarstvennyi Komitet SSSR po Nauke i Tekhnike, Moscow, USSR) (COSPAR, WMO, URSI, et al., Plenary Meeting, 26th, Symposium 3, Workshop V,

and Topical Meeting A2 on Remote Sensing from Space, Toulouse, France, June 30-July 11, 1986) Advances in Space Research (ISSN 0273-1177), vol. 7, no. 11, 1987, p. 59-63.

Methodological aspects of setting up remote sensing observations for assessing and controlling the state of agricultural resources at the regional level are discussed. The strategy of samples is based on selection of areas with the relevant agricultural parameters, identification of representative test sites grid, remote sensing from aerospace platforms, and ground truth data acquisition. The use of the derived data in automatic interactive imagery processing is addressed. C.D.

A88-27805

SPECTRAL AND BOTANICAL CLASSIFICATION OF GRASSLANDS - AUXOIS EXAMPLE

C. M. GIRARD (Institut National Agronomique Paris-Grignon, Thiverval-Grignon, France) (COSPAR, WMO, URSI, et al., Plenary Meeting, 26th, Symposium 3, Workshop V, and Topical Meeting A2 on Remote Sensing from Space, Toulouse, France, June 30-July 11, 1986) Advances in Space Research (ISSN 0273-1177), vol. 7, no. 11, 1987, p. 67-70. refs

Botanical observations made in the field and in situ reflectance measurements made over Auxois in Burgundy were obtained. Principal components analysis of the reflectance data showed that the most important wavelengths for spectral classification of grasslands are: 550, 675, 850, and 1400 nm, while the most important period is mid-April at the beginning of plant growth. Factorial analysis of botanical data is used to define grasslands associations, which are in turn transformed into agroecological units which may be spectrally characterized. C.D.

A88-27806

COMPARATIVE STUDY OF TEMPERATURE DATA FROM NOAA7-AVHRR AND WMO - AN INTERPRETATION THROUGH THE USE OF A SOIL-VEGETATION MODEL

Y. V. SERAFINI (IBM France, S. A., Paris) (COSPAR, WMO, URSI, et al., Plenary Meeting, 26th, Symposium 3, Workshop V, and Topical Meeting A2 on Remote Sensing from Space, Toulouse, France, June 30-July 11, 1986) Advances in Space Research (ISSN 0273-1177), vol. 7, no. 11, 1987, p. 71-76. refs

NOAA7-AVHRR IR images on clear days of various seasons are used to derive surface temperatures over France. These temperatures are then compared to the shelter-height temperatures collected at the WMO standard meteorological stations during the time of satellite overpass. The difference between the two temperatures varies both with season and latitude. To analyze those results, a model of the soil-vegetation interface, forced by a reconstruction of the surface fluxes derived from the WMO data, is used. The model simulates reasonably well the seasonal trends in the difference between satellite surface temperature and surface-air temperature, and provides a physical interpretation of the latitudinal variation in summer as resulting from a north-south gradient in the soil moisture conditions. Author

A88-27807* Rutgers Univ., New Brunswick, N. J.

DETERMINATION OF VEGETATED FRACTION OF SURFACE FROM SATELLITE MEASUREMENTS

ERNESTINE CARY (Rutgers University, New Brunswick, NJ) and CYNTHIA ROSENZWEIG (NASA, Goddard Institute for Space Studies, New York) (COSPAR, WMO, URSI, et al., Plenary Meeting, 26th, Symposium 3, Workshop V, and Topical Meeting A2 on Remote Sensing from Space, Toulouse, France, June 30-July 11, 1986) Advances in Space Research (ISSN 0273-1177), vol. 7, no. 11, 1987, p. 77-80. refs

One input to the ground hydrology component of general circulation models is the fraction of gridbox covered (i.e., shaded) by vegetation. The FV is needed in order to specify the partitioning of evaporation between vegetated and nonvegetated surfaces. Satellite data could provide global and seasonally varying specification of FV. In this work, FV is derived from Landsat data for a site in western Kenya; the accuracy of the estimate is evaluated and then compared to the accuracy requirements of a ground hydrology model. Results show that the accuracy of Landsat

estimation of FV is + or - 5 percent and that transpiration, evaporation from bare soil and the seasonality of evapotranspiration are strongly dependent on FV. Author

A88-27808

MONITORING OF GLOBAL VEGETATION DYNAMICS FOR ASSESSMENT OF PRIMARY PRODUCTIVITY USING NOAA ADVANCED VERY HIGH RESOLUTION RADIOMETER

J. U. HIELKEMA (UN, Remote Sensing Centre, Rome, Italy), S. D. PRINCE, and W. L. ASTLE (Queen Mary College, London, England) (COSPAR, WMO, URSI, et al., Plenary Meeting, 26th, Symposium 3, Workshop V, and Topical Meeting A2 on Remote Sensing from Space, Toulouse, France, June 30-July 11, 1986) *Advances in Space Research* (ISSN 0273-1177), vol. 7, no. 11, 1987, p. 81-88. refs

A88-27809* National Aeronautics and Space Administration. Lyndon B. Johnson Space Center, Houston, Tex.

ESTIMATION OF BIOPHYSICAL PROPERTIES OF FOREST CANOPIES USING C-BAND MICROWAVE DATA

DAVID E. PITTS, GAUTAM D. BADHWAR (NASA, Johnson Space Center, Houston, TX), and E. REYNA (Lockheed Engineering and Management Services Co., Inc., Houston, TX) (COSPAR, WMO, URSI, et al., Plenary Meeting, 26th, Symposium 3, Workshop V, and Topical Meeting A2 on Remote Sensing from Space, Toulouse, France, June 30-July 11, 1986) *Advances in Space Research* (ISSN 0273-1177), vol. 7, no. 11, 1987, p. 89-95. refs

A scatterometer ranging experiment is described in which C-band data and bore-sight photography were collected using a helicopter so as to provide a capability to study scattering processes in forest canopies in the Superior National Forest in Minnesota. An inversion scheme is used to determine C-band volume extinction and scattering coefficients for high density aspen sites. Analysis of data through the season indicates that VV, HH, and VH volume extinction coefficients change during the year and are presumably affected by the emergence and senescence of leaves. A linear relationship was observed between $\sigma(0)$ (VV) and leaf area index for low and medium density aspen sites, but a large decrease occurred in $\sigma(0)$ for both high density sites. Calculations using the Fung disk model, which accounts only for the leaves, shows an underestimate of $\sigma(0)$ by a factor of two or three indicating that scattering by branches and soil background may be important at C-band. Author

A88-27810

A NEW STRATEGY FOR VEGETATION MAPPING WITH THE AID OF LANDSAT MSS DATA

O. G. MALAN (Council for Scientific and Industrial Research, National Physical Research Laboratory, Pretoria, Republic of South Africa) and R. H. WESTFALL (Directorate of Agricultural Research, Botanical Research Institute, Pretoria, Republic of South Africa) (COSPAR, WMO, URSI, et al., Plenary Meeting, 26th, Symposium 3, Workshop V, and Topical Meeting A2 on Remote Sensing from Space, Toulouse, France, June 30-July 11, 1986) *Advances in Space Research* (ISSN 0273-1177), vol. 7, no. 11, 1987, p. 97-103. refs

The use of almost orthographic scale-related vegetation-enhanced Landsat MSS imagery to facilitate stratification and make it more objective is demonstrated. The digital enhancement of the imagery by principal component analysis, display in Munsell color space, and filtering for scale-related product is described. An application to plant communities in the Transvaal is discussed. C.D.

A88-27811

PRELIMINARY STUDY OF THE CHARACTERIZATION OF THE RIVERINE FORESTS OF THE GARONNE USING LANDSAT MSS AND TM DATA (ETUDE PRELIMINAIRE A LA CARACTERISATION DES FORETS RIVERAINES DU FLEUVE GARONNE A L'AIDE DE DONNEES LANDSAT MSS ET TM)

G. GONZALES and H. CASANOVA (Centre d'Ecologie des Ressources Renouvelables, Toulouse, France) (COSPAR, WMO, URSI, et al., Plenary Meeting, 26th, Symposium 3, Workshop V,

and Topical Meeting A2 on Remote Sensing from Space, Toulouse, France, June 30-July 11, 1986) *Advances in Space Research* (ISSN 0273-1177), vol. 7, no. 11, 1987, p. 105-108. refs

A88-27817* National Aeronautics and Space Administration. Goddard Space Flight Center, Greenbelt, Md.

TECHNIQUES OF GROUND-TRUTH MEASUREMENTS OF DESERT-SCRUB STRUCTURE

J. OTTERMANN, D. DEERING (NASA, Goddard Space Flight Center, Greenbelt, MD), T. ECK (Science Applications Research, Lanham, MD), and S. RINGROSE (University of Botswana, Gaborone) (COSPAR, WMO, URSI, et al., Plenary Meeting, 26th, Symposium 3, Workshop V, and Topical Meeting A2 on Remote Sensing from Space, Toulouse, France, June 30-July 11, 1986) *Advances in Space Research* (ISSN 0273-1177), vol. 7, no. 11, 1987, p. 153-158. refs

Inversion of remote sensing data taken over a desert scrub surface in Texas with a multidirectionally viewing field radiometer, PARABOLA, yields the value of 0.12 for the protrusion parameter, s , (the projection on a vertical plane of plants per unit area) if isotropy (Lambert law) is assumed for the underlying soil. However, a significantly higher value of s , in the range 0.15 to 0.20, can be inferred if the soil is assumed anisotropic. It is concluded that in remote sensing of sparse vegetation, it is important to know the reflectance characteristics of the underlying soil. Other techniques that can be used to infer desert scrub vegetation structure include various photographic techniques, and measurements of reflected radiance from zenith for a range of solar elevation angles on a clear day. Author

A88-27818

ESTIMATION OF EVAPOTRANSPIRATION IN THE SAHELIAN ZONE BY USE OF METEOSAT AND NOAA AVHRR DATA

Y. H. KERR (CNES and CNRS, Laboratoire d'Etudes et de Recherches en Teledetection Spatiale, Toulouse, France), E. ASSAD, J. P. FRETEAUD (Institut de Recherches en Agronomie Tropicale, Montpellier, France), J. P. LAGUARDE, and B. SEGUIN (Institut National de Recherches Agronomiques, Montfavet, France) (COSPAR, WMO, URSI, et al., Plenary Meeting, 26th, Symposium 3, Workshop V, and Topical Meeting A2 on Remote Sensing from Space, Toulouse, France, June 30-July 11, 1986) *Advances in Space Research* (ISSN 0273-1177), vol. 7, no. 11, 1987, p. 161-164. EEC-supported research. refs

Using data collected by the Meteosat and NOAA satellites and ground data during the years 1983 to 1985, a simplified relationship has been established between surface temperature and the hydric characteristics of the soil in the Sahelian area (Senegal), which led to the elaboration of a regional map of evapotranspiration. In order to achieve this result, satellite data were processed and confronted to ground data during three rainy seasons. This paper deals with the data processing, the extraction of the physical parameters of the surface, and the processing of ground data through models. It is followed by the analysis of the results together with a discussion about the limits of the method. Author

A88-27819* Maryland Univ., College Park.

EVALUATING NORTH AMERICAN NET PRIMARY PRODUCTIVITY WITH SATELLITE OBSERVATIONS

SAMUEL N. GOWARD (Maryland, University, College Park) and DENNIS G. DYE (NASA, Goddard Space Flight Center, Greenbelt, MD) (COSPAR, WMO, URSI, et al., Plenary Meeting, 26th, Symposium 3, Workshop V, and Topical Meeting A2 on Remote Sensing from Space, Toulouse, France, June 30-July 11, 1986) *Advances in Space Research* (ISSN 0273-1177), vol. 7, no. 11, 1987, p. 165-174. refs

(Contract NCC5-26)
An ecological model is developed to estimate annual net primary productivity (NPP) in 12 North American biomes. The model combines existing models which address canopy photosynthesis in response to light, temperature, and moisture availability, and account for respiration. Climate data, solar radiation data, and spectral vegetation index data are utilized. Estimates of NPP from

01 AGRICULTURE AND FORESTRY

the model compare well with data in the literature, but a systematic error is suspected. Difficulties encountered in specifying certain model parameters are discussed as possible sources of this error. The results of this study suggest the promise of remotely sensed measurements for macroscale evaluation and modeling of NPP.

C.D.

A88-27820

ANALYZING LONG-TERM CHANGES IN VEGETATION WITH GEOGRAPHIC INFORMATION SYSTEM AND REMOTELY SENSED DATA

LOUIS R. IVERSON (Illinois Natural History Survey, Champaign) and PAUL G. RISSER (New Mexico, University, Albuquerque) (COSPAR, WMO, URSI, et al., Plenary Meeting, 26th, Symposium 3, Workshop V, and Topical Meeting A2 on Remote Sensing from Space, Toulouse, France, June 30-July 11, 1986) *Advances in Space Research* (ISSN 0273-1177), vol. 7, no. 11, 1987, p. 183-194. refs

A88-27821

COMPREHENSIVE STUDIES OF THE DYNAMICS OF GEOSYSTEMS WITH THE USE OF REMOTE SENSING TECHNIQUES

L. N. VASIL'EV (AN SSSR, Institut Geografii, Moscow, USSR), R. KACZYNSKI, and B. I. NEY (Instytut Geodezji i Kartografii, Warsaw, Poland) (COSPAR, WMO, URSI, et al., Plenary Meeting, 26th, Symposium 3, Workshop V, and Topical Meeting A2 on Remote Sensing from Space, Toulouse, France, June 30-July 11, 1986) *Advances in Space Research* (ISSN 0273-1177), vol. 7, no. 11, 1987, p. 195-199. refs

A research program on changes occurring within geosystems, part of the Interkosmos program, is described. The results of previous studies of geosystems under anthropogenic stress within the framework of the Interkosmos program are reviewed. Multifactor characteristics of soil and crops obtained in completed studies on agricultural geosystems are discussed.

C.D.

A88-27835

X-BAND FEATURES OF CANOPY COVER - AN UP TO DATE SUMMARY OF ACTIVE AND PASSIVE MEASUREMENTS

S. PALOSCIA and P. PAMPALONI (CNR, Florence, Italy) (COSPAR, WMO, URSI, et al., Plenary Meeting, 26th, Symposium 3, Workshop V, and Topical Meeting A2 on Remote Sensing from Space, Toulouse, France, June 30-July 11, 1986) *Advances in Space Research* (ISSN 0273-1177), vol. 7, no. 11, 1987, p. 305-308. CNR-supported research. refs

A88-27836*

Purdue Univ., West Lafayette, Ind. CHARACTERIZING FOREST STANDS WITH MULTI-INCIDENCE ANGLE AND MULTI-POLARIZED SAR DATA

R. M. HOFFER, D. F. LOZANO-GARCIA, and D. D. GILLESPIE (Purdue University, West Lafayette, IN) (COSPAR, WMO, URSI, et al., Plenary Meeting, 26th, Symposium 3, Workshop V, and Topical Meeting A2 on Remote Sensing from Space, Toulouse, France, June 30-July 11, 1986) *Advances in Space Research* (ISSN 0273-1177), vol. 7, no. 11, 1987, p. 309-312. (Contract JPL-956952; NAS7-918)

The potential for using HH-polarized L-band SAR data obtained at different incidence angles from satellite altitudes to identify and map different forest cover types and stand density classes is studied. Reasonably accurate results are obtained if the speckle characteristics of the data are suppressed by low-pass spatial filters and a contextual classification algorithm. Multipolarized L-band SAR data obtained from aircraft altitudes over the same test site are also analyzed to assess the relationships between polarization and forest stand characteristics. It is found that incidence angle controls, to a very large extent, the characteristics of the data and the type of information that can be obtained from L-band, HH-polarized satellite SAR data. Cross-polarization of L-band SAR data enhances and differentiates various forest stand characteristics which cannot be defined using only the like-polarized data, and vice-versa.

C.D.

A88-28010

MEASUREMENT OF CANOPY INTERCEPTION OF SOLAR RADIATION BY STANDS OF TREES IN SPARSELY WOODED SAVANNA

S. D. PRINCE (Queen Mary College, London, England) *International Journal of Remote Sensing* (ISSN 0143-1161), vol. 8, Dec. 1987, p. 1747-1766. refs

A88-28011* National Aeronautics and Space Administration. Goddard Space Flight Center, Greenbelt, Md.

DETERMINING THE RATE OF FOREST CONVERSION IN MATO GROSSO, BRAZIL, USING LANDSAT MSS AND AVHRR DATA

ROSS NELSON (NASA, Goddard Space Flight Center, Greenbelt, MD), NED HORNING (Science Applications Research, Lanham, MD), and THOMAS A. STONE (Marine Biological Laboratory, Woods Hole, MA) *International Journal of Remote Sensing* (ISSN 0143-1161), vol. 8, Dec. 1987, p. 1767-1784. refs (Contract DE-AC05-84OR-21400)

AVHRR-LAC thermal data and Landsat MSS and TM spectral data were used to estimate the rate of forest clearing in Mato Grosso, Brazil, between 1981 and 1984. The Brazilian state was stratified into forest and nonforest. A list sampling procedure was used in the forest stratum to select Landsat MSS scenes for processing based on estimates of fire activity in the scenes. Fire activity in 1984 was estimated using AVHRR-LAC thermal data. State-wide estimates of forest conversion indicate that between 1981 and 1984, 353,966 ha + or - 77,000 ha (0.4 percent of the state area) were converted per year. No evidence of reforestation was found in this digital sample. The relationship between forest clearing rate (based on MSS-TM analysis) and fire activity (estimated using AVHRR data) was noisy (R-squared = 0.41). The results suggest that AVHRR data may be put to better use as a stratification tool than as a subsidiary variable in list sampling.

Author

A88-28012*

Michigan State Univ., East Lansing. EVALUATION OF SEVERAL CLASSIFICATION SCHEMES FOR MAPPING FOREST COVER TYPES IN MICHIGAN

W. D. HUDSON (Michigan State University, East Lansing) *International Journal of Remote Sensing* (ISSN 0143-1161), vol. 8, Dec. 1987, p. 1785-1796. refs (Contract NGL-23-004-083)

Landsat MSS data were evaluated for mapping forest cover types in the northern Lower Peninsula of Michigan. The study examined seasonal variations, interpretation procedures and vegetation composition/distribution and their effect on overall classification accuracy and ability to identify individual pine species. Photographic images were used for visual interpretations while digital analysis was performed using a common (ERDAS) microcomputer image processing system. The classification schemes were evaluated using contingency tables and were ranked using the KAPPA statistic. The various classification schemes were ranked differentially according to study site location. Visual interpretation procedures ranked best, or least accurate, depending on the spatial distribution and complexity of the forest cover. Supervised classification techniques were more accurate than unsupervised clustering over all sites and seasons. Maximum likelihood classification of June data was superior to any digital classification technique of February data. The study indicates that classification accuracy is more dependent on the composition and distribution of forests in the northern lower Peninsula of Michigan than on the selection of a particular classification scheme.

Author

A88-28015

MAPPING NOAA-AVHRR IMAGERY USING EQUAL-AREA RADIAL PROJECTIONS

DANIEL LLOYD and GILES D'SOUZA (Bristol, University, England) *International Journal of Remote Sensing* (ISSN 0143-1161), vol. 8, Dec. 1987, p. 1869-1878. refs

The advantages of registering NOAA-AVHRR imagery to the world graticule of latitude and longitude using equal area radial

projections are discussed and are illustrated with normalized difference vegetation index imagery. It is noted that the practical advantages of the rectilinear graticule provided by radial projections are complemented by the egalitarian representation of the earth's surface that only an equal-area map can provide. The Peters (1982) Map radial construction is shown to be well suited to provide the base map array for products such as the Global Vegetation Index because it can be remapped to any other preferred radial construction with no data duplication and with minimal data redundancy. R.R.

A88-28016* National Aeronautics and Space Administration. Goddard Space Flight Center, Greenbelt, Md.

ESTIMATES OF PRIMARY PRODUCTIVITY OVER THE THAR DESERT BASED UPON NIMBUS-7 37 GHZ DATA - 1979-1985

B. J. CHOUDHURY (NASA, Goddard Space Flight Center, Greenbelt, MD) International Journal of Remote Sensing (ISSN 0143-1161), vol. 8, Dec. 1987, p. 1885-1890. refs

An empirical relationship has been determined between the difference of vertically and horizontally polarized brightness temperatures noted at the 37 GHz frequency of the Nimbus-7 SMMR and primary productivity over hot arid and semiarid regions of Africa and Australia. This empirical relationship is applied to estimate the primary productivity over the Thar Desert between 1979 and 1985, giving an average value of 0.271 kg/sq m per yr. The spatial variability of the productivity values is found to be quite significant, with a standard deviation about the mean of 0.08 kg/sq m per yr. R.R.

A88-28270*# National Aeronautics and Space Administration. Ames Research Center, Moffett Field, Calif.

REMOTE SENSING OF FOREST CANOPY AND LEAF BIOCHEMICAL CONTENTS

DAVID L. PETERSON, PAMELA A. MATSON, DON H. CARD (NASA, Ames Research Center, Moffett Field, CA), JOHN D. ABER, CAROL WESSMAN (Wisconsin, University, Madison), NANCY SWANBERG, and MICHAEL SPANNER (NASA, Ames Research Center; TGS Technology, Inc., Moffett Field, CA) Remote Sensing of Environment (ISSN 0034-4257), vol. 24, Feb. 1988, p. 85-108. refs

Recent research on the remote sensing of forest leaf and canopy biochemical contents suggests that the shortwave IR region contains this information; laboratory analyses of dry ground leaves have yielded reliable predictive relationships between both leaf nitrogen and lignin with near-IR spectra. Attention is given to the application of these laboratory techniques to a limited set of spectra from fresh, whole leaves of conifer species. The analysis of Airborne Imaging Spectrometer data reveals that total water content variations in deciduous forest canopies appear as overall shifts in the brightness of raw spectra. O.C.

A88-28271* New Hampshire Univ., Durham.
COMPARISON OF IN SITU AND AIRBORNE SPECTRAL MEASUREMENTS OF THE BLUE SHIFT ASSOCIATED WITH FOREST DECLINE

B. N. ROCK (New Hampshire, University, Durham), T. HOSHIZAKI (California Institute of Technology, Jet Propulsion Laboratory, Pasadena), and J. R. MILLER (York University, North York, Canada) Remote Sensing of Environment (ISSN 0034-4257), vol. 24, Feb. 1988, p. 109-127. refs

Visible IR Intelligent Spectrometer (VIRIS) reflectance data have been found to have similar features that are related to air-pollution-induced forest decline and visible damage in both the red spruce of Vermont and the Norway spruce of Baden-Wuerttemberg; the similarity suggests a common source of damage. Spectra of both species include a 5-nm blueshifting of the red-edge inflection point, while pigment data for both species indicate a loss of total chlorophylls. The blue shift of the chlorophyll absorption maximum, as well as the increased red radiance and decreased near-IR radiance of the damaged spruce, may be used to delineate and map damage areas. O.C.

A88-28272* Ludwig-Maximilians-Universitaet, Munich (West Germany).

PRELIMINARY ASSESSMENT OF AIRBORNE IMAGING SPECTROMETER AND AIRBORNE THEMATIC MAPPER DATA ACQUIRED FOR FOREST DECLINE AREAS IN THE FEDERAL REPUBLIC OF GERMANY

KARIN HERRMANN, ULRICH AMMER (Muenchen, Universitaet, Munich, Federal Republic of Germany), BARRETT ROCK (New Hampshire, University, Durham), and HELEN N. PALEY (California Institute of Technology, Jet Propulsion Laboratory, Pasadena) Remote Sensing of Environment (ISSN 0034-4257), vol. 24, Feb. 1988, p. 129-149. DFVLR-supported research. refs

This study evaluated the utility of data collected by the high-spectral resolution airborne imaging spectrometer (AIS-2, tree mode, spectral range 0.8-2.2 microns) and the broad-band Daedalus airborne thematic mapper (ATM, spectral range 0.42-13.0 micron) in assessing forest decline damage at a predominantly Scotch pine forest in the FRG. Analysis of spectral radiance values from the ATM and raw digital number values from AIS-2 showed that higher reflectance in the near infrared was characteristic of high damage (heavy chlorosis, limited needle loss) in Scotch pine canopies. A classification image of a portion of the AIS-2 flight line agreed very well with a damage assessment map produced by standard aerial photointerpretation techniques. Author

A88-28682* National Aeronautics and Space Administration. Lyndon B. Johnson Space Center, Houston, Tex.

THE USE OF A HELICOPTER MOUNTED RANGING SCATTEROMETER FOR ESTIMATION OF EXTINCTION AND BACKSCATTERING PROPERTIES OF FOREST CANOPIES-I: EXPERIMENTAL APPROACH AND CALIBRATION

DAVID E. PITTS, GAUTAM D. BADHWAR (NASA, Johnson Space Center, Houston, TX), EDDIE REYNA (Lockheed Engineering and Management Services Co., Inc., Houston, TX), FAWWAZ T. ULABY (Michigan, University, Ann Arbor), and DAVID R. BRUNFELDT (Applied Microwave Corp., Lawrence, KS) IEEE Transactions on Geoscience and Remote Sensing (ISSN 0196-2892), vol. 26, March 1988, p. 140-143. refs

A helicopter-borne C-band scatterometer with the capability of collecting the backscattered power as a function of range is described. This instrument was repeatedly flown from May to September 1984 to study the microwave properties of forest canopies of aspen and black spruce in the Superior National Forest in Minnesota. The characteristics of the instrument, its calibration, the data collection, and preprocessing, are described. I.E.

A88-28683* National Aeronautics and Space Administration. Lyndon B. Johnson Space Center, Houston, Tex.

THE USE OF A HELICOPTER MOUNTED RANGING SCATTEROMETER FOR ESTIMATION OF EXTINCTION AND BACKSCATTERING PROPERTIES OF FOREST CANOPIES-II: EXPERIMENTAL RESULTS FOR HIGH-DENSITY ASPEN

DAVID E. PITTS, GAUTAM D. BADHWAR (NASA, Johnson Space Center, Houston, TX), and EDDIE REYNA (Lockheed Engineering and Management Services Co., Inc., Houston, TX) IEEE Transactions on Geoscience and Remote Sensing (ISSN 0196-2892), vol. 26, March 1988, p. 144-152. refs

An analytic expression is derived that describes the backscatter power from a semi-infinite plane parallel homogeneous canopy as a function of distance from an airborne radar. This model is fitted to observed data for a high-density aspen canopy by a modification of a technique developed by Tyapkin (1960). This inversion of the model provides unbiased estimates of the canopy extinction and backscattering parameters. An active radar calibrator located underneath the canopy provides an independent method of determining the volume extinction coefficient. The results reported indicate that the coefficients change throughout the year. A comparison of these coefficients with Eom and Funk's (1984) disk model, using measured canopy properties, shows that at C-band frequency, only a part of the scattering and absorption can be attributed to the canopy leaves. I.E.

A88-28705* National Aeronautics and Space Administration. Ames Research Center, Moffett Field, Calif.

ABOVEGROUND BIOMASS, SURFACE AREA, AND PRODUCTION RELATIONS OF RED FIR (ABIES MAGNIFICA) AND WHITE FIR (A. CONCOLOR)

WALTER E. WESTMAN (NASA, Ames Research Center; TGS Technology, Inc., Moffett Field, CA; California, University, Los Angeles) Canadian Journal of Forest Research (ISSN 0045-5067), vol. 17, 1987, p. 311-319. Research supported by the California Air Resources Board. refs
(Contract NCA2-IR-390-402)

A88-29277

AIRCRAFT MSS DATA REGISTRATION AND VEGETATION CLASSIFICATION FOR WETLAND CHANGE DETECTION

E. J. CHRISTENSEN (EG&G Energy Measurements, Inc., Las Vegas, NV), J. R. JENSEN, E. W. RAMSEY (South Carolina, University, Columbia), and H. E. MACKEY, JR. (Du Pont de Nemours and Co., Inc., Savannah River Laboratory, Aiken, SC) International Journal of Remote Sensing (ISSN 0143-1161), vol. 9, Jan. 1988, p. 31-38. refs
(Contract DE-AC09-76SR-00001)

Portions of the Savannah River floodplain swamp were evaluated for vegetation change using high resolution (5.6 m) aircraft multispectral scanner (MSS) data. Image distortion from aircraft movement prevented precise image-to-image registration in some areas. However, when small scenes were used (200-250 ha), a first-order linear transformation provided registration accuracies of less than or equal to one pixel. A larger area was registered using a piecewise linear method. Five major wetland classes were identified and evaluated for change. Phenological differences and the variable distribution of vegetation limited wetland type discrimination. Using unsupervised methods and ground-collected vegetation data, overall classification accuracies ranged from 84 percent to 87 percent for each scene. Results suggest that high-resolution aircraft MSS data can be precisely registered, if small areas are used, and that wetland vegetation change can be accurately detected and monitored. Author

A88-29278

LANDSAT IMAGERY FOR MAPPING SALINE SOILS AND WETLANDS IN NORTH-WEST INDIA

R. C. SHARMA and G. P. BHARGAVA (Central Soil Salinity Research Institute, Karnal, India) International Journal of Remote Sensing (ISSN 0143-1161), vol. 9, Jan. 1988, p. 39-44. refs

A88-29280

FORECASTING PATTERNS OF SOIL EROSION IN ARID LANDS FROM LANDSAT MSS DATA

G. PICKUP and V. H. CHEWINGS (CSIRO, Central Australian Laboratory, Alice Springs, Australia) International Journal of Remote Sensing (ISSN 0143-1161), vol. 9, Jan. 1988, p. 69-84. refs

A model for forecasting large-scale patterns of soil erosion and deposition from Landsat MSS data in arid grazing lands is described. The model is based on the erosion cell mosaic approach and exploits the high degree of temporal and spatial autocorrelation in the erosion process on flat alluvial plains. Testing of the model against observed change indicates that it is reasonably accurate as long as the underlying pattern series is obtained from imagery in which there is sufficient vegetation cover for the soil stability index to be a sensitive indicator of the state of the landscape. B.J.

A88-29282* Marine Biological Lab., Woods Hole, Mass.

SHUTTLE IMAGING RADAR A ANALYSIS OF LAND USE IN AMAZONIA

THOMAS A. STONE (Marine Biological Laboratory, Woods Hole, MA) and GEORGE M. WOODWELL (Woods Hole Oceanographic Institution, MA) International Journal of Remote Sensing (ISSN 0143-1161), vol. 9, Jan. 1988, p. 95-105. NASA-DOE-supported research. refs

Over large areas in the tropics, satellite imagery is the principal

source of data on the area, current stature, and extent of disturbance of the forests. The information from imagery that covers large areas at low resolution is greatly enhanced when different types of imagery can be compared. The paper presents a comparison of data from Landsat MSS and from the Shuttle Imaging Radar (SIR-A) L band HH polarization data for sites in the Amazon Basin. Results indicate that SIR-A backscatter from the undisturbed forest was lower than that from some disturbed areas and from flooded forests and that SIR-A brightness, increases nonlinearly with the Landsat normalized difference vegetation index. It is hypothesized that the brightest radar returns in southern Amazonia are from newly cleared forests that are littered with standing and fallen tree boles that function as corner reflectors; and that backscatter will diminish from disturbed areas over time as fields are burned repeatedly. Author

A88-29288

EXPLORING THE RELATIONSHIPS BETWEEN LEAF NITROGEN CONTENT, BIOMASS AND THE NEAR-INFRARED/RED REFLECTANCE RATIO

S. E. PLUMMER (Sheffield, University, England) International Journal of Remote Sensing (ISSN 0143-1161), vol. 9, Jan. 1988, p. 177-183. refs

Results of a pilot study that sought to explore the links between biomass, leaf 'kjeldahl' nitrogen (LKN), and R and NIR reflectance are presented. It was found that biomass was related to R and NIR reflectance and LKN but the variance in each relationship was high despite taking into account leaf and soil moisture and site topography. It is suggested that much of the unexplained variance is due to different proportions of live, dead, erectophile, and planophile biomass at each site. B.J.

A88-29494

INTERMEDIATE-SCALE VEGETATION MAPPING OF INNOKO NATIONAL WILDLIFE REFUGE, ALASKA USING LANDSAT MSS DIGITAL DATA

STEPHEN S. TALBOT (U.S. Fish and Wildlife Service, Anchorage, AK) and CARL J. MARKON (TGS Technology, Inc., Anchorage, AK) Photogrammetric Engineering and Remote Sensing (ISSN 0099-1112), vol. 54, March 1988, p. 377-383. refs

A Landsat-derived vegetation map was prepared for Innoko National Wildlife Refuge. The refuge lies within the northern boreal subzone of northwestern central Alaska. Six major vegetation classes and 21 subclasses were recognized: forest (closed needleleaf, open needleleaf, needleleaf woodland, mixed, and broadleaf); broadleaf scrub (lowland, upland burn regeneration, subalpine); dwarf scrub (prostrate dwarf shrub tundra, erect dwarf shrub heath, dwarf shrub-graminoid peatland, dwarf shrub-graminoid tussock peatland, dwarf shrub raised bog with scattered trees, dwarf shrub-graminoid marsh); herbaceous (graminoid bog, graminoid marsh, graminoid tussock-dwarf shrub peatland); scarcely vegetated areas (scarcely vegetated scree and floodplain); and water (clear, sedimented). The methodology employed a cluster-block technique. Sample areas were described based on a combination of helicopter-ground survey, aerial photointerpretation, and digital Landsat data. Major steps in the Landsat analysis involved preprocessing (geometric correction), derivation of statistical parameters for spectral classes, spectral class labeling of sample areas, preliminary classification of the entire study area using a maximum-likelihood algorithm, and final classification utilizing ancillary information such as digital elevation data. The final product is 1:250,000-scale vegetation map representative of distinctive regional patterns and suitable for use in comprehensive conservation planning. Author

A88-29495

MEASURING CROWN COVER IN INTERIOR ALASKA VEGETATION TYPES

KENNETH C. WINTERBERGER and FREDERIC R. LARSON (USDA, Anchorage Forestry Sciences Laboratory, AK) Photogrammetric Engineering and Remote Sensing (ISSN 0099-1112), vol. 54, March 1988, p. 385-387. refs

Various aerial and ground methods used to estimate crown

closure are described. Consideration is given to the applicability of ocular estimation, the comparison method, the use of stereograms or dot grids, plane-table surveying, and the Klier (1969) method based on the Bitterlich principle for crown closure measurement. The use of remote sensing data to estimate crown closure in the interior of Alaska is examined. The difficulties involved in estimating from the images, and various procedures for alleviating these problems, such as the use of the Caylor method, are discussed. I.F.

A88-30087

ADAPTIVE COMPUTER-AIDED SYSTEM FOR CROP INVENTORY ACCORDING TO SPACE PHOTOGRAPHS
[ADAPTIVNAIA AVTOMATIZIROVANNAIA SISTEMA INVENTARIZATSII SEL'SKOKHOZIAISTVENNYKH KUL'TUR PO KOSMICHESKIM SNIMKAM]

V. V. ASMUS, V. VADAS, A. B. KARASEV, and L. KECHKEMETI (Gosudarstvennyi Nauchno-Issledovatel'skii Tsentr Izucheniia Prirodnykh Resursov, Moscow, USSR; Orszagos Meteorologiai Szolgálat, Budapest, Hungary) *Issledovanie Zemli iz Kosmosa* (ISSN 0205-9614), Nov.-Dec. 1987, p. 79-88. In Russian. refs

A88-30439

CALCULATION OF CANOPY BIDIRECTIONAL REFLECTANCE USING THE MONTE CARLO METHOD

IU. K. ROSS and A. L. MARSHAK (AN ESSR, Institut Astrofiziki i Fiziki Atmosfery, Toravere, Estonian SSR) (*Issledovanie Zemli iz Kosmosa*, July-Aug. 1987, p. 86-93) *Remote Sensing of Environment* (ISSN 0034-4257), vol. 24, March 1988, p. 213-225. Translation. Previously cited in issue 06, p. 834, Accession no. A88-19572. refs

A88-30440* Jet Propulsion Lab., California Inst. of Tech., Pasadena.

ASSESSING FOREST DAMAGE IN HIGH-ELEVATION CONIFEROUS FORESTS IN VERMONT AND NEW HAMPSHIRE USING THEMATIC MAPPER DATA

JAMES E. VOGELMANN and BARRETT N. ROCK (California Institute of Technology, Jet Propulsion Laboratory, Pasadena) *Remote Sensing of Environment* (ISSN 0034-4257), vol. 24, March 1988, p. 227-246. refs

This study evaluates the potential of measuring/mapping forest damage in spruce-fir forests in the Green Mountains of Vermont and White Mountains of New Hampshire using Landsat Thematic Mapper (TM) data. The TM 1.65/0.83-micron (TM5/4) and 2.22/0.83-micron (TM7/4) band ratios were found to correlate well with ground-based measurements of forest damage (a measure of percentage foliar loss) at 11 spruce-fir stands located on Camels Hump, a mountain in northern Vermont. Images using 0.56 and 1.65-micron bands with 1.65/0.83-micron band ratios indicated locations of heavy conifer forest damage. Both 1.65/0.83 and 2.22/0.83-micron band ratios were used to quantify levels of conifer forest damage among individual mountains throughout many of the Green and White Mountains. Damage was found to be consistently higher for the Green than the White Mountains.

Author

A88-30441* National Aeronautics and Space Administration. Goddard Space Flight Center, Greenbelt, Md.

ESTIMATING FOREST BIOMASS AND VOLUME USING AIRBORNE LASER DATA

ROSS NELSON (NASA, Goddard Space Flight Center, Greenbelt, MD), WILLIAM KRABILL (NASA, Wallops Flight Center, Wallops Island, VA), and JOHN TONELLI (International Paper Corporate Research Center, Tuxedo Park, NY) *Remote Sensing of Environment* (ISSN 0034-4257), vol. 24, March 1988, p. 247-267. refs

An airborne pulsed laser system was used to obtain canopy height data over a southern pine forest in Georgia in order to predict ground-measured forest biomass and timber volume. Although biomass and volume estimates obtained from the laser data were variable when compared with the corresponding ground measurements site by site, the present models are found to predict

mean total tree volume within 2.6 percent of the ground value, and mean biomass within 2.0 percent. The results indicate that species stratification did not consistently improve regression relationships for four southern pine species. R.R.

A88-30444* National Aeronautics and Space Administration. Goddard Space Flight Center, Greenbelt, Md.

RELATIVE SENSITIVITY OF NORMALIZED DIFFERENCE VEGETATION INDEX (NDVI) AND MICROWAVE POLARIZATION DIFFERENCE INDEX (MPDI) FOR VEGETATION AND DESERTIFICATION MONITORING

FRANCOIS BECKER and BHASKAR J. CHOUDHURY (NASA, Goddard Space Flight Center, Greenbelt, MD) *Remote Sensing of Environment* (ISSN 0034-4257), vol. 24, March 1988, p. 297-311. refs

A simple equation relating the Microwave Polarization Difference Index (MPDI) and the Normalized Difference Vegetation Index (NDVI) is proposed which represents well data obtained from Nimbus 7/SMMR at 37 GHz and NOAA/AVHRR Channels 1 and 2. It is found that there is a limit which is characteristic of a particular type of cover for which both indices are equally sensitive to the variation of vegetation, and below which MPDI is more efficient than NDVI. The results provide insight into the relationship between water content and chlorophyll absorption at pixel size scales. R.R.

A88-30446* National Aeronautics and Space Administration. Goddard Space Flight Center, Greenbelt, Md.

ESTIMATING SURFACE SOIL MOISTURE FROM SATELLITE MICROWAVE MEASUREMENTS AND A SATELLITE DERIVED VEGETATION INDEX

MANFRED OWE, ALFRED CHANG (NASA, Goddard Space Flight Center, Greenbelt, MD), and ROBERT E. GOLUS (Science Applications Research, Lanham, MD) *Remote Sensing of Environment* (ISSN 0034-4257), vol. 24, March 1988, p. 331-345. refs

Normalized 18-GHz microwave brightness temperatures, T(B), and a vegetation index determined from satellite radiometer data are combined with climatically modeled surface moisture estimates to constrain a simple physically based soil moisture model. It is found that the normalized T(B) values correlated well with soil moisture when the data were segregated by vegetation index range, but less so when all the data were combined. By using the vegetation index parameter, the model is shown to account for about 70 percent of the variability in modeled surface soil moisture. R.R.

A88-30447* Montana Univ., Missoula.

RELATING SEASONAL PATTERNS OF THE AVHRR VEGETATION INDEX TO SIMULATED PHOTOSYNTHESIS AND TRANSPIRATION OF FORESTS IN DIFFERENT CLIMATES

STEVEN W. RUNNING and RAMAKRISHNA R. NEMANI (Montana, University, Missoula) *Remote Sensing of Environment* (ISSN 0034-4257), vol. 24, March 1988, p. 347-367. refs (Contract NAGW-952; NCA2-138; NCA2-27)

Weekly AVHRR Normalized Difference Vegetation Index (NDVI) values for 1983-1984 for seven sites of diverse climate in North America were correlated with results of an ecosystem simulation model of a hypothetical forest stand for the corresponding period at each site. The tendency of raw NDVI data to overpredict photosynthesis and transpiration on water limited sites was shown to be partially corrected by using an aridity index of annual radiation/annual precipitation. The results suggest that estimates of vegetation productivity using the global vegetation index are only accurate as annual integrations, unless unsampled local area coverage NDVI data can be tested against forest photosynthesis, transpiration and aboveground net primary production data measured at shorter time intervals. R.R.

A88-30448* San Diego State Univ., Calif.

ESTIMATION OF WHEAT CANOPY RESISTANCE USING COMBINED REMOTELY SENSED SPECTRAL REFLECTANCE AND THERMAL OBSERVATIONS

01 AGRICULTURE AND FORESTRY

A. S. HOPE (San Diego State University, CA) Remote Sensing of Environment (ISSN 0034-4257), vol. 24, March 1988, p. 369-383. USDA-NASA-supported research. refs

A88-32658* National Aeronautics and Space Administration. Goddard Space Flight Center, Greenbelt, Md.

MICROWAVE VEGETATION INDEX - A NEW LONG-TERM

GLOBAL DATA SET FOR BIOSPHERIC STUDIES

BHASKAR J. CHOUDHURY (NASA, Goddard Space Flight Center, Greenbelt, MD) International Journal of Remote Sensing (ISSN 0143-1161), vol. 9, Feb. 1988, p. 185, 186.

A88-32660

SIMULATION OF SOLAR ZENITH ANGLE EFFECT ON GLOBAL VEGETATION INDEX (GVI) DATA

S. M. SINGH (NERC, Reading, England) International Journal of Remote Sensing (ISSN 0143-1161), vol. 9, Feb. 1988, p. 237-248. refs

(Contract NERC-F60/G6/12)

The effect of solar zenith angle on the normalized difference vegetation index (NDVI) derived from the AVHRR channel 1 (red) and channel 2 (near-IR) data is studied. Four classes of surface-cover types (high, moderate, and low vegetation densities and bare soil) are considered. For each class, the NDVI was simulated for solar zenith angles up to 90 deg. The results reveal that the NDVI for bare soil remains constant for solar zenith angles up to about 60 deg, then decreases for solar zenith angles above this. The NDVIs for high, moderate, and low green-leaf vegetation densities remain constant up to a solar zenith angle of 30 deg. In the case of larger solar zenith angles, these NDVIs decrease significantly. K.K.

A88-32661

VEGETATIVE AND OPTICAL CHARACTERISTICS OF FOUR-ROW CROP CANOPIES

D. F. WANJURA and J. L. HATFIELD (USDA, Cropping Systems Research Laboratory, Lubbock, TX) International Journal of Remote Sensing (ISSN 0143-1161), vol. 9, Feb. 1988, p. 249-258. refs

The row crop canopies of cotton, soya beans, grain sorghum, and sunflower were characterized on the basis of plant height, ground cover, leaf area index, leaf overlap index, foliage density, and leaf angle. It was found that, in all crops, plant height was highly correlated with ground cover and leaf area index, and leaf area index was highly correlated with leaf overlap index. Increasing the leaf area increased the radiation scattering coefficient value for band TM 4 while the band TM 3 coefficient value stayed the same. K.K.

A88-32662

RADIOMETRIC LEAF AREA INDEX

P. J. CURRAN and N. W. WARDLEY (Sheffield, University, England) International Journal of Remote Sensing (ISSN 0143-1161), vol. 9, Feb. 1988, p. 259-274. refs

The geometrical structure of a vegetation canopy determines the amount of foliage presented to a sensor and the form of the relationship between reflectance and vegetation amount. The aim of this study was to develop a practical measure of vegetation amount that was sensitive to canopy geometry. This measure was termed the radiometric leaf area index (RLAI) and comprised measurements of leaf area index (LAI), leaf inclination or curvature and the area of the canopy visible to the sensor. RLAI, evaluated on simulated and laboratory-derived data, was sensitive to canopy geometry but, like LAI, suffered from a high measurement error. Primarily as a result of error in these data sets reflectance was similarly correlated to both RLAI and LAI and therefore RLAI offered no advantage over LAI for the measurement of vegetation amount. It was concluded that future formulations of RLAI should be more complex and accurate. Author

A88-32663

EVALUATION OF MIDDLE AND THERMAL INFRARED RADIANCE IN INDICES USED TO ESTIMATE GLAI

H. D. WILLIAMSON (Adelaide, University, Australia) International Journal of Remote Sensing (ISSN 0143-1161), vol. 9, Feb. 1988, p. 275-283. refs

(Contract NERC-GR3/5046)

The remote sensing of agricultural crops has concentrated on the use of red and near-infrared radiance. The increasing availability of middle and thermal infrared radiance data has opened up a new source of spectral information. In grassland areas middle and thermal infrared radiance are usually negatively related to green leaf area index (GLAI). These data can be used in vegetation indices (in addition to red and near-infrared radiance data) to model the GLAI-radiance relationship empirically. The accuracy of GLAI estimation was significantly increased using such indices rather than a red/near-infrared based index. These increases were masked when applying a methodology to allow for sampling error and it is suggested that this was due to this section of the methodology rather than insufficient spectral information from the middle and thermal infrared wavebands. Author

A88-32664

CROP CANOPY SPECTRAL REFLECTANCE

MAHENDRA KUMAR (Nottingham, University, Loughborough, England) International Journal of Remote Sensing (ISSN 0143-1161), vol. 9, Feb. 1988, p. 285-294. refs

A simple model based on the Kubelka-Munk theory of scattering is used to describe a relationship between reflection ratios in two contrasting wavebands and fractional light absorption by a canopy. The analysis reveals that while the relationship between ratio and vegetation is curvilinear, it varies linearly with the fraction of photosynthetically active radiation absorbed by vegetation. Author

A88-32665

LARGE AREA CROP CLASSIFICATION IN NEW SOUTH WALES, AUSTRALIA, USING LANDSAT DATA

KEN W. DAWBIN and JOHN C. EVANS (New South Wales Department of Agriculture, Haymarket, Australia) International Journal of Remote Sensing (ISSN 0143-1161), vol. 9, Feb. 1988, p. 295-301. refs

A88-32666

AN INTEGRATED CAMERA AND RADIOMETER FOR AERIAL MONITORING OF VEGETATION

S. D. PRINCE, P. J. WILLSON, D. M. HUNT, and P. HALSTEAD (Queen Mary College, London, England) International Journal of Remote Sensing (ISSN 0143-1161), vol. 9, Feb. 1988, p. 303-318. Research supported by the United Nations and NERC. refs

The design requirements for a broad-band red and near infrared radiometer for monitoring vegetation from a light aircraft are discussed and an instrument which incorporates these characteristics, called an integrated camera and radiometer (ICAR), is described. It consists of two downward-looking, spectral radiometers and a solar radiometer coupled with a 35 mm camera and a data-logger in a convenient payload for mounting in a light aircraft. The distinctive features of the ICAR are the synchronization of the camera and radiometers, the equivalence of their fields of view and the integral microcomputer which controls the instrument and acts as a programmable data-logger. The simultaneous aerial photographs are used to locate the data geographically, to select the fields of view which are of the desired target, to interpret the radiometer data, and to act as a record of the terrain conditions for visual interpretation. ICAR data are compared with data from an Exotech 100BX radiometer mounted in an aircraft and also with satellite imaging radiometer data for the same locations. Author

N88-16113# Joint Publications Research Service, Arlington, Va. MONTE CARLO METHOD CALCULATION OF SPECTRAL BRIGHTNESS COEFFICIENT OF VEGETATION COVER AS FUNCTION OF ILLUMINATION CONDITIONS Abstract Only

YU. K. ROSS and A. L. MARSHAK In its JPRS Report: Science and Technology. USSR: Space p 133 24 Nov. 1987 Transl. into ENGLISH from Issledovaniye Zemli iz Kosmosa (Moscow,

USSR), no. 2, Mar. - Apr. 1987 p 96-105 Original language document was announced in IAA as A87-48190
 Avail: NTIS HC A08/MF A01

Results are presented from calculation of the variation of spectral brightness coefficient or index of reflection of a model of a vegetation cover as a function of the viewing direction. The influence of repetition of scattering and the fraction of scattered sky radiation in the total incident solar radiation is estimated. The variation of spectral brightness coefficient with zenith angle, azimuth of the Sun and brightness of the soil is analyzed. Calculations are performed for the area of photosynthetically active radiation at 380 to 710 nm. Vegetation is modeled by horizontal matte leaves and vertical nontransparent stems. It is found that the model can be limited to one time scattering, multiple scattering increasing the brightness by only 5 percent. The indices of reflection calculated for total and direct solar radiation differ little. Author

N88-16182*# Bionetics Corp., Cocoa Beach, Fla.
EFFECTS OF FIRE ON COMPOSITION, BIOMASS, AND NUTRIENTS IN OAK SCRUB VEGETATION ON JOHN F. KENNEDY SPACE CENTER, FLORIDA

PAUL A. SCHMALZER and C. ROSS HINKLE Jul. 1987 149 p
 (NASA-TM-100305; NAS 1.15:100305) Avail: NTIS HC A07/MF A01 CSCL 02F

Four stands of oak scrub two, four, eight, and 25 years since fire were sampled with permanent 15 m line transects. Percent cover by species was determined. Plant samples were analyzed for a variety of substances. Transects were resurveyed in 1985 for vegetation parameters. Nutrient pools in biomass were calculated from biomass data and tissue nutrient concentrations. Soil nutrient pools were calculated from nutrient concentrations and bulk density. Species distribution and soil chemical properties were found to be closely related to water table depth. The following fire-related conclusions are reached: (1) major structural changes occur in scrub after fire in that shrub height is reduced and requires four to six years to exceed 1 m; (2) reduction in shrub height affects the suitability of scrub for the Florida scrub jay (3) live biomass increases with time since fire; (4) nutrient concentrations in live biomass do not change with time since fire; (5) species composition and richness are little changed after fire; and (6) imposition of a continued regime of burning on a three-year cycle may have adverse impacts not indicated by the recovery of scrub from a single fire. J.P.B.

N88-17098# Deutsche Forschungs- und Versuchsanstalt fuer Luft- und Raumfahrt, Freiburg (West Germany).

INVESTIGATIONS ON THE APPLICATION OF SPACE PHOTOGRAPHS (SPACELAB METRIC CAMERA) FOR ROUTINE INVENTORIES OF EXTENSIVELY MANAGED FOREST AREAS Thesis - Freiburg Univ., Fed. Republic of Germany

WOLF FORSTREUTER Dec. 1986 252 p In GERMAN; ENGLISH summary Original contains color illustrations (DFVLR-FB-87-22; ISSN-0171-1342; ETN-88-91447) Avail: NTIS HC A12/MF A01; DFVLR, Cologne, Fed. Republic of Germany DM 135

The applicability of photos for forest inventories was investigated. The pictures were taken with a metric camera in space, and are comparable with LANDSAT data in many respects. The characteristics of the Spacelab pictures and their information content with respect to large-area inventories are discussed. The results demonstrate the applicability for forest inventories. The different data processing possibilities, and the availability of the data are discussed. ESA

N88-17103*# Utah Univ., Salt Lake City. Center for Remote Sensing and Cartography.

DETECTION OF SOIL EROSION WITH THEMATIC MAPPER (TM) SATELLITE DATA WITHIN PINYON-JUNIPER WOODLANDS

KEVIN PAUL PRICE Dec. 1987 210 p Sponsored in part by USDA Soil Conservation Service

(Contract NAGW-95)

(NASA-CR-182476; NAS 1.26:182476; CRSC-87-2) Avail: NTIS HC A10/MF A01 CSCL 02F

Pinyon-Juniper woodlands dominate approximately 24.3 million hectares (60 million acres) in the western United States. The overall objective was to test the sensitivity of the LANDSAT Thematic Mapper (TM) spectral data for detecting varying degrees of soil erosion within the Pinyon-Juniper woodlands. A second objective was to assess the potential of the spectral data for assigning the Universal Soil Loss Equation (USLE) crop management (C) factor values to varying cover types within the woodland. Thematic Mapper digital data for June 2, 1984 on channels 2, 3, 4, and 5 were used. Digital data analysis was performed using the ELAS software package. Best results were achieved using CLUS, an unsupervised clustering algorithm. Fifteen of the 40 Pinyon-Juniper signatures were identified as being relatively pure Pinyon-Juniper woodland. Final analysis resulted in the grouping of the 15 signatures into three major groups. Ten study sites were selected from each of the three groups and located on the ground. At each site the following field measurements were taken: percent tree canopy and percent understory cover, soil texture, total soil loss, and soil erosion rate estimates. A technique for measuring soil erosion within Pinyon-Juniper woodlands was developed. A theoretical model of site degradation after Pinyon-Juniper invasion is presented. Author

N88-18049*# California Univ., Santa Barbara. Dept. of Geography.

IMPROVED CANOPY REFLECTANCE MODELING AND SCENE INFERENCE THROUGH IMPROVED UNDERSTANDING OF SCENE PATTERN Final Report

JANET FRANKLIN and DAVID SIMONETT 31 Jan. 1988 56 p
 (Contract NGT-05-010-804)
 (NASA-CR-182488; NAS 1.26:182488) Avail: NTIS HC A04/MF A01 CSCL 02F

The Li-Strahler reflectance model, driven by LANDSAT Thematic Mapper (TM) data, provided regional estimates of tree size and density within 20 percent of sampled values in two bioclimatic zones in West Africa. This model exploits tree geometry in an inversion technique to predict average tree size and density from reflectance data using a few simple parameters measured in the field (spatial pattern, shape, and size distribution of trees) and in the imagery (spectral signatures of scene components). Trees are treated as simply shaped objects, and multispectral reflectance of a pixel is assumed to be related only to the proportions of tree crown, shadow, and understory in the pixel. These, in turn, are a direct function of the number and size of trees, the solar illumination angle, and the spectral signatures of crown, shadow and understory. Given the variance in reflectance from pixel to pixel within a homogeneous area of woodland, caused by the variation in the number and size of trees, the model can be inverted to give estimates of average tree size and density. Because the inversion is sensitive to correct determination of component signatures, predictions are not accurate for small areas. Author

N88-18991# Los Alamos National Lab., N. Mex.

THE ANGULAR REFLECTANCE SIGNATURE OF THE CANOPY HOT SPOT IN THE OPTICAL REGIME

S. A. W. GERSTL 1988 5 p Presented at the 4th International Colloquium on Spectral Signatures of Objects in Remote Sensing, Aussois, France, 18 Jan. 1988

(Contract W-7405-ENG-36)
 (DE88-005385; LA-UR-88-145; CONF-880154-1) Avail: NTIS HC A02/MF A01

When any three-dimensional surface, e.g., a plant canopy is illuminated by a directional light source such as the sun, an angular reflectance distribution results that shows a narrow intensity peak in the direction of retro-reflection. This is called the Heiligenschein or hot spot (HS) of vegetation canopies and is caused by the absence of mutual shading of leaves when the observation direction coincides with the illumination direction. The angular intensity distribution of this hot spot, its brightness and contrast against the background, are therefore indicators of the plant's geometry.

01 AGRICULTURE AND FORESTRY

We show from experimental data and by modeling that the hot spot angular reflectance signature carries information about plant stand architecture that is often more distinctive for different plant species than their spectral signatures. DOE

N88-19801# Instituto de Pesquisas Espaciais, Sao Jose dos Campos (Brazil).

CROP FORECASTING IN BRAZIL: A SHORT HISTORY OF PRODUCTIVITY MODELS [PREVISAO DE SAFRAS NO BRASIL: UM BREVE HISTORICO DOS MODELOS DE PRODUTIVIDADE]

FAUSTO C. DEALMEIDA and LEONARDO D. DEABREUSA Apr. 1987 15 p In PORTUGUESE; ENGLISH summary (INPE-4150-PRE/1056) Avail: NTIS HC A03/MF A01

Crop forecasting is of fundamental importance to economic planning and in the commercial exchanges between Brazil and other countries. However, in Brazil this activity is still developing, especially when compared to such efforts in the United States, Canada, and Europe. A brief review of research done in Brazil in the area of crop yield modeling is presented. Author

N88-19802# Instituto de Pesquisas Espaciais, Sao Jose dos Campos (Brazil).

REPORT OF THE PARTICIPATION IN THE INTERNATIONAL TRAINING COURSE: REMOTE SENSING IN VILLAGE FORESTRY

FLAVIO JORGE PONZONI and JOSE SIMEAO DEMEDEIROS Feb. 1988 52 p In ENGLISH and PORTUGUESE Course held in the Fed. Republic of Germany, 7 May - 3 Jun. 1987; sponsored by the Deutsche Stiftung fuer International Entwicklung, United Nation FAO, and the Bavarian State Forest Service (INPE-4476-NTE/278) Avail: NTIS HC A04/MF A01

A report on and an evaluation of INPE personnel participation in the International Training Course: Remote Sensing and Village Forestry are presented. The course took place from May 7 to June 3 1987 in West Germany, and was conducted by the Deutsche Stiftung fur International Entwicklung (DSE) in cooperation with the FAO of the UN and the Bavarian State Forest Service. Author

N88-19804# Instituto de Pesquisas Espaciais, Sao Jose dos Campos (Brazil).

MAPPING OF THE MANGROVES OF THE GUANABARRA BAY THROUGH THE UTILIZATION OF REMOTE SENSING TECHNIQUES M.S. Thesis [MAPEAMENTOS DOS MANGUEZAIS DO RECONCAVO DA BAIJA DE GUANABARA ATRAVES DA UTILIZACAO DE TECNICAS DE SENSORIAMENTO REMOTO]

IVAN DEOLIVEIRA PIRES Jul. 1986 104 p In PORTUGUESE; ENGLISH summary Contains map as supplement (INPE-3942-TDL/229) Avail: NTIS HC A06/MF A01

The mangrove forests of Guanabara Bay (Rio de Janeiro State) were mapped using remote sensing techniques. The materials used were MSS-LANDSAT imagery and aerial photography. The following techniques of image processing were used to enhance the imagery: atmospheric and radiometric corrections, scaling, rationing, and contrast stretch. In addition, the usual photointerpretation procedures were used. The Interactive Multispectral Image Analysis System (Image-100) from INPE was used for digital classification (maximum likelihood classifier - MAXVER). Detailed field work was done to check the preliminary classifications. Finally, the importance of integrating various remote sensing techniques in the study of coastal ecosystems such as mangroves using orbital data is emphasized. Author

N88-19807# Instituto de Pesquisas Espaciais, Sao Jose dos Campos (Brazil).

REPORT ON PHASE 1 OF THE PROJECT ESTIMATE DEVELOPMENT OF A MODEL FOR YIELD ESTIMATION OF SUGAR CANE BASED ON LANDSAT AND AGROMET DATA [RELATORIO DA FASE 1 DO PROJETO ESTIMA DESENVOLVIMENTO DE UM MODELO PARA ESTIMATIVA DA PRODUTIVIDADE AGRICOLA DA CANA-DE-ACUCAR BASEADO EM DADOS LANDSAT E AGROMETEOROLOGICOS]

BERNARDO FRIEDRICH T RUDORFF and GETULIO TEIXEIRA BATISTA Feb. 1988 133 p In PORTUGUESE; ENGLISH summary Sponsored by Fundo de Incentivo a Pesquisa Tecnico-Cientifica (FIPIC) (INPE-4466-RPE/560) Avail: NTIS HC A07/MF A01

The objective was the development of a model for sugar cane (*Saccharum officinarum*) yield estimation in a test site corresponding to the sugar cane crop production area of an industrial plant, based on LANDSAT and Agromet data. Information on agricultural production system of the Barra Grande Plant located at the municipal area of Lencois Paulista, Sao Paulo State, for the crop year of 1983/84, 1984/85, and 1985/86 was obtained. Initially, the spectral response of the main varieties at different stages (number of harvesting cuts) was analyzed based on LANDSAT MSS data. The correlation between LANDSAT MSS and actual yield, estimated at the plant was investigated for the main planted varieties and development stages. Afterwards, a representative sample of the production system taking into account the different varieties and growth stages was selected for each crop year. Digital counts of the LANDSAT imagery analyzed were extracted using an image processing laboratory implemented at INPE. Vegetation indices based on the digital counts of the sugar cane selected fields were computed and correlated to the actual observed at the plant. The yield variation explained by the vegetation index was 41 percent. Estimated yield based on an Agromet model was correlated to the actual yield as well, and 57 percent of yield variation was explained by this model. When the vegetation index and the Agromet data were jointly correlated to the actual yield, 72 percent of the yield variation explanation resulted. This result is as accurate as the yield estimation done at the field level for the plant operation management purposes. Author

N88-19817*# Oregon State Univ., Corvallis. Environmental Remote Sensing Applications Lab.

RESEARCH IN REMOTE SENSING OF VEGETATION Final Technical Report, 1 Aug. 1986 - 31 Mar. 1988

BARRY J. SCHRUMPF, WILLIAM J. RIPPLE, and DENNIS L. ISAACSON 31 Mar. 1988 40 p (Contract NAGW-924)

(NASA-CR-182663; NAS 1.26:182663; REPT-16) Avail: NTIS HC A03/MF A01 CSCL 13B

The research topics undertaken were primarily selected to further the understanding of fundamental relationships between electromagnetic energy measured from Earth orbiting satellites and terrestrial features, principally vegetation. Vegetation is an essential component in the soil formation process and the major factor in protecting and holding soil in place. Vegetation plays key roles in hydrological and nutrient cycles. Awareness of improvement or deterioration in the capacity of vegetation and the trends that those changes may indicate are, therefore, critical detections to make. A study of the relationships requires consideration of the various portions of the electromagnetic spectrum; characteristics of detector system; synergism that may be achieved by merging data from two or more detector systems or multiple dates of data; and vegetational characteristics. The vegetation of Oregon is sufficiently diverse as to provide ample opportunity to investigate the relationships suggested above several vegetation types. B.G.

N88-19824# Department of Energy, Washington, D. C. Office of Energy Research.

PROCEEDINGS OF THE FOREST-ATMOSPHERE INTERACTION WORKSHOP

HARRY MOSES, ed., VOLKER A. MOHNEN, ed., WILLIAM E. REIFSNEYDER, ed., and DAVID H. SLADE, ed. May 1987 254 p Workshop held at Lake Placid, N.Y., 1-4 Oct. 1985 Prepared in cooperation with State Univ. of New York, Albany, and Yale Univ., New Haven, Conn.

(CONF-8510250) Avail: NTIS HC A12/MF A01

The essential ideas of the papers presented at the Forest Atmosphere Interaction Workshop are presented. These range from remote sensing to the impact of viruses, bacteria and pests to the effects of severe climate/weather conditions. Also presented are the recommendations for research from three deliberative panels for each of the three main sections of the Workshop: (1) Forest Science and Management; (2) Atmosphere-Canopy Exchange; and (3) Biomass Decline. There is some overlap in the research recommendations as may have been expected but the essential ideas on what ought to be done are included. Author

N88-19855*# Michigan Univ., Ann Arbor. Radiation Lab.
MESOSCALE MONITORING OF THE SOIL FREEZE/THAW BOUNDARY FROM ORBITAL MICROWAVE RADIOMETRY
Semiannual Progress Report

FAWWAZ T. ULABY, M. CRAIG DOBSON, and WILLIAM R. KUHN Jan. 1988 7 p

(Contract NAG5-852)

(NASA-CR-182659; NAS 1.26:182659) Avail: NTIS HC A02/MF A01 CSDL 08M

The fundamental objectives are to test the feasibility of delineating the lateral boundary between frozen and thawed condition in the surface layer of soil from orbital microwave radiometry and secondly to examine the sensitivity of general circulation models to an explicit parameterization of the boundary condition. Physical models were developed to relate emissivity to scene properties and a simulation package was developed to predict brightness temperature as a function of emissivity and physical temperature in order to address issues of heterogeneity, scaling, and scene dynamics. Radiative transfer models were developed for both bare soil surfaces and those obscured by an intervening layer of vegetation or snow. These models relate the emissivity to the physical properties of the soil and to those of the snow or vegetation cover. A SMMR simulation package was developed to evaluate the adequacy of the emission models and the limiting effects of scaling for realistic scenarios incorporating spatially heterogeneous scenes with dynamic moisture and temperature gradients at the pixel scale. B.G.

N88-20023# Instituto de Pesquisas Espaciais, Sao Jose dos Campos (Brazil).

A VARIANT OF THE ISODATA ALGORITHM FOR APPLICATION TO AGRICULTURAL TARGETS [UMA VARIANTE DO ALGORITMO ISODATA PARA APLICACAO EM ALVOS AGRICOLAS]

LEONARDO SANTANNABINS and FLAVIO ROBERTO DIASVELASCO Nov. 1987 17 p In PORTUGUESE; ENGLISH summary Presented at the 2nd Latin-American Symposium on Remote Sensing, Bogota, Colombia, 16-21 Nov. 1987 (INPE-4436-PRE/1235) Avail: NTIS HC A03/MF A01

A variant is presented of the ISODATA algorithm for automatic clustering of agricultural targets in multispectral images. In the same way as ISODATA, the algorithm dispenses with a priori knowledge of the number of classes. Compared to ISODATA, the algorithm has the following advantages: it depends on less parameters, it converges quicker and is guaranteed to terminate. The proposed algorithm start with a single class and, in the following iterations, splits classes for which the variance is greater than a given constant C. The algorithm terminates when all classes have variances within the desired limit. To minimize the mean square error, at each iteration, a k-means algorithm is performed where k is the iteration index. Examples are shown of the application of the algorithm for LANDSAT/TM images. Author

ENVIRONMENTAL CHANGES AND CULTURAL RESOURCES

Includes land use analysis, urban and metropolitan studies, environmental impact, air and water pollution, geographic information systems, and geographic analysis.

A88-21012

A REMOTE SENSING BASED METHODOLOGY FOR QUANTIFYING THE SPATIAL AND FUNCTIONAL RELATIONSHIPS AMONGST INDUSTRIAL LAND USES DELINEATED AROUND THE PORT OF BALTIMORE

THOMAS D. MORELLI (Florida Atlantic University, McLean, VA) IN: American Society for Photogrammetry and Remote Sensing and ACSM, Annual Convention, Baltimore, MD, Mar. 29-Apr. 3, 1987, Technical Papers. Volume 1. Falls Church, VA, American Society for Photogrammetry and Remote Sensing and ACSM, 1987, p. 104-112. refs

A88-21014

INTERRELATIONSHIPS BETWEEN SPATIAL RESOLUTION AND PER-PIXEL CLASSIFIERS FOR EXTRACTING INFORMATION CLASSES. I - THE URBAN ENVIRONMENT. II - THE NATURAL ENVIRONMENT

JOHN R. JENSEN and MICHAEL E. HODGSON (South Carolina, University, Columbia) IN: American Society for Photogrammetry and Remote Sensing and ACSM, Annual Convention, Baltimore, MD, Mar. 29-Apr. 3, 1987, Technical Papers. Volume 1. Falls Church, VA, American Society for Photogrammetry and Remote Sensing and ACSM, 1987, p. 121-139. refs

This paper discusses methodology for examining remotely sensed imagery for the relationship between spatial resolution, minimum mapping unit, and the fundamental components of each land-use category in an urban environment. Three resolutions of MSS data (15 x 15, 30 x 30, and 60 x 60 meter) were analyzed for mapping U.S.G.S. urban land use classes. The same methodology was used to determine the relationship between spatial resolution, minimum mapping unit, and the fundamental biophysical components of information classes in a natural wetland environment, analyzing 3 x 3, 6 x 6, and 12 x 12 meter resolutions of the MSS data. The analysis of environment mapping from high resolution imagery using a simple per-pixel classifier and brightness values indicated the presence of a number of fundamental problems inherent to the classifier. I.S.

A88-21023

COMPUTER-ASSISTED MAP ANALYSIS - A SET OF PRIMITIVE OPERATORS FOR A FLEXIBLE APPROACH

JOSEPH K. BERRY (Yale University, New Haven, CT) and KENNETH L. REED (Spatial Information Systems, Inc., Omaha, NE) IN: American Society for Photogrammetry and Remote Sensing and ACSM, Annual Convention, Baltimore, MD, Mar. 29-Apr. 3, 1987, Technical Papers. Volume 1. Falls Church, VA, American Society for Photogrammetry and Remote Sensing and ACSM, 1987, p. 206-218. refs

This paper describes a software package, termed the professional Map Analysis Package (pMAP) which is a set of computer programs providing for the encoding, storage, analysis, and display of spatial information. The pMAP combines the capabilities of conventional map processing involving traditional maps and drafting aids, with advanced database and analytic capabilities such as geographic searches, spatial statistics, and cartographic modeling. Input data may be in the form of grid-cells, digitizer points, or lines of polygons; the output is 'raster-pattern' graphics. I.S.

A88-21041

LARGE-SCALE HURRICANE HAZARD MAPPING ALONG THE COASTAL PLAIN OF HONDURAS USING LANDSAT DATA

02 ENVIRONMENTAL CHANGES AND CULTURAL RESOURCES

DONALD R. WIESNET (Satellite Hydrology, Inc., Vienna, VA) and STEPHEN O. BENDER (Organization of American States, Washington, DC) IN: American Society for Photogrammetry and Remote Sensing and ACSM, Annual Convention, Baltimore, MD, Mar. 29-Apr. 3, 1987, Technical Papers. Volume 1. Falls Church, VA, American Society for Photogrammetry and Remote Sensing and ACSM, 1987, p. 402-411. Research supported by the U.S. Agency for International Development. refs

A88-21044

AUTOMATED ROAD NETWORK EXTRACTION FROM LANDSAT TM IMAGERY

J. F. WANG and P. J. HOWARTH (Waterloo, University, Canada) IN: American Society for Photogrammetry and Remote Sensing and ACSM, Annual Convention, Baltimore, MD, Mar. 29-Apr. 3, 1987, Technical Papers. Volume 1. Falls Church, VA, American Society for Photogrammetry and Remote Sensing and ACSM, 1987, p. 429-438. Research supported by the International Development Research Centre. refs

(Contract NSERC-A-0766)

In this paper a sequential line extraction method for identifying road networks on high resolution digital satellite images is described. The method considers line following as graph searching and an 'acuteness operator' is proposed to obtain the magnitude and direction of local line likeness. The graph searching starts at the most prominent locations within lines and uses an heuristic depth-first search to trace lines. The method has been successfully applied to road network extraction from Landsat TM images. The methodology and some experimental results are reported in this paper. Author

A88-21060* Jet Propulsion Lab., California Inst. of Tech., Pasadena.

AN AUTOMATED SYSTEM FOR TERRAIN DATABASE CONSTRUCTION

L. F. JOHNSON, R. K. FRETZ, T. L. LOGAN, and N. A. BRYANT (California Institute of Technology, Jet Propulsion Laboratory, Pasadena) IN: American Society for Photogrammetry and Remote Sensing and ACSM, Annual Convention, Baltimore, MD, Mar. 29-Apr. 3, 1987, Technical Papers. Volume 4. Falls Church, VA, American Society for Photogrammetry and Remote Sensing and ACSM, 1987, p. 167-176. refs

An automated Terrain Database Preparation System (TDPS) for the construction and editing of terrain databases used in computerized wargaming simulation exercises has been developed. The TDPS system operates under the TAE executive, and it integrates VICAR/IBIS image processing and Geographic Information System software with CAD/CAM data capture and editing capabilities. The terrain database includes such features as roads, rivers, vegetation, and terrain roughness. R.R.

A88-21071

LAND COVER CHANGE DETECTION WITH LANDSAT MSS AND TM DATA IN THE KITCHENER-WATERLOO AREA, CANADA

TUNG FUNG and ELLSWORTH LEDREW (Waterloo, University, Canada) IN: American Society for Photogrammetry and Remote Sensing and ACSM, Annual Convention, Baltimore, MD, Mar. 29-Apr. 3, 1987, Technical Papers. Volume 6. Falls Church, VA, American Society for Photogrammetry and Remote Sensing and ACSM, 1987, p. 81-89. Research supported by the Board of Industrial Leaderships and Development and NSERC. refs

A88-21073* Michigan State Univ., East Lansing.

LAND COVER CHANGE DETECTION USING A GIS-GUIDED, FEATURE-BASED CLASSIFICATION OF LANDSAT THEMATIC MAPPER DATA

WILLIAM R. ENSLIN, JEZCHING TON, and ANIL JAIN (Michigan State University, East Lansing) IN: American Society for Photogrammetry and Remote Sensing and ACSM, Annual Convention, Baltimore, MD, Mar. 29-Apr. 3, 1987, Technical Papers. Volume 6. Falls Church, VA, American Society for Photogrammetry and Remote Sensing and ACSM, 1987, p. 108-120. Research

supported by the Michigan Department of Natural Resources. refs

(Contract NGL-23-004-083)

Landsat TM data were combined with land cover and planimetric data layers contained in the State of Michigan's geographic information system (GIS) to identify changes in forestlands, specifically new oil/gas wells. A GIS-guided feature-based classification method was developed. The regions extracted by the best image band/operator combination were studied using a set of rules based on the characteristics of the GIS oil/gas pads. K.K.

A88-24511

USING REMOTELY SENSED DATA FOR CENSUS SURVEYS AND POPULATION ESTIMATION IN DEVELOPING COUNTRIES - EXAMPLES FROM NIGERIA

PETER O. ADENIYI (Lagos, University, Nigeria) Geocarto International (ISSN 1010-6049), vol. 2, Dec. 1987, p. 11-31. Research supported by the International Development Research Centre. refs

The conduct of conventional census surveys in most developing countries and the rational use of the results obtained have been impaired largely by the lack of basic infrastructures. These infrastructures include up-to-date administrative and topographic maps, settlement and land use information and geographically referenced enumeration areas (EAs). Using examples from Nigeria, this paper demonstrates how remotely sensed data can be used to acquire some of the basic data requirements for census surveys and to estimate population. The result obtained shows that visual identification of settlements on Landsat MSS and TM is more accurate and economical than equivalent digital classification techniques. Black and white aerial photographs were used to estimate the population of a model town and to establish EAs. The population estimation method employed can be used to obtain intercensal population estimates for the rapidly growing central places, while the established EAs for the study area have created a permanent base for future census surveys and census cross-validation, population estimation and other social surveys. Author

A88-24512

A STUDY ON THE UTILIZATION OF SIR-A DATA FOR POPULATION ESTIMATION IN THE EASTERN PART OF SPAIN

J. MELIA and J. A. SOBRINO (Valencia, Universidad, Burjasot, Spain) Geocarto International (ISSN 1010-6049), vol. 2, Dec. 1987, p. 33-37. refs

In this work a study has been carried out in order to estimate population on a strip of land of 100 km length and 50 km width, placed in the Eastern part of Spain. Use has been made of an SIR-A image obtained from the Columbia Shuttle on November 1981 and referred to the mentioned area. It is shown the difficulty of estimating population in coast nuclei due to the large number of touristic buildings which deceive the population census. Nuclei with less than 2000 people may be identified in many cases but it is hardly difficult to estimate their surface. With the remaining nuclei a twofold classification has been carried out according to the number of people. The surfaces of semiurban nuclei (of less than 10,000 people) show a dependency on the number of people between three and four times below that for urban nuclei (of more than 20,000 people). Author

A88-27265*

Max-Planck-Inst. fuer Chemie, Mainz (West Germany).

BIOMASS-BURNING EMISSIONS AND ASSOCIATED HAZE LAYERS OVER AMAZONIA

M. O. ANDREA (Max-Planck-Institut fuer Chemie, Mainz, Federal Republic of Germany), E. V. BROWELL, G. L. GREGORY, R. C. HARRISS, G. F. HILL, G. W. SACHSE, R. W. TALBOT (NASA, Langley Research Center, Hampton, VA), M. GARSTANG (Virginia, University, Charlottesville), D. J. JACOB (Harvard University, Cambridge, MA), A. L. TORRES (NASA, Wallops Flight Center, Wallops Island, VA) et al. Journal of Geophysical Research

(ISSN 0148-0227), vol. 93, Feb. 20, 1988, p. 1509-1527. NASA-supported research. refs
(Contract NSF ATM-84-07137)

The characteristics of haze layers, which were visually observed over the central Amazon Basin during many of the Amazon Boundary Layer Experiment 2A flights in July/August 1985, were investigated by remote and in situ measurements, using the broad range of instrumentation and sampling equipment on board the Electra aircraft. It was found that these layers strongly influenced the chemical and optical characteristics of the atmosphere over the eastern Amazon Basin. Relative to the regional background, the concentrations of CO, CO₂, O₃, and NO were significantly elevated in the plumes and haze layers, with the NO/CO ratio in fresh plumes much higher than in the aged haze layers. The haze aerosol was composed predominantly of organic material, NH₄, K(+), NO₃(-), SO₄(2-), and organic anions (formate, acetate, and oxalate). I.S.

A88-27803* National Aeronautics and Space Administration. Goddard Space Flight Center, Greenbelt, Md.

PROBLEMS RELATED TO THE DETERMINATION OF LAND SURFACE PARAMETERS AND FLUXES OVER HETEROGENEOUS MEDIA FROM SATELLITE DATA

F. BECKER (NASA, Goddard Space Flight Center, Greenbelt, MD) and M. RAFFY (Strasbourg I, Université, France) (COSPAR, WMO, URSI, et al., Plenary Meeting, 26th, Symposium 3, Workshop V, and Topical Meeting A2 on Remote Sensing from Space, Toulouse, France, June 30-July 11, 1986) *Advances in Space Research* (ISSN 0273-1177), vol. 7, no. 11, 1987, p. 45-57. CNES-CNRS-supported research. refs

Problems encountered in the definition of relevant parameters which can describe heterogeneous media as a whole are discussed. A procedure to extend the definition of parameters from local to regional scales via inversion of appropriate models is tentatively proposed. The adequacy of these models for describing physical processes at the earth/atmosphere interface as observed with satellite systems is addressed. C.D.

A88-28014
IDENTIFICATION AND MEASUREMENT OF THE AREAL EXTENT OF SETTLEMENTS FROM LANDSAT - AN EXPLORATION INTO THE NIGERIAN CASE

J. FUNSO OOLORUNFEMI (Ilorin, University, Nigeria) *International Journal of Remote Sensing* (ISSN 0143-1161), vol. 8, Dec. 1987, p. 1839-1843. Research supported by the British Council. refs

A88-28603
REMOTE SENSING AND GEOGRAPHIC INFORMATION SYSTEM TECHNIQUES FOR AQUATIC RESOURCE EVALUATION

R. WELCH, M. MADDEN REMILLARD (Georgia, University, Atlanta), and R. B. SLACK (EPA, Atlanta, GA) *Photogrammetric Engineering and Remote Sensing* (ISSN 0099-1112), vol. 54, Feb. 1988, p. 177-185. Research supported by the South Carolina Department of Health and Environmental Control and Lockheed Engineering and Management Services Co. refs
(Contract EPA-5R-1301-NAEX)

A88-28606
LAND-COVER MONITORING WITH SPOT FOR LANDFILL INVESTIGATIONS

WARREN R. PHILIPSON (USDA, Agricultural Research Service, Beltsville, MD), EUGENIA M. BARNABA, ARLYNN INGRAM (Cornell University, Ithaca, NY), and VICKI L. WILLIAMS (SPOT Image Corp., Reston, VA) *Photogrammetric Engineering and Remote Sensing* (ISSN 0099-1112), vol. 54, Feb. 1988, p. 223-228. Research supported by the Suffolk County Department of Health Services. refs

As an extension of an airphoto-based inventory of active and inactive waste storage and disposal sites in a New York county, SPOT satellite images were evaluated to determine their capacity for monitoring land-cover changes that could be significant in landfill investigations. A panchromatic and a multispectral image of 25

1.5- by 1.5-km sites were displayed and minimally enhanced (contrast stretched and enlarged) on a digital image processing system, where the imaged test sites were compared visually to the most recent 1:24,000-scale U.S. Geological Survey topographic maps. Significant changes - disturbed, reclaimed, and developed land; recently exposed soil; ponded water; and new or removed structures - were interpreted and delineated, based only on the images and maps. Airphoto and field (helicopter) verification found the accuracy of SPOT interpretations to be approximately 95 percent. SPOT images are judged to be a cost-effective tool for county or regional monitoring programs. Author

A88-28684* California Univ., Santa Barbara.
REQUIREMENTS AND PRINCIPLES FOR THE IMPLEMENTATION AND CONSTRUCTION OF LARGE-SCALE GEOGRAPHIC INFORMATION SYSTEMS

TERENCE R. SMITH, SUDHAKAR MENON, JEFFREY L. STAR, and JOHN E. ESTES (California, University, Santa Barbara) *International Journal of Geographical Information Systems*, vol. 1, no. 1, 1987, p. 13, 15, 17 (7 ff.). refs
(Contract NAGW-455)

This paper provides a brief survey of the history, structure and functions of 'traditional' geographic information systems (GIS), and then suggests a set of requirements that large-scale GIS should satisfy, together with a set of principles for their satisfaction. These principles, which include the systematic application of techniques from several subfields of computer science to the design and implementation of GIS and the integration of techniques from computer vision and image processing into standard GIS technology, are discussed in some detail. In particular, the paper provides a detailed discussion of questions relating to appropriate data models, data structures and computational procedures for the efficient storage, retrieval and analysis of spatially-indexed data. Author

A88-29427
METHODS FOR PROCESSING RADIO-PHYSICAL MEASUREMENT DATA IN STUDIES OF THE ENVIRONMENT [METODY OBRABOTKI DANNYKH RADIOFIZICHESKOGO ISSLEDOVANIYA OKRUZHAIUSHCHEI SREDY]

NEON ALEKSANDROVICH ARMAND, VLADIMIR FEDOROVICH KRAPIVIN, and FERDINAND ANUSHAVANO MKRTCHIAN Moscow, Izdatel'stvo Nauka, 1987, 272 p. In Russian. refs

Airborne and satellite-borne microwave-radiometer monitoring of the environment is described. Attention is given to methods for the sorting, classification, and thematic processing of microwave remote-sensing data using different types of computers. Problems connected with the detection and spatial-temporal identification of anomalous formations on land and ocean surfaces are examined. Particular emphasis is placed on the monitoring of water systems and biogeochemical fields. B.J.

A88-31103
ABSOLUTE INFRARED INTENSITIES FOR F-113 AND F-114 AND AN ASSESSMENT OF THEIR GREENHOUSE WARMING POTENTIAL RELATIVE TO OTHER CHLOROFLUOROCARBONS

JERRY D. ROGERS and ROBERT D. STEPHENS (GM Research Laboratories, Warren, MI) *Journal of Geophysical Research* (ISSN 0148-0227), vol. 93, March 20, 1988, p. 2423-2428. refs

The literature concerning the 'greenhouse' warming potentials of chlorofluorocarbons F-11, F-12, F-22, F-113, F-114, F-134a, and F-142b is reviewed. Additionally, infrared intensities are reported for each of the fundamental absorption bands of F-113 (CF₂ClCFCl₂) and F-114 (CF₂ClCF₂Cl) in the region between 8 and 20 microns. The total intensities measured for this region were 4905/sq cm/atm for F-113 and 6064/sq cm/atm for F-114, compared to a total intensity of 3404/sq cm/atm for F-12 (CF₂Cl₂) in the same region. On the basis of these infrared intensities and the atmospheric lifetimes of F-113 and of F-114 relative to F-12, and on a per unit mass basis, F-113 and F-114 are about 0.8 and 1.9 times as effective, respectively, as F-12 in the 'greenhouse' warming of the earth. Author

02 ENVIRONMENTAL CHANGES AND CULTURAL RESOURCES

A88-32659* Maryland Univ., College Park.

SELECTING THE SPATIAL RESOLUTION OF SATELLITE SENSORS REQUIRED FOR GLOBAL MONITORING OF LAND TRANSFORMATIONS

J. R. G. TOWNSHEND (NERC, Reading, England) and C. O. JUSTICE (Maryland, University, College Park) International Journal of Remote Sensing (ISSN 0143-1161), vol. 9, Feb. 1988, p. 187-236. refs

(Contract NAG5-399; NERC-F60/G6/12)

The paper provides preliminary evidence for the spatial resolutions required to monitor land transformations at broad scales. This is obtained from simulations of imagery at various spatial resolutions between 125 and 4000 m derived from Landsat MSS imagery. Consideration is given to the various types of spatial images detectable by remotely-sensed systems, as well as to the difficulties associated in disentangling permanent land transformations from shorter term changes such as phenological and interannual changes. K.K.

N88-15278# Naval Postgraduate School, Monterey, Calif.

MODEL-BASED BUILDING VERIFICATION IN AERIAL PHOTOGRAPHS Annual Report, Oct. 1985 - Sep. 1986

CHIN-HWA LEE and HSI-JIAN LEE Sep. 1987 40 p

(Contract MIPR-HM0050-6-357)

(AD-A186010; NPS-82-87-001) Avail: NTIS HC A03/MF A01 CSCL 08B

This paper concerns the design of a computer vision system for change detection. Here, change detection is defined as figuring out the differences between an object model and the newly sensed image. The target objects are confined to the cultural features, such as roads and buildings. We divide the task into two modules: model verification and image interpretation. In this report, the verification stage will be discussed in detail. In general there exists a lot of domain specific heuristics to judge the status of changes. For example, to verify the existence of a building, we can check its shape, size, height, surface direction, and surface material, etc. The expert system approach is a natural approach which can code all information together. While different photo interpreters and field specialists may have different viewpoints about the status of an object, expert systems can be modified easily to reflect a particular viewpoint. GRA

N88-17119# Pacific Northwest Labs., Richland, Wash.

USER'S GUIDE TO A DATA BASE OF CURRENT ENVIRONMENTAL MONITORING PROJECTS IN THE US-CANADIAN TRANSBOUNDARY REGION

M. Y. BALLINGER, J. DEFFERDING, E. G. CHAPMAN, M. D. BETTINSON, and C. S. GLANTZ Nov. 1987 84 p

(Contract DE-AC06-76RL-01830)

(DE88-002476; PNL-6377) Avail: NTIS HC A05/MF A01

This document describes how to use a data base of current transboundary region environmental monitoring projects. The data base was prepared from data provided by Glantz et al. (1986) and Concord Scientific Corporation (1985), and contains information on 226 projects with monitoring stations located within 400 km (250 mi) of the US-Canadian border. The data base is designed for use with the dBASE III PLUS data management systems on IBM-compatible personal computers. Data-base searches are best accomplished using an accompanying command file called RETRIEVE or the dBASE command LIST. The user must carefully select the substrings on which the search is to be based. Example search requests and subsequent output are presented to illustrate substring selections and applications of the data base. DOE

N88-18079# National Oceanic and Atmospheric Administration, Silver Spring, Md. Air Resources Lab.

METEOROLOGICAL AND AEROSOL MEASUREMENTS FROM THE NOAA WP-3D AIRCRAFT DURING WATOX-86, JANUARY 4-9, 1986

H. BRIDGMAN, B. STUNDER, R. ARTZ, G. ROLPH, and R. SCHNELL Jul. 1987 76 p Prepared in cooperation with Colorado Univ., Boulder

(PB88-120860; NOAA-TM-ERL-ARL-156) Avail: NTIS HC

A05/MF A01 CSCL 13B

On January 4, 6, 8, and 9, 1986, NOAA WP-3D research flights were conducted over the Western Atlantic Ocean, two to three hundred km off the coast of North America. Flights were made perpendicular to NW airflow to establish the flux of gas and aerosol emissions from the east coast of North America. The following data is presented for each flight: a horizontal projection of the flight track on a latitude-longitude grid; the relevant synoptic situation; air-parcel back-trajectories; a flight log; vertical cross sections of condensation nuclei (CN) and aerosol scattering extinction (b sub sp); and representative aerosol size distributions. GRA

N88-19826# United Nations Environment Program, Nairobi (Kenya). Administrative Committee on Co-ordination.

SYSTEM-WIDE MEDIUM-TERM ENVIRONMENT PROGRAMME FOR THE PERIOD 1990-1995: STRATEGIES OF THE UNITED NATIONS SYSTEM FOR THE ENVIRONMENT

1 Dec. 1987 133 p

(UNEP/GCSS.I/2) Avail: NTIS HC A07/MF A01

Misuse of natural resources and degradation of the environment threaten human survival so long as they proceed unchecked. The environment program of the United Nations comprises a wide range of activities aimed at correcting these abuses and achieving sustainable development. Sustainable development rests upon the wise use of resources, prudent management of the environment and rehabilitation of degraded environments. To ensure that development will be sustainable, environmental and developmental activities of the United Nations system must become more fully integrated and more closely co-ordinated. Environmental action must respond to priority requirements and become more visible. The environment program reflects these principles. The thrust of these environmental programs are outlined. B.G.

03

GEODESY AND CARTOGRAPHY

Includes mapping and topography.

A88-21054

AMERICAN SOCIETY FOR PHOTOGRAMMETRY AND REMOTE SENSING AND ACSM, ANNUAL CONVENTION, BALTIMORE, MD, MAR. 29-APR. 3, 1987, TECHNICAL PAPERS. VOLUME 3 - SURVEYING

Convention sponsored by the American Society for Photogrammetry and Remote Sensing and ACSM. Falls Church, VA, American Society for Photogrammetry and Remote Sensing and ACSM, 1987, 327 p. For individual items see A88-21055 to A88-21057.

Recent advances in surveying technology and data processing are discussed in reviews and reports. Topics addressed include survey networks; control survey; marine surveying and mapping; multipurpose cadaster and global positioning systems; surveying evidence, standards, and instrumentation; and surveying water boundaries. Consideration is given to simultaneous determination of astronomic position and azimuth from observations of zenith distances and horizontal directions, trigonometric leveling using electronic distance measurement, GPS survey techniques for deformation analysis, electronic theodolites and tacheometers, and high-speed cm-accuracy GPS surveys. T.K.

A88-21055

SIMULTANEOUS DETERMINATION OF ASTRONOMIC POSITION AND AZIMUTH FROM OBSERVATIONS OF ZENITH DISTANCES AND HORIZONTAL DIRECTIONS

DAVID J. LEHMAN (DMA, Fort Clayton, Panama) IN: American Society for Photogrammetry and Remote Sensing and ACSM, Annual Convention, Baltimore, MD, Mar. 29-Apr. 3, 1987, Technical

Papers. Volume 3 . Falls Church, VA, American Society for Photogrammetry and Remote Sensing and ACSM, 1987, p. 37-51. Army-supported research. refs

A88-21057

GPS SURVEY TECHNIQUES FOR DEFORMATION ANALYSIS

TODD PORTER and JIM MCLELLAN (McElhanney Group, Ltd., Calgary, Canada) IN: American Society for Photogrammetry and Remote Sensing and ACSM, Annual Convention, Baltimore, MD, Mar. 29-Apr. 3, 1987, Technical Papers. Volume 3 . Falls Church, VA, American Society for Photogrammetry and Remote Sensing and ACSM, 1987, p. 194-207. refs

The use of three-dimensional positioning data from the Navstar GPS satellite network in monitoring the deformation of topographical features or manmade structures is discussed and demonstrated. The design and operation of GPS are reviewed; the receivers used in the present test surveys are described; and the observation and data-processing methods employed are explained in detail. Results for a high-pressure gas pipeline (interstation baselines of 10-800 m) and a mountain slide area near a hydroelectric facility (1-3 km) are presented in tables and graphs and compared with conventional survey data. In the pipeline survey, the 95-percent-confidence ellipses with GPS (5-20 mm) were acceptably close to those for conventional methods (3-6 mm). T.K.

A88-21058

AMERICAN SOCIETY FOR PHOTOGRAMMETRY AND REMOTE SENSING AND ACSM, ANNUAL CONVENTION, BALTIMORE, MD, MAR. 29-APR. 3, 1987, TECHNICAL PAPERS. VOLUME 4 - CARTOGRAPHY

Convention sponsored by the American Society for Photogrammetry and Remote Sensing and ACSM. Falls Church, VA, American Society for Photogrammetry and Remote Sensing and ACSM, 1987, 260 p. For individual items see A88-21059 to A88-21061.

Cartographic applications of photogrammetry and remote sensing are discussed in reviews and reports of recent investigations. Sections are devoted to general cartography, digital cartography, education, and digital terrain and elevation modeling. Consideration is given to the perception of three-dimensional cartographic representations, presentation-quality exploration-geology maps, hypsography in digital line graph format, graphic syntax and expert systems for map design, micro-based CAD systems in surveying and mapping education, standards for digital elevation models, and digital terrain analysis employing X-Y-Z point vectors as input data. T.K.

A88-24289

GEODETIC APPLICATION OF THE GLOBAL POSITIONING SYSTEM

P. WILLIS and C. BOUCHER (Institut Geographique National, Saint-Mande, France) Annales Geophysicae, Series B - Terrestrial and Planetary Physics (ISSN 0980-8760), vol. 5, Dec. 1987, p. 517-521. refs

The Global Positioning System (GPS) can presently be used for geodesy and geophysics. The French Institut Geographique National (IGNF) has developed its own software (named GDVS) for processing GPS data. The basic capabilities of this software are discussed. In this paper, the more important observing campaigns related to geophysics and oceanography (terrestrial reference frame, tide gauge connections, local and regional deformation networks) are reviewed and plans for the future are given. Author

A88-25224

ON THE ACCURACY OF MARINE GRAVITY MEASUREMENTS

PAL WESSEL and ANTHONY B. WATTS (Lamont-Doherty Geological Observatory, Palisades, New York) Journal of Geophysical Research (ISSN 0148-0227), vol. 93, Jan. 10, 1988, p. 393-413. Navy-supported research. refs

The accuracy of Lamont-Doherty Geological Observatory's global marine gravity data bank has been assessed by examining the crossover errors (COEs) at intersecting ship tracks. More than

63,000 COEs were found, having a standard deviation of 22.43 mGal. The COEs are used to find and remove linear drifts and DC shifts present in the data set. This adjustment reduces the standard deviation to 13.96 mGal. COEs generally decrease with latitude, which is attributed to uncertainties in the Eotvos correction. High COEs occur in areas of high gravity gradients. These two features point to poor navigation as the principal source of error in marine gravity surveys. COEs have generally been decreasing during the last two decades, reflecting improvements in instrumentation and quality of navigation. A comparison of the shipboard gravity data to Seasat derived gravity data revealed a 9-mGal bias in the terrestrial data, which probably reflects uncertainties in the choice of reference field. The adjusted data set was used to generate a gravimetric geoid for the NW Atlantic Ocean. By removing this geoid from the Seasat sea surface heights, a residual 'geoid' was obtained. A special feature of this map is an elongate ENE trend that appears to correlate with the edge of the Gulf Stream. Author

A88-25225* Bologna Univ. (Italy).

MANTLE RHEOLOGY AND SATELLITE SIGNATURES FROM PRESENT-DAY GLACIAL FORCINGS

ROBERTO SABADINI (Bologna, Università, Italy), DAVID A. YUEN (Minnesota, University, Minneapolis), and PAOLO GASPERINI (Istituto Nazionale di Geofisica, Rome, Italy) Journal of Geophysical Research (ISSN 0148-0227), vol. 93, Jan. 10, 1988, p. 437-447. refs

(Contract CNR-PSN-86,060; NAG5-770; NSF EAR-85-11200)

Changes in the long-wavelength region of the earth's gravity field resulting from both present-day glacial discharges and the possible growth of the Antarctic ice sheet are considered. Significant differences in the responses between the Maxwell and Burger body rheologies are found for time spans of less than 100 years. The quantitative model for predicting the secular variations of the gravitational potential, and means for incorporating glacial forcings, are described. Results are given for the excitation of the degree two harmonics. It is suggested that detailed satellite monitoring of present-day ice movements in conjunction with geodetic satellite missions may provide a reasonable alternative for the estimation of deep mantle viscosity. R.R.

A88-25850

ON DIFFERENTIAL SCALE CHANGES AND THE SATELLITE DOPPLER SYSTEM Z-SHIFT

TOMAS SOLER (NOAA, National Geodetic Survey, Rockville, MD) and BOUDEWIJN H. W. VAN GELDER (Delft, Technische Hogeschool, Netherlands) Geophysical Journal (ISSN 0016-8009), vol. 91, Dec. 1987, p. 639-656. refs

General differential transformation equations are reviewed and a comparison is made between scaling methods and their effects on geodetic heights. Particular attention is given to the z-shift of the Doppler-derived satellite system. It is concluded that proper adoption of a global reference scale is necessary for a complete interrelation between different geodetic and/or geophysical products to be rigorously ascertained. K.K.

A88-26347

THE DOWNWARD CONTINUATION OF AERIAL GRAVIMETRIC DATA WITHOUT DENSITY HYPOTHESIS

CHRISTOPHER JEKELI (USAF, Geophysics Laboratory, Hanscom AFB, MA) Bulletin Geodesique (ISSN 0007-4632), vol. 61, no. 4, 1987, p. 319-329. refs

A method for determining the gravity disturbance on the earth's surface given its vertical gradient everywhere at some fixed aircraft altitude is presented. It is assumed that the earth's surface has a nontrivial shape corresponding to the actual topography, which is itself assumed to be a known and well defined, differentiable function of two spatial variables. Although the method requires terrain elevations, it does not require the specification of density information. R.R.

03 GEODESY AND CARTOGRAPHY

A88-27299

A METHOD FOR THE ESTIMATE OF BROADBAND DIRECTIONAL SURFACE ALBEDO FROM A GEOSTATIONARY SATELLITE

B. PINTY and D. RAMOND (Clermont-Ferrand II, Universite, Aubiere, France) *Journal of Climate and Applied Meteorology* (ISSN 0733-3021), vol. 26, Dec. 1987, p. 1709-1722. refs

Surface albedo can be inferred from geostationary satellite measurements as long as the effects due to the atmosphere, the spectral response of the sensor, and the angular anisotropy of the reflected field are corrected. In this paper, a method which includes ad hoc correction procedures for the three categories of effects is developed. An application of the method is conducted over the Sahara and the African Sahel using Meteosat radiances together with auxiliary data derived from other satellites (Tiros-N and Nimbus-7) and standard meteorological observations. The surface albedo maps are estimated over this region, at a spatial resolution compatible with one used in climate models, for two days representative of the dry and the wet seasons, respectively. The observed seasonal surface albedo change and the relationships between the surface and the planetary albedos are discussed in order to examine the validity of the method and the correction procedures. Author

A88-27465

AN INVESTIGATION OF SMALL-OFFSET FRACTURE ZONE GEOID WAVEFORMS

PETER R. SHAW (Woods Hole Oceanographic Institution, MA) *Geophysical Research Letters* (ISSN 0094-8276), vol. 15, Feb. 1988, p. 192-195. refs
(Contract NSF OCE-86-14512)

Approximately 1,500 geoid cross sections across 15 small-offset South Atlantic fracture zones (FZs) are compiled from Seasat altimeter data and organized according to crustal age; these profiles provide a basis for the comparison of the different FZs, and the evolution of each over geological time. An empirical orthogonal function decomposition is used to investigate the dependence of profile shape and amplitude on crustal age. The geoid cross sections are found to be coherent in form down the length of each FZ, and possess amplitudes that are inversely related to the relative spreading rate at the time of formation. This observation is consistent with a simple model in which the active portion of a fracture zone (the transform fault) remains a fixed spatial length, yielding a variable age offset across the FZ. Author

N88-15289 Deutsche Geodaetische Kommission, Munich (West Germany).

OPTIMIZATION OF PHOTOGRAMMETRIC IMAGE ADJUSTMENT Ph.D. Thesis - Stuttgart Univ., West Germany [OPTIMIERUNG DER PHOTOGRAMMETRISCHEN AUFNAHMEANORDNUNG]

STEPHAN ZINNDORF 1986 79 p In GERMAN (SER-C-323; ISBN-3-7696-9373-6; ISSN-0065-5325; ETN-88-90801) Avail: Issuing Activity

Optimization processes used in geodetic surveys are introduced. Weighted optimization is useful for getting an optimal geodetic network. Analytic optimization is emphasized and is associated with the data definition of the network. The data problem must be solved, especially for weighted optimization. A clear storage of the network surveys is important. An optimization process can be used in free or associated networks. This process approaches the real covariance matrix of the network to an ideal matrix: the criterion matrix. This approach allows an improvement of the geometric arrangement of the shots. ESA

N88-15291 Deutsche Geodaetische Kommission, Munich (West Germany).

OBSERVATIONS OF EARTH TIDES BY THE GERMAN GEODETIC RESEARCH INSTITUTE, DIVISION 1, IN THE PERIOD 1979-1985 AT THE BERCHTESGADEN AND WETTZELL STATIONS [ERDGEZEITENBEOBACHTUNGEN DES DEUTSCHEN GEODAETISCHEN FORSCHUNGSINSTITUTS, ABT. 1, IM ZEITRAUM 1979-1985 AUF DEN STATIONEN BERCHTESGADEN UND WETTZELL] HARALD SCHMITZ-HUEBSCH 1986 79 p In GERMAN; ENGLISH summary Original contains color illustrations (SER-B-280; ISBN-3-7696-8565-2; ISSN-0065-5317; ETN-88-90804) Avail: Issuing Activity

Temporal variations of the gravity vector were observed, using a gravity meter and a vertical pendulum of 30 m length in a salt mine in Berchtesgaden (West Germany) and 2 borehole-tiltmeters at the satellite observation station in Wettzell (West Germany). A comparison between both stations shows that the Earth tide parameters depend on the geological structure. The amplitude factors of the partial tide M2 obtained from the pearl gneiss at Wettzell are lower by 18 percent in N-S direction and 4 percent in E-W direction than those derived from the softer clay anhydrite mixture at Berchtesgaden. For both stations stable preferential directions of the long-term drift can be given; they are consistent with the direction obtained from tectonic model computations and with the direction of the Central European stress field. ESA

N88-16104# Joint Publications Research Service, Arlington, Va. **SPACE APPLICATIONS IN GEOGRAPHY**

A. M. GRIN *In its* JPRS Report: Science and Technology. USSR: Space p 114-124 24 Nov. 1987 Transl. into ENGLISH from Zemlya i Vselennaya (Moscow, USSR), no. 2, Mar. - Apr. 1987 p 19-25

Avail: NTIS HC A08/MF A01

As the Earth's surface is being photographed from the Salyut-7 station, a survey of the Earth is being conducted by artificial Earth satellites, flying laboratories, and helicopters, and ground based observation points are helping out. These things help in the development of the science that studies the surface of the Earth, geography. Geographers have strived in recent years to replace graphic descriptions with quantitative values obtained by means and methods used by the precise sciences, primarily physics and chemistry. The addition of space based techniques to science's arsenal for studying the Earth's surface has made it possible for geographers to obtain an image of whatever natural or economic complex they are studying that is measured within an extremely wide range of electromagnetic waves, including not only the entire visible-optical range, but also those far beyond it, those encompassing thermal and radio emission. The effects of these techniques on the development of geography is examined. Author

N88-16105# Joint Publications Research Service, Arlington, Va. **METHOD FOR JOINT ADJUSTMENT OF SATELLITE AND SURFACE GEODETIC NETWORKS Abstract Only**

B. M. KLENITSKIY, K. K. NASRETDINOV, and M. M. KHOTIN *In its* JPRS Report: Science and Technology. USSR: Space p 125 24 Nov. 1987 Transl. into ENGLISH from Geodeziya i Kartografiya (Moscow, USSR), no. 5, May 1987 p 12-15

Avail: NTIS HC A08/MF A01

The purpose of joint adjustment of satellite and surface geodetic networks constructed in different coordinate systems is to obtain adjusted coordinates of stations in each network, taking into account the results of adjustments of other networks and transformation elements in such a way that the adopted coordinate systems are not changed. An effort was made to develop an adjustment method which takes maximum advantage of newly available methods for processing measurements of extensive geodetic networks with minimum need for additional software. The proposed algorithm is readily integrated with traditional schemes for adjustment of such networks, such as the Pranis-Pranevich method, with solution of normal equations by the successive exclusions of unknowns. In comparison with the known method

for integrating solutions, based on summing of the weighting matrices of individual networks, the new method does not require a procedure for obtaining a weighting matrix for the initial station of the surface geodetic network because it is based on the summing of correlation matrices. Author

N88-16116# Joint Publications Research Service, Arlington, Va.
NEW POSSIBILITIES FOR USING GRAVITY DATA IN DEVELOPING GEODETIC COORDINATE SYSTEMS Abstract Only

L. P. PELLINEN *In its* JPRS Report: Science and Technology. USSR: Space p 136 24 Nov. 1987 Transl. into ENGLISH from *Geodeziya i Kartografiya* (Moscow, USSR), no. 3, Mar. 1987 p 10-13 Original language document was announced in IAA as A87-42939

Avail: NTIS HC A08/MF A01

Radio altimeter observations from GEOS-3 and Seasat as well as laser tracking observations of Lageos have opened new possibilities for the realization of geodetic coordinate system by the joint processing of ground measurements and satellite observations. A method is proposed for the processing of geodetic data which makes it possible to use height anomalies that are completely free of the indirect effect of geodetic coordinate errors. Author

N88-16279*# National Aeronautics and Space Administration. Goddard Space Flight Center, Greenbelt, Md.

CRUSTAL DYNAMICS PROJECT DATA ANALYSIS, 1987. VOLUME 1: FIXED STATION VLBI GEODETIC RESULTS, 1979-1986

J. W. RYAN and C. MA Sep. 1987 169 p
 (NASA-TM-100682; REPT-87-B-0480; NAS 1.15:100682) Avail: NTIS HC A08/MF A01 CSCL 08G

The Goddard VLBI group reports the results of analyzing Mark III data sets from fixed observatories through the end of 1986 and available to the Crustal Dynamics Project. All full-day data from POLARIS/IRIS are included. The mobile VLBI sites at Platteville (Colorado), Penticton (British Columbia), and Yellowknife (Northwest Territories) are also included since these occupations bear on the study of plate stability. Two large solutions, GLB121 and GLB122, were used to obtain Earth rotation parameters and baseline evolutions, respectively. Radio source positions were estimated globally while nutation offsets were estimated from each data set. The results include 25 sites and 108 baselines. Author

N88-16280*# National Aeronautics and Space Administration. Goddard Space Flight Center, Greenbelt, Md.

CRUSTAL DYNAMICS PROJECT DATA ANALYSIS, 1987. VOLUME 2: MOBILE VLBI GEODETIC RESULTS, 1982-1986

C. MA and J. W. RYAN Nov. 1987 130 p
 (NASA-TM-100689-VOL-2; REPT-88-B-0042; NAS 1.15:100689-VOL-2) Avail: NTIS HC A07/MF A01 CSCL 08G

The Goddard VLBI group reports the results of analyzing 101 Mark III data sets acquired from mobile observing sites through the end of 1986 and available to the Crustal Dynamics Project. The fixed VLBI observations at Hat Creek, Ft. Davis, Mojave, and OVRO are included as they participate heavily in the mobile schedules. One large solution GLB171 was used to obtain baseline length and transverse evolutions. Radio source positions were estimated globally, while nutation offsets were estimated from each data set. The results include 28 mobile sites. Author

N88-18054# Nova Univ., Dania, Fla.
FIVE-DIAGONAL WEIGHTING SCHEME FOR GEOIDAL PROFILES

GEORGES BLAHA Mar. 1987 21 p
 (Contract F19628-86-K-0006)
 (AD-A188033) Avail: NTIS HC A03/MF A01 CSCL 08E

Rigorous weighting of geoidal observations along profiles, such as encountered, for example, in satellite altimetry, would be a task exceedingly demanding in terms of computer run-time. A profile with m observation points would require an inversion of an (mxm) variance-covariance matrix, whose entries are correlated and

depend almost entirely on the geoidal covariance function. However, if the observations are uniformly distributed, a slight modification of this function can greatly facilitate the formation of the weight matrix of observations, which subsequently enters the least-squares adjustment process. In the suggested method this matrix is five-diagonal. Its six distinct entries are known beforehand for any number of observations. GRA

N88-18055# Vexcell Corp., Boulder, Colo.

A SMART, MAPPING, CHARTING AND GEODESY CONTROL GENERATOR, PHASE 1 Final Report, Aug. 1986 - Mar. 1987

FRANZ LEBERL, WOODY KOBER, and MARK HARJES Mar. 1987 72 p

(Contract DACA72-86-C-0008)

(AD-A188184; ETL-0458) Avail: NTIS HC A04/MF A01 CSCL 08B

The real-time automated registration of multi-sensor imagery begins with the generation of control information. A specific application may require the registration of newly acquired data to an existing spatial database (absolute registration), or to other images of a series (relative registration). This study examines the feasibility and upper-level design of a system capable of providing the control information required for a range of image registration tasks and image types. In general, the control generator we suggest will be guided by a spatial database maintaining information about the feature content of the area of interest. A rule based query generator will extract candidate ground control optimized for the particular image type and geometry at hand. GRA

N88-18993# Institut fuer Angewandte Geodaesie, Frankfurt am Main (West Germany).

REPORTS ON CARTOGRAPHY AND GEODESY. SERIES 1, REPORT 98 [NACHRICHTEN AUS DEM KARTEN- UND VERMESSUNGSWESEN. REIHE 1: HEFT 98]

1987 105 p In GERMAN; ENGLISH summary
 (ISSN-0469-4236; ETN-88-91098) Avail: NTIS HC A06/MF A01

The significance of orientation unknowns in station and net adjustments was treated. The application of Global Positioning System time receivers to the fundamental station Wettzell is presented. The datum problem of global networks, determined by satellite techniques, was investigated. ESA

N88-19037*# National Aeronautics and Space Administration. Goddard Space Flight Center, Greenbelt, Md.

CRUSTAL DYNAMICS PROJECT: CATALOGUE OF SITE INFORMATION

CAREY E. NOLL, ed. Mar. 1988 539 p
 (NASA-RP-1198; REPT-88B9999; NAS 1.61:1198) Avail: NTIS HC A23/MF A01 CSCL 08G

This document represents a catalog of site information for the Crustal Dynamics Project. It contains information on and descriptions of those sites used by the Project as observing stations for making the precise geodetic measurements necessary for studies of the Earth's crustal movements and deformation. Author

N88-19844*# European Space Agency, Paris (France).

PROCEEDINGS OF AN ESA-NASA WORKSHOP ON A JOINT SOLID EARTH PROGRAM

T. D. GUYENNE, ed. and J. J. HUNT, ed. Oct. 1987 53 p
 Workshop held in Matera, Italy, 29-30 Apr. 1987; sponsored by ESA and NASA
 (NASA-CR-182642; NAS 1.26:182642; ESA-SP-1094; ISSN-0379-6566; ETN-88-91781) Avail: NTIS HC A04/MF A01 CSCL 08G

The NASA geodynamics program; spaceborne magnetometry; spaceborne gravity gradiometry (characterizing the data type); terrestrial gravity data and comparisons with satellite data; GRADIO three-axis electrostatic accelerometers; gradiometer accommodation on board a drag-free satellite; gradiometer mission spectral analysis and simulation studies; and an opto-electronic

03 GEODESY AND CARTOGRAPHY

accelerometer system were discussed.

ESA

N88-19845*# National Aeronautics and Space Administration, Washington, D.C.

NASA'S GEODYNAMICS PROGRAM

D. C. MCADOO /In ESA, Proceedings of an ESA-NASA Workshop on a Joint Solid Earth Program p 11-16 Oct. 1987

Avail: NTIS HC A04/MF A01 CSCL 08G

The NASA geodynamics program covers dynamics of the core; dynamics and structure of the mantle; dynamics and structure of the lithosphere; evolution and composition of the Earth; and comparative planetology. Projects include crustal dynamics/Earth observations; gravity field modelling; and magnetic field studies. Planned space flights include global gravity and magnetic field mapping; magnetic field secular changes; gravity gradiometer mission; LAGEOS-2; and Earth Observing System. ESA

N88-19846*# National Aeronautics and Space Administration, Goddard Space Flight Center, Greenbelt, Md.

SPACEBORNE MAGNETOMETRY

P. T. TAYLOR /In ESA, Proceedings of an ESA-NASA Workshop on a Joint Solid Earth Program p 17-21 Oct. 1987

Avail: NTIS HC A04/MF A01 CSCL 08E

Low orbit (160 km altitude) satellite magnetometry is discussed. Magnetic field simulations and theoretical analyses were performed. They suggest that at 160 km, resolution value is 10, compared to 0.6 for Magsat, and that the satellite can reveal significant information on crustal tectonics. Vector and scalar magnetometers should be carried. ESA

N88-19847*# Jet Propulsion Lab., California Inst. of Tech., Pasadena.

SPACEBORNE GRAVITY GRADIOMETRY CHARACTERIZING THE DATA TYPE

D. SONNABEND /In ESA, Proceedings of an ESA-NASA Workshop on a Joint Solid Earth Program p 23-25 Oct. 1987

Avail: NTIS HC A04/MF A01 CSCL 08E

Satellite gravity gradiometers, particularly the two stage drag free carrier vehicle are discussed. An inner stage, carrying the tracking antenna(s), measures the relative position of the internal free proof mass, and feeds this to a set of magnetic forcers, acting against the outer or main vehicle. As the external forces on the inner stage are low, and as the position relative to the proof mass is tightly controlled, carrier phase disturbances are greatly reduced. The arrangement lowers instantaneous accelerations. It is stressed that gravity gradiometers do not measure gradients, they measure components of an intrinsic tensor. ESA

N88-19848*# Ohio State Univ., Columbus. Dept. of Geodetic Science and Surveying.

TERRESTRIAL GRAVITY DATA AND COMPARISONS WITH SATELLITE DATA

R. H. RAPP /In ESA, Proceedings of an ESA-NASA Workshop on a Joint Solid Earth Program p 27-30 Oct. 1987

Avail: NTIS HC A04/MF A01 CSCL 08G

Figures that demonstrate the state of terrestrial gravity coverage, and comparisons between satellite derived gravity field and terrestrial gravity data are presented. It is shown that only a few areas of the world have information accurate enough for geodesy and geophysics. A gravity field mapping space mission is recommended. ESA

N88-19851*# Bureau Gravimetrique International, Toulouse (France).

GRADIOMETER MISSION SPECTRAL ANALYSIS AND SIMULATION STUDIES: PAST AND FUTURE

G. BALMINO /In ESA, Proceedings of an ESA-NASA Workshop on a Joint Solid Earth Program p 45-47 Oct. 1987

Avail: NTIS HC A04/MF A01 CSCL 08G

Sensitivity analysis and simulation studies performed for a

satellite gravity gradiometer (SGG) mission, and ideas about necessary future numerical simulations are reviewed. ESA

04

GEOLOGY AND MINERAL RESOURCES

Includes mineral deposits, petroleum deposits, spectral properties of rocks, geological exploration, and lithology.

A88-20878

FLUVIAL PERTURBANCE IN THE WESTERN AMAZON BASIN - REGULATION BY LONG-TERM SUB-ANDEAN TECTONICS

MATTI E. RASANEN, JUKKA S. SALO, and RISTO J. KALLIOLA (Turku, University, Finland) Science (ISSN 0036-8075), vol. 238, Dec. 4, 1987, p. 1398-1401. Research supported by the Academy of Finland and Finnida. refs

Haffer's refuge theory proposes that during the arid climatic phases of the late Pleistocene, tropical lowland forests of Amazonia were reduced to isolated patches contributing to the high species richness of the present-day forest. The theory was developed because no obvious historic or modern geomorphic isolation barriers were recorded in Amazonia. Analyses of radar images combined with stratigraphical data show that in the basinal forelands of the tectonically active Andes the geological setting causes long-term fluvial perturbation. This leads to a temporally structured highly complex mosaic of fossil and present floodplains. These dynamics have been present with varying activity and geographic range during the Tertiary and Quaternary, providing site-turnover that has not been recognized by the biographic tradition of the Amazon basin. Author

A88-20902

DETECTION OF SUBSURFACE GEOLOGIC STRUCTURES IN THE THARTHAR AREA OF CENTRAL IRAQ USING LANDSAT IMAGES

NAZAR M. S. NUMAN and GEORGE Y. B. BAKOS (Mosul University, Iraq) ITC Journal (ISSN 0303-2434), no. 2, 1987, p. 145-152. refs

A88-21009

REMOTE SENSING APPLICATIONS BY CONSULTING ENGINEERS - THREE CASE HISTORIES

ALICE E. REDFIELD, RONALD L. FREW, JOSEPH J. UDWARI, and GREG H. DEEVER (Dames and Moore, Bethesda, MD) IN: American Society for Photogrammetry and Remote Sensing and ACSM, Annual Convention, Baltimore, MD, Mar. 29-Apr. 3, 1987, Technical Papers. Volume 1. Falls Church, VA, American Society for Photogrammetry and Remote Sensing and ACSM, 1987, p. 78-85.

The paper discusses the application of conventional image interpretation techniques to three typical engineering or hydrogeologic projects. These include interpretations of 1:24,000-scale black-and-white photography for the determination of rock resistance, zones of weakness in the rock, and slope stability of a cut-slope for a proposed commercial development; of low-altitude photography of the areas of highly plastic soils for a proposed transportation facility; and of historic aerial photographs seeking the location and the extent of an old landfill. The use of remote sensing made it possible to fill basic gaps in existing data sources and to identify key engineering characteristics and potential problem areas not shown on traditional geologic and soil maps, such as the occurrence and distribution of bedrock outcrop; faulting, jointing, and highly fractured rock; severe erosion; and hidden gully features. I.S.

A88-21034

GEOLOGIC APPLICATIONS OF SIDE-LOOKING AIRBORNE RADAR IMAGES IN THE APPALACHIAN VALLEY AND RIDGE PROVINCE

C. SCOTT SOUTHWORTH (USGS, Reston, VA) IN: American Society for Photogrammetry and Remote Sensing and ACSM, Annual Convention, Baltimore, MD, Mar. 29-Apr. 3, 1987, Technical Papers. Volume 1. Falls Church, VA, American Society for Photogrammetry and Remote Sensing and ACSM, 1987, p. 329-338. refs

Examples of specific geologic features of the Appalachian Valley and Ridge Province that are strongly expressed on SLAR images are presented. The topographically expressed geologic features, identified by tonal and textural patterns, include faults, folds, fractures, cross-strike structural discontinuities, and giant rockslides. It is noted, however, that complex geologic features can be suggested by artifacts inherent in SLAR images and image mosaics, requiring field verification. V.L.

A88-21036

APPLICATION OF DATA FROM THE U.S. GEOLOGICAL SURVEY'S SIDE-LOOKING AIRBORNE RADAR PROGRAM

JOHN EDWIN JONES and ALLAN N. KOVER (USGS, Reston, VA) IN: American Society for Photogrammetry and Remote Sensing and ACSM, Annual Convention, Baltimore, MD, Mar. 29-Apr. 3, 1987, Technical Papers. Volume 1. Falls Church, VA, American Society for Photogrammetry and Remote Sensing and ACSM, 1987, p. 348-354. refs

Since the U.S. Geological Survey began its side-looking airborne radar (SLAR) acquisition program in 1980, high quality data have been collected for more than 2 million sq km. The special attributes of SLAR, especially selective relief enhancement, have resulted in significant contributions to geology, hydrology, geography, and cartography. The almost complete SLAR coverage of the Appalachians has greatly improved understanding of the complex structural relationships and may aid in location of additional natural gas deposits. Potentially hazardous, previously unmapped rockslide areas have been identified on SLAR mosaics. The radar has been used in upgrading structural mapping in the Adirondacks. The data have also been used in hydrologic studies for hazardous waste disposal, mapping marine terraces, in merges with other data sets to increase interpretability, and in investigations of mineral potential of ancient basins. Author

A88-21043

GEOBOTANICAL DETECTION OF LINEAR FEATURES IN THE SILVER MINE AREA OF SOUTHEASTERN MISSOURI

GARY J. COWICK, MICHAEL P. BISHOP, and ROBERT C. HOWE (Indiana State University, Terre Haute) IN: American Society for Photogrammetry and Remote Sensing and ACSM, Annual Convention, Baltimore, MD, Mar. 29-Apr. 3, 1987, Technical Papers. Volume 1. Falls Church, VA, American Society for Photogrammetry and Remote Sensing and ACSM, 1987, p. 420-428. refs

An evaluation of Landsat-4 TM digital data has revealed the presence of several linear features in the Silver Mine area of southeastern Missouri. The most prominent linear feature trends approximately N 24 deg E and is believed to be a vegetative expression of a previously mapped shear zone. This feature appears in stretched TM Band 6 (2.08-2.35 microns) data but is most clearly delineated using a band ratio involving Bands 6 and 4 (0.76-0.90 microns). Interpretation of black and white, color, and color infrared aerial photography as well as SIR-B data data has provided no additional evidence for the existence of the feature. However, the results of reconnaissance sampling of vegetation indicate that the feature is identifiable on the TM imagery because it is probably related to canopy areas having a higher leaf moisture content. The geobotanical detection and identification of linear features utilizing TM data may prove as an important aid to future exploration in this area, and may provide further insight into the location of tin, tungsten, lead, and zinc mineralization. Author

A88-21045* National Aeronautics and Space Administration. Goddard Space Flight Center, Greenbelt, Md.

ENGIMA OF A THERMAL ANOMALY - A TM/AVHRR STUDY OF THE VOLCANIC ARABIAN HIGHLANDS

H. W. BLODGET (NASA, Goddard Space Flight Center, Greenbelt, MD), C. G. ANDRE (Smithsonian Institution, Washington, DC), and

P. M. MASUOKA (Science Applications Research, Lanham, MD) IN: American Society for Photogrammetry and Remote Sensing and ACSM, Annual Convention, Baltimore, MD, Mar. 29-Apr. 3, 1987, Technical Papers. Volume 1. Falls Church, VA, American Society for Photogrammetry and Remote Sensing and ACSM, 1987, p. 439-451. refs

Discovery of a large thermal anomaly in the western Arabian highlands on Landsat TM imagery is reported. The anomaly, 15 C warmer than surroundings, forms a 2-km-wide arc around the southern flank of Jebel Chada, a volcano active in 1256 AD. It is recorded by AVHRR imagery as well, despite the 1.1-km spatial resolution of this sensor. Air photos and geologic maps show no bedrock unit that corresponds to the anomaly. Digital techniques were applied to the TM and AVHRR data, including contrast enhancement, density slicing, principal components analysis, and construction of multiband composite images. It is concluded that the anomaly results from a thin cover of volcanic ash or cinder that is optically indistinguishable from underlying basalt, rather than from internal (volcanic or hydrologic) heat sources. Author

A88-22616

CONTRIBUTION OF SPOT IMAGES TO THE GEOLOGICAL MAPPING OF ARID COUNTRIES - EXAMPLE OF THE YEMEN ARAB REPUBLIC [APPORT DE L'IMAGERIE SPOT A LA CARTOGRAPHIE GEOLOGIQUE EN PAYS ARIDE - EXEMPLE DE LA REPUBLIQUE ARABE DU YEMEN]

P. CHRISTMANN and J. Y. SCANVIE (Bureau de Recherches Geologiques et Minières, Orleans, France) Societe Francaise de Photogrammetrie et de Teledetection, Bulletin (ISSN 0244-6014), no. 106, 1987, p. 23-32. In French.

R.R.

A88-24781

THE SPACE METAL: ALL ABOUT TITANIUM [KOSMICHESKII METALL: VSE O TITANE]

LEONID BORISOVICH ZUBKOV Moscow, Izdatel'stvo Nauka, 1987, 128 p. In Russian. refs

The history of the discovery and study of titanium, its occurrence in space and on earth, and its applications are discussed in a popular manner. Attention is given to the physicochemical properties of titanium and titanium alloys, geochemistry and mineralogy of titanium, main titanium deposits, titanium mining and concentration of titanium ores, and titanium alloys. The properties and applications of titanium alloys are discussed with particular reference to titanium-based alloys with aluminum, iron, copper, manganese, molybdenum, chromium, and other metals. V.L.

A88-25045

EVOLUTION OF THE JUAN FERNANDEZ MICROPLATE DURING THE LAST THREE MILLION YEARS

A. YELLES-CHAUOUCHE, J. FRANCHETEAU, and PH. PATRIAT (Paris VII, Universite, France) Earth and Planetary Science Letters (ISSN 0012-821X), vol. 86, no. 2-4, Dec. 1987, p. 269-286. NSF-CNRS-sponsored research. refs

Magnetic and SEABEAM bathymetric data obtained during the 'Thomas Washington' survey of the area north of the Antarctic-Nazca-Pacific triple junction at 35 deg S have confirmed the existence of the Juan Fernandez microplate. An analysis is presently conducted of the magnetic anomaly data. The origin of the microplate lies at about 2 million years ago, when the western boundary began to accrete. The evolution of the microplate corresponds to a transfer of accretion from the eastern boundary to the western axis. O.C.

A88-25217*# Arizona State Univ., Tempe.

TALEMZANE - ALGERIAN IMPACT CRATER DETECTED ON SIR-A ORBITAL IMAGING RADAR

JOHN F. MCHONE and RONALD GREELEY (Arizona State University, Tempe) Meteoritics (ISSN 0026-1114), vol. 22, Sept. 30, 1987, p. 253-264. refs

(Contract JPL-956428; NSG-7415)

In November, 1981, NASA's first Shuttle Imaging Radar mission (SIR-A) began producing maplike photographic strips of Earth

04 GEOLOGY AND MINERAL RESOURCES

scenes from orbital altitude. A Saharan radar image acquired over Algeria clearly delineates two sedimentary basins, Erg Occidental and Erg Oriental, separated by an elongated zone of exposed bedrock, the M'Zab Chebka. At the NE margin of the Chebka, rimrocks, slopes, and ejecta deposits of Talemzane meteorite impact crater appear as a distinct two km wide radar-bright ring. This unique circle of strong radar backscatter distinguishes the solitary impact structure from numerous dayas (similarly appearing karstic depressions) which characterize the region. The crater is prominent on radar, but is obscure on optically obtained satellite and aircraft images, as are partly buried fluvial drainage systems and fault-block traces developed in bedrocks of the Chebka. Radar detection of an annular drainage system indicates possible presence of a ring graben at the crater. Brightest radar signals on the image are cultural features at recently developed gas fields near Hassi er R'Mel. Author

A88-25448

GEOSTRUCTURAL EVOLUTION OF THE SOUTHERN ALPS - LINEAMENTS TRENDS DETECTED ON LANDSAT IMAGES

EUGENIO ZILIOLI and MASSIMO ANTONINETTI (CNR, Istituto per la Geofisica della Litosfera, Milan, Italy) Remote Sensing of Environment (ISSN 0034-4257), vol. 23, Dec. 1987, p. 479-492. refs

The plutonic body of Mount Adamello in the central part of the Southern Calcareous Alps seems to have played a very important role in driving and controlling forces and tectonic events, since Upper Oligocene at the height of Alpine orogenesis. The intrusion is confined by the main tectonic alpine lineaments and is contiguous to the Austroalpine domain. This makes the area a rigid mechanical impediment to the advancing Adriatic microplate from whose movements different domains of lineaments originate, some of which have been recorded in recent studies on neotectonics. Stress fields that are still present have been suggested in this paper by using digitally enhanced Landsat image data to analyze lineaments. Author

A88-25551

CHARACTERISTICS OF THE SUBSURFACE RADAR SOUNDING OF NATURAL OBJECTS [OSOBENOSTI PODPOVERKHNOSTNOGO RADIOLOKatsIONNOGO ZONDIROVANIYA PRIRODNYKH OB'EKTOV]

A. I. TIMCHENKO (AN USSR, Institut Radiofiziki i Elektroniki, Kharkov, Ukrainian SSR) Akademiia Nauk SSSR, Doklady (ISSN 0002-3264), vol. 297, no. 5, 1987, p. 1091-1094. In Russian. refs

The features characterizing the subsurface radar sounding of natural objects are examined with reference to the spaceborne (e.g., Cosmos-1500) sidelooking-radar sounding of desert areas. Three important characteristics are identified: (1) an angular dependence for scattering from deep formations that is smoother than that for scattering from the upper surface; (2) the isotropization of the angular dependence of the backscattering cross section due to the inclination of subsurface structures with respect to the sounding beam; and (3) the possibility of observing objects with an angle of inclination of more than 90 deg with respect to the sounding beam in the case of scattering by a rough upper surface. B.J.

A88-26337* Nevada Univ., Reno.

GEOLOGICAL AND VEGETATIONAL APPLICATIONS OF SHUTTLE IMAGING RADAR-B, MINERAL COUNTY, NEVADA

M. X. BORENGASSER, E. F. KLEINER, F. F. PETERSON, H. KLIEFORTH (Nevada, University, Reno), P. VREELAND (Western Analytical Biogeographers, Inc., Reno, NV) et al. Photogrammetric Engineering and Remote Sensing (ISSN 0099-1112), vol. 54, Jan. 1988, p. 71-76. refs
(Contract NASA ORDER L-61130-C)

Multiple-incidence angle and multi-azimuth radar data were acquired from a Shuttle platform over test sites in Nevada in October 1984. An attempt was made to correlate these data with ground features for the purpose of evaluating the use of such data for geological and vegetational assessment. Standard

ecological parameters with respect to the flora (community composition, dominance, and relative cover) were recorded in the field at the time of overflight. Although a total of 33 species representing 11 plant families were recognized, and plant cover ranged from 13 to 26 percent, radar data could not be used to separate plant communities. The signal return is more a function of abiotic conditions than vegetative characteristics. Illumination geometry plays an important role in the ability to detect strike-slip and dip-slip faults. Local incidence angle is the most important parameter, and SIR-B data takes with small incidence angles are superior for identifying certain styles of faulting. Look direction is critical for detecting faults with a dip-slip component. New structural features were not observed. Problems with radar antenna power and recording significantly affected data quality. Author

A88-26708

TECHNIQUES OF GEOMORPHOLOGICAL MAPPING ON THE BASIS OF SPACE PHOTOGRAPHS [TEKHNOLOGIIA SOSTAVLENIIA GEOMORFOLOGICHESKIKH KART PO MATERIALAM KOSMICHESKIKH S'EMOK]

S. A. SLADKOPEVTSEV (Moskovskii Institut Inzhenerov Geodezii, Aerofotos'emki i Kartografii, Moscow, USSR) Geodeziia i Aerofotos'emka (ISSN 0536-101X), no. 4, 1987, p. 54-61. In Russian. refs

A plan for the organization of geomorphological-mapping work using space photographic data is described. Particular emphasis is placed on the definition of the mapping principle, the selection and evaluation of space photographs, photointerpretation, and the organization of field work. B.J.

A88-28024

PROBLEMS IN GEOLOGIC AND GEOMORPHIC INTERPRETATION AND GEOMETRIC MODELING OF RADAR IMAGES USING A DIGITAL TERRAIN MODEL [PROBLEMES D'INTERPRETATION GEOMORFOLOGIQUE ET GEOLOGIQUE ET MODELISATION GEOMETRIQUE D'IMAGES RADAR A PARTIR D'UN MODELE NUMERIQUE DE TERRAIN]

JEAN-PAUL RUDANT, JEAN CHOROWICZ, and PHILIPPE DURAND (Paris VI, Universite, France) Academie des Sciences (Paris), Comptes Rendus, Serie II - Mecanique, Physique, Chimie, Sciences de l'Univers, Sciences de la Terre (ISSN 0249-6305), vol. 306, Jan. 7, 1988, p. 15-20. In French.

Radar image models of the Sainte-Victoire mountain in southern France have been constructed using a digital terrain model in order to assess the efficiency of speckle filtering and to point out difficulties in interpretation. The images reveal the presence of artifacts which yield false escarpments. While speckle filtering produces less grainy images, the process results in the disappearance of many surface features. It is noted that the smoothing effect of speckle filtering aids in geomorphologic interpretation. R.R.

A88-28267

USE OF AIRBORNE IMAGING SPECTROMETER DATA TO MAP MINERALS ASSOCIATED WITH HYDROTHERMALLY ALTERED ROCKS IN THE NORTHERN GRAPEVINE MOUNTAINS, NEVADA, AND CALIFORNIA

FRED A. KRUSE (USGS, Denver, CO) Remote Sensing of Environment (ISSN 0034-4257), vol. 24, Feb. 1988, p. 31-51. Research supported by USGS, Colorado School of Mines and ASPRS. refs

An algorithm was developed to automatically calculate absorption band parameters for the strongest absorption feature in each pixel of data from three airborne imaging spectrometer flightlines from which vertical stripping had been removed and normalized. These parameters (band position, depth, and bandwidth) were mapped onto an intensity/hue/saturation color system in order to produce a single-color image summarizing absorption-band information. The image was then used to map areas of potential alteration on the basis of the predicted relationships between the color image and mineral absorption band. Areas of quartz-sericite-pyrite alteration were identified. O.C.

A88-28268* Nevada Univ., Reno.

DISCRIMINATION OF HYDROTHERMAL ALTERATION MINERAL ASSEMBLAGES AT VIRGINIA CITY, NEVADA, USING THE AIRBORNE IMAGING SPECTROMETER

AMY HUTSINPILLER (Nevada, University, Reno) Remote Sensing of Environment (ISSN 0034-4257), vol. 24, Feb. 1988, p. 53-66. refs

(Contract NASW-4050)

The purpose of this study is to use airborne imaging spectrometer data to discriminate hydrothermal alteration mineral assemblages associated with silver and gold mineralization at Virginia City, NV. The data is corrected for vertical striping and sample gradients, and converted to flat-field logarithmic residuals. Log residual spectra from areas known to be altered are compared to field spectra for kaolinitic, illitic, sericitic, and propylitic alteration types. The areal distributions of these alteration types are estimated using a spectral matching technique. Both visual examination of spectra and the matching techniques are effective in distinguishing kaolinitic, illitic, and propylitic alteration types from each other. However, illitic and sericitic alteration cannot be separated using these techniques because the spectra of illite and sericite are very similar. A principal components analysis of 14 channels in the 2.14-2.38 micron wavelength region is also successful in discriminating and mapping illitic, kaolinitic, and propylitic alteration types. Author

A88-28269* Nevada Univ., Reno.

COMPARISON OF TECHNIQUES FOR DISCRIMINATING HYDROTHERMAL ALTERATION MINERALS WITH AIRBORNE IMAGING SPECTROMETER DATA

SANDRA C. FELDMAN and JAMES V. TARANIK (Nevada, University, Reno) Remote Sensing of Environment (ISSN 0034-4257), vol. 24, Feb. 1988, p. 67-83. NASA-AIME-supported research. refs

Hydrothermal alteration mineralogy in the Tybo mining district of Nevada has been mapped on the basis of high spectral and spatial resolution Airborne Imaging Spectrometer (AIS) data, using band ratios, principal component analysis, and a signature-matching algorithm to delineate the alteration zones and limestone foundations. The signature-matching algorithm is found to be the most effective method of discriminating alteration minerals, and is noted to be able to identify mineralogy by matching AIS image spectra with library reference spectra. AIS bands in the 2048-2337-nm portion of the spectrum accounted for the greatest amount of variance. O.C.

A88-28273* Brown Univ., Providence, R. I.

EXPLORATION OF CRUSTAL/MANTLE MATERIAL FOR THE EARTH AND MOON USING REFLECTANCE SPECTROSCOPY

CARLE M. PIETERS and JOHN F. MUSTARD (Brown University, Providence, RI) Remote Sensing of Environment (ISSN 0034-4257), vol. 24, Feb. 1988, p. 151-178. refs (Contract NASW-4048; NAGW-28; NAGW-738)

Near-infrared reflectance spectra have been acquired (1) for Moses Rock diatreme in SE Utah using an airborne imaging spectrometer (AIS) and (2) for small areas in and around the large lunar impact crater Copernicus using a spectrometer on earth-based telescopes. The high spectral resolution and precision of these data allow several mineral components of surface material to be identified and analyzed in a spatial context. The derived mineralogical information is used to address specific geological problems. For the terrestrial study the distribution of the measured abundance of mantle derived ultramafic microbreccia across Moses Rock dike indicates that flow stabilized into a few channels during the violent eruption. For the lunar study the variety of rock types identified in crustal material of deep-seated origin is distinct from the dominant rock types sampled from the upper lunar crust and suggests a complex crustal evolution. Author

A88-29281

COMPARISON OF LANDSAT MSS AND SIR-A DATA FOR GEOLOGICAL APPLICATIONS IN PAKISTAN

S. A. K. ALIZAI and JAWED ALI (SUPARCO, Remote Sensing

Applications Centre, Karachi, Pakistan) International Journal of Remote Sensing (ISSN 0143-1161), vol. 9, Jan. 1988, p. 85-94. refs

A88-29431

GEOCHEMISTRY OF CONTINENTAL VOLCANISM

[GEOKHIMIYA KONTINENTAL'NOGO VULKANIZMA]

S. V. GRIGORIAN, ED. Moscow, Izdatel'stvo Nauka, 1987, 240 p. In Russian. No individual items are abstracted in this volume. refs

The laws governing the distribution of petrogenic and rare elements in volcanic rocks are examined on the basis of the geochemical characteristics of volcanic and basaltic rocks from different regions of the USSR. Attention is given to geochemical trends in the basaltoid series and the rare-element clarkes in these rocks as well as to the types of alkaline basaltoids of the Russian platform. Special consideration is given to the geochemical characteristics and the formation conditions of the volcanic associations of the Maimecha-Kotui and the Baikal regions, the trends of the magmatic differentiation of the alkaline basalts of the Kuzneki Alatau region, and the geochemistry and genesis of the youngest volcanites in the Caucasus region. The petrochemical typification of the alkaline-basaltic continental series is presented. I.S.

A88-29489

LANDSAT DETERMINED GEOGRAPHIC CHANGE

W. J. STRINGER, J. E. GROVES, and C. OLMSTED (Alaska, University, Fairbanks) Photogrammetric Engineering and Remote Sensing (ISSN 0099-1112), vol. 54, March 1988, p. 347-351.

Geomorphic changes in the Yukon River Delta occurring over a thirty-five year span have been detected through comparison of a recent Landsat image with earlier maps compiled from aerial photography. Island formation or growth and channel migration were found to have taken place with a calculated location precision of around 200 m. Geographic control of the Landsat image was established through digitization of surveyed control points used for control of aerial photography for mapping. Tide stage considerations were found to be useful in these low-lying areas, even though the astronomical tide range here is relatively small. Author

A88-30079

THE USE OF METEOR-PRIRODA SPACE PHOTOGRAPHS FOR THE COMPILATION OF SMALL-SCALE AND MEDIUM-SCALE TECTONIC AND GEOLOGICAL MAPS [ISPOL'ZOVANIE KOSMICHESKIKH SNIMKOV SISTEMY 'METEOR-PRIRODA' PRI SOSTAVLENNII TEKTONICHESKIKH I GEOLOGICHESKIKH KART MELKIKH I SREDNIKH MASSHTABOV]

T. P. ONUFRIIUK (Moskovskii Gosudarstvennyi Universitet, Moscow, USSR) Issledovanie Zemli iz Kosmosa (ISSN 0205-9614), Nov.-Dec. 1987, p. 23-30. In Russian. refs

A88-30081

INVESTIGATION OF THE FOCI OF POWERFUL EARTHQUAKES AND SEISMICALLY HAZARDOUS AREAS ON SPACE PHOTOGRAPHS FOR THE BAIKAL-ALDAN REGION [IZUCHENIE OCHAGOV SIL'NYKH ZEMLETRIASENII I SEISMOOPASNYKH ZON PO KOSMICHESKIM SNIMKAM V BAIKALO-ALDANSKOM REGIONE]

A. F. PETROV (AN SSSR, Otdel Okhrani Prirody, Yakutsk, USSR) and A. M. BOROVNIKOV (Novosibirski Gosudarstvennyi Universitet, Novosibirsk, USSR) Issledovanie Zemli iz Kosmosa (ISSN 0205-9614), Nov.-Dec. 1987, p. 34-41. In Russian. refs

A88-31125*

IDENTIFICATION AND SPECTRAL CHARACTERISTICS OF HYDROTHERMAL ALTERATION ON LANDSAT TM IMAGERY OF NORTH CHILE

MICHAEL C. W. BAKER Australasian Institute of Mining and Metallurgy, International Congress on the Geology, Structure,

04 GEOLOGY AND MINERAL RESOURCES

Mineralization, and Economics of the Pacific Rim, Broadbeach, Australia, Aug. 26-29, 1987, Paper. 4 p.
(Contract NASW-4066)

This study examines the application of Landsat TM data to the identification of hydrothermal alteration in the arid terrain of the El Salvador region of north Chile. Numerical reflectance values were extracted from the digital Landsat TM data for a variety of rock surfaces, including four parts of the El Salvador gossan, for each of six spectral bands. These reflectance values were analyzed statistically in order to select the three spectral bands, combined as a color composite image, that are most efficient in discriminating different varieties of alteration and for general geological interpretation. The most cost effective composite image for this area is a combination of bands 1, 4 and 7 as the blue, green and red components respectively, with simple contrast enhancement. This image is superior to some much more expensive enhancement techniques and allows unambiguous identification of areas of hydrothermal alteration larger than about 50 m. The display includes a practical guide to the use of Landsat TM imagery for volcanic gold exploration. Author

N88-15288 Deutsche Geodaetische Kommission, Munich (West Germany).

THE AEROPHOTOGRAMMETRIC DETERMINATION OF EARTH SURFACE DEFORMATIONS Ph.D. Thesis - Technische Univ., Brunswick, West Germany [ZUR

AEROPHOTOGRAMMETRISCHEN ERMITTLUNG VON VERFORMUNGEN DER ERDOBERFLAECHE]

PETER LADSTAETTER 1986 59 p In GERMAN
(SER-C-321; ISBN-3-7696-9371-X; ISSN-0065-5325;
ETN-88-90800) Avail: Issuing Activity

The deformation of a part of the tectonically active Krafla fissure swarms in Iceland was studied using the aerophotogrammetric method. Measurement of the image coordinates, calibration of the plotter, and the correction software are described. The determination of object coordinates and displacement vectors is explained. The aerotriangulation shows a 10 cm accuracy of the coordinates, suitable for the deformation analysis of phases with strong rifting. The vertical movement analysis requires a critical evaluation. Software improvements and the use of artificial covariance matrices are necessary. The mathematical model of bundle block adjustment has to be improved regarding self-calibration and image coordinate weighting. ESA

N88-16103# Joint Publications Research Service, Arlington, Va.
SATELLITE MONITORING OF EARTHQUAKE PRECURSOR EFFECTS IN MAGNETOSPHERE

YU. I. ZAYTSEV In its JPRS Report: Science and Technology. USSR: Space p 106-113 24 Nov. 1987 Transl. into ENGLISH from Zemlya i Vselennaya (Moscow, USSR), no. 3, May - Jun. 1987 p 45-50

Avail: NTIS HC A08/MF A01

During satellite overflights of seismically active regions of the Earth, special equipment is recording bursts of electromagnetic radiation in the Earth's ionosphere and magnetosphere. These bursts frequently not only accompany a seismic shock, but also precede it. How these bursts can be used to predict earthquakes is addressed. Author

N88-16108# Joint Publications Research Service, Arlington, Va.
SPACE PHOTOGRAPHS OF THE ONEGA-LADOGA ISTHMUS AND PREDICTION OF USEFUL MINERALS

Z. A. BAGROVA and I. B. ANTONOVA In its JPRS Report: Science and Technology. USSR: Space p 128 24 Nov. 1987 Transl. into ENGLISH from Issledovaniye Zemli iz Kosmosa (Moscow, USSR), no. 2, Mar. - Apr. 1987 p 66-72 Original language document was announced in IAA as A87-48185

Avail: NTIS HC A08/MF A01

The geological structural characteristics of the Onega-Ladoga isthmus as interpreted from space imagery is considered. Fault systems and ring structures were identified. This information along with available geological and geophysical data makes it possible

to recognize signs of explosive magmatism and to predict the occurrence of bauxites and other minerals. Author

N88-16109# Joint Publications Research Service, Arlington, Va.
USE OF SPACE PHOTOGRAPHS FOR GEOMORPHOLOGICAL STUDIES IN SOUTHWESTERN TAJIKISTAN

V. P. LOZIYEV and M. S. SAIDOV In its JPRS Report: Science and Technology. USSR: Space p 129 24 Nov. 1987 Transl. into ENGLISH from Issledovaniye Zemli iz Kosmosa (Moscow, USSR), no. 2, Mar. - Apr. 1987 p 73-80 Original language document was announced in IAA as A87-48186

Avail: NTIS HC A08/MF A01

Since 1977, complex studies of natural resources in Tajikistan have been performed based on space survey materials, space photographs of varying levels of generalization obtained onboard the Salyut manned spacecraft and the Cosmos automatic spacecraft. The results of these studies have shown that the materials of space photographic surveys can be successfully used for geomorphological mapping. The materials can be used in many cases to reproduce relief forms which have been destroyed by human economic activity and recognize buried elements which determine the lithologic and structural characteristics of sedimentary basins. The quality of transparency of the photographs allows determination of certain deep structural elements not observed by visual mapping. A table illustrates the relationship of recent tectonic movement and development of epiplatform relief in the area. Author

N88-16110# Joint Publications Research Service, Arlington, Va.
USE OF SPACE PHOTOGRAPHS FOR PALEOSEISMOGEOLOGICAL STUDIES (ON THE EXAMPLE OF MONGOLIAN ALTAY) Abstract Only

A. L. STROM In its JPRS Report: Science and Technology. USSR: Space p 130 24 Nov. 1987 Transl. into ENGLISH from Issledovaniye Zemli iz Kosmosa (Moscow, USSR), no. 2, Mar. - Apr. 1987 p 81-84 Original language document was announced in IAA as A87-48187

Avail: NTIS HC A08/MF A01

It is demonstrated that, in Central Asia, young faults observed by space photographs can be reliably interpreted as paleoseismodislocations. Such faults are characterized by their manifestations as scarps and the presence of displacements of river beds or deluvial/proluvial cones. Author

N88-16111# Joint Publications Research Service, Arlington, Va.
STUDY OF RELIEF OF ORE REGIONS USING SPACE IMAGES (ON THE EXAMPLE OF EASTERN YAKUTIA) Abstract Only

V. A. BALANDIN In its JPRS Report: Science and Technology. USSR: Space p 131 24 Nov. 1987 Transl. into ENGLISH from Issledovaniye Zemli iz Kosmosa (Moscow, USSR), no. 2, Mar. - Apr. 1987 p 85-89 Original language document was announced in IAA as A87-48188

Avail: NTIS HC A08/MF A01

A study of many mining regions of Eastern Yakutia has shown that most of them coincide with areas of granitoids, associated with circular formations produced by endogenous structure forming factors. The method of locating these formations from space photographs is simple, involving a search for concentric sectors of divides and valleys, arch shaped image elements associated with changes in facies and intensity of jointing, isometric and arch shaped landscape zones and other similar characteristics. Ore zones are usually found around the outer contour of local circular formations or are associated with radially concentric cracks at their centers. The circular formations and lineaments of meridional, latitudinal and diagonal directions are found to be ore controlling characteristics. The space photographs agree with, but are more diagnostic than, structural geomorphological constructions in locating ore zones. Author

N88-16281*# National Academy of Sciences - National Research Council, Washington, D. C.

INTERNATIONAL ROLE OF US GEOSCIENCE Final Report

Jun. 1987 104 p Sponsored in part by NASA; National Geodetic

Survey, Rockville, Md.

(Contract NA84-AA-D-00009)

(NASA-CR-182407; NAS 1.26:182407; PB88-113683) Avail:
NTIS HC A06/MF A01 CSCL 08G

Geologic processes are global in scope and no country or continent has areas that encompass all the phenomena. Joint participation between U.S. and foreign scientists is indispensable for advancing basic scientific concepts and their application to economic and policy issues in the U.S. Up-to-date knowledge is critical to assure an adequate flow of industrial minerals and to assure an adequate supply of strategic minerals. GRA

N88-17099# Deutsche Forschungs- und Versuchsanstalt fuer Luft- und Raumfahrt, Oberpfaffenhofen (West Germany). Abteilung Meteorologische Fernerkundung.

STATISTICS OF TWO-DIMENSIONAL STRUCTURE ELEMENTS OF MOUNTAINOUS RANGES (MOOSAIC MODEL) FOR CALCULATING THREE-DIMENSIONAL REFLECTION FUNCTIONS

RUEDIGER H. BUELL Sep. 1987 66 p In GERMAN; ENGLISH summary

(DFVLR-FB-87-33; ISSN-0171-1342; ETN-88-91693) Avail:

NTIS HC A04/MF A01; DFVLR, Cologne, Federal Republic of Germany, DM 23.50

Three-dimensional reflection functions were calculated in order to determine the albedo of an orographically partitioned terrain from satellite data. Quantities such as valley statistics and synthetic valley cross sections were determined by the analysis of two-dimensional structure elements of the terrain. These quantities allow the calculation of three-dimensional reflection functions. The methods of the computer program system for such an analysis are described. The application of the program system to two regions of the Alps yields acceptable results. ESA

N88-17140*# Nevada Univ., Reno. Dept. of Geological Sciences.

NATURE AND ORIGIN OF MINERAL COATINGS ON VOLCANIC ROCKS OF THE BLACK MOUNTAIN, STONEWALL MOUNTAIN, AND KANE SPRINGS WASH VOLCANIC CENTERS, SOUTHERN NEVADA Semiannual Progress Report, Jul. 1987 - Jan. 1988

JAMES V. TARANIK, LIANG C. HSU, and DAVID SPATZ Jan. 1988 53 p

(Contract NAS5-28765)

(NASA-CR-181437; NAS 1.26:181437) Avail: NTIS HC A04/MF A01 CSCL 08G

Comparative lab spectra and Thematic Mapper imagery investigations at 3 Tertiary calderas in southern Nevada indicate that desert varnish is absorbant relative to underlying host rocks below about 0.7 to 1.3 microns, depending on mafic affinity of the sample, but less absorbant than mafic host rocks at higher wavelengths. Desert varnish occurs chiefly as thin impregnating films. Distribution of significant varnish accumulations is sparse and localized, occurring chiefly in surface recesses. These relationships result in the longer wavelength bands and high 5/2 values over felsic units with extensive desert varnish coatings. These lithologic, petrochemical, and desert varnish controlled spectral responses lead to characteristic TM band relationships which tend to correlate with conventionally mappable geologic formations. The concept of a Rock-Varnish Index (RVI) is introduced to help distinguish rocks with a potentially detectable varnish. Felsic rocks have a high RVI, and those with extensive desert varnish behave differently, spectrally, from those without extensive varnish. The spectrally distinctive volcanic formations at Stonewall Mountain provide excellent statistical class segregation on supervised classification images. A binary decision rule flow-diagram is presented to aid TM imagery analysis over volcanic terrane in semi-arid environments. Author

N88-18047# Utah Univ., Salt Lake City.

THREE-DIMENSIONAL TRANSIENT ELECTROMAGNETIC MODELING FOR EXPLORATION GEOPHYSICS Ph.D. Thesis

GREGORY ALEX NEWMAN 1987 242 p

Avail: Univ. Microfilms Order No. DA8722653

The three-dimensional (3-D) electromagnetic scattering problem is first formulated in the frequency domain in terms of an electric-field volume-integral equation. Three-dimensional responses are then Fourier-transformed with sine and cosine digital filters. The digital-filter technique is applied to a sparsely sampled frequency sounding, which is replaced by a cubic-spline interpolating function prior to convolution with the digital filters. A 3-D solution is used to study the galvanic response of a 3-D conductor energized by a large rectangular loop. In addition, the solution is applied to the central-loop sounding method for 3-D structural interpretation with layered-earth models and horizontal-field measurements. An integral-equation solution for the transient electromagnetic (TEM) scattering of prisms in layered half-spaces is formulated to provide meaningful results when the prisms are in highly resistive layers. The solution provides meaningful results over a wide range of layered-host resistivities, including that of free space. The solution is used to investigate the effect of conductive overburden on 3-D TEM responses and the lateral resolution of two conductors for the fixed-loop and central-loop configurations. Dissert. Abstr.

N88-18048# Geoexplorers International, Inc., Denver, Colo. **GEOLOGICAL EVOLUTION AND ANALYSIS OF CONFIRMED OR SUSPECTED GAS HYDRATE LOCALITIES. VOLUME 10: BASIN ANALYSIS, FORMATION AND STABILITY OF GAS HYDRATES OF THE ALEUTIAN TRENCH AND THE BERING SEA**

J. KRASON and M. CIESNIK Jan. 1987 183 p

(Contract DE-AC21-84MC-21181)

(DE88-001008; DOE/MC-21181/1950-VOL-10) Avail: NTIS HC A09/MF A01

Four major areas with inferred gas hydrates are the subject of this study. Two of these areas, the Navarin and the Norton Basins, are located within the Bering Sea shelf, whereas the remaining areas of the Atka Basin in the central Aleutian Trench system and the eastern Aleutian Trench represent a huge region of the Aleutian Trench-Arc system. All four areas are geologically diverse and complex. Particularly the structural features of the accretionary wedge north of the Aleutian Trench still remain the subjects of scientific debates. Prior to this study, suggested presence of the gas hydrates in the four areas was based on seismic evidence, i.e., presence of bottom simulating reflectors (BSRs). Although the disclosure of the BSRs is often difficult, particularly under the structural conditions of the Navarin and Norton basins, it can be concluded that the identified BSRs are mostly represented by relatively weak and discontinuous reflectors. Under thermal and pressure conditions favorable for gas hydrate formation, the relative scarcity of the BSRs can be attributed to insufficient gas supply to the potential gas hydrate zone. Hydrocarbon gas in sediment may have biogenic, thermogenic or mixed origin. In the four studied areas, basin analysis revealed limited biogenic hydrocarbon generation. The migration of the thermogenically derived gases is probably diminished considerably due to the widespread diagenetic processes in diatomaceous strata. The latter processes resulted in the formation of the diagenetic horizons. The identified gas hydrate-related BSRs seem to be located in the areas of increased biogenic methanogenesis and faults acting as the pathways for thermogenic hydrocarbons. DOE

N88-18050# Geoexplorers International, Inc., Denver, Colo. **GEOLOGICAL EVOLUTION AND ANALYSIS OF CONFIRMED OR SUSPECTED GAS HYDRATE LOCALITIES. VOLUME 9: FORMATION AND STABILITY OF GAS HYDRATES OF THE MIDDLE AMERICA TRENCH**

P. FINLEY and J. KRASON Dec. 1986 261 p

(Contract DE-AC21-84MC-21181)

(DE88-001007; DOE/MC-21181/1950-VOL-9) Avail: NTIS HC A12/MF A01

This report presents a geological description of the Pacific margin of Mexico and Central America, including regional and local

04 GEOLOGY AND MINERAL RESOURCES

structural settings, geomorphology, geological history, stratigraphy, and physical properties. It provides the necessary regional and geological background for more in-depth research of the area. Detailed discussion of bottom simulating acoustic reflectors, sediment acoustic properties, and distribution of hydrates within the sediments are also included in this report. The formation and stabilization of gas hydrates in sediments are considered in terms of phase relations, nucleation, and crystallization constraints, gas solubility, pore fluid chemistry, inorganic diagenesis, and sediment organic content. Together with a depositional analysis of the area, this report gives a better understanding of the thermal evolution of the locality. It should lead to an assessment of the potential for both biogenic and thermogenic hydrocarbon generation.

DOE

N88-18984*# Cornell Univ., Ithaca, N.Y. Dept. of Geological Sciences.

THEMATIC MAPPER STUDY OF ALASKAN OPHIOLITES Final Report

JOHN M. BIRD Feb. 1988 296 p

(Contract NAS5-28739)

(NASA-CR-182554; NAS 1.26:182554) Avail: NTIS HC A13/MF A01 CSCL 08G

The two principle objectives of the project Thematic Mapper Study of Alaskan Ophiolites were to further develop techniques for producing geologic maps, and to study the tectonics of the ophiolite terrains of the Brooks Range and Ruby Geanticline of northern Alaska. Ophiolites, sections of oceanic lithosphere emplaced along island arcs and continental margins, are important to the understanding of mountain belt evolution. Ophiolites also provide an opportunity to study the structural, lithologic, and geochemical characteristics of ocean lithosphere, yielding a better understanding of the processes forming lithosphere. The first part of the report is a description of the methods and results of the TM mapping and gravity modeling. The second part includes papers being prepared for publication. These papers are the following: (1) an analysis of basalt spectral variations; (2) a study of basalt geochemical variations; (3) an examination of the cooling history of the ophiolites using radiometric data; (4) an analysis of shortening produced by thrusting during the Brooks Range orogeny; and (5) a study of an ophiolite using digital aeromagnetic and topographic data. Additional papers are in preparation.

F.M.R.

N88-18988# Bureau of Mines, Pittsburgh, Pa. Research Center.

CHARACTER OF FIVE SELECTED LANDSAT LINEAMENTS IN SOUTHWESTERN PENNSYLVANIA: REPORT OF INVESTIGATIONS, 1987

N. N. MOEBS and G. P. SAMES 1987 31 p

(PB88-133517; BM-RI-9104; LC-86-607593) Avail: NTIS HC A03/MF A01 CSCL 05B

Five LANDSAT lineaments in the coal mining region of southwestern Pennsylvania were investigated by the Bureau of Mines to determine their geologic character, relation to subsurface conditions, and the means of discriminating one from another. The investigation included earth resistivity and very low frequency electromagnetic traverses, soil moisture sampling, and a correlation with coal mine roof conditions. The lineaments could not be detected by the methods used, suggesting that they might be a surface phenomenon unrelated to subsurface geologic structures or roof stability in coal mine workings beneath.

GRA

05

OCEANOGRAPHY AND MARINE RESOURCES

Includes sea-surface temperature, ocean bottom surveying imagery, drift rates, sea ice and icebergs, sea state, fish location.

A88-20942#

MEASURING OCEAN WAVES FROM SPACE

ROBERT C. BEAL (Johns Hopkins University, Laurel, MD) Aerospace America (ISSN 0740-722X), vol. 26, Jan. 1988, p. 34-36, 38.

During the coming decade, several nations will monitor various properties of the ocean surface with active radars in space. The Europeans will launch ERS-1, the Japanese will launch JERS-1, the U.S. will launch TOPEX and possibly NROSS, and the Canadians will launch Radarsat. NASA is planning two SIR-C flights in the early 1990's; these flights are expected to demonstrate the potential of SAR for the validation and refinement of ocean wave models over global scales. Attention is given to the Spectrasat concept, involving a low-altitude, free-flying SAR with a three-year orbital lifetime using active drag compensation combined with a small spacecraft frontal cross section. Another approach is the addition of an off-nadir ROWS (radar ocean wave spectrometer) to one of the planned higher-altitude missions.

B.J.

A88-20978

NORTH ATLANTIC THERMOHALINE CIRCULATION DURING THE PAST 20,000 YEARS LINKED TO HIGH-LATITUDE SURFACE TEMPERATURE

EDWARD A. BOYLE (MIT, Cambridge, MA) and LLOYD KEIGWIN (Woods Hole Oceanographic Institution, MA) Nature (ISSN 0028-0836), vol. 330, Nov. 5, 1987, p. 35-40. NSF-supported research. refs

A88-21003

REMOTE SENSING OF CHESAPEAKE BAY WATER QUALITY REQUIRED FOR HEALTHY OYSTER BEDS

PAUL V. RIGTERINK (Computer Sciences Corp., Silver Spring, MD) IN: American Society for Photogrammetry and Remote Sensing and ACSM, Annual Convention, Baltimore, MD, Mar. 29-Apr. 3, 1987, Technical Papers. Volume 1. Falls Church, VA, American Society for Photogrammetry and Remote Sensing and ACSM, 1987, p. 18-26. refs

A88-22154*# National Aeronautics and Space Administration. Goddard Space Flight Center, Greenbelt, Md.

SATELLITE MAPS OF ANTARCTIC TOTAL OZONE

ARLIN J. KRUEGER (NASA, Goddard Space Flight Center, Greenbelt, MD) AIAA, Aerospace Sciences Meeting, 26th, Reno, NV, Jan. 11-14, 1988. 5 p. refs
(AIAA PAPER 88-0210)

Satellite remote sensing techniques for ozone have made it possible to observe the detailed, daily horizontal structure of atmospheric ozone at all locations where sunlight is present. The Antarctic ozone 'hole' has been observed with the Total Ozone Mapping Spectrometer (TOMS) instrument since launch of Nimbus 7 in 1978. This feature is a continental-size ozone minimum found in the Antarctic winter and spring seasons which has generally deepened in recent years to levels in 1985 and 1987 far below the lowest values ever observed elsewhere. The minimum appears to be produced by atmospheric circulations, but the deepening almost certainly involves chemistry which is unique to cold, dark conditions.

Author

A88-22911

THE WESTERN EQUATORIAL PACIFIC OCEAN CIRCULATION STUDY

ERIC LINDSTROM, STUART GODFREY (CSIRO, Div. of Oceanography, Hobart, Australia), ROGER LUKAS, ERIC FIRING (Hawaii, University, Honolulu), RANA FINE (Miami, University, FL)

et al. *Nature* (ISSN 0028-0836), vol. 330, Dec. 10, 1987, p. 533-537. NSF-CSIRO-supported research. refs

A recent set of oceanographic measurements in the western equatorial Pacific has revealed the existence of previously undescribed major ocean currents and upper-ocean mixed-layer structure. The measurements also confirm a 20-year-old hypothesis on the water-mass origins of the Equatorial Undercurrent in the Pacific Ocean.

Author

A88-22947

SEA RETURN AT C AND KU BANDS

B. FISCELLA, P. P. LOMBARDINI, P. TRIVERO, C. CAPPÀ (Torino, Università; CNR, Istituto di Cosmogeofisica, Turin, Italy), and R. CINI (Firenze, Università, Florence, Italy) *Nuovo Cimento C, Serie 1* (ISSN 0390-5551), vol. 10, July-Aug. 1987, p. 381-385. refs

The effect of surface oil on C and Ku fan beam Doppler airborne scatterometers used for measuring sea clutter return is investigated with reference to recently published results (Singh et al., 1986) obtained in flights over crude oil artificial spills. It is demonstrated that, in the Ku band, the mechanism of sea clutter is due to the second-order Bragg term.

V.L.

A88-23544

AN APPROXIMATE MODEL FOR THE MICROWAVE BRIGHTNESS TEMPERATURE OF THE SEA

A. GUISSARD and P. SOBIESKI (Louvain, Université Catholique, Louvain-la-Neuve, Belgium) *International Journal of Remote Sensing* (ISSN 0143-1161), vol. 8, Nov. 1987, p. 1607-1627. refs

(Contract ESA-5285/82)

A modified two-scale model is proposed for scattering and emissivity calculations for certain classes of random rough surfaces. It is based on an approach by Burrows (1973) and by Brown (1978), but it has been extended to bistatic scattering by lossy dielectric surfaces, and it incorporates modified Fresnel reflection coefficients and a simple correction for multiple-scattering effects. The method is shown to be applicable to the ocean surface for light and moderate winds. A contracted form of the radiative-transfer equation is proposed and the included Wentz correction for surface scattering is discussed. This could lead to a method that could be both simple and accurate enough for real-time inversion algorithms in microwave remote sensing.

Author

A88-23545

REMOTE SENSING OF WAVE PATTERNS WITH OCEANOGRAPHIC IMPLICATIONS

DAVID SHERES, DAVIDSON T. CHEN, and GASPAR R. VALENZUELA (U.S. Navy, Naval Research Laboratory, Washington, DC) *International Journal of Remote Sensing* (ISSN 0143-1161), vol. 8, Nov. 1987, p. 1629-1640. Research supported by the U.S. National Research Council. refs

First, a general review is presented of wave-current interaction processes (for horizontal shears) and their effect on radar backscatter and radar imagery (SAR/RAR). Then numerical results on the refraction of wave energy trajectories by complex bottom topography (finite depth) and a linear shear current are presented. For deep water, the wave-energy trajectories are given for mesoscale currents (e.g. eddies and double-vortex configurations). The focusing of wave energy by variable currents found here should have important influence on the spatial scale of wind stress over the ocean, and on optical and acoustic properties of the upper layer of the ocean.

Author

A88-23546* Jet Propulsion Lab., California Inst. of Tech., Pasadena.

WIND-FETCH DEPENDENCE OF SEASAT SCATTEROMETER MEASUREMENTS

ROMAN E. GLAZMAN (California Institute of Technology, Jet Propulsion Laboratory, Pasadena) *International Journal of Remote Sensing* (ISSN 0143-1161), vol. 8, Nov. 1987, p. 1641-1647. refs

This work is focused on the effects of large-scale wind-generated gravity waves on scatterometer wind-measurement

accuracy. Theoretical and experimental evidence of the important role played by the degree of wind-wave coupling in surface geometry and therefore in microwave signatures is presented. Seasat scatterometer wind-measurement errors are analyzed, and an error bias is found to be related to the degree of wind-wave development. Attention is focused on a dynamic measure of wind-wave development that characterizes the rate of energy transfer from the mean wind to the energy-carrying portion of the wave spectrum. An explanation of the bias is suggested based on the consideration of an additional component of surface scattering caused by electromagnetic-wave diffraction at the crests of individual, sufficiently steep wavelets.

Author

A88-23547

INTERPRETATION OF SEASAT RADAR-ALTIMETER DATA OVER SEA ICE USING NEAR-SIMULTANEOUS SAR IMAGERY

LARS M. H. ULANDER (Chalmers Tekniska Högskola, Göteborg, Sweden) *International Journal of Remote Sensing* (ISSN 0143-1161), vol. 8, Nov. 1987, p. 1679-1686. Research supported by the Swedish Board for Space Activities. refs

(Contract ESA-6617/85/F/FL(SC))

The backscatter properties of Seasat altimeter data in the Beaufort Sea on October 3, 1978 show distinct zones, which are interpreted in terms of geophysical characteristics. An overlapping and near-simultaneous synthetic-aperture radar image shows regions of open water, new ice, and multi-year sea ice which correspond to the different zones. It is found that the altimeter signal is sensitive to the ocean-ice boundary and that it indicates the ice type. The pulse-echo waveforms also suggest that several scattering components are present in the returned power over sea ice.

Author

A88-23762

POTENTIAL APPLICATIONS OF DIGITAL IMAGE ANALYSIS SYSTEMS FOR DISPLAYING SATELLITE ALTIMETRY DATA

ROSTAM YAZDANI, NIKOLAOS CHRISTOU, and EUGENE DERENYI (New Brunswick, University, Fredericton, Canada) *Photogrammetric Engineering and Remote Sensing* (ISSN 0099-1112), vol. 53, Nov. 1987, p. 1545-1548. Research supported by the Department of Supply and Services. refs

DIPIX ARIES II and Perceptron EASI/PACE digital image analysis systems were used for displaying geoidal and sea-surface heights. These data sets were transferred to image files for display. Black-and-white and color density slicing, and enhanced color display techniques were employed to better visualize these surfaces. An analytical relief shading program was developed to make the small local undulations in height visible. The shape and orientation of the various surfaces were compared by a differencing program specifically written for this purpose. The processing and display techniques employed offered additional capabilities in examining and interpreting the displayed surfaces. They also offered better discrimination of certain features which were not discernible from the conventional contour displays.

Author

A88-23988#

A MULTI-FREQUENCY-MULTI-NADIR-ANGLE PUSHBROOM-RADIOMETER FOR OIL SPILL DETECTION AND MAPPING (ON THE SURFACE OF THE SEA)

D. SALZER, W. BIRKMAYER, and G. BRAUN (Messerschmitt-Boelkow-Blohm GmbH, Munich, Federal Republic of Germany) *International Colloquium on Remote Sensing of Ocean Properties, Oldenburg, Federal Republic of Germany, Mar. 31-Apr. 3, 1987, Paper. 15 p.* refs

(MBB-UR-952-87)

Scanning single-frequency radiometers have been used in the past to measure the thickness of oil layers. The proposed radiometer includes two improvements to the present systems. One is the use of the pushbroom concept where the scanning antenna is replaced by a multifeed antenna and the other improvement is the observation of the oil spill at two different angles to the surface. Since the differences in the radiometric temperatures of the water and the oil are a function of the observation angle the temperatures measured at different angles

provide information about the oil type. The described system works simultaneously at two different frequencies to measure oil layers with thicknesses between 0.1 and 2.5 mm. So that both frequency channels simultaneously illuminate the same spots on the surface of the water dual-frequency horns are used. Author

A88-24456

A SNAPSHOT OF THE LABRADOR CURRENT INFERRED FROM ICE-FLOE MOVEMENT IN NOAA SATELLITE IMAGERY
INGRID PETERSON (Bedford Institute of Oceanography, Dartmouth, Canada) Atmosphere - Ocean (ISSN 0705-5900), vol. 25, Dec. 1987, p. 402-415. Research supported by the Canadian Federal Panel on Energy Research and Development. refs

Ice floes along the Labrador Coast were tracked using visible NOAA satellite images on two consecutive days (26 and 27 April, 1984) when the ice-pack extended beyond the Labrador Current, and winds were weak. The resulting 'snapshot' of the velocity field reveals strong topographic steering of the Labrador Current, such that the current speed and width in different areas are dependent on the steepness of the continental slope, and the current deflects into and out of Hopedale Saddle. Between 55 and 58 deg N, the main core of the current is 60-90 km wide, with speeds of 30-55 cm/s. The overall circulation pattern is in good agreement with historical water mass analyses over the shelf and slope, and with estimates of the speed of the Labrador Current obtained by other methods. Author

A88-24457

THE BAROCLINIC CIRCULATION IN HUDSON STRAIT
JOSEF CHERNIAWSKY and PAUL H. LEBLOND (British Columbia, University, Vancouver, Canada) Atmosphere - Ocean (ISSN 0705-5900), vol. 25, Dec. 1987, p. 416-426. NSERC-supported research. refs

Results on the flow of semigeostrophic currents around indented coastlines are used to model the baroclinic circulation in the mouth of the Hudson Strait. A realistic representation of the circulation is achieved by expanding the basic T-junction model to include the sharp northern tip of Labrador, the southwestern tip of Baffin Island, and part of Ungava Bay. It is found that the mouth of the Hudson does not form a significant obstacle to baroclinic flows in and out of it, indicating the recirculation noted by LeBlond et al. (1981) cannot be due to the effects of the geometry of the coastline on the baroclinic part of the flow. It is suggested that bathymetric influences on the barotropic component may contribute to this recirculation. R.R.

A88-24582

GEOSAT ALTIMETER OBSERVATIONS OF KELVIN WAVES AND THE 1986-87 EL NINO
LAURY MILLER, ROBERT E. CHENEY, and BRUCE C. DOUGLAS (NOAA, National Ocean Service, Rockville, MD) Science (ISSN 0036-8075), vol. 239, Jan. 1, 1988, p. 52-54. refs

Two years of Geosat altimeter observations are used to investigate the response of sea level to anomalous westerly wind bursts in the tropical Pacific Ocean before and during the 1986-87 El Nino. Sea level time series along the equator show examples of both positive and negative anomalies of 10-centimeter amplitude and 2- to 4-week time scale propagating across the Pacific with phase speeds of 2.4 to 2.8 meters per second, suggesting downwelling and upwelling Kelvin waves, respectively. A comparison of island wind observations with sea level indicates one instance (May 1986) in which a positive sea level anomaly can be related to westerly winds caused by a cross-equatorial cyclone pair in the western Pacific. This episode was followed by additional wind bursts later in the year, and finally by sustained westerlies in the western Pacific during November-December 1986, at the height of El Nino. The Geosat observations reveal the sea level response to these meteorological events and provide a synoptic description of the El Nino oceanographic phenomenon. Author

A88-24654

FEATURES OF HYDROLOGICAL ANOMALIES IN CONNECTION WITH THE SEARCH FOR DEEP-WATER POLYMETALLIC SULFIDES [OSOBENNOSTI GIDROLOGICHESKIKH ANOMALII V SVIAZI S POISKAMI GLUBOKOVODNYKH POLIMETALLICHESKIKH SUL'FIDOV]
I. S. GRAMBERG, I. N. GORIAINOV, A. E. OVSIANNIKOV, and I. M. MIRCHINK (Severnoe Proizvodstvennoe Ob'edinenie po Morskim Geologorazvedochnym Rabotam, Leningrad, USSR) Akademiia Nauk SSSR, Doklady (ISSN 0002-3264), vol. 297, no. 4, 1987, p. 961-963. In Russian. refs

Data from the Eastern Pacific are used in an effort to develop a model for the structure and evolution of hydrological anomalies (HAs) connected with active hydrothermal sources on the ocean bottom. Two types of HAs are identified: (1) an extended plumage type whose roots are connected with the emergence of the source on the ocean bottom and (2) a successive 'free' eddy type with different time intervals between eddies. B.J.

A88-24655

SURFACE TEMPERATURE VARIATIONS OF THE WORLD OCEAN IN THE EOCENE [IZMENENIE TEMPERATUR POVERKHNOSTNYKH VODNYKH MASS MIROVOGO OKEANA V EOTSENE]

S. D. NIKOLAEV, N. S. BLIUM, and V. I. NIKOLAEV (Moskovskii Gosudarstvennyi Universitet; AN SSSR, Institut Geografii, Moscow, USSR) Akademiia Nauk SSSR, Doklady (ISSN 0002-3264), vol. 297, no. 4, 1987, p. 967-969. In Russian.

A88-24933

SYNTHETIC APERTURE RADAR IMAGERY OF RANGE TRAVELING OCEAN WAVES
KAZUO OUCHI (King's College, London, England) IEEE Transactions on Geoscience and Remote Sensing (ISSN 0196-2892), vol. 26, Jan. 1988, p. 30-37. SERC-supported research. refs

In synthetic-aperture radar (SAR) imagery of ocean waves, an image modulation by radar foreshortening exists in addition to backscatter radar cross sections. The foreshortening effect is due to surface-height differences making sections of a rough surface fall into different range bins than they would if the surface were flat. Since the degree of this modulation changes according to the local wave height, foreshortening alone could produce the image pattern corresponding to the wave field. The effect, termed range bunching, is maximum for range traveling ocean waves and vanishes for azimuth traveling waves. It also increases with decreasing radar look angle. The imaging processes of range traveling waves are investigated by taking account of both the cross section and range bunching. The SAR transfer function and image modulation functions are defined to describe the relative importance and the coupling effects of the two contributions. It is shown that in low to moderate sea states, where the major variation in backscatter arises from local surface tilt, the image modulation by the cross section is enhanced by range bunching and the effect increases with increasing wave slope and also with decreasing look angle. For ocean waves in high sea states with a small variation in the cross section and steep wave slopes, range bunching may become an important mechanism for the interpretation of the images formed by SAR with small look angles. I.E.

A88-24934* Stanford Univ., Calif.

OBSERVATION OF SEA-ICE DYNAMICS USING SYNTHETIC APERTURE RADAR IMAGES: AUTOMATED ANALYSIS
JOHN F. VESECKY, RAMIN SAMADANI, MARTHA P. SMITH, JASON M. DAIDA, and RONALD N. BRACEWELL (Stanford University, CA) IEEE Transactions on Geoscience and Remote Sensing (ISSN 0196-2892), vol. 26, Jan. 1988, p. 38-48. Navy-supported research. refs

(Contract NAGW-419)

The European Space Agency's ERS-1 satellite, as well as others planned to follow, is expected to carry synthetic-aperture radars (SARs) over the polar regions beginning in 1989. A key

component in utilization of these SAR data is an automated scheme for extracting the sea-ice velocity field from a time sequence of SAR images of the same geographical region. Two techniques for automated sea-ice tracking, image pyramid area correlation (hierarchical correlation) and feature tracking, are described. Each technique is applied to a pair of Seasat SAR sea-ice images. The results compare well with each other and with manually tracked estimates of the ice velocity. The advantages and disadvantages of these automated methods are pointed out. Using these ice velocity field estimates it is possible to construct one sea-ice image from the other member of the pair. Comparing the reconstructed image with the observed image, errors in the estimated velocity field can be recognized and a useful probable error display created automatically to accompany ice velocity estimates. It is suggested that this error display may be useful in segmenting the sea ice observed into regions that move as rigid plates of significant ice velocity shear and distortion. I.E.

A88-25289

SIZE DISTRIBUTIONS OF SEA-SOURCE AEROSOL PARTICLES - A PHYSICAL EXPLANATION OF OBSERVED NEARSHORE VERSUS OPEN-SEA DIFFERENCES

H. SIEVERING (Colorado, University, Denver; NOAA, Environmental Research Laboratories, Boulder, CO), J. BOATMAN, L. GUNTER, D. WELLMAN (NOAA, Environmental Research Laboratories, Boulder, CO), H. HORVATH (NOAA, Environmental Research Laboratories, Boulder, CO; Wien, Universitaet, Vienna, Austria) et al. *Journal of Geophysical Research* (ISSN 0148-0227), vol. 92, Dec. 20, 1987, p. 14850-14860. NOAA-supported research. refs

Log-normal size distribution fits to aerosol probe data collected by the NOAA's King Air aircraft were obtained by a new computer fitting routine. The average fit to western Atlantic nearshore data and open-sea data showed a marked difference in the volume geometric median diameter (VGMD) of the coarse-particle sea-salt mode. Analysis of seven separate near-shore flights during offshore flow showed the average VGMD to be 8.1 microns, with a geometric median standard deviation $\sigma(g)$ of 2.1. Six separate open-sea flights showed the average VGMD to be 5.6 microns, with a $\sigma(g)$ of 1.7. It is shown that atmospheric state conditions, near-shore versus open sea, could not have caused the significant difference between the nearshore and open-sea VGMD values. It is demonstrated that sea-derived aerosol size distributions nearshore may often be expected to have more large aerosol particles present than sea-derived aerosol distributions over the open sea. Author

A88-25445

SATELLITE-DERIVED COLOR-TEMPERATURE RELATIONSHIP IN THE ALBORAN SEA

ROBERT A. ARNONE (U.S. Navy, Naval Ocean Research and Development Activity, Bay Saint Louis, MS) *Remote Sensing of Environment* (ISSN 0034-4257), vol. 23, Dec. 1987, p. 417-437. Navy-supported research. refs

Improved understanding of biooptical responses to physical and chemical processes in the ocean can be obtained through the analyses of ocean color-temperature relationships using satellite data. These data can be used to trace the mixing of water masses along frontal zones and to suggest patterns of subsurface and horizontal advection. To illustrate this concept, the ocean color and sea surface temperature relationships in the Alboran Sea are derived from CZCS color and AVHRR sea-surface temperature (SST) data. Near-coincident (2.5 h) images are registered and converted into quantitative estimates of biooptical properties and SST. Water masses are classified based on unsupervised clustering analyses of these parameters. The classes appear to describe sequences of phytoplankton populations distributed along the Alboran Sea front and gyre. The color-SST signature is shown to provide a method to assess mixing between water masses. The water-mass classifications also appear to be associated with different biological and physical processes. Author

A88-25726

EL NINO EVENTS AND THEIR RELATION TO THE SOUTHERN OSCILLATION - 1925-1986

CLARA DESER and JOHN M. WALLACE (Washington, University, Seattle) *Journal of Geophysical Research* (ISSN 0148-0227), vol. 92, Dec. 15, 1987, p. 14189-14196. refs
(Contract NSF ATM-83-18853)

Relationships among sea surface temperatures (SSTs) at the coast of Peru and offshore, river discharge in northern Peru, and sea level pressure at Darwin, Australia, during the period 1925-1986 are investigated using time series plots, frequency distributions, and a simple statistical analysis. It is shown that SSTs undergo a larger seasonal cycle offshore than at the coast, exhibit more interannual variability during the warm than the cool season, are positively skewed during much of the year, and exhibit greatest month-to-month persistence during the cool season. Many, but not all, episodes of above normal coastal SSTs are accompanied by enhanced river discharge in northern Peru. Comparison of the Darwin pressure and coastal SST records during the past 60 years shows that El Nino events (episodes of above normal SSTs along the coast of Peru) have occurred both in advance of and subsequent to major negative swings of the Southern Oscillation (and associated climatic changes in the central equatorial Pacific). In addition, El Nino events and negative swings of the Southern Oscillation have occurred separately. Hence El Nino and the Southern Oscillation are more loosely coupled than other studies would imply. Author

A88-25727#

LONGITUDINAL VARIATIONS IN TROPICAL TROPOPAUSE PROPERTIES IN RELATION TO TROPICAL CONVECTION AND EL NINO-SOUTHERN OSCILLATION EVENTS

K. S. GAGE and G. C. REID (NOAA, Aeronomy Laboratory, Boulder, CO) *Journal of Geophysical Research* (ISSN 0148-0227), vol. 92, Dec. 15, 1987, p. 14197-14203. refs

The longitudinal variations in tropical tropopause properties that might be expected to accompany a zonally nonuniform distribution of convection in the equatorial zone were investigated, analyzing over 30 years of radiosonde temperature soundings from six tropical Pacific stations to obtain tropopause height and potential temperature. Both these parameters show a clear year-to-year variation in response to changes in tropical convection associated with El Nino-Southern Oscillation events, with the tropopause potential temperature being particularly sensitive to the longitude of major convective activity. It was found that the sense of the tropopause potential temperature difference between the two stations, Koror and Majuro, was consistent with the hypothesis that systematic increases in tropical tropopause temperature occur away from major centers of convection, provided the centers of active convection are found to the west of the station network during non-El Nino years and to the east of it during El Nino years. I.S.

A88-25728*

Research and Data Systems, Inc., Lanham, Md.
REMOTE SENSING OF WATER VAPOR CONVERGENCE, DEEP CONVECTION, AND PRECIPITATION OVER THE TROPICAL PACIFIC OCEAN DURING THE 1982-1983 EL NINO
PHILIP E. ARDANUY (Research and Data Systems Corp., Lanham, MD), PRABHAKARA CUDDAPAH, and H. LEE KYLE (NASA, Goddard Space Flight Center, Greenbelt, MD) *Journal of Geophysical Research* (ISSN 0148-0227), vol. 92, Dec. 15, 1987, p. 14204-14216. refs

Using data collected by SMMR on board the Nimbus 7 satellite, estimates of atmospheric water vapor were obtained over the tropical Pacific Ocean during the 1982-1983 El Nino. A parameterization that physically relates the synoptic and convective scales was employed, making it possible to explicitly resolve convective elements and rain cells for poorly resolvable measurements. The derived water vapor flux convergences were analyzed during the El Nino episode to map the inferred deep convection and estimated rainfall over regions impacted by the event, and the inferred monthly rainfall amounts were compared

with observations for 14 island and coastal stations in the Pacific Ocean. I.S.

A88-25729

SEA SURFACE TEMPERATURE, LOW-LEVEL MOISTURE, AND CONVECTION IN THE TROPICAL PACIFIC, 1982-1985

ELLEN J. STEINER and SIRI JODHA SINGH KHALSA (Colorado, University, Boulder) Journal of Geophysical Research (ISSN 0148-0227), vol. 92, Dec. 15, 1987, p. 14217-14224. NOAA-supported research. refs

The relationships between sea surface temperature (SST), low-level precipitable water (LLPW), and deep convection in the tropical Pacific are examined for the January 1982 through December 1985 period, using partially or wholly satellite-derived data, and these relationships are compared for El Nino Southern Oscillation (ENSO) and non-ENSO years. Monthly means of LLPW and highly reflective clouds (HRCs) were computed from daily data to correspond to the averaging period of SST. Maxima and minima of the three variables were found to be offset in both time and space; in the eastern equatorial Pacific, increases of SST and LLPW were found to precede the rises of HRC by one or more months. Variability of all three parameters in the eastern Pacific was dominated by the 1982-1983 ENSO and the seasonal cycle, whereas in the western and the central Pacific, the seasonal cycle of all parameters was weak. I.S.

A88-25731

AN INVESTIGATION OF THE EL NINO-SOUTHERN OSCILLATION CYCLE WITH STATISTICAL MODELS. I - PREDICTOR FIELD CHARACTERISTICS. II - MODEL RESULTS

NICHOLAS E. GRAHAM, JOEL MICHAELSEN (California, University, Santa Barbara), and TIM P. BARNETT (California, University, San Diego) Journal of Geophysical Research (ISSN 0148-0227), vol. 92, Dec. 15, 1987, p. 14251-14289. refs (Contract NSF ATM-85-13713; NOAA-NA-85AADAC132)

A combination of extended empirical orthogonal function (EEOF) analysis and canonical correlation analysis (CCA) was used to construct two sets of linear models for predicting equatorial Pacific sea surface temperatures (SSTs) from the Indo-Pacific trade wind field and the near-global sea level pressure (SLP) field. The EEOF analysis was used to compress and reexpress the predictor fields; it made it possible to predict temporal evolution of dominant modes in these fields. The CCA was used to calculate the SST forecast models and to highlight those aspects of the predictor fields that provide the observed model skill. The method was also applied in an analysis of the contemporaneous covariance between the two predictor fields. The details of model construction and the forecast modeling results are presented. The results provide insights into the development of anomalies in the wind and SLP fields through the El Nino Southern Oscillation period. I.S.

A88-25732

REMOTE FORCING OF SEA SURFACE TEMPERATURE IN THE EL NINO REGION

PABLO LAGOS, JOHN M. WALLACE, and TODD P. MITCHELL (Washington, University, Seattle) Journal of Geophysical Research (ISSN 0148-0227), vol. 92, Dec. 15, 1987, p. 14291-14296. refs (Contract NSF ATM-83-18853)

The relationship between oceanic Kelvin waves forced over the western equatorial Pacific and seasonal and nonseasonal sea surface temperature (SST) variability at the South American coast is investigated using harmonic dial analysis and lag correlation statistics. The seasonal cycle of coastal SST is adequately described by the first two harmonics and is very regular in both El Nino and non-El Nino years. In contrast, the seasonal cycle of zonal wind over the western equatorial Pacific varies from year to year and is dominated by years of large negative swings of the Southern Oscillation index. Hence it seems unlikely that the winds over the western equatorial Pacific contribute strongly to the seasonal cycle of coastal SST. For nonseasonal variability the winds with periods shorter than 15 months precede fluctuations in coastal SST by two to four months, consistent with the remote

forcing hypothesis, while for the lower frequencies the SST leads the winds by two to three months, similar to El Nino composite zonal winds of Rasmusson and Carpenter (1982). Author

A88-25733

A HEAT BUDGET FOR THE NORTHERN CALIFORNIA SHELF DURING CODE 2

STEVEN J. LENTZ (Woods Hole Oceanographic Institution, MA) Journal of Geophysical Research (ISSN 0148-0227), vol. 92, Dec. 15, 1987, p. 14491-14509. refs (Contract NSF OCE-84-17769)

The heat budget for the northern California shelf was investigated using moored current, water temperature, and meteorological observations made in the summer of 1982 during the second phase of the Coastal Ocean Dynamics Experiment (CODE 2). Two modes of alongshore heat flux variability were observed. The dominant mode, characterized by large equatorward heat fluxes over the outer shelf during the early part of the upwelling season, is associated with strong vertical shears in alongshore velocity in the vicinity of the upwelling front, which results in equatorward flow of the warm surface water relative to the colder deep water. The second mode, concentrated over the inner half of the shelf, is related to the wind such that poleward heat fluxes occur in the northern portion of the volume during periods of weak winds. I.S.

A88-25734

THE ICE THICKNESS DISTRIBUTION ACROSS THE ATLANTIC SECTOR OF THE ANTARCTIC OCEAN IN MIDWINTER

PETER WADHAMS (Cambridge, University, England), MANFRED A. LANGE (Alfred-Wegener-Institut fuer Polar- und Meeresforschung, Bremerhaven, Federal Republic of Germany), and STEPHEN F. ACKLEY (U.S. Army, Cold Regions Research and Engineering Laboratory, Hanover, NH) Journal of Geophysical Research (ISSN 0148-0227), vol. 92, Dec. 15, 1987, p. 14535-14552. NERC-supported research. refs (Contract NSF DPP-85-12728)

A88-25736

SIMULTANEITY OF RESPONSE OF ATLANTIC OCEAN TROPICAL CYCLONES AND INDIAN MONSOONS

PAUL HANDLER and BRIDGET O'NEILL (Illinois, University, Urbana) Journal of Geophysical Research (ISSN 0148-0227), vol. 92, Dec. 15, 1987, p. 14621-14630. Research supported by the University of Illinois.

The degree of correlation between two seasonal climate events, namely, the frequency of tropical cyclones in the north Atlantic and the Indian summer monsoon precipitation, was determined using data available for two time series for the Indian monsoon (1871-1986 and 1875-1984) and for the tropical cyclones between the years of 1871 and 1985. Using several analytical methods to show the simultaneity of the climate events in these two regions separated by about 180 deg longitude, it is demonstrated that the events correlate with a significance greater than 99.75 percent and that there is little chance that this correlation is due to random events. Noting a correlation between the two climatic events and the presence of reported volcanic aerosols in the stratosphere, it is hypothesized that the causal element of the observed simultaneity of the Atlantic Ocean tropical cyclones and the Indian monsoons is the presence of low-latitude volcanic aerosols. I.S.

A88-25737

ON THE PARAMETERIZATION OF IRRADIANCE FOR OPEN OCEAN PHOTOPROCESSES

DAVID A. SIEGEL and T. D. DICKEY (Southern California, University, Los Angeles, CA) Journal of Geophysical Research (ISSN 0148-0227), vol. 92, Dec. 15, 1987, p. 14648-14662. Navy-supported research. refs

Using data on downwelling spectral radiance taken in the eastern North Pacific Ocean during the Optical Dynamics Experiment in the fall of 1982, vertical profiles were constructed for downwelling irradiance of visible energy (400-700nm) and photosynthetic available radiation (PAR). The profiles, which

indicate that the attenuation of visible energy and PAR are primarily dependent upon chlorophyll pigment concentration and depth, did not agree with the results of commonly used parameterization methods for radiant fluxes and their attenuation. Therefore, a new parameterization method was developed for the estimation of open ocean in situ radiant fluxes, which produced results that agreed with the observations. The method assumes that chlorophyll pigments and pure seawater control the attenuation of spectral irradiance and that the downwelling radiant fluxes just beneath the sea surface are directly proportional to the incident solar flux. I.S.

A88-25738

MULTIYEAR SEA ICE FLOE DISTRIBUTION IN THE CANADIAN ARCTIC OCEAN

RICK D. HUDSON (Polar Tech, Ltd., Sidney, Canada) *Journal of Geophysical Research* (ISSN 0148-0227), vol. 92, Dec. 15, 1987, p. 14663-14669. Research supported by Gulf Canada Resources, Ltd. refs

A88-26065

THE ROLE OF SYNOPTIC SCALE PROCESSES IN THE TRANSFER OF SEA SURFACE TEMPERATURE ANOMALIES [O ROLI PROTSESSOV SINOPTICHESKOGO MASSHTABA V PERENOSIE ANOMALII TEMPERATURY POVERKHNOSTI OKEANA]

L. I. PITERBARG and S. V. SEMOVSKII (AN SSSR, Institut Okeanologii, Moscow, USSR) *Meteorologiya i Gidrologiya* (ISSN 0130-2906), Jan. 1988, p. 126-130. In Russian. refs

A method of estimating the contribution of synoptic processes to the transfer of anomalous heat is described. The proposed procedure is used to analyze data on the sea surface temperature in the Kuroshio region. Frequency spectra are presented for the meridional component of the anomalous heat advection rate. K.K.

A88-26099

OBSERVATIONS OF OCEAN AND SEA BOTTOM RELIEF FROM SPACE [NABLIUDENIYA REL' EFA DNA MOREI I OKEANOV IZ KOSMOSA]

A. LAZAREV, V. KOVALENOK, T. DAMINOVA, and CH. VILLMANN (AN ESSR, Institut Astrofiziki i Fiziki Atmosfery, Tartu, Estonian SSR; Gosudarstvennyi Opticheskii Institut, Leningrad, USSR) *Eesti NSV Teaduste Akadeemia Toimetised, Füüsika-Matemaatika* (ISSN 0367-1429), vol. 36, no. 4, 1987, p. 398-404. In Russian.

Visual observations of the bottom relief of the open ocean made by cosmonauts aboard the Salyut-6 orbital station are analyzed. Under certain conditions, it is possible to study the bottom relief at a depth of 100 meters. It is shown that agitation of the ocean does not significantly affect the possibility of observing submerged objects and formations whose angular dimensions exceed the resolving power of the cosmonaut's visual system. K.K.

A88-26131

SEA ICE AND SEA-SURFACE TEMPERATURES IN THE STRAIT OF FRAM ACCORDING TO NOAA-AVHRR DATA [GLACES DE MER ET TEMPERATURES DE SURFACE DE LA MER DANS LE DETROIT DE FRAM D'APRES LES DONNEES NOAA-AVHRR]

CL. KEROMARD (Lille I, Université, Villeneuve-d'Ascq, France) *Photo Interpretation* (ISSN 0031-8523), vol. 25, Nov.-Dec. 1986, p. 39-43, 45-49, 51, 52. In French, English, and Spanish.

NOAA-AVHRR data obtained during the 1984 MIZEX experiment are used to study the sea ice and sea-surface temperatures in the Strait of Fram. The data reveal four types of ice formations: (1) fixed land ice; (2) rounded floes in the continuous and relatively uniform polar pack ice; (3) small concentrations of ice between the polar pack ice the sea ice; and (4) denser pack ice consisting of large floes encased in a matrix of small floes. The distribution of sea surface temperatures reveals eddy dynamics which can be explained by the shearing between the eastern Greenland current

and the western Spitsbergen current, which run parallel to each other but in opposite directions. R.R.

A88-26149

THE LEGAL PROBLEMS OF THE COMMERCIALIZATION OF SATELLITE REMOTE SENSING [PROBLEMY PRAWNE KOMERCJALIZACJI TELEDETEKCJI SATELITARNEJ]

JERZY RZYMANEK (Instytut Prawa Międzynarodowego, Warsaw, Poland) *Postępy Astronautyki* (ISSN 0373-5982), vol. 20, no. 1-2, 1987, p. 129-143. In Polish. refs

The advent of remote sensing commercialization is discussed with attention given to the launching of the SPOT-1 satellite and the establishment of a company responsible for marketing its imagery. SPOT activity is examined within the framework of remote sensing principles approved by the Committee on the Peaceful Uses of Outer Space. K.K.

A88-26346

DIGITIZED GLOBAL LAND-SEA MAP AND ACCESS SOFTWARE

C. K. SHUM, B. E. SCHUTZ, J. C. RIES, and B. D. TAPLEY (Texas, University, Austin) *Bulletin Geodesique* (ISSN 0007-4632), vol. 61, no. 4, 1987, p. 311-317.

A computer-efficient global data file, which contains digitized information that enables identification of a given latitude/longitude defined point as being over land or over water, was generated from a data base which defines the world's shoreline. The method used in the generation of this land-sea boundary data map and its data structure are discussed. The land-sea boundary map also includes information on islands and inland lakes. The resolution of this map is 5 x 5 arcmin or an equivalent of 9 km square surface blocks at the equator. The software to access this data base is structured to be easily transportable to different computers. This data base was used in the generation of the Seasat Geophysical Data Record to identify whether a spaceborne radar altimeter measurement was over-land or over-ocean. Author

A88-26676

ON THE PROBLEM OF EVOLUTION OF OCEANIC WATER COMPOSITION IN THE PHANEROZOIC [K PROBLEME EVOLIUTSII SOSTAVA OKEANICHESKOI VODY V FANEROZOE]

V. M. KOVALEVICH (AN USSR, Institut Geologii i Geokhimii Goriuchikh Iskopaemykh, Lvov, Ukrainian SSR) *Geokhimiya* (ISSN 0016-7525), Nov. 1987, p. 1527-1536. In Russian. refs

Compositional changes undergone by oceanic waters during the Phanerozoic are examined on the basis of data published on the age-related changes during the Phanerozoic in the halogen salts of the sediments and brine of ancient basins, including the Eastern Siberian, Dnepr-Donets, Eastern European, Preddobrudzh, Erevan', and Cis-Carpathian basins. It is shown that the evolution of halogenesis during the phanerozoic proceeded in parallel with evolutionary changes in the composition of the sedimentary earth crust, atmosphere, and oceanic water. It is suggested that the primary cause of the changes in the composition of ocean water was the change in the intensity of volcanism (and thus of CO₂ generation). Related to the degree of volcanism are also changes in the ocean level, water temperature, climate, biogenic processes, the composition of the atmosphere, and the degree of erosion, which all contributed to the evolution of the ocean water composition. I.S.

A88-26911*# National Aeronautics and Space Administration. Goddard Space Flight Center, Greenbelt, Md.

AIRBORNE MEASUREMENTS OF SURFACE LAYER TURBULENCE OVER THE OCEAN DURING COLD AIR OUTBREAKS

SHU-SHIEN CHOU and EUENG-NAN YEH (NASA, Goddard Space Flight Center, Greenbelt, MD) *Journal of the Atmospheric Sciences* (ISSN 0022-4928), vol. 44, Dec. 15, 1987, p. 3721-3733. refs

The spectral characteristics of surface layer turbulence for the near-shore cloud street regions over the Atlantic Ocean were examined using 50-m level data of airborne measurements of

atmospheric turbulence spectra above the western Atlantic Ocean during cold air outbreaks. The present study, performed for the Mesoscale Air-Sea Exchange (MASEX) experiment, extends and completes the preliminary analyses of Chou and Yeh (1987). In the inertial subrange, a near 4/3 ratio was observed between velocity spectra normal to and those along the aircraft heading. A comparison of the turbulent kinetic energy budgets with those of Wyngaard and Cote (1971) and Caughey and Wyngaard (1979) data indicates that the turbulent kinetic energy in the surface layer is dissipated less in the MASEX data than in data obtained by the previous groups. I.S.

A88-26923

ON THE EVOLUTION OF THE SOUTHERN OSCILLATION

KEVIN E. TRENBERTH and DENNIS J. SHEA (National Center for Atmospheric Research, Boulder, CO) Monthly Weather Review (ISSN 0027-0644), vol. 115, Dec. 1987, p. 3078-3096. refs

The evolution of the Southern Oscillation (SO) is examined in the time domain for the post-1941 period by computing lagged cross correlations between sea level pressures at Darwin and sea level or surface pressures at selected stations. The dominant pattern reveals the two poles of the traditional standing oscillation or seesaw of the SO, with centers of opposite sign over Indonesia and the central South Pacific Ocean. There are significant phase variations within each center and clear indications that changes over the South Pacific lead the opposite changes in the Indonesian pole by one to two seasons. For the post-1950 period, the SO was dominated by a three-six year quasi-periodicity which leads to ambiguity in interpreting phase relationships. The importance of the tendency for changes over the South Pacific to lead the SO lies in the probable role of associated processes in setting up tropical SST anomalies, especially during the onset stage of El Nino events. C.D.

A88-27010#

SATELLITE OBSERVATIONS OF A WESTERN BOUNDARY CURRENT IN THE BAY OF BENGAL

RICHARD LEGECKIS (NOAA, National Environmental Satellite Data Information Service, Washington, DC) Journal of Geophysical Research (ISSN 0148-0227), vol. 92, Nov. 15, 1987, p. 12974-12978, 13199, 13200. refs

Satellite infrared observations of the Bay of Bengal during the latter part of February 1985 reveal the existence of two bands of warm water that resemble western boundary currents along the east coasts of India and Sri Lanka. A recently formed elliptical warm core eddy, with a major axis of nearly 150 km, appears at longitude 90 deg E and latitude 19 deg N at the end of the axis of the current. Color infrared images of sea surface temperature are used to illustrate the sea surface temperature patterns and to estimate their displacements with time. Author

A88-27011

COASTAL UPWELLING AND EDDY DEVELOPMENT OFF NOVA SCOTIA

BRIAN PETRIE, BRENDA J. TOPLISS, and DANIEL G. WRIGHT (Bedford Institute of Oceanography, Dartmouth, Canada) Journal of Geophysical Research (ISSN 0148-0227), vol. 92, Nov. 15, 1987, p. 12979-12991, 13201, 13202. refs

The time of appearance, the broadening rate, and the bottom temperature evolution of a band of cool water observed in satellite photographs along the seaward coast of Nova Scotia during a month-long upwelling period are in agreement with an idealized two-layer model of the wind-driven shelf circulation. The results obtained suggest that the wavelike features observed are primarily the result of baroclinic instability of the upwelling-associated base state; estimates suggest that both upwelling and subsequent eddy development are important factors in supplying nutrients to the surface waters of the shelf. O.C.

A88-27012

PROCESSING AND ANALYSIS OF LARGE VOLUMES OF SATELLITE-DERIVED THERMAL INFRARED DATA

PETER CORNILLON, CRAIG GILMAN (Rhode Island, University,

Narragansett), LOTHAR STRAMMA (Kiel, Universitaet, Federal Republic of Germany), OTIS BROWN, ROBERT EVANS (Miami, University, FL) et al. Journal of Geophysical Research (ISSN 0148-0227), vol. 92, Nov. 15, 1987, p. 12993-13002, 13203, 13204. refs

(Contract N00014-81-C-0062; NSF OCE-85-10828)

Preprocessing and data reduction steps are proposed for the application of TIROS-N AVHRR-derived data to regional physical oceanographic studies. The preprocessing procedure can reduce the data volume/satellite pass by over 98 percent for full-resolution data; the output is a set of sea surface temperature fields covering about 2000 x 4000 km. The data reduction procedure reduces the number of such fields to a set that is manageable from the analyst's perspective by compositing the data into 1- or 2-day groups. Mean Gulf Stream position and meandering envelope, and its cold core ring trajectories, are typical of the phenomena addressed by these procedures. O.C.

A88-27013

SHELF WATER ENTRAINMENT BY GULF STREAM WARM-CORE RINGS

NEWELL GARFIELD, III (Rhode Island, University, Kingston) and DAVID L. EVANS (U.S. Navy, Office of Naval Research, Arlington, VA) Journal of Geophysical Research (ISSN 0148-0227), vol. 92, Nov. 15, 1987, p. 13003-13012, 13205. Research sponsored by the University of Rhode Island, NSF, and U.S. Navy. refs

Seven years of AVHRR imagery indicate that shelf water removal by entrainment adjacent to Gulf Stream warm core rings is a common occurrence that is important for shelf water budgets; these data also indicate little mean seasonal variability, but substantial interannual variability, in streamer occurrences south of the Georges Bank. Streamers may be incorporated into the warm core ring or detrained from the ring, with either the formation of cold cyclonic rings in the slope water or entrainment into the northern edge of the Gulf Stream. O.C.

A88-27014* Washington Univ., Seattle.

SATELLITE PASSIVE MICROWAVE STUDIES OF THE SEA OF OKHOTSK ICE COVER AND ITS RELATION TO OCEANIC PROCESSES, 1978-1982

MICHAEL A. ALFULTIS and SEELYE MARTIN (Washington, University, Seattle) Journal of Geophysical Research (ISSN 0148-0227), vol. 92, Nov. 15, 1987, p. 13013-13028, 13207-13209. refs

(Contract NR PROJECT 083-012; N00014-84-C-0111; NAGW-700; NAGW-1045)

A88-27015* Alaska Univ., Fairbanks.

MULTIPLE DIPOLE EDDIES IN THE ALASKA COASTAL CURRENT DETECTED WITH LANDSAT THEMATIC MAPPER DATA

KRISTINA AHLNAS, THOMAS C. ROYER, and THOMAS H. GEORGE (Alaska, University, Fairbanks) Journal of Geophysical Research (ISSN 0148-0227), vol. 92, Nov. 15, 1987, p. 13041-13047, 13213, 13214. refs

(Contract NAS5--28762)

Seventeen dipole eddies, including five large, well-formed ones, three second-generation eddies, and two double eddies, were observed in the Alaska Coastal Current near Kayak Island in one single scene of the Landsat thematic mapper (TM) on April 22, 1985. The digital Landsat TM satellite data were computer analyzed to extract details in the near coastal circulation in the northern Gulf of Alaska. Enhancement techniques were applied to the visible and thermal IR bands. The features are evident only in the visible bands because of the ability of these bands to detect the distribution of sediments in the near surface. These eddies did not have a significant thermal signature. The sources of these sediments are the glacial streams found throughout the Gulf of Alaska coast. Eddies of this configuration and frequency have never been observed here previously. However, the oceanographic and meteorological conditions are typical for this time of year. These eddies should be important to the cross-shelf mixing processes in

the Alaska Coastal Current and are an indicator that the flow here can be unstable at certain times of the year. Author

A88-27016* Scripps Institution of Oceanography, La Jolla, Calif.
THE ONSET OF SPRING MELT IN FIRST-YEAR ICE REGIONS OF THE ARCTIC AS DETERMINED FROM SCANNING MULTICHANNEL MICROWAVE RADIOMETER DATA FOR 1979 AND 1980

MARK R. ANDERSON (California, University, Scripps Institution of Oceanography, La Jolla) Journal of Geophysical Research (ISSN 0148-0227), vol. 92, Nov. 15, 1987, p. 13153-13163. refs (Contract NSF DPP-82-17265; NAGW-363; NAG2-36; NAG1-028)

A88-27036
REMANENT MAGNETIZATION OF THE OCEANIC UPPER MANTLE

JAFAR ARKANI-HAMED (Brock University, Saint Catharines, Canada) Geophysical Research Letters (ISSN 0094-8276), vol. 15, Jan. 1988, p. 48-51. refs (Contract NSERC-A-2037)

Skewnesses of the marine and Magsat magnetic anomalies of the Atlantic Ocean are explained in terms of the remanent magnetization gradually acquired by the oceanic lithosphere during its cooling. Magnetizations of the lower crust and the upper mantle are about 20-50 and 10-30 percent of the magnetization of the oceanic basaltic layer 2A, respectively. The oceanic upper mantle controls the skewness of the Magsat anomalies, whereas the skewness of the marine anomalies arise primarily from the oceanic lower crust. Author

A88-27201
INTERPRETATION OF THE VISIBLE MANIFESTATIONS OF SEA WATER DYNAMICS FROM SPACE IMAGERS OF THE CASPIAN SEA [INTERPRETATSIYA VIDIMYKH PROIYAVLENIY DINAMIKI VOD PO KOSMICHESKIM SNIMKAM KASPIISKOGO MORIA]

V. I. KRAVTSOVA and V. V. TARAKANCHIKOV (Moskovskii Gosudarstvennyi Universitet, Moscow, USSR) Issledovanie Zemli iz Kosmosa (ISSN 0205-9614), Sept.-Oct. 1987, p. 3-13. In Russian. refs

The dynamics of Caspian Sea waters was investigated by analyzing a series of 16 scanner images (on 1:5,000,000 and 1:12,000,000 scale) obtained by the Meteor-30 satellite during the spring and summer of 1983 and 1984. The resulting maps show frontal zones and confluence fronts in the northern Caspian Sea, upwelling frontal zones off its eastern shore, mushroom-like currents, eddies, and internal waves. The interpretation of these phenomena depended on {1} contrasts resulting from varying concentrations of sea-water suspensions and {2} differences in sea-surface roughness. I.S.

A88-27202
INVESTIGATING THE NORTHERN CASPIAN SEA ICE REGIME FROM METEOROLOGICAL-SATELLITE DATA [IZUCHENIE LEDOVOGO REZHIMA SEVERNOGO KASPIIA PO DANNYM METEOROLOGICHESKIKH SPUTNIKOV ZEMLI]

G. F. KRASNOZHON and K. S. LIUBOMIROVA (AN SSSR, Institut Vodnykh Problem, Moscow, USSR) Issledovanie Zemli iz Kosmosa (ISSN 0205-9614), Sept.-Oct. 1987, p. 14-17. In Russian.

A88-27203
THE RELATIONSHIP BETWEEN THE TEMPORAL VARIABILITY OF OCEAN TEMPERATURE AND THE MERIDIONAL SHIFTS OF THE INTERTROPICAL CONVERGENCE ZONE [VZAIMOSVIAZ' VREMENNOI IZMENCHIVOSTI TEMPERATURY OKEANA S MERIDIONAL'NYMI BLUZHDAIAMI VNUTRITROPICHESKOI ZONY KONVERGENTSII]

G. S. DVORIANINOV, A. V. PRUSOV, and M. V. SHOKUROV (AN USSR, Morskoi Gidrofizicheskii Institut, Sevastopol, Ukrainian SSR) Issledovanie Zemli iz Kosmosa (ISSN 0205-9614), Sept.-Oct. 1987, p. 18-24. In Russian. refs

The relationship between meridional shifts of the intertropical

convergence zone (ITCZ) and anomalies in sea-surface temperature (SST) was investigated using Meteosat data on ITCZ position and on monthly averaged SSTs of a near-equatorial zone (between 2 S and 2 N) of the Atlantic Ocean obtained for the period between 1974 and 1984. Spectral analysis of these data disclosed the presence of an interannual variation in the behaviors of both the meridional ITCZ shifts and the ocean temperature anomalies. Both types of variations had a quasi-two-year cyclic pattern and were interrelated. It is suggested that this relationship can be utilized for estimating SST variability from data on ITCZ shifts. I.S.

A88-27204
CALCULATIONS OF OCEAN-ATMOSPHERE RADIANCE ON THE BASIS OF REMOTE SENSING [K RASCHETU IARKOSTI SISTEMY OKEAN-ATMOSFERA PRI DISTANTSIONNOM ZONDIROVANII]

I. M. LEVIN, T. M. RADOMYSLSKAIA, and K. S. SHIFRIN (AN SSSR, Institut Okeanologii, Leningrad, USSR) Issledovanie Zemli iz Kosmosa (ISSN 0205-9614), Sept.-Oct. 1987, p. 25-29. In Russian. refs

Errors that can result from the use of well-known expressions for calculating the sea surface radiance using total radiance figures, obtained for the ocean-atmosphere system by remote sensing, are discussed, and some modifications for these formulas are suggested. The equation of Sobolev (1956) for atmospheric haze radiance is modified with due regard to different sea-surface albedos for direct and scattered light. In the equations for the radiance reflected from sea surface and that emerging from the sea, the surface reflection anisotropy and multiple scattering in the atmosphere are taken into account. I.S.

A88-27205
VARIATIONS IN THE INTENSITY OF EMITTED AND SCATTERED MICROWAVE RADIATION OF THE SEA SURFACE SENSED AT GRAZING ANGLES IN A FIELD OF SURFACE MANIFESTATIONS OF INTERNAL WAVES [VARIATSIY INTENSIVNOSTI SOBSTVENNOGO I RASSEIANNOGO SVCH-IZLUCHENIYA PRI NASTIL'NYKH UGLAKH ZONDIROVANIYA OKEANA V POLE POVERKHNOSTNYKH PROIYAVLENIY VNUTRENNIKH VOLN]

V. B. VENSLAVSKII, V. E. GERSHENZON, V. K. GROMOV, S. S. SEMENOV, Z. E. ENTIN (AN SSSR, Institut Kosmicheskikh Issledovaniy, Moscow, USSR) et al. Issledovanie Zemli iz Kosmosa (ISSN 0205-9614), Sept.-Oct. 1987, p. 30-34. In Russian. refs

Data on variations in microwave emission of and microwave scattering by the sea surface, induced by internal wave activity, were obtained with an experimental vessel for three Pacific Ocean zones of internal wave generation: the Nintoku Mountain (at a depth of 950 m), the Makarov Mountain (1300 m), and the Ramapo shoal (85-90 m). Internal waves were registered by an automatic thermoprofilograph pulled in tow or by distributed temperature sensors. The intensity of microwave radiation from the sea surface was measured using a system which included two radiometers and a radiometer-scatterometer (operating at a 78-deg angle) installed on a hydrostabilized platform. Data showing relationships between variations of the emitted and scattered microwave radiation at different conditions of sea turbulence and wind speed at these locations are presented. I.S.

A88-27209
CHOOSING CONDITIONS FOR THE REMOTE SENSING OF OCEAN FEATURES IN THE VISIBLE SPECTRUM, WITH THE EFFECT OF COASTAL ZONE TAKEN INTO ACCOUNT [VYBOR USLOVIIY DISTANTSIONNOGO ZONDIROVANIYA OKEANICHESKIKH OBRAZOVANIY V VIDIMOY OBLASTI SPEKTRA S UCHETOM EFFEKTA BEREGOVOY ZONY]

A. B. KARASEV, S. V. PANTIUKHOV, and V. G. SLASHCHEV (Moskovskii Fiziko-Tekhnicheskii Institut, Moscow, USSR) Issledovanie Zemli iz Kosmosa (ISSN 0205-9614), Sept.-Oct. 1987, p. 56-65. In Russian. refs

The process of selecting optimal conditions for the observation of ocean surface features is discussed, using, as an example, the

results of an analysis of a numerical model for the remote sensing of phytoplankton pigments and river-mud suspensions in the coastal zone. The effects of these two factors on the localization of eddies and internal ocean waves are demonstrated. The analysis takes into account the optical properties of the earth surface, the state of the atmosphere, and the instrumentation parameters. I.S.

A88-27210

THE EFFICIENCY OF POLARIZATION MEASUREMENTS IN PASSIVE REMOTE SENSING OF THE OCEAN IN THE VISIBLE SPECTRUM [OB EFFEKTIVNOSTI POLIARIZATSIONNYYKH IZMERENII PRI PASSIVNOM DISTANTSIONNOM ZONDIROVANII OKEANA V VIDIMOI OBLASTI SPEKTRA]

A. P. VASIL'KOV, T. V. KONDRANIN, and N. A. KROTKOV (AN SSSR, Institut Okeanologii; Moskovskii Fiziko-Tekhnicheskii Institut, Moscow, USSR) Issledovanie Zemli iz Kosmosa (ISSN 0205-9614), Sept.-Oct. 1987, p. 66-74. In Russian. refs

The effects of the atmosphere and the sea surface conditions on the polarization characteristics of visible radiation scattered from the ocean-atmosphere system were investigated for different observation conditions. It is shown that the degree of polarization of the upward Brewster radiation follows a nonmonotonic function of height above sea-level and depends upon the angles of sighting, the position of the sun, and the radiation wavelength. The conditions at which the use of a polarizer for remote sensing yields best signal-to-noise results are discussed. I.S.

A88-27213

COMPUTER-AIDED MAPPING OF ANTARCTIC SEA ICE USING ALONG-THE-COURSE RADIOMETRIC MEASUREMENTS ABOARD THE COSMOS-1500 SATELLITE

[AVTOMATIZIROVANNOE POSTROENIE KART MORSKIKH L'DOV IUZHNOGO OKEANA PO DANNYM TRASSOVYKH RADIOMETRICHESKIKH IZMERENII S ISZ 'KOSMOS-1500']

P. A. NIKITIN, I. U. G. SPIRIDONOV, and N. B. TRAPEZNIKOVA (Gosudarstvennyi Nauchno-Issledovatel'skii Tsentr Izucheniia Prirodnykh Resursov, Moscow, USSR) Issledovanie Zemli iz Kosmosa (ISSN 0205-9614), Sept.-Oct. 1987, p. 92-98. In Russian. refs

A88-27492

SPRAY DROPLET GENERATION, TRANSPORT, AND EVAPORATION IN A WIND WAVE TUNNEL DURING THE HUMIDITY EXCHANGE OVER THE SEA EXPERIMENTS IN THE SIMULATION TUNNEL

PATRICE MESTAYER and CLAUDE LEFAUCCONNIER (CNRS; Aix-Marseille II, Universite, Marseille, France) Journal of Geophysical Research (ISSN 0148-0227), vol. 93, Jan. 15, 1988, p. 572-586. CNRS-NATO-Navy-supported research. refs

The processes of spray droplet generation, transport, and evaporation in a wind tunnel were studied, as part of the Humidity Exchange Over the Sea (HEXOS) program experiments. In order to study separately the generation of droplets, their transport and diffusion by turbulence, their evaporation, and their deposition, an experimental setup was designed in which spray droplets were generated by the bursting of bubbles produced by aeration devices immersed in the water tank of a large air-sea interaction simulation tunnel. Numerical modeling was carried out using a subprogram of HEXOS, HEXIST, which focuses on the effects of spray droplet transport and evaporation. The governing equations of the program HEXIST are presented together with the results of the feasibility experiments. I.S.

A88-27493

DOWNWARD LONGWAVE IRRADIANCE AT THE OCEAN SURFACE FROM SATELLITE DATA - METHODOLOGY AND IN SITU VALIDATION

ROBERT FROUIN, CATHERINE GAUTIER (California, University, La Jolla), and JEAN-JACQUES MORCRETTE (National Center for Atmospheric Research, Boulder, CO) Journal of Geophysical Research (ISSN 0148-0227), vol. 93, Jan. 15, 1988, p. 597-619. refs

(Contract N00014-80-C-0440; N00014-85-C-0140)

The paper presents a radiative transfer model for estimating downward longwave irradiance at the ocean surface from satellite radiance data. The model is based on the Morcrette et al. (1986) routine for global circulation models. Temperature and water vapor mixing ratio were obtained from NOAA Tiros operational vertical sounder data, while cloud parameters were retrieved from GOES visible and infrared spin scan radiometer data. Satellite-derived irradiances were compared to those measured in situ during the Mixed Layer Dynamic Experiment, with the results indicating a similarity between the estimated and the measured values, with the estimate errors corresponding to 6 to 8 percent of the measured ones. I.S.

A88-27494

THE NATAL PULSE - AN EXTREME TRANSIENT ON THE AGULHAS CURRENT

J. R. E. LUTJEHARMS and H. R. ROBERTS (Council for Scientific and Industrial Research, National Research Institute for Oceanology, Stellenbosch, Republic of South Africa) Journal of Geophysical Research (ISSN 0148-0227), vol. 93, Jan. 15, 1988, p. 631-645. refs

An analysis of satellite data collected over a period of nine years as well as historic hydrographic data show that the northern Agulhas Current is subject to large, intermittent, and solitary meanders. These transient events, collectively named the Natal pulse, progress downstream at consistent rates of 21 cm/s. Upon reaching the area where the shelf broadens, their rate of progression slackens to 5 cm/s. They are present in some stages of development at least 17 percent of the time, extend offshore by about 170 km on average, and show a continuous lateral growth on moving downstream. With few exceptions, the pulses are spawned as cold core, cyclonic, trapped lee eddies in the Natal Bight. They are held responsible for the intermittent coastal counter currents observed inshore of the Agulhas Current along the southern African coast and may play a crucial role in sediment distribution of the shelf. Author

A88-27495

MARINE BOUNDARY LAYER MODIFICATION ACROSS THE EDGE OF THE AGULHAS CURRENT

MARK JURY (Cape Town, University, Rondebosch, Republic of South Africa) and NAN WALKER (Council for Scientific and Industrial Research, National Research Institute for Oceanology, Stellenbosch, Republic of South Africa) Journal of Geophysical Research (ISSN 0148-0227), vol. 93, Jan. 15, 1988, p. 647-654. Research supported by the Council for Scientific and Industrial Research and Sea Fisheries Research Institute. refs

Aerial survey results are presented which show a modification of the lower atmosphere on crossing the edge of the Agulhas Current near 37 deg S, 20 deg E. Profiles of air temperature and dewpoint show increases in marine boundary layer heights of about 400 m, as sea surface temperatures rise suddenly from 18 to 24 C. Westerly winds increase across the NE-SW aligned sea surface temperature front by 7 m/s, in a sea breeze-like circulation. Surface latent and sensible heat fluxes to the atmosphere change from 100 W/sq m to 340 W/sq m on entering the Agulhas Current because of feedback processes between warmer sea surface temperatures, turbulence, and wind stress. The data sample is small and statistically limited, but the case study results indicate that the response of the lower atmosphere to the Agulhas Current is similar to that found over the Gulf Stream and other warm western boundary currents. Author

A88-27812* Jet Propulsion Lab., California Inst. of Tech., Pasadena.

SATELLITE OBSERVATION OF ATMOSPHERE AND SURFACE INTERACTION PARAMETERS

MOUSTAFA T. CHAHINE, ROBERT D. HASKINS (California Institute of Technology, Jet Propulsion Laboratory, Pasadena), JOEL SUSSKIND, and DENNIS REUTER (NASA, Goddard Space Flight Center, Greenbelt, MD) (COSPAR, WMO, URSI, et al., Plenary Meeting, 26th, Symposium 3, Workshop V, and Topical

Meeting A2 on Remote Sensing from Space, Toulouse, France, June 30-July 11, 1986) *Advances in Space Research* (ISSN 0273-1177), vol. 7, no. 11, 1987, p. 111-117, 119. refs

Atmosphere and ocean surface parameters are being derived from weather satellite data acquired by the High Resolution Infrared Sounder and the Microwave Sounding Unit. In this paper, the global distribution and accuracy of the derived parameters are described, and the satellite-derived skin surface temperature is compared with available shelter temperature. Seasonal and interannual changes are examined to study the response time of large-scale atmospheric changes to changes in surface conditions. C.D.

A88-27837

RADAR ALTIMETER DATA QUALITY FLAGGING

S. W. LAXON and C. G. RAPLEY (London, University College, Dorking, England) (COSPAR, WMO, URSI, et al., Plenary Meeting, 26th, Symposium 3, Workshop V, and Topical Meeting A2 on Remote Sensing from Space, Toulouse, France, June 30-July 11, 1986) *Advances in Space Research* (ISSN 0273-1177), vol. 7, no. 11, 1987, p. 315-318. refs

The Seasat radar altimeter was designed to provide precise and accurate surface height measurements over the ocean. These data have been used in studies of the ocean geoid, tides, and currents. Several factors can affect the quality of the height measurements produced by the on-board processor. In particular, radar returns with time profiles which depart from a standard form can introduce significant errors. These arise over very calm seas, over rain cells or when sea ice or land are present within the altimeter footprint. Blunder point algorithms are used in the ground processing to flag outlying data points, but these fail to identify some of the anomalies that are observed. An alternative method for flagging poor quality data using a simple algorithm based on pulse shape is presented. It is demonstrated that the algorithm provides a sensitive means of editing altimeter ocean data. Furthermore, changes in surface type, such as transitions between open water and sea ice can be accurately located. Author

A88-27838

SWATH ALTIMETRY OF OCEANS AND TERRAIN

C. G. RAPLEY (London, University College, Dorking, England) and H. D. GRIFFITHS (University College, London, England) (COSPAR, WMO, URSI, et al., Plenary Meeting, 26th, Symposium 3, Workshop V, and Topical Meeting A2 on Remote Sensing from Space, Toulouse, France, June 30-July 11, 1986) *Advances in Space Research* (ISSN 0273-1177), vol. 7, no. 11, 1987, p. 319-322. refs

(Contract ESA-6001/84/NL/BI)

Satellite radar altimeters have demonstrated a wide range of scientific capabilities over oceans and ice, and have considerable potential over land and inland water. However, the universal adoption of the single-beam, pulse-limited mode of operation limits the spatial and temporal sampling achievable and makes the generation of surface elevation maps critically dependent on the accuracy of the satellite orbit reconstruction. Also, over topographic surfaces, the data can be difficult, sometimes impossible, to interpret. With the advent of the Columbus polar platform, previous limitations on the size and complexity of space instruments will not apply. What types of swath altimeter might take advantage of this possibility are considered, and it is concluded that both multifeed, large antenna instruments and an interferometric design could provide valuable advances. Ultimately, a scanning beam, phased array instrument could provide full global coverage with high spatial resolution. Author

A88-27839 Paris VI Univ. (France).

QUANTITATIVE USE OF SATELLITE SAR IMAGERY OF SEA ICE

M. FILY (Paris VI, Université, France) and D. A. ROTHROCK (Washington, University, Seattle) (COSPAR, WMO, URSI, et al., Plenary Meeting, 26th, Symposium 3, Workshop V, and Topical Meeting A2 on Remote Sensing from Space, Toulouse, France,

June 30-July 11, 1986) *Advances in Space Research* (ISSN 0273-1177), vol. 7, no. 11, 1987, p. 323-326. NASA-Navy-ESA-supported research. refs

An automatic technique to obtain ice motion based on maximizing cross-correlation and employing a strategy of nested calculations has been developed and used to obtain displacements of more than 2000 tie-points on a 2 km mesh grid. The mean displacement error is 250 m and is as low as manual data error of 150 m on rigid pieces. The method allows tie-points to be found on a regular grid in a fully automatic fashion. Full resolution data are not needed to maximize the accuracy of displacement measurements, a result which is significant for SAR images, with their large amounts of data. C.D.

A88-27840

DETECTION OF OIL FILMS BY ACTIVE AND PASSIVE MICROWAVE SENSORS

W. KEYDEL (DFVLR, Institut fuer Hochfrequenztechnik, Oberpfaffenhofen, Federal Republic of Germany) and W. ALPERS (Bremen, Universität, Federal Republic of Germany) (COSPAR, WMO, URSI, et al., Plenary Meeting, 26th, Symposium 3, Workshop V, and Topical Meeting A2 on Remote Sensing from Space, Toulouse, France, June 30-July 11, 1986) *Advances in Space Research* (ISSN 0273-1177), vol. 7, no. 11, 1987, p. 327-333. refs

This paper tries to point out the possibilities, the advantages and disadvantages of microwave systems for detection of oil films on sea surfaces on the basis of measurement results gained with both radar and microwave radiometers in several frequency bands. Author

A88-27841* National Aeronautics and Space Administration. Goddard Space Flight Center, Greenbelt, Md.

FUTURE RESEARCH DIRECTIONS IN THE QUANTITATIVE RADAR REMOTE SENSING OF LAND AND OCEANIC SURFACE FEATURES

VINCENT V. SALOMONSON (NASA, Goddard Space Flight Center, Greenbelt, MD) and H. OETTL (DFVLR, Institut fuer Hochfrequenztechnik, Wessling, Federal Republic of Germany) (COSPAR, WMO, URSI, et al., Plenary Meeting, 26th, Symposium 3, Workshop V, and Topical Meeting A2 on Remote Sensing from Space, Toulouse, France, June 30-July 11, 1986) *Advances in Space Research* (ISSN 0273-1177), vol. 7, no. 11, 1987, p. 335, 336.

A88-28850

MICROWAVE REMOTE SENSING OF ICE IN LAKE MELVILLE AND THE LABRADOR SEA

SUSAN A. DIGBY-ARGUS, ROBERT K. HAWKINS, and KESHA P. SINGH (Canada Centre for Remote Sensing, Ottawa) IEEE Journal of Oceanic Engineering (ISSN 0364-9059), vol. OE-12, July 1987, p. 503-517. refs

Results from a microwave remote-sensing experiment conducted in March 1982 on the pack ice and young ice of the Labrador Sea and the brackish ice of Lake Melville are reported. The relationship of the microwave response to the ice types of this region and to specific features such as icebergs and icebreaker tracks is examined and characterized. Some aspects of wave propagation in pack ice are discussed along with radar contrast measurements of icebergs surrounded by pack ice giving the effect of incidence angle. C.D.

A88-29276

PRELIMINARY ASSESSMENT OF RADIOMETRIC ACCURACIES FOR MOS-1 SENSORS

KOHEI ARAI (National Space Development Agency of Japan, Earth Observation Center, Saitama) International Journal of Remote Sensing (ISSN 0143-1161), vol. 9, Jan. 1988, p. 5-21. refs

The radiometric characteristics of the sensors on the Japanese Marine Observation Satellite 1 (MOS-1) were assessed using prelaunch data and simulations, taking into account sea surface conditions, sun-glitter effects, and atmospheric effects. Specifically, input radiances for the MESSR and VTIR instruments and

brightness temperatures for the MSR instruments on the MOS-1 were estimated taking atmospheric effects into account. In addition, attention was also given to the effect of sun glitter on MESSR and VTIR data, the effect due to rim darkening on VTIR data, the emissivity change due to antenna rotation, and the sidelobe effect on MSR data. B.J.

A88-29279

COMPARISON OF SUBMARINE RELIEF FEATURES ON A RADAR SATELLITE IMAGE AND ON A SKYLAB SATELLITE PHOTOGRAPH

INGO HENNINGS (GKSS Forschungszentrum Geesthacht GmbH; Bremen, Universitaet, Federal Republic of Germany), ROLAND DOERFFER (GKSS Forschungszentrum Geesthacht GmbH, Federal Republic of Germany), and WERNER ALPERS (Bremen, Universitaet, Federal Republic of Germany) International Journal of Remote Sensing (ISSN 0143-1161), vol. 9, Jan. 1988, p. 45-67. refs

Satellite imagery obtained by an optical sensor and that obtained by an SAR for a shallow ocean area showing submarine relief features are compared. A Skylab photograph and a Seasat radar image of the North American east coast (Nantucket Shoals) taken at different dates but at the same tidal phase and under comparable weather conditions are analyzed. It is found that both the radar imaging and the optical imaging are caused by roughness variations of the water surface due to tidal flow over submarine relief. It is concluded from the analysis of the densities in the blue, green, and red layers of the Skylab color film that specularly reflected sunlight at the rough ocean surface is the dominant imaging mechanism. B.J.

A88-29283

ATMOSPHERIC CORRECTION OF THERMAL INFRARED IMAGES

ZHIRONG LI and M. J. MCDONNELL (Department of Scientific and Industrial Research, Div. of Information Technology, Lower Hutt, New Zealand) International Journal of Remote Sensing (ISSN 0143-1161), vol. 9, Jan. 1988, p. 107-121. refs

A method for estimating SST from a single IR channel together with an atmospheric model is investigated. Based on a simulated atmospheric height profile, the precipitable water and transmittance can be calculated as a function of height from the known atmospheric pressure, temperature and relative humidity on the ground. An effective transmittance is used to correct the effect of off-nadir scanner angle. Various data from the Heat Capacity Mapping Mission, the advanced very high resolution radiometer, and other sources are used to evaluate the accuracy of the method. The SST derived agrees with available ground truth with a rms error of about 1 deg K. Author

A88-29323* Columbia Univ., New York, N.Y.

A MODEL OF THE TROPICAL PACIFIC SEA SURFACE TEMPERATURE CLIMATOLOGY

RICHARD SEAGER (Columbia University, New York), STEPHEN E. ZEBIAK, and MARK A. CANE (Lamont-Doherty Geological Observatory, Palisades, NY) Journal of Geophysical Research (ISSN 0148-0227), vol. 93, Feb. 15, 1988, p. 1265-1280. refs (Contract NCC5-29; NSF ATM-86-12570; NAGW-916)

A model for the climatological mean sea surface temperature (SST) of the tropical Pacific Ocean is developed. The upper ocean response is computed using a time dependent, linear, reduced gravity model, with the addition of a constant depth frictional surface layer. The full three-dimensional temperature equation and a surface heat flux parameterization that requires specification of only wind speed and total cloud cover are used to evaluate the SST. Specification of atmospheric parameters, such as air temperature and humidity, over which the ocean has direct influence, is avoided. The model simulates the major features of the observed tropical Pacific SST. The seasonal evolution of these features is generally captured by the model. Analysis of the results demonstrates the control the ocean has over the surface heat flux from ocean to atmosphere and the crucial role that dynamics play in determining the mean SST in the equatorial Pacific. The

sensitivity of the model to perturbations in the surface heat flux, cloud cover specification, diffusivity, and mixed layer depth is discussed. Author

A88-29324

ICE FLOE COLLISIONS AND THEIR RELATION TO ICE DEFORMATION IN THE BERING SEA DURING FEBRUARY 1983

SEELYE MARTIN and PAUL BECKER (Washington, University, Seattle) Journal of Geophysical Research (ISSN 0148-0227), vol. 93, Feb. 15, 1988, p. 1303-1315. refs (Contract NAVY TASK NR-083-012; N00014-84-C-0111)

The nature of the ice floe collisions and their relation to ice deformation were investigated during a field study conducted in the Bering Sea in February 1983, during which four radar-tracked buoys, three of which were equipped with triaxial accelerometers, were deployed on selected ice floes. Two classes of collisions were observed. The first type constitutes major collisions, which occur infrequently (two were observed during the 4-d sampling period) and are associated with the large-scale deformation; these collisions were shown to have mean square velocities of 0.1-1 sq mm/sq sec order. The second type of collisions are periodic collisions, which recur at the ocean swell frequency. The observations suggest that their onset and magnitude are correlated with the periods of ice convergence. I.S.

A88-29325* Jet Propulsion Lab., California Inst. of Tech., Pasadena.

SCATTEROMETER WIND SPEED BIAS INDUCED BY THE LARGE-SCALE COMPONENT OF THE WAVE FIELD

R. E. GLAZMAN, G. G. PIHOS, and J. IP (California Institute of Technology, Jet Propulsion Laboratory, Pasadena) Journal of Geophysical Research (ISSN 0148-0227), vol. 93, Feb. 15, 1988, p. 1317-1328. refs

In order to determine if an environmental bias exists in the winds measured by the Seasat A satellite scatterometer (SASS), the SASS wind speed observations, $U(s)$, colocated with the buoy wind speed data, $U(b)$, were analyzed. There was a trend in the SASS wind speed error, $U(b) - U(s)$, which was found to be related to the degree of the development of wind-generated gravity waves; this trend (estimated to be 0.5 m/sec per 100 km of the generalized wind fetch) is capable of introducing a well-pronounced environmental bias into the scatterometer-produced global distributions of wind. I.S.

A88-29492* Alaska Univ., Fairbanks.

DETECTION AND IDENTIFICATION OF ARCTIC LANDFORMS - AN ASSESSMENT OF REMOTELY SENSED DATA

KENNESON G. DEAN (Alaska, University, Fairbanks) and LESLIE A. MORRISSEY (TGS Technology, Inc., Moffett Field, CA) Photogrammetric Engineering and Remote Sensing (ISSN 0099-1112), vol. 54, March 1988, p. 363-371. NASA-supported research. refs

The use of remote sensing data to monitor and analyze the arctic environment is examined. Landsat MSS, TM simulated, NS001, Seasat, and airborne radar are employed to investigate the Strand and Dune areas on the Arctic Coastal Plain in Alaska. The Strand area contains landforms associated with permafrost and the Dune area is dominated by eolian deposits consisting of large longitudinal dunes. The remote sensing data are compared to baseline geomorphic maps derived from aerial photography. It is observed that the multispectral data are better than the radar data for the detection and recognition of arctic landforms, and the NS001 data provided the highest spatial resolution and correlated well with the high-altitude aerial photography. I.F.

A88-29766* Jet Propulsion Lab., California Inst. of Tech., Pasadena.

MEASUREMENT OF GLOBAL OCEANIC WINDS FROM SEASAT-SMMR AND ITS COMPARISON WITH SEASAT-SASS AND ALT DERIVED WINDS

PREM C. PANDEY (California Institute of Technology, Jet

Propulsion Laboratory, Pasadena) IEEE Transactions on Geoscience and Remote Sensing (ISSN 0196-2892), vol. GE-25, Nov. 1987, p. 670-676. refs

The retrieval of ocean-surface wind speed from different channel combinations of Seasat SMMR measurements is demonstrated. Wind speeds derived using the best two channel subsets (10.6 H and 18.0 V) were compared with in situ data collected during the Joint Air-Sea Interaction (JASIN) experiment and an rms difference of 1.5 m/s was found. Global maps of wind speed generated with the present algorithm show that the averaged winds are arranged in well-ordered belts. K.K.

A88-30077

BLOCKING OF THE BENGUELA CURRENT BY A SINGLE ANTICYCLONE - ANALYSIS OF SATELLITE AND SHIP DATA [BLOKIROVANIE BENGEL'SKOGO TECHENIIA ODINOCHNYM ANTITSIKLONOM: ANALIZ SPUTNIKOVOI I SUDOVOI INFORMATSII]

A. S. KAZ'MIN and G. G. SUTYRIN (AN SSSR, Institut Okeanologii, Moscow, USSR) Issledovanie Zemli iz Kosmosa (ISSN 0205-9614), Nov.-Dec. 1987, p. 9-14. In Russian. refs

A88-30078

THE USE OF THE OPTICAL CLASSIFICATION OF OCEAN WATERS TO ESTIMATE CORRELATIONS BETWEEN THE CONCENTRATIONS OF VARIABLE COMPONENTS WITH REFERENCE TO THE DEVELOPMENT OF REMOTE-SENSING METHODS [ISPOL'ZOVANIE OPTICHESKOI KLASSIFIKATSII OKEANSKIKH VOD DLIA OTSENKI SOOTNOSHENII MEZHDU KONTSENTRATSIIAMI PEREMENNYKH KOMPONENT PRIMENITEL'NO K RAZVITIUI DISTANTSIONNYKH METODOV]
V. P. LEVENTUEV (Vsesoiuznyi Nauchno-Issledovatel'skii Institut Morskogo Rybnogo Khoziaistva i Okeanografii, Moscow, USSR) Issledovanie Zemli iz Kosmosa (ISSN 0205-9614), Nov.-Dec. 1987, p. 15-22. In Russian. refs

A88-30083

DETECTION OF INTERNAL WAVES USING DATA FROM SATELLITE MICROWAVE RADIOMETRY AND THE RESEARCH SHIP ACADEMICIAN ALEXANDER NESMEIANOV [REGISTRATSIYA VNUTRENNIKH VOLN PO DANNYM RADIOFIZICHESKOGO ZONDIROVANIYA S ISZ I NIS 'AKADEMIK ALEKSANDR NESMEIANOV']

L. M. MITNIK (AN SSSR, Tikhookeanski Okeanologicheski Institut, Vladivostok, USSR) Issledovanie Zemli iz Kosmosa (ISSN 0205-9614), Nov.-Dec. 1987, p. 49-56. In Russian. refs

A88-30084

ESTIMATION OF THE ACCURACY OF DETERMINING ATMOSPHERIC TEMPERATURE PROFILES FROM MICROWAVE REMOTE SENSING AT FREQUENCIES OF 117-118.5 GHZ [OTSENKA TOCHNOSTI VOSSTANOVLENIYA TEMPERATURNOGO PROFILIA ATMOSFERY PO DISTANTSIONNYM IZMERENIYAM V MIKROVOLNOVOM DIAPAZONE SPEKTRA 117-118,5 GGTS]

I. B. KOTLIAR and B. L. NOVAK (AN SSSR, Institut Kosmicheskikh Issledovaniy, Moscow, USSR) Issledovanie Zemli iz Kosmosa (ISSN 0205-9614), Nov.-Dec. 1987, p. 57-62. In Russian. refs

A88-30085

THE USE OF REGRESSION ANALYSIS TO DETERMINE SEA SURFACE TEMPERATURES FROM COSMOS-1151 MEASUREMENTS OF IR RADIATION [ISPOL'ZOVANIE REGRESSIONNOGO ANALIZA DLIA OPREDELENIYA TEMPERATURY POVERKHNOSTI OKEANA PO IZMERENIYAM IK-IZLUCHEENIYA SO SPUTNIKA 'KOSMOS-1151']

V. S. SUETIN and S. N. KOROLEV (AN USSR, Morskoi Gidrofizicheskii Institut, Sevastopol, Ukrainian SSR) Issledovanie Zemli iz Kosmosa (ISSN 0205-9614), Nov.-Dec. 1987, p. 63-72. In Russian. refs

A88-30089

CURRENT STATUS AND PROBLEMS OF SATELLITE INVESTIGATIONS OF THE OCEAN (REVIEW OF NON-SOVIET PUBLICATIONS) [SOVREMENNOE SOSTOYANIE I PROBLEMY SPUTNIKOVIKH ISSLEDOVANIY OKEANA /OBZOR ZARUBEZHNYKH RABOT/]

G. A. GRISHIN (AN USSR, Morskoi Gidrofizicheskii Institut, Sevastopol, Ukrainian SSR) Issledovanie Zemli iz Kosmosa (ISSN 0205-9614), Nov.-Dec. 1987, p. 94-110. In Russian. refs

The performance characteristics of cameras on existing satellites and those planned for future satellite systems are described. Examples are presented which illustrate the application of satellite data in oceanography. Attention is given to space programs for the study of the world ocean planned by developed countries for the next decade. Methodological, scientific, and organizational problems connected with satellite-borne ocean studies are examined. B.J.

A88-30199

PRINCIPAL COMPONENT ANALYSIS OF SATELLITE PASSIVE MICROWAVE DATA OVER SEA ICE

D. A. ROTHROCK, DONALD R. THOMAS (Washington, University, Seattle), and ALAN S. THORNDIKE (University of Puget Sound, Tacoma, WA) Journal of Geophysical Research (ISSN 0148-0227), vol. 93, March 15, 1988, p. 2321-2332. refs
(Contract N00014-81-K-0095; NSF DPP-86-17176)

Correlation, multiple regression, and principal component analyses of 10 channels of SMMR data for the Arctic are presented, showing correlations of greater than 0.8 for most of the channels. Three channels are shown to explain between 94.0 and 99.6 percent of the total variance. It is suggested that only the first two principal components contain variance, due to the mixture of surface types. It is shown that three-component mixtures of water, first-year ice, and multiyear ice can be resolved in two dimensions, and that the presence of other ice types makes determination of ice age ambiguous in some regions. The small variance in principal components 3-10 is due to variability in the pure type signatures. R.R.

A88-30200

ICE BREAKUP - OBSERVATIONS OF THE ACOUSTIC SIGNAL

S. R. WADDELL and D. M. FARMER (Institute of Ocean Sciences, Sidney, Canada) Journal of Geophysical Research (ISSN 0148-0227), vol. 93, March 15, 1988, p. 2333-2342. refs

Observations of ambient sound beneath landfast ice in the Canadian Arctic Archipelago are described, and its evolution over the period June-August is interpreted in terms of ice cracking and disintegration. The data were recorded on six bands between 50 and 14,500 Hz for the period Apr. 2 to Aug. 7, 1986, in Delphin and Union Strait. The frequency dependence of the attenuation of sound in water allows separation of distant and local noise sources. In conjunction with satellite imagery and meteorological data, it is shown that strong signals in the acoustic time series are associated with major breakup events. The acoustic signal can provide predictive information about ice conditions and the approach of breakup. Author

A88-30415* Miami Univ., Coral Gables, Fla.

EXACT RAYLEIGH SCATTERING CALCULATIONS FOR USE WITH THE NIMBUS-7 COASTAL ZONE COLOR SCANNER

HOWARD R. GORDON, JAMES W. BROWN (Miami, University, Coral Gables, FL), and ROBERT H. EVANS (Miami, University, FL) Applied Optics (ISSN 0003-6935), vol. 27, March 1, 1988, p. 862-871. refs
(Contract NAGW-273; NAS5-28798)

The radiance reflected from a plane-parallel atmosphere and flat sea surface in the absence of aerosols has been determined with an exact multiple scattering code to improve the analysis of Nimbus-7 CZCS imagery. It is shown that the single scattering approximation normally used to compute this radiance can result in errors of up to 5 percent for small and moderate solar zenith angles. A scheme to include the effect of variations in the surface pressure in the exact computation of the Rayleigh radiance is

05 OCEANOGRAPHY AND MARINE RESOURCES

discussed. The results of an application of these computations to CZCS imagery suggest that accurate atmospheric corrections can be obtained for solar zenith angles at least as large as 65 deg.

R.R.

A88-30445

EMISSIVITY OF PURE AND SEA WATERS FOR THE MODEL SEA SURFACE IN THE INFRARED WINDOW REGIONS

K. MASUDA, T. TAKASHIMA, and Y. TAKAYAMA (Meteorological Research Institute, Tsukuba, Japan) Remote Sensing of Environment (ISSN 0034-4257), vol. 24, March 1988, p. 313-329. refs

Emissivity of pure and sea waters for the model sea surface is tabulated as a function of the zenith angle of observed radiation (θ) and the surface wind speed in the infrared window regions, 3.5-4.1 and 8-13 microns. The sea surface is simulated by many facets whose slopes are changed according to the isotropic Gaussian distribution with respect to surface wind. Emissivity is also computed for the plane surface condition. Computational results show that: (1) emissivity decreases slowly with the increase of θ , (2) little effect of the surface wind is noted on emissivity for θ equal to or less than 30 deg, whereas this effect greatly appears for θ equal to or greater than 70 deg, and (3) relative difference of emissivities between pure water and sea water is less than 0.1 percent within $\theta = 50$ deg for wind speed less than 15 m/s. Finally, the corresponding apparent temperatures are also examined.

Author

A88-30662

REMOTE SENSING OF THE SEA SURFACE

O. M. PHILLIPS (Johns Hopkins University, Baltimore, MD) IN: Annual review of fluid mechanics. Volume 20. Palo Alto, CA, Annual Reviews, Inc., 1988, p. 89-109. refs (Contract N00014-84-K-0080)

An account is given of the operating principles of radar altimeter and radar spectrometer devices employed in the remote probing of the sea surface, as well as of the sea surface characteristics that influence the return signals. Attention is given to the application of these principles to various aspects of dynamic oceanography, including the measurement of surface currents, oceanic tides, and the spectrum of wind-generated waves. The estimation of surface wind-stress distributions, and the detection of small-scale surface-current features together with their interpretation in terms of current velocity gradients, are also undertaken by these methods.

O.C.

A88-30836

GRAVITY FIELD MAPPING FROM SATELLITE ALTIMETRY, SEA-GRAVIMETRY AND BATHYMETRY IN THE EASTERN MEDITERRANEAN

D. ARABELOS (Salonika, University, Greece) and C. C. TSCHERNING (Geodaetisk Institut, Charlottenlund, Denmark) Geophysical Journal (ISSN 0952-4592), vol. 92, Feb. 1988, p. 195-206. refs

(Contract EEC-ST2J-39-DK(EDB))

Data from the Eastern Mediterranean were used to show how different data types may improve the quality of a gravity field approximation; a detailed geoid was computed for the area. Available data types included bias-adjusted satellite altimetry, sea gravimetry, bathymetry and heights, and the spherical harmonic coefficient set OSU81. A trend analysis of the altimeter data revealed a tilt of 0.0026 m/km toward the east and 0.0067 m/km toward the north.

K.K.

A88-31111

THE GENESIS OF ATLANTIC LOWS EXPERIMENT - THE PLANETARY-BOUNDARY-LAYER SUBPROGRAM OF GALE

SETHU RAMAN and ALLEN J. RIORDAN (North Carolina State University, Raleigh) American Meteorological Society, Bulletin (ISSN 0003-0007), vol. 69, Feb. 1988, p. 161-172. refs (Contract NSF ATM-83-11812; N00014-84-K-0620)

The Genesis of Atlantic Lows Experiment (GALE), focused an intensive data-gathering effort along the mid-Atlantic coast of the

United States from January 15 to March 15, 1986. Here, the general objectives and experimental layout are described with special emphasis on the planetary-boundary-layer (PBL) component of GALE. Instrumentation is described for buoys, ships, research aircraft, and towers. The networks of the cross-chain long range aid to navigation (LORAN) atmospheric sounding system (CLASS) and the portable automated mesonet (PAM II) are described and their impact on the operation of GALE is outlined. Special use of dual-Doppler radar to obtain detailed wind measurements in the PBL is discussed. Preliminary analyses for a selected observational period are given. Detailed observations of the offshore coastal front reveal direct mesoscale circulations imbedded in the frontal zone. Later in the period during an intense cold-air outbreak, sensible-heat and latent-heat fluxes over the coastal ocean each attain values of about 500 W/sq m. Coordinated aircraft operations are outlined for this case and a few early findings are given.

Author

A88-31793*# National Aeronautics and Space Administration. Goddard Space Flight Center, Greenbelt, Md.

SOURCE OF THE AUSTRALASIAN TEKITE STREWN FIELD - A POSSIBLE OFF-SHORE IMPACT SITE

C. C. SCHNETZLER, L. S. WALTER, and J. G. MARSH (NASA, Goddard Space Flight Center, Greenbelt, MD) Geophysical Research Letters (ISSN 0094-8276), vol. 15, April 1988, p. 357-360. refs

Although there is a preponderance of evidence that tektites were formed by asteroid impacts on the earth, no source crater has been found for the largest and youngest of the strewn fields - the Australasian strewn field. A combined Seasat/Geos 3 altimeter data set of sea surface heights in the northern portion of the Australasian strewn field has been examined for negative gravity anomalies on the continental shelf and slope which might be related to the source crater for these tektites. A large negative anomaly called the Qui Nhon Slope Anomaly is a sea surface depression of approximately 1.5 meters over an area of 100 km diameter. It corresponds to a gravity anomaly of about -50 mgal. It is proposed that this anomaly may be due to the impact structure that produced the Australasian strewn field.

Author

A88-32508

THERMAL EXPANSION OF A RIG

L. CAVALERI, S. CURIOTTO, and P. LIONELLO (CNR, Istituto per lo Studio della Dinamica delle Grandi Masse, Venice, Italy) Nuovo Cimento C, Serie 1 (ISSN 0390-5551), vol. 10, Sept-Oct. 1987, p. 573-576.

The thermal expansion of the CNR oceanographic tower in the northern Adriatic {a steel structure with 16 m submerged and 12 m exposed} was measured on two successive sunny days in August 1987, to determine its suitability as a reference target for the altimeter of the ESA ERS-1 remote-sensing satellite. The measurements were obtained by monitoring the relative positions of reference marks on a 1-mm-diameter steel wire suspended outside the tower. No variations in position were observed, indicating that thermal expansion was less than 1 mm, and a computation accounting for seasonal temperature changes predicts a maximum expansion of 5.6 mm (well below the ERS-1 requirement of 1 cm).

T.K.

N88-15101# Naval Research Lab., Washington, D.C.

TEXTURE STUDY OF SYNTHETIC APERTURE RADAR (SAR) IMAGES OF OCEAN SURFACES Interim Report

LI-JEN DU 20 Aug. 1987 29 p (AD-A186021; NRL-MR-6005) Avail: NTIS HC A03/MF A01 CSDL 171

This report describes the first phase of a study whose objective is to establish the relation between the texture in SAR images of the ocean surface and the relevant physical conditions giving rise to this texture. The initial concern is the selection of a technique which leads to a reliable separation of images into regions of different texture. Section 2 of the report discusses the role of texture in image analysis. Section 3 introduces the concept of a feature and establishes rationale for the selection of gray level

co-occurrence matrix approach to feature extraction. Section 4 describes the proposed classification algorithm and Section 5 gives the results for several test images. It is found that this approach works well in classification of land scenes. For ocean images which exhibit only subtle differences between regions the approach's discriminating power is less satisfactory than for land scenes. In Section 6 alternate approaches are suggested for ocean images.

GRA

N88-15280# Institute of Oceanographic Sciences, Birkenhead (England).

REVIEW OF THE POTENTIAL OF SATELLITE REMOTE SENSING FOR MARINE FLOOD PROTECTION

J. M. HUTHNANCE, ed., T. D. ALLAN, T. F. BAKER, P. G. CHALLENGER, K. R. DYER, R. A. FLATHER, T. H. GUYMER, I. D. JAMES, and P. L. WOODWORTH 1987 61 p Prepared for the Ministry of Agriculture, Fisheries and Food, United Kingdom (IOS-237; ETN-88-90937) Avail: NTIS HC A04/MF A01

Flood protection in the UK using satellite remote sensing techniques is discussed. Operational use is limited by widely spaced orbits with repeat periods of several days for any one polar-orbiting satellite, or by cloud cover for visible and infrared imagery spanning the orbit separation. Geostationary satellites have limited resolution at 50 to 60N. Research and design applications are numerous, with potential for monitoring climate and mean sea level change, overviews of coastal development, sediment movement and wave behavior, and establishing global wind and wave climatology. Flooding may be imaged over that part of the UK sensed by ERS-1 in SAR mode at the time. Useful surge and wave data assimilation for forecasts awaits the Columbus program and requires its altimeters to have 0(2 cm) accuracy and to cover a swath 0(100 km) or more, as well as rapid data transmission and forecast model development. ESA

N88-15285*# Scripps Institution of Oceanography, La Jolla, Calif.

GEOSAT CROSSOVER ANALYSIS IN THE TROPICAL PACIFIC. PART 1: CONSTRAINED SINUSOIDAL CROSSOVER ADJUSTMENT Final Technical Report

CHANG-KOU TAI 3 Feb. 1988 24 p

(Contract NAGW-808)

(NASA-CR-182391; NAS 1.26:182391) Avail: NTIS HC A03/MF A01 CSCL 22A

A new method (constrained sinusoidal crossover adjustment) for removing the orbit error in satellite altimetry is tested (using crossovers accumulated in the first 91 days of the Geosat non-repeat era in the tropical Pacific) and found to have excellent qualities. Two features distinguish the new method from the conventional bias-and-tilt crossover adjustment. First, a sine wave (with wavelength equaling the circumference of the Earth) is used to represent the orbit error for each satellite revolution, instead of the bias-and-tilt (and curvature, if necessary) approach for each segment of the satellite ground track. Secondly, the indeterminacy of the adjustment process is removed by a simple constraint minimizing the amplitudes of the sine waves, rather than by fixing selected tracks. Overall the new method is more accurate, more efficient, and much less cumbersome than the old. The idea of restricting the crossover adjustment to crossovers between tracks that are less than certain days apart in order to preserve the large-scale long-term oceanic variability is also tested with inconclusive results because the orbit error was unusually nonstationary in the initial 91 days of the GEOSAT mission.

Author

N88-15286*# Scripps Institution of Oceanography, La Jolla, Calif.

AN EFFICIENT ALGORITHM FOR COMPUTING THE CROSSOVERS IN SATELLITE ALTIMETRY Final Technical Report

CHANG-KOU TAI 3 Feb. 1988 15 p

(Contract NAGW-808)

(NASA-CR-182389; NAS 1.26:182389) Avail: NTIS HC A03/MF A01 CSCL 22A

An efficient algorithm has been devised to compute the crossovers in satellite altimetry. The significance of the crossovers is twofold. First, they are needed to perform the crossover adjustment to remove the orbit error. Secondly, they yield important insight into oceanic variability. Nevertheless, there is no published algorithm to make this very time consuming task easier, which is the goal of this report. The success of the algorithm is predicated on the ability to predict (by analytical means) the crossover coordinates to within 6 km and 1 sec of the true values. Hence, only one interpolation/extrapolation step on the data is needed to derive the crossover coordinates in contrast to the many interpolation/extrapolation operations usually needed to arrive at the same accuracy level if deprived of this information. Author

N88-15292# GKSS-Forschungszentrum Geesthacht (West Germany).

THE INFLUENCE OF YELLOW SUBSTANCES ON REMOTE SENSING OF SEA WATER CONSTITUENTS FROM SPACE. VOLUME 1: SUMMARY

R. DOERFFER, J. FISCHER, H. GRASSL, I. HENNINGS, R. REUTER, D. DIEBEL-LANGOHR, V. AMANN, H. V.D. PIEPEN, V. ITTEKOT, and A. SPITZY (Hamburg Univ., West Germany) Paris, France ESA Dec. 1986 24 p (Contract ESA-5953/84-NL-MD) (ESA-CR(P)-2443-VOL-1; ETN-88-91138) Avail: NTIS HC A03/MF A01

The impact of Gelbstoff (yellow substance) on radiance spectra of the sea, and methods to incorporate Gelbstoff in an evaluation procedure of ocean color spectra measured at satellite altitude are discussed. Due to a large number of overlapping absorption bands Gelbstoff shows a continuous absorption decreasing exponentially from the blue to the red wavelengths without any minima; consequently there is no characteristic band for the location of a Gelbstoff channel in a spectrometer. The fluorescence shows a similar broad emission spectrum. The main fraction of Gelbstoff in the sea stems from river discharge; it can therefore be used as a tracer for investigations of water mass distribution and transport. The decay rate of Gelbstoff in the sea is slow and allows tracer studies in the time range of at least 15 to 20 days. Gelbstoff has a strong impact on water leaving radiance spectra: typical concentrations in estuaries reduce the radiance in the blue-green part of the spectrum by a factor 2 to 3. ESA

N88-15293# GKSS-Forschungszentrum Geesthacht (West Germany).

THE INFLUENCE OF YELLOW SUBSTANCES ON REMOTE SENSING OF SEA WATER CONSTITUENTS FROM SPACE. VOLUME 2: APPENDICES

R. DOERFFER, J. FISCHER, H. GRASSL, I. HENNINGS, R. REUTER, D. DIEBEL-LANGOHR, V. AMANN, H. V.D. PIEPEN, V. ITTEKOT, and A. SPITZY (Hamburg Univ., West Germany) Paris, France ESA Dec. 1986 257 p (Contract ESA-5953/84-NL-MD) (ESA-CR(P)-2443-VOL-2; ETN-88-91139) Avail: NTIS HC A12/MF A01

An uncharacterized fraction of dissolved organic carbon; the influence of yellow substance (Gelbstoff) on remote monitoring of water substances in coastal waters; optical properties of Gelbstoff; an inverse technique for remote detection and separation of substances in ocean water; an inverse technique for remote detection of suspended matter, phytoplankton, and yellow substances from CZCS measurements; long term stability of Gelbstoff concerning its optical properties; the selection of an optimized channel for measuring yellow substance from space within the 380 to 475 nm domain; ground truth techniques and procedures for Gelbstoff measurements; and airborne laser fluorosensor measurements of Gelbstoff are discussed. ESA

N88-15294# GKSS-Forschungszentrum Geesthacht (West Germany).

THE USE OF CHLOROPHYLL FLUORESCENCE MEASUREMENTS FROM SPACE FOR SEPARATING CONSTITUENTS OF SEA WATER. VOLUME 1: SUMMARY

05 OCEANOGRAPHY AND MARINE RESOURCES

R. DOERFFER, J. FISCHER, H. GRASSL, I. HENNINGS, U. KRONFELD, K. GUENTHER, H. HAARDT, P. KOSKE, V. AMANN, H. V.D.PIEPEN (Deutsche Forschungs- und Versuchsanstalt fuer Luft- und Raumfahrt, Oberpfaffenhofen, West Germany) et al. Paris, France ESA Dec. 1986 41 p
(Contract ESA-5952/84-NL-MD)
(ESA-CR(P)-2444-VOL-1; ETN-88-91140) Avail: NTIS HC A03/MF A01

Sunlight stimulated fluorescence of marine phytoplankton and the transport of this signal to the top of the atmosphere as a method to map the distribution of phytoplankton in coastal areas of the sea from space were examined. Sun stimulated chlorophyll-a fluorescence at 685 nm is a generally detectable though small spectral feature in upward radiation spectra over the sea containing chlorophyll-a concentrations down to at least 1 mg/cum. Under typical coastal conditions very simple extraction algorithms give a linear dependence of chlorophyll fluorescence on chlorophyll concentration with a relatively low standard deviation. The primary productivity of marine algae is inversely related to in situ chlorophyll-a fluorescence. Suspended matter and Gelbstoff may induce problems. ESA

N88-15295# GKSS-Forschungszentrum Geesthacht (West Germany).

THE USE OF CHLOROPHYLL FLUORESCENCE MEASUREMENTS FROM SPACE FOR SEPARATING CONSTITUENTS OF SEA WATER. VOLUME 2: APPENDICES

R. DOERFFER, J. FISCHER, H. GRASSL, I. HENNINGS, U. KRONFELD, K. GUENTHER, H. HAARDT, P. KOSKE, V. AMANN, H. V.D.PIEPEN (Deutsche Forschungs- und Versuchsanstalt fuer Luft- und Raumfahrt, Oberpfaffenhofen, West Germany) et al. Paris, France ESA Dec. 1986 467 p
(Contract ESA-5952/84-NL-MD)
(ESA-CR(P)-2444-VOL-2; ETN-88-91141) Avail: NTIS HC A20/MF A01

Biophysical processes of chlorophyll-a fluorescence; Sun stimulated chlorophyll fluorescence within a day-cycle; the daily cycle of in vivo chlorophyll-a fluorescence stimulated by artificial light sources; the effect of short term illumination changes on the Sun stimulated fluorescence of phytoplankton; chlorophyll fluorescence within the visible spectrum; horizontal and seasonal variability of species composition and phytoplankton chlorophyll in the Baltic and North Seas; scales of horizontal variability of chlorophyll-a phytoplankton; the influence of exceptional phytoplankton blooms on remote sensing of chlorophyll; masking of chlorophyll fluorescence by the atmosphere; ground truth measurement for primary production, production capacity, and fluorescence; use of airborne laser fluorometer as ground truth for satellite data evaluation; factor analysis of multispectral radiance over coastal and open ocean water based on radiative transfer calculations; effect of environmental factors and species composition on chlorophyll fluorescence of phytoplankton; and variability of excitation, emission, and absorption spectra normalized to the chlorophyll concentration are discussed. ESA

N88-15346# Royal Australian Navy Research Lab., Edgely. Cliff.

THE OCEAN HEAT BUDGET

J. W. HILL May 1987 49 p
(AD-A186130; RANRL-TN-3/87; AR-003-469) Avail: NTIS HC A03/MF A01 CSCL 08C

Methods are assembled for calculating the components of ocean heating/cooling from above, viz. short-wave radiation, albedo, longwave radiation, and evaporative and sensible heat exchange with the atmosphere. The aim is to secure the best possible balance between precision and simplicity, bearing in mind the inherent limitations of meteorological information. Much of the material comes from the literature, but a consolidation of the radiant heating input parameters and a simplification of the atmospheric heat exchange calculation are believed to be original developments. GRA

N88-15348# World Climate Programme, Geneva (Switzerland).

WOCE CORE PROJECT 2 PLANNING MEETING: THE SOUTHERN OCEAN

May 1987 64 p Meeting held in Bremerhaven, Federal Republic of Germany, 20-23 May 1986 Prepared in cooperation with the International Council of Scientific Unions, Rome, Italy (WCP-138; WMO/TD-181; ETN-88-90773) Avail: NTIS MF A01; print copy available from WMO, Geneva, Switzerland

The role of the Southern Ocean in transporting heat, salt and other properties; and the strong ocean-atmosphere interactions and consequent water mass transformations were discussed. The Antarctic circumpolar current; meridional fluxes; and air sea ice interactions were treated. Scientific objectives; observational programs; and modeling requirements of field studies were determined. ESA

N88-15352*# Scripps Institution of Oceanography, La Jolla, Calif.

ON ESTIMATING THE BASIN-SCALE OCEAN CIRCULATION FROM SATELLITE ALTIMETRY. PART 1:

STRAIGHTFORWARD SPHERICAL HARMONIC EXPANSION

Final Technical Report

CHANG-KOU TAI 3 Feb. 1988 34 p
(Contract NAGW-808)
(NASA-CR-182387; NAS 1.26:182387) Avail: NTIS HC A03/MF A01 CSCL 08C

Direct estimation of the absolute dynamic topography from satellite altimetry has been confined to the largest scales (basically the basin-scale) owing to the fact that the signal-to-noise ratio is more unfavorable everywhere else. But even for the largest scales, the results are contaminated by the orbit error and geoid uncertainties. Recently a more accurate Earth gravity model (GEM-T1) became available, providing the opportunity to examine the whole question of direct estimation under a more critical limelight. It is found that our knowledge of the Earth's gravity field has indeed improved a great deal. However, it is not yet possible to claim definitively that our knowledge of the ocean circulation has improved through direct estimation. Yet, the improvement in the gravity model has come to the point that it is no longer possible to attribute the discrepancy at the basin scales between altimetric and hydrographic results as mostly due to geoid uncertainties. A substantial part of the difference must be due to other factors; i.e., the orbit error, or the uncertainty of the hydrographically derived dynamic topography. Author

N88-16107# Joint Publications Research Service, Arlington, Va.

LIMITING ACCURACY OF SCATTEROMETER

DETERMINATION OF WIND SPEED OVER OCEAN FROM SATELLITE Abstract Only

G. N. KHRISTOFOROV, A. S. ZAPEVALOV, and V. YE. SMOLOV *In its* JPRS Report: Science and Technology. USSR: Space p 127 24 Nov. 1987 Transl. into ENGLISH from Issledovaniye Zemli iz Kosma (Moscow, USSR), no. 2, Mar. - Apr. 1987 p 57-65 Original language document was announced in IAA as A87-48184 Avail: NTIS HC A08/MF A01

Errors in determining wind velocities from scatterometer measurements are assessed, and it is shown that the highest accuracy of wind field determination is about + or - 1 m/s over the 4 to 17 m/s range. It is found that the velocity of weak winds cannot be accurately determined from remote measurements of sea ripple, while for velocities higher than 4 m/s the accuracy of scatterometer measurement is limited by a statistical spread of + or - 1 to 2 m/s. Author

N88-16152# Ludwig-Maximilians-Universitaet, Munich (West Germany). Inst. fuer Meteorologie.

VERTICAL SOUNDING OF THE AIR LAYER CLOSE TO A GLACIER ON MOUNT VERNAGFERNER IN THE OETZAL ALPS, TYROL (EXPERIMENT LUZIVER 1983)

[VERTIKALSONDIERUNGEN DER EISNAHEN LUFTSCHICHT AM VERNAGTFFERNER (LUZIVER 1983)]

MARKUS WEBER *In its* Research Work at the Meteorological

Institute of the University of Munich (Federal Republic of Germany)
p 68-72 Mar. 1987 In GERMAN
Avail: NTIS HC A11/MF A01

The vertical profiles of wind, temperature, and moisture close to a glacier were measured between 300 and 2979 m using captive probes, pilot balloon ascensions, and mast measurements. Time-height wind velocity plots are explained. A distinct separation between glacier wind layer and cross wind is difficult using only the wind velocity profiles. Therefore, the equivalent-potential temperature isoline, obtained from mast measurements, are needed. The correlation between temperature gradients and glacier wind is explained. The range of the glacier wind in the foreland is discussed. The results show that the development of the glacier wind regime in the last decameter above the glacier is determined by the synoptic situation and the orography. ESA

N88-16180*# GKSS-Forschungszentrum Geesthacht (West Germany).
THEMATIC MAPPER RESEARCH IN THE EARTH SCIENCES: SMALL SCALE PATCHES OF SUSPENDED MATTER AND PHYTOPLANKTON IN THE ELBE RIVER ESTUARY, GERMAN BIGHT AND TIDAL FLATS Progress Report
H. GRASSL, R. DOERFFER, J. FISCHER, C. BROCKMANN, and M. STOESEL 9 Oct. 1987 40 p Sponsored by NASA (NASA-CR-182378; NAS 1.26:182378) Avail: NTIS HC A03/MF A01 CSCL 08B

A Thematic Mapper (TM) field experiment was followed by a data analysis to determine TM capabilities for analysis of suspended matter and phytoplankton. Factor analysis showed that suspended matter concentration, atmospheric scattering, and sea surface temperature can be retrieved as independent factors which determine the variation in the TM data over water areas. Spectral channels in the near infrared open the possibility of determining the Angstrom exponent better than for the coastal zone color scanner. The suspended matter distribution may then be calculated by the absolute radiance of channel 2 or 3 or the ratio of both. There is no indication of whether separation of chlorophyll is possible. The distribution of suspended matter and sea surface temperature can be observed with the expected fine structure. A good correlation between water depth and suspended matter distribution as found from ship data can now be analyzed for an entire area by the synoptic view of the TM scenes. J.P.B.

N88-16292# European Space Agency, Paris (France).
OCEAN COLOUR WORKSHOP
T. D. GUYENNE, ed. Jul. 1987 119 p Workshop held at Villefranche-sur-Mer, France, 5-6 Nov. 1986 Original contains color illustrations (ESA-SP-1083; ISSN-0379-6566; ETN-88-91135) Avail: NTIS HC A06/MF A01

The use of ocean color to study biological productivity and biochemical cycles; ocean dynamics and coastal processes; and technical aspects of ocean color remote sensing were discussed. ESA

N88-16293# European Space Agency, Paris (France). Earth Observation and Microgravity Directorate.
EUROPE'S POSITION CONCERNING OCEAN COLOUR ACTIVITIES
G. DUCHOSSOIS In its Ocean Colour Workshop p 7-8 Jul. 1987
Avail: NTIS HC A06/MF A01

The NIMBUS-7 Coastal Zone Color Scanner, and the ERS-1 Ocean Color Monitor studies are recalled, and ocean color studies on Columbus are suggested. An imaging spectrometer consisting of a high spatial resolution sensor for local, coastal monitoring, and a medium resolution, large swath instrument for continuous and global monitoring on a daily basis is proposed. It could fly on Polar Platforms. ESA

N88-16294# European Space Agency. European Space Research and Technology Center, ESTEC, Noordwijk (Netherlands). Earth Observation Dept.
OVERVIEW OF ESA'S ACTIVITIES IN OCEAN COLOUR REMOTE SENSING

M. RAST and M. REYNOLDS In its Ocean Colour Workshop p 9-11 Jul. 1987
Avail: NTIS HC A06/MF A01

The NIMBUS-7 Coastal Zone Color Scanner, and ERS-1 Ocean Color Monitor studies are recalled, and a pushbroom CCD imaging spectrometer is introduced. Ground pixel size is 300 m, swath width is 1071 km, and it has 8 spectral bands going from 0.4 to 1 micron. Studies on chlorophylls and yellow substances in sea water are mentioned. ESA

N88-16295*# National Aeronautics and Space Administration, Washington, D.C.
UPDATE OF NASA'S OCEAN COLOUR ACTIVITIES
J. A. YODER In ESA, Ocean Colour Workshop p 13-15 Jul. 1987 Original contains color illustrations
Avail: NTIS HC A06/MF A01 CSCL 08C

The NIMBUS-7 Coastal Zone Color Scanner (CZCS) status and processing are reviewed, and future American ocean color instruments are introduced. The CZCS is probably dead, but an attempt to restart it is planned. A wide field instrument for LANDSAT-6 and 7 (WIFS) and a whiskbroom imaging spectrometer (MODIS-T) for Columbus Polar Platforms are outlined. The WIFS and MODIS-T specifications are similar: 64 bands in the range 400 to 1030 nm, with 15 to 30 nm bandwidth; 1 km resolution from 850 km altitude; 64 km footprint along track; 1500 km scan across track; and 10 yr continuous operation life. ESA

N88-16296# Marine Biological Association of the United Kingdom, Plymouth (England).
REMOTE SENSING OF OCEAN COLOUR FOR STUDIES OF BIOLOGICAL PRODUCTIVITY AND BIOCHEMICAL CYCLES
P. M. HOLLIGAN and A. MOREL (Laboratoire d'Océanographie Physique, Paris, France) In ESA, Ocean Colour Workshop p 19-22 Jul. 1987 Original contains color illustrations
Avail: NTIS HC A06/MF A01

The use of ocean color to assess marine biological resources, to study photosynthetic processes (biomass primary production), and to follow biogeochemical cycles (such as CO₂ exchange between atmosphere and ocean, and phytoplankton effects on the carbon cycle) is discussed. Aerosol and sediment studies using narrow band visible scanners such as the Coastal Zone Color Scanner to examine materials exchange are mentioned. Steps which must be taken to exploit ocean color imagery in prediction of global environmental change are listed. ESA

N88-16297# Southampton Univ. (England). Dept. of Oceanography.
OCEAN COLOUR APPLICATIONS IN OCEAN DYNAMICS AND COASTAL PROCESSES
I. S. ROBINSON and D. SPITZER (Ministry of Transport and Waterways, The Hague, Netherlands) In ESA, Ocean Colour Workshop p 23-26 Jul. 1987
Avail: NTIS HC A06/MF A01

Use of ocean color as a tracer of ocean dynamics, in climate studies, and in coastal bathymetry was reviewed. Ideal spatial and temporal resolutions for studies of ocean basin circulation, mesoscale phenomena (ocean fronts and eddies), shelf sea processes, coastal and beach processes, and estuarine dynamics were established. Priority sensor requirements are for a medium resolution ocean color instrument for ocean, mesoscale, and shelf sea dynamics (Columbus Polar Platform) and a high resolution color sensor for coastal and estuarine studies (not necessarily a marine-dedicated instrument). ESA

05 OCEANOGRAPHY AND MARINE RESOURCES

N88-16298# European Space Agency. European Space Research and Technology Center, ESTEC, Noordwijk (Netherlands).

TECHNICAL ASPECTS OF FUTURE OCEAN COLOUR REMOTE SENSING

M. RAST *In its* Ocean Colour Workshop p 27-28 Jul. 1987
Avail: NTIS HC A06/MF A01

Performance requirements for a Polar Platform Ocean color sensor are given. Spatial resolution = 0.5×0.5 km; swath width is at least 1500 km; spectral bandwidth = 10 nm (nominal) 5 nm (goal); radiometric resolution = 12 bit; q spectral bands minimum (visible/near infrared); global daily coverage; tilt mode to avoid sunlight; sensitivity sufficient for low reflecting targets (e.g., ocean surface at high latitude) in order to get data at low solar illumination conditions; and it is essential that the sensor is insensitive to polarization conditions of scattered light. ESA

N88-16299# Joint Research Centre of the European Communities, Ispra (Italy).

STATUS AND PROSPECTS OF THE JOINT RESEARCH COMMITTEE (JRC) WORK ON THE APPLICATION OF OCEAN COLOUR MONITORING FROM SPACE

B. STURM, A. BECKERING, G. FRAYSSE, S. GALLIDEPARATESI, B. M. HENRY, G. MARACCI, L. NYKJAER, P. SCHLITTENHARDT, and S. TASSAN *In* ESA, Ocean Colour Workshop p 35-46 Jul. 1987

Avail: NTIS HC A06/MF A01

The status of activity on ocean color analysis is given. The main achievements are an operational software package for the evaluation of CZCS data and site specific interpretation algorithms for case 2-type water of the Northern Adriatic Sea which allow the elaboration of geometrically corrected maps of pigment and total suspended matter concentrations and of diffuse attenuation coefficient. Applying these techniques to an extensive archive of CZCS data from the Adriatic Sea, the ultimate goal is to assess remote sensing of anthropogenic pollutants; and to develop a methodology to predict the movement and dispersion of pollutants in estuarine and coastal zones. ESA

N88-16300# Institute of Ocean Sciences, Sidney (British Columbia).

CANADIAN ACTIVITIES AND GOALS IN REMOTE SENSING OF OCEAN COLOUR AND FLUORESCENCE FROM SPACE

J. F. R. GOWER *In* ESA, Ocean Colour Workshop p 41-48 Jul. 1987 Original contains color illustrations

Avail: NTIS HC A06/MF A01

Uses of ocean color remote sensing in oceanography, fisheries research and management, coastal zone mapping, and bathymetry are described. The importance of this work, and the development of an airborne phytoplankton mapping technique based on solar-stimulated chlorophyll fluorescence, led to development of an imaging spectrometer as a prototype satellite sensor. Results from this instrument are shown. Examples of airborne hydrography with passive and active sensors are also presented. ESA

N88-16301# Geneva Univ. (Switzerland). Dept. de Geologie et de Paleontologie.

RESEARCH IN SWITZERLAND ON OCEAN AND INLAND-WATER COLOUR MONITORING

J.-M. JAQUET *In* ESA, Ocean Colour Workshop p 49-52 Jul. 1987 Original contains color illustrations

Avail: NTIS HC A06/MF A01

Research in water color monitoring is reviewed. The development of algorithms addressing the complexity of inland waters is discussed. ESA

N88-16302# Deutsche Forschungs- und Versuchsanstalt fuer Luft- und Raumfahrt, Oberpfaffenhofen (West Germany). Inst. fuer Optoelektronik.

FEDERAL REPUBLIC OF GERMANY'S INTERESTS, ACTIVITIES AND GOALS IN REMOTE SENSING OF OCEAN COLOUR/FLUORESCENCE FROM SPACE

H. VANDERPIEPEN *In* ESA, Ocean Colour Workshop p 53-58 Jul. 1987 Original contains color illustrations

Avail: NTIS HC A06/MF A01

Scientific research and technical developments concerning natural fluorescence in context of with an ocean color monitor as payload on the polar platforms of the Columbus program are reviewed. Application programs, scientific and user communities, and government involvement in oceanography are described. ESA

N88-16303# Centre National d'Etudes Spatiales, Paris (France). **FRENCH ACTIVITIES IN OCEAN COLOUR OBSERVATIONS**

J.-L. FELLOUS and A. MOREL *In* ESA, Ocean Colour Workshop p 59-69 Jul. 1987 Original contains color illustrations

Avail: NTIS HC A06/MF A01

The use of CZCS data as well as AVHRR and high resolution LANDSAT-TM and SPOT imagery in ocean color studies is reviewed. Main research programs and experiments are coordinated with international efforts such as TOGA, WOCE, and GOFS. Plans to fly a large-swath visible and near IR sensor (named Vegetation) on the remote sensing satellite SPOT-4 (mid-1992) for vegetation and ocean color monitoring are revealed. ESA

N88-16304# Consiglio Nazionale delle Ricerche, Venice (Italy). Lab. per lo Studio della Dinamica delle Grande Masse.

ITALIAN ACTIVITIES IN OCEAN COLOUR REMOTE SENSING

R. FRASSETTO and L. PANTANI (Consiglio Nazionale delle Ricerche, Florence, Italy) *In* ESA, Ocean Colour Workshop p 71-72 Jul. 1987 Original contains color illustrations

Avail: NTIS HC A06/MF A01

The potential of ocean color remote sensing over coastal and offshore areas of Italy in providing valuable information for planning and decision making of public administrative agencies is demonstrated. The principal interest is in pollution monitoring, including thermal pollution near shore and in forecast of eutrophication. Technological research is directed to the development of instruments for in-situ or airborne measurements in air and water. User activity and interests in ocean color are described. ESA

N88-16305# Ministry of Transport and Waterways, The Hague (Netherlands). Tidal Waters Div.

NATIONAL REMOTE SENSING PROGRAM (NRSP) OF THE NETHERLANDS

D. SPITZER *In* ESA, Ocean Colour Workshop p 83-90 Jul. 1987 Sponsored by the Netherlands Remote Sensing Board, the National Aerospace Lab. and Netherlands Inst. for Sea Research Original contains color illustrations

Avail: NTIS HC A06/MF A01

Structure and organization of remote sensing are outlined. Priorities and projects are mentioned with respect to operationalization, commercialization, applied and fundamental research, technology development, and infrastructure. Progress in remote sensing of ocean color is highlighted. Applications of the pushbroom airborne scanner CAESAR having spectral characteristic similar to the OCM, including the fluorescence channels, are emphasized. Underwater and low altitude radiometers were developed allowing an improved interpretation of the remotely sensed imagery. ESA

N88-16306# Southampton Univ. (England). Dept. of Oceanography.

DEVELOPMENTS IN OCEAN COLOUR RESEARCH IN THE UNITED KINGDOM

I. S. ROBINSON and P. M. HOLLIGAN (Marine Biological Association of the United Kingdom, Plymouth, England) *In* ESA, Ocean Colour Workshop p 91-99 Jul. 1987 Original contains color illustrations

Avail: NTIS HC A06/MF A01

Requirements for ocean color sensors are outlined. Coordinated programs for marine science, having an ocean color component, are mentioned. Details of the Ocean Fluxes study are given. ESA

N88-16307# GKSS-Forschungszentrum Geesthacht (West Germany).

THE USE OF CHLOROPHYLL FLUORESCENCE MEASUREMENTS FROM SPACE FOR SEPARATING CONSTITUENTS OF SEA WATER

H. GRASSL *In* ESA, Ocean Colour Workshop p 103-109 Jul. 1987

Avail: NTIS HC A06/MF A01

Remote sensing of chlorophyll-a is reviewed. Chlorophyll-a shows a Sun stimulated fluorescence line peaking at 685 nm wavelength. This spectral feature is detectable from airplanes at all chlorophyll-a concentrations at least down to a chlorophyll-a content of 1 g/cum, also in turbid coastal waters. For space applications absorption by atmospheric gases for wavelengths above 688 nm forces a fluorescence channel to the shortwave part of the fluorescence line. The influence of nonchlorophyllous suspensions and of Gelbstoff on fluorescence is small. Fluorescence efficiency dependence on insolation is small at Sun elevations above 20 to 30 deg, the typical remote sensing conditions. Recommendations for a space application are listed.

ESA

N88-16308# GKSS-Forschungszentrum Geesthacht (West Germany).

THE INFLUENCE OF YELLOW SUBSTANCES ON REMOTE SENSING OF SEA-WATER CONSTITUENTS FROM SPACE

H. GRASSL *In* ESA, Ocean Colour Workshop p 111-118 Jul. 1987 Original contains color illustrations

(Contract ESA-RFQ-3-5060/84-NL-MD)

Avail: NTIS HC A06/MF A01

Gelbstoff influence on upward radiance spectra at the surface as well as at satellite altitude, and on the use of Gelbstoff as a tracer for salinity were studied. Results show that only inverse modeling using absolutely calibrated multichannel radiance values is able to separate Gelbstoff from phytoplankton and suspended matter, and that Gelbstoff is stable enough to be used as a tracer for salinity in coastal waters as long as the riverine concentration is known. Recommendations for a satellite Gelbstoff sensor are made.

ESA

N88-17155# Naval Postgraduate School, Monterey, Calif.
SEA SURFACE CURRENT ESTIMATES OFF CENTRAL CALIFORNIA AS DERIVED FROM ENHANCED AVHRR (ADVANCED VERY HIGH RESOLUTION RADIOMETER) INFRARED IMAGES M.S. Thesis

CHUNG-MING FANG Sep. 1987 51 p

(AD-A186867) Avail: NTIS HC A04/MF A01 CSCL 08C

A technique is presented which uses an interactive computer program to estimate sea surface current velocities from the displacement of Sea Surface Temperature (SST) patterns apparent in enhanced sequential infrared images obtained from the NOAA-6 Advanced Very High Resolution Radiometer (AVHRR). This technique was applied to the surface currents of the California current system using IR image data from 27 and 28 April 1981. This technique, which uses enhanced pseudocolor gradient imagery, produced more current vectors than an earlier technique developed by O'Hara (1987) which used unenhanced gray scale imagery. The resultant surface vectors agree well in direction but underestimate velocities obtained from Doppler Acoustic Log (DAL) measurements taken during the same period. The two methods produced closest agreement of current velocities of less than 40 cm/sec and with satellite-derived velocities obtained with sequential 12 hour images rather than sequential 24 hour images. Satellite-derived velocities in the rapid flow area (larger than 40 cm/sec) showed poor correspondence to DAL-measured velocities. The strong current shear in these areas may distort the surface SST patterns making identification of features between two images more difficult.

GRA

N88-17158# Royal Australian Navy Research Lab., Edgecliff.
OCEANOGRAPHIC FEATURES OF THE EAST AND SOUTHEAST INDIAN OCEAN FOR JUNE 1983

L. J. HAMILTON Feb. 1987 31 p

(AD-A186948; RANRL-TM-3/87; DODA-AR-003-463) Avail: NTIS HC A03/MF A01 CSCL 08C

During the period late May to late June 1983 two research vessels and seven ships of opportunity transited sections of the south-east and east Indian Ocean. Expendable bathy thermographs were deployed and several Nansen stations occupied, providing a rare occasion of wide-spread quasisynoptic data coverage for the area. Satellite imagery is available from two sources and three satellite tracked drifting buoys were in the area. Data are used to form a broad scale description of oceanographic conditions for the period, with more detailed analysis possible in the area north-west of Australia. Comparisons are made with data from the Indian Ocean Expedition of early 1960s and other sources. The relation of surface thermal patterns to circulation is examined.

GRA

N88-17159# Coastal Engineering Research Center, Vicksburg, Miss.

NEARSHORE WAVE TRANSFORMATION STUDY OF SITES NEAR PORT CANAVERAL INLET, FLORIDA Final Report

WILLIE A. BROWN, REBECCA M. BROOKS, and EDWARD F. THOMPSON Sep. 1987 48 p

(AD-A186965; CERC-MP-87-16) Avail: NTIS HC A03/MF A01 CSCL 08C

This report describes a 20-year summary of nearshore wave estimates of shoaling and transformation of waves in the vicinity of Cape Canaveral. The objective of this study was to obtain data which could be used in determining sediment transport in the Port Canaveral Inlet. These data consisted of breaking wave conditions at five different sites along the coastline near Port Canaveral Inlet.

GRA

N88-17160# Washington Univ., Seattle. School of Oceanography.

NORTH PACIFIC OCEAN. CENTRAL PACIFIC TRANSITION ZONE, R/V THOMAS G. THOMPSON: 25 MARCH - 3 MAY 1968. STD DATA REPORT

GUNNAR I. RODEN and WILLIAM J. FREDERICKS 1987 284 p

(Contract N00014-67-A-0103; N00014-84-C-0111)

(AD-A186570; CONTRIB-1716) Avail: NTIS HC A13/MF A01 CSCL 08C

During March and April 1968, scientists aboard the R/V Thomas G. Thompson studied the thermohaline and density structures in the subarctic-subtropical transition zone of the central North Pacific. Additional hydrographic sections were made north of Kahuka Point, Oahu. Of the 130 STD stations planned for this area, 127 were completed and 3 were lost because of weather. The primary objectives of the field study were: (1) to investigate the mesoscale thermohaline and density structures in long meridional resolution sections across the subarctic and subtropical boundaries; (2) to determine the mesoscale signatures of the subarctic and subtropical fronts at the boundaries of the transition zone; (3) to study the mesoscale dynamic height and baroclinic flow structures across the transition zone; and (4) to access the submesoscale thermohaline and baroclinic flow variability in the vicinity of the Hawaiian Ridge.

GRA

N88-17162# Massachusetts Inst. of Tech., Cambridge. Research Lab. of Electronics.

ACTIVE AND PASSIVE REMOTE SENSING OF ICE Semiannual Report, 1 Feb. - 31 Jul. 1987

JIN A. KONG 31 Jul. 1987 11 p

(Contract N00014-83-K-0258)

(AD-A186685) Avail: NTIS HC A03/MF A01 CSCL 08L

We have studied volume scattering effects of snow-covered sea ice with a three-layer random medium model for microwave remote sensing. Strong fluctuation theory and bilocal approximation are applied to calculate the effective permittivities for snow and sea ice. Wave scattering theory, in conjunction with the distorted Born approximation, is then used to compute bistatic coefficients and backscattering cross sections. We also derived a general

05 OCEANOGRAPHY AND MARINE RESOURCES

mixing formula for discrete scatterers immersed in a host medium. The results are applicable to general multiphase mixtures, and the scattering ellipsoids of the different phases can have different sizes and arbitrary ellipticity distribution and axis orientation, i.e., the mixture may be isotropic or anisotropic. The Mueller matrix and polarization covariance matrix are described for polarimetric radar systems. Clutter is modelled by a layer of random permittivity, described by a three-dimensional correlation function, with variance, and horizontal and vertical correlation lengths. Study of the strong fluctuation theory for a bounded layer of random discrete scatterers is extended to include high-order co-polarized and cross-polarized second moments. We have derived the dyadic Green's function for a two-layer anisotropic medium. GRA

N88-17163 GKSS-Forschungszentrum Geesthacht (West Germany). Inst. fuer Physik.

INVESTIGATION OF THE QUANTITATIVE DETERMINATION OF TWO DIMENSIONAL SEA SURFACE WAVE SPECTRA FROM SHIPBORNE RADAR MEASUREMENTS Thesis - Hamburg Univ., Fed. Republic of Germany [UNTERSUCHUNG ZUR QUANTITATIVEN BESTIMMUNG ZWEIDIMENSIONALER SEEANGANGSSPEKTREN AUS MESSUNGEN MIT NAUTISCHEM RADAR]

F. ZIEMER 3 Dec. 1987 158 p In GERMAN; ENGLISH summary

(GKSS-87/E/10; ISSN-0344-9629; ETN-88-91047) Avail:

Fachinformationszentrum, Karlsruhe, Fed. Republic of Germany

A shipborne microwave system (X-band) for routine imaging of sea surface waves is presented. The applied measurement and analysis technique provides the asymmetric energy density spectra versus wavenumber components with a very high signal to noise ratio. Deviations of the wave energy from the dispersion shell give the amount and direction of near-surface current. The radar results agree well with those of other measurements. The image transfer function was investigated by measurements and computer simulations. The observed effects of antenna viewing direction, distance from the imaged scene, and average wave height were parameterized, providing a first step toward the development of a self calibrating system. ESA

N88-17164# Kiel Univ. (West Germany). Inst. fuer Meereskunde.

HYDROGRAPHIC AND CURRENT MEASUREMENTS IN THE NORTH-EAST ATLANTIC OCEAN. DATA REPORT ON F.S. METEOR CRUISES 69/5 AND 69/6, OCTOBER TO NOVEMBER 1984

T. J. MUELLER, M. FINKE, W. DASCH, and R.-R. WITTSTOCK 1987 110 p (REPT-166; ISSN-0341-8561; ETN-88-91471) Avail: NTIS HC A06/MF A01

Hydrographic data and 1 year long records from 6 mooring sites in the NE Atlantic Ocean between 20 N and 41 N and east of 27 W were collected. Sections of temperature, salinity, and density by an in situ calibrated CTD-system; sections from expendable bathythermograph casts; measurements of a geomagnetic electro-kinetograph, and near surface temperature and salinity are shown. From current meter mooring site (33 N, 22 W) the continuation of low pass filtered time series started in 1980 is shown. Five further sites along 28 N were equipped with 2 long (400 m) thermistor cable moorings and a current meter in the main thermocline. ESA

N88-17165# Kiel Univ. (West Germany). Inst. fuer Meereskunde.

ANALYSIS OF LOW FREQUENCY CURRENT FLUCTUATIONS IN THE NORTH-EAST ATLANTIC OCEAN Thesis

T. J. MUELLER 1987 146 p In GERMAN; ENGLISH summary (REPT-170; ISSN-0341-8561; ETN-88-91472) Avail: NTIS HC A07/MF A01

Eulerian current measurements from 13 positions in the Atlantic between 28 N and 42 N and east of 27 W are analyzed. Most of the time series are from the main thermocline and 200 to 380

days long; for position N1, (33 N, 22 W) the series are 2049 days long. Mean current vectors confirm the mean baroclinic circulation pattern inferred from historical data but show higher velocities. Integral time scales of the fluctuating part of the currents are of the order of 20 to 30 days. Only the east component on position N1 has an extremely long integral time scale (70 days). The level of the fluctuating part of kinetic energy is moderate according to position and depth. In the northern Canary basin it has a maximum in the range 50 to 200 days. Neither in the currents nor in their variances is a seasonal signal detected. The zonal component at N1 shows a very slowly varying signal of 3.5 year period. Barotropic and the first baroclinic mode contain greater than 80 percent of the fluctuating part of the energy. ESA

N88-17166# Old Dominion Univ., Norfolk, Va. Research Foundation.

CONTINENTAL SHELF PROCESSES AFFECTING THE OCEANOGRAPHY OF THE SOUTH ATLANTIC BIGHT Progress Report, 1 Jun. 1987 - 31 May 1988

L. P. ATKINSON Jan. 1988 37 p

(Contract DE-FG05-85ER-60348)

(DE88-004102; DOE/ER-60348/7; TR-87-12) Avail: NTIS HC A03/MF A01

This study of continental shelf processes affecting the oceanography of the South Atlantic Bight (SAB) is part of the interdisciplinary DOE-sponsored South Atlantic Bight Program. Our part of the program involves hydrographic and nutrient characteristics of the region. Current research efforts in the SAB Program are being focused on the inner shelf region where effects of bottom friction, local wind forcing, river and estuarine discharge, and tides, which are all small scale processes, are important. Our major accomplishment during the past year was the completion of the FLEX (Fall Experiment) field study. Since most of our data collection is computerized, preliminary hydrographic data analysis was done on board ship during the cruise and preliminary results are available. These results will be presented in this report. We are just beginning our standard data processing and data analysis procedures. We continued the processing and analysis of SPREX data collected during April 1985. Work has also continued on the older GABEX I and II data sets. DOE

N88-17167# Academy of Sciences (USSR), Moscow. Soviet Geophysical Committee.

MATERIALS OF THE WORLD DATA CENTER B. DEEP SEISMIC SOUNDING (DSS): PACIFIC DATA

1987 108 p In RUSSIAN; ENGLISH summary

Avail: NTIS HC A06/MF A01

The catalog contains results obtained by the method of deep seismic sounding in the Pacific Ocean in experiments begun in 1948 to 1950 and then continued into the early 1980's. The tables of velocity values and thickness of Earth crustal layers, the parameters of the M boundary as well as schemes of seismic sections for more detailed studies are presented. The tables are compiled on the basis of previous publications and available summaries. The distinctive feature of the catalog is that the tables give the information based on observational methods. To demonstrate, the legend chosen on the basis of the analysis of the system of travel-time curves, and the characteristics of sources and receivers are taken into account. This approach allows the scientists to evaluate the relative reliability of each section. The peculiarities of the method are indicated in the study map showing the areas of investigations. Author

N88-18109# National Aeronautics and Space Administration, Washington, D.C.

NASA OCEANIC PROCESSES PROGRAM Biennial Report, fiscal years 1986 and 1987

Feb. 1988 183 p

(NASA-TM-4025; NAS 1.15:4025) Avail: NTIS HC A09/MF A01 CSDL 08C

An overview of the recent accomplishments, present activities, and future plans is provided. Sections following the introduction provides summaries of current flight projects and definition studies,

brief descriptions of individual research activities, and a bibliography of referred Journal Articles appearing within the last three years.

Author

N88-18110# Skidaway Inst. of Oceanography, Savannah, Ga.
COORDINATION: SOUTHEAST CONTINENTAL SHELF STUDIES Progress Report, 1 Jun. 1986 - 31 Dec. 1987

D. W. MENZEL 11 Dec. 1987 31 p

(Contract DE-FG09-86ER-60450)

(DE88-003680; DOE/ER-60450/T1) Avail: NTIS HC A03/MF A01

The principal investigator coordinated activities associated with the conduct of research on the oceanography of the southeastern continental shelf. These activities included serving as a contact between program managers at DOE and principal investigators associated with the program, developing long-range research plans, providing DOE with summaries of the results of past and current research activities, conducting planning/reporting meetings involving principal investigators and interested agency personnel, and consolidating and scheduling the use of research vessels.

DOE

N88-19057# Woods Hole Oceanographic Institution, Mass.
ESTIMATION OF SEA SURFACE WAVE SPECTRA USING ACOUSTIC TOMOGRAPHY Ph.D. Thesis

JAMES H. MILLER Sep. 1987 176 p

(Contract N00014-87-K-0017)

(AD-A187837; WHOI-87-31) Avail: NTIS HC A09/MF A01

CSCS 08C

This thesis develops a new technique for estimating quasi-homogeneous and quasi-stationary sea surface wave frequency-direction spectra using acoustic tomography. The analysis of acoustic (mode and ray) phase and travel time perturbations due to a rough sea surface is presented. Two canonical waveguides (ideal shallow water and linear squared index of refraction) are used as examples for the mode perturbation. The analysis is used to explain high mode coherence measured in the FRAM IV experiment. The forward problem of computing the acoustic phase and travel time perturbation spectra given the surface wave spectrum is solved to first order. An application of the technique to ray phase data taken during the MIZEX '84 experiment is shown. The inverse problems for the homogeneous and quasi-homogeneous frequency-direction spectrum are introduced. The theory is applied to synthetic data which simulate a fetch-dependent sea. The estimates made agree well with the actual (synthetic data) spectrum. The effect of noise in the travel time estimates is studied. The sensitivity of the technique to the number of rays used in the inversion is investigated and the resolution and variance of the inverse method are addressed.

GRA

N88-19058 Maryland Univ., College Park.
SPATIAL-TEMPORAL VARIABILITY OF NORTH PACIFIC SEA SURFACE TEMPERATURE ANOMALY PATTERNS Ph.D. Thesis

JOHN ALBERT ERNST 1987 310 p

Avail: Univ. Microfilms Order No. DA8725499

General Circulation Models were used in the diagnostic mode to assess the importance of the underlying initial boundary condition under the hypothesis that North Pacific sea surface temperature anomalies are an important link in the teleconnective specification of downstream atmospheric weather patterns. The objectives of this study are: to specify the North Pacific sea surface temperature anomaly patterns over the period 1947 to 1983; to determine quantitatively the geographic distribution of the spatial-temporal variability associated with each type of anomaly pattern; and to assess the significance of the resultant type patterns in terms of cloud amount anomaly changes at selected geographic areas. An objective classification of seasonally composited gridpoint values of sea surface temperature anomalies was performed using linear correlation to identify 18 patterns in the North Pacific. The first five types were found to have comprised more than 62 percent

of the total number of seasonal anomaly composite maps.

Dissert. Abstr.

N88-19059 New South Wales Univ., Sydney (Australia).
FIVE NEW SOUTH WALES BARRIER LAGOONS: THEIR MACROBENTHIC FAUNA AND SEAGRASS COMMUNITIES Abstract Only. Ph.D. Thesis

PHILIP JOHN GIBBS Dec. 1986 244 p

Avail: Issuing Activity

The distribution of sea grasses was determined in five lagoons: Queens Lake, Lake Macquarie, Lake Illawarra, Burrill Lake, and Merimbula Lake. The macrobenthic invertebrates were sampled in 1976 and 1977 at 15 sites in the 3 major sedimentary habitats, the marine sand entrance channel, the sublittoral fringe and the central mud basin of each lagoon. Temporal variability in the flora, nutrients, and fauna of the sublittoral fringe habitat of Merimbula Lake was assessed bimonthly over 3 years, 1978 to 1982. Hypotheses relating the biota of barrier lagoons to their geological evolution, biogeography, and coastal zone management are tested. The lagoons span the 2A type in the estuarine evolutionary model of Roy. Elements of the estuarine faunas have cosmopolitan, subtropical northern or cool to cold temperate southern distributions, which cross the boundaries of accepted biogeographic provinces defined for the southeastern Australian exposed rocky shores. A model relating estuarine faunal distribution patterns and offshore ocean currents is presented. Low level sewage enrichment in the sublittoral fringe of Merimbula Lake was compared with levels for the agricultural catchment. Bacteriological studies, however, indicated inadequate management of foreshore effluent disposal systems. Eutrophication is a future consequence for the lagoon.

Author

N88-19060 New South Wales Univ., Sydney (Australia).
MESOSCALE COASTAL OCEAN DYNAMICS Abstract Only Ph.D. Thesis

DAVID A. GRIFFIN Nov. 1986 146 p

Avail: Issuing Activity

An analysis of observed circulation over the continental shelf and slope of the southern Great Barrier Reef (GBR), and a theoretical examination of wind driven flow in an infinite channel are presented. Current meters and water level recorders were deployed in the Capricornia section of the GBR from June to December, 1983. Tidal analyses of the hourly data set reveal an amplification of the semidiurnal tides as they propagate north-westward into the Capricorn Channel. The observed M sub 2 tidal heights and currents are in excellent agreement with the results of a barotropic numerical model. The longer period fluctuations of current, sea level, temperature, and wind stress are interpreted by comparison with coastal trapped wave (CTW) theories. Near-coastal currents and sea levels are modeled with some success by a theory of locally wind-forced barotropic continental shelf waves. Recorded temperatures and CTD data reveal that both tidal and longer period currents contribute to periodic upwelling onto the shelf. Secondly, the steady, wind driven, barotropic flow in long frictional channels of parabolic depth profile is examined analytically. Driven by spatially sinusoidal along-channel wind stress, the nature of the circulation depends mainly on the dimensionless channel width. The predicted steady wind driven circulation of Lake Ontario is in accord with observations.

Author

N88-19262# Scripps Institution of Oceanography, La Jolla, Calif. Visibility Lab.

REMOTE SENSING OF ATMOSPHERIC OPTICAL THICKNESS AND SEA-WATER ATTENUATION WHEN SUBMERGED: WAVELENGTH SELECTION AND ANTICIPATED ERRORS Final Report, 1 Jul. 1978 - 30 Apr. 1986

T. J. PETZOLD and R. W. AUSTIN Jul. 1987 84 p

(Contract N00014-78-C-0556)

(AD-A187609; SIO-REF-87-18) Avail: NTIS HC A05/MF A01

CSCS 20F

Prior analysis and experimentation has provided strong support for determining the attenuation of optical radiation for the

atmosphere and the water column above a submerged platform by measuring the absolute downwelling irradiance at two wavelengths. The technique requires knowing the two irradiance values and also: (1) the spectral irradiance of the Sun outside the atmosphere; (2) the solar zenith angle; and (3) the depth at which the irradiances are measured. With this capability in hand, the questions considered in this report are which wavelengths to use and the effect of errors in the measurement of irradiance and other parameters. GRA

N88-19879# Army Cold Regions Research and Engineering Lab., Hanover, N.H.

AIRBORNE ELECTROMAGNETIC SOUNDING OF SEA ICE THICKNESS AND SUB-ICE BATHYMETRY

AUSTIN KOVACS, NICHOLAS C. VALLEAU, and J. S. HOLLADAY Dec. 1987 47 p
(AD-A188939; CRREL-87-23) Avail: NTIS HC A03/MF A01 CSCL 08L

A study was made in May 1985 to determine the feasibility of using an airborne electromagnetic sounding system for profiling sea ice thickness and the sub-ice water depth and conductivity. The study was made in the area of Prudhoe Bay, Alaska. The multifrequency airborne electromagnetic sounding system consisted of control and recording electronics and an antenna. The electronics module was installed in a helicopter, and the 7 m long tubular antenna was towed beneath the helicopter at about 35 m above the ice surface. For this electromagnetic system, both first-year and second-year sea ice could be profiled, but the resolution of ice thickness decreased as the ice became rough. This decrease was associated with the large footprint of the system, which effectively smoothed out the sea ice relief. Under-ice water depth was determined, as was seawater conductivity. The results of the feasibility study were encouraging, and further system development is therefore warranted. GRA

N88-19882# SACLANT ASW Research Center, La Spezia (Italy).

THE EFFECTS OF ATMOSPHERIC AND THERMOHALINE VARIABILITY ON THE VALIDATION OF THE GEOSAT ALTIMETER OCEANOGRAPHIC SIGNAL BETWEEN SCOTLAND AND ICELAND

P. J. MINNETT Oct. 1987 39 p
(AD-A189324; SACLANTCEN-SR-128) Avail: NTIS HC A03/MF A01 CSCL 08C

Atmospheric and oceanographic profiles from the area between Scotland and Iceland are analyzed in order to predict the magnitudes of the errors they can induce in satellite altimeter measurements of sea-surface topography. This is the area where the second phase of the COMPASS project will take place in early 1988, and the aim is to provide absolute calibration data for the GEOSAT altimeter by using coastal land-based active microwave transponders. While most of the variability in the sea-surface topography can be ascribed to variations in the temperature profile, the spatial changes in the temperature-salinity relationship are such that errors in the sea-surface topography predicted from measured temperature profiles can not be neglected. This means that the validation of the altimeter oceanographic signal can not be done in this area by using only the more readily-available temperature profiles from expendable probes. The atmospheric variability characteristic of this area can induce errors in the altimeter range measurement comparable to the oceanographic signal, and careful corrections are necessary. These will have to faithfully reflect the changes in atmospheric properties along the COMPASS arc. GRA

HYDROLOGY AND WATER MANAGEMENT

Includes snow cover and water runoff in rivers and glaciers, saline intrusion, drainage analysis, geomorphology of river basins, land uses, and estuarine studies.

A88-21002

DEVELOPMENT OF MULTIDATE ESTUARINE WATER QUALITY MODELS USING LANDSAT 2 AND 4 MSS DATA

PATRICK D. PELKEY (Integrat Corp., Huntsville, AL) and SIAMAK KHORRAM (North Carolina State University, Raleigh) IN: American Society for Photogrammetry and Remote Sensing and ACSM, Annual Convention, Baltimore, MD, Mar. 29-Apr. 3, 1987, Technical Papers. Volume 1. Falls Church, VA, American Society for Photogrammetry and Remote Sensing and ACSM, 1987, p. 1-17. Research supported by the California State Resources Agency. refs

(Contract NOAA-NA-80AAD00120)

Predictive multivariate water-quality models developed for 1980 and 1983 turbidity, total suspended solid (TSS), and salinity concentrations in the San Pablo Bay, San Francisco Bay and Delta regions, California, on the basis of Landsat MSS reflectance values were tested for statistical significance, the quality of the fit, and structural consistency. The results of data analysis indicate that Landsat MSS could detect differences in hydrodynamic conditions between the San Francisco Bay and Delta for the 1980 and 1983 scenes. Water quality models were successful in predicting distributions of 1980 and 1983 Delta turbidity, 1983 Delta TSS, and 1980 Delta salinity. The Delta TSS models were the only functions which could be expressed in a generalized form, where one model could describe both dates despite differences in Delta flow conditions, tide phases, satellite sensors, and sun elevation. The restricted applicability of regional generalized models may be limited because of extreme differences in physical conditions on the two dates. It is suggested that seasonal models may be more appropriate. I.S.

A88-21004

COMPARISON OF LANDSAT MSS PIXEL ARRAY SIZES FOR ESTIMATING WATER QUALITY VARIABLES IN SMALL LAKES

JERRY C. RITCHIE (USDA, Hydrology Laboratory, Beltsville, MD) and CHARLES M. COOPER (USDA, Sedimentation Laboratory, Oxford, MS) IN: American Society for Photogrammetry and Remote Sensing and ACSM, Annual Convention, Baltimore, MD, Mar. 29-Apr. 3, 1987, Technical Papers. Volume 1. Falls Church, VA, American Society for Photogrammetry and Remote Sensing and ACSM, 1987, p. 27-36. refs

Different Landsat MSS-pixel array sizes for estimating water quality variables were analyzed for the Moon Lake, Mississippi, water to determine the extent to which pixels of different size are representative of the whole area. Nested arrays of pixels with sizes of 5 x 5, 3 x 3, and 2 x 2, and the single center pixel of the 5 x 5 array were sampled at five different locations where water quality variables had been measured; 14 different Landsat scenes for the period between January 1983 and June 1985 were analyzed. Pixel values were significantly correlated with water quality variables, such as total suspended solids and chlorophyll-a, for all array sizes. However a paired T-test of the mean of the differences between array pairs showed that the single center pixel and 2 x 2 pixel arrays may not be representative of the larger pixel arrays. I.S.

A88-21006

MONITORING NORTH CAROLINA'S NUTRIENT-SENSITIVE RESERVOIRS USING LANDSAT TM DIGITAL DATA

H. M. CHESHIRE and S. KHORRAM (North Carolina State University, Raleigh) IN: American Society for Photogrammetry and Remote Sensing and ACSM, Annual Convention, Baltimore,

MD, Mar. 29-Apr. 3, 1987, Technical Papers. Volume 1. Falls Church, VA, American Society for Photogrammetry and Remote Sensing and ACSM, 1987, p. 47-56. refs

A88-21007

REMOTE SENSING OF AQUATIC MACROPHYTE DISTRIBUTION IN SELECTED SOUTH CAROLINA RESERVOIRS

JOHN R. JENSEN and BRUCE A. DAVIS (South Carolina, University, Columbia) IN: American Society for Photogrammetry and Remote Sensing and ACSM, Annual Convention, Baltimore, MD, Mar. 29-Apr. 3, 1987, Technical Papers. Volume 1. Falls Church, VA, American Society for Photogrammetry and Remote Sensing and ACSM, 1987, p. 57-65. refs

Several state agencies are responsible for monitoring the spread of aquatic macrophytes throughout South Carolina lakes and streams. Remote sensing research was conducted on six reservoirs to determine the identity and geographic distribution of aquatic macrophytes. Color infrared aerial photography acquired at 5,200 and 10,000 feet above ground level provided detailed coverage of each reservoir. Aquatic macrophyte maps derived from the aerial photography were transferred to a UTM projection and then digitized. Results show that identification of both submergent and emergent vegetation was possible but that species identification was restricted to emergent vegetation only. In addition to the basic identification and mapping of aquatic macrophytes, it was also possible to identify cause and effect relationships between aquatic macrophyte distribution and water quality parameters in selected reservoirs. Furthermore, the polygonal macrophyte data represent a comprehensive data set which can be accessed, maintained, and updated by state agencies for use in resource management decisions. Author

A88-21011

GROUNDWATER IDENTIFICATION USING DIGITALLY ENHANCED NHAP

SIMA BAGHERI (New Jersey Institute of Technology, Newark) and ROBERT M. HORDON (Rutgers University, New Brunswick, NJ) IN: American Society for Photogrammetry and Remote Sensing and ACSM, Annual Convention, Baltimore, MD, Mar. 29-Apr. 3, 1987, Technical Papers. Volume 1. Falls Church, VA, American Society for Photogrammetry and Remote Sensing and ACSM, 1987, p. 94-103. refs

This study investigates the utilization of digitally enhanced National High Altitude Photography (NHAP) for identification of groundwater resources in the Sourland Mountain area of New Jersey. The Sourlands are underlain by diabase and argillite rocks which form one of the poorest areas in the state in terms of groundwater availability. A selected variety of microcomputer-based techniques were used to identify and enhance the fracture traces (faults, fractures and joints) as an aid in the determination of their geologic and hydrologic significance. Fracture traces in consolidated rock formations are usually associated with higher yielding wells since the secondary porosity is greater. NHAP color infrared transparencies were selected for their better resolution and fidelity in distinguishing between subtle differences in soil moisture and vegetation type. The goal of the research is to see if the delineated fracture traces are associated with known well yields so that future wells could be better located. Author

A88-21021

THE USE OF REMOTE SENSING IN DEVELOPING AND VALIDATING A GROUND HYDROLOGY/VEGETATION MODEL FOR GCM3

CYNTHIA ROSENZWEIG (Columbia University, New York) IN: American Society for Photogrammetry and Remote Sensing and ACSM, Annual Convention, Baltimore, MD, Mar. 29-Apr. 3, 1987, Technical Papers. Volume 1. Falls Church, VA, American Society for Photogrammetry and Remote Sensing and ACSM, 1987, p. 185-194. refs

Remotely sensed data may be used in the development of a ground hydrology model (GHM) for a general circulation model (GCM) through the prescription of land-surface characteristics and

for validation studies. Accuracy requirements for some GHM inputs and accuracy estimates for remotely sensed observations of these inputs are compared, and studies using satellite data to measure hydrological variables are considered as possible validation datasets for the GHM. Accuracy requirements for the GHM inputs studied are higher than satellite data can provide, although satellite prescription of fraction of land surface covered with vegetation may be feasible. GHM validation studies using satellite data are potentially useful, but may be hampered by low accuracy and other problems. Author

A88-21038

EVALUATION OF X-BAND SAR IMAGERY FOR MAPPING OPEN SURFACE WATER IN THE NORTHEASTERN UNITED STATES

FLOYD M. HENDERSON (New York, State University, Albany) IN: American Society for Photogrammetry and Remote Sensing and ACSM, Annual Convention, Baltimore, MD, Mar. 29-Apr. 3, 1987, Technical Papers. Volume 1. Falls Church, VA, American Society for Photogrammetry and Remote Sensing and ACSM, 1987, p. 365-370. refs

A88-21039

A TIME-LAPSE ANALYSIS OF THE MISSISSIPPI DELTA USING LANDSAT MSS BAND 4 (IR2) PHOTOGRAPHIC IMAGERY

RONALD J. WASOWSKI and STEPHEN B. FERRETTI (Notre Dame, University, IN) IN: American Society for Photogrammetry and Remote Sensing and ACSM, Annual Convention, Baltimore, MD, Mar. 29-Apr. 3, 1987, Technical Papers. Volume 1. Falls Church, VA, American Society for Photogrammetry and Remote Sensing and ACSM, 1987, p. 386-392. refs

Land area changes in the Mississippi Delta are examined on the basis of an analysis of Landsat MSS Band 4 (IR2) positive transparencies at a scale of 1:1,000,000 obtained on January 28, 1976, December 9, 1981, and February 13, 1985. The results of image interpretation confirm the usefulness of optical satellite remote sensing imagery for monitoring land area changes within the Mississippi delta. It is also suggested that radar imagery immune to the frequent cloud cover might be even more useful. V.L.

A88-21042

SPECTRAL ENHANCEMENTS OF LANDSAT MSS AND TM IMAGERY APPLIED TO GROUND WATER INVESTIGATIONS IN KENYA

MORRIS DEUTSCH (Satellite Hydrology, Inc., Vienna, VA) and HOWARD L. HEYDT (General Electric Co., Space Div., Lanham, MD) IN: American Society for Photogrammetry and Remote Sensing and ACSM, Annual Convention, Baltimore, MD, Mar. 29-Apr. 3, 1987, Technical Papers. Volume 1. Falls Church, VA, American Society for Photogrammetry and Remote Sensing and ACSM, 1987, p. 412-419.

A88-24198* Jet Propulsion Lab., California Inst. of Tech., Pasadena.

LANDSAT CLASSIFICATION OF THE BARREN HYDROLITTORAL AREAS OF LAKE YLI-KITKA, NORTH-EASTERN FINLAND

J. RAITALA (California Institute of Technology, Jet Propulsion Laboratory, Pasadena; Oulu, University, Finland), H. JANTUNEN, and J. LAMPINEN (Oulu, University, Finland) Space Technology - Industrial and Commercial Applications (ISSN 0277-4488), vol. 7, no. 4, 1987, p. 265-272. Research supported by the Foundation for Research of Natural Resources in Finland. refs

As a part of the project 'Landsat-studies for Mapping the Variables within Water Areas' this study deals with the classification possibilities of evaluating and mapping depth relations and bottom materials within the barren and clear-watered shores of Lake Yli-Kitka, North-Eastern Finland. It has been discovered that it is possible to distinguish open water areas with a water depth of more than about half of the Secchi disk depth from those of shallower hydrolittoral areas. The morainic, sandy and only slightly vegetated subareas of the shallow shores and shoals can possibly

be identified by using a simple classification procedure. The data used were recorded by the coarse-resolution Landsat MSS imagery system, and better results are expected after the experiences of the Landsat TM data and the availability of the SPOT material.

Author

A88-24662

EFFECT OF ICE-GRAIN SIZE DISTRIBUTION ON THE THERMAL EMISSION OF SNOW COVER [VLIANIE RASPREDELENIYA LEDIANYKH ZEREN PO RAZMERAM NA TEPLOVOE IZLUCHENIE SNEZHNOGO POKROVA]

V. V. DMITRIYEV, N. I. KLIORIN, V. G. MIROVSKII, and V. S. ETKIN (Moskovskii Gosudarstvennyi Pedagogicheskii Institut, Moscow, USSR) Akademiia Nauk SSSR, Doklady (ISSN 0002-3264), vol. 297, no. 6, 1987, p. 1363-1366. In Russian. refs

The influence of ice-grain size distribution on the thermal microwave emissivity of snow cover is studied with reference to remote-sensing studies. It is shown that the brightness temperature of snow depends strongly on its statistical characteristics. An increase in variance is associated with an increase in the number of small and large grains. In the long-wavelength region, where scattering is low, large particles lead to an increase in the variance, which leads in turn to a slight decrease in the brightness temperature. The effect of small particles is most pronounced in the short-wavelength region, where they substantially enhance absorption.

B.J.

A88-25730* National Aeronautics and Space Administration. Goddard Space Flight Center, Greenbelt, Md.

CHARACTERISTICS OF EXTREME RAINFALL EVENTS IN NORTHWESTERN PERU DURING THE 1982-1983 EL NINO PERIOD

R. A. GOLDBERG, G. M. TISNADO (NASA, Goddard Space Flight Center, Greenbelt, MD), and R. A. SCOFIELD (NOAA, Satellite Applications Laboratory, Washington, DC) Journal of Geophysical Research (ISSN 0148-0227), vol. 92, Dec. 15, 1987, p. 14225-14241. Research supported by the Instituto Nacional de Investigacion de Transportes of Peru, NOAA, and NASA. refs

Histograms and contour maps describing the daily rainfall characteristics of a northwestern Peru area most severely affected by the 1982-1983 El Nino event were prepared from daily rainfall data obtained from 66 stations in this area during the El Nino event, and during the same 8-month intervals for the two years preceding and following the event. These data were analyzed, in conjunction with the analysis of visible and IR satellite images, for cloud characteristics and structure. The results present a comparison of the rainfall characteristics as a function of elevation, geographic location, and the time of year for the El Nino and non-El Nino periods.

I.S.

A88-25735*

GAS EXCHANGE ON MONO LAKE AND CROWLEY LAKE, CALIFORNIA

RIK WANNINKHOF, JAMES R. LEDWELL, and WALLACE S. BROECKER (Lamont-Doherty Geological Observatory, Palisades, NY) Journal of Geophysical Research (ISSN 0148-0227), vol. 92, Dec. 15, 1987, p. 14567-14580. refs (Contract NAGW-667)

Gas exchange coefficients (k) have been determined for freshwater Crowley Lake and saline Mono Lake through the use of a man-made purposefully injected gas, SF₆. The concentration decreased from an initial value of 40 to 4 pmol/L for Mono Lake and from 20 to 1 pmol/L for Crowley lake over a period of 6 wks. Wind-speed (u) records from anemometers on the shore of each lake made it possible to determine the relationship between k and u . The average u and k values for the experiment were identical for the two lakes, despite the large chemical differences. It is estimated that, for the u values observed over Mono Lake from July to December 1984, the exchange of CO₂ occurred 2.5 times faster than without chemical enhancement. This is a factor of 4 lower than needed to explain the high invasion rate of C-14 produced by nuclear bomb tests.

Author

A88-27741

COMPLEX REMOTE MONITORING OF LAKES [KOMPLEKSNYI DISTANTSIONNYI MONITORING OZER]

K. IA. KONDRAT'EV, ED. Leningrad, Izdatel'stvo Nauka, 1987, 296 p. In Russian. No individual items are abstracted in this volume.

Papers are presented on remote-sensing investigations of lakes, with emphasis on the remote monitoring of the optical properties of lake waters and anthropogenic eutrophication; the study of thermal and radiative regimes; and the investigation of ice cover. Particular consideration is given to the remote sensing of chlorophyll in natural reservoirs, the comparative characterization of the radiative temperature and surface water temperature of lakes, microwave measurements of melting ice cover on lakes, and the organization of comprehensive remote monitoring of factors determining the eutrophication of Lake Ladoga.

B.J.

A88-27815

REMOTE SENSING OF SOIL MOISTURE

H. L. MCKIM, T. PANGBURN (U.S. Army, Cold Regions Research and Engineering Laboratory, Hanover, NH), J. E. WALSH, and P. J. LAPOTIN (Dartmouth College, Hanover, NH) (COSPAR, WMO, URSI, et al., Plenary Meeting, 26th, Symposium 3, Workshop V, and Topical Meeting A2 on Remote Sensing from Space, Toulouse, France, June 30-July 11, 1986) Advances in Space Research (ISSN 0273-1177), vol. 7, no. 11, 1987, p. 139-145. refs

A solid state, durable radiofrequency soil moisture probe is described that can be interrogated via a remote monitoring system. The probe can be used to monitor soil moisture changes in the field to an accuracy of + or - 5 percent by volume. The soil moisture data can be placed automatically into a geographic information system and used via a system dynamics approach to spatially average soil moisture changes over large areas. This integrated approach to provide water resource personnel with a data base for calculating soil storage required for flood forecasting and trafficability/mobility models.

C.D.

A88-27816

MONITORING HYDROCLIMATIC CHARACTERISTICS USING SATELLITE OBSERVATIONS FROM WEST AFRICA

O. OJO (Lagos, University, Nigeria) (COSPAR, WMO, URSI, et al., Plenary Meeting, 26th, Symposium 3, Workshop V, and Topical Meeting A2 on Remote Sensing from Space, Toulouse, France, June 30-July 11, 1986) Advances in Space Research (ISSN 0273-1177), vol. 7, no. 11, 1987, p. 147-151. refs

A88-29493

MULTITEMPORAL LANDSAT MULTISPECTRAL SCANNER AND THEMATIC MAPPER DATA OF THE HUBBARD GLACIER REGION, SOUTHEAST ALASKA

KIM-MARIE WALKER (TGS Technology, Inc., Anchorage, AK) and CHESTER ZENONE (USGS, Water Resources Div., Anchorage, AK) Photogrammetric Engineering and Remote Sensing (ISSN 0099-1112), vol. 54, March 1988, p. 373-376. refs

N88-16143# Ludwig-Maximilians-Universitaet, Munich (West Germany). Inst. fuer Meteorologie.

USE OF THE THERMODYNAMIC EVAPORATION FORMULA OF HOFFMANN IN ENERGY BALANCE MODELS FOR FLOWING WATER [DIE ANWENDUNG DER THERMODYNAMISCHEN VERDUNSTUNGSFORMEL NACH HOFMANN IN ENERGIEBILANZMODELLEN VON FLIESSGEWASSERN]

NORBERT BEIER In its Research Work at the Meteorological Institute of the University of Munich (Federal Republic of Germany) p 10-17 Mar. 1987 In GERMAN
 Avail: NTIS HC A11/MF A01

A linearized model equation of the first order nonlinear differential equation for the calculation of flowing water temperature was deduced. The assumptions leading to the linearized model equation are discussed. The introduction of the thermodynamic evaporation formula of Hoffmann leads to a piecewise analytically model equation, suitable for operational use. The resulting

approximation is only sufficiently accurate if air and water temperature differ only slightly. Otherwise, the model equation has to be expanded around the residual term of the Taylor expansion. However, the obtained accuracy is generally sufficient for the applications, given the limited accuracy of the meteorological and hydrological input quantities of the energy balance models. ESA

N88-16145# Ludwig-Maximilians-Universitaet, Munich (West Germany). Inst. fuer Meteorologie.

ENERGY BALANCE AND DISCHARGE OF AN ALPINE GLACIER, ILLUSTRATED BY MOUNT VERNAGTFERNER IN THE OETZAL ALPS, TYROL [ENERGIEBILANZ UND ABFLUSS EINES ALPENGLETSCHERS DARGESTELLT AM BEISPIEL DES VERNAGTFERNERS IN DEN OETZTALER ALPEN/TIROL] HEIDI ESCHER-VETTER *In its* Research Work at the Meteorological Institute of the University of Munich (Federal Republic of Germany) p 24-29 Mar. 1987 In GERMAN
Avail: NTIS HC A11/MF A01

A meteorological-hydrological glacier discharge model was developed. The model approximation for the energy balance from which the available melted snow and ice are deduced is presented. The simulation of the discharge at a weather station using a mathematical model is explained. The results show that a simple energy balance model allows the calculation of the melted snow and ice production in a limited area, with a time and superficial resolution sufficient to use the data as input for a discharge model. Although not all phenomena were modeled in detail, there is good agreement between the modelled and the measured discharge.

ESA

N88-16147# Ludwig-Maximilians-Universitaet, Munich (West Germany). Inst. fuer Meteorologie.

THE UNSTEADY GROUND HEAT FLOW AT THE CONTACT SURFACE BETWEEN A GLACIER RUN AND THE SUBSOIL [DER INSTATIONAERE BODENWAERMESTROM AN DER KONTAKTFLAECHE EINES GLETSCHERBACHES ZUM UNTERGRUND]

WALDEMAR GEREKE *In its* Research Work at the Meteorological Institute of the University of Munich (Federal Republic of Germany) p 37-42 Mar. 1987 In GERMAN
Avail: NTIS HC A11/MF A01

A method for the estimation of the heat conducted from the glacier subsoil into the glacier run water was developed. The bed profile of the glacier run was modeled using a Schwarz-Christoffel conformal mapping. The proposed method calculates the heat flow in the case of a semi-infinite flat surface, and hence the increase of the water temperature of the glacier run. The comparison between calculated and measured data shows good agreement.

ESA

N88-16185# Instituto de Pesquisas Espaciais, Sao Jose dos Campos (Brazil).

EVALUATION OF THE FLOODING AREAS OF THE SAO GONCALO CANAL THROUGH LANDSAT 5 THEMATIC MAPPER IMAGES [AVALIACAO DA AREA DE INUNDACAO DO CANAL DE SAO GONCALO ATRAVES DE IMAGENS TM-LANDSAT 5]

CARLOS HARTMANN (Fundacao Univ. do Rio Grande, Brazil), R. A. C. LAMPARELLI, R. ROSA, and E. E. SANO 1988 15 p In PORTUGUESE; ENGLISH summary
(INPE-4118-PRE/1039) Avail: NTIS HC A03/MF A01

Two LANDSAT TM images were digitally processed on the I-100 Image Analyzer of INPE (Sao Jose dos Campos, Sao Paulo). The floodable area of the canal de Sao Goncalo was studied: one image associated to an exceptionally high inundation (06-11-84) and one image associated with a normal water level (12-04-84) were compared. The digital classification (1:50,000 scale) led to a map (1:100,000 scale) showing the limits of the flooding areas. This work demonstrated the usefulness of remote sensing techniques to delimitate and identify floodable areas.

Author

N88-17147# World Climate Programme, Geneva (Switzerland).

REPORT OF THE WORKSHOP ON SPACE SYSTEMS POSSIBILITIES FOR A GLOBAL ENERGY AND WATER CYCLE EXPERIMENT

May 1987 128 p Workshop held in Columbia, Md., 19-23 Jan. 1987

(WCP-137; WMO/TD-180; ETN-88-91683) Avail: NTIS MF A01; print copy available from WMO, Geneva, Switzerland

An experiment to study the transport of water (vapor, liquid, and solid) and energy fluxes in the global atmosphere and at the underlying surface; and to develop methods of predicting changes in the distribution of water (vapor, liquid, and solid) within the global atmosphere and on the underlying surface, which may occur naturally or through man's activity is presented. Global atmospheric models are reviewed. Techniques for global observation, and the contribution of spaceborne techniques are discussed. ESA

N88-17156# Army Cold Regions Research and Engineering Lab., Hanover, N.H.

PHYSICAL PROPERTIES OF SUMMER SEA ICE IN THE FRAM STRAIT, JUNE-JULY 1984

ANTHONY J. GOW, WALTER B. TUCKER, III, and WILFORD F. WEEKS Sep. 1987 92 p
(AD-A186937; CRREL-87-16) Avail: NTIS HC A05/MF A01
CSCL 08L

Most of the ice sampled was multi-year; it is estimated to represent at least 84 percent by volume of the total ice discharged from Fram Strait during June and July. Thicknesses and other properties indicated that none of the multi-year ice was older than 4 to 5 years. Snow cover on the multi-year ice averaged 29 cm deep while that on first-year averaged only 8 cm. Much of this difference appears to be the result of enhanced sublimation of the snow on the thinner first-year ice. Salinity profiles of first-year ice clearly show the effects of ongoing brine drainage in that profiles from cores drilled later in the experiment were substantially less saline than earlier cores. Bulk salinities of multi-year ice are generally much lower than those of first-year ice. This difference furnished a reliable means of distinguishing between the two ice types. Thin section examinations of crystal structure indicate that about 75 percent of the ice consisted of congelation ice with typically columnar crystal structure. The remaining 25 percent consisted of granular ice with only a few occurrences of snow ice. The granular ice consisted primarily of frazil, found in small amounts at the top of floes, but mainly observed in multi-year ridges where it occurred as the major component of ice in interblock voids. The horizontally oriented crystal c-axes showed varying degrees of alignment, from negligible to strong, in which the alignment direction changed with depth, implying a change in floe orientation with respect to the ocean current at the ice/water interface during ice growth. GRA

N88-19865# Virginia Univ., Charlottesville. Dept. of Environmental Sciences.

DESIGN OF THE PRIMARY PRE-TRMM AND TRMM GROUND TRUTH SITE Annual Report

MICHAEL GARSTANG 1 Apr. 1988 56 p
(Contract NAG5-870)

(NASA-CR-182609; NAS 1.26:182609) Avail: NTIS HC A04/MF A01 CSCL 04B

The primary objective of the Tropical Rain Measuring Mission (TRMM) were to: integrate the rain gage measurements with radar measurements of rainfall using the KSFC/Patrick digitized radar and associated rainfall network; delineate the major rain bearing systems over Florida using the Weather Service reported radar/rainfall distributions; combine the integrated measurements with the delineated rain bearing systems; use the results of the combined measurements and delineated rain bearing systems to represent patterns of rainfall which actually exist and contribute significantly to the rainfall to test sampling strategies and based on the results of these analyses decide upon the ground truth network; and complete the design begun in Phase 1 of a multi-scale (space and time) surface observing precipitation network centered upon KSFC. Work accomplished and in progress is discussed.

B.G.

DATA PROCESSING AND DISTRIBUTION SYSTEMS

Includes film processing, computer technology, satellite and aircraft hardware, and imagery.

A88-20841

HIERARCHICAL SEGMENTATION USING A COMPOSITE CRITERION FOR REMOTELY SENSED IMAGERY

MORRIS GOLDBERG and JINYUN ZHANG (Ottawa, University, Canada) Photogrammetria (ISSN 0031-8663), vol. 42, Dec. 1987, p. 87-96. refs

An image segmentation algorithm based upon hierarchical step-wise optimization with a composite merge criterion is presented. In hierarchical step-wise optimization, at each step, the two segments which optimize a criterion/cost function are found and merged. The main innovation proposed in this paper is that different criteria are employed at different stages in the hierarchical process. At the lowest stage, when the segment size is still small, the segment mean is the main information and is used in the merge criterion. For the intermediate stages, with increasing segment size, the mean is no longer sufficient to describe the characteristics of a segment and, therefore, a criterion related to the mean and the variance is considered. At the final stage, additional information such as the edge information is included in the criterion. In other words, with increasing segment size, more information is required to describe the characteristics of the segments and is incorporated into a composite criterion. Experimental results on a Landsat image show that improved segmentations can result when a composite criterion is employed.

Author

A88-20901

OPERATIONAL REVISION OF NATIONAL TOPOGRAPHIC MAPS IN CANADA USING LANDSAT IMAGES

ANTHONY M. TURNER (Gregory Geoscience, Ltd., Ottawa, Canada) and DAVID R. STAFFORD (Department of Energy, Mines and Resources, Topographical Survey Div., Ottawa, Canada) ITC Journal (ISSN 0303-2434), no. 2, 1987, p. 123-128. refs

A88-21025* National Aeronautics and Space Administration. Earth Resources Lab., Bay St. Louis, Miss.

DEVELOPMENT OF A 32-BIT UNIX-BASED ELAS WORKSTATION

BRUCE A. SPIERING, RONNIE W. PEARSON (NASA, Earth Resources Laboratory, Bay Saint Louis, MS), and THOMAS D. CHENG IN: American Society for Photogrammetry and Remote Sensing and ACSM, Annual Convention, Baltimore, MD, Mar. 29-Apr. 3, 1987, Technical Papers. Volume 1. Falls Church, VA, American Society for Photogrammetry and Remote Sensing and ACSM, 1987, p. 227-235. refs

A mini/microcomputer UNIX-based image analysis workstation has been designed and is being implemented to use the Earth Resources Laboratory Applications Software (ELAS). The hardware system includes a MASSCOMP 5600 computer, which is a 32-bit UNIX-based system (compatible with AT&T System V and Berkeley 4.2 BSD operating system), a floating point accelerator, a 474-megabyte fixed disk, a tri-density magnetic tape drive, and an 1152 by 910 by 12-plane color graphics/image interface. The software conversion includes reconfiguring the ELAS driver Master Task, recompiling and then testing the converted application modules. This hardware and software configuration is a self-sufficient image analysis workstation which can be used as a stand-alone system, or networked with other compatible workstations.

Author

A88-21026

IMPLEMENTATION OF THE LAND ANALYSIS SYSTEM ON A WORKSTATION

LYNDON R. OLESON (USGS, EROS Data Center, Sioux Falls, SD) IN: American Society for Photogrammetry and Remote Sensing and ACSM, Annual Convention, Baltimore, MD, Mar. 29-Apr. 3, 1987, Technical Papers. Volume 1. Falls Church, VA, American Society for Photogrammetry and Remote Sensing and ACSM, 1987, p. 236-244.

The Land Analysis System (LAS) provides a broad range of functional capabilities in the general areas of image processing and analysis, tabular data processing and analysis, geographic data input and manipulation, and custom product generation. To enhance the functionality and utility of LAS to its users, implementations of LAS are being extended to microprocessor-based workstations. The LAS host-computer and workstation implementation approach centers on the development of highly transportable and functionally modular software and the utilization of hardware-independent interfaces and integration techniques. This includes the conversion of LAS to the UNIX operating system environment to further reduce hardware dependencies and to expand the utility of LAS to users on a broad range of processors.

Author

A88-21027

AUTOMATED PHOTOINTERPRETATION - A STEREOSCOPIC WORKSTATION

ARTHUR V. MASELLI, FRANK L. SCARPACE, and RALPH W. KIEFER (Wisconsin, University, Madison) IN: American Society for Photogrammetry and Remote Sensing and ACSM, Annual Convention, Baltimore, MD, Mar. 29-Apr. 3, 1987, Technical Papers. Volume 1. Falls Church, VA, American Society for Photogrammetry and Remote Sensing and ACSM, 1987, p. 245-254. refs

Manual aerial photographic interpretation often employs stereoscopic viewing techniques to improve image interpretability. Stereoscopic viewing on a computer monitor offers several advantages over stereoscopic viewing on prints or transparencies. These include image enhancement, text overlay, and automated image pan, scroll, zoom capability, and rapid information transfer rates from interpreted images to data bases. This paper reviews various stereoscopic viewing techniques for computer CRTs. The paper describes a computerized stereoscopic approach for terrain feature identification, developed at the Environmental Remote Sensing Center of the University of Wisconsin-Madison. The technique employs a split screen approach to stereoscopic viewing on an IBM PC-AT microcomputer monitor, and has the advantage of low computer system cost, minimal viewing discomfort for the interpreter, and limited preprocessing computer time.

Author

A88-21030

PRINCIPAL COMPONENT ANALYSIS OF AERIAL VIDEO IMAGERY

WILLIAM J. KRAMBER, KAMLESH LULLA (Indiana State University, Terre Haute), ARTHUR J. RICHARDSON, and PAUL R. NIXON (USDA, Agricultural Research Service, Weslaco, TX) IN: American Society for Photogrammetry and Remote Sensing and ACSM, Annual Convention, Baltimore, MD, Mar. 29-Apr. 3, 1987, Technical Papers. Volume 1. Falls Church, VA, American Society for Photogrammetry and Remote Sensing and ACSM, 1987, p. 275-284. refs

Aerial video images of an agricultural test site were analyzed using principal component analysis and image processing techniques. The site - six treatments and four replications of cotton, sorghum, cantaloupe, johnsongrass, pigweed, and soil - was imaged using blue, yellow-green, red, and infrared filters over the lenses of four black-and-white video cameras, on May 31 and July 24, 1983. Separate principal component analysis procedures were applied to the May and July data as part of a methodology to assess data dimensionality and structure. Supervised minimum Euclidean distance classification procedures were conducted on sets of data that consisted of all four principal components, the first three principal components, the first two principal components, and the first principal component. Results indicated that the number of components required to accurately represent the four band data sets was three for the May data and two for the July data.

Scatter diagrams of principal components 1 and 2 showed good potential for determining the relative level of plant development.

Author

A88-21037* Vexcell Corp., Boulder, Colo.

IMAGE BASED SAR PRODUCT SIMULATION FOR ANALYSIS
G. DOMIK and F. LEBERL (Vexcel Corp., Boulder, CO) IN: American Society for Photogrammetry and Remote Sensing and ACSM, Annual Convention, Baltimore, MD, Mar. 29-Apr. 3, 1987, Technical Papers. Volume 1. Falls Church, VA, American Society for Photogrammetry and Remote Sensing and ACSM, 1987, p. 355-364. refs
(Contract JPL-957549)

SAR product simulation serves to predict SAR image gray values for various flight paths. Input typically consists of a digital elevation model and backscatter curves. A new method is described of product simulation that employs also a real SAR input image for image simulation. This can be denoted as 'image-based simulation'. Different methods to perform this SAR prediction are presented and advantages and disadvantages discussed. Ascending and descending orbit images from NASA's SIR-B experiment were used for verification of the concept: input images from ascending orbits were converted into images from a descending orbit; the results are compared to the available real imagery to verify that the prediction technique produces meaningful image data. Author

A88-21047

A SATELLITE IMAGE MOSAIC OF ILLINOIS

RICHARD E. DAHLBERG, DONALD E. LUMAN (Northern Illinois University, DeKalb, IL), ALDEN WARREN (USGS, National Mapping Div., Reston, VA), and CHRISTOPHER J. STOHR (Illinois State Geological Survey, Champaign, IL) IN: American Society for Photogrammetry and Remote Sensing and ACSM, Annual Convention, Baltimore, MD, Mar. 29-Apr. 3, 1987, Technical Papers. Volume 2. Falls Church, VA, American Society for Photogrammetry and Remote Sensing and ACSM, 1987, p. 91-101. refs

An account is given of the creation and publication of a 'Satellite Image Map of Illinois' (Illinois State Geological Survey, 1985). The image map was created in color from 12 TM scenes acquired in autumn. It is found that sharpened half-tone positives provide better quality control than sharpened half-tone negative films do for lithographic platemaking. Attention is given to the concept and design of the image map product, the entities involved in preparation and publication, the production processes employed, and the response of the public. K.K.

A88-21048

COMPUTER-ASSISTED COLOR GENERATION FOR THEMATIC MAPPING

THOMAS M. MCCULLOCH, BRIAN S. BENNETT, and DOUGLAS S. AITKEN (USGS, Menlo Park, CA) IN: American Society for Photogrammetry and Remote Sensing and ACSM, Annual Convention, Baltimore, MD, Mar. 29-Apr. 3, 1987, Technical Papers. Volume 2. Falls Church, VA, American Society for Photogrammetry and Remote Sensing and ACSM, 1987, p. 102-107.

New techniques for computer-assisted color generation have been developed as part of thematic map production within the USGS. Inherent to the techniques is the raster scanning of color boundary linework using the Scitex system; the linework is then converted to vector data and processed through the National Mapping Division's Production System software. The computer-assisted approach guarantees that all polygons within the map can have their color generated automatically; moreover, it greatly reduces the amount of interactive work required at the Scitex raster edit station. K.K.

A88-21049

COMPARISON OF THE GRIDDED FINITE ELEMENT AND THE POLYNOMIAL INTERPOLATIONS FOR GEOMETRIC RECTIFICATION AND MOSAICKING OF LANDSAT DATA

JUNE M. THORMODSGARD (USGS, EROS Data Center, Sioux Falls, SD) and THOMAS LILLESAND (Wisconsin, University, Madison) IN: American Society for Photogrammetry and Remote

Sensing and ACSM, Annual Convention, Baltimore, MD, Mar. 29-Apr. 3, 1987, Technical Papers. Volume 2. Falls Church, VA, American Society for Photogrammetry and Remote Sensing and ACSM, 1987, p. 139-151. refs

A88-21053

AN EXPERT SYSTEM FOR THE COMPUTER-ASSISTED ANALYSIS OF RADAR IMAGERY

RICHARD F. PASCUCCI (Autometric, Inc., Falls Church, VA) IN: American Society for Photogrammetry and Remote Sensing and ACSM, Annual Convention, Baltimore, MD, Mar. 29-Apr. 3, 1987, Technical Papers. Volume 2. Falls Church, VA, American Society for Photogrammetry and Remote Sensing and ACSM, 1987, p. 355-363. Army-supported research.

Automated identification of features on radar imagery was carried out. The following steps were involved: (1) the detection of descriptors, (2) the application of condition/action rules to organize the descriptors into descriptor sets, and (3) the application of if-then rules to infer feature identity from descriptor sets. K.K.

A88-21059

METHODS AND ACCURACY OF OPERATIONAL DIGITAL IMAGE MAPPING WITH AIRCRAFT SAR

F. W. LEBERL, G. DOMIK (Vexcel Corp., Boulder, CO), and B. MERCER (INTERA Technologies, Ltd., Calgary, Canada) IN: American Society for Photogrammetry and Remote Sensing and ACSM, Annual Convention, Baltimore, MD, Mar. 29-Apr. 3, 1987, Technical Papers. Volume 4. Falls Church, VA, American Society for Photogrammetry and Remote Sensing and ACSM, 1987, p. 149-158. refs

An airborne sidelooking Synthetic Aperture Radar (SAR) system, STAR-1, has been complemented by processing techniques to create a new type of cartographic product: a 1:50,000 radar image map with 100 m contour lines. This product is denoted as STARMAP. The paper describes the system, processing steps and some results. Author

A88-21061

DIGITAL TERRAIN ANALYSIS EMPLOYING X-Y-Z POINT VECTORS AS INPUT DATA

ANDREW A. ROST (Delta Data Systems, Inc., Picayune, MS) IN: American Society for Photogrammetry and Remote Sensing and ACSM, Annual Convention, Baltimore, MD, Mar. 29-Apr. 3, 1987, Technical Papers. Volume 4. Falls Church, VA, American Society for Photogrammetry and Remote Sensing and ACSM, 1987, p. 228-237. refs

Software for producing a smooth, digital terrain model in a raster image file has been developed based on the application of a cubic spline interpolation on an X-Y-Z sample input. The method finds the best approximation for the Z value for each X-Y point in the data set, with the interpolator calculating a smooth approximation for elevation for points falling between the contour intervals. Terrain analysis software is then used to calculate slope, aspect, and slope length. R.R.

A88-21062

AMERICAN SOCIETY FOR PHOTOGRAMMETRY AND REMOTE SENSING AND ACSM, ANNUAL CONVENTION, BALTIMORE, MD, MAR. 29-APR. 3, 1987, TECHNICAL PAPERS. VOLUME 6 - IMAGE DATA PROCESSING

Convention sponsored by the American Society for Photogrammetry and Remote Sensing and ACSM. Falls Church, VA, American Society for Photogrammetry and Remote Sensing and ACSM, 1987, 163 p. For individual items see A88-21063 to A88-21075.

The conference presents papers on a proposed semisupervised two-stage classification technique, detecting subpixel woody features using simulated multispectral and panchromatic spot imagery, a semiautomated training sample selector for multispectral land cover classification, and a comparison of the hierarchical cluster and homogeneous training field detection methods in classifying urban land covers from TM data. Other topics include the use of automated computer vision techniques for the recognition of features of radar imagery, and the application of frequency

07 DATA PROCESSING AND DISTRIBUTION SYSTEMS

filtering in remotely sensed imagery. Consideration is also given to land cover change detection using a GIS-guided feature-based classification of Landsat TM mapper data, the Landsat remote sensing imagery analysis program, and a microcomputer processing system utilizing currently available hardware. K.K.

A88-21063

A PROPOSED SEMI-SUPERVISED TWO STAGE CLASSIFICATION TECHNIQUE

DANIEL A. TOOMEY and FRANK L. SCARPACE (Wisconsin, University, Madison) IN: American Society for Photogrammetry and Remote Sensing and ACSM, Annual Convention, Baltimore, MD, Mar. 29-Apr. 3, 1987, Technical Papers. Volume 6 . Falls Church, VA, American Society for Photogrammetry and Remote Sensing and ACSM, 1987, p. 1-6. refs

A two step Semi-Supervised classifier is being developed on an IBM PC-AT microcomputer at the Environmental Remote Sensing Center, University of Wisconsin-Madison. This technique is used to classify images of digitized aerial photographs. This is a hybrid classification technique that offers the advantage of an unsupervised classification with the direction of a supervised classification scheme. The first step identifies training sets in an image utilizing a limited number of training 'areas', so that an unsupervised clustering algorithm can identify a user defined number of spectral clusters to segment the scene. After the scene is classified spectrally the second step potentially increases classification accuracy by reclassifying certain cover types according to ancillary data. Author

A88-21064

RESULTS OF TESTING DIGITAL IMAGE MEASUREMENTS AND ENHANCEMENTS ON THE REMOTE WORK PROCESSING FACILITY

HERBERT JOHNSON, CHRISTOPHER GILES, ROBERT BROCK, and GERALD KINN (New York, State University, Syracuse) IN: American Society for Photogrammetry and Remote Sensing and ACSM, Annual Convention, Baltimore, MD, Mar. 29-Apr. 3, 1987, Technical Papers. Volume 6 . Falls Church, VA, American Society for Photogrammetry and Remote Sensing and ACSM, 1987, p. 7-14.

(Contract DMA800-85-C-0033)

The Digital Image Measurements and Enhancement (DIME) compendium is an effort to document the image measurements available on the Defense Mapping Agency's Remote Work Processing Facility (RWPF). Various test images were systematically processed using each of the available measures. Training and classification experiments were also performed on the images and the results subjectively reviewed. It was found that most texture measures were sensitive to image resolution. It was also noted that some measures were sensitive to the orientation of features to be segmented. Insights were provided as to the choice of window size parameters required by some measures. Information was also gained with respect to the use of edge-preserving measures, highly correlated texture measures, and cascaded measures (i.e., the output of one measure used as input to a second measure). Author

A88-21066

A SEMI-AUTOMATED TRAINING SAMPLE SELECTOR FOR MULTISPECTRAL LAND COVER CLASSIFICATION

MARTIN P. BUCHHEIM and THOMAS M. LILLESAND (Wisconsin, University, Madison) IN: American Society for Photogrammetry and Remote Sensing and ACSM, Annual Convention, Baltimore, MD, Mar. 29-Apr. 3, 1987, Technical Papers. Volume 6 . Falls Church, VA, American Society for Photogrammetry and Remote Sensing and ACSM, 1987, p. 23-34. refs

A semiautomated training sample selector was developed to address problems encountered in the application of conventional image analysis techniques to high-resolution multispectral imagery and to eliminate more general problems associated with conventional classification approaches. The procedure can be implemented in either a supervised or unsupervised mode. Preliminary testing of the procedure with SPOT imagery simulation

and TM imagery attests to its ability to produce accurate image classifications while simultaneously reducing image analyst time requirements. K.K.

A88-21067

A COMPARISON OF THE HIERARCHICAL CLUSTER AND HOMOGENEOUS TRAINING FIELD DETECTION METHODS IN CLASSIFYING URBAN LANDCOVERS FROM TM DATA

DOUGLAS J. WHEELER (Utah State University, Logan) IN: American Society for Photogrammetry and Remote Sensing and ACSM, Annual Convention, Baltimore, MD, Mar. 29-Apr. 3, 1987, Technical Papers. Volume 6 . Falls Church, VA, American Society for Photogrammetry and Remote Sensing and ACSM, 1987, p. 35-44. refs

A88-21068* Hunter Coll., New York.

REFINING IMAGE SEGMENTATION BY POLYGON SKELETONIZATION

KEITH C. CLARKE (Hunter College, New York) IN: American Society for Photogrammetry and Remote Sensing and ACSM, Annual Convention, Baltimore, MD, Mar. 29-Apr. 3, 1987, Technical Papers. Volume 6 . Falls Church, VA, American Society for Photogrammetry and Remote Sensing and ACSM, 1987, p. 45-52. NASA-supported research. refs

A skeletonization algorithm was encoded and applied to a test data set of land-use polygons taken from a USGS digital land use dataset at 1:250,000. The distance transform produced by this method was instrumental in the description of the shape, size, and level of generalization of the outlines of the polygons. A comparison of the topology of skeletons for forested wetlands and lakes indicated that some distinction based solely upon the shape properties of the areas is possible, and may be of use in an intelligent automated land cover classification system. K.K.

A88-21069

THE USE OF AUTOMATED COMPUTER VISION TECHNIQUES FOR THE RECOGNITION OF FEATURES ON RADAR IMAGERY

DANIEL K. GORDON (Autometric, Inc., Falls Church, VA) IN: American Society for Photogrammetry and Remote Sensing and ACSM, Annual Convention, Baltimore, MD, Mar. 29-Apr. 3, 1987, Technical Papers. Volume 6 . Falls Church, VA, American Society for Photogrammetry and Remote Sensing and ACSM, 1987, p. 63-72. Army-supported research. refs

Computer vision techniques were identified and developed to automatically recognize descriptor sets being used by image analysts for the characterization of features found in radar imagery. This was accomplished via careful selection of existing raster and vector image processing tools that provided reliable edge information. It is concluded that the ability to identify points, lines, areas, and their associated patterns provides a substantial image processing foundation on which the computer-assisted analysis of radar imagery of various forms can be conducted. K.K.

A88-21070* Vexcel Corp., Boulder, Colo.

MATCHING OF DISSIMILAR RADAR IMAGES USING MARR-HILDRETH ZERO CROSSINGS

ROSS M. MCCONNELL (Vexcel Corp., Boulder, CO) IN: American Society for Photogrammetry and Remote Sensing and ACSM, Annual Convention, Baltimore, MD, Mar. 29-Apr. 3, 1987, Technical Papers. Volume 6 . Falls Church, VA, American Society for Photogrammetry and Remote Sensing and ACSM, 1987, p. 73-80. refs

(Contract JPL-957363)

Two alternatives to the classical method for finding corresponding points in opposite-side synthetic aperture radar imagery are presented. These new methods focus on matching the shapes of large-scale features in the images rather than on correlating high-frequency pixel gray values. One of the methods may be of use in matching radar images to optical images. The large-scale features are extracted using the Marr-Hildreth operator. K.K.

A88-21072

APPLICATION OF FREQUENCY FILTERING IN REMOTELY SENSED IMAGERY

C. F. CHEN, KURT J. WORRELL, WILLIAM R. BERGEN, and FRANK L. SCARPACE (Wisconsin, University, Madison) IN: American Society for Photogrammetry and Remote Sensing and ACSM, Annual Convention, Baltimore, MD, Mar. 29-Apr. 3, 1987, Technical Papers. Volume 6. Falls Church, VA, American Society for Photogrammetry and Remote Sensing and ACSM, 1987, p. 98-107. refs

The two-dimensional Fourier transform allows conceptual examination of an image from another coordinate space, known as the frequency domain. It is easier and more efficient to study some image characteristics and perform some operations, such as filtering, in the frequency domain than in the spatial domain. A software package for a two-dimensional fast Fourier transform (FFT) and frequency filtering was implemented on a microcomputer at the Environmental Remote Sensing Center, University of Wisconsin-Madison. In filtering operations, the discontinuity caused by the ideal filter with a specific cut-off frequency normally generates ringing in the filtered image. In order to reduce ringing, the ideal filter is modified by a window function. A series of experiments were conducted to illustrate the importance of choosing the proper window function to minimize the ringing in the filtered image. This frequency filtering technique was successfully applied to remove periodic noise in a digital thermal image and satellite data. Author

A88-21075

LANDSAT REMOTE SENSING IMAGERY ANALYSIS PROGRAM

SCOTT A. LOOMER (U.S. Army, Military Academy, West Point, NY) IN: American Society for Photogrammetry and Remote Sensing and ACSM, Annual Convention, Baltimore, MD, Mar. 29-Apr. 3, 1987, Technical Papers. Volume 6. Falls Church, VA, American Society for Photogrammetry and Remote Sensing and ACSM, 1987, p. 131-139.

A multispectral image processing program has been developed that fully utilizes the improved graphics and processor capabilities of AT-class microcomputers with enhanced graphics. With no requirements for specialized hardware, the program provides high resolution gray-level displays of single bands of multispectral data, color displays of multiband scenes, statistical analysis of the data, selection of training areas, and supervised classification of up to seven bands of data utilizing a maximum probable likelihood classifier. The program can work with subscenes as large as 3600 pixels wide by essentially unlimited height. Output of both single band displays and classified images is supported on several popular graphics printers. The menu-driven user interface makes the program particularly suited as an introduction to the concepts of remote sensing image classification. The program has been placed in the public domain and is available for noncommercial purposes. Author

A88-23502#

INTERPRETATION OF SATELLITE IMAGERY OF A RAPIDLY DEEPENING CYCLONE

M. V. YOUNG, G. A. MONK, and K. A. BROWNING (Meteorological Office, Bracknell, England) Royal Meteorological Society, Quarterly Journal (ISSN 0035-9009), vol. 113, Oct. 1987, p. 1089-1115. refs

Model output and observational data are used to interpret, in detail, satellite images of a distinctive cloud system several hundred kilometers long, which was observed before and during rapid cyclonic development that occurred over England. Conceptual models which account for the structure of the major cloud areas and upper-level moisture fields immediately prior to and following the onset of vigorous cyclogenesis are forwarded. The cloud system corresponded to what R. B. Weldon (1979) refers to as a baroclinic leaf cloud and was characterized by 'ana' cold frontal ascent. The baroclinic leaf lay within an area of enhanced ascent ahead of a major upper-level trough. A jet streak which originated upstream, propagated rapidly around the base of the upper trough.

A tongue of dry air centered on the left flank of this jet streak lay immediately upstream of the leaf cloud and had a major influence on its subsequent development. This intrusion of dry air was well represented by the Meteorological Office fine mesh model, which showed it as a pronounced tongue of recently descended air with high potential vorticity, which originated in the upper troposphere and lower stratosphere. Rapid cyclogenesis occurred as the dry intrusion overran low-level air of high theta(W) within a warm conveyor belt at the southern tip of the leaf cloud. Interaction of the dry intrusion and baroclinic leaf cloud is shown to be particularly important in accounting for the detailed distribution of weather. It also suggests a way of pinpointing the location and timing of vigorous cyclogenesis. Author

A88-23760

GEOMETRIC ACCURACY TESTING OF ORBITAL RADAR IMAGERY

ABDALLA ELSADIG ALI (Khartoum, University, Sudan) Photogrammetric Engineering and Remote Sensing (ISSN 0099-1112), vol. 53, Nov. 1987, p. 1533-1537. refs

Two spaceborne synthetic aperture side-looking radar (SLR) images covering two different areas were tested for geometric accuracy in order to assess the suitability of the present spaceborne radar systems for topographic mapping applications. The results confirm that the geometric accuracy of SLR imagery falls far below that of conventional photographic images. The attainable accuracy is dependent on many factors, the most important of which are the method of processing SAR data and the nature and topography of the area being mapped. The results also show that metric information can be extracted from spaceborne radars at an accuracy standard sufficient for the purposes of many developing countries, particularly those with continuous cloud cover which makes acquisition of photographic images impossible. C.D.

A88-23761

ASSESSMENT OF SIR-B FOR TOPOGRAPHIC MAPPING

P. J. WISE (Division of National Mapping, Belconnen, Australia) and J. C. TRINDER (New South Wales, University, Kensington, Australia) Photogrammetric Engineering and Remote Sensing (ISSN 0099-1112), vol. 53, Nov. 1987, p. 1539-1544. Research supported by the Division of National Mapping. refs

The geometric accuracy of features derived from SIR-B (Shuttle Imaging Radar-B) data and the detectability of features required for cartographic map scales in Australia are experimentally investigated. The geometric accuracy of the SIR-B radar is found to be suitable only for 1:250,000-scale mapping and smaller because the rms vector error from the first-order polynomial used to transform the radar data to the map grid is about four pixels, or about 50 m on the ground. Analysis of the content shows that at best the radar images contain only 60 percent of the detail depicted on a 1:100,000 map. C.D.

A88-23768

APPLICATION OF PREDICTIVE COMPRESSION METHODS TO SYNTHETIC APERTURE RADAR IMAGERY I

SUSAN A. S. WERNESS (Michigan, Environmental Research Institute, Ann Arbor) Optical Engineering (ISSN 0091-3286), vol. 26, Dec. 1987, p. 1200-1218. refs

In this paper, it is demonstrated that strip map SAR imagery can be characterized by correlations that can be used in a design of a prediction compression system. Using 6-m resolution SAR data obtained by the Sea Ice and Terrain Assessment Radar system described by Nichols et al. (1984), it is shown that simple predictive coding system utilizing an unadaptive moving-average (MA) predictor and a Gaussian optimal quantizer can result in satisfactory reconstructed imagery at compression ratios of 2:1 to 4:1. It is also shown that an MA predictor is more suitable for SAR prediction than the commonly used autoregressive predictor; the advantages of MA predictors are their lack of stability problems and their limited memory in the presence of channel errors. I.S.

A88-24935

THE APPLICATION OF PERCEPTUAL COLOR SPACES TO THE DISPLAY OF REMOTELY SENSED IMAGERY

PHILIP K. ROBERTSON and JOHN F. O'CALLAGHAN (CSIRO, Div. of Information Technology, Canberra, Australia) IEEE Transactions on Geoscience and Remote Sensing (ISSN 0196-2892), vol. 26, Jan. 1988, p. 49-59. refs

An attempt is made to show how perceptually uniform color spaces can improve significantly the interpretability of displays and remotely sensed geoscientific imagery. A computational framework encompassing the mapping of data into perceptually uniform color spaces is presented, and practical application of this framework to various types of geophysical data is described. Applications include the depiction of informative data variables in specified lightness and saturation ranges, the effective utilization of chromatic contrast in multispectral data displays, and representations of more complex integrated data sets. I.E.

A88-24936

REGISTRATION OF IMAGES WITH GEOMETRIC DISTORTIONS

ARDESHIR GOSHATSBY (Kentucky, University, Lexington) IEEE Transactions on Geoscience and Remote Sensing (ISSN 0196-2892), vol. 26, Jan. 1988, p. 60-64. Research supported by the University of Kentucky. refs

A technique for registration of images with geometric distortions is described. This technique uses two surface splines to represent the X-component and the Y-component of a mapping function. A mapping function is described in such a way that it would map corresponding control points in the images exactly on top of each other and map other points in the images by interpolation using information and local geometric distortion between the images. I.E.

A88-24937

A TRANSFORMATION FOR ORDERING MULTISPECTRAL DATA IN TERMS OF IMAGE QUALITY WITH IMPLICATIONS FOR NOISE REMOVAL

ANDREW A. GREEN, MAURICE D. CRAIG (CSIRO, Div. of Mineral Physics and Mineralogy, North Ryde, Australia), MARK BERMAN (CSIRO, Div. of Mathematics and Statistics, Lindfield, Australia), and PAUL SWITZER (Stanford University, CA) IEEE Transactions on Geoscience and Remote Sensing (ISSN 0196-2892), vol. 26, Jan. 1988, p. 65-74. refs

A transformation known as the maximum noise fraction (MNF) transformation, which always produces new components ordered by image quality, is presented. It can be shown that this transformation is equivalent to principal components transformations when the noise variance is the same in all bands and that it reduces to a multiple linear regression when noise is in one band only. Noise can be effectively removed from multispectral data by transforming to the MNF space, smoothing or rejecting the most noisy components, and then retransforming to the original space. In this way, more intense smoothing can be applied to the MNF components with high noise and low signal content than could be applied to each band of the original data. The MNF transformation requires knowledge of both the signal and noise covariance matrices. Except when the noise is in one band only, the noise covariance matrix needs to be estimated. One procedure for doing this is discussed and examples of cleaned images are presented. I.E.

A88-27822* National Aeronautics and Space Administration. Goddard Space Flight Center, Greenbelt, Md.

ATMOSPHERIC EFFECT ON SPECTRAL SIGNATURE - MEASUREMENTS

YORAM J. KAUFMAN (NASA, Goddard Space Flight Center, Greenbelt, MD; Technion - Israel Institute of Technology, Haifa) (COSPAR, WMO, URSI, et al., Plenary Meeting, 26th, Symposium 3, Workshop V, and Topical Meeting A2 on Remote Sensing from Space, Toulouse, France, June 30-July 11, 1986) Advances in Space Research (ISSN 0273-1177), vol. 7, no. 11, 1987, p. 203-206. refs

In order to study the spectral atmospheric effect on remote sensing, measurements of the spectral signature of surface cover were conducted during hazy conditions. Simultaneous measurements of the aerosol optical thickness and its vertical distribution were carried out. The upward radiance in high flight were also simulated by radiative transfer computations, and the results were compared with the measurements. It is suggested that the radiances over dark areas can be used to derive the aerosol optical thickness. Combined with climatological information, the derived optical thickness can be used to perform corrections of the atmospheric effect. C.D.

A88-27824* National Aeronautics and Space Administration. Goddard Space Flight Center, Greenbelt, Md.

RECENT DATA QUALITY AND EARTH SCIENCE RESULTS FROM THE LANDSAT THEMATIC MAPPER

VINCENT V. SALOMONSON and JOHN L. BARKER (NASA, Goddard Space Flight Center, Greenbelt, MD) (COSPAR, WMO, URSI, et al., Plenary Meeting, 26th, Symposium 3, Workshop V, and Topical Meeting A2 on Remote Sensing from Space, Toulouse, France, June 30-July 11, 1986) Advances in Space Research (ISSN 0273-1177), vol. 7, no. 11, 1987, p. 217-226. refs

The results of the NASA Landsat Image Data Quality Analysis (LIDQA) program are reviewed. Landsat-4 and Landsat-5 TM data quality with regard to image geometry and radiometry are discussed. The results indicate that the TM provides excellent imagery that can be used in the form of satellite image maps meeting cartographic standards at scales of 1:100,000 or smaller. These data can be used to locate features or guide the revision or updating of maps for scales up to 1:24,000. The TM sensor is also providing data of good radiometric quality and stability, with radiometric uncertainties of 1 percent or smaller. The temperature dependence in the absolute radiometry is on the order of 1 to 5 percent of full scale. In terms of bidirectional reflectance estimated at the satellite, the error is estimated at under 6 percent and commonly 3 percent. Preliminary results also corroborate the utility of the TM data for geological or geographical studies. C.D.

A88-27825

DIGITAL STEREO PROCESSING OF SATELLITE IMAGE DATA

R. SIMARD (Canada Centre for Remote Sensing, Ottawa) (COSPAR, WMO, URSI, et al., Plenary Meeting, 26th, Symposium 3, Workshop V, and Topical Meeting A2 on Remote Sensing from Space, Toulouse, France, June 30-July 11, 1986) Advances in Space Research (ISSN 0273-1177), vol. 7, no. 11, 1987, p. 227-235. refs

Currently, space image data of the earth's surface is being primarily used with emphasis on two-dimensional information content. Three-dimensional image data acquisition is now emerging through the multilateral viewing capability of new spaceborne Visible/Infrared and SAR imaging systems. While visual relief perception from stereo pairs is easily achievable using low-level processed data, more advanced digital stereo processing techniques can be used as versatile tools to extract information out of three-dimensional input data. A completely automated approach is presented for digital generation of elevation data from stereo pairs. The emphasis will be on the reliability and precision of results obtained from digital image data. Author

A88-27830

SIMULATION OF SPACEBORNE SAR IMAGERY FROM AIRBORNE SAR DATA

H. KIMURA, N. MOTOMURA, and N. KODAIRA (Remote Sensing Technology Centre of Japan, Tokyo) (COSPAR, WMO, URSI, et al., Plenary Meeting, 26th, Symposium 3, Workshop V, and Topical Meeting A2 on Remote Sensing from Space, Toulouse, France, June 30-July 11, 1986) Advances in Space Research (ISSN 0273-1177), vol. 7, no. 11, 1987, p. 281-284.

This paper discusses the simulation of the spaceborne SAR imagery using airborne SAR data obtained by the SAR-580 experiments of 1983 in Japan. Simulation parameters are spatial resolution, received signal-to-noise ratio, the number of bits in the

raw data sample, and the number of looks. The simulation method is described, and first analysis results are given on the received signal-to-noise ratio. Author

A88-27831

SIMULATION OF BIT-QUANTIZATION INFLUENCE ON SAR IMAGES

A. P. WOLFRAMM and T. K. PIKE (DFVLR, Institut fuer Hochfrequenztechnik, Oberpfaffenhofen, Federal Republic of Germany) (COSPAR, WMO, URSI, et al., Plenary Meeting, 26th, Symposium 3, Workshop V, and Topical Meeting A2 on Remote Sensing from Space, Toulouse, France, June 30-July 11, 1986) *Advances in Space Research* (ISSN 0273-1177), vol. 7, no. 11, 1987, p. 285-288. refs

The influence of two-bit and four-bit quantization schemes on the ocean wave spectra obtained in the wave imaging mode of the first European Remote Sensing Satellite ERS-1 is analyzed. The SAR images utilized were obtained through simulation using a static ocean-wave radar model and a comprehensive software SAR system simulation model. The results indicate that spectra produced by the four-bit quantization are not significantly degraded from the optimum, but that the two-bit quantization requires some gain adjustment for optimal spectral reproduction. The conclusions are supported by images and spectral plots covering the various options simulated. C.D.

A88-27834

SPECKLE IN SAR IMAGES - AN EVALUATION OF FILTERING TECHNIQUES

J. M. DURAND (CNES and CNRS, Laboratoire d'Etudes et de Recherche en Teledetection Spatiale, Toulouse, France), B. J. GIMONET (ONERA, Centre d'Etudes et de Recherches de Toulouse, France), and J. R. PERBOS (CNES, Toulouse, France) (COSPAR, WMO, URSI, et al., Plenary Meeting, 26th, Symposium 3, Workshop V, and Topical Meeting A2 on Remote Sensing from Space, Toulouse, France, June 30-July 11, 1986) *Advances in Space Research* (ISSN 0273-1177), vol. 7, no. 11, 1987, p. 301-304. refs
(Contract ESA-6153/85/NL/MS)

This study compares five usual filtering techniques to remove speckle noise in remote-sensing synthetic aperture radar images. All algorithms were tested on real remote-sensing images with vegetation and urban areas. The comparison includes brief theoretical analysis, visual interpretation, computing time, and classification results. The study shows the necessity of filtering SAR images for classification purposes and selects an adaptive filter based on nonlinear local statistics as the best one for agricultural images. Author

A88-28009* National Aeronautics and Space Administration. Goddard Space Flight Center, Greenbelt, Md.

EXTRACTION OF SPECTRAL HEMISPHERICAL REFLECTANCE (ALBEDO) OF SURFACES FROM NADIR AND DIRECTIONAL REFLECTANCE DATA

D. S. KIMES (NASA, Goddard Space Flight Center, Greenbelt, MD), P. J. SELLERS (Maryland, University, College Park), and D. J. DINER (California Institute of Technology, Jet Propulsion Laboratory, Pasadena) *International Journal of Remote Sensing* (ISSN 0143-1161), vol. 8, Dec. 1987, p. 1727-1746. refs

A radiative transfer model is used to investigate how the error of spectral hemispherical reflectance data obtained from nadir reflectance values varies with wavelength, solar zenith angle, leaf area index, and leaf orientation distribution. Several techniques employing multiple off-nadir view angles taken in azimuth planes are found to accurately infer spectral hemispherical reflectances, and to be well suited to sensor systems that scan in a known azimuth plane or view fore and aft in a known azimuth plane. The effects of errors in hemispherical reflectance on terrestrial energy budget and productivity calculations is also considered. R.R.

A88-28602

THEMATIC MAPPER AND SPOT INTEGRATION WITH A GEOGRAPHIC INFORMATION SYSTEM

DAVID G. GOODENOUGH (Canada Centre for Remote Sensing, Ottawa) *Photogrammetric Engineering and Remote Sensing* (ISSN 0099-1112), vol. 54, Feb. 1988, p. 167-176. Research supported by the Canada Centre for Remote Sensing. refs

The integration of remote sensing and geographic information systems GIS is essential for effective resource management. The volume of remote sensing imagery for managing a provincial resource is such that one must use digital image analysis systems. By combining remote sensing image analysis and geographic information systems, resource managers can have timely and accurate knowledge of a renewable resource. In addition, satellite imagery with higher resolution can be used to update road network information in a GIS for a city. There are, however, several scientific and technical problems that reduce the success of this integration. This paper describes several integration problems and the Landsat Digital Image Analysis System (LDIAS) used at the Canada Centre for Remote Sensing (CCRS). Experiments have been conducted integrating a forestry geographic information system for the province of British Columbia with LDIAS and SPOT imagery with city information. Some of the difficulties encountered require the use of nonalgorithmic solutions which use symbolic reasoning. Author

A88-28604

THE POTENTIAL FOR AUTOMATED MAPPING FROM GEOCODED DIGITAL IMAGE DATA

RICHARD SWANN, DAVE HAWKINS, ANDREW WESTWELL-ROPER, and WILLIAM JOHNSTONE (MacDonald, Dettwiler and Associates, Ltd., Richmond, Canada) *Photogrammetric Engineering and Remote Sensing* (ISSN 0099-1112), vol. 54, Feb. 1988, p. 187-193. refs

Recent improvements in the resolution of available commercial satellite imagery, combined with new techniques for high-precision geometric image correction, now make production of accurate topographic maps from satellite imagery possible. This paper discusses the technical considerations of using imagery from existing satellites such as Landsat and SPOT. Author

A88-28605

EVALUATION OF THE STEREOSCOPIC ACCURACY OF THE SPOT SATELLITE

V. RODRIGUEZ, P. GIGORD, A. C. DE GAUJAC, P. MUNIER (Institut Geographique National, Toulouse, France), and G. BEGNI (CNES, Toulouse, France) *Photogrammetric Engineering and Remote Sensing* (ISSN 0099-1112), vol. 54, Feb. 1988, p. 217-221.

The methods used for the in-flight assessment of the SPOT 1 satellite are described. The sequence of operations, including the checkout organization, determination of a network of control points, image acquisition programming, and processing of stereopairs, is discussed. The results, including quality of plotting, of modeling, and of restitution are examined. Future prospects for the photogrammetric exploitation of SPOT images are addressed. C.D.

A88-28680

RADIOMETRIC CORRECTION OF C-BAND IMAGERY FOR TOPOGRAPHIC EFFECTS IN REGIONS OF MODERATE RELIEF

MARIO HINSE, Q. H. J. GWYN, and F. BONN (Sherbrooke, Universite, Canada) *IEEE Transactions on Geoscience and Remote Sensing* (ISSN 0196-2892), vol. 26, March 1988, p. 122-132. Research supported by NSERC and Ministere de l'Education du Quebec. refs

The combined effects of topography, slope, look angle, and aspect on C-band synthetic-aperture radar (SAR) data on the radiometric quality of SAR images in a region of moderate relief are examined. A correction method was used to attenuate the change of illumination across the swath due to the antenna pattern. Ground data were integrated into the analysis using a digital terrain model (DTM). Correction functions based on the cosine of the incidence angle were applied to the thematic classes and to the grouped classes in order to reduce the effects related to

topography. It was found that it is possible to eliminate part of the radiometric variations created by moderate topographic relief. After the corrections were applied, a reduction was noted of the variance in the radiometric values of the spectral signatures of the cover types, which ranged between 3.03 and 9.47 percent, depending on the correction function used. No noticeable correction occurred of pixels with slopes less than 6 deg and at local incident angles less than 26 deg. However, the closer the slopes are to being perpendicular to the look direction, the stronger is the correlation between backscatter and slope angle. I.E.

A88-28681

SAR IMAGING OF VOLUME SCATTERERS

N. D. TAKET, T. J. HALL, and R. E. BURGE (King's College, London, England) IEEE Transactions on Geoscience and Remote Sensing (ISSN 0196-2892), vol. 26, March 1988, p. 133-139. Research supported by the Ministry of Defence. refs

The first renormalization scattering method is used to obtain an expression for the synthetic-aperture radar (SAR) complex image amplitude of a volume scatterer with an undulating boundary surface. This expression is then used to derive further expressions for correlations of such an image when the boundary is either deterministic or random. I.E.

A88-29286

THE ACQUISITION OF SPOT-1 HRV IMAGERY OVER SOUTHERN BRITAIN AND NORTHERN FRANCE, MAY 1986-MAY 1987

JANIS CUSHNIE (Reading, University, England) International Journal of Remote Sensing (ISSN 0143-1161), vol. 9, Jan. 1988, p. 159-167.

The number and spatial distribution of SPOT-1 HRV images acquired over southern Britain and northern France during the first commercial year of the SPOT system have been assessed in response to concern about the lack of cloud-free imagery. It is confirmed that, despite large numbers of images being acquired per scene (1 panchromatic and 12 multispectral on average over northern France; 8 panchromatic and 12 multispectral over southern Britain), most are of limited use because of cloud cover. Only 30 percent of the images collected have at least one quadrant with less than 25 percent cloud cover and 10 percent have less than 10 percent cloud cover in each quadrant. Recommendations on what can be done are presented. B.J.

A88-29287* National Aeronautics and Space Administration. Goddard Space Flight Center, Greenbelt, Md.

RELATING NIMBUS-7 37 GHZ DATA TO GLOBAL LAND-SURFACE EVAPORATION, PRIMARY PRODUCTIVITY AND THE ATMOSPHERIC CO2 CONCENTRATION

B. J. CHOUDHURY (NASA, Goddard Space Flight Center, Greenbelt, MD) International Journal of Remote Sensing (ISSN 0143-1161), vol. 9, Jan. 1988, p. 169-176. refs

Global observations at 37 GHz by the Nimbus-7 SMMR are related to zonal variations of land surface evaporation and primary productivity, as well as to temporal variations of atmospheric CO2 concentration. The temporal variation of CO2 concentration and the zonal variations of evaporation and primary productivity are shown to be highly correlated with the satellite sensor data. The potential usefulness of the 37-GHz data for global biospheric and climate studies is noted. B.J.

A88-29479

ACCURACY OF MAPPING BY PANORAMIC PHOTOGRAPHY

S. PITERI (Athens, University, Greece) Earth, Moon, and Planets (ISSN 0167-9295), vol. 40, Jan. 1988, p. 29-44. refs

An effort has been made to estimate the accuracy of mapping with the use of panoramic photography. The analysis includes a formulation of the equations that give the ground coordinates of objects imaged on two panoramic photographs. The effect of errors in the acquisition of the data on the estimation of the ground coordinates of the objects has been calculated and it is shown that the accuracy of the resulting maps or profiles will be diminished

for objects near the horizon and for objects imaged at the ends of the film strip. Author

A88-29490

AN AUTOCAD-BASED MAPPING SYSTEM FOR ENCODED STEREOPLOTTERS

JAMES A. ROGERS (North Pacific Aerial Surveys, Inc., Anchorage, AK) and ROBERT M. BENNETT (ComRim Systems, Inc., Anchorage, AK) Photogrammetric Engineering and Remote Sensing (ISSN 0099-1112), vol. 54, March 1988, p. 353-355.

Microcomputer CAD technology can be applied to the growing field of digital mapping through an encoder interface to existing analog stereoplotters. One such approach, developed by DAT/EM Systems, links the stereoplotter directly to the AutoCAD software. The use of low cost, general purpose PC equipment for photogrammetric data capture is discussed. Author

A88-29491

AN INTEGRATED APPROACH FOR AUTOMATED COVER-TYPE MAPPING OF LARGE INACCESSIBLE AREAS IN ALASKA

MICHAEL D. FLEMING (TGS Technology, Inc., Anchorage, AK) Photogrammetric Engineering and Remote Sensing (ISSN 0099-1112), vol. 54, March 1988, p. 357-362. refs

An integrated approach to computer-aided analysis is described by illustrating the development of a cover-type map for the 1.43 million acre Kanuti National Wildlife Refuge in Alaska. This method combines field data with spatial data sets consisting of Landsat MSS data, digital elevation data, and high-altitude color-IR aerial photographs. Consideration is given to the data selection and definition process; the selection of training blocks and plots; the collection of the field data; the preprocessing of the spectral classes; the processing of the field data; the labeling and stratification of the spectral classes; and the evaluation of the cover-type classification. The benefits of this integrated procedure employed to generate cover-type maps are discussed. I.F.

A88-29496

THE ARSUP DATABASE AND ITS ACCESS THROUGH THE CMCIRS CATALOG - MAKING AVAILABLE TO THE PUBLIC DIGITAL MAPS FROM THE ARSUP PROCESS

THOMAS FRANK EIDEL and JANICE L. CROUCH (U.S. Department of the Interior, Bureau of Land Management, Anchorage, AK) Photogrammetric Engineering and Remote Sensing (ISSN 0099-1112), vol. 54, March 1988, p. 389-394. refs

A88-29499

INFORMATION CONTENT OF SPECTRAL SIGNATURES AND TEXTURES AND STRUCTURES FOR REMOTE SENSING OF THE EARTH [ZUM INFORMATIONSGEHALT VON SPECTRALEN SIGNATURMERKMALEN SOWIE TEXTUREN UND STRUKTUREN FÜR DIE GEOFERNERKUNDUNG]

R. SOELLNER (Akademie der Wissenschaften der DDR, Zentralinstitut fuer Physik der Erde, Potsdam, German Democratic Republic) Gerlands Beitrage zur Geophysik (ISSN 0016-8696), vol. 96, no. 6, 1987, p. 478-488. In German. refs

The use of spectral signatures to determine the textural and structural characteristics of natural objects in remote sensing is discussed. It is shown how the different properties of the biosphere and the lithosphere can be determined point by point using broadband measurements of target surfaces in the visible and in the near-infrared, infrared, far-infrared, and microwave regions. A classification of the textures of natural objects for purposes of remote sensing is proposed. C.D.

A88-30080

KARST AND EROSION TOPOGRAPHY ON SPACE PHOTOGRAPHS (WITH REFERENCE TO THE USTIURT PLATEAU) [EROZIONNO-KARSTOVYE FORMY REL'EF'A NA KOSMICHESKIKH SNIMKAKH /NA PRIMERE PLATO USTIURT/]

M. I. BURLESHIN and A. G. CHIKISHEV (Proizvodstvennoe

Geologicheskoe Ob'edinenie, Moscow, USSR) Issledovanie Zemli iz Kosmosa (ISSN 0205-9614), Nov.-Dec. 1987, p. 31-33. In Russian. refs

A88-30086

THE USE OF SUCCESSIVE CLUSTERING TO ANALYZE MULTISPECTRAL IMAGERY [PRIMENENIE POSLEDOVATEL'NOI KLASTERIZATSII DLIA ANALIZA MNOGOZONAL'NYKH IZOBRAZHENII]

M. D. BREIDO, A. N. POTAPOV, A. V. SHATALOV, and R. I. EL'MAN (Vsesoiuznoe Aerofotolesoustroitel'noe Ob'edinenie, Moscow, USSR) Issledovanie Zemli iz Kosmosa (ISSN 0205-9614), Nov.-Dec. 1987, p. 73-78. In Russian. refs

This paper considers an algorithm of successive classification without training and its application in the analysis of multispectral imagery. The method essentially relies on the iterative use of clustering analysis to extract image regions with spectrally uniform brightness and to assign them to specific classes. At the end of each iteration the regions recognized are labeled with the name of a corresponding class and are no longer considered. The contrast of the rest of the image is enhanced and the analysis procedure is repeated. The advantages of this method are illustrated with reference to the condition of pine forests estimated using multispectral images. Author

A88-32167

A COMPARISON BETWEEN PANORAMIC PHOTOGRAPHY AND CONVENTIONAL AERIAL PHOTOGRAPHY IN TERMS OF MAPPING ACCURACY

S. PITERI (Athens, University, Greece) Earth, Moon, and Planets (ISSN 0167-9295), vol. 40, March 1988, p. 295-302.

The accuracy of estimation of ground coordinates of objects imaged using aerial photography is compared with that of objects imaged using panoramic photography. Errors in the data used to evaluate the ground coordinates affect the accuracy of mapping from both types of photography in a similar way when the image points have small radial distances. The mapping accuracy from panoramic photography will be lessened when the image points of the ground objects appear near the edges of the photograph, although this is also the case for tilted aerial photographs. R.R.

N88-15287* Pacific Northwest Labs., Richland, Wash.

LANDSAT THEMATIC MAPPER RADIOMETRIC CALIBRATION STUDY

G. E. WUKELIC, D. E. GIBBONS, H. P. FOOTE, and L. M. MARTUCCI Aug. 1987 7 p Presented at the Annual LANDSAT TM Investigators' Workshop, Santa Barbara, Calif., 1 Sep. 1987 (Contract DE-AC06-76RL-01830) (NASA-CR-182410; NAS 1.26:182410; DE88-001965; PNL-SA-15199; CONF-8709179-1) Avail: NTIS HC A02/MF A01 CSDL 08B

The intent was to develop and test analytical techniques that will enhance the scientific and technical exploitation of digital multispectral data. The thrust involved radiometric calibration efforts aimed at determining the bias and validity in absolute temperature determinations using TM band 6 data. Other objectives included: looking at spectral characterization; change detection; combined reflective and emissive data use; and mixed pixel and atmospheric adjustments. To date, six TM data sets (five day scenes and one night scene) have been analyzed. Calibration accuracy of the water and non-water satellite-determined temperatures, using atmospherically corrected radiance values determined from LOWTRAN 6 with local radiosonde, non-local radiosonde, and LOWTRAN 6 model atmospheres, have been studied. Thermal values for non-water pixels have recently been determined. Extensive progress has been made in validating our calibration methodology, analyzing TM5-band 6 data sets for water and non-water pixels, verifying the mixed pixel and atmospheric adjustment methodologies, considering the quantitative effects of clouds and emissivities on absolute temperature determinations, and in conducting initial experiments relative to band 7 calibration. DOE

N88-15290 Deutsche Geodaetische Kommission, Munich (West Germany).

THEORY AND RESEARCH ON THE DISJUNCTION OF CROSS PASSAGE ERRORS AND SYSTEMATIC IMAGE ERRORS IN PHOTOGRAMMETRIC POINT DETERMINATION Ph.D. Thesis - Stuttgart Univ., West Germany [THEORIE UND UNTERSUCHUNG DER TRENNBARKEIT VON GROBEN PASSPUNKTFEHLERN UND SYSTEMATISCHEN BILDFEHLERN BEI DER PHOTOGRAMMETRISCHEN PUNKTBESTIMMUNG]

DEREN LI 1987 123 p In GERMAN (SER-C-324; ISBN-3-7696-9374-4; ISSN-0065-5325; ETN-88-90802) Avail: Issuing Activity

Image error compensation is discussed. Ways for a better separation of gross passage errors and the systematic ones are: cross aerial photography with 20 percent superposing which gives the best performances (nearly equal to the double flight results with 60 percent superposing); the measuring of the double points especially when the passage points are weakly lined up; equalizing with a large group, the bundle presenting several images per surface. The gross passage errors are easier to separate from systematic image errors than gross passage points errors in between. ESA

N88-16115# Joint Publications Research Service, Arlington, Va. **MULTISTEP COMPONENT ANALYSIS OF CORRELATIONS**

Abstract Only

V. A. KOTTSOV and E. A. GORBUSHINA In its JPRS Report: Science and Technology. USSR: Space p 135 24 Nov. 1987 Transl. into ENGLISH from Issledovaniye Zemli iz Kosmosa (Moscow, USSR), no. 2, Mar. - Apr. 1987 p 118-122 Original language document was announced in IAA as A87-48193 Avail: NTIS HC A08/MF A01

The feasibility of using the principal component method to select optimal combinations of spectral channels in the multispectral remote sensing of the Earth is discussed. The optimization procedure employs differences in the indeterminacies of correlation matrix elements and eliminates them successively by comparison with a given accuracy threshold. The potential of the method is demonstrated by analysis of multispectral imagery obtained with the MKF-6 camera on Soyuz-22. Author

N88-16135# Joint Publications Research Service, Arlington, Va. **PHOTOGRAMMETRIC PRINCIPLES FOR COMBINING REMOTE SOUNDING AND THREE-DIMENSIONAL MAPPING Abstract Only**

O. R. MUSIN, B. A. NOVAKOVSKIY, and S. N. SERBENYUK In its USSR Report: Earth Sciences p 42-43 30 Mar. 1987 Transl. into ENGLISH from Vestnik Moskovskogo Universiteta: Seriya 5, Geografiya (Moscow, USSR), no. 6, Nov. - Dec. 1986 p 56-64 Avail: NTIS HC A04/MF A01

Some aspects of automated three-dimensional mapping of the relief image of the earth's surface on the basis of photogrammetric digital terrain models are described. Attention is given to the role of photogrammetry in the further introduction of remote sounding in cartographic work and geographical research. The possibilities afforded by combining remote sounding and three-dimensional mapping are illustrated in the example of cartometric interpretation of a fragment of a digital terrain model using the AKS-MGU automated cartographic system. The user is supplied with a definite set of mutually supplementing metric and nonmetric components of three-dimensional mapping which may or may not be matched with the initial photographic image. The photogrammetric methods make it possible to introduce remote sounding into geographical research by a quantitative interpretation of aerial and space photographs. This is an effective means for forming a digital data base which can be used in obtaining a wide range of cartometric and morphometric indices, which are key elements of three-dimensional mapping. Author

07 DATA PROCESSING AND DISTRIBUTION SYSTEMS

N88-16169# Ludwig-Maximilians-Universitaet, Munich (West Germany). Inst. fuer Meteorologie.

THE ROLE OF ANISOTROPY IN THE LONG RANGE RECONNAISSANCE OF THE ALBEDO OF LAND SURFACES [DIE ROLLE DER ANISOTROPIE BEI DER FERNERKUNDUNG DER ALBEDO VON LANDOBERFLAECHEEN]

PETER KOEPKE *In its* Research Work at the Meteorological Institute of the University of Munich (Federal Republic of Germany) p 157-160 Mar. 1987 In GERMAN
Avail: NTIS HC A11/MF A01

The determination of the albedo of land surfaces, varying in space and time, from radiation density satellite measurements, was investigated. The anisotropy at the radiation field is described by an anisotropy factor, depending on the angles of Sun and satellite in the measuring point. The anisotropy factors spectrally depend on the characteristics of soil and atmosphere. The errors resulting from the assumption that the land surfaces can be treated as isotropic reflectors are discussed. For large land surfaces average anisotropy factors can be measured from satellites. For smaller land surfaces with different types of vegetation, specific anisotropy factors, calculated by numerically simulated radiation density fields, have to be used. ESA

N88-16171# Ludwig-Maximilians-Universitaet, Munich (West Germany). Inst. fuer Meteorologie.

THE ANISOTROPY OF REFLECTED SOLAR RADIATION OVER SEVERAL TYPES OF LAND SURFACE [DIE ANISOTROPIE REFLEKTIERTER SOLARER STRAHLUNG UEBER VERSCHIEDENEN LANDOBERFLAECHEENTYPEN]

RALF MEERKOEETTER *In its* Research Work at the Meteorological Institute of the University of Munich (Federal Republic of Germany) p 165-171 Mar. 1987 In GERMAN
Avail: NTIS HC A11/MF A01

A set of spectral reflection functions for the description of the most important surface types of the Earth was developed using computer simulations and results of measurements. The developed model is based on a geometrical approach, supposing that the anisotropy in the reflected radiation field of natural surfaces is essentially determined by the geometrical structure of the surface components. The application possibilities of the model are discussed. The results of the model show the superimposed effects of the macro and microstructure on the anisotropy of the reflected radiation. ESA

N88-16181# Instituto de Pesquisas Espaciais, Sao Jose dos Campos (Brazil).

TEXTURAL FEATURES FOR IMAGE CLASSIFICATION IN REMOTE SENSING

VITOR HAERTEL (Universidade Federale do Rio Grand do Sul, Porto Alegre, Brazil) and YOSIO EDEMIR SHIMABUKURO May 1987 47 p Presented at the 4th Brazilian Symposium on Remote Sensing, Gramado, Brazil, 10-15 Aug. 1986 (INPE-4169-PRE/1066) Avail: NTIS HC A03/MF A01

Texture is an important characteristic in identifying regions of interest in an image. Several methods to quantify image texture were reported in literature. Experiments aimed to extract textural features from digital images by calculating statistical properties in and around each pixel are described. This moving window concept is implemented, and tests using LANDSAT MSS and TM imagery are presented. Author

N88-16760# European Space Agency. European Space Research and Technology Center, ESTEC, Noordwijk (Netherlands). Data Handling Div.

EARTHNET'S EXPERIENCE WITH SEASAT SAR IMAGE PROCESSING

J. P. GUIGNARD *In its* ESA Bulletin No. 24 p 40-45 Nov. 1980
Avail: NTIS HC A05/MF A01

Synthetic aperture radar (SAR) data transmitted by the Seasat-4 spacecraft was acquired in Europe and processed using optical and digital techniques. Valuable experience was gained at system level with hardware and processing algorithms. Delivery of data

was regularly complemented by the organization of workshops aimed at facilitating the dialogue with the potential users of such data, to simulate European user and applications-oriented initiatives. As the different and often unexpected applications of SAR images emerged, optimum extraction of information content become more and more the crucial issue, not just for the Seasat data but more particularly for future SAR-carrying satellite missions, such as a European Earth-resources satellite. Author (ESA)

N88-16761# European Space Agency. ESRIN, Frascati (Italy). Earthnet Program Office.

THE EARTHNET HEAT CAPACITY MAPPING MISSION (HCMM) DATA-PROCESSING SYSTEM AT LANNION (FRANCE)

L. FUSCO *In its* ESA Bulletin No. 24 p 46-52 Nov. 1980
Avail: NTIS HC A05/MF A01

Within the framework of the Earthnet Program and the Memorandum of Understanding between ESA and NASA, the French Space Meteorology Center is acquiring, archiving, and preprocessing data from NASA's Heat-Capacity Mapping Mission (HCMM) spacecraft. The data from the HCMM support scientific investigations to establish the feasibility of using thermal infrared measurements of the Earth's surface to determine soil thermal inertia. Author (ESA)

N88-17152*# Illinois State Water Survey, Champaign. Climate and Meteorology Section.

APPLICATION OF SATELLITE DATA IN VARIATIONAL ANALYSIS FOR GLOBAL CYCLONIC SYSTEMS Status Report

G. L. ACHEMEIER Feb. 1988 28 p
(Contract NAG8-059)
(NASA-CR-182468; NAS 1.26:182468) Avail: NTIS HC A03/MF A01 CSCL 04B

The goal of the research is a variational data assimilation method that incorporates as dynamical constraints, the primitive equations for a moist, convectively unstable atmosphere and the radiative transfer equation. Variables to be adjusted include the three-dimensional vector wind, height, temperature, and moisture from rawinsonde data, and cloud-wind vectors, moisture, and radiance from satellite data. In order to facilitate thorough analysis of each of the model components, four variational models that divide the problem naturally according to increasing complexity were defined. The research performed during the second year fall into four areas: sensitivity studies involving Model 1; evaluation of Model 2; reformation of Model 1 for greater compatibility with Model 2; development of Model 3 (radiative transfer equation); and making the model more responsive to the observations. B.G.

N88-18056# Army Engineer Topographic Labs., Fort Belvoir, Va.

AUTOCORRELATION OF CONTROL POINTS ON 11-BAND MULTISPECTRAL IMAGERY

ROBERT S. RAND Aug. 1987 31 p
(AD-A188185; ETL-0473) Avail: NTIS HC A03/MF A01 CSCL 12I

The use of multispectral imagery with other types of imagery requires that the combined set be accurately registered. This study investigates correlation properties between bands of an 11-channel multispectral scanner for 37 control points in support of interband registration that can later be extended to dissimilar image registration. The results show a high degree of correlation between channels 1 through 7, but a lower and unpredictable correlation for other combinations. In addition to providing information about interband registration, the results also have implications for multispectral segmentation algorithms. GRA

N88-18978# Defense Mapping Agency Aerospace Center, St. Louis, Mo.

THE DIGITAL LANDMASS SIMULATION PRODUCTION OVERVIEW

RICHARD V. HALBERT 1987 8 p
(AD-A187978) Avail: NTIS HC A02/MF A01 CSCL 08B

The Defense Mapping Agency (DMA) pioneered in the

development and production of Digital Landmass (DLMS) data to support various simulation systems for operational training. A variety of production techniques, procedures, software, and equipment have been developed by DMA since 1977. The Agency is currently responsible for the publication and distribution of product specifications for DLMS data and is also responsible for Multination agreement establishing standardized production and exchange of DLMS data. This presentation explores some of this production methodology. While not an historical treatment of the subject, production and methodology will be discussed in an evolutionary context. Finally, the presentation will explore some future considerations involving further evolution of the production methodology as well as comment on anticipated changes to the nature of DLMS data. GRA

N88-18979# Naval Postgraduate School, Monterey, Calif.
THREE-DIMENSIONAL IMAGE GENERATION FROM AN AERIAL PHOTOGRAPH M.S. Thesis

LELAND G. COLEMAN Sep. 1987 106 p
 (AD-A188039) Avail: NTIS HC A06/MF A01 CSCL 08B

This thesis concerns developing a program that takes an aerial photograph, and a set of Digital Terrain Elevation Data (DTED) that is defined over the area of the photograph, and generates a synthesized view that represents what a camera would see from a different location. The elevation data points are grouped into triangular panels that are projected to the reference image by three dimensional transformation equations. Shading for the synthesized image is determined from the reference image. The pixels of the reference image that fall within a triangular panel are collected and averaged. When a new observer location is selected, the panels are projected to the new synthesized image plane. A z-buffer approach and a polygon fill algorithm were used to remove hidden surfaces of the synthesized view. This program is tested on both artificial and real data. Other characteristics and performance measurements of the program are also analyzed here. The quality of the synthesized image from real data was affected by the low resolution of the terrain elevation data, and yielded less desirable results than could be expected of a high resolution. GRA

N88-18983# Army Engineer Topographic Labs., Fort Belvoir, Va.

RADAR DESCRIPTORS FOR THE CLASSIFICATION OF TERRAIN FEATURES

FREDERICK W. ROHDE 16 Sep. 1987 17 p
 (AD-A188145; USAETL-R-109) Avail: NTIS HC A03/MF A01 CSCL 171

An approach toward the automated extraction of terrain features from synthetic aperture radar (SAR) imagery is the development of sets of descriptors that uniquely and unambiguously characterize each feature. This investigation involves a detailed examination of 701 SAR image examples covering 29 types of man-made and natural terrain features. The descriptors represent attributes of the radar signatures from terrain features. The descriptors are developed by means of which image analysts identify the terrain features. The development of descriptors is guided by the objectives that the descriptors can be easily recognized and identified by untrained personnel and that they provide a baseline for interactive and automated feature extraction. The number of selected descriptors at this point is 52 and may change as the research progresses. A feature class is characterized by specific sets of descriptors. Because radar signatures of the same type of terrain feature will vary it is necessary to establish combination rules for descriptor sets. GRA

N88-18985 New South Wales Univ., Kensington (Australia). School of Electrical Engineering and Computer Science.

MULTISOURCE CONTEXT CLASSIFICATION METHODS IN REMOTE SENSING Abstract Only. Ph.D. Thesis

TONG LEE Oct. 1986 264 p
 Avail: Issuing Activity

The problem of multisource data analysis in remote sensing is concerned with the extraction of information embodied in different

sources of spatial data to allow a composite decision to be made concerning the class membership of pixels in the data. Methodologies for solving this problem were in the past mostly ad hoc, and only little attention was given to deriving means for machine-assisted or semi-automated analysis of multisensor and multisource spatial data. Two approaches, one probabilistic and the other evidential, are described for addressing this important problem. The concepts developed in both multisource classification approaches are evaluated with LANDSAT image data and the results demonstrate their effectiveness. An essential feature common to both approaches is the ability to incorporate uncertainties regarding the data and analysis qualities into the process of making composite inferences, a property not shared with other established techniques. Author

N88-18987# Instituto de Pesquisas Espaciais, Sao Jose dos Campos (Brazil).

A DIGITAL TERRAIN SYSTEM FOR MICROCOMPUTERS [UM SISTEMA DIGITAL DE TERRENO PARA MICROCOMPUTADORES]

CARLOS ALBERTO FELGUEIRAS, GUARACI JOSE ERTHAL, LUIZ ALBERT VIEIRA DIAS, JOAO ARGEMIRO C. PAIVA, and GILBERTO CAMARA NETO May 1987 8 p In PORTUGUESE; ENGLISH summary Presented at the 14th Integrated Software and Hardware Seminar, Salvador, Bahia, 11-19 Jul. 1987 (INPE-4170-PRE/1067) Avail: NTIS HC A02/MF A01

This paper describes theoretical and implementation features of a Digital Terrain Modeling System (DTM). This system runs on a microcomputer and is integrated with a Geographic Information System which allows the combination of DTM data with thematic maps, satellite images, and so on, to obtain new derived maps. Author

N88-18996# Institut fuer Angewandte Geodaesie, Frankfurt am Main (West Germany).

THE ORIENTATION OF GLOBAL SATELLITE NETWORKS [ZUR ORIENTIERUNG VON GLOBALEN SATELLITENNETZEN]

GERHARD SOLTAU In its Reports on Cartography and Geodesy. Series 1, Report 98 p 95-105 1987 In GERMAN, ENGLISH summary Avail: NTIS HC A06/MF A01

The datum problem of global networks, determined by satellite techniques, is treated. The conditions for the derivation of the Bender-Goad formulas for the orientation of global networks are given. It is shown that these can be derived on the basis of the fictitious transformation of Reissmann. The datum problem can be removed by a combination of the adjustment of the measured value and a Helmert coordinate transformation to a compatible approximation system. ESA

N88-19810# Carnegie-Mellon Univ., Pittsburgh, Pa. Dept. of Computer Science.

AUTOMATIC KNOWLEDGE ACQUISITION FOR AERIAL IMAGE INTERPRETATION Interim Report

DAVID M. MCKEOWN, JR. and WILSON A. HARVEY Dec. 1987 45 p
 (Contract F33615-84-K-1520)
 (AD-A188616; CMU-CS-87-102; AFWAL-TR-87-1165) Avail: NTIS HC A03/MF A01 CSCL 08B

The interpretation of aerial photographs requires a lot of knowledge about the scene under consideration. Knowledge about the type of scene: airport, suburban housing development, urban city, aids in low-level and intermediate level image analysis, and will drive high-level interpretation by constraining search for plausible consistent scene models. Collecting and representing large knowledge bases requires specialized tools. In this paper we describe the organization of a set of tools for interactive knowledge acquisition of scene primitives and spatial constraints for interpretation of aerial imagery. These tools include a user interface for interactive knowledge acquisition, the automated compilation of that knowledge from a schema-based representation into productions that are directly executable by our interpretation system, and a performance analysis tool that generates a critique

07 DATA PROCESSING AND DISTRIBUTION SYSTEMS

of the final interpretation. Finally, the generality of these tools is demonstrated by the generation of rules for a new task, suburban house scenes, and the analysis of a set of imagery by our interpretation system. GRA

N88-20124# Instituto de Pesquisas Espaciais, Sao Jose dos Campos (Brazil).

PHOTOGRAPHIC FILTERS [FILTROS FOTOGRAFICOS]

JOSE EDUARDO RODRIGUES and WAGNER SANTOSDEALMEIDA
Dec. 1987 98 p In PORTUGUESE; ENGLISH summary
(INPE-4448-RPE/558) Avail: NTIS HC A05/MF A01

Some of the main aspects related to photographic filters are examined and prepared as a reference for researchers and students of remote sensing. A large range of information about the filters including their basic fundamentals, classification, and main types is presented. The theme cannot be exhausted in this or any other individual publication because of its great complexity, profound theoretical publication, and dynamic technological development. The subject does not deal only with filter applications in remote sensing. As much as possible, additional information about the utilization of these products in other professional areas, as pictorial photography, photographic processing, and optical engineering, were included. Author

08

INSTRUMENTATION AND SENSORS

Includes data acquisition and camera systems and remote sensors.

A88-20903

THE DEVELOPMENT AND STATE OF THE ART OF REMOTE SENSING

GOTTFRIED KONECNY (Hannover, Universitaet, Hanover, Federal Republic of Germany) (International Society for Photogrammetry and Remote Sensing, Symposium, Enschede, Netherlands, Aug. 1986) ITC Journal (ISSN 0303-2434), no. 2, 1987, p. 153-156.

Advances in the field of remote sensing are described. Remote sensing is defined in terms of photogrammetry. Events related to the development of remote sensing are discussed. The capabilities of the Landsat MSS and TM, and future trends in remote sensing are examined. The roles of various institutions and societies in promoting remote sensing activities are considered. I.F.

A88-20904

REMOTE SENSING APPLICATIONS - AN OUTLOOK FOR THE FUTURE

HERMAN TH. VERSTAPPEN (International Institute for Aerospace Survey and Earth Sciences, Enschede, Netherlands) (International Society for Photogrammetry and Remote Sensing, Symposium, Enschede, Netherlands, Aug. 1986) ITC Journal (ISSN 0303-2434), no. 2, 1987, p. 157-164.

Future trends in remote sensing are described. Current remote sensing techniques, such as the use of satellite data, mapping projects, and resource assessment, are compared with methods employed in the 1960's. Some of the advances in remote sensing include: more diverse sensors and recording altitudes, the use of digital methods, the availability of topographic and thematic information, and the meteorological and oceanographic use of remote sensing data. Consideration is given to resource surveying, image interpretation, multitemporal recording, quantitative relief analysis, and photogrammetry. Three types of resource satellite systems (high-resolution satellites with multispectral capacity, a low-resolution system, and a system for resource mapping at scales of 1:250,000 to 1:500,000) are examined. The costs involved in implementing new remote sensing techniques, and the need for joint cooperation between nations in order to fulfill future remote sensing goals are discussed. I.F.

A88-21001

AMERICAN SOCIETY FOR PHOTOGRAMMETRY AND REMOTE SENSING AND ACSM, ANNUAL CONVENTION, BALTIMORE, MD, MAR. 29-APR. 3, 1987, TECHNICAL PAPERS. VOLUME 1 - REMOTE SENSING

Convention sponsored by the American Society for Photogrammetry and Remote Sensing and ACSM. Falls Church, VA, American Society for Photogrammetry and Remote Sensing and ACSM, 1987, 460 p. For individual items see A88-21002 to A88-21045.

Topics discussed in this volume include hydrospheric sciences; the applications of photointerpretation to resource assessments; earth-system science remote sensing research on global change; developments in workstations for image processing and geographic data handling; plant sciences; use of satellites for assessing forest cover; the techniques and applications of radar/sonar; and geography, land use, and land cover remote sensing. Papers are presented on the development of multistage estuarine water quality models using Landsat 2 and 4 MSS data, technical considerations in software design for scene catalog geographic searches, multistage remote sensing as a tool for Minnesota natural resources management, and modeling interactions between the terrestrial biosphere and the global atmosphere. Other papers include those on software and workstation design considerations for grass, the principal component analysis of aerial video imagery, the definition of forest stand characteristics based on multiincidence angle SIR-B data, image-based SAR product simulation for analysis, and automated road network extraction from Landsat TM data. I.S.

A88-21018

MULTI-STAGE REMOTE SENSING - A TOOL FOR MINNESOTA NATURAL RESOURCES MANAGEMENT

LEE M. WESTFIELD (State of Minnesota, Dept. of Natural Resources, Grand Rapids) IN: American Society for Photogrammetry and Remote Sensing and ACSM, Annual Convention, Baltimore, MD, Mar. 29-Apr. 3, 1987, Technical Papers. Volume 1. Falls Church, VA, American Society for Photogrammetry and Remote Sensing and ACSM, 1987, p. 160-165.

Minnesota natural resources managers use several remote sensing products in combination to effectively and efficiently manage the resource. Photography in 35 mm format is used to monitor and update management activities. This photography is produced at scales of 1:200 to 1:31,680 using the optimal film type, and flown in the optimal season and on a critical schedule. Applications include: (1) configuration and acreage determination for timber sales and mechanical site preparations; (2) qualitative evaluation of plantations, herbicide applications, aspen regeneration density, fire and windthrow; (3) time critical data such as the seasonal wild rice cover crop for the waterfowl migration, water levels of lakes and rivers and insect or disease infections; and (4) species identification of vegetation. This format (35 mm) along with National High Altitude Photography (NHAP) greatly enhances the traditional photography; 1:15,840, black-and-white (B&W) infrared, 9-in. contact prints. All of these photographic resources are important for monitoring management activities, accurately updating a continuous inventory system and management planning. Author

A88-21019

OBSERVATIONS OF SURFACE AND ATMOSPHERIC FEATURES FROM PASSIVE MICROWAVE SATELLITE MEASUREMENTS

RALPH R. FERRARO (Research and Data Systems Corp., Lanham, MD), JOHN C. ALISHOUSE, NORMAN C. GRODY, and J. D. TARPLEY (NOAA, National Environmental Satellite and Data Information Service, Washington, DC) IN: American Society for Photogrammetry and Remote Sensing and ACSM, Annual Convention, Baltimore, MD, Mar. 29-Apr. 3, 1987, Technical Papers. Volume 1. Falls Church, VA, American Society for Photogrammetry and Remote Sensing and ACSM, 1987, p. 166-175. NOAA-supported research. refs

Passive microwave measurements from satellites have been applied to the retrieval of geophysical parameters over land and ocean. Specifically, data at five different frequencies (6.6, 10.7,

18, 21, and 37 GHz) from the Scanning Multichannel Microwave Radiometer (SMMR) aboard the Nimbus-7 satellite have been used. At dual polarization, this array of ten different measurements allows for the retrieval of snow cover, soil moisture, and rain over land. Over oceans, the SMMR data have been used to derive water vapor, cloud water content, rain rate, sea ice concentration, surface temperature, and wind speed. In this paper, algorithms for determining oceanic rain rates and separating various geophysical parameters will be presented. They were developed empirically by comparing the SMMR measurements with available ground truth sources (such as rain gauge, snow depth, and radar measurements). Despite the empirical nature of the algorithms, each has a strong physical basis. The application of the algorithms to various SMMR case studies, displayed as color enhanced images, will be presented. Author

A88-21022

EXTENDED ABSTRACT MODELLING INTERACTIONS BETWEEN THE TERRESTRIAL BIOSPHERE AND THE GLOBAL ATMOSPHERE

PIERS J. SELLERS (Maryland, University, College Park) IN: American Society for Photogrammetry and Remote Sensing and ACSM, Annual Convention, Baltimore, MD, Mar. 29-Apr. 3, 1987, Technical Papers. Volume 1. Falls Church, VA, American Society for Photogrammetry and Remote Sensing and ACSM, 1987, p. 195-205. refs

The philosophy and formulation of a model of the terrestrial biosphere designed for use within atmospheric General Circulation Models (GCMs) are outlined. The Simple Biosphere (SiB) of Sellers et al. (1986) was formulated to provide a biophysically realistic description of the processes governing the transfers of momentum, radiation, and heat (both sensible and latent terms) between the land surface and the atmosphere. It replaces a range of existing formulations which are based on the 'bucket' hydrological model. The SiB model has been extensively tested offline using micrometeorological data sets collected above a variety of vegetated surfaces. The model is in the process of being implemented in three atmospheric GCMs. Recent studies have demonstrated that satellite data may be directly useful in initializing and validating the model. Author

A88-21050

GEOGRAPHICAL POSITION PLOTTING BY PHOTO INTERPRETERS FROM SPACE SHUTTLE LARGE FORMAT CAMERA PHOTOGRAPHY

GLEN C. GUSTAFSON (James Madison University, Harrisonburg, VA), JOHN INKSTER, and JAMES O'HEAR IN: American Society for Photogrammetry and Remote Sensing and ACSM, Annual Convention, Baltimore, MD, Mar. 29-Apr. 3, 1987, Technical Papers. Volume 2. Falls Church, VA, American Society for Photogrammetry and Remote Sensing and ACSM, 1987, p. 233-240. refs

Large Format Camera (LFC) images from Space Shuttle, and Metritek-21 aircraft images were used by photointerpreters for the photogrammetric plotting of geographical positions. Ground control for the orientation of the airphotos came primarily from U.S. Geological Survey topographic quadrangles of two different scales. For image measuring, a standard roll-film light table, with X-Y mensuration system and zoom stereoscope was used. Monoplotting software, on a mainframe computer supports the photointerpretation work station. The effort is made to evaluate the quality of the image-plotted ground coordinates, in relation to the quality of the input ground control. Author

A88-21051

PARALLAX BAR HEIGHTING ACCURACY OF LARGE FORMAT CAMERA PHOTOGRAPHY

C. P. LO (Georgia, University, Athens) IN: American Society for Photogrammetry and Remote Sensing and ACSM, Annual Convention, Baltimore, MD, Mar. 29-Apr. 3, 1987, Technical Papers. Volume 2. Falls Church, VA, American Society for Photogrammetry and Remote Sensing and ACSM, 1987, p. 251-257. Research supported by the University of Georgia.

The x-parallax of the large format camera (LFC) photographs

of the Cape Cod area was measured using a precision parallax bar and a mirror stereoscope under 6X enlargement to obtain height information on terrains and buildings in cities. The use of the y-squared term in the model deformation correction formula and an appropriate distribution of six control points produced an rmse of + or - 63.0 m (+ or - 0.27 per mil of the flying height). Enlarged portions (18X) of the LFC photographs led to even better height results because of their more restricted coverage and less severe error in base alignment. K.K.

A88-21168* Jet Propulsion Lab., California Inst. of Tech., Pasadena.

INTRODUCTION TO THE PHYSICS AND TECHNIQUES OF REMOTE SENSING

CHARLES ELACHI (California Institute of Technology, Jet Propulsion Laboratory, Pasadena) New York, Wiley-Interscience, 1987, 444 p. refs

This book presents a comprehensive overview of the basics behind remote-sensing physics, techniques, and technology. The physics of wave/matter interactions, techniques of remote sensing across the electromagnetic spectrum, and the concepts behind remote sensing techniques now established and future ones under development are discussed. Applications of remote sensing are described for a wide variety of earth and planetary atmosphere and surface sciences. Solid surface sensing across the electromagnetic spectrum, ocean surface sensing, basic principles of atmospheric sensing and radiative transfer, and atmospheric remote sensing in the microwave, millimeter, submillimeter, and infrared regions are examined. C.D.

A88-21382

RELATIONSHIPS BETWEEN MONTHLY PRECIPITATION AND SST VARIATIONS IN THE TROPICAL PACIFIC REGION

BRYAN C. WEARE (California, University, Davis) Monthly Weather Review (ISSN 0027-0644), vol. 115, Nov. 1987, p. 2687-2698. NSF-supported research. refs

The relationships between the patterns of monthly sea surface temperature (SST) variations and those of precipitation in the tropical Pacific Ocean region are examined. The rainfall data utilized are derived from satellite observations of outgoing longwave radiation. A composite empirical orthogonal function analysis of SST and rainfall perturbations is presented which indicates a dominant mode of variation linking SST variations in the eastern equatorial region with those of rainfall about 30 deg westward. One-point correlation analyses show that this general relationship is present for all points in the eastern and central ocean, but that no significant SST-rainfall correlations are evident for SST points west about the dateline. The results are used to formulate possible statistical models for using observed SST anomalies to specify rainfall departure patterns. C.D.

A88-21660

AUTONOMOUS CONTROL OF IMAGE SENSOR FOR THE OPTIMAL ACQUISITION OF GROUND INFORMATION FOR DYNAMIC ANALYSIS

SING T. BOW (Pennsylvania State University, University Park) IN: Space Station automation II; Proceedings of the Meeting, Cambridge, MA, Oct. 28-30, 1986. Bellingham, WA, Society of Photo-Optical Instrumentation Engineers, 1987, p. 260-264. refs

In this paper an attempt is made to improve the overall performance of a stripmap image sensor through an implementation with AI. The virtual range of scanning thus obtained could be two to three times as large as the original range. The approach suggested is mainly a predictive control with which the viewing direction of the sensor is intermittently centered at the centroid of the target information acquired during the preceding scans so that maximum amount of information on the successive target segments can be obtained. Simulation experiment conducted verifies the feasibility of the suggested approach. Author

A88-21784

CORRELATION CHARACTERISTICS OF IMAGES OF THE EARTH SURFACE OBTAINED WITH A SYNTHETIC-APERTURE RADAR [KORRELIATSIONNYE KHARAKTERISTIKI IZOBRAZHENII ZEMNOI POVERKHNOSTI, POLUCHAEMYKH RADIOLOKATOROM S SINTEZIROVANNOMI APERTUROI]

A. L. IL'IN, M. N. MAROV, and G. V. KORSUNOV Radiotekhnika i Elektronika (ISSN 0033-8494), vol. 32, Nov. 1987, p. 2332-2341. In Russian. refs

The relationship between the correlation characteristics of two types of intensity fluctuations of synthetic-aperture radar images is examined: (1) intraelement fluctuations arising within an image resolution element in the Doppler frequency range and (2) interelement fluctuations due to the random character of images of the earth surface. The correlation intervals are related to the focusing degree and the size of the synthetic aperture, as well as to the interval of incoherent signal accumulation. It is shown that both intraelement and interelement fluctuations can be caused by interference intensity modulation due to the phase part of the complex field of the radar image. B.J.

A88-22724#

THE EARTH-OBSERVATION PREPARATORY PROGRAMME

B. PFEIFFER and R. F. BONNEFOY (ESA, Earth Observation Programmes Dept., Noordwijk, Netherlands) ESA Bulletin (ISSN 0376-4265), no. 51, Aug. 1987, p. 34-38.

The purpose of the ESA Earth-Observation Preparatory Programme (EOPP) is to develop the programs that have been identified in the European Long-Term Space Plan to a level of proven overall system feasibility (Phase-A level). The programs to be prepared to Phase-A level in the framework of EOPP are: a solid-earth program to cover missions for precise positioning and geopotential field measurements; a second-generation Meteosat program; a polar-orbit earth observation program; and a flight-opportunity program providing flight opportunities for instruments developed nationally. Interfaces with the science and applications user community are examined along with organization and schedule. B.J.

A88-23511#

A SEQUENTIAL ESTIMATION APPROACH TO CLOUD-CLEARING FOR SATELLITE TEMPERATURE SOUNDING

J. R. EYRE and P. D. WATTS (Meteorological Office, Oxford, England) Royal Meteorological Society, Quarterly Journal (ISSN 0035-9009), vol. 113, Oct. 1987, p. 1349-1376. refs

After discussing current cloud-clearing methods for temperature sounding of the troposphere, using satellite-borne IR radiometers, a novel approach to cloud-clearing that is based on optimal estimation methods is developed and applied to data from the High-resolution IR Sounder (HIRS) of the Tiros-N/NOAA satellite series. Having obtained preliminary estimates of clear-column radiances and their expected errors at each HIRS spot, the horizontal consistency properties expected in the clear-column radiance field are used to improve the initial estimates using a sequential estimation procedure. Details are presented for the new scheme and for the scheme replaced by it. O.C.

A88-23772

SINGLE-SOURCE THREE-DIMENSIONAL IMAGING SYSTEM FOR REMOTE SENSING

A. PORTER MCLAURIN, EDWIN R. JONES, and LECONTE CATHEY (South Carolina, University, Columbia) Optical Engineering (ISSN 0091-3286), vol. 26, Dec. 1987, p. 1251-1256. Research supported by the University of South Carolina and Carolina Research and Development Foundation. refs

A recent development in three-dimensional imaging is the application of VISIDEP technology to surveillance and reconnaissance. The results of initial efforts to develop a single-source system using a moving platform are reported. These tests clearly demonstrate the feasibility of such a system. Although film was used to achieve the present results, electronic imaging can be used to generate near-real-time three-dimensional video

images with delays of less than 3 s. With the continued development of high density video and digital imaging, improved image resolution is easily achievable. The theoretical basis, testing results, and projections for future development are presented in full detail. Potential applications and expectations are discussed briefly as a part of the conclusion drawn from this basic effort.

Author

A88-24818

ASIAN CONFERENCE ON REMOTE SENSING, 7TH, SEOUL, REPUBLIC OF KOREA, OCT. 23-28, 1986, PROCEEDINGS

Conference sponsored by the Asian Association on Remote Sensing, Korean Society of Remote Sensing, and Japan Association of Remote Sensing. Tokyo, Asian Association on Remote Sensing, 1986, 581 p. No individual items are abstracted in this volume.

Methods, hardware, and applications of remote sensing are discussed in reviews and reports of recent investigations. Topics addressed include the status of remote sensing in individual Asian countries, geographic information systems, land-use cartography, water resources and hydrology, agriculture and forestry, oceanography and meteorology, geology and geomorphology, data processing, and microcomputer applications to education and training. Diagrams, graphs, maps, sample images, and tables of numerical data are provided. T.K.

A88-26050

REMOTE SENSING METHODS AND INSTRUMENTATION FOR OBTAINING DATA ON EARTH RESOURCES AND THE ENVIRONMENT [DISTANTSIONNYE METODY I APPARATURA POLUCHENIIA DANNYKH O PRIRODNYKH RESURSAKH ZEMLI I OKRUZHAIUSHCHEI SREDE]

A. M. VOLKOV, ED. and V. F. TULINOV, ED. Leningrad, Gidrometeoizdat (Gosudarstvennyi Nauchno-Issledovatel'skii Tsentr Izučeniia Prirodnikh Resursov. Trudy, No. 28), 1987, 160 p. In Russian. No individual items are abstracted in this volume.

The development of methods and different types of instruments for obtaining remote sensing data is considered in an attempt to study the atmosphere and natural resources and to monitor the state of the environment. The effect of the solar zenith angle on the reflection properties of the soil is studied as well as the determination of the parameters of the atmosphere and the underlying surface from multichannel microwave measurements with the Meteor-Priroda satellite over land. Attention is also given to the requirements placed on radiometer parameters to ensure the accuracy of brightness temperature measurements. Satellite data coding and conversion problems are examined as well as operational automated planning for optimal satellite data collection and transmission to ground data receiving and processing centers. K.K.

A88-26166

SPOT 1 - EARTH OBSERVING SATELLITE [SPOT 1 - SATELLITE D'OBSERVATION DE LA TERRE]

ROGER FERLET (CNRS, Institut d'Astrophysique, Paris, France) L'Astronomie (ISSN 0004-6302), vol. 101, Nov. 1987, p. 567-571. In French.

The on-board instrumentation and orbital parameters of the SPOT 1 earth observing satellite are discussed. Total earth coverage is achieved by SPOT in a circular sun-synchronous orbit at 822 km altitude with an orbital inclination of 98.7 deg. SPOT makes $14 + 5/26$ revolutions per day, and completes its cycle of earth coverage each 26 days. The high-resolution (20-10 m) optical instruments on-board SPOT can produce 1/100,000 topographic maps. The ability to obtain views of a single region many times during the 26-day cycle allows the study of rapidly changing phenomena. The series of 6000 CCD detectors can simultaneously image a 60-km field at 10-m resolution. R.R.

A88-27027*#

National Environmental Satellite Service, Washington, D. C.

COMPARISON OF TOTAL OZONE AMOUNTS DERIVED FROM SATELLITE AND GROUND-BASED MEASUREMENTS

WALTER G. PLANET (NOAA, National Environmental Satellite, Data, and Information Service, Washington, DC), ALVIN J. MILLER (NOAA, National Weather Service, Silver Spring, MD), and JAMES K. ANGELL (NOAA, Office of Oceanic and Atmospheric Research, Boulder, CO) *Geophysical Research Letters* (ISSN 0094-8276), vol. 15, Jan. 1988, p. 5-8. NASA-supported research. refs

Total ozone amounts derived from the NOAA operational sounder (TOVS) are compared to measurements from Nimbus-7 SBUV and ground-based Dobson spectrophotometer observations over a seven-year period. The global trends of the data, in terms of deviations from long-term averages, derived from measurements by each satellite instrument show qualitative agreement until mid-1984 when the data diverge with the TOVS-derived data showing higher values. Additionally, more significant differences appear in both the north and south temperate zones' records. The trends derived from the satellite systems' measurements also show differences from that of the Dobson instrument measurements with the trend of the TOVS measurements showing generally better overall agreement with the Dobson data record. Author

A88-27214

A METHOD FOR SYNTHESIZING OPTIMAL SPACE SYSTEMS FOR EARTH SURVEYING [METOD SINTEZA OPTIMAL'NYKH STRUKTUR KOSMICHESKIKH SISTEM ZEMLEOBZORA]

V. I. MILOVANOV and O. P. NESTERENKO *Issledovanie Zemli iz Kosmosa* (ISSN 0205-9614), Sept.-Oct. 1987, p. 99-105. In Russian. refs

A method for designing optimal space systems for earth observations is proposed. The design is done in two stages: (1) the preliminary selection of optimal configuration alternatives and (2) the evaluation of selected systems for efficiency. The method is illustrated on an example of an earth-survey system designed for the prediction of the approach of catastrophic events that would threaten Pacific coast. I.S.

A88-27215

THE RELATIONSHIPS BETWEEN ORBIT PARAMETERS AND THE GEOMETRY OF THE TRAJECTORY FOR REMOTE SENSING SATELLITES [ZAVISIMOSTI MEZHDU PARAMETRAMI ORBITY I GEOMETRIEY TRASSY DLIA ISZ DISTANTSIONNOGO ZONDIROVANIYA]

N. S. RAMM and A. K. RYNSKAIA (Vsesoiuznyi Nauchno-Issledovatel'skii Institut Kosmoaerogeologicheskikh Metodov, Leningrad, USSR) *Issledovanie Zemli iz Kosmosa* (ISSN 0205-9614), Sept.-Oct. 1987, p. 106-113. In Russian. refs

A class of orbits with an appropriate number of revolutions per day is identified in the set of satellite near-circular orbits, and the trajectory geometry of such orbits is studied. Also derived are relationships between the number of revolutions, the repetition ratio order, and some other orbit characteristics. These relationships provide for easy selection of an orbit for a specific remote sensing problem. I.S.

A88-27216

IDENTICAL-ROUTE SATELLITE ORBITS FOR LONG-TERM PERIODIC GLOBAL SURVEY OF THE EARTH, NOT DEPENDENT ON SOLAR ILLUMINATION [IZOMARSHRUTNYE ORBITY ISZ DLIA DOLGOVREMENNOGO PERIODICHESKOGO GLOBAL'NOGO OBZORA ZEMLI, NE ZAVISIASHCHEGO OT SOLNECHNOGO OSVESHCHENIYA]

A. K. RYNSKAIA (Vsesoiuznyi Nauchno-Issledovatel'skii Institut Kosmoaerogeologicheskikh Metodov, Leningrad, USSR) *Issledovanie Zemli iz Kosmosa* (ISSN 0205-9614), Sept.-Oct. 1987, p. 114-120. In Russian. refs

This paper considers the problem of selecting circular orbits for long-term periodic global surveys by detectors that do not require solar illumination. A methodology is proposed for the calculation of identical-route orbits that provide for global coverage in a specified time interval with a minimum detector survey zone. I.S.

A88-27497* Maryland Univ., College Park.
THE FIRST ISLSCP FIELD EXPERIMENT (FIFE)

P. J. SELLERS (Maryland, University, College Park), F. G. HALL (NASA, Goddard Space Flight Center, Greenbelt, MD), G. ASRAR (Kansas State University, Manhattan), D. E. STREBEL (Science Applications Research, Lanham, MD), and R. E. MURPHY (NASA, Washington, DC) *American Meteorological Society, Bulletin* (ISSN 0003-0007), vol. 69, Jan. 1988, p. 22-27.

The background and planning of the first International Satellite Land Surface Climatology Project (ISLSCP) field experiment (FIFE) are discussed. In FIFE, the NOAA series of satellites and GOES will be used to provide a moderate-temporal resolution coarse-spatial resolution data set, with SPOT and aircraft data providing the high-spatial resolution pointable-instrument capability. The paper describes the experiment design, the measurement strategy, the configuration of the site of the experiment (which will be at and around the Konza prairie near Manhattan, Kansas), and the experiment's operations and execution. I.S.

A88-27801* Maryland Univ., College Park.

REMOTE SENSING FROM SPACE; PROCEEDINGS OF SYMPOSIUM 3, WORKSHOP V, AND TOPICAL MEETING A2 OF THE TWENTY-SIXTH COSPAR PLENARY MEETING, TOULOUSE, FRANCE, JUNE 30-JULY 11, 1986

S. N. GOWARD, ED. (Maryland, University, College Park), S. G. UNGAR, ED. (NASA, Goddard Institute for Space Studies, New York), J. NITHACK, ED. (DFVLR, Wessling, Federal Republic of Germany), and A. F. HASLER, ED. (NASA, Goddard Space Flight Center, Greenbelt, MD) *Symposium, Workshop, and Meetings sponsored by COSPAR, WMO, URSI, et al. Advances in Space Research* (ISSN 0273-1177), vol. 7, no. 11, 1987, 398 p. In English and French. For individual items see A88-27802 to A88-27849.

Various papers on remote sensing from space are presented. The use of such remote sensing to study terrestrial patterns and processes is examined, including the relevant processes and theories, observed vegetation and surface climate parameters, derived terrestrial processes, atmospheric effects, and new sensors. Quantitative radar remote sensing of land and oceanic surface features is addressed, including systems, calibration, simulation, data evaluation for vegetational studies, altimetry, sea ice monitoring, and oil slick detection. The use of satellite observations for weather prediction is discussed. C.D.

A88-27813* National Aeronautics and Space Administration. Goddard Space Flight Center, Greenbelt, Md.

IMPORTANCE OF A REMOTE MEASUREMENT OF SPECTRAL THERMAL INFRARED EMISSIVITIES - PRESENTATION AND VALIDATION OF SUCH A DETERMINATION

F. BECKER (NASA, Goddard Space Flight Center, Greenbelt, MD), F. NERRY, P. RAMANANTSIHENA, and M. P. STOLL (Strasbourg, Ecole Nationale Supérieure de Physique, France) (COSPAR, WMO, URSI, et al., Plenary Meeting, 26th, Symposium 3, Workshop V, and Topical Meeting A2 on Remote Sensing from Space, Toulouse, France, June 30-July 11, 1986) *Advances in Space Research* (ISSN 0273-1177), vol. 7, no. 11, 1987, p. 121-127. CNES-supported research. refs

A88-27814

A GLOBAL SURVEY OF SURFACE CLIMATE PARAMETERS FROM SATELLITE OBSERVATIONS - PRELIMINARY RESULTS OVER AFRICA

G. DEDIEU, P. Y. DESCHAMPS, Y. H. KERR, and P. RABERANTO (CNES and CNRS, Laboratoire d'Etudes et de Recherches en Teledetection Spatiale, Toulouse, France) (COSPAR, WMO, URSI, et al., Plenary Meeting, 26th, Symposium 3, Workshop V, and Topical Meeting A2 on Remote Sensing from Space, Toulouse, France, June 30-July 11, 1986) *Advances in Space Research* (ISSN 0273-1177), vol. 7, no. 11, 1987, p. 129-137. CNRS-CNES-supported research. refs

A88-27823

SIMULATIONS OF THE METEOSAT VISIBLE SENSOR RESPONSE TO CHANGING BOUNDARY CONDITIONS

R. T. PINKER (Maryland, University, College Park) (COSPAR, WMO, URSI, et al., Plenary Meeting, 26th, Symposium 3, Workshop

V, and Topical Meeting A2 on Remote Sensing from Space, Toulouse, France, June 30-July 11, 1986) *Advances in Space Research* (ISSN 0273-1177), vol. 7, no. 11, 1987, p. 211-216. refs

Computational experiments have been conducted to simulate the Meteosat visible sensor's response to varying surfaces and clear-sky atmospheric conditions, as a function of solar zenith angle. The possible bias in observations obtained with this limited spectral response sensor was assessed. The filtered clear-sky planetary albedo, as observed with the Meteosat was compared with the unfiltered planetary albedo, under the same environmental conditions. Four cases of wavelength-independent surface albedo and four cases of realistic wavelength dependent surface albedo have been simulated. The complexity of the narrow/broadband spectral relationship of the clear-sky planetary albedo has been demonstrated. The simulations have shown that while under certain assumptions the two were in close agreement, the relationship would strongly depend on the assumptions made on the spectral dependence of the surface reflectivity. Author

A88-27826

A STUDY TO PRODUCE 1:100,000 SCALE LFC COLOR PHOTOMAP

S. TANAKA, T. SUGIMURA (Remote Sensing Technology Center of Japan, Tokyo), M. HIGASHI (Tokyo Inshoken Printing Co., Ltd., Japan), and M. YOSHIMURA (Hosei University, Koganei, Japan) (COSPAR, WMO, URSI, et al., Plenary Meeting, 26th, Symposium 3, Workshop V, and Topical Meeting A2 on Remote Sensing from Space, Toulouse, France, June 30-July 11, 1986) *Advances in Space Research* (ISSN 0273-1177), vol. 7, no. 11, 1987, p. 237-240. refs

Three independent components exist for the photomap presentation. These are spatial resolution, field of view, and the variety of map information added to the space image. The technical direction of the photomap is to advance the level of these three component stages simultaneously. Spatial resolution was investigated by digitizing the LFC color transparency. It was estimated to be better than 30 lines/mm. Next, map information added to the space image was discussed. The optimum solution may be found in the application of computer graphics technology, rather than in the application of the conventional printing presentation. Author

A88-27832

DESIGN CONCEPT OF THE SAR INSTALLED ON ERS-1

N. KODAIRA (Remote Sensing Technology Center of Japan, Tokyo), S. NIWA (Technology Research Association of Resources Remote Sensing System, Japan), Y. ISHIZAWA, S. MORIMOTO (National Space Development Agency of Japan, Tokyo), J. KOMAI (Earth Resources Satellite Data Analysis Center, Japan) et al. (COSPAR, WMO, URSI, et al., Plenary Meeting, 26th, Symposium 3, Workshop V, and Topical Meeting A2 on Remote Sensing from Space, Toulouse, France, June 30-July 11, 1986) *Advances in Space Research* (ISSN 0273-1177), vol. 7, no. 11, 1987, p. 289-292.

The mission equipment of the ERS-1 is briefly described, emphasizing the SAR system. Data are given on the main characteristics of the SAR, the planned orbit, the mission data recorder, and the mission transmitter, and the development schedule of ERS-1 is shown. The user requirements, frequency and polarization, swath width, off-nadir angle, PRFs, and data rate reduction pertaining to the SAR are examined. C.D.

A88-27833

PROPOSED USES OF ERS-1

G. DUCHOSSOIS and J.-P. GUIGNARD (ESA, Paris, France) (COSPAR, WMO, URSI, et al., Plenary Meeting, 26th, Symposium 3, Workshop V, and Topical Meeting A2 on Remote Sensing from Space, Toulouse, France, June 30-July 11, 1986) *Advances in Space Research* (ISSN 0273-1177), vol. 7, no. 11, 1987, p. 293-298.

The first European Remote Sensing Satellite (ERS-1) is one of the major programs of the European Space Agency (ESA) in the

field of earth observation. It is due to be launched in December 1989 and will embark a very comprehensive set of radar instruments designed to observe the surface wind and wave structure over the oceans and to provide high resolution all-weather images of the ice caps, coastal zones and land surface. The paper briefly describes the main features and expected geophysical performances of these various instruments; it provides examples for the utilization of ERS-1 data for scientific research in such fields as physical oceanography, glaciology and climatology, as well as in application demonstrations for offshore activities and land resources management. Author

A88-27844

THE USE OF DIRECT READOUT, HIGH RESOLUTION TOVS DATA IN SHORT AND MEDIUM RANGE WEATHER PREDICTIONS

J. N. RICKETS, R. J. ALLAM (Meteorological Office, Bracknell, England), and J. TURNER (NERC, British Antarctic Survey, Cambridge, England) (COSPAR, WMO, URSI, et al., Plenary Meeting, 26th, Symposium 3, Workshop V, and Topical Meeting A2 on Remote Sensing from Space, Toulouse, France, June 30-July 11, 1986) *Advances in Space Research* (ISSN 0273-1177), vol. 7, no. 11, 1987, p. 347-350. refs

Since 1983, the UK Meteorological Office has been receiving the direct readout transmissions of TIROS-N Operational Vertical Sounder (TOVS) data from the NOAA satellites and routinely deriving high resolution temperature and humidity profiles for the North Atlantic/European area. The process of deriving these profiles using locally derived regression coefficients is described with a brief account of a new cloud clearing process now being tested. Characteristics of profiles and 1000-500MB thickness fields derived from the retrieval data when compared with conventional profiles and fields, which have been noted over a two year period, are described. An example of a comparison of profiles from TOVS data with collocated radiosonde profiles is also shown. Finally, work on new retrieval methods is outlined. Author

A88-27846

ASSESSMENT OF THE USE OF SATELLITE DERIVED WINDS IN MONSOON FORECASTING USING A GENERAL CIRCULATION MODEL

P. C. JOSHI, C. M. KISHTWAL, M. S. NARAYANAN (ISRO, Space Applications Centre, Ahmedabad, India), O. P. SHARMA, and H. C. UPADHYAY (Indian Institute of Technology, New Delhi, India) (COSPAR, WMO, URSI, et al., Plenary Meeting, 26th, Symposium 3, Workshop V, and Topical Meeting A2 on Remote Sensing from Space, Toulouse, France, June 30-July 11, 1986) *Advances in Space Research* (ISSN 0273-1177), vol. 7, no. 11, 1987, p. 353-356. refs

A88-28013

PRINCIPLES OF FIELD SPECTROSCOPY

E. J. MILTON (Southampton, University, England) *International Journal of Remote Sensing* (ISSN 0143-1161), vol. 8, Dec. 1987, p. 1807-1827. refs

Field spectroscopy involves the study of the interrelationships between the spectral characteristics of objects and their biophysical attributes in the field environment. It is a technique of fundamental importance in remote sensing, yet its full potential is rarely exploited. In this article the principles of the subject are explained and its historical development reviewed with reference to the instruments and methods adopted. Field spectroscopy has a role to play in at least three areas of remote sensing. Firstly, it acts as a bridge between laboratory measurements of spectral reflectance and the field situation and is thus useful in the calibration of airborne and satellite sensors. Secondly, it is useful in predicting the optimum spectral bands, viewing configuration and time to perform a particular remote sensing task. Thirdly, it provides a tool for the development, refinement and testing of models relating biophysical attributes to remotely-sensed data. Author

A88-28266* Jet Propulsion Lab., California Inst. of Tech., Pasadena.

TERRESTRIAL IMAGING SPECTROSCOPY

GREGG VANE (California Institute of Technology, Jet Propulsion Laboratory, Pasadena) and ALEXANDER F. H. GOETZ (Colorado, University, Boulder) Remote Sensing of Environment (ISSN 0034-4257), vol. 24, Feb. 1988, p. 1-29. refs

Recent advances in imaging spectroscopy for remote sensing applications are discussed, reviewing the results of recent investigations. The advantages offered by the higher spectral resolution of imaging spectroscopy relative to scanners such as Landsat MSS and TM are explained; the design and performance of the Airborne Imaging Spectrometer (Vane et al., 1984) are described and illustrated with drawings, photographs, and sample images; data processing and analysis techniques are outlined; and applications to geological and botanical research are considered.

T.K.

A88-28447

THE USE OF SPACE TECHNOLOGY FOR THE REMOTE SENSING OF EARTH RESOURCES AND MAPPING [ISPOL'ZOVANIE KOSMICHESKOI TEKHNIKI DLIA PRIRODOVEDENIIA I KARTOGRAFIROVANIIA]

IU. P. KIENKO Geodeziia i Kartografiia (ISSN 0016-7126), Nov. 1987, p. 30-35. In Russian.

The organization of remote sensing and satellite mapping activities in the Soviet Union is examined. The Soviet remote sensing system comprises the Cosmos satellites, manned space stations, aircraft for subsatellite measurements, and facilities for the processing of remote-sensing data. Emphasis is placed on the development of a national system for the automated control of earth-resources utilization.

B.J.

A88-28679* Johns Hopkins Univ., Laurel, Md.

ANALYSIS OF ALGORITHMS FOR THE RETRIEVAL OF RAIN-RATE PROFILES FROM A SPACEBORNE DUAL-WAVELENGTH RADAR

JULIUS GOLDBIRSH (Johns Hopkins University, Laurel, MD) IEEE Transactions on Geoscience and Remote Sensing (ISSN 0196-2892), vol. 26, March 1988, p. 98-114. NASA-supported research. refs

(Contract N00039-87-C-5301)

The ability to retrieve rain-rate profiles from a dual-wavelength spaceborne radar system operating at 13.6 and 35 GHz is analyzed. The fundamental problem of extracting either the attenuation and/or the reflectivity from the backscatter echo, which contains both contributions, is addressed. Three algorithms, the backscatter, the attenuation coefficient, and the dual-wavelength methods, are examined. These algorithms are tested using four rain-rate profiles derived from radar measurements. In particular, measured (true) values are compared with calculated (retrieved) rain rates applying the algorithms with superimposed uncertainties assuming a suggested spaceborne dual-wavelength radar system. Error values of rain rates are determined where these values reflect failure of the assumptions utilized in the derivation of the algorithms, rain backscatter noise, and instrument noise. It is concluded that no single technique gives rise to a panacea in the making of accurate rain measurements and that difficulties exist with each method.

I.E.

A88-29235* National Aeronautics and Space Administration. Goddard Space Flight Center, Greenbelt, Md.

LOOKING AT THE EARTH FROM SPACE

MARVIN A. GELLER (NASA, Goddard Space Flight Center, Greenbelt, MD) British Interplanetary Society, Journal (NASA Space Science) (ISSN 0007-084X), vol. 41, Jan.-Feb. 1988, p. 95-102. refs

Some of the scientific accomplishments attained in observing the earth from space are discussed. A brief overview of findings concerning the atmosphere, the oceans and sea ice, the solid earth, and the terrestrial hydrosphere and biosphere is presented, and six examples are examined in which space data have provided unique information enabling new knowledge concerning the

workings of the earth to be derived. These examples concern stratospheric water vapor, hemispheric differences in surface and atmosphere parameters, Seasat altimeter mesoscale variability, variability of Antarctic sea ice, variations in the length of day, and spaceborne radar imaging of ancient rivers. Future space observations of the earth are briefly addressed.

C.D.

A88-29284

AN IMPROVED METHOD FOR DETECTING CLEAR SKY AND CLOUDY RADIANCES FROM AVHRR DATA

R. W. SAUNDERS (Meteorological Office, Oxford, England) and K. T. KRIEBEL (DFVLR, Institut fuer Physik der Atmosphaere, Oberpfaffenhofen, Federal Republic of Germany) International Journal of Remote Sensing (ISSN 0143-1161), vol. 9, Jan. 1988, p. 123-150. refs

A scheme which identifies cloud-free and cloud-filled pixels has been devised in order to obtain accurate estimates of surface and cloud parameters from satellite radiance data. This scheme has been developed for application to high-resolution (1 x 1 km pixel) images recorded over Western Europe and the North Atlantic by the AVHRR on the TIROS-N/NOAA polar orbiters. The scheme consists of five daytime or five nighttime tests applied to each individual pixel to determine whether that pixel is cloud-free, partly cloudy, or cloud-filled.

B.J.

A88-30082

RELATIONSHIP BETWEEN BRIGHTNESS TEMPERATURE IN THE RF RANGE AND THE RADIATIVE DRYNESS INDEX [O VZAIMOSVIAZI IARKOSTNOI TEMPERATURY V RADIODIAPAZONE S RADIATSIONNYM INDEKSNOM SUKHOSTI]

E. A. REUTOV and A. M. SHUTKO (AN SSSR, Institut Radiotekhniki i Elektroniki, Moscow, USSR) Issledovanie Zemli iz Kosmosa (ISSN 0205-9614), Nov.-Dec. 1987, p. 42-48. In Russian. refs

A relationship between radio brightness temperature and the radiative dryness index (RDI) is established on the basis of model calculations and aerial and satellite-borne microwave radiometry. The relationship between brightness temperature at a wavelength of 30 cm and the RDI is evaluated for various types of regions, including southern and forest tundra, northern and southern taiga, deciduous forest, steppe, semiarid region, and desert. Possible applications of the proposed approach are examined.

B.J.

A88-30670#

APPLICATIONS OF MICROWAVES TO REMOTE SENSING

ERWIN SCHANDA (Bern, Universitaet, Switzerland) (European Microwave Conference and Workshop, 17th, Rome, Italy, Sept. 7-11, 1987) Alta Frequenza (English Edition) (ISSN 0002-6557), vol. 56, Dec. 1987, p. 399-403. refs

The interaction of microwaves with the molecular properties and geometric features of media emerge from theoretical, laboratory, and field investigations of rough-surface scattering and emission from agricultural soil and sea surface, as well as of volume scattering and emission from snow and vegetation. Algorithms are derived for the interpretation of airborne and spaceborne radiometer and radar data in terms of natural parameters. The mm-wave range absorption lines of atmospheric constituents can be used to measure various trace gases, and such parameters as temperature, throughout the mesosphere and stratosphere.

O.C.

A88-30731

ESTIMATION OF ATMOSPHERIC LIQUID-WATER AMOUNT BY NIMBUS 7 SMMR DATA - A NEW METHOD AND ITS APPLICATION TO THE WESTERN NORTH-PACIFIC REGION

TAKAO TAKEDA and GUOSHENG LIU (Nagoya University, Japan) Meteorological Society of Japan, Journal (ISSN 0026-1165), vol. 65, Dec. 1987, p. 931-947. refs

08 INSTRUMENTATION AND SENSORS

N88-15282*# National Aeronautics and Space Administration. Goddard Space Flight Center, Greenbelt, Md.

HIRIS (HIGH-RESOLUTION IMAGING SPECTROMETER: SCIENCE OPPORTUNITIES FOR THE 1990S. EARTH OBSERVING SYSTEM. VOLUME 2C: INSTRUMENT PANEL REPORT

1987 89 p Original document contains color illustrations (NASA-TM-89703; NAS 1.15:89703) Avail: NTIS HC A05/MF A01 CSCL 14B

The high-resolution imaging spectrometer (HIRIS) is an Earth Observing System (EOS) sensor developed for high spatial and spectral resolution. It can acquire more information in the 0.4 to 2.5 micrometer spectral region than any other sensor yet envisioned. Its capability for critical sampling at high spatial resolution makes it an ideal complement to the MODIS (moderate-resolution imaging spectrometer) and HMMR (high-resolution multifrequency microwave radiometer), lower resolution sensors designed for repetitive coverage. With HIRIS it is possible to observe transient processes in a multistage remote sensing strategy for Earth observations on a global scale. The objectives, science requirements, and current sensor design of the HIRIS are discussed along with the synergism of the sensor with other EOS instruments and data handling and processing requirements. Author

N88-15283*# National Aeronautics and Space Administration. Goddard Space Flight Center, Greenbelt, Md.

FROM PATTERN TO PROCESS: THE STRATEGY OF THE EARTH OBSERVING SYSTEM: VOLUME 2: EOS SCIENCE STEERING COMMITTEE REPORT

1987 153 p Original document contains color illustrations (NASA-TM-89702; NAS 1.15:89702) Avail: NTIS HC A08/MF A01 CSCL 12B

The Earth Observing System (EOS) represents a new approach to the study of the Earth. It consists of remotely sensed and correlative in situ observations designed to address important, interrelated global-scale processes. There is an urgent need to study the Earth as a complete, integrated system in order to understand and predict changes caused by human activities and natural processes. The EOS approach is based on an information system concept and designed to provide a long-term study of the Earth using a variety of measurement methods from both operational and research satellite payloads and continuing ground-based Earth science studies. The EOS concept builds on the foundation of the earlier, single-discipline space missions designed for relatively short observation periods. Continued progress in our understanding of the Earth as a system will come from EOS observations spanning several decades using a variety of contemporaneous measurements. F.M.R.

N88-15284*# National Aeronautics and Space Administration. Goddard Space Flight Center, Greenbelt, Md.

SAR (SYNTHETIC APERTURE RADAR). EARTH OBSERVING SYSTEM. VOLUME 2F: INSTRUMENT PANEL REPORT

1987 260 p Original document contains color illustrations (NASA-TM-89701; NAS 1.15:89701) Avail: NTIS HC A12/MF A01 CSCL 17I

The scientific and engineering requirements for the Earth Observing System (EOS) imaging radar are provided. The radar is based on Shuttle Imaging Radar-C (SIR-C), and would include three frequencies: 1.25 GHz, 5.3 GHz, and 9.6 GHz; selectable polarizations for both transmit and receive channels; and selectable incidence angles from 15 to 55 deg. There would be three main viewing modes: a local high-resolution mode with typically 25 m resolution and 50 km swath width; a regional mapping mode with 100 m resolution and up to 200 km swath width; and a global mapping mode with typically 500 m resolution and up to 700 km swath width. The last mode allows global coverage in three days. The EOS SAR will be the first orbital imaging radar to provide multifrequency, multipolarization, multiple incidence angle observations of the entire Earth. Combined with Canadian and Japanese satellites, continuous radar observation capability will

be possible. Major applications in the areas of glaciology, hydrology, vegetation science, oceanography, geology, and data and information systems are described. J.P.B.

N88-16112# Joint Publications Research Service, Arlington, Va.

STATISTICAL MODEL OF INTERACTION OF ELECTROMAGNETIC WAVES WITH NATURAL OBJECTS BEING SENSED Abstract Only

V. V. YEGOROV *In its* JPRS Report: Science and Technology. USSR: Space p 132 24 Nov. 1987 Transl. into ENGLISH from *Issledovaniye Zemli iz Kosmosa* (Moscow, USSR), no. 2, Mar. - Apr. 1987 p 90-95 Avail: NTIS HC A08/MF A01

A study is made of a model of objects being sensed and the processes of interaction between the objects and the sensing electromagnetic field, utilizing models of tropospheric and ionospheric scatter communications channels. A statistical method of analysis is used, assuming scattering of the field to be Gaussian with zero mean and noncoherent summation of partial fields. The model includes the pulse response of the transmission path, which is demonstrated to be influenced by the spectral reflection properties of the object being sensed. Determination of the transfer functions of all elements involved in remote sensing makes possible a description of the entire monitoring loop and control of the status of natural and man made objects. Author

N88-16136# Joint Publications Research Service, Arlington, Va. **LASER SYSTEM FOR AUTOMATING TOPOGRAPHIC TERRAIN SURVEY Abstract Only**

V. S. GOLOV, YU. M. DESYATYKH, A. S. FEDOROV, and A. G. PARAMONOV *In its* USSR Report: Earth Sciences p 47 30 Mar. 1987 Transl. into ENGLISH from *Geodeziya i Kartografiya* (Moscow, USSR), no. 10, Oct. 1986 p 38-41 Avail: NTIS HC A04/MF A01

An experimental model of a system based on a helium-neon laser was developed for the purpose of finding ways to automate a topographic survey. The system consists of a transmitter mounted over a point with known coordinates (theodolite traverse station) and a receiver which during the course of the survey is moved along the line. The transmitter includes a laser transmitter with a rotating head and a radio transmitter. The laser transmitter shapes two beams, one of which is horizontal, whereas the other slants at the angle beta to the horizon. The lower beam during rotation of the head creates a horizontal plane, whereas the upper beam creates a conical surface. In the form of pulses the radio transmitter transmits information on the angle of rotation of the rotating head relative to the initial direction. The initial direction is the direction to the second theodolite station, at which the receiver is placed prior to onset of the survey. The receiver consists of a photodetector with a circular-scan objective which is attached on a telescopic rod which is used for moving it vertically. It has a movement-code converter and a computer with a digital display for indicating the three determined coordinates. In the base there is an electromechanical drive for raising and lowering the photodetector. The working principles and procedures are described. Author

N88-16179*# National Aeronautics and Space Administration, Washington, D.C.

COMMERCIAL APPLICATIONS AND SCIENTIFIC RESEARCH REQUIREMENTS FOR THERMAL-INFRARED OBSERVATIONS OF TERRESTRIAL SURFACES

SAMUEL N. GOWARD, JAMES V. TARANIK, DANIEL LAPORTE, and EVELYN S. PUTNAM, ed. (Santa Barbara Research Center, Goleta, Calif.) Aug. 1986 150 p Prepared in cooperation with Maryland Univ., College Park (NASA-TM-89704; NAS 1.15:89704) Avail: NTIS HC A07/MF A01 CSCL 08B

In the spring of 1986 the EOSAT Company and NASA Headquarters organized a workshop to consider: (1) the potential value of space-acquired multiband thermal remote sensing in terrestrial research and commercial applications, and (2) the scientific and technological requirements for conducting such

observations from the LANDSAT platform. The workshop defined the instrument characteristics of three types of sensors that would be needed to expand the use of thermal information for Earth observation and new commercial opportunities. The panels from two disciplines, geology and evapotranspiration/botany, along with the instrument panel, presented their recommendations to the workshop. The findings of these meetings are presented. Author

N88-16916# Helsinki Univ. of Technology, Espoo (Finland). Radio Lab.

CONSTRUCTION OF AIRBORNE RADARS FOR REMOTE SENSING Progress Report, 1 Jul. 1986 - 30 Jun. 1987

M. HALLIKAINEN, J. HYYPPAE, M. TOIKKA, T. FORSELL, and J. HAAPANEN 1987 24 p
(PB88-113063; S-171; ISBN-951-754-210-0) Avail: NTIS HC A03/MF A01 CSCL 20N

The progress made in the radar construction project from 1 July 1986 through 30 June 1987 is described. The project includes the design and construction of two airborne systems for microwave remote sensing. The dual-frequency scatterometer system will operate at 5 and 10 GHz and it will be used both for extensive data collection campaigns and for detailed investigations of the scattering properties of various targets. The primary uses of the 10 GHz side-looking airborne radar (SLAR) will be detection of oil slicks and mapping of sea ice. GRA

N88-17101# Physics and Electronics Lab. TNO, The Hague (Netherlands). Divisie 1: Operationele Research.

DESIGN AND IMPLEMENTATION OF A DATA BASE SYSTEM FOR DIGITAL LAND MASS SYSTEM (DLMS) DATA

J. C. BRON, J. KIEVIT, and M. R. SCHURINK May 1987 54 p
In DUTCH; ENGLISH summary Original contains color illustrations

(FEL-IR-1987-19; ETN-88-91563) Avail: NTIS HC A04/MF A01

Highly detailed and multipurpose digital terrain data was produced for a large part of Europe. These so-called Digital Land Mass System (DLMS) data are delivered on raw-format tapes. The design, implementation, and use of a data base system to transform DLMS-data to structured files, needed for specific applications are described. ESA

N88-17143# European Space Agency. European Space Operations Center, Darmstadt (West Germany). Meteosat Exploitation Project.

METEOROLOGICAL INFORMATION EXTRACTION CENTER (MIEC) PROCESSING

W. R. BURKE, ed. Sep. 1987 27 p
(ESA-STR-224; ISSN-0379-4067; ETN-88-91412) Avail: NTIS HC A03/MF A01

Radiative transfer, segment processing, and semitransparency correction of Meteosat images is described. Cloud motion vectors, sea surface temperatures, cloud analysis, cloud-top height, upper tropospheric humidity, and precipitation index are considered. The climate data set and the International Satellite Cloud Climatology Project are mentioned. ESA

N88-17964*# Ithaco, Inc., Ithaca, N.Y.

ISTP SBIR PHASE 1 FULL-SKY SCANNER: A FEASIBILITY STUDY Final Report

6 Aug. 1986 60 p
(Contract NAS5-29276)
(NASA-CR-180749; NAS 1.26:180749; REPT-93226) Avail: NTIS HC A04/MF A01 CSCL 14B

The objective was to develop a Full-Sky Sensor (FSS) to detect the Earth, Sun and Moon from a spinning spacecraft. The concept adopted has infinitely variable resolution. A high-speed search mode is implemented on the spacecraft. The advantages are: (1) a single sensor determines attitude parameters from Earth, Sun and Moon, thus eliminating instrument mounting errors; (2) the bias between the actual spacecraft spin axis and the intended spin axis can be determined; (3) cost is minimized; and (4) ground processing is straightforward. The FSS is a modification of an existing flight-proven sensor. Modifications to the electronics are

necessary to accommodate the amplitude range and signal width range of the celestial bodies to be detected. Potential applications include ISTP missions, Multi-Spacecraft Satellite Program (MSSP), dual-spin spacecraft at any altitude, spinning spacecraft at any altitude, and orbit parameter determination for low-Earth orbits.

J.P.B.

N88-18052# Oregon Graduate Center for Study and Research, Beaverton. Dept. of Applied Physics and Electrical Engineering.

REMOTE SENSING OF ATMOSPHERIC CROSSWINDS BY UTILIZING SPECKLE-TURBULENCE INTERACTION AND OPTICAL HETERODYNE DETECTION Final Report, 1 Jan. 1986 - 30 Jun. 1987

J. F. HOLMES 16 Sep. 1987 33 p

(Contract DAAL03-86-K-0022)

(AD-A187580; ARO-23313.5-GS) Avail: NTIS HC A03/MF A01 CSCL 17K

Speckle-turbulence interaction can be utilized to measure the vector wind in a plane perpendicular to the line of sight from a laser transmitter to a target. A continuous wave source of around one watt and operating at 10.6 microns, in conjunction with an optical heterodyne receiver, has been used to measure atmospheric winds along horizontal paths. A theoretical basis, the experimental apparatus, processing techniques, and experimental results are presented. The technique has been demonstrated for remote sensing of atmospheric winds along horizontal paths and has potential for global remote sensing of atmospheric winds and for on-board wind shear detection systems for aircraft. GRA

N88-18053# Johns Hopkins Univ., Laurel, Md. Applied Physics Lab.

EVALUATION OF A TEMPERATURE REMOTE SENSING TECHNIQUE

S. A. GEARHART and M. E. THOMAS Jul. 1987 29 p

(Contract N00039-87-C-5301)

(AD-A187885; JHU/APL/TG-1365) Avail: NTIS HC A03/MF A01 CSCL 14B

A noninvasive technique for measuring temperature in hot gases is evaluated as an alternative to conventional mechanical probing techniques. The technique uses a diode laser spectrometer to measure the line-center absorption coefficient ratio of two absorption lines that originate from different vibrational energy levels of the same absorbing species. The temperature is calculated without knowledge of the pressure, absorber concentration, or optical path length. A previous study demonstrated temperature measurements at about 200K at atmospheric pressure. The results of this evaluation suggest that the technique is also applicable for temperatures as low as 400 K and at pressures well below 1 atm. GRA

N88-18986 New South Wales Univ., Kensington (Australia).

SURVEYING WITH GPS IN AUSTRALIA Abstract Only. Ph.D. Thesis

ROD ECKELS Nov. 1986 222 p

Avail: Issuing Activity

This thesis describes the Global Positioning System (GPS) and how it can be used for surveying in Australia. The basic component parts of the system and the role they play are outlined. The satellite signal measurement process is described and currently available receivers are reviewed. Field procedures and processing techniques that should be followed to achieve surveying accuracies are discussed. As GPS surveys refer to a satellite reference datum, the relationship between this datum and the Australian datum is given. With the knowledge about GPS provided here, the surveyor should be able to use GPS confidently. Author

N88-18995# Institut fuer Angewandte Geodaesie, Frankfurt am Main (West Germany).

APPLICATION OF THE GLOBAL POSITIONING SYSTEM (GPS) TIME RECEIVERS TO THE FUNDAMENTAL STATION WETZELL [ZUM EINSATZ VON GPS-ZEITEMPFAENGERNAUF DER FUNDAMENTALSTATION WETZELL]

WOLFGANG SCHLUETER In its Reports on Cartography and

08 INSTRUMENTATION AND SENSORS

Geodesy. Series 1, Report 98 p 87-95 1987 In GERMAN;
ENGLISH summary
Avail: NTIS HC A06/MF A01

The first experiences with two GPS receivers for time transfer are presented. The GPS that works presently with seven operational satellites is described. Test measurements show that time transfer between stations with a precision of better than 20nsec is possible, if the common view technique is applied and if the receivers are calibrated
ESA

N88-18997# National Oceanic and Atmospheric Administration, Washington, D. C. Satellite Research Lab.
GENERAL DETERMINATION OF EARTH SURFACE TYPE AND CLOUD AMOUNT USING MULTISPECTRAL AVHRR DATA
IRWIN RUFF and ARNOLD GRUBER Feb. 1988 36 p
(NOAA-TR-NESDIS-39) Avail: NTIS HC A03/MF A01

A method is presented for determining the type of daylight scene viewed by every resolution element of the Advanced Very High Resolution Radiometer (AVHRR) for routine, large-scale processing, using mainly values from the various spectral channels of AVHRR. The specification of scene types was restricted to the broad categories of vegetation, non-vegetated land, snow/ice, and cloud. The method appears to be sufficiently sensitive, however, to permit it to be extended to finer specification of scene type.
Author

N88-19863# National Severe Storms Lab., Norman, Okla.
NATIONAL SEVERE STORMS LABORATORY, FISCAL YEAR 1987 Annual Report, 1 Oct. 1986 - 30 Sep. 1987
Oct. 1987 55 p
(PB88-140108) Avail: NTIS HC A04/MF A01 CSCL 04B

The National Severe Storm Laboratory (NSSL) develops improved means for weather observing and forecasting through studies of storm processes, numerical and conceptual modeling of storm phenomena, and applications of technologies in remote sensing. Recent studies have drawn heavily on observations by Doppler radar and lightning-mapping systems, and more effective methods for using Doppler radar and lightning data for forecasts and warnings of severe storms were developed. The work at NSSL, probably the most substantial precursor of the major national initiative NEXRAD, continues to support that program in critical ways. The annual report describes the accomplishments of the previous year.
GRA

09

GENERAL

Includes economic analysis.

N88-16133# Joint Publications Research Service, Arlington, Va.
ACADEMIC COURSE SPACE METHODS FOR STUDYING MODERN LANDSCAPES OF CONTINENTS
YE. V. GLUSHKO *In its* USSR Report: Earth Sciences p 41
30 Mar. 1987 Transl. into ENGLISH from Vestnik Moskovskogo Universiteta: Seriya 5, Geografiya (Moscow, USSR), no. 6, Nov. - Dec. 1986 p 78-82
Avail: NTIS HC A04/MF A01

In this course the emphasis is on the study via space photographs of present-day landscapes incorporating both natural and anthropogenic components. The following topics are included: (1) theoretical principles of space methods for landscape research, including optical properties of landscapes, and the system for the classification of modern landscapes; (2) study of the structure of modern landscapes by means of interpretations of space photographs and subsequent mapping; (3) natural and anthropogenic landscape components and principal types of environmental pollution identifiable on space photographs; (4) study of present-day analogue landscapes; and (5) study of natural and anthropogenic processes, as well as rhythmic, dynamic and

evolutionary changes of landscapes from space photographs. In their practical work, students use space photographs in the interpretation of Quaternary deposits, relief, hydrographic network, soils, vegetation and land use.
Author

N88-16577*# National Academy of Sciences - National Research Council, Washington, D. C.

CRITICAL ISSUES IN NASA INFORMATION SYSTEMS Final Report

Jun. 1987 68 p

(Contract NASW-4124)

(NASA-CR-182380; NAS 1.26:182380; PB88-101027) Avail: NTIS HC A04/MF A01 CSCL 05B

The National Aeronautics and Space Administration has developed a globally-distributed complex of earth resources data bases since LANDSAT 1 was launched in 1972. NASA envisages considerable growth in the number, extent, and complexity of such data bases, due to the improvements expected in its remote sensing data rates, and the increasingly multidisciplinary nature of its scientific investigations. Work already has begun on information systems to support multidisciplinary research activities based on data acquired by the space station complex and other space-based and terrestrial sources. In response to a request from NASA's former Associate Administrator for Space Science and Applications, the National Research Council convened a committee in June 1985 to identify the critical issues involving information systems support to space science and applications. The committee has suggested that OSSA address four major information systems issues; centralization of management functions, interoperability of user involvement in the planning and implementation of its programs, and technology.
GRA

N88-18046*# National Aeronautics and Space Administration, Washington, D.C.

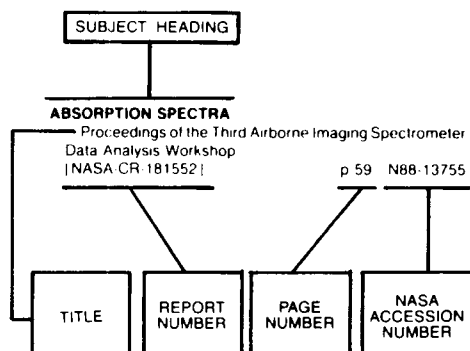
SPACE-BASED REMOTE SENSING OF THE EARTH: A REPORT TO THE CONGRESS

Sep. 1987 147 p Original document contains color illustrations
Prepared in cooperation with National Oceanic and Atmospheric Administration, Washington, D.C.

(NASA-TM-89709; NAS 1.15:89709) Avail: SOD HC \$9.00 as 033-000-00983-6; NTIS MF A01 CSCL 08B

The commercialization of the LANDSAT Satellites, remote sensing research and development as applied to the Earth and its atmosphere as studied by NASA and NOAA is presented. Major gaps in the knowledge of the Earth and its atmosphere are identified and a series of space based measurement objectives are derived. The near-term space observations programs of the United States and other countries are detailed. The start is presented of the planning process to develop an integrated national program for research and development in Earth remote sensing for the remainder of this century and the many existing and proposed satellite and sensor systems that the program may include are described.
Author

Typical Subject Index Listing



The subject heading is a key to the subject content of the document. The title is used to provide a description of the subject matter. When the title is insufficiently descriptive of document content, a title extension is added, separated from the title by three hyphens. The (NASA or AIAA) accession number and the page number are included in each entry to assist the user in locating the abstract in the abstract section. If applicable, a report number is also included as an aid in identifying the document. Under any one subject heading, the accession numbers are arranged in sequence with the AIAA accession numbers appearing first.

A

ACCURACY

- Methods and accuracy of operational digital image mapping with aircraft SAR p 55 A88-21059
- Limiting accuracy of scatterometer determination of wind speed over ocean from satellite p 44 N88-16107

ACOUSTIC MEASUREMENT

- Ice breakup - Observations of the acoustic signal p 41 A88-30200

ACOUSTIC SCATTERING

- Estimation of sea surface wave spectra using acoustic tomography [AD-A187837] p 49 N88-19057

ADJUSTING

- Method for joint adjustment of satellite and surface geodetic networks p 22 N88-16105

AERIAL PHOTOGRAPHY

- Remote sensing applications by consulting engineers - Three case histories p 24 A88-21009
- Groundwater identification using digitally enhanced NHAP - national high altitude photography p 51 A88-21011
- A remote sensing based methodology for quantifying the spatial and functional relationships amongst industrial land uses delineated around the port of Baltimore p 17 A88-21012

- Difficulties and recommendations for obtaining very large scale 70 mm aerial photography for rangeland monitoring p 1 A88-21017

- Multi-stage remote sensing - A tool for Minnesota natural resources management p 64 A88-21018

- Automated photointerpretation - A stereoscopic workstation p 54 A88-21027

- Principal component analysis of aerial video imagery p 54 A88-21030

- A proposed semi-supervised two stage classification technique p 56 A88-21063

- Results of testing digital image measurements and enhancements on the remote work processing facility p 56 A88-21064

- Correlation between aircraft MSS and lidar remotely sensed data on a forested wetland p 6 A88-24513

- A new strategy for vegetation mapping with the aid of Landsat MSS data p 9 A88-27810

- Microwave remote sensing of ice in Lake Melville and the Labrador Sea p 39 A88-28850

- Accuracy of mapping by panoramic photography p 60 A88-29479

- Measuring crown cover in interior Alaska vegetation types p 12 A88-29495

- A comparison between panoramic photography and conventional aerial photography in terms of mapping accuracy p 61 A88-32167

- Model-based building verification in aerial photographs [AD-A186010] p 20 N88-15278

- The aerophotogrammetric determination of Earth surface deformations p 28 N88-15288

- Photogrammetric principles for combining remote sounding and three-dimensional mapping p 61 N88-16135

- Three-dimensional image generation from an aerial photograph [AD-A188039] p 63 N88-18979

- Automatic knowledge acquisition for aerial image interpretation [AD-A188616] p 63 N88-19810

AEROSOLS

- Size distributions of sea-source aerosol particles - A physical explanation of observed nearshore versus open-sea differences p 33 A88-25289

- Simultaneity of response of Atlantic Ocean tropical cyclones and Indian monsoons p 34 A88-25736

- Spray droplet generation, transport, and evaporation in a wind wave tunnel during the humidity exchange over the sea experiment: in the simulation tunnel p 38 A88-27492

- Meteorological and aerosol measurements from the NOAA WP-3D aircraft during WATOX-86, January 4-9, 1986 p 20 N88-18079

- [PB88-120860] p 20 N88-18079

AGRICULTURE

- Remote sensing surveys design in regional agricultural inventories p 8 A88-27804

- Adaptive computer-aided system for crop inventory according to space photographs p 13 A88-30087

- Crop forecasting in Brazil: A short history of productivity models [INPE-4150-PRE/1056] p 16 N88-19801

AIR LAND INTERACTIONS

- Structure and growth of the mixing layer over the Amazonian rain forest p 8 A88-27252

AIR POLLUTION

- Absolute infrared intensities for F-113 and F-114 and an assessment of their greenhouse warming potential relative to other chlorofluorocarbons p 19 A88-31103

- Meteorological and aerosol measurements from the NOAA WP-3D aircraft during WATOX-86, January 4-9, 1986 p 20 N88-18079

- [PB88-120860] p 20 N88-18079

- Proceedings of the Forest-Atmosphere Interaction Workshop [CONF-8510250] p 17 N88-19824

AIR WATER INTERACTIONS

- Characteristics of extreme rainfall events in northwestern Peru during the 1982-1983 El Nino period p 52 A88-25730

- Airborne measurements of surface layer turbulence over the ocean during cold air outbreaks p 35 A88-26911

- Calculations of ocean-atmosphere radiance on the basis of remote sensing p 37 A88-27204

- Satellite observation of atmosphere and surface interaction parameters p 38 A88-27812

- Measurement of global oceanic winds from Seasat-SMMR and its comparison with Seasat-SASS and ALT derived winds p 40 A88-29766

- The ocean heat budget [AD-A186130] p 44 N88-15346

- WOCE Core Project 2 Planning Meeting: The Southern Ocean [WCP-138] p 44 N88-15348

- Report of the Workshop on Space Systems Possibilities for a Global Energy and Water Cycle Experiment [WCP-137] p 53 N88-17147

- NASA Oceanic Processes Program [NASA-TM-4025] p 48 N88-18109

AIRBORNE EQUIPMENT

- Methods and accuracy of operational digital image mapping with aircraft SAR p 55 A88-21059

- Discriminating semiarid vegetation using airborne imaging spectrometer data - A preliminary assessment p 4 A88-21359

- Multiband-scatterometer data analysis of forests p 5 A88-23548

- The DUT airborne scatterometer p 5 A88-23549

- Measurements of the backscatter and attenuation properties of forest stands at X-, C- and L-band p 7 A88-25444

- The use of a helicopter mounted ranging scatterometer for estimation of extinction and backscattering properties of forest canopies-I: Experimental approach and calibration p 11 A88-28682

- The use of a helicopter mounted ranging scatterometer for estimation of extinction and scattering properties of forest canopies-II: Experimental results for high-density aspen p 11 A88-28683

- Aircraft MSS data registration and vegetation classification for wetland change detection p 12 A88-29277

- An integrated camera and radiometer for aerial monitoring of vegetation p 14 A88-32666

AIRBORNE LASERS

- Estimating forest biomass and volume using airborne laser data p 13 A88-30441

AIRCRAFT INSTRUMENTS

- Methods for processing radio-physical measurement data in studies of the environment - Russian book p 19 A88-29427

ALASKA

- An integrated approach for automated cover-type mapping of large inaccessible areas in Alaska p 60 A88-29491

- Thematic mapper study of Alaskan ophiolites [NASA-CR-182554] p 30 N88-18984

ALEUTIAN ISLANDS (US)

- Geological evolution and analysis of confirmed or suspected gas hydrate localities. Volume 10: Basin analysis, formation and stability of gas hydrates of the Aleutian Trench and the Bering Sea [DE88-001008] p 29 N88-18048

ALGORITHMS

- Analysis of algorithms for the retrieval of rain-rate profiles from a spaceborne dual-wavelength radar p 69 A88-28679

- An efficient algorithm for computing the crossovers in satellite altimetry [NASA-CR-182389] p 43 N88-15286

- A variant of the ISODATA algorithm for application to agricultural targets [INPE-4436-PRE/1235] p 17 N88-20023

ALPINE METEOROLOGY

- Energy balance and discharge of an Alpine glacier, illustrated by Mount Vernaghtferner in the Oetzal Alps, Tyrol p 53 N88-16145

- Vertical sounding of the air layer close to a glacier on Mount Vernaghtferner in the Oetzal Alps, Tyrol (experiment LUZIVER 1983) p 44 N88-16152

ALPS MOUNTAINS (EUROPE)

- Geostrophical evolution of the Southern Alps - Lineaments trends detected on Landsat images p 26 A88-25448

- Energy balance and discharge of an Alpine glacier, illustrated by Mount Vernaghtferner in the Oetzal Alps, Tyrol p 53 N88-16145

- Statistics of two-dimensional structure elements of mountainous ranges (mosaic model) for calculating three-dimensional reflection functions [DFVLR-FB-87-33] p 29 N88-17099

ALTIMETERS

Source of the Australasian tektite strewn field - A possible off-shore impact site p 42 A88-31793

AMAZON REGION (SOUTH AMERICA)

Structure and growth of the mixing layer over the Amazonian rain forest p 8 A88-27252
Biomass-burning emissions and associated haze layers over Amazonia p 18 A88-27265
Shuttle imaging radar A analysis of land use in Amazonia p 12 A88-29282

ANALOG TO DIGITAL CONVERTERS

An autoCAD-based mapping system for encoded stereoplotters p 60 A88-29490

ANGLES (GEOMETRY)

The angular reflectance signature of the canopy hot spot in the optical regime [DE88-005385] p 15 N88-18991

ANIMALS

Five New South Wales barrier lagoons: Their macrobenthic fauna and seagrass communities p 49 N88-19059

ANISOTROPY

The role of anisotropy in the long range reconnaissance of the albedo of land surfaces p 62 N88-16169
The anisotropy of reflected solar radiation over several types of land surface p 62 N88-16171

ANNUAL VARIATIONS

Satellite observed seasonal and inter-annual variation of vegetation over the Kalahari, the Great Victoria Desert, and the Great Sandy Desert - 1979-1984 p 3 A88-21356

Satellite observation of atmosphere and surface interaction parameters p 38 A88-27812
Monitoring hydroclimatic characteristics using satellite observations from West Africa p 52 A88-27816
Relating seasonal patterns of the AVHRR vegetation index to simulated photosynthesis and transpiration of forests in different climates p 13 A88-30447
Spatial-temporal variability of North Pacific sea surface temperature anomaly patterns p 49 N88-19058

ANOMALIES

Spatial-temporal variability of North Pacific sea surface temperature anomaly patterns p 49 N88-19058

ANOMALOUS TEMPERATURE ZONES

The role of synoptic scale processes in the transfer of sea surface temperature anomalies p 35 A88-26065

ANTARCTIC OCEAN

The ice thickness distribution across the Atlantic sector of the Antarctic Ocean in midwinter p 34 A88-25734

ANTARCTIC REGIONS

Satellite maps of Antarctic total ozone [AIAA PAPER 88-0210] p 30 A88-22154
WOCE Core Project 2 Planning Meeting: The Southern Ocean [WCP-138] p 44 N88-15348

ANTICYCLONES

Blocking of the Benguela Current by a single anticyclone - Analysis of satellite and ship data p 41 A88-30077

APPROXIMATION

Active and passive remote sensing of ice [AD-A186685] p 47 N88-17162

ARCTIC OCEAN

Multiyear sea ice floe distribution in the Canadian Arctic Ocean p 35 A88-25738
Sea ice and sea-surface temperatures in the Strait of Fram according to NOAA-AVHRR data p 35 A88-26131

The onset of spring melt in first-year ice regions of the Arctic as determined from scanning multichannel microwave radiometer data for 1979 and 1980 p 37 A88-27016

ARCTIC REGIONS

Detection and identification of Arctic landforms - An assessment of remotely sensed data p 40 A88-29492
Ice breakup - Observations of the acoustic signal p 41 A88-30200

AREA

Aboveground biomass, surface area, and production relations of red fir (*Abies magnifica*) and white fir (*A. concolor*) p 12 A88-28705

ARID LANDS

Remote sensing science applications in arid environments p 3 A88-21351
Suitability of spectral indices for evaluating vegetation characteristics on arid rangelands p 3 A88-21355
The use of spectral and spatial variability to monitor cover change on inert landscapes p 4 A88-21363
Reflectance modeling of semiarid woodlands p 4 A88-21364

A method for the estimate of broadband directional surface albedo from a geostationary satellite p 22 A88-27299
Forecasting patterns of soil erosion in arid lands from Landsat MSS data p 12 A88-29280

Identification and spectral characteristics of hydrothermal alteration on Landsat TM imagery of north Chile p 27 A88-31125

Improved canopy reflectance modeling and scene inference through improved understanding of scene pattern [NASA-CR-182488] p 15 N88-18049

ARTIFICIAL INTELLIGENCE

Autonomous control of image sensor for the optimal acquisition of ground information for dynamic analysis p 65 A88-21660

ARTIFICIAL SATELLITES

Space applications in geography p 22 N88-16104
Five-diagonal weighting scheme for geoidal profiles [AD-A188033] p 23 N88-18054

ASTROMETRY

Simultaneous determination of astronomic position and azimuth from observations of zenith distances and horizontal directions p 20 A88-21055

ATLANTIC OCEAN

North Atlantic thermohaline circulation during the past 20,000 years linked to high-latitude surface temperature p 30 A88-20978
Simultaneity of response of Atlantic Ocean tropical cyclones and Indian monsoons p 34 A88-25736
Remanent magnetization of the oceanic upper mantle p 37 A88-27036

An investigation of small-offset fracture zone geoid waveforms p 22 A88-27465
The Genesis of Atlantic Lows Experiment - The planetary-boundary-layer subprogram of GALE p 42 A88-31111

Hydrographic and current measurements in the North-East Atlantic Ocean. Data report on F.S. Meteor cruises 69/5 and 69/6, October to November 1984 [REPT-166] p 48 N88-17164

Analysis of low frequency current fluctuations in the North-East Atlantic Ocean [REPT-170] p 48 N88-17165

Meteorological and aerosol measurements from the NOAA WP-3D aircraft during WATOX-86, January 4-9, 1986 [PB88-120860] p 20 N88-18079

ATMOSPHERIC ATTENUATION

Remote sensing of atmospheric optical thickness and sea-water attenuation when submerged: Wavelength selection and anticipated errors [AD-A187609] p 49 N88-19262

ATMOSPHERIC BOUNDARY LAYER

Structure and growth of the mixing layer over the Amazonian rain forest p 8 A88-27252
Biomass-burning emissions and associated haze layers over Amazonia p 18 A88-27265
Simulations of the Meteorosol visible sensor response to changing boundary conditions p 67 A88-27823

ATMOSPHERIC CHEMISTRY

Applications of microwaves to remote sensing p 69 A88-30670

ATMOSPHERIC CIRCULATION

Extended abstract modelling interactions between the terrestrial biosphere and the global atmosphere p 65 A88-21022

Remote sensing of water vapor convergence, deep convection, and precipitation over the tropical Pacific Ocean during the 1982-1983 El Nino p 33 A88-25728
Gas exchange on Mono Lake and Crowley Lake, California p 52 A88-25735
On the evolution of the southern oscillation p 36 A88-26923

Assessment of the use of satellite derived winds in monsoon forecasting using a general circulation model p 68 A88-27846

ATMOSPHERIC COMPOSITION

Satellite maps of Antarctic total ozone [AIAA PAPER 88-0210] p 30 A88-22154
Relating Nimbus-7 37 GHz data to global land-surface evaporation, primary productivity and the atmospheric CO2 concentration p 60 A88-29287

ATMOSPHERIC CORRECTION

Atmospheric correction of thermal infrared images p 40 A88-29283

ATMOSPHERIC EFFECTS

Atmospheric effect on spectral signature - Measurements p 58 A88-27822
Proceedings of the Forest-Atmosphere Interaction Workshop [CONF-8510250] p 17 N88-19824

ATMOSPHERIC MODELS

Extended abstract modelling interactions between the terrestrial biosphere and the global atmosphere p 65 A88-21022

Interpretation of satellite imagery of a rapidly deepening cyclone p 57 A88-23502
An investigation of the El Nino-Southern Oscillation Cycle with statistical models. I - Predictor field characteristics. II - Model results p 34 A88-25731

Remote forcing of sea surface temperature in the El Nino region p 34 A88-25732
Comparative study of temperature data from NOAA7-AVHRR and WMO - An interpretation through the use of a soil-vegetation model p 8 A88-27806
Assessment of the use of satellite derived winds in monsoon forecasting using a general circulation model p 68 A88-27846

Atmospheric correction of thermal infrared images p 40 A88-29283
National Severe Storms Laboratory, fiscal year 1987 [PB88-140108] p 72 N88-19863

ATMOSPHERIC MOISTURE

Estimation of atmospheric liquid-water amount by Nimbus 7 SMMR data - A new method and its application to the western North-Pacific region p 69 A88-30731
Report of the Workshop on Space Systems Possibilities for a Global Energy and Water Cycle Experiment [WCP-137] p 53 N88-17147

ATMOSPHERIC OPTICS

An improved method for detecting clear sky and cloudy radiances from AVHRR data p 69 A88-29284

ATMOSPHERIC PHYSICS

The ocean heat budget [AD-A186130] p 44 N88-15346

ATMOSPHERIC PRESSURE

On the evolution of the southern oscillation p 36 A88-26923

ATMOSPHERIC SCATTERING

Statistical model of interaction of electromagnetic waves with natural objects being sensed p 70 N88-16112

ATMOSPHERIC SOUNDING

Airborne measurements of surface layer turbulence over the ocean during cold air outbreaks p 35 A88-26911
Comparison of total ozone amounts derived from satellite and ground-based measurements p 66 A88-27027

The first ISLSCP field experiment (FIFE) - International Satellite Land Surface Climatology Project p 67 A88-27497

Vertical sounding of the air layer close to a glacier on Mount Vernagferner in the Oetzal Alps, Tyrol (experiment LUZIVER 1983) p 44 N88-16152

Report of the Workshop on Space Systems Possibilities for a Global Energy and Water Cycle Experiment [WCP-137] p 53 N88-17147

ATMOSPHERIC TEMPERATURE

A sequential estimation approach to cloud-clearing for satellite temperature sounding p 66 A88-23511
Marine boundary layer modification across the edge of the Agulhas Current p 38 A88-27495
Satellite observation of atmosphere and surface interaction parameters p 38 A88-27812
Estimation of the accuracy of determining atmospheric temperature profiles from microwave remote sensing at frequencies of 117-118.5 GHz p 41 A88-30084

ATMOSPHERIC TURBULENCE

Airborne measurements of surface layer turbulence over the ocean during cold air outbreaks p 35 A88-26911

AUSTRALIA

Satellite remote sensing of Australian rangelands p 4 A88-21361
Detection of yearly cover change with Landsat MSS on pastoral landscapes in central Australia p 4 A88-21362
The use of spectral and spatial variability to monitor cover change on inert landscapes p 4 A88-21363
Mesoscale coastal ocean dynamics p 49 N88-19060

AUSTRALITES

Source of the Australasian tektite strewn field - A possible off-shore impact site p 42 A88-31793

AUTOCORRELATION

Autocorrelation of control points on 11-band multispectral imagery [AD-A188185] p 62 N88-18056

AUTOMATIC CONTROL

A semi-automated training sample selector for multispectral land cover classification p 56 A88-21066

The use of automated computer vision techniques for the recognition of features on radar imagery p 56 A88-21069

An autoCAD-based mapping system for encoded stereoplotters p 60 A88-29490

A smart, mapping, charting and geodesy control generator, phase 1 [AD-A188184] p 23 N88-18055

AUTONOMY

Autonomous control of image sensor for the optimal acquisition of ground information for dynamic analysis p 65 A88-21660

AUTOREGRESSIVE PROCESSES

Application of predictive compression methods to synthetic aperture radar imagery I p 57 A88-23768

AZIMUTH

- The orientation of global satellite networks
p 63 N88-18996

B

BACKSCATTERING

- Modelling radar backscatter from vegetation
p 5 A88-21501
Sea return at C and Ku bands p 31 A88-22947
Measurements of the backscatter and attenuation
properties of forest stands at X-, C- and L-band
p 7 A88-25444

BAROCLINIC WAVES

- The baroclinic circulation in Hudson Strait
p 32 A88-24457

BAROCLINITY

- North Pacific Ocean. Central Pacific Transition Zone,
R/V Thomas G. Thompson: 25 March - 3 May 1968. STD
data report
[AD-A186570] p 47 N88-17160

BATHYMETERS

- Evolution of the Juan Fernandez microplate during the
last three million years p 25 A88-25045
Gravity field mapping from satellite altimetry,
sea-gravimetry and bathymetry in the Eastern
Mediterranean p 42 A88-30836
Airborne electromagnetic sounding of sea ice thickness
and sub-ice bathymetry
[AD-A188939] p 50 N88-19879

BAYS (TOPOGRAPHIC FEATURES)

- Continental shelf processes affecting the oceanography
of the South Atlantic Bight
[DE88-004102] p 48 N88-17166

BERING SEA

- Ice floe collisions and their relation to ice deformation
in the Bering Sea during February 1983
p 40 A88-29324

BIOCHEMISTRY

- Remote sensing of forest canopy and leaf biochemical
contents p 11 A88-28270

BIOMASS

- Quantification of biomass of the marsh grass *Spartina
alterniflora* Loisel using Landsat Thematic Mapper
imagery p 6 A88-23765
Biomass-burning emissions and associated haze layers
over Amazonia p 18 A88-27265
Estimates of primary productivity over the Thar Desert
based upon Nimbus-7 37 GHz data - 1979-1985
p 11 A88-28016
Aboveground biomass, surface area, and production
relations of red fir (*Abies magnifica*) and white fir (*A.
concolor*) p 12 A88-28705
Exploring the relationships between leaf nitrogen
content, biomass and the near-infrared/red reflectance
ratio p 12 A88-29288
Estimating forest biomass and volume using airborne
laser data p 13 A88-30441

BIOMETRICS

- Use of microwave radiometry for measuring the biometric
characteristics of vegetation cover p 7 A88-27207

BIOSPHERE

- Extended abstract modelling interactions between the
terrestrial biosphere and the global atmosphere
p 65 A88-21022
Estimates of primary productivity over the Thar Desert
based upon Nimbus-7 37 GHz data - 1979-1985
p 11 A88-28016
Microwave vegetation index - A new long-term global
data set for biospheric studies p 14 A88-32658

BISTATIC REFLECTIVITY

- Active and passive remote sensing of ice
[AD-A186685] p 47 N88-17162

BOTANY

- Spectral and botanical classification of grasslands -
Auxois example p 8 A88-27805

BOTSWANA

- Spectral assessment of indicators of range degradation
in the Botswana hardveld environment
p 5 A88-21365

BOUNDARY LAYER FLOW

- Marine boundary layer modification across the edge of
the Agulhas Current p 38 A88-27495

BOUNDARY VALUE PROBLEMS

- Spatial-temporal variability of North Pacific sea surface
temperature anomaly patterns p 49 N88-19058
Mesoscale monitoring of the soil freeze/thaw boundary
from orbital microwave radiometry
[NASA-CR-182659] p 17 N88-19855

BRAZIL

- Crop forecasting in Brazil: A short history of productivity
models
[INPE-4150-PRE/1056] p 16 N88-19801

- Mapping of the mangroves of the Guanabarra Bay
through the utilization of remote sensing techniques
[INPE-3942-TDL/229] p 16 N88-19804

BRAZILIAN SPACE PROGRAM

- Report of the participation in the International Training
Course: Remote Sensing in Village Forestry
[INPE-4476-NTE/278] p 16 N88-19802

BRIGHTNESS

- Monte Carlo method calculation of spectral brightness
coefficient of vegetation cover as function of illumination
conditions p 14 N88-16113

BRIGHTNESS TEMPERATURE

- An approximate model for the microwave brightness
temperature of the sea p 31 A88-23544
Estimates of primary productivity over the Thar Desert
based upon Nimbus-7 37 GHz data - 1979-1985
p 11 A88-28016
Relationship between brightness temperature in the RF
range and the radiative dryness index p 69 A88-30082

- LANDSAT thematic mapper radiometric calibration
study
[NASA-CR-182410] p 61 N88-15287

- Mesoscale monitoring of the soil freeze/thaw boundary
from orbital microwave radiometry
[NASA-CR-182659] p 17 N88-19855

C

C BAND

- Sea return at C and Ku bands p 31 A88-22947
Estimation of biophysical properties of forest canopies
using C-band microwave data p 9 A88-27809
Radiometric correction of C-band imagery for
topographic effects in regions of moderate relief
p 59 A88-28680

CALIBRATING

- LANDSAT thematic mapper radiometric calibration
study
[NASA-CR-182410] p 61 N88-15287

CAMERAS

- An integrated camera and radiometer for aerial
monitoring of vegetation p 14 A88-32666

CANADIAN SPACE PROGRAM

- Canadian activities and goals in remote sensing of ocean
colour and fluorescence from space p 46 N88-16300

CANOPIES (VEGETATION)

- An evaluation of the use of TM digital data for updating
the land cover component of the SCS 1987 multisource
inventory of New Jersey --- soil conservation service
p 1 A88-21013
Modelling radar backscatter from vegetation
p 5 A88-21501
Canopy reflectance of seven rangeland plant species
with variable leaf pubescence p 5 A88-23764
A canopy reflectance model based on an analytical
solution to the multiple scattering equation
p 7 A88-25447
Geological and vegetational applications of Shuttle
Imaging Radar-B, Mineral County, Nevada
p 26 A88-26337

- Use of microwave radiometry for measuring the biometric
characteristics of vegetation cover p 7 A88-27207

- Relations between canopy reflectance, photosynthesis
and transpiration - Links between optics, biophysics and
canopy architecture p 8 A88-27802

- Estimation of biophysical properties of forest canopies
using C-band microwave data p 9 A88-27809

- Techniques of ground-truth measurements of
desert-scrub structure p 9 A88-27817

- Evaluating North American net primary productivity with
satellite observations p 9 A88-27819

- X-band features of canopy cover - An up to date summary
of active and passive measurements p 10 A88-27835

- Measurement of canopy interception of solar radiation
by stands of trees in sparsely wooded savanna
p 10 A88-28010

- Remote sensing of forest canopy and leaf biochemical
contents p 11 A88-28270

- The use of a helicopter mounted ranging scatterometer
for estimation of extinction and backscattering properties
of forest canopies-I: Experimental approach and
calibration p 11 A88-28682

- The use of a helicopter mounted ranging scatterometer
for estimation of extinction and scattering properties of
forest canopies-II: Experimental results for high-density
aspen p 11 A88-28683

- Measuring crown cover in interior Alaska vegetation
types p 12 A88-29495

- Calculation of canopy bidirectional reflectance using the
Monte Carlo method p 13 A88-30439

- Estimating forest biomass and volume using airborne
laser data p 13 A88-30441

- Estimation of wheat canopy resistance using combined
remotely sensed spectral reflectance and thermal
observations p 13 A88-30448

- Vegetative and optical characteristics of four-row crop
canopies p 14 A88-32661

- Radiometric leaf area index p 14 A88-32662

- Crop canopy spectral reflectance p 14 A88-32664

- Monte Carlo method calculation of spectral brightness
coefficient of vegetation cover as function of illumination
conditions p 14 N88-16113

- Detection of soil erosion with Thematic Mapper (TM)
satellite data within Pinyon-Juniper woodlands
[NASA-CR-182476] p 15 N88-17103

- Improved canopy reflectance modeling and scene
inference through improved understanding of scene
pattern
[NASA-CR-182488] p 15 N88-18049

- The angular reflectance signature of the canopy hot spot
in the optical regime
[DE88-005385] p 15 N88-18991

- Proceedings of the Forest-Atmosphere Interaction
Workshop
[CONF-8510250] p 17 N88-19824

CARBON

- The influence of yellow substances on remote sensing
of sea-water constituents from space
p 47 N88-16308

CARBON DIOXIDE CONCENTRATION

- Relating Nimbus-7 37 GHz data to global land-surface
evaporation, primary productivity and the atmospheric CO2
concentration p 60 A88-29287

CASPIAN SEA

- Interpretation of the visible manifestations of sea water
dynamics from space imagers of the Caspian Sea
p 37 A88-27201

- Investigating the northern Caspian Sea ice regime from
meteorological-satellite data p 37 A88-27202

CATHODE RAY TUBES

- Automated photointerpretation - A stereoscopic
workstation p 54 A88-21027

CELESTIAL GEODESY

- New possibilities for using gravity data in developing
geodetic coordinate systems p 23 N88-16116

CENSUS

- Using remotely sensed data for census surveys and
population estimation in developing countries - Examples
from Nigeria p 18 A88-24511

CENTRAL AMERICA

- Geological evolution and analysis of confirmed or
suspected gas hydrate localities. Volume 9: Formation and
stability of gas hydrates of the Middle America Trench
[DE88-001007] p 29 N88-18050

CHANGE DETECTION

- Land cover change detection with Landsat MSS and
TM data in the Kitchener-Waterloo area, Canada
p 18 A88-21071

- Land cover change detection using a GIS-guided,
feature-based classification of Landsat thematic mapper
data --- Geographic Information System
p 18 A88-21073

- Analyzing long-term changes in vegetation with
geographic information system and remotely sensed
data p 10 A88-27820

- Land-cover monitoring with SPOT for landfill
investigations p 19 A88-28606

- Aircraft MSS data registration and vegetation
classification for wetland change detection
p 12 A88-29277

CHEMICAL COMPOSITION

- On the problem of evolution of oceanic water
composition in the Phanerozoic p 35 A88-26676

- The use of chlorophyll fluorescence measurements from
space for separating constituents of sea water
p 47 N88-16307

CHESAPEAKE BAY (US)

- Remote sensing of Chesapeake Bay water quality
required for healthy oyster beds p 30 A88-21003

CHLOROCARBONS

- Absolute infrared intensities for F-113 and F-114 and
an assessment of their greenhouse warming potential
relative to other chlorofluorocarbons p 19 A88-31103

CHLOROPHYLLS

- On the parameterization of irradiance for open ocean
photoprocesses p 34 A88-25737

- The use of chlorophyll fluorescence measurements from
space for separating constituents of sea water. Volume
1: Summary
[ESA-CR(P)-2444-VOL-1] p 43 N88-15294

- The use of chlorophyll fluorescence measurements from
space for separating constituents of sea water. Volume
2: Appendices
[ESA-CR(P)-2444-VOL-2] p 44 N88-15295

- The use of chlorophyll fluorescence measurements from
space for separating constituents of sea water
p 47 N88-16307

CIRCULATION DISTRIBUTION

On estimating the basin-scale ocean circulation from satellite altimetry. Part 1: Straightforward spherical harmonic expansion
[NASA-CR-182387] p 44 N88-15352

CITIES

Interrelationships between spatial resolution and per-pixel classifiers for extracting information classes. I - The urban environment. II - The natural environment p 17 A88-21014
Identification and measurement of the areal extent of settlements from Landsat - An exploration into the Nigerian case p 19 A88-28014

CLASSIFICATIONS

Interrelationships between spatial resolution and per-pixel classifiers for extracting information classes. I - The urban environment. II - The natural environment p 17 A88-21014
The use of digital Landsat data for wildlife management on the Warm Springs Indian Reservation of Oregon p 2 A88-21029
Definition of forest stand characteristics based on multi-incidence angle SIR-B data p 2 A88-21031
An application of divergence measurement using transformed video data p 6 A88-24510
A study on the utilization of SIR-A data for population estimation in the eastern part of Spain p 18 A88-24512
Radar descriptors for the classification of terrain features [AD-A188145] p 63 N88-18983
Multisource context classification methods in remote sensing p 63 N88-18985

CLASSIFYING

A proposed semi-supervised two stage classification technique p 56 A88-21063

CLIMATOLOGY

Fluvial perturbation in the western Amazon basin - Regulation by long-term sub-Andean tectonics p 24 A88-20878
The first ISLSCP field experiment (FIFE) --- International Satellite Land Surface Climatology Project p 67 A88-27497
A global survey of surface climate parameters from satellite observations - Preliminary results over Africa p 67 A88-27814
Proposed uses of ERS-1 p 68 A88-27833

CLOUD COVER

A sequential estimation approach to cloud-clearing for satellite temperature sounding p 66 A88-23511
An improved method for detecting clear sky and cloudy radiances from AVHRR data p 69 A88-29284
The acquisition of SPOT-1 HRV imagery over southern Britain and northern France, May 1986-May 1987 p 60 A88-29286

Estimation of atmospheric liquid-water amount by Nimbus 7 SMMR data - A new method and its application to the western North-Pacific region p 69 A88-30731
General determination of Earth surface type and cloud amount using multispectral AVHRR data [NOAA-TR-NESDIS-39] p 72 N88-18997

CLOUD PHYSICS

Interpretation of satellite imagery of a rapidly deepening cyclone p 57 A88-23502

CLUSTER ANALYSIS

A comparison of the hierarchical cluster and homogeneous training field detection methods in classifying urban landcovers from TM data p 56 A88-21067
The use of successive clustering to analyze multispectral imagery p 61 A88-30086

CLUTTER

Active and passive remote sensing of ice [AD-A186685] p 47 N88-17162

COAL

Character of five selected LANDSAT lineaments in southwestern Pennsylvania: Report of investigations, 1987 [PB88-133517] p 30 N88-18988

COASTAL CURRENTS

Multiple dipole eddies in the Alaska Coastal Current detected with Landsat thematic mapper data p 36 A88-27015

COASTAL ECOLOGY

Mapping of the mangroves of the Guanabarra Bay through the utilization of remote sensing techniques [INPE-3942-TDL/229] p 16 N88-19804

COASTAL PLAINS

Large-scale hurricane hazard mapping along the coastal plain of Honduras using Landsat data p 17 A88-21041

COASTAL WATER

Coastal upwelling and eddy development off Nova Scotia p 36 A88-27011

Choosing conditions for the remote sensing of ocean features in the visible spectrum, with the effect of coastal zone taken into account p 37 A88-27209

The use of chlorophyll fluorescence measurements from space for separating constituents of sea water. Volume 1: Summary [ESA-CR(P)-2444-VOL-1] p 43 N88-15294

The use of chlorophyll fluorescence measurements from space for separating constituents of sea water. Volume 2: Appendices [ESA-CR(P)-2444-VOL-2] p 44 N88-15295
Ocean colour applications in ocean dynamics and coastal processes p 45 N88-16297

COASTAL ZONE COLOR SCANNER

Exact Rayleigh scattering calculations for use with the Nimbus-7 Coastal Zone Color Scanner p 41 A88-30415
Update of NASA's ocean colour activities p 45 N88-16295

COASTS

A heat budget for the northern California shelf during CODE 2 p 34 A88-25733
Digitized global land-sea map and access software p 35 A88-26346
Nearshore wave transformation study of sites near Port Canaveral Inlet, Florida [AD-A186965] p 47 N88-17159

COLD WEATHER

Airborne measurements of surface layer turbulence over the ocean during cold air outbreaks p 35 A88-26911

COLLISION PARAMETERS

Ice floe collisions and their relation to ice deformation in the Bering Sea during February 1983 p 40 A88-29324

COLOR

Computer-assisted color generation for thematic mapping p 55 A88-21048
Status and prospects of the Joint Research Committee (JRC) work on the application of ocean colour monitoring from space p 46 N88-16299
Canadian activities and goals in remote sensing of ocean colour and fluorescence from space p 46 N88-16300
Research in Switzerland on ocean and inland-water colour monitoring p 46 N88-16301

COLOR PHOTOGRAPHY

The application of perceptual color spaces to the display of remotely sensed imagery p 58 A88-24935
A study to produce 1:100,000 scale LFC color photomap --- Large Format Camera p 68 A88-27826

COLOR VISION

The application of perceptual color spaces to the display of remotely sensed imagery p 58 A88-24935

COLUMBUS SPACE STATION

Technical aspects of future ocean colour remote sensing p 46 N88-16298

COMBUSTION PRODUCTS

Biomass-burning emissions and associated haze layers over Amazonia p 18 A88-27265

COMPONENTS

Aboveground biomass, surface area, and production relations of red fir (*Abies magnifica*) and white fir (*A. concolor*) p 12 A88-28705

COMPUTATION

An efficient algorithm for computing the crossovers in satellite altimetry [NASA-CR-182389] p 43 N88-15286

COMPUTER AIDED DESIGN

An autoCAD-based mapping system for encoded stereoplotters p 60 A88-29490

COMPUTER AIDED MAPPING

Computer-assisted map analysis - A set of primitive operators for a flexible approach --- in geographic information systems p 17 A88-21023
Computer-assisted color generation for thematic mapping p 55 A88-21048
Methods and accuracy of operational digital image mapping with aircraft SAR p 55 A88-21059
Digitized global land-sea map and access software p 35 A88-26346

Computer-aided mapping of Antarctic Sea ice using along-the-course radiometric measurements aboard the Cosmos-1500 satellite p 38 A88-27213
Thematic mapper and SPOT integration with a geographic information system p 59 A88-28602
An autoCAD-based mapping system for encoded stereoplotters p 60 A88-29490

An integrated approach for automated cover-type mapping of large inaccessible areas in Alaska p 60 A88-29491
The ARSUP database and its access through the CMCIRES catalog - Making available to the public digital maps from the ARSUP process --- Computerized Map Cataloging and Information Retrieval System p 60 A88-29496

The digital landmass simulation production overview [AD-A187978] p 62 N88-18978

COMPUTER GRAPHICS

Landsat remote sensing imagery analysis program p 57 A88-21075

COMPUTER NETWORKS

Development of a 32-bit UNIX-based ELAS workstation p 54 A88-21025

COMPUTER PROGRAMMING

Application of satellite data in variational analysis for global cyclonic systems [NASA-CR-182468] p 62 N88-17152

COMPUTER PROGRAMS

Computer-assisted map analysis - A set of primitive operators for a flexible approach --- in geographic information systems p 17 A88-21023
Development of a 32-bit UNIX-based ELAS workstation p 54 A88-21025
Sea surface current estimates off central California as derived from enhanced AVHRR (Advanced Very High Resolution Radiometer) infrared images [AD-A186867] p 47 N88-17155

COMPUTER SYSTEMS PROGRAMS

Implementation of the Land Analysis System on a workstation p 54 A88-21026

COMPUTER TECHNIQUES

Automated photointerpretation - A stereoscopic workstation p 54 A88-21027
An expert system for the computer-assisted analysis of radar imagery p 55 A88-21053
An application of divergence measurement using transformed video data p 6 A88-24510
Assessment of thematic mapper imagery for forestry applications under Lake States conditions p 7 A88-26336

Model-based building verification in aerial photographs [AD-A186010] p 20 N88-15278
Automatic knowledge acquisition for aerial image interpretation [AD-A188616] p 63 N88-19810

COMPUTER VISION

The use of automated computer vision techniques for the recognition of features on radar imagery p 56 A88-21069

COMPUTERIZED SIMULATION

The digital landmass simulation production overview [AD-A187978] p 62 N88-18978

CONDUCTIVE HEAT TRANSFER

The unsteady ground heat flow at the contact surface between a glacier run and the subsoil p 53 N88-16147

CONFERENCES

American Society for Photogrammetry and Remote Sensing and ACSM, Annual Convention, Baltimore, MD, Mar. 29-Apr. 3, 1987, Technical Papers. Volume 1 - Remote sensing p 64 A88-21001
American Society for Photogrammetry and Remote Sensing and ACSM, Annual Convention, Baltimore, MD, Mar. 29-Apr. 3, 1987, Technical Papers. Volume 2 - Photogrammetry p 2 A88-21046
American Society for Photogrammetry and Remote Sensing and ACSM, Annual Convention, Baltimore, MD, Mar. 29-Apr. 3, 1987, Technical Papers. Volume 3 - Surveying p 20 A88-21054
American Society for Photogrammetry and Remote Sensing and ACSM, Annual Convention, Baltimore, MD, Mar. 29-Apr. 3, 1987, Technical Papers. Volume 4 - Cartography p 21 A88-21058
American Society for Photogrammetry and Remote Sensing and ACSM, Annual Convention, Baltimore, MD, Mar. 29-Apr. 3, 1987, Technical Papers. Volume 6 - Image data processing p 55 A88-21062
Asian Conference on Remote Sensing, 7th, Seoul, Republic of Korea, Oct. 23-28, 1986, Proceedings p 66 A88-24818

Remote sensing from space; Proceedings of Symposium 3, Workshop V, and Topical Meeting A2 of the Twenty-sixth COSPAR Plenary Meeting, Toulouse, France, June 30-July 11, 1986 p 67 A88-27801

Ocean Colour Workshop --- conference [ESA-SP-1083] p 45 N88-16292

Proceedings of the Forest-Atmosphere Interaction Workshop [CONF-8510250] p 17 N88-19824

Proceedings of an ESA-NASA Workshop on a Joint Solid Earth Program [NASA-CR-182642] p 23 N88-19844

CONIFERS

Spectral changes in conifers subjected to air pollution and water stress: Experimental studies p 6 A88-24932

Aboveground biomass, surface area, and production relations of red fir (*Abies magnifica*) and white fir (*A. concolor*) p 12 A88-28705

Assessing forest damage in high-elevation coniferous forests in Vermont and New Hampshire using Thematic Mapper data p 13 A88-30440

- CONSERVATION**
Effects of fire on composition, biomass, and nutrients in oak scrub vegetation on John F. Kennedy Space Center, Florida
[NASA-TM-100305] p 15 N88-16182
- CONTACTS (GEOLOGY)**
The unsteady ground heat flow at the contact surface between a glacier run and the subsoil p 53 N88-16147
- CONTINENTAL DRIFT**
Crustal dynamics project data analysis, 1987. Volume 2: Mobile VLBI geodetic results, 1982-1986
[NASA-TM-100689-VOL-2] p 23 N88-16280
- CONTINENTAL SHELVES**
Shelf water entrainment by Gulf Stream warm-core rings p 36 A88-27013
Continental shelf processes affecting the oceanography of the South Atlantic Bight
[DE88-004102] p 48 N88-17166
Coordination: Southeast continental shelf studies
[DE88-003680] p 49 N88-18110
Mesoscale coastal ocean dynamics p 49 N88-19060
- CONTINENTS**
Geochemistry of continental volcanism --- Russian book p 27 A88-29431
- CONVECTION CURRENTS**
Sea surface temperature, low-level moisture, and convection in the tropical Pacific, 1982-1985 p 34 A88-25729
- CORAL REEFS**
Mesoscale coastal ocean dynamics p 49 N88-19060
- COSMOCHEMISTRY**
The space metal: All about titanium --- Russian book p 25 A88-24781
- COST ANALYSIS**
Multi-stage remote sensing - A tool for Minnesota natural resources management p 64 A88-21018
- COVARIANCE**
Five-diagonal weighting scheme for geoidal profiles
[AD-A188033] p 23 N88-18054
- CROP GROWTH**
Vegetative and optical characteristics of four-row crop canopies p 14 A88-32661
Report on phase 1 of the project estimate development of a model for yield estimation of sugar cane based on LANDSAT and agromet data
[INPE-4466-RPE/560] p 16 N88-19807
- CROP IDENTIFICATION**
Operational interpretation of AVHRR vegetation indices for world crop information p 7 A88-26335
X-band features of canopy cover - An up to date summary of active and passive measurements p 10 A88-27835
Evaluation of middle and thermal infrared radiance in indices used to estimate GLAI p 14 A88-32663
Large area crop classification in New South Wales, Australia, using Landsat data p 14 A88-32665
- CROP INVENTORIES**
Remote sensing surveys design in regional agricultural inventories p 8 A88-27804
Adaptive computer-aided system for crop inventory according to space photographs p 13 A88-30087
Calculation of canopy bidirectional reflectance using the Monte Carlo method p 13 A88-30439
Crop forecasting in Brazil: A short history of productivity models
[INPE-4150-PRE/1056] p 16 N88-19801
- CROP VIGOR**
Crop forecasting in Brazil: A short history of productivity models
[INPE-4150-PRE/1056] p 16 N88-19801
- CROSSOVERS**
Geosat crossover analysis in the tropical Pacific. Part 1: Constrained sinusoidal crossover adjustment
[NASA-CR-182391] p 43 N88-15285
An efficient algorithm for computing the crossovers in satellite altimetry
[NASA-CR-182389] p 43 N88-15286
- CRUDE OIL**
Sea return at C and Ku bands p 31 A88-22947
- CRUSTAL FRACTURES**
An investigation of small-offset fracture zone geoid waveforms p 22 A88-27465
- CRYSTAL STRUCTURE**
Physical properties of summer sea ice in the Fram Strait, June-July 1984
[AD-A186937] p 53 N88-17156
- CYCLOGENESIS**
The Genesis of Atlantic Lows Experiment - The planetary-boundary-layer subprogram of GALE p 42 A88-31111
- CYCLOONES**
Interpretation of satellite imagery of a rapidly deepening cyclone p 57 A88-23502
- Simultaneity of response of Atlantic Ocean tropical cyclones and Indian monsoons p 34 A88-25736
- D**
- DAMAGE ASSESSMENT**
Comparison of in situ and airborne spectral measurements of the blue shift associated with forest decline p 11 A88-28271
Preliminary assessment of airborne imaging spectrometer and airborne thematic mapper data acquired for forest decline areas in the Federal Republic of Germany p 11 A88-28272
- DATA ACQUISITION**
Autonomous control of image sensor for the optimal acquisition of ground information for dynamic analysis p 65 A88-21660
Remote sensing methods and instrumentation for obtaining data on earth resources and the environment p 66 A88-26050
Aircraft MSS data registration and vegetation classification for wetland change detection p 12 A88-29277
The acquisition of SPOT-1 HRV imagery over southern Britain and northern France, May 1986-May 1987 p 60 A88-29286
Accuracy of mapping by panoramic photography p 60 A88-29479
- DATA BASE MANAGEMENT SYSTEMS**
Requirements and principles for the implementation and construction of large-scale geographic information systems p 19 A88-28684
Critical issues in NASA information systems
[NASA-CR-182380] p 72 N88-16577
Design and implementation of a data base system for Digital Land Mass System (DLMS) data
[FEL-IR-1987-19] p 71 N88-17101
- DATA BASES**
An automated system for terrain database construction p 18 A88-21060
Digital terrain analysis employing X-Y-Z point vectors as input data p 55 A88-21061
Requirements and principles for the implementation and construction of large-scale geographic information systems p 19 A88-28684
The ARSUP database and its access through the CMCIRS catalog - Making available to the public digital maps from the ARSUP process --- Computerized Map Cataloging and Information Retrieval System p 60 A88-29496
User's guide to a data base of current environmental monitoring projects in the US-Canadian transboundary region
[DE88-002476] p 20 N88-17119
- DATA CONVERSION ROUTINES**
Design and implementation of a data base system for Digital Land Mass System (DLMS) data
[FEL-IR-1987-19] p 71 N88-17101
- DATA CORRELATION**
Method for joint adjustment of satellite and surface geodetic networks p 22 N88-16105
- DATA FLOW ANALYSIS**
Multiband-scatterometer data analysis of forests p 5 A88-23548
- DATA MANAGEMENT**
Landsat classification of the barren hydrolittoral areas of Lake Yli-Kitka, north-eastern Finland p 51 A88-24198
National Severe Storms Laboratory, fiscal year 1987
[PB88-140108] p 72 N88-19863
- DATA PROCESSING**
Implementation of the Land Analysis System on a workstation p 54 A88-21026
American Society for Photogrammetry and Remote Sensing and ACSM, Annual Convention, Baltimore, MD, Mar. 29-Apr. 3, 1987, Technical Papers. Volume 6 - Image data processing p 55 A88-21062
Refining image segmentation by polygon skeletonization p 56 A88-21068
Land cover change detection with Landsat MSS and TM data in the Kitchener-Waterloo area, Canada p 18 A88-21071
Method for joint adjustment of satellite and surface geodetic networks p 22 N88-16105
Application of satellite data in variational analysis for global cyclonic systems
[NASA-CR-182468] p 62 N88-17152
Multisource context classification methods in remote sensing p 63 N88-18985
Spaceborne gravity gradiometry characterizing the data type p 24 N88-19847
Design of the primary pre-TRMM and TRMM ground truth site
[NASA-CR-182609] p 53 N88-19865
- DATA REDUCTION**
Processing and analysis of large volumes of satellite-derived thermal infrared data --- for physical oceanographic studies p 36 A88-27012
- DATA RETRIEVAL**
Requirements and principles for the implementation and construction of large-scale geographic information systems p 19 A88-28684
- DATA SAMPLING**
A semi-automated training sample selector for multispectral land cover classification p 56 A88-21066
- DATA SIMULATION**
Image based SAR product simulation for analysis p 55 A88-21037
Differences in vegetation indices for simulated Landsat-5 MSS and TM, NOAA-9 AVHRR, and SPOT-1 sensor systems p 7 A88-25446
Simulation of spaceborne SAR imagery from airborne SAR data p 58 A88-27830
- DATA STRUCTURES**
Digitized global land-sea map and access software p 35 A88-26346
- DEFORMATION**
The aerophotogrammetric determination of Earth surface deformations
[SER-C-321] p 28 N88-15288
- DELTA S**
Landsat determined geographic change p 27 A88-29489
- DEPTH**
Airborne electromagnetic sounding of sea ice thickness and sub-ice bathymetry
[AD-A188939] p 50 N88-19879
- DESERTIFICATION**
Relative sensitivity of Normalized Difference Vegetation Index (NDVI) and Microwave Polarization Difference Index (MPDI) for vegetation and desertification monitoring p 13 A88-30444
- DESERTS**
Satellite observed seasonal and inter-annual variation of vegetation over the Kalahari, the Great Victoria Desert, and the Great Sandy Desert - 1979-1984 p 3 A88-21356
Aircraft and satellite remote sensing of desert soils and landscapes p 3 A88-21358
Contribution of SPOT images to the geological mapping of arid countries - Example of the Yemen Arab Republic p 25 A88-22616
Techniques of ground-truth measurements of desert-scrub structure p 9 A88-27817
Estimates of primary productivity over the Thar Desert based upon Nimbus-7 37 GHz data - 1979-1985 p 11 A88-28016
Karst and erosion topography on space photographs (With reference to the Ustiurt plateau) p 60 A88-30080
- DETECTION**
Model-based building verification in aerial photographs
[AD-A186010] p 20 N88-15278
- DEVELOPING NATIONS**
Using remotely sensed data for census surveys and population estimation in developing countries - Examples from Nigeria p 18 A88-24511
- DIGITAL DATA**
The use of digital Landsat data for wildlife management on the Warm Springs Indian Reservation of Oregon p 2 A88-21029
Definition of forest stand characteristics based on multi-incidence angle SIR-B data p 2 A88-21031
Digital terrain analysis employing X-Y-Z point vectors as input data p 55 A88-21061
Results of testing digital image measurements and enhancements on the remote work processing facility p 56 A88-21064
Digitized global land-sea map and access software p 35 A88-26346
The potential for automated mapping from Geocoded digital image data p 59 A88-28604
An integrated approach for automated cover-type mapping of large inaccessible areas in Alaska p 60 A88-29491
Textural features for image classification in remote sensing
[INPE-4169-PRE/1066] p 62 N88-16181
Critical issues in NASA information systems
[NASA-CR-182380] p 72 N88-16577
The digital landmass simulation production overview
[AD-A187978] p 62 N88-18978
Report on phase 1 of the project estimate development of a model for yield estimation of sugar cane based on LANDSAT and agromet data
[INPE-4466-RPE/560] p 16 N88-19807

DIGITAL SIMULATION

- Detecting subpixel woody features using simulated multispectral and panchromatic SPOT imagery p 3 A88-21065

DIGITAL TECHNIQUES

- Potential applications of digital image analysis systems for displaying satellite altimetry data p 31 A88-23762
Radiometric correction of C-band imagery for topographic effects in regions of moderate relief p 59 A88-28680
Evaluation of the flooding areas of the Sao Goncalo Canal through LANDSAT 5 thematic mapper images [INPE-4118-PRE/1039] p 53 N88-16185

DIODES

- Evaluation of a temperature remote sensing technique [AD-A187885] p 71 N88-18053

DISPLAY DEVICES

- Potential applications of digital image analysis systems for displaying satellite altimetry data p 31 A88-23762
The application of perceptual color spaces to the display of remotely sensed imagery p 58 A88-24935

DOPPLER EFFECT

- On differential scale changes and the satellite Doppler system z-shift p 21 A88-25850

DRAINAGE PATTERNS

- Detection of subsurface geologic structures in the Tharthar area of central Iraq using Landsat images p 24 A88-20902

DRILLING

- Geological evolution and analysis of confirmed or suspected gas hydrate localities. Volume 9: Formation and stability of gas hydrates of the Middle America Trench [DE88-001007] p 29 N88-18050

DROPS (LIQUIDS)

- Spray droplet generation, transport, and evaporation in a wind wave tunnel during the humidity exchange over the sea experiments in the simulation tunnel p 38 A88-27492

DROUGHT

- Satellite remote sensing of drought conditions p 3 A88-21357

E

EARTH ALBEDO

- A method for the estimate of broadband directional surface albedo from a geostationary satellite p 22 A88-27299
A global survey of surface climate parameters from satellite observations - Preliminary results over Africa p 67 A88-27814
Simulations of the Meteosat visible sensor response to changing boundary conditions p 67 A88-27823
Extraction of spectral hemispherical reflectance (albedo) of surfaces from nadir and directional reflectance data p 59 A88-28009
The role of anisotropy in the long range reconnaissance of the albedo of land surfaces p 62 N88-16169

EARTH ATMOSPHERE

- Extended abstract modelling interactions between the terrestrial biosphere and the global atmosphere p 65 A88-21022
Remote sensing of atmospheric optical thickness and sea-water attenuation when submerged: Wavelength selection and anticipated errors p 49 N88-19262
The effects of atmospheric and thermohaline variability on the validation of the GEOSAT altimeter oceanographic signal between Scotland and Iceland [AD-A189324] p 50 N88-19882

EARTH CRUST

- Geodetic application of the Global Positioning System p 21 A88-24289
An investigation of small-offset fracture zone geoid waveforms p 22 A88-27465
Exploration of crustal/mantle material for the earth and moon using reflectance spectroscopy p 27 A88-28273

- Crustal dynamics project data analysis, 1987. Volume 1: Fixed station VLBI geodetic results, 1979-1986 [NASA-TM-100682] p 23 N88-16279

- Crustal dynamics project data analysis, 1987. Volume 2: Mobile VLBI geodetic results, 1982-1986 [NASA-TM-100689-VOL-2] p 23 N88-16280

- Materials of the World Data Center B. Deep Seismic Sounding (DSS): Pacific data p 48 N88-17167

- Crustal Dynamics Project: Catalogue of site information [NASA-RP-1198] p 23 N88-19037

EARTH IONOSPHERE

- Satellite monitoring of earthquake precursor effects in magnetosphere p 28 N88-16103

EARTH MAGNETOSPHERE

- Satellite monitoring of earthquake precursor effects in magnetosphere p 28 N88-16103

EARTH MANTLE

- Mantle rheology and satellite signatures from present-day glacial forcings p 21 A88-25225
Remanent magnetization of the oceanic upper mantle p 37 A88-27036
Exploration of crustal/mantle material for the earth and moon using reflectance spectroscopy p 27 A88-28273

EARTH OBSERVATIONS (FROM SPACE)

- American Society for Photogrammetry and Remote Sensing and ACSM, Annual Convention, Baltimore, MD, Mar. 29-Apr. 3, 1987, Technical Papers. Volume 1 - Remote sensing p 64 A88-21001
Introduction to the physics and techniques of remote sensing --- Book p 65 A88-21168
The Earth-Observation Preparatory Programme p 66 A88-22724
SPOT 1 - Earth observing satellite p 66 A88-26166
A method for synthesizing optimal space systems for earth surveying p 67 A88-27214
Identical-route satellite orbits for long-term periodic global survey of the earth, not dependent on solar illumination p 67 A88-27216
Terrestrial imaging spectroscopy p 69 A88-28266
Looking at the earth from space p 69 A88-29235
Methods for processing radio-physical measurement data in studies of the environment --- Russian book p 19 A88-29427

- From pattern to process: The strategy of the Earth Observing System: Volume 2: EOS Science Steering Committee report [NASA-TM-89702] p 70 N88-15283

- Academic course Space Methods for Studying Modern Landscapes of Continents p 72 N88-16133

- Status and prospects of the Joint Research Committee (JRC) work on the application of ocean colour monitoring from space p 46 N88-16299

- Canadian activities and goals in remote sensing of ocean colour and fluorescence from space p 46 N88-16300

- Federal Republic of Germany's interests, activities and goals in remote sensing of ocean colour/fluorescence from space p 46 N88-16302

- French activities in ocean colour observations p 46 N88-16303
The use of chlorophyll fluorescence measurements from space for separating constituents of sea water p 47 N88-16307

- Report of the Workshop on Space Systems Possibilities for a Global Energy and Water Cycle Experiment [WCP-137] p 53 N88-17147

- Space-based remote sensing of the Earth: A report to the Congress [NASA-TM-89709] p 72 N88-18046

- NASA's geodynamics program p 24 N88-19845

EARTH OBSERVING SYSTEM (EOS)

- HIRIS (High-Resolution Imaging Spectrometer: Science opportunities for the 1990s. Earth observing system. Volume 2C: Instrument panel report [NASA-TM-89703] p 70 N88-15282
From pattern to process: The strategy of the Earth Observing System: Volume 2: EOS Science Steering Committee report [NASA-TM-89702] p 70 N88-15283
SAR (Synthetic Aperture Radar). Earth observing system. Volume 2F: Instrument panel report [NASA-TM-89701] p 70 N88-15284

EARTH RESOURCES

- A semi-automated training sample selector for multispectral land cover classification p 56 A88-21066

- A comparison of the hierarchical cluster and homogeneous training field detection methods in classifying urban landcovers from TM data p 56 A88-21067

- Land cover change detection with Landsat MSS and TM data in the Kitchener-Waterloo area, Canada p 18 A88-21071

- Land cover change detection using a GIS-guided, feature-based classification of Landsat thematic mapper data --- Geographic Information System p 18 A88-21073

- An application of divergence measurement using transformed video data p 6 A88-24510

- The space metal: All about titanium --- Russian book p 25 A88-24781

- Characteristics of the subsurface radar sounding of natural objects p 26 A88-25551

- Remote sensing methods and instrumentation for obtaining data on earth resources and the environment p 66 A88-26050

- The use of space technology for the remote sensing of earth resources and mapping p 69 A88-28447

- Space photographs of the Omega-Ladoga isthmus and prediction of useful minerals p 28 N88-16108
Use of space photographs for geomorphological studies in southwestern Tajikistan p 28 N88-16109

- Critical issues in NASA information systems [NASA-CR-182380] p 72 N88-16577
System-wide medium-term environment programme for the period 1990-1995: Strategies of the United Nations system for the environment [UNEP/GCSS.1/2] p 20 N88-19826

EARTH ROTATION

- Crustal dynamics project data analysis, 1987. Volume 1: Fixed station VLBI geodetic results, 1979-1986 [NASA-TM-100682] p 23 N88-16279

EARTH SURFACE

- Correlation characteristics of images of the earth surface obtained with a synthetic-aperture radar p 66 A88-21784

- Talemzane - Algerian impact crater detected on SIR-A orbital imaging radar p 25 A88-25217

- A method for the estimate of broadband directional surface albedo from a geostationary satellite p 22 A88-27299

- Comparative study of temperature data from NOAA7-AVHRR and WMO - An interpretation through the use of a soil-vegetation model p 8 A88-27806

- Aboveground biomass, surface area, and production relations of red fir (*Abies magnifica*) and white fir (*A. concolor*) p 12 A88-28705

- Information content of spectral signatures and textures and structures for remote sensing of the earth p 60 A88-29499

- Relationship between brightness temperature in the RF range and the radiative dryness index p 69 A88-30082

- Applications of microwaves to remote sensing p 69 A88-30670

- The aerophotogrammetric determination of Earth surface deformations [SER-C-321] p 28 N88-15288

- Space applications in geography p 22 N88-16104
Multistep component analysis of correlations p 61 N88-16115

- General determination of Earth surface type and cloud amount using multispectral AVHRR data [NOAA-TR-NESDIS-39] p 72 N88-18997

EARTH TIDES

- Observations of Earth tides by the German Geodetic Research Institute, division 1, in the period 1979-1985 at the Berchtesgaden and Wettzell stations [SER-B-280] p 22 N88-15291

EARTHQUAKES

- Investigation of the foci of powerful earthquakes and seismically hazardous areas on space photographs for the Baikal-Aldan region p 27 A88-30081

- Satellite monitoring of earthquake precursor effects in magnetosphere p 28 N88-16103

ECOLOGICAL

- The first ISLSCP field experiment (FIFE) --- International Satellite Land Surface Climatology Project p 67 A88-27497

- Detection of soil erosion with Thematic Mapper (TM) satellite data within Pinyon-Juniper woodlands [NASA-CR-182476] p 15 N88-17103

ECOSYSTEMS

- Comprehensive studies of the dynamics of geosystems with the use of remote sensing techniques p 10 A88-27821

EDUCATION

- Academic course Space Methods for Studying Modern Landscapes of Continents p 72 N88-16133
Report of the participation in the International Training Course: Remote Sensing in Village Forestry [INPE-4476-NTE/278] p 16 N88-19802

EFFICIENCY

- An efficient algorithm for computing the crossovers in satellite altimetry [NASA-CR-182389] p 43 N88-15286

EL NINO

- Geosat altimeter observations of Kelvin waves and the 1986-87 El Nino p 32 A88-24582

- El Nino events and their relation to the Southern Oscillation - 1925-1986 p 33 A88-25726

- Longitudinal variations in tropical tropopause properties in relation to tropical convection and El Nino-Southern Oscillation events p 33 A88-25727

- Remote sensing of water vapor convergence, deep convection, and precipitation over the tropical Pacific Ocean during the 1982-1983 El Nino p 33 A88-25728

- Characteristics of extreme rainfall events in northwestern Peru during the 1982-1983 El Nino period p 52 A88-25730

- An investigation of the El Nino-Southern Oscillation Cycle with statistical models. I - Predictor field characteristics. II - Model results p 34 A88-25731

- Remote forcing of sea surface temperature in the El Nino region p 34 A88-25732

ELECTROMAGNETIC INTERACTIONS

- Statistical model of interaction of electromagnetic waves with natural objects being sensed p 70 N88-16112

ELECTROMAGNETIC PROPERTIES

Research in remote sensing of vegetation
[NASA-CR-182663] p 16 N88-19817

ELECTROMAGNETIC RADIATION

Parametric analysis of synthetic aperture radar data for
characterization of deciduous forest stands

p 2 A88-21033
Satellite monitoring of earthquake precursor effects in
magnetosphere p 28 N88-16103
Statistical model of interaction of electromagnetic waves
with natural objects being sensed p 70 N88-16112
Airborne electromagnetic sounding of sea ice thickness
and sub-ice bathymetry p 50 N88-19879

ELECTROMAGNETIC SCATTERING

Three-dimensional transient electromagnetic modeling
for exploration geophysics p 29 N88-18047

ELECTROMAGNETIC WAVE TRANSMISSION

Active and passive remote sensing of ice
[AD-A186685] p 47 N88-17162

EMISSION

The emissivity of the vegetation-soil system
p 8 A88-27208
Importance of a remote measurement of spectral
thermal infrared emissivities - Presentation and validation
of such a determination p 67 A88-27813
Emissivity of pure and sea waters for the model sea
surface in the infrared window regions p 42 A88-30445

ENERGY BUDGETS

Use of the thermodynamic evaporation formula of
Hoffmann in energy balance models for flowing water
p 52 N88-16143
Energy balance and discharge of an Alpine glacier,
illustrated by Mount Vernagferner in the Oetzal Alps,
Tyrol p 53 N88-16145

ENERGY SPECTRA

Investigation of the quantitative determination of two
dimensional sea surface wave spectra from shipborne
radar measurements [GKSS-87/E/10] p 48 N88-17163

ENGINEERING MANAGEMENT

Remote sensing applications by consulting engineers -
Three case histories p 24 A88-21009

ENTRAINMENT

Shelf water entrainment by Gulf Stream warm-core
rings p 36 A88-27013

ENVIRONMENT EFFECTS

Effects of fire on composition, biomass, and nutrients
in oak scrub vegetation on John F. Kennedy Space Center,
Florida [NASA-TM-100305] p 15 N88-16182

ENVIRONMENT POLLUTION

System-wide medium-term environment programme for
the period 1990-1995: Strategies of the United Nations
system for the environment [UNEP/GCSS.1/2] p 20 N88-19826

ENVIRONMENT PROTECTION

System-wide medium-term environment programme for
the period 1990-1995: Strategies of the United Nations
system for the environment [UNEP/GCSS.1/2] p 20 N88-19826

ENVIRONMENTAL MONITORING

The Earth-Observation Preparatory Programme
p 66 A88-22724
Remote sensing methods and instrumentation for
obtaining data on earth resources and the environment
p 66 A88-26050
Principles of field spectroscopy p 68 A88-28013
Methods for processing radio-physical measurement
data in studies of the environment --- Russian book
p 19 A88-29427

User's guide to a data base of current environmental
monitoring projects in the US-Canadian transboundary
region [DE88-002476] p 20 N88-17119

Meteorological and aerosol measurements from the
NOAA WP-3D aircraft during WATOX-86, January 4-9,
1986 [PB88-120860] p 20 N88-18079

System-wide medium-term environment programme for
the period 1990-1995: Strategies of the United Nations
system for the environment [UNEP/GCSS.1/2] p 20 N88-19826

ENVIRONMENTAL QUALITY

User's guide to a data base of current environmental
monitoring projects in the US-Canadian transboundary
region [DE88-002476] p 20 N88-17119

EQUATORIAL REGIONS

The western equatorial Pacific Ocean circulation study
p 30 A88-22911

EROSION

Detection of soil erosion with Thematic Mapper (TM)
satellite data within Pinyon-Juniper woodlands
[NASA-CR-182476] p 15 N88-17103

ERROR ANALYSIS

Accuracy of mapping by panoramic photography
p 60 A88-29479

A comparison between panoramic photography and
conventional aerial photography in terms of mapping
accuracy p 61 A88-32167

Geostat crossover analysis in the tropical Pacific. Part
1: Constrained sinusoidal crossover adjustment
[NASA-CR-182391] p 43 N88-15285

Limiting accuracy of scatterometer determination of wind
speed over ocean from satellite p 44 N88-16107

Design of the primary pre-TRMM and TRMM ground
truth site [NASA-CR-182609] p 53 N88-19865

The effects of atmospheric and thermohaline variability
on the validation of the GEOSAT altimeter oceanographic
signal between Scotland and Iceland [AD-A189324] p 50 N88-19882

ERS-1 (ESA SATELLITE)

Observation of sea-ice dynamics using synthetic
aperture radar images: Automated analysis p 32 A88-24934

Simulation of bit-quantization influence on SAR
images p 59 A88-27831

Design concept of the SAR installed on ERS-1
p 68 A88-27832

Proposed uses of ERS-1 p 68 A88-27833

ESTIMATES

On estimating the basin-scale ocean circulation from
satellite altimetry. Part 1: Straightforward spherical
harmonic expansion [NASA-CR-182387] p 44 N88-15352

Sea surface current estimates off central California as
derived from enhanced AVHRR (Advanced Very High
Resolution Radiometer) infrared images [AD-A186867] p 47 N88-17155

ESTIMATION

A study on the utilization of SIR-A data for population
estimation in the eastern part of Spain p 18 A88-24512

ESTUARIES

Development of multivariate estuarine water quality models
using Landsat 2 and 4 MSS data p 50 A88-21002

EUROPEAN SPACE AGENCY

Overview of ESA's activities in ocean colour remote
sensing p 45 N88-16294

EUROPEAN SPACE PROGRAMS

Europe's position concerning ocean colour activities
p 45 N88-16293

Overview of ESA's activities in ocean colour remote
sensing p 45 N88-16294

Federal Republic of Germany's interests, activities and
goals in remote sensing of ocean colour/fluorescence from
space p 46 N88-16302

EVAPORATION

Relating Nimbus-7 37 GHz data to global land-surface
evaporation, primary productivity and the atmospheric CO2
concentration p 60 A88-29287

Use of the thermodynamic evaporation formula of
Hoffmann in energy balance models for flowing water
p 52 N88-16143

EVAPOTRANSPIRATION

Estimation of evapotranspiration in the Sahelian zone
by use of Meteosat and NOAA AVHRR data p 9 A88-27818

EVOLUTION (DEVELOPMENT)

On the problem of evolution of oceanic water
composition in the Phanerozoic p 35 A88-26676

Five New South Wales barrier lagoons: Their
macrobenthic fauna and seagrass communities p 49 N88-19059

EXPERIMENT DESIGN

The first ISLSCP field experiment (FIFE) --- International
Satellite Land Surface Climatology Project p 67 A88-27497

EXPERT SYSTEMS

An expert system for the computer-assisted analysis of
radar imagery p 55 A88-21053

F**FARM CROPS**

Adaptive computer-aided system for crop inventory
according to space photographs p 13 A88-30087

Vegetative and optical characteristics of four-row crop
canopies p 14 A88-32661

Evaluation of middle and thermal infrared radiance in
indices used to estimate GLAI p 14 A88-32663

Crop canopy spectral reflectance p 14 A88-32664

Large area crop classification in New South Wales,
Australia, using Landsat data p 14 A88-32665

FINITE ELEMENT METHOD

Comparison of the gridded finite element and the
polynomial interpolations for geometric rectification and
mosaicking of Landsat data p 55 A88-21049

FINLAND

Landsat classification of the barren hydrolittoral areas
of Lake Yli-Kitka, north-eastern Finland p 51 A88-24198

FIRE DAMAGE

Effects of fire on composition, biomass, and nutrients
in oak scrub vegetation on John F. Kennedy Space Center,
Florida [NASA-TM-100305] p 15 N88-16182

FISSURES (GEOLOGY)

The aerophotogrammetric determination of Earth
surface deformations [SER-C-321] p 28 N88-15288

FLOOD CONTROL

Review of the potential of satellite remote sensing for
marine flood protection [IOS-237] p 43 N88-15280

FLOOD PREDICTIONS

Review of the potential of satellite remote sensing for
marine flood protection [IOS-237] p 43 N88-15280

FLOODS

Radar flood inundation mapping of upper Benue Trough,
Nigeria p 2 A88-21035

Evaluation of the flooding areas of the Sao Goncalo
Canal through LANDSAT 5 thematic mapper images
[INPE-4118-PRE/1039] p 53 N88-16185

FLORIDA

Nearshore wave transformation study of sites near Port
Canaveral Inlet, Florida [AD-A186965] p 47 N88-17159

Design of the primary pre-TRMM and TRMM ground
truth site [NASA-CR-182609] p 53 N88-19865

FLUORESCENCE

The use of chlorophyll fluorescence measurements from
space for separating constituents of sea water p 47 N88-16307

FLUOROCARBONS

Absolute infrared intensities for F-113 and F-114 and
an assessment of their greenhouse warming potential
relative to other chlorofluorocarbons p 19 A88-31103

FOREST FIRES

Mid-infrared (1.45 to 2.0 microns) video - A potential
aid in wildfire mop-up operations p 1 A88-21016

FOREST MANAGEMENT

Effects of fire on composition, biomass, and nutrients
in oak scrub vegetation on John F. Kennedy Space Center,
Florida [NASA-TM-100305] p 15 N88-16182

Investigations on the application of space photographs
(Spacelab metric camera) for routine inventories of
extensively managed forest areas [DFVLR-FB-87-22] p 15 N88-17098

Report of the participation in the International Training
Course: Remote Sensing in Village Forestry
[INPE-4476-NTE/278] p 16 N88-19802

FORESTS

Fluvial perturbation in the western Amazon basin -
Regulation by long-term sub-Andean tectonics p 24 A88-20878

Multispectral video survey of a Northern Ontario forest
p 1 A88-21015

Estimating forest productivity in southern Illinois using
Landsat Thematic Mapper data and geographic
information system analysis techniques p 2 A88-21028

Definition of forest stand characteristics based on
multi-incidence angle SIR-B data p 2 A88-21031

Parametric analysis of synthetic aperture radar data for
characterization of deciduous forest stands p 2 A88-21033

Reflectance modeling of semiarid woodlands p 4 A88-21364

Multiband-scatterometer data analysis of forests
p 5 A88-23548

The DUT airborne scatterometer p 5 A88-23549

Correlation between aircraft MSS and lidar remotely
sensed data on a forested wetland p 6 A88-24513

Remote sensing of forest cover distribution in the Phu
Wiang watershed area of Khon Kaen Province, Northeast
of Thailand p 6 A88-24514

Measurements of the backscatter and attenuation
properties of forest stands at X-, C- and L-band p 7 A88-25444

Assessment of thematic mapper imagery for forestry
applications under Lake States conditions p 7 A88-26336

Estimation of biophysical properties of forest canopies
using C-band microwave data p 9 A88-27809

Preliminary study of the characterization of the riverine
forests of the Garonne using Landsat MSS and TM data p 9 A88-27811

Characterizing forest stands with multi-incidence angle
and multi-polarized SAR data p 10 A88-27836

- Determining the rate of forest conversion in Mato Grosso, Brazil, using Landsat MSS and AVHRR data p 10 A88-28011
- Evaluation of several classification schemes for mapping forest cover types in Michigan p 10 A88-28012
- Remote sensing of forest canopy and leaf biochemical contents p 11 A88-28270
- Comparison of in situ and airborne spectral measurements of the blue shift associated with forest decline p 11 A88-28271
- Preliminary assessment of airborne imaging spectrometer and airborne thematic mapper data acquired for forest decline areas in the Federal Republic of Germany p 11 A88-28272
- The use of a helicopter mounted ranging scatterometer for estimation of extinction and backscattering properties of forest canopies-I: Experimental approach and calibration p 11 A88-28682
- The use of a helicopter mounted ranging scatterometer for estimation of extinction and scattering properties of forest canopies-II: Experimental results for high-density aspen p 11 A88-28683
- Measuring crown cover in interior Alaska vegetation types p 12 A88-29495
- Assessing forest damage in high-elevation coniferous forests in Vermont and New Hampshire using Thematic Mapper data p 13 A88-30440
- Estimating forest biomass and volume using airborne laser data p 13 A88-30441
- Relating seasonal patterns of the AVHRR vegetation index to simulated photosynthesis and transpiration of forests in different climates p 13 A88-30447
- Improved canopy reflectance modeling and scene inference through improved understanding of scene pattern [NASA-CR-182488] p 15 A88-18049
- Mapping of the mangroves of the Guanabarra Bay through the utilization of remote sensing techniques [INPE-3942-TDL/229] p 16 A88-19804
- Proceedings of the Forest-Atmosphere Interaction Workshop [CONF-8510250] p 17 A88-19824
- FOSSILS**
- Fluvial perturbation in the western Amazon basin - Regulation by long-term sub-Andean tectonics p 24 A88-20878
- FOURIER TRANSFORMATION**
- Application of frequency filtering in remotely sensed imagery p 57 A88-21072
- FREEZING**
- Mesoscale monitoring of the soil freeze/thaw boundary from orbital microwave radiometry [NASA-CR-182659] p 17 A88-19855
- FRENCH SPACE PROGRAMS**
- French activities in ocean colour observations p 46 A88-18303
- The Earthnet Heat Capacity Mapping Mission (HCMM) data-processing system at Lannion (France) p 62 A88-18761
- FRESH WATER**
- Evaluation of X-band SAR imagery for mapping open surface water in the northeastern United States p 51 A88-21038
- Gas exchange on Mono Lake and Crowley Lake, California p 52 A88-25735
- Emissivity of pure and sea waters for the model sea surface in the infrared window regions p 42 A88-30445
- FRONTS (METEOROLOGY)**
- North Pacific Ocean. Central Pacific Transition Zone, R/V Thomas G. Thompson: 25 March - 3 May 1968. STD data report [AD-A186570] p 47 A88-17160
- FUNCTIONAL DESIGN SPECIFICATIONS**
- Construction of airborne radars for remote sensing [PB88-113063] p 71 A88-16916
- G**
- GAS EXCHANGE**
- Gas exchange on Mono Lake and Crowley Lake, California p 52 A88-25735
- GEOCHEMISTRY**
- Geochemistry of continental volcanism --- Russian book p 27 A88-29431
- Nature and origin of mineral coatings on volcanic rocks of the Black Mountain, Stonewall Mountain, and Kane Springs Wash volcanic centers, Southern Nevada [NASA-CR-181437] p 29 A88-17140
- GEODESY**
- Simultaneous determination of astronomic position and azimuth from observations of zenith distances and horizontal directions p 20 A88-21055
- On differential scale changes and the satellite Doppler system z-shift p 21 A88-25850

- Five-diagonal weighting scheme for geoidal profiles [AD-A188033] p 23 A88-18054
- A smart, mapping, charting and geodesy control generator, phase 1 [AD-A188184] p 23 A88-18055
- Reports on cartography and geodesy. Series 1, report 98 [ISSN-0469-4236] p 23 A88-18993
- GEODEIC COORDINATES**
- On differential scale changes and the satellite Doppler system z-shift p 21 A88-25850
- Method for joint adjustment of satellite and surface geodetic networks p 22 A88-16105
- New possibilities for using gravity data in developing geodetic coordinate systems p 23 A88-16116
- Reports on cartography and geodesy. Series 1, report 98 [ISSN-0469-4236] p 23 A88-18993
- The orientation of global satellite networks p 63 A88-18996
- GEODEIC SATELLITES**
- Geodetic application of the Global Positioning System p 21 A88-24289
- On differential scale changes and the satellite Doppler system z-shift p 21 A88-25850
- GEODEIC SURVEYS**
- American Society for Photogrammetry and Remote Sensing and ACSM, Annual Convention, Baltimore, MD, Mar. 29-Apr. 3, 1987, Technical Papers. Volume 3 - Surveying p 20 A88-21054
- GPS survey techniques for deformation analysis p 21 A88-21057
- Observations of Earth tides by the German Geodetic Research Institute, division 1, in the period 1979-1985 at the Berchtesgaden and Wettzell stations [SER-B-280] p 22 A88-15291
- Crustal dynamics project data analysis, 1987. Volume 1: Fixed station VLBI geodetic results, 1979-1986 [NASA-TM-100682] p 23 A88-16279
- Crustal dynamics project data analysis, 1987. Volume 2: Mobile VLBI geodetic results, 1982-1986 [NASA-TM-100689-VOL-2] p 23 A88-16280
- Crustal Dynamics Project: Catalogue of site information [NASA-RP-1198] p 23 A88-19037
- GEODYNAMICS**
- Geodetic application of the Global Positioning System p 21 A88-24289
- Crustal dynamics project data analysis, 1987. Volume 1: Fixed station VLBI geodetic results, 1979-1986 [NASA-TM-100682] p 23 A88-16279
- Crustal dynamics project data analysis, 1987. Volume 2: Mobile VLBI geodetic results, 1982-1986 [NASA-TM-100689-VOL-2] p 23 A88-16280
- Crustal Dynamics Project: Catalogue of site information [NASA-RP-1198] p 23 A88-19037
- Proceedings of an ESA-NASA Workshop on a Joint Solid Earth Program [NASA-CR-182642] p 23 A88-19844
- NASA's geodynamics program p 24 A88-19845
- GEOGRAPHIC INFORMATION SYSTEMS**
- Computer-assisted map analysis - A set of primitive operators for a flexible approach --- in geographic information systems p 17 A88-21023
- Estimating forest productivity in southern Illinois using Landsat Thematic Mapper data and geographic information system analysis techniques p 2 A88-21028
- An automated system for terrain database construction p 18 A88-21060
- Land cover change detection using a GIS-guided, feature-based classification of Landsat thematic mapper data --- Geographic Information System p 18 A88-21073
- Geographic information systems for resource management: A compendium --- Book p 5 A88-23253
- Analyzing long-term changes in vegetation with geographic information system and remotely sensed data p 10 A88-27820
- Comprehensive studies of the dynamics of geosystems with the use of remote sensing techniques p 10 A88-27821
- Thematic mapper and SPOT integration with a geographic information system p 59 A88-28602
- Remote sensing and geographic information system techniques for aquatic resource evaluation p 19 A88-28603
- Requirements and principles for the implementation and construction of large-scale geographic information systems p 19 A88-28684
- GEOGRAPHY**
- Landsat determined geographic change p 27 A88-29489
- Space applications in geography p 22 A88-16104

- GEOIDS**
- Potential applications of digital image analysis systems for displaying satellite altimetry data p 31 A88-23762
- An investigation of small-offset fracture zone geoid waveforms p 22 A88-27465
- Five-diagonal weighting scheme for geoidal profiles [AD-A188033] p 23 A88-18054
- GEOLOGICAL FAULTS**
- Space photographs of the Onega-Ladoga isthmus and prediction of useful minerals p 28 A88-16108
- Use of space photographs for paleoseismogeological studies (on the example of Mongolian Altay) p 28 A88-16110
- GEOLOGICAL SURVEYS**
- Detection of subsurface geologic structures in the Tharthar area of central Iraq using Landsat images p 24 A88-20902
- Geologic applications of side-looking airborne radar images in the Appalachian Valley and Ridge Province p 24 A88-21034
- Application of data from the U.S. Geological Survey's side-looking airborne radar program p 25 A88-21036
- Contribution of SPOT images to the geological mapping of arid countries - Example of the Yemen Arab Republic p 25 A88-22616
- Geological and vegetational applications of Shuttle Imaging Radar-B, Mineral County, Nevada p 26 A88-26337
- Comparison of Landsat MSS and SIR-A data for geological applications in Pakistan p 27 A88-29281
- The use of Meteor-Priroda space photographs for the compilation of small-scale and medium-scale tectonic and geological maps p 27 A88-30079
- Space photographs of the Onega-Ladoga isthmus and prediction of useful minerals p 28 A88-16108
- International role of US geoscience [NASA-CR-182407] p 28 A88-16281
- GEOLOGY**
- Geobotanical detection of linear features in the Silver Mine area of southeastern Missouri p 25 A88-21043
- Problems in geologic and geomorphic interpretation and geometric modeling of radar images using a digital terrain model p 26 A88-28024
- Geological evolution and analysis of confirmed or suspected gas hydrate localities. Volume 10: Basin analysis, formation and stability of gas hydrates of the Aleutian Trench and the Bering Sea [DE88-001008] p 29 A88-18048
- GEOMAGNETISM**
- Remanent magnetization of the oceanic upper mantle p 37 A88-27036
- Proceedings of an ESA-NASA Workshop on a Joint Solid Earth Program [NASA-CR-182642] p 23 A88-19844
- Spaceborne magnetometry p 24 A88-19846
- Terrestrial gravity data and comparisons with satellite data p 24 A88-19848
- Gradiometer mission spectral analysis and simulation studies: Past and future p 24 A88-19851
- GEOMETRIC ACCURACY**
- Geometric accuracy testing of orbital radar imagery p 57 A88-23760
- Assessment of SIR-B for topographic mapping p 57 A88-23761
- Evaluation of the stereoscopic accuracy of the SPOT satellite p 59 A88-28605
- GEOMETRIC RECTIFICATION (IMAGERY)**
- Comparison of the gridded finite element and the polynomial interpolations for geometric rectification and mosaicking of Landsat data p 55 A88-21049
- Registration of images with geometric distortions p 58 A88-24936
- GEOMORPHOLOGY**
- Detection of subsurface geologic structures in the Tharthar area of central Iraq using Landsat images p 24 A88-20902
- Techniques of geomorphological mapping on the basis of space photographs p 26 A88-26708
- Problems in geologic and geomorphic interpretation and geometric modeling of radar images using a digital terrain model p 26 A88-28024
- Landsat determined geographic change p 27 A88-29489
- Detection and identification of Arctic landforms - An assessment of remotely sensed data p 40 A88-29492
- Use of space photographs for geomorphological studies in southwestern Tajikistan p 28 A88-16109
- Use of space photographs for paleoseismogeological studies (on the example of Mongolian Altay) p 28 A88-16110
- Geological evolution and analysis of confirmed or suspected gas hydrate localities. Volume 10: Basin analysis, formation and stability of gas hydrates of the Aleutian Trench and the Bering Sea [DE88-001008] p 29 A88-18048

- Geological evolution and analysis of confirmed or suspected gas hydrate localities. Volume 9: Formation and stability of gas hydrates of the Middle America Trench [DE88-001007] p 29 N88-18050
- GEOPHYSICS**
Proposed uses of ERS-1 p 68 A88-27833
Looking at the earth from space p 69 A88-29235
Three-dimensional transient electromagnetic modeling for exploration geophysics p 29 N88-18047
Proceedings of an ESA-NASA Workshop on a Joint Solid Earth Program [NASA-CR-182642] p 23 N88-19844
- GEOPOTENTIAL**
The downward continuation of aerial gravimetric data without density hypothesis p 21 A88-26347
- GEOPOTENTIAL HEIGHT**
New possibilities for using gravity data in developing geodetic coordinate systems p 23 N88-16116
- GEOSAT SATELLITES**
Geosat altimeter observations of Kelvin waves and the 1986-87 El Nino p 32 A88-24582
Geosat crossover analysis in the tropical Pacific. Part 1: Constrained sinusoidal crossover adjustment [NASA-CR-182391] p 43 N88-15285
- GEOSTROPHIC WIND**
The baroclinic circulation in Hudson Strait p 32 A88-24457
- GEOTEMPERATURE**
Importance of a remote measurement of spectral thermal infrared emissivities - Presentation and validation of such a determination p 67 A88-27813
A global survey of surface climate parameters from satellite observations - Preliminary results over Africa p 67 A88-27814
- GEO THERMAL ANOMALIES**
Engima of a thermal anomaly - A TM/AVHRR study of the volcanic Arabian highlands p 25 A88-21045
- GLACIAL DRIFT**
Observation of sea-ice dynamics using synthetic aperture radar images: Automated analysis p 32 A88-24934
The unsteady ground heat flow at the contact surface between a glacier run and the subsoil p 53 N88-16147
- GLACIERS**
Multitemporal Landsat multispectral scanner and Thematic Mapper data of the Hubbard Glacier region, southeast Alaska p 52 A88-29493
Energy balance and discharge of an Alpine glacier, illustrated by Mount Vernagferner in the Oetzal Alps, Tyrol p 53 N88-16145
Vertical sounding of the air layer close to a glacier on Mount Vernagferner in the Oetzal Alps, Tyrol (experiment LUZIVER 1983) p 44 N88-16152
- GLACIOLOGY**
Mantle rheology and satellite signatures from present-day glacial forcings p 21 A88-25225
NASA Oceanic Processes Program [NASA-TM-4025] p 48 N88-18109
- GLOBAL POSITIONING SYSTEM**
GPS survey techniques for deformation analysis p 21 A88-21057
Geodetic application of the Global Positioning System p 21 A88-24289
Surveying with GPS in Australia p 71 N88-18986
Application of the Global Positioning System (GPS) time receivers to the fundamental station Wettzell p 71 N88-18995
- GRASSES**
Quantification of biomass of the marsh grass *Spartina alterniflora* Loisel using Landsat Thematic Mapper imagery p 6 A88-23765
- GRASSLANDS**
Difficulties and recommendations for obtaining very large scale 70 mm aerial photography for rangeland monitoring p 1 A88-21017
Preliminary SPOT results in Lorraine related to permanent grasslands p 5 A88-22617
The first ISLSCP field experiment (FIFE) -- International Satellite Land Surface Climatology Project p 67 A88-27497
Spectral and botanical classification of grasslands - Auxois example p 8 A88-27805
Radiometric leaf area index p 14 A88-32662
- GRAVIMETRY**
The downward continuation of aerial gravimetric data without density hypothesis p 21 A88-26347
Gravity field mapping from satellite altimetry, sea-gravimetry and bathymetry in the Eastern Mediterranean p 42 A88-30836
- GRAVITATIONAL FIELDS**
Gravity field mapping from satellite altimetry, sea-gravimetry and bathymetry in the Eastern Mediterranean p 42 A88-30836
New possibilities for using gravity data in developing geodetic coordinate systems p 23 N88-16116
- GRAVITY GRADIOMETERS**
Spaceborne gravity gradiometry characterizing the data type p 24 N88-19847
- GRAVITY WAVES**
Wind-fetch dependence of Seasat scatterometer measurements p 31 A88-23546
- GREENHOUSE EFFECT**
Absolute infrared intensities for F-113 and F-114 and an assessment of their greenhouse warming potential relative to other chlorofluorocarbons p 19 A88-31103
- GROUND BASED CONTROL**
Evaluation of the stereoscopic accuracy of the SPOT satellite p 59 A88-28605
- GROUND STATIONS**
The Earthnet Heat Capacity Mapping Mission (HCMM) data-processing system at Lannion (France) p 62 N88-16761
Application of the Global Positioning System (GPS) time receivers to the fundamental station Wettzell p 71 N88-18995
Crustal Dynamics Project: Catalogue of site information [NASA-RP-1196] p 23 N88-19037
- GROUND TRUTH**
Techniques of ground-truth measurements of desert-scrub structure p 9 A88-27817
From pattern to process: The strategy of the Earth Observing System: Volume 2: EOS Science Steering Committee report [NASA-TM-89702] p 70 N88-15283
- GROUND WATER**
Groundwater identification using digitally enhanced NMAP -- national high altitude photography p 51 A88-21011
Spectral enhancements of Landsat MSS and TM imagery applied to ground water investigations in Kenya p 51 A88-21042
- GULF STREAM**
Shelf water entrainment by Gulf Stream warm-core rings p 36 A88-27013
- H**
- HALOGENS**
On the problem of evolution of oceanic water composition in the Phanerozoic p 35 A88-26676
- HAWAII**
North Pacific Ocean. Central Pacific Transition Zone, R/V Thomas G. Thompson: 25 March - 3 May 1968. STD data report [AD-A186570] p 47 N88-17160
- HAZE**
Biomass-burning emissions and associated haze layers over Amazonia p 18 A88-27265
Atmospheric effect on spectral signature - Measurements p 58 A88-27822
- HEAT BUDGET**
A heat budget for the northern California shelf during CODE 2 p 34 A88-25733
The ocean heat budget [AD-A186130] p 44 N88-15346
- HEAT CAPACITY MAPPING MISSION**
The Earthnet Heat Capacity Mapping Mission (HCMM) data-processing system at Lannion (France) p 62 N88-16761
- HELICOPTERS**
The use of a helicopter mounted ranging scatterometer for estimation of extinction and backscattering properties of forest canopies-I: Experimental approach and calibration p 11 A88-28682
The use of a helicopter mounted ranging scatterometer for estimation of extinction and scattering properties of forest canopies-II: Experimental results for high-density aspen p 11 A88-28683
- HELIUM-NEON LASERS**
Laser system for automating topographic terrain survey p 70 N88-16136
- HIGH RESOLUTION**
The acquisition of SPOT-1 HRV imagery over southern Britain and northern France, May 1986-May 1987 p 60 A88-29286
General determination of Earth surface type and cloud amount using multispectral AVHRR data [NOAA-TR-NESDIS-39] p 72 N88-18997
- HIGH TEMPERATURE GASES**
Evaluation of a temperature remote sensing technique [AD-A187885] p 71 N88-18053
- HONDURAS**
Large-scale hurricane hazard mapping along the coastal plain of Honduras using Landsat data p 17 A88-21041
- HUDSON BAY (CANADA)**
The baroclinic circulation in Hudson Strait p 32 A88-24457
- HUMIDITY**
Sea surface temperature, low-level moisture, and convection in the tropical Pacific, 1982-1985 p 34 A88-25729
- HURRICANES**
Large-scale hurricane hazard mapping along the coastal plain of Honduras using Landsat data p 17 A88-21041
- HYDRATES**
Geological evolution and analysis of confirmed or suspected gas hydrate localities. Volume 9: Formation and stability of gas hydrates of the Middle America Trench [DE88-001007] p 29 N88-18050
- HYDROGEOLOGY**
Remote sensing applications by consulting engineers - Three case histories p 24 A88-21009
Landsat classification of the barren hydrothermal areas of Lake Yli-Kitka, north-eastern Finland p 51 A88-24198
Multitemporal Landsat multispectral scanner and Thematic Mapper data of the Hubbard Glacier region, southeast Alaska p 52 A88-29493
- HYDROGRAPHY**
The Natal pulse - An extreme transient on the Agulhas Current p 38 A88-27494
North Pacific Ocean. Central Pacific Transition Zone, R/V Thomas G. Thompson: 25 March - 3 May 1968. STD data report [AD-A186570] p 47 N88-17160
Hydrographic and current measurements in the North-East Atlantic Ocean. Data report on F.S. Meteor cruises 69/5 and 69/6, October to November 1984 [REPT-166] p 48 N88-17164
- HYDROLOGICAL CYCLE**
Remote sensing of soil moisture p 52 A88-27815
Report of the Workshop on Space Systems Possibilities for a Global Energy and Water Cycle Experiment [WCP-137] p 53 N88-17147
- HYDROLOGY**
Complex remote monitoring of lakes -- Russian book p 52 A88-27741
Comprehensive studies of the dynamics of geosystems with the use of remote sensing techniques p 10 A88-27821
Evaluation of the flooding areas of the Sao Goncalo Canal through LANDSAT 5 thematic mapper images [INPE-4118-PRE/1039] p 53 N88-16185
- HYDROLOGY MODELS**
The use of remote sensing in developing and validating a ground hydrology/vegetation model for GCM3 -- general circulation models p 51 A88-21021
Determination of vegetated fraction of surface from satellite measurements p 8 A88-27807
Use of the thermodynamic evaporation formula of Hoffmann in energy balance models for flowing water p 52 N88-16143
- HYDROMETEOROLOGY**
Monitoring hydroclimatic characteristics using satellite observations from West Africa p 52 A88-27816
- HYDROTHERMAL SYSTEMS**
Identification and spectral characteristics of hydrothermal alteration on Landsat TM imagery of north Chile p 27 A88-31125
- I**
- ICE**
Effect of ice-grain size distribution on the thermal emission of snow cover p 52 A88-24662
- ICE ENVIRONMENTS**
The ice thickness distribution across the Atlantic sector of the Antarctic Ocean in midwinter p 34 A88-25734
Quantitative use of satellite SAR imagery of sea ice p 39 A88-27839
- ICE FLOES**
A snapshot of the Labrador current inferred from ice-floe movement in NOAA satellite imagery p 32 A88-24456
The ice thickness distribution across the Atlantic sector of the Antarctic Ocean in midwinter p 34 A88-25734
Multiyear sea ice floe distribution in the Canadian Arctic Ocean p 35 A88-25738
- ICE MAPPING**
Computer-aided mapping of Antarctic Sea ice using along-the-course radiometric measurements aboard the Cosmos-1500 satellite p 38 A88-27213
- ICE REPORTING**
Multiyear sea ice floe distribution in the Canadian Arctic Ocean p 35 A88-25738
Satellite passive microwave studies of the Sea of Okhotsk ice cover and its relation to oceanic processes, 1978-1982 p 36 A88-27014
Investigating the northern Caspian Sea ice regime from meteorological-satellite data p 37 A88-27202
Microwave remote sensing of ice in Lake Melville and the Labrador Sea p 39 A88-28850

Ice floe collisions and their relation to ice deformation in the Bering Sea during February 1983 p 40 A88-29324

ILLINOIS

A satellite image mosaic of Illinois p 55 A88-21047

ILLUMINANCE

Monte Carlo method calculation of spectral brightness coefficient of vegetation cover as function of illumination conditions p 14 N88-16113

IMAGE ANALYSIS

Remote sensing applications by consulting engineers - Three case histories p 24 A88-21009

Principal component analysis of aerial video imagery p 54 A88-21030

Image based SAR product simulation for analysis p 55 A88-21037

Geobotanical detection of linear features in the Silver Mine area of southeastern Missouri p 25 A88-21043

Automated road network extraction from Landsat TM imagery p 18 A88-21044

An expert system for the computer-assisted analysis of radar imagery p 55 A88-21053

American Society for Photogrammetry and Remote Sensing and ACSM, Annual Convention, Baltimore, MD, Mar. 29-Apr. 3, 1987, Technical Papers, Volume 6 - Image data processing p 55 A88-21062

A proposed semi-supervised two stage classification technique p 56 A88-21063

A semi-automated training sample selector for multispectral land cover classification p 56 A88-21066

A comparison of the hierarchical cluster and homogeneous training field detection methods in classifying urban landcovers from TM data p 56 A88-21067

The use of automated computer vision techniques for the recognition of features on radar imagery p 56 A88-21069

Application of frequency filtering in remotely sensed imagery p 57 A88-21072

Landsat remote sensing imagery analysis program p 57 A88-21075

Potential applications of digital image analysis systems for displaying satellite altimetry data p 31 A88-23762

Evaluation of several classification schemes for mapping forest cover types in Michigan p 10 A88-28012

Identification and measurement of the areal extent of settlements from Landsat - An exploration into the Nigerian case p 19 A88-28014

Comparison of submarine relief features on a radar satellite image and on a Skylab satellite photograph p 40 A88-29279

Comparison of Landsat MSS and SIR-A data for geological applications in Pakistan p 27 A88-29281

Shuttle imaging radar A analysis of land use in Amazonia p 12 A88-29282

An improved method for detecting clear sky and cloudy radiances from AVHRR data p 69 A88-29284

The use of successive clustering to analyze multispectral imagery p 61 A88-30086

Space photographs of the Onega-Ladoga isthmus and prediction of useful minerals p 28 N88-16108

Study of relief of ore regions using space images (on the example of Eastern Yakutia) p 28 N88-16111

Thematic mapper research in the earth sciences: Small scale patches of suspended matter and phytoplankton in the Elbe River Estuary, German Bight and Tidal Flats [NASA-CR-182378] p 45 N88-16180

Textural features for image classification in remote sensing [INPE-4169-PRE/1066] p 62 N88-16181

Nature and origin of mineral coatings on volcanic rocks of the Black Mountain, Stonewall Mountain, and Kane Springs Wash volcanic centers, Southern Nevada [NASA-CR-181437] p 29 N88-17140

IMAGE ENHANCEMENT

Results of testing digital image measurements and enhancements on the remote work processing facility p 56 A88-21064

Refining image segmentation by polygon skeletonization p 56 A88-21068

IMAGE FILTERS

Application of frequency filtering in remotely sensed imagery p 57 A88-21072

Photographic filters [INPE-4448-RPE/558] p 64 N88-20124

IMAGE PROCESSING

Groundwater identification using digitally enhanced NHAP --- national high altitude photography p 51 A88-21011

Development of a 32-bit UNIX-based ELAS workstation p 54 A88-21025

Implementation of the Land Analysis System on a workstation p 54 A88-21026

Comparison of the gridded finite element and the polynomial interpolations for geometric rectification and mosaicking of Landsat data p 55 A88-21049

Methods and accuracy of operational digital image mapping with aircraft SAR p 55 A88-21059

An automated system for terrain database construction p 18 A88-21060

Results of testing digital image measurements and enhancements on the remote work processing facility p 56 A88-21064

Matching of dissimilar radar images using Marr-Hildreth zero crossings p 56 A88-21070

Land cover change detection using a GIS-guided, feature-based classification of Landsat thematic mapper data --- Geographic Information System p 18 A88-21073

The application of perceptual color spaces to the display of remotely sensed imagery p 58 A88-24935

Registration of images with geometric distortions p 58 A88-24936

On the accuracy of marine gravity measurements p 21 A88-25224

Digital stereo processing of satellite image data p 58 A88-27825

Speckle in SAR images - An evaluation of filtering techniques p 59 A88-27834

The potential for automated mapping from Geocoded digital image data p 59 A88-28604

Texture study of Synthetic Aperture Radar (SAR) images of ocean surfaces p 42 N88-15101

[AD-A186021] Model-based building verification in aerial photographs [AD-A186010] p 20 N88-15278

Optimization of photogrammetric image adjustment [SER-C-323] p 22 N88-15289

Theory and research on the disjunction of cross passage errors and systematic image errors in photogrammetric point determination p 61 N88-15290

[SER-C-324] Textural features for image classification in remote sensing [INPE-4169-PRE/1066] p 62 N88-16181

Evaluation of the flooding areas of the Sao Goncalo Canal through LANDSAT 5 thematic mapper images [INPE-4118-PRE/1039] p 53 N88-16185

Earthnet's experience with Seasat SAR image processing p 62 N88-16760

The Earthnet Heat Capacity Mapping Mission (HCMM) data-processing system at Lannion (France) p 62 N88-16761

Nature and origin of mineral coatings on volcanic rocks of the Black Mountain, Stonewall Mountain, and Kane Springs Wash volcanic centers, Southern Nevada [NASA-CR-181437] p 29 N88-17140

Meteorological Information Extraction Center (MIEC) processing --- Meteosat imagery [ESA-STR-224] p 71 N88-17143

Sea surface current estimates off central California as derived from enhanced AVHRR (Advanced Very High Resolution Radiometer) infrared images [AD-A186867] p 47 N88-17155

A smart, mapping, charting and geodesy control generator, phase 1 [AD-A188184] p 23 N88-18055

Autocorrelation of control points on 11-band multispectral imagery [AD-A188185] p 62 N88-18056

Three-dimensional image generation from an aerial photograph [AD-A188039] p 63 N88-18979

Report on phase 1 of the project estimate development of a model for yield estimation of sugar cane based on LANDSAT and agromet data [INPE-4466-RPE/560] p 16 N88-19807

Automatic knowledge acquisition for aerial image interpretation [AD-A188616] p 63 N88-19810

IMAGE RESOLUTION Interrelationships between spatial resolution and per-pixel classifiers for extracting information classes. I - The urban environment. II - The natural environment p 17 A88-21014

Matching of dissimilar radar images using Marr-Hildreth zero crossings p 56 A88-21070

IMAGERY Theory and research on the disjunction of cross passage errors and systematic image errors in photogrammetric point determination [SER-C-324] p 61 N88-15290

Autocorrelation of control points on 11-band multispectral imagery [AD-A188185] p 62 N88-18056

Three-dimensional image generation from an aerial photograph [AD-A188039] p 63 N88-18979

IMAGING SPECTROMETERS

Discriminating semiarid vegetation using airborne imaging spectrometer data - A preliminary assessment p 4 A88-21359

Terrestrial imaging spectroscopy p 69 A88-28266

Use of airborne imaging spectrometer data to map minerals associated with hydrothermally altered rocks in the Northern Grapevine Mountains, Nevada, and California p 26 A88-28267

Discrimination of hydrothermal alteration mineral assemblages at Virginia City, Nevada, using the airborne imaging spectrometer p 27 A88-28268

Comparison of techniques for discriminating hydrothermal alteration minerals with Airborne Imaging Spectrometer data p 27 A88-28269

Remote sensing of forest canopy and leaf biochemical contents p 11 A88-28270

Comparison of in situ and airborne spectral measurements of the blue shift associated with forest decline p 11 A88-28271

Preliminary assessment of airborne imaging spectrometer and airborne thematic mapper data acquired for forest decline areas in the Federal Republic of Germany p 11 A88-28272

Exploration of crustal/mantle material for the earth and moon using reflectance spectroscopy p 27 A88-28273

HIRIS (High-Resolution Imaging Spectrometer: Science opportunities for the 1990s. Earth observing system. Volume 2C: Instrument panel report [NASA-TM-89703] p 70 N88-15282

IMAGING TECHNIQUES

Single-source three-dimensional imaging system for remote sensing p 66 A88-23772

Textural features for image classification in remote sensing [INPE-4169-PRE/1066] p 62 N88-16181

Multisource context classification methods in remote sensing p 63 N88-18985

Photographic filters [INPE-4448-RPE/558] p 64 N88-20124

IMPACT DAMAGE

Talemzane - Algerian impact crater detected on SIR-A orbital imaging radar p 25 A88-25217

INDIAN OCEAN

The Natal pulse - An extreme transient on the Agulhas Current p 38 A88-27494

Marine boundary layer modification across the edge of the Agulhas Current p 38 A88-27495

Oceanographic features of the east and southeast Indian Ocean for June 1983 [AD-A186948] p 47 N88-17158

INDUSTRIAL MANAGEMENT

A remote sensing based methodology for quantifying the spatial and functional relationships amongst industrial land uses delineated around the port of Baltimore p 17 A88-21012

INFORMATION RETRIEVAL

The ARSUP database and its access through the CMCIRS catalog - Making available to the public digital maps from the ARSUP process --- Computerized Map Cataloging and Information Retrieval System p 60 A88-29496

User's guide to a data base of current environmental monitoring projects in the US-Canadian transboundary region [DE88-002476] p 20 N88-17119

INFORMATION SYSTEMS

Critical issues in NASA information systems [NASA-CR-182380] p 72 N88-16577

INFRARED IMAGERY

Mid-infrared (1.45 to 2.0 microns) video - A potential aid in wildfire mop-up operations p 1 A88-21016

A snapshot of the Labrador current inferred from ice-floe movement in NOAA satellite imagery p 32 A88-24456

Correlation between aircraft MSS and lidar remotely sensed data on a forested wetland p 6 A88-24513

Satellite observations of a western boundary current in the Bay of Bengal p 36 A88-27010

Processing and analysis of large volumes of satellite-derived thermal infrared data --- for physical oceanographic studies p 36 A88-27012

Atmospheric correction of thermal infrared images p 40 A88-29283

Commercial applications and scientific research requirements for thermal-infrared observations of terrestrial surfaces [NASA-TM-89704] p 70 N88-16179

Sea surface current estimates off central California as derived from enhanced AVHRR (Advanced Very High Resolution Radiometer) infrared images [AD-A186867] p 47 N88-17155

INFRARED PHOTOGRAPHY

Groundwater identification using digitally enhanced NHAP --- national high altitude photography p 51 A88-21011

INFRARED PHOTOMETRY

- Remote sensing of aquatic macrophyte distribution in selected South Carolina reservoirs p 51 A88-21007

INFRARED RADIATION

- The emissivity of the vegetation-soil system p 8 A88-27208

INFRARED RADIOMETERS

- Engima of a thermal anomaly - A TM/AVHRR study of the volcanic Arabian highlands p 25 A88-21045
- Monitoring of global vegetation dynamics for assessment of primary productivity using NOAA advanced very high resolution radiometer p 9 A88-27808
- Determining the rate of forest conversion in Mato Grosso, Brazil, using Landsat MSS and AVHRR data p 10 A88-28011
- An improved method for detecting clear sky and cloudy radiances from AVHRR data p 69 A88-29284
- Simulation of solar zenith angle effect on global vegetation index (GVI) data p 14 A88-32660
- An integrated camera and radiometer for aerial monitoring of vegetation p 14 A88-32666

INFRARED REFLECTION

- Exploring the relationships between leaf nitrogen content, biomass and the near-infrared/red reflectance ratio p 12 A88-29288

INFRARED WINDOWS

- Emissivity of pure and sea waters for the model sea surface in the infrared window regions p 42 A88-30445

INLAND WATERS

- Research in Switzerland on ocean and inland-water colour monitoring p 46 A88-16301

INORGANIC SULFIDES

- Features of hydrological anomalies in connection with the search for deep-water polymetallic sulfides p 32 A88-24654

INTERNAL WAVES

- Variations in the intensity of emitted and scattered microwave radiation of the sea surface sensed at grazing angles in a field of surface manifestations of internal waves p 37 A88-27205
- Detection of internal waves using data from satellite microwave radiometry and the research ship Academician Alexandr Nesmelanov p 41 A88-30083

INTERNATIONAL COOPERATION

- International role of US geoscience [NASA-CR-182407] p 28 A88-16281
- System-wide medium-term environment programme for the period 1990-1995: Strategies of the United Nations system for the environment [UNEP/GCSS.I/2] p 20 A88-19826

INTERPOLATION

- Comparison of the gridded finite element and the polynomial interpolations for geometric rectification and mosaicking of Landsat data p 55 A88-21049

INTERTROPICAL CONVERGENT ZONES

- The relationship between the temporal variability of ocean temperature and the meridional shifts of the intertropical convergence zone p 37 A88-27203

INVENTORIES

- Investigations on the application of space photographs (Spacelab metric camera) for routine inventories of extensively managed forest areas [DFVLR-FB-87-22] p 15 A88-17098

INVERSIONS

- Improved canopy reflectance modeling and scene inference through improved understanding of scene pattern [NASA-CR-182488] p 15 A88-18049

INVERTEBRATES

- Five New South Wales barrier lagoons: Their macrobenthic fauna and seagrass communities p 49 A88-19059

IRRADIANCE

- On the parameterization of irradiance for open ocean photoprocesses p 34 A88-25737
- Downward longwave irradiance at the ocean surface from satellite data - Methodology and in situ validation p 38 A88-27493

ITALY

- Italian activities in ocean colour remote sensing p 46 A88-16304

JAPANESE SPACECRAFT

- Preliminary assessment of radiometric accuracies for MOS-1 sensors p 39 A88-29276

K**KARST**

- Karst and erosion topography on space photographs (With reference to the Ustiurt plateau) p 60 A88-30080

KNOWLEDGE

- Automatic knowledge acquisition for aerial image interpretation [AD-A188616] p 63 A88-19810

L**LAGOONS**

- Five New South Wales barrier lagoons: Their macrobenthic fauna and seagrass communities p 49 A88-19059

LAKES

- Gas exchange on Mono Lake and Crowley Lake, California p 52 A88-25735
- Complex remote monitoring of lakes --- Russian book p 52 A88-27741

LAND

- Problems related to the determination of land surface parameters and fluxes over heterogeneous media from satellite data p 19 A88-27803
- The role of anisotropy in the long range reconnaissance of the albedo of land surfaces p 62 A88-16169
- The anisotropy of reflected solar radiation over several types of land surface p 62 A88-16171

LAND USE

- A remote sensing based methodology for quantifying the spatial and functional relationships amongst industrial land uses delineated around the port of Baltimore p 17 A88-21012
- A comparison of the hierarchical cluster and homogeneous training field detection methods in classifying urban landcovers from TM data p 56 A88-21067
- Refining image segmentation by polygon skeletonization p 56 A88-21068
- A global survey of surface climate parameters from satellite observations - Preliminary results over Africa p 67 A88-27814
- Analyzing long-term changes in vegetation with geographic information system and remotely sensed data p 10 A88-27820
- Comprehensive studies of the dynamics of geosystems with the use of remote sensing techniques p 10 A88-27821
- Identification and measurement of the areal extent of settlements from Landsat - An exploration into the Nigerian case p 19 A88-28014
- Land-cover monitoring with SPOT for landfill investigations p 19 A88-28606
- Shuttle imaging radar A analysis of land use in Amazonia p 12 A88-29282
- Design and implementation of a data base system for Digital Land Mass System (DLMS) data [FEL-IR-1987-19] p 71 A88-17101

LANDFORMS

- Detection and identification of Arctic landforms - An assessment of remotely sensed data p 40 A88-29492
- The digital landmass simulation production overview [AD-A187978] p 62 A88-18978

LANDSAT SATELLITES

- Operational revision of national topographic maps in Canada using Landsat images p 54 A88-20901
- Detection of subsurface geologic structures in the Tharthar area of central Iraq using Landsat images p 24 A88-20902
- Development of multirate estuarine water quality models using Landsat 2 and 4 MSS data p 50 A88-21002
- Comparison of Landsat MSS pixel array sizes for estimating water quality variables in small lakes p 50 A88-21004
- Monitoring North Carolina's nutrient-sensitive reservoirs using Landsat TM digital data p 50 A88-21006
- Estimating forest productivity in southern Illinois using Landsat Thematic Mapper data and geographic information system analysis techniques p 2 A88-21028
- The use of digital Landsat data for wildlife management on the Warm Springs Indian Reservation of Oregon p 2 A88-21029
- A time-lapse analysis of the Mississippi Delta using Landsat MSS Band 4 (IR2) photographic imagery p 51 A88-21039
- Evaluation of Thematic Mapper data for mapping tidal wetlands in South Carolina p 2 A88-21040
- Large-scale hurricane hazard mapping along the coastal plain of Honduras using Landsat data p 17 A88-21041

- Spectral enhancements of Landsat MSS and TM imagery applied to ground water investigations in Kenya p 51 A88-21042

- Detection of yearly cover change with Landsat MSS on pastoral landscapes in central Australia p 4 A88-21362

- Quantification of biomass of the marsh grass *Spartina alterniflora* Loisel using Landsat Thematic Mapper imagery p 6 A88-23765

- Integrating sphere transmissometer for field measurement of leaf transmittance p 6 A88-23766

- Using remotely sensed data for census surveys and population estimation in developing countries - Examples from Nigeria p 18 A88-24511

- Remote sensing of forest cover distribution in the Phu Wiang watershed area of Khon Kaen Province, Northeast of Thailand p 6 A88-24514

- Registration of images with geometric distortions p 58 A88-24936

- A transformation for ordering multispectral data in terms of image quality with implications for noise removal p 58 A88-24937

- Operational interpretation of AVHRR vegetation indices for world crop information p 7 A88-26335

- A new strategy for vegetation mapping with the aid of Landsat MSS data p 9 A88-27810

- Landsat imagery for mapping saline soils and wet lands in north-west India p 12 A88-29278

- Landsat determined geographic change p 27 A88-29489

- Intermediate-scale vegetation mapping of Innoko National Wildlife Refuge, Alaska using Landsat MSS digital data p 12 A88-29494

- Large area crop classification in New South Wales, Australia, using Landsat data p 14 A88-32665

- LANDSAT thematic mapper radiometric calibration study [NASA-CR-182410] p 61 A88-15287

- Space-based remote sensing of the Earth: A report to the Congress [NASA-TM-89709] p 72 A88-18046

- Thematic mapper study of Alaskan ophiolites [NASA-CR-182554] p 30 A88-18984

LASER APPLICATIONS

- Laser system for automating topographic terrain survey p 70 A88-16136
- Evaluation of a temperature remote sensing technique [AD-A187885] p 71 A88-18053

LASER INDUCED FLUORESCENCE

- The use of chlorophyll fluorescence measurements from space for separating constituents of sea water. Volume 1: Summary [ESA-CR(P)-2444-VOL-1] p 43 A88-15294
- The use of chlorophyll fluorescence measurements from space for separating constituents of sea water. Volume 2: Appendices [ESA-CR(P)-2444-VOL-2] p 44 A88-15295

LASER OUTPUTS

- Evaluation of a temperature remote sensing technique [AD-A187885] p 71 A88-18053

LEAF AREA INDEX

- Exploring the relationships between leaf nitrogen content, biomass and the near-infrared/red reflectance ratio p 12 A88-29288
- Radiometric leaf area index p 14 A88-32662
- Evaluation of middle and thermal infrared radiance in indices used to estimate GLAI p 14 A88-32663
- Crop canopy spectral reflectance p 14 A88-32664

LEAVES

- Canopy reflectance of seven rangeland plant species with variable leaf pubescence p 5 A88-23764
- Integrating sphere transmissometer for field measurement of leaf transmittance p 6 A88-23766
- Spectral changes in conifers subjected to air pollution and water stress: Experimental studies p 6 A88-24932

- Polarized and non-polarized leaf reflectances of *Coleus blumei* p 7 A88-26624

LIGHT SCATTERING

- Monte Carlo method calculation of spectral brightness coefficient of vegetation cover as function of illumination conditions p 14 A88-16113

LIGHT TRANSMISSION

- Remote sensing of atmospheric optical thickness and sea-water attenuation when submerged: Wavelength selection and anticipated errors [AD-A187609] p 49 A88-19262

LITHOLOGY

- Nature and origin of mineral coatings on volcanic rocks of the Black Mountain, Stonewall Mountain, and Kane Springs Wash volcanic centers, Southern Nevada [NASA-CR-181437] p 29 A88-17140

J

- Geological evolution and analysis of confirmed or suspected gas hydrate localities. Volume 10: Basin analysis, formation and stability of gas hydrates of the Aleutian Trench and the Bering Sea [DE88-001008] p 29 N88-18048
- Geological evolution and analysis of confirmed or suspected gas hydrate localities. Volume 9: Formation and stability of gas hydrates of the Middle America Trench [DE88-001007] p 29 N88-18050

LITHOSPHERE

- Thematic mapper study of Alaskan ophiolites [NASA-CR-182554] p 30 N88-18984

LITTORAL TRANSPORT

- Nearshore wave transformation study of sites near Port Canaveral Inlet, Florida [AD-A186965] p 47 N88-17159

LUNAR GEOLOGY

- Exploration of crustal/mantle material for the earth and moon using reflectance spectroscopy p 27 A88-28273

M**MAGNETIC ANOMALIES**

- Evolution of the Juan Fernandez microplate during the last three million years p 25 A88-25045

MAGNETIC MEASUREMENT

- Spaceborne magnetometry p 24 N88-19846
- Terrestrial gravity data and comparisons with satellite data p 24 N88-19848

MAGNETOMETERS

- Gradiometer mission spectral analysis and simulation studies: Past and future p 24 N88-19851

MAGSAT SATELLITES

- Remanent magnetization of the oceanic upper mantle p 37 A88-27036
- Spaceborne magnetometry p 24 N88-19846

MAN ENVIRONMENT INTERACTIONS

- System-wide medium-term environment programme for the period 1990-1995: Strategies of the United Nations system for the environment [UNEP/GCSS.1/2] p 20 N88-19826

MAN-COMPUTER INTERFACE

- Requirements and principles for the implementation and construction of large-scale geographic information systems p 19 A88-28684

MAPPING

- American Society for Photogrammetry and Remote Sensing and ACSM, Annual Convention, Baltimore, MD, Mar. 29-Apr. 3, 1987, Technical Papers. Volume 4 - Cartography p 21 A88-21058
- Assessment of SIR-B for topographic mapping p 57 A88-23761
- Intermediate-scale vegetation mapping of Innoko National Wildlife Refuge, Alaska using Landsat MSS digital data p 12 A88-29494
- Gravity field mapping from satellite altimetry, sea-gravimetry and bathymetry in the Eastern Mediterranean p 42 A88-30836
- Photogrammetric principles for combining remote sounding and three-dimensional mapping p 61 N88-16135
- Laser system for automating topographic terrain survey p 70 N88-16136
- Construction of airborne radars for remote sensing [PB88-113063] p 71 N88-16916
- A smart, mapping, charting and geodesy control generator, phase 1 [AD-A186184] p 23 N88-18055
- A digital terrain system for microcomputers [INPE-4170-PRE/1067] p 63 N88-18987
- Reports on cartography and geodesy. Series 1, report 98 [ISSN-0469-4236] p 23 N88-18993

MAPS

- Satellite maps of Antarctic total ozone [AIAA PAPER 88-0210] p 30 A88-22154
- A digital terrain system for microcomputers [INPE-4170-PRE/1067] p 63 N88-18987

MARINE BIOLOGY

- Remote sensing of Chesapeake Bay water quality required for healthy oyster beds p 30 A88-21003
- Remote sensing of aquatic macrophyte distribution in selected South Carolina reservoirs p 51 A88-21007
- Remote sensing of ocean colour for studies of biological productivity and biochemical cycles p 45 N88-16296

MARINE CHEMISTRY

- Remote sensing of ocean colour for studies of biological productivity and biochemical cycles p 45 N88-16296
- The use of chlorophyll fluorescence measurements from space for separating constituents of sea water p 47 N88-16307

MARINE ENVIRONMENTS

- On the accuracy of marine gravity measurements p 21 A88-25224

- The ocean heat budget [AD-A186130] p 44 N88-15346

- The effects of atmospheric and thermohaline variability on the validation of the GEOSAT altimeter oceanographic signal between Scotland and Iceland [AD-A189324] p 50 N88-19882

MARINE METEOROLOGY

- Relationships between monthly precipitation and SST variations in the tropical Pacific region p 65 A88-21382

- Airborne measurements of surface layer turbulence over the ocean during cold air outbreaks p 35 A88-26911

- The onset of spring melt in first-year ice regions of the Arctic as determined from scanning multichannel microwave radiometer data for 1979 and 1980 p 37 A88-27016

- A model of the tropical Pacific sea surface temperature climatology p 40 A88-29323

- Measurement of global oceanic winds from Seasat-SMMR and its comparison with Seasat-SASS and ALT derived winds p 40 A88-29766

- The Genesis of Atlantic Lows Experiment - The planetary-boundary-layer subprogram of GALE p 42 A88-31111

- Review of the potential of satellite remote sensing for marine flood protection [IOS-237] p 43 N88-15280

MARINE RESOURCES

- Remote sensing of ocean colour for studies of biological productivity and biochemical cycles p 45 N88-16296

MARITIME SATELLITES

- Preliminary assessment of radiometric accuracies for MOS-1 sensors p 39 A88-29276

MARSHLANDS

- Evaluation of Thematic Mapper data for mapping tidal wetlands in South Carolina p 2 A88-21040
- Quantification of biomass of the marsh grass *Spartina alterniflora* Loisel using Landsat Thematic Mapper imagery p 6 A88-23765

MATCHING

- Matching of dissimilar radar images using Marr-Hildreth zero crossings p 56 A88-21070

MATHEMATICAL MODELS

- Problems in geologic and geomorphic interpretation and geometric modeling of radar images using a digital terrain model p 26 A88-28024
- Forecasting patterns of soil erosion in arid lands from Landsat MSS data p 12 A88-29280

The ocean heat budget

- [AD-A186130] p 44 N88-15346

- Statistical model of interaction of electromagnetic waves with natural objects being sensed p 70 N88-16112
- Statistics of two-dimensional structure elements of mountainous ranges (mosaic model) for calculating three-dimensional reflection functions [DFVLR-FB-87-33] p 29 N88-17099

- Application of satellite data in variational analysis for global cyclonic systems [NASA-CR-182468] p 62 N88-17152

- Multisource context classification methods in remote sensing p 63 N88-18985

- Five New South Wales barrier lagoons: Their macrobenthic fauna and seagrass communities p 49 N88-19059

- Report on phase 1 of the project estimate development of a model for yield estimation of sugar cane based on LANDSAT and agromet data [INPE-4466-RPE/560] p 16 N88-19807

- Mesoscale monitoring of the soil freeze/thaw boundary from orbital microwave radiometry [NASA-CR-182659] p 17 N88-19855

MATRICES (MATHEMATICS)

- Method for joint adjustment of satellite and surface geodetic networks p 22 N88-16105

MEDITERRANEAN SEA

- Satellite-derived color-temperature relationship in the Alboran Sea p 33 A88-25445
- Gravity field mapping from satellite altimetry, sea-gravimetry and bathymetry in the Eastern Mediterranean p 42 A88-30836
- Italian activities in ocean colour remote sensing p 46 N88-16304

MELTING

- Mesoscale monitoring of the soil freeze/thaw boundary from orbital microwave radiometry [NASA-CR-182659] p 17 N88-19855

MERIDIONAL FLOW

- The relationship between the temporal variability of ocean temperature and the meridional shifts of the intertropical convergence zone p 37 A88-27203

MESOSCALE PHENOMENA

- Characteristics of extreme rainfall events in northwestern Peru during the 1982-1983 El Nino period p 52 A88-25730
- Mesoscale coastal ocean dynamics p 49 N88-19060

- National Severe Storms Laboratory, fiscal year 1987 [PB88-140108] p 72 N88-19863

METAL COMPOUNDS

- Features of hydrological anomalies in connection with the search for deep-water polymetallic sulfides p 32 A88-24654

METALLURGY

- The space metal: All about titanium --- Russian book p 25 A88-24781

METEORITE CRATERS

- Talezmaze - Algerian impact crater detected on SIR-A orbital imaging radar p 25 A88-25217

METEOROLOGICAL PARAMETERS

- Observations of surface and atmospheric features from passive microwave satellite measurements p 64 A88-21019

NASA Oceanic Processes Program

- [NASA-TM-4025] p 48 N88-18109

METEOROLOGY

- Application of satellite data in variational analysis for global cyclonic systems [NASA-CR-182468] p 62 N88-17152

METEOSAT SATELLITE

- Estimation of evapotranspiration in the Sahelian zone by use of Meteosat and NOAA AVHRR data p 9 A88-27818

- Simulations of the Meteosat visible sensor response to changing boundary conditions p 67 A88-27823

- Meteorological Information Extraction Center (MIEC) processing --- Meteosat imagery [ESA-STR-224] p 71 N88-17143

METHANE

- Geological evolution and analysis of confirmed or suspected gas hydrate localities. Volume 9: Formation and stability of gas hydrates of the Middle America Trench [DE88-001007] p 29 N88-18050

METRIC PHOTOGRAPHY

- Investigations on the application of space photographs (Spacelab metric camera) for routine inventories of extensively managed forest areas [DFVLR-FB-87-22] p 15 N88-17098

MICROPROCESSORS

- Development of a 32-bit UNIX-based ELAS workstation p 54 A88-21025

MICROWAVE IMAGERY

- Microwave vegetation index - A new long-term global data set for biospheric studies p 14 A88-32658

MICROWAVE RADIOMETERS

- Observations of surface and atmospheric features from passive microwave satellite measurements p 64 A88-21019

- Validating regional differences in modelled satellite microwave signatures p 1 A88-21020

- A multi-frequency-multi-nadir-angle pushbroom-radiometer for oil spill detection and mapping (On the surface of the sea) [MBB-UR-952-87] p 31 A88-23988

- Satellite passive microwave studies of the Sea of Okhotsk ice cover and its relation to oceanic processes, 1978-1982 p 36 A88-27014

- Use of microwave radiometry for measuring the biometric characteristics of vegetation cover p 7 A88-27207

- Estimates of primary productivity over the Thar Desert based upon Nimbus-7 37 GHz data - 1979-1985 p 11 A88-28016

- Relating Nimbus-7 37 GHz data to global land-surface evaporation, primary productivity and the atmospheric CO₂ concentration p 60 A88-29287

- Methods for processing radio-physical measurement data in studies of the environment --- Russian book p 19 A88-29427

- Measurement of global oceanic winds from Seasat-SMMR and its comparison with Seasat-SASS and ALT derived winds p 40 A88-29766

- Principal component analysis of satellite passive microwave data over sea ice p 41 A88-30199

- Estimating surface soil moisture from satellite microwave measurements and a satellite derived vegetation index p 13 A88-30446

- Estimation of atmospheric liquid-water amount by Nimbus 7 SMMR data - A new method and its application to the western North-Pacific region p 69 A88-30731

MICROWAVE SCATTERING

- An approximate model for the microwave brightness temperature of the sea p 31 A88-23544

- Measurements of the backscatter and attenuation properties of forest stands at X-, C- and L-band p 7 A88-25444

- Variations in the intensity of emitted and scattered microwave radiation of the sea surface sensed at grazing angles in a field of surface manifestations of internal waves p 37 A88-27205

- Estimation of biophysical properties of forest canopies using C-band microwave data p 9 A88-27809

- The use of a helicopter mounted ranging scatterometer for estimation of extinction and backscattering properties of forest canopies-I: Experimental approach and calibration p 11 A88-28682
- Applications of microwaves to remote sensing p 69 A88-30670
- Active and passive remote sensing of ice [AD-A186685] p 47 N88-17162
- MICROWAVE SENSORS**
- Wind-fetch dependence of Seasat scatterometer measurements p 31 A88-23546
- Multiband-scatterometer data analysis of forests p 5 A88-23548
- The DUT airborne scatterometer p 5 A88-23549
- Detection of oil films by active and passive microwave sensors p 39 A88-27840
- Estimation of the accuracy of determining atmospheric temperature profiles from microwave remote sensing at frequencies of 117-118.5 Ghz p 41 A88-30084
- MICROWAVES**
- Microwave remote sensing of ice in Lake Melville and the Labrador Sea p 39 A88-28650
- Relative sensitivity of Normalized Difference Vegetation Index (NDVI) and Microwave Polarization Difference Index (MPDI) for vegetation and desertification monitoring p 13 A88-30444
- Construction of airborne radars for remote sensing [PB88-113063] p 71 N88-16916
- MIDDLE ATMOSPHERE**
- Applications of microwaves to remote sensing p 69 A88-30670
- MINERAL DEPOSITS**
- Geobotanical detection of linear features in the Silver Mine area of southeastern Missouri p 25 A88-21043
- Space photographs of the Onega-Ladoga isthmus and prediction of useful minerals p 28 N88-16108
- Study of relief of ore regions using space images (on the example of Eastern Yakutia) p 28 N88-16111
- Character of five selected LANDSAT lineaments in southwestern Pennsylvania: Report of investigations, 1987 [PB88-133517] p 30 N88-18988
- MINERAL EXPLORATION**
- Use of airborne imaging spectrometer data to map minerals associated with hydrothermally altered rocks in the Northern Grapevine Mountains, Nevada, and California p 26 A88-28267
- Discrimination of hydrothermal alteration mineral assemblages at Virginia City, Nevada, using the airborne imaging spectrometer p 27 A88-28268
- Comparison of techniques for discriminating hydrothermal alteration minerals with Airborne Imaging Spectrometer data p 27 A88-28269
- Exploration of crustal/mantle material for the earth and moon using reflectance spectroscopy p 27 A88-28273
- Study of relief of ore regions using space images (on the example of Eastern Yakutia) p 28 N88-16111
- International role of US geoscience [NASA-CR-182407] p 28 N88-16281
- Three-dimensional transient electromagnetic modeling for exploration geophysics p 29 N88-18047
- MINING**
- Character of five selected LANDSAT lineaments in southwestern Pennsylvania: Report of investigations, 1987 [PB88-133517] p 30 N88-18988
- MISSISSIPPI DELTA (LA)**
- A time-lapse analysis of the Mississippi Delta using Landsat MSS Band 4 (IR2) photographic imagery p 51 A88-21039
- MODELS**
- Improved canopy reflectance modeling and scene inference through improved understanding of scene pattern [NASA-CR-182488] p 15 N88-18049
- A digital terrain system for microcomputers [INPE-4170-PRE/1067] p 63 N88-18987
- MOISTURE CONTENT**
- Canopy reflectance of seven rangeland plant species with variable leaf pubescence p 5 A88-23764
- Spectral changes in conifers subjected to air pollution and water stress: Experimental studies p 6 A88-24932
- Relationship between brightness temperature in the RF range and the radiative dryness index p 69 A88-30082
- Estimation of atmospheric liquid-water amount by Nimbus 7 SMMR data - A new method and its application to the western North-Pacific region p 69 A88-30731
- Detection of soil erosion with Thematic Mapper (TM) satellite data within Pinyon-Juniper woodlands [NASA-CR-182476] p 15 N88-17103
- MOISTURE METERS**
- Remote sensing of soil moisture p 52 A88-27815
- MONSOONS**
- Simultaneity of response of Atlantic Ocean tropical cyclones and Indian monsoons p 34 A88-25736
- Assessment of the use of satellite derived winds in monsoon forecasting using a general circulation model p 68 A88-27846
- MONT CARLO METHOD**
- Calculation of canopy bidirectional reflectance using the Monte Carlo method p 13 A88-30439
- MOSAICS**
- A satellite image mosaic of Illinois p 55 A88-21047
- MOUNTAINS**
- Assessing forest damage in high-elevation coniferous forests in Vermont and New Hampshire using Thematic Mapper data p 13 A88-30440
- Thematic mapper study of Alaskan ophiolites [NASA-CR-182554] p 30 N88-18984
- MULTISENSOR APPLICATIONS**
- From pattern to process: The strategy of the Earth Observing System: Volume 2: EOS Science Steering Committee report [NASA-TM-89702] p 70 N88-15283
- MULTISPECTRAL BAND SCANNERS**
- Operational revision of national topographic maps in Canada using Landsat images p 54 A88-20901
- Remote sensing applications - An outlook for the future p 64 A88-20904
- Comparison of Landsat MSS pixel array sizes for estimating water quality variables in small lakes p 50 A88-21004
- Multispectral video survey of a Northern Ontario forest p 1 A88-21015
- The use of digital Landsat data for wildlife management on the Warm Springs Indian Reservation of Oregon p 2 A88-21029
- A time-lapse analysis of the Mississippi Delta using Landsat MSS Band 4 (IR2) photographic imagery p 51 A88-21039
- Spectral enhancements of Landsat MSS and TM imagery applied to ground water investigations in Kenya p 51 A88-21042
- Detecting subpixel woody features using simulated multispectral and panchromatic SPOT imagery p 3 A88-21065
- A semi-automated training sample selector for multispectral land cover classification p 56 A88-21066
- Land cover change detection with Landsat MSS and TM data in the Kitchener-Waterloo area, Canada p 18 A88-21071
- Detection of yearly cover change with Landsat MSS on pastoral landscapes in central Australia p 4 A88-21362
- Spectral assessment of indicators of range degradation in the Botswana hardveld environment p 5 A88-21365
- Using remotely sensed data for census surveys and population estimation in developing countries - Examples from Nigeria p 18 A88-24511
- Correlation between aircraft MSS and lidar remotely sensed data on a forested wetland p 6 A88-24513
- Remote sensing of forest cover distribution in the Phu Wiang watershed area of Khon Kaen Province, Northeast of Thailand p 6 A88-24514
- A transformation for ordering multispectral data in terms of image quality with implications for noise removal p 58 A88-24937
- Operational interpretation of AVHRR vegetation indices for world crop information p 7 A88-26335
- Assessment of thematic mapper imagery for forestry applications under Lake States conditions p 7 A88-26336
- A new strategy for vegetation mapping with the aid of Landsat MSS data p 9 A88-27810
- Preliminary study of the characterization of the riverine forests of the Garonne using Landsat MSS and TM data p 9 A88-27811
- Determining the rate of forest conversion in Mato Grosso, Brazil, using Landsat MSS and AVHRR data p 10 A88-28011
- Evaluation of several classification schemes for mapping forest cover types in Michigan p 10 A88-28012
- Identification and measurement of the areal extent of settlements from Landsat - An exploration into the Nigerian case p 19 A88-28014
- Use of airborne imaging spectrometer data to map minerals associated with hydrothermally altered rocks in the Northern Grapevine Mountains, Nevada, and California p 26 A88-28267
- Aircraft MSS data registration and vegetation classification for wetland change detection p 12 A88-29277
- Forecasting patterns of soil erosion in arid lands from Landsat MSS data p 12 A88-29280
- Comparison of Landsat MSS and SIR-A data for geological applications in Pakistan p 27 A88-29281
- Multitemporal Landsat multispectral scanner and Thematic Mapper data of the Hubbard Glacier region, southeast Alaska p 52 A88-29493
- Intermediate-scale vegetation mapping of Innoko National Wildlife Refuge, Alaska using Landsat MSS digital data p 12 A88-29494
- Commercial applications and scientific research requirements for thermal-infrared observations of terrestrial surfaces [NASA-TM-89704] p 70 N88-16179
- Autocorrelation of control points on 11-band multispectral imagery [AD-A188185] p 62 N88-18056
- MULTISPECTRAL PHOTOGRAPHY**
- An application of divergence measurement using transformed video data p 6 A88-24510
- The use of successive clustering to analyze multispectral imagery p 61 A88-30086
- Multistep component analysis of correlations p 61 N88-16115
- Commercial applications and scientific research requirements for thermal-infrared observations of terrestrial surfaces [NASA-TM-89704] p 70 N88-16179
- A variant of the ISODATA algorithm for application to agricultural targets [INPE-4436-PRE/1235] p 17 N88-20023
- MULTISPECTRAL RADAR**
- Development of multivariate estuarine water quality models using Landsat 2 and 4 MSS data p 50 A88-21002
- Analysis of algorithms for the retrieval of rain-rate profiles from a spaceborne dual-wavelength radar p 69 A88-28679
- MULTIVARIATE STATISTICAL ANALYSIS**
- A variant of the ISODATA algorithm for application to agricultural targets [INPE-4436-PRE/1235] p 17 N88-20023
- N**
- NASA SPACE PROGRAMS**
- Update of NASA's ocean colour activities p 45 N88-16295
- NASA's geodynamics program p 24 N88-19845
- NATURAL GAS**
- Geological evolution and analysis of confirmed or suspected gas hydrate localities. Volume 9: Formation and stability of gas hydrates of the Middle America Trench [DE88-001007] p 29 N88-18050
- NEAR INFRARED RADIATION**
- Exploring the relationships between leaf nitrogen content, biomass and the near-infrared/red reflectance ratio p 12 A88-29288
- NEARSHORE WATER**
- Shelf water entrainment by Gulf Stream warm-core rings p 36 A88-27013
- NETHERLANDS**
- National Remote Sensing Program (NRSP) of the Netherlands p 46 N88-16305
- NEVADA**
- Spectral characteristics of selected soils and vegetation in northern Nevada and their discrimination using band ratio techniques p 3 A88-21352
- NIGERIA**
- Radar flood inundation mapping of upper Benue Trough, Nigeria p 2 A88-21035
- NIMBUS 7 SATELLITE**
- Observations of surface and atmospheric features from passive microwave satellite measurements p 64 A88-21019
- Validating regional differences in modelled satellite microwave signatures p 1 A88-21020
- Exact Rayleigh scattering calculations for use with the Nimbus-7 Coastal Zone Color Scanner p 41 A88-30415
- NITROGEN**
- Exploring the relationships between leaf nitrogen content, biomass and the near-infrared/red reflectance ratio p 12 A88-29288
- NOAA SATELLITES**
- Interpretation of satellite imagery of a rapidly deepening cyclone p 57 A88-23502
- A snapshot of the Labrador current inferred from ice-floe movement in NOAA satellite imagery p 32 A88-24456
- Monitoring of global vegetation dynamics for assessment of primary productivity using NOAA advanced very high resolution radiometer p 9 A88-27808
- Estimation of evapotranspiration in the Sahelian zone by use of Meteosat and NOAA AVHRR data p 9 A88-27818
- Mapping NOAA-AVHRR imagery using equal-area radial projections p 10 A88-28015

NOAA 7 SATELLITE

- Comparative study of temperature data from NOAA7-AVHRR and WMO - An interpretation through the use of a soil-vegetation model p 8 A88-27806
Evaluating North American net primary productivity with satellite observations p 9 A88-27819

NOISE REDUCTION

- A transformation for ordering multispectral data in terms of image quality with implications for noise removal p 58 A88-24937
Speckle in SAR images - An evaluation of filtering techniques p 59 A88-27834

NORTH AMERICA

- Meteorological and aerosol measurements from the NOAA WP-3D aircraft during WATOX-86, January 4-9, 1986 [PB88-120860] p 20 N88-18079

NUMERICAL ANALYSIS

- Multisource context classification methods in remote sensing p 63 N88-18985
Gradiometer mission spectral analysis and simulation studies: Past and future p 24 N88-19851

NUMERICAL WEATHER FORECASTING

- A sequential estimation approach to cloud-clearing for satellite temperature sounding p 66 A88-23511

O

OCEAN BOTTOM

- North Atlantic thermohaline circulation during the past 20,000 years linked to high-latitude surface temperature p 30 A88-20978

Features of hydrological anomalies in connection with the search for deep-water polymetallic sulfides

- p 32 A88-24654
Surface temperature variations of the world ocean in the Eocene p 32 A88-24655
Observations of ocean and sea bottom relief from space p 35 A88-26099

Comparison of submarine relief features on a radar satellite image and on a Skylab satellite photograph p 40 A88-29279

Source of the Australasian tektite strewn field - A possible off-shore impact site p 42 A88-31793

Thematic mapper study of Alaskan ophiolites [NASA-CR-182554] p 30 N88-18984

OCEAN COLOR SCANNER

- Satellite-derived color-temperature relationship in the Alboran Sea p 33 A88-25445

OCEAN CURRENTS

- The western equatorial Pacific Ocean circulation study p 30 A88-22911

A snapshot of the Labrador current inferred from ice-floe movement in NOAA satellite imagery p 32 A88-24456

Satellite observations of a western boundary current in the Bay of Bengal p 36 A88-27010

Marine boundary layer modification across the edge of the Agulhas Current p 38 A88-27495

Blocking of the Benguela Current by a single anticyclone - Analysis of satellite and ship data p 41 A88-30077

On estimating the basin-scale ocean circulation from satellite altimetry. Part 1: Straightforward spherical harmonic expansion [NASA-CR-182387] p 44 N88-15352

Sea surface current estimates off central California as derived from enhanced AVHRR (Advanced Very High Resolution Radiometer) infrared images [AD-A186867] p 47 N88-17155

Oceanographic features of the east and southeast Indian Ocean for June 1983 [AD-A186948] p 47 N88-17158

Hydrographic and current measurements in the North-East Atlantic Ocean. Data report on F.S. Meteor cruises 69/5 and 69/6, October to November 1984 [REPT-166] p 48 N88-17164

Analysis of low frequency current fluctuations in the North-East Atlantic Ocean [REPT-170] p 48 N88-17165

Mesoscale coastal ocean dynamics p 49 N88-19060

Thermal expansion of a rig --- oceanographic platform for satellite altimetry p 42 A88-32508

Status and prospects of the Joint Research Committee (JRC) work on the application of ocean colour monitoring from space p 46 N88-16299

Overview of ESA's activities in ocean colour remote sensing p 45 N88-16294

Update of NASA's ocean colour activities p 45 N88-16295

Remote sensing of ocean colour for studies of biological productivity and biochemical cycles p 45 N88-16296

Ocean colour applications in ocean dynamics and coastal processes p 45 N88-16297

Technical aspects of future ocean colour remote sensing p 46 N88-16298

Status and prospects of the Joint Research Committee (JRC) work on the application of ocean colour monitoring from space p 46 N88-16299

Canadian activities and goals in remote sensing of ocean colour and fluorescence from space p 46 N88-16300

Federal Republic of Germany's interests, activities and goals in remote sensing of ocean colour/fluorescence from space p 46 N88-16302

French activities in ocean colour observations p 46 N88-16303

Developments in ocean colour research in the United Kingdom p 46 N88-16306

Oceanographic features of the east and southeast Indian Ocean for June 1983 [AD-A186948] p 47 N88-17158

North Pacific Ocean. Central Pacific Transition Zone, R/V Thomas G. Thompson: 25 March - 3 May 1968. STD data report [AD-A186570] p 47 N88-17160

The effects of atmospheric and thermohaline variability on the validation of the GEOSAT altimeter oceanographic signal between Scotland and Iceland [AD-A189324] p 50 N88-19882

Oceanography Measuring ocean waves from space p 30 A88-20942

Sea ice and sea-surface temperatures in the Strait of Fram according to NOAA-AVHRR data p 35 A88-26131

Proposed uses of ERS-1 p 68 A88-27833

Radar altimeter data quality flagging p 39 A88-27837

WOCE Core Project 2 Planning Meeting: The Southern Ocean [WCP-138] p 44 N88-15348

Sea surface current estimates off central California as derived from enhanced AVHRR (Advanced Very High Resolution Radiometer) infrared images [AD-A186867] p 47 N88-17155

Oceanographic features of the east and southeast Indian Ocean for June 1983 [AD-A186948] p 47 N88-17158

Continental shelf processes affecting the oceanography of the South Atlantic Bight [DE88-004102] p 48 N88-17166

NASA Oceanic Processes Program [NASA-TM-4025] p 48 N88-18109

Coordination: Southeast continental shelf studies [DE88-003680] p 49 N88-18110

Mesoscale coastal ocean dynamics p 49 N88-19060

The effects of atmospheric and thermohaline variability on the validation of the GEOSAT altimeter oceanographic signal between Scotland and Iceland [AD-A189324] p 50 N88-19882

OCEANS On the problem of evolution of oceanic water composition in the Phanerozoic p 35 A88-26676

OFFSHORE PLATFORMS Thermal expansion of a rig --- oceanographic platform for satellite altimetry p 42 A88-32508

OCEAN MODELS

- A model of the tropical Pacific sea surface temperature climatology p 40 A88-29323
Emissivity of pure and sea waters for the model sea surface in the infrared window regions p 42 A88-30445

The Genesis of Atlantic Lows Experiment - The planetary-boundary-layer subprogram of GALE p 42 A88-31111

NASA Oceanic Processes Program [NASA-TM-4025] p 48 N88-18109

Spatial-temporal variability of North Pacific sea surface temperature anomaly patterns p 49 N88-19058

OCEAN SURFACE Sea return at C and Ku bands p 31 A88-22947

An approximate model for the microwave brightness temperature of the sea p 31 A88-23544

Remote sensing of wave patterns with oceanographic implications p 31 A88-23545

The DUT airborne scatterometer p 5 A88-23549

Potential applications of digital image analysis systems for displaying satellite altimetry data p 31 A88-23762

A multi-frequency-multi-nadir-angle pushbroom-radiometer for oil spill detection and mapping (On the surface of the sea) [MBB-UR-952-87] p 31 A88-23988

Surface temperature variations of the world ocean in the Eocene p 32 A88-24655

The role of synoptic scale processes in the transfer of sea surface temperature anomalies p 35 A88-26065

Airborne measurements of surface layer turbulence over the ocean during cold air outbreaks p 35 A88-26911

Calculations of ocean-atmosphere radiance on the basis of remote sensing p 37 A88-27204

Variations in the intensity of emitted and scattered microwave radiation of the sea surface sensed at grazing angles in a field of surface manifestations of internal waves p 37 A88-27205

Choosing conditions for the remote sensing of ocean features in the visible spectrum, with the effect of coastal zone taken into account p 37 A88-27209

The efficiency of polarization measurements in passive remote sensing of the ocean in the visible spectrum p 38 A88-27210

Downward longwave irradiance at the ocean surface from satellite data - Methodology and in situ validation p 38 A88-27493

Future research directions in the quantitative radar remote sensing of land and oceanic surface features p 39 A88-27841

Exact Rayleigh scattering calculations for use with the Nimbus-7 Coastal Zone Color Scanner p 41 A88-30415

Remote sensing of the sea surface p 42 A88-30662

Source of the Australasian tektite strewn field - A possible off-shore impact site p 42 A88-31793

Texture study of Synthetic Aperture Radar (SAR) images of ocean surfaces [AD-A186021] p 42 N88-15101

The ocean heat budget [AD-A186130] p 44 N88-15346

Limiting accuracy of scatterometer determination of wind speed over ocean from satellite p 44 N88-16107

Sea surface current estimates off central California as derived from enhanced AVHRR (Advanced Very High Resolution Radiometer) infrared images [AD-A186867] p 47 N88-17155

Investigation of the quantitative determination of two dimensional sea surface wave spectra from shipborne radar measurements [GKSS-87/E/10] p 48 N88-17163

Estimation of sea surface wave spectra using acoustic tomography [AD-A187837] p 49 N88-19057

The effects of atmospheric and thermohaline variability on the validation of the GEOSAT altimeter oceanographic signal between Scotland and Iceland [AD-A189324] p 50 N88-19882

OCEAN TEMPERATURE An approximate model for the microwave brightness temperature of the sea p 31 A88-23544

Surface temperature variations of the world ocean in the Eocene p 32 A88-24655

The relationship between the temporal variability of ocean temperature and the meridional shifts of the intertropical convergence zone p 37 A88-27203

OCEANOGRAPHIC PARAMETERS Observations of ocean and sea bottom relief from space p 35 A88-26099

Processing and analysis of large volumes of satellite-derived thermal infrared data --- for physical oceanographic studies p 36 A88-27012

The use of the optical classification of ocean waters to estimate correlations between the concentrations of variable components with reference to the development of remote-sensing methods p 41 A88-30078
Detection of internal waves using data from satellite microwave radiometry and the research ship Academician Alexander Nesmejanov p 41 A88-30083
Current status and problems of satellite investigations of the ocean (Review of non-Soviet publications) p 41 A88-30089

Remote sensing of the sea surface p 42 A88-30662

The influence of yellow substances on remote sensing of sea water constituents from space. Volume 1: Summary [ESA-CR(P)-2443-VOL-1] p 43 N88-15292

The influence of yellow substances on remote sensing of sea water constituents from space. Volume 2: Appendices [ESA-CR(P)-2443-VOL-2] p 43 N88-15293

Ocean Colour Workshop --- conference [ESA-SP-1083] p 45 N88-16292

Europe's position concerning ocean colour activities p 45 N88-16293

Overview of ESA's activities in ocean colour remote sensing p 45 N88-16294

Update of NASA's ocean colour activities p 45 N88-16295

Remote sensing of ocean colour for studies of biological productivity and biochemical cycles p 45 N88-16296

Ocean colour applications in ocean dynamics and coastal processes p 45 N88-16297

Technical aspects of future ocean colour remote sensing p 46 N88-16298

Status and prospects of the Joint Research Committee (JRC) work on the application of ocean colour monitoring from space p 46 N88-16299

Canadian activities and goals in remote sensing of ocean colour and fluorescence from space p 46 N88-16300

Federal Republic of Germany's interests, activities and goals in remote sensing of ocean colour/fluorescence from space p 46 N88-16302

French activities in ocean colour observations p 46 N88-16303

Developments in ocean colour research in the United Kingdom p 46 N88-16306

Oceanographic features of the east and southeast Indian Ocean for June 1983 [AD-A186948] p 47 N88-17158

North Pacific Ocean. Central Pacific Transition Zone, R/V Thomas G. Thompson: 25 March - 3 May 1968. STD data report [AD-A186570] p 47 N88-17160

The effects of atmospheric and thermohaline variability on the validation of the GEOSAT altimeter oceanographic signal between Scotland and Iceland [AD-A189324] p 50 N88-19882

OCEANOGRAPHY Measuring ocean waves from space p 30 A88-20942

Sea ice and sea-surface temperatures in the Strait of Fram according to NOAA-AVHRR data p 35 A88-26131

Proposed uses of ERS-1 p 68 A88-27833

Radar altimeter data quality flagging p 39 A88-27837

WOCE Core Project 2 Planning Meeting: The Southern Ocean [WCP-138] p 44 N88-15348

Sea surface current estimates off central California as derived from enhanced AVHRR (Advanced Very High Resolution Radiometer) infrared images [AD-A186867] p 47 N88-17155

Oceanographic features of the east and southeast Indian Ocean for June 1983 [AD-A186948] p 47 N88-17158

Continental shelf processes affecting the oceanography of the South Atlantic Bight [DE88-004102] p 48 N88-17166

NASA Oceanic Processes Program [NASA-TM-4025] p 48 N88-18109

Coordination: Southeast continental shelf studies [DE88-003680] p 49 N88-18110

Mesoscale coastal ocean dynamics p 49 N88-19060

The effects of atmospheric and thermohaline variability on the validation of the GEOSAT altimeter oceanographic signal between Scotland and Iceland [AD-A189324] p 50 N88-19882

OCEANS On the problem of evolution of oceanic water composition in the Phanerozoic p 35 A88-26676

OFFSHORE PLATFORMS Thermal expansion of a rig --- oceanographic platform for satellite altimetry p 42 A88-32508

- Geological evolution and analysis of confirmed or suspected gas hydrate localities. Volume 9: Formation and stability of gas hydrates of the Middle America Trench [DE88-001007] p 29 N88-18050
- OIL EXPLORATION**
Three-dimensional transient electromagnetic modeling for exploration geophysics p 29 N88-18047
- OIL POLLUTION**
Detection of oil films by active and passive microwave sensors p 39 A88-27840
- OIL SLICKS**
A multi-frequency-multi-nadir-angle pushbroom-radiometer for oil spill detection and mapping (On the surface of the sea) [MBB-UR-952-87] p 31 A88-23988
Detection of oil films by active and passive microwave sensors p 39 A88-27840
- ONBOARD DATA PROCESSING**
Radar altimeter data quality flagging p 39 A88-27837
- OPERATIONAL PROBLEMS**
Difficulties and recommendations for obtaining very large scale 70 mm aerial photography for rangeland monitoring p 1 A88-21017
- OPERATORS (MATHEMATICS)**
Matching of dissimilar radar images using Marr-Hildreth zero crossings p 56 A88-21070
- OPTICAL EQUIPMENT**
Remote sensing of atmospheric crosswinds by utilizing speckle-turbulence interaction and optical heterodyne detection [AD-A187580] p 71 N88-18052
- OPTICAL FILTERS**
Photographic filters [INPE-4448-RPE/558] p 64 N88-20124
- OPTICAL HETERODYNING**
Remote sensing of atmospheric crosswinds by utilizing speckle-turbulence interaction and optical heterodyne detection [AD-A187580] p 71 N88-18052
- OPTICAL MEASUREMENT**
Evaluation of a temperature remote sensing technique [AD-A187885] p 71 N88-18053
- OPTICAL PROPERTIES**
Vegetative and optical characteristics of four-row crop canopies p 14 A88-32661
- OPTICAL RADAR**
Correlation between aircraft MSS and lidar remotely sensed data on a forested wetland p 6 A88-24513
Estimating forest biomass and volume using airborne laser data p 13 A88-30441
- OPTICAL THICKNESS**
Remote sensing of atmospheric optical thickness and sea-water attenuation when submerged: Wavelength selection and anticipated errors [AD-A187609] p 49 N88-19262
- OPTIMIZATION**
Hierarchical segmentation using a composite criterion for remotely sensed imagery p 54 A88-20841
Optimization of photogrammetric image adjustment [SER-C-323] p 22 N88-15289
- ORBIT CALCULATION**
Identical-route satellite orbits for long-term periodic global survey of the earth, not dependent on solar illumination p 67 A88-27216
- ORBITAL ELEMENTS**
The relationships between orbit parameters and the geometry of the trajectory for remote sensing satellites p 67 A88-27215
- ORBITAL MECHANICS**
Geosat crossover analysis in the tropical Pacific. Part 1: Constrained sinusoidal crossover adjustment [NASA-CR-182391] p 43 N88-15285
- OROGRAPHY**
Geostrophical evolution of the Southern Alps - Lineaments trends detected on Landsat images p 26 A88-25448
Statistics of two-dimensional structure elements of mountainous ranges (mosaic model) for calculating three-dimensional reflection functions [DFVLR-FB-87-33] p 29 N88-17099
- OZONE**
Comparison of total ozone amounts derived from satellite and ground-based measurements p 66 A88-27027
- OZONE DEPLETION**
Satellite maps of Antarctic total ozone [AIAA PAPER 88-0210] p 30 A88-22154
- PACIFIC OCEAN**
Relationships between monthly precipitation and SST variations in the tropical Pacific region p 65 A88-21382

P

- The western equatorial Pacific Ocean circulation study p 30 A88-22911
- Remote sensing of water vapor convergence, deep convection, and precipitation over the tropical Pacific Ocean during the 1982-1983 El Nino p 33 A88-25728
Sea surface temperature, low-level moisture, and convection in the tropical Pacific, 1982-1985 p 34 A88-25729
- Geosat crossover analysis in the tropical Pacific. Part 1: Constrained sinusoidal crossover adjustment [NASA-CR-182391] p 43 N88-15285
North Pacific Ocean. Central Pacific Transition Zone, R/V Thomas G. Thompson: 25 March - 3 May 1968. STD data report [AD-A186570] p 47 N88-17160
Materials of the World Data Center B. Deep Seismic Sounding (DSS): Pacific data p 48 N88-17167
Geological evolution and analysis of confirmed or suspected gas hydrate localities. Volume 9: Formation and stability of gas hydrates of the Middle America Trench [DE88-001007] p 29 N88-18050
- PALEONTOLOGY**
Use of space photographs for paleoseismogeological studies (on the example of Mongolian Altay) p 28 N88-16110
- PANORAMIC CAMERAS**
Accuracy of mapping by panoramic photography p 60 A88-29479
A comparison between panoramic photography and conventional aerial photography in terms of mapping accuracy p 61 A88-32167
- PARALLAX**
Parallax bar heighting accuracy of large format camera photography p 65 A88-21051
Single-source three-dimensional imaging system for remote sensing p 66 A88-23772
- PARALLEL PROCESSING (COMPUTERS)**
Automated photointerpretation - A stereoscopic workstation p 54 A88-21027
- PARAMETERIZATION**
On the parameterization of irradiance for open ocean photoprocesses p 34 A88-25737
- PARTICLE SIZE DISTRIBUTION**
Effect of ice-grain size distribution on the thermal emission of snow cover p 52 A88-24662
Size distributions of sea-source aerosol particles - A physical explanation of observed nearshore versus open-sea differences p 33 A88-25289
- PARTICULATES**
Biomass-burning emissions and associated haze layers over Amazonia p 18 A88-27265
- PATTERN RECOGNITION**
Results of testing digital image measurements and enhancements on the remote work processing facility p 56 A88-21064
Detecting subpixel woody features using simulated multispectral and panchromatic SPOT imagery p 3 A88-21065
The use of automated computer vision techniques for the recognition of features on radar imagery p 56 A88-21069
Land cover change detection using a GIS-guided, feature-based classification of Landsat thematic mapper data --- Geographic Information System p 18 A88-21073
Problems related to the determination of land surface parameters and fluxes over heterogeneous media from satellite data p 19 A88-27803
Spectral and botanical classification of grasslands - Auxois example p 8 A88-27805
Atmospheric effect on spectral signature - Measurements p 58 A88-27822
Forecasting patterns of soil erosion in arid lands from Landsat MSS data p 12 A88-29280
- PATTERN REGISTRATION**
A smart, mapping, charting and geodesy control generator, phase 1 [AD-A188184] p 23 N88-18055
Autocorrelation of control points on 11-band multispectral imagery [AD-A188185] p 62 N88-18056
- PERIODIC VARIATIONS**
An investigation of the El Nino-Southern Oscillation Cycle with statistical models. I - Predictor field characteristics. II - Model results p 34 A88-25731
Analysis of low frequency current fluctuations in the North-East Atlantic Ocean [REPT-170] p 48 N88-17165
- PERSONAL COMPUTERS**
Computer-assisted map analysis - A set of primitive operators for a flexible approach --- in geographic information systems p 17 A88-21023
- PERSONNEL**
Report of the participation in the International Training Course: Remote Sensing in Village Forestry [INPE-4476-NTE/278] p 16 N88-19802

PETROLOGY

- Geochemistry of continental volcanism --- Russian book p 27 A88-29431
Nature and origin of mineral coatings on volcanic rocks of the Black Mountain, Stonewall Mountain, and Kane Springs Wash volcanic centers, Southern Nevada [NASA-CR-181437] p 29 N88-17140

PHOSPHORESCENCE

- Canadian activities and goals in remote sensing of ocean colour and fluorescence from space p 46 N88-16300
Federal Republic of Germany's interests, activities and goals in remote sensing of ocean colour/fluorescence from space p 46 N88-16302

PHOTO GEOLOGY

- Geostrophical evolution of the Southern Alps - Lineaments trends detected on Landsat images p 26 A88-25448

- Use of airborne imaging spectrometer data to map minerals associated with hydrothermally altered rocks in the Northern Grapevine Mountains, Nevada, and California p 26 A88-28267
Discrimination of hydrothermal alteration mineral assemblages at Virginia City, Nevada, using the airborne imaging spectrometer p 27 A88-28268
Comparison of techniques for discriminating hydrothermal alteration minerals with Airborne Imaging Spectrometer data p 27 A88-28269

- Exploration of crustal/mantle material for the earth and moon using reflectance spectroscopy p 27 A88-28273
Landsat determined geographic change p 27 A88-29489
The use of Meteor-Priroda space photographs for the compilation of small-scale and medium-scale tectonic and geological maps p 27 A88-30079
Investigation of the foci of powerful earthquakes and seismically hazardous areas on space photographs for the Baikal-Aldan region p 27 A88-30081

- PHOTOGRAMMETRY**
Remote sensing applications - An outlook for the future p 64 A88-20904
American Society for Photogrammetry and Remote Sensing and ACSM, Annual Convention, Baltimore, MD, Mar. 29-Apr. 3, 1987, Technical Papers. Volume 2 - Photogrammetry p 2 A88-21046
Geographical position plotting by photo interpreters from Space Shuttle Large Format Camera photography p 65 A88-21050
American Society for Photogrammetry and Remote Sensing and ACSM, Annual Convention, Baltimore, MD, Mar. 29-Apr. 3, 1987, Technical Papers. Volume 6 - Image data processing p 55 A88-21062
A comparison between panoramic photography and conventional aerial photography in terms of mapping accuracy p 61 A88-32167
The aerophotogrammetric determination of Earth surface deformations [SER-C-321] p 28 N88-15288
Optimization of photogrammetric image adjustment [SER-C-323] p 22 N88-15289
Theory and research on the disjunction of cross passage errors and systematic image errors in photogrammetric point determination [SER-C-324] p 61 N88-15290
Photogrammetric principles for combining remote sounding and three-dimensional mapping p 61 N88-16135

- PHOTOGRAPHS**
Academic course Space Methods for Studying Modern Landscapes of Continents p 72 N88-16133

PHOTOGRAPHY

- Photographic filters [INPE-4448-RPE/558] p 64 N88-20124

PHOTOINTERPRETATION

- Automated photointerpretation - A stereoscopic workstation p 54 A88-21027
Geographical position plotting by photo interpreters from Space Shuttle Large Format Camera photography p 65 A88-21050

- Problems in geologic and geomorphic interpretation and geometric modeling of radar images using a digital terrain model p 26 A88-28024
Detection and identification of Arctic landforms - An assessment of remotely sensed data p 40 A88-29492
The use of successive clustering to analyze multispectral imagery p 61 A88-30086
Large area crop classification in New South Wales, Australia, using Landsat data p 14 A88-32665
Model-based building verification in aerial photographs [AD-A186010] p 20 N88-15278
Study of relief of ore regions using space images (on the example of Eastern Yakutia) p 28 N88-16111
Automatic knowledge acquisition for aerial image interpretation [AD-A188616] p 63 N88-19810

PHOTOMAPPING

- Computer-aided mapping of Antarctic Sea ice using along-the-course radiometric measurements aboard the Cosmos-1500 satellite p 38 A88-27213
- A study to produce 1:100,000 scale LFC color photomap --- Large Format Camera p 68 A88-27826
- Evaluation of several classification schemes for mapping forest cover types in Michigan p 10 A88-28012
- Mapping NOAA-AVHRR imagery using equal-area radial projections p 10 A88-28015
- The use of space technology for the remote sensing of earth resources and mapping p 69 A88-28447
- The potential for automated mapping from Geocoded digital image data p 59 A88-28604
- Accuracy of mapping by panoramic photography p 60 A88-29479
- An integrated approach for automated cover-type mapping of large inaccessible areas in Alaska p 60 A88-29491
- A comparison between panoramic photography and conventional aerial photography in terms of mapping accuracy p 61 A88-32167
- Use of space photographs for geomorphological studies in southwestern Tajikistan p 28 A88-16109

PHOTOMAPS

- The ARSUP database and its access through the CMCIRS catalog - Making available to the public digital maps from the ARSUP process --- Computerized Map Cataloging and Information Retrieval System p 60 A88-29496

PHOTOMETERS

- Remote sensing of atmospheric optical thickness and sea-water attenuation when submerged: Wavelength selection and anticipated errors [AD-A187609] p 49 A88-19262

PHOTORECONNAISSANCE

- Space applications in geography p 22 A88-16104

PHOTOSYNTHESIS

- On the parameterization of irradiance for open ocean photoprocesses p 34 A88-25737
- Relations between canopy reflectance, photosynthesis and transpiration - Links between optics, biophysics and canopy architecture p 8 A88-27802
- Relating seasonal patterns of the AVHRR vegetation index to simulated photosynthesis and transpiration of forests in different climates p 13 A88-30447

PHYTOPLANKTON

- Thematic mapper research in the earth sciences: Small scale patches of suspended matter and phytoplankton in the Elbe River Estuary, German Bight and Tidal Flats [NASA-CR-182378] p 45 A88-16180

PIXELS

- Hierarchical segmentation using a composite criterion for remotely sensed imagery p 54 A88-20841
- Comparison of Landsat MSS pixel array sizes for estimating water quality variables in small lakes p 50 A88-21004
- Interrelationships between spatial resolution and per-pixel classifiers for extracting information classes. I - The urban environment. II - The natural environment p 17 A88-21014
- Textural features for image classification in remote sensing [INPE-4169-PRE/1066] p 62 A88-16181

PLANETARY BOUNDARY LAYER

- The Genesis of Atlantic Lows Experiment - The planetary-boundary-layer subprogram of GALE p 42 A88-31111

PLANETARY GRAVITATION

- On the accuracy of marine gravity measurements p 21 A88-25224
- Mantle rheology and satellite signatures from present-day glacial forcings p 21 A88-25225

PLANKTON

- The use of chlorophyll fluorescence measurements from space for separating constituents of sea water. Volume 2: Appendices [ESA-CR(P)-2444-VOL-2] p 44 A88-15295

PLANTS (BOTANY)

- Five New South Wales barrier lagoons: Their macrobenthic fauna and seagrass communities p 49 A88-19059

PLATES (TECTONICS)

- Evolution of the Juan Fernandez microplate during the last three million years p 25 A88-25045

PLOTTERS

- An autoCAD-based mapping system for encoded stereoplotters p 60 A88-29490

POINTS (MATHEMATICS)

- Digital terrain analysis employing X-Y-Z point vectors as input data p 55 A88-21061

POLAR REGIONS

- Observation of sea-ice dynamics using synthetic aperture radar images: Automated analysis p 32 A88-24934

POLARIMETRY

- The efficiency of polarization measurements in passive remote sensing of the ocean in the visible spectrum p 38 A88-27210

POLARIZATION CHARACTERISTICS

- Parametric analysis of synthetic aperture radar data for characterization of deciduous forest stands p 2 A88-21033

- Polarized and non-polarized leaf reflectances of *Coleus blumei* p 7 A88-26624

POLARIZED ELECTROMAGNETIC RADIATION

- Relative sensitivity of Normalized Difference Vegetation Index (NDVI) and Microwave Polarization Difference Index (MPDI) for vegetation and desertification monitoring p 13 A88-30444

POLLUTION MONITORING

- A multi-frequency-multi-nadir-angle pushbroom-radiometer for oil spill detection and mapping (On the surface of the sea) [MBB-UR-952-87] p 31 A88-23988

POLYGONS

- Refining image segmentation by polygon skeletonization p 56 A88-21068

POLYNOMIALS

- Comparison of the gridded finite element and the polynomial interpolations for geometric rectification and mosaicking of Landsat data p 55 A88-21049

POPULATIONS

- Using remotely sensed data for census surveys and population estimation in developing countries - Examples from Nigeria p 18 A88-24511
- A study on the utilization of SIR-A data for population estimation in the eastern part of Spain p 18 A88-24512

PRECIPITATION (METEOROLOGY)

- Relationships between monthly precipitation and SST variations in the tropical Pacific region p 65 A88-21382

- Remote sensing of water vapor convergence, deep convection, and precipitation over the tropical Pacific Ocean during the 1982-1983 El Nino p 33 A88-25728
- Estimation of atmospheric liquid-water amount by Nimbus 7 SMMR data - A new method and its application to the western North-Pacific region p 69 A88-30731

PREDICTION ANALYSIS TECHNIQUES

- Application of predictive compression methods to synthetic aperture radar imagery I p 57 A88-23768

PREDICTIONS

- Satellite monitoring of earthquake precursor effects in magnetosphere p 28 A88-16103
- Crop forecasting in Brazil: A short history of productivity models [INPE-4150-PRE/1056] p 16 A88-19801

PRINCIPAL COMPONENTS ANALYSIS

- Principal component analysis of aerial video imagery p 54 A88-21030
- Comparison of techniques for discriminating hydrothermal alteration minerals with Airborne Imaging Spectrometer data p 27 A88-28269
- Principal component analysis of satellite passive microwave data over sea ice p 41 A88-30199
- Multistep component analysis of correlations p 61 A88-16115

PRODUCTIVITY

- Report on phase 1 of the project estimate development of a model for yield estimation of sugar cane based on LANDSAT and agromet data [INPE-4466-RPE/560] p 16 A88-19807

PROJECT MANAGEMENT

- Coordination: Southeast continental shelf studies [DE88-003680] p 49 A88-18110

PROJECT PLANNING

- Critical issues in NASA information systems [NASA-CR-182380] p 72 A88-16577
- Coordination: Southeast continental shelf studies [DE88-003680] p 49 A88-18110

PROPANE

- Geological evolution and analysis of confirmed or suspected gas hydrate localities. Volume 9: Formation and stability of gas hydrates of the Middle America Trench [DE88-001007] p 29 A88-18050

PULSE CODE MODULATION

- Application of predictive compression methods to synthetic aperture radar imagery I p 57 A88-23768

PUSHBROOM SENSOR MODES

- A multi-frequency-multi-nadir-angle pushbroom-radiometer for oil spill detection and mapping (On the surface of the sea) [MBB-UR-952-87] p 31 A88-23988
- HIRIS (High-Resolution Imaging Spectrometer: Science opportunities for the 1990s. Earth observing system. Volume 2C: Instrument panel report [NASA-TM-89703] p 70 A88-15282

Q

QUALITY CONTROL

- Operational revision of national topographic maps in Canada using Landsat images p 54 A88-20901

R

RADAR

- Active and passive remote sensing of ice [AD-A186685] p 47 A88-17162

RADAR CROSS SECTIONS

- Modelling radar backscatter from vegetation p 5 A88-21501

RADAR DATA

- Application of data from the U.S. Geological Survey's side-looking airborne radar program p 25 A88-21036

RADAR IMAGERY

- Fluvial perturbation in the western Amazon basin - Regulation by long-term sub-Andean tectonics p 24 A88-20878
- Characterization of vegetation with combined Thematic Mapper (TM) and Shuttle Imaging Radar (SIR-B) image data p 2 A88-21032
- Parametric analysis of synthetic aperture radar data for characterization of deciduous forest stands p 2 A88-21033
- Geologic applications of side-looking airborne radar images in the Appalachian Valley and Ridge Province p 24 A88-21034
- Image based SAR product simulation for analysis p 55 A88-21037
- Evaluation of X-band SAR imagery for mapping open surface water in the northeastern United States p 51 A88-21038
- An expert system for the computer-assisted analysis of radar imagery p 55 A88-21053
- The use of automated computer vision techniques for the recognition of features on radar imagery p 56 A88-21069
- Matching of dissimilar radar images using Marr-Hildreth zero crossings p 56 A88-21070
- Modelling radar backscatter from vegetation p 5 A88-21501
- Correlation characteristics of images of the earth surface obtained with a synthetic-aperture radar p 66 A88-21784
- Remote sensing of wave patterns with oceanographic implications p 31 A88-23545
- Interpretation of Seasat radar-altimeter data over sea ice using near-simultaneous SAR imagery p 31 A88-23547
- Geometric accuracy testing of orbital radar imagery p 57 A88-23760
- Application of predictive compression methods to synthetic aperture radar imagery I p 57 A88-23768
- A study on the utilization of SIR-A data for population estimation in the eastern part of Spain p 18 A88-24512
- Synthetic aperture radar imagery of range traveling ocean waves p 32 A88-24933
- Observation of sea-ice dynamics using synthetic aperture radar images: Automated analysis p 32 A88-24934
- Characteristics of the subsurface radar sounding of natural objects p 26 A88-25551
- X-band features of canopy cover - An up to date summary of active and passive measurements p 10 A88-27835
- Problems in geologic and geomorphic interpretation and geometric modeling of radar images using a digital terrain model p 26 A88-28024
- Radiometric correction of C-band imagery for topographic effects in regions of moderate relief p 59 A88-28680
- SAR imaging of volume scatterers p 60 A88-28681
- Comparison of submarine relief features on a radar satellite image and on a Skylab satellite photograph p 40 A88-29279
- Texture study of Synthetic Aperture Radar (SAR) images of ocean surfaces [AD-A186021] p 42 A88-15101
- Earthnet's experience with Seasat SAR image processing p 62 A88-16760

RADAR MAPS

- Radar flood inundation mapping of upper Benue Trough, Nigeria p 2 A88-21035
- Evaluation of X-band SAR imagery for mapping open surface water in the northeastern United States p 51 A88-21038

- Methods and accuracy of operational digital image mapping with aircraft SAR p 55 A88-21059

RADAR MEASUREMENT

- Analysis of algorithms for the retrieval of rain-rate profiles from a spaceborne dual-wavelength radar p 69 A88-28679

- Investigation of the quantitative determination of two dimensional sea surface wave spectra from shipborne radar measurements [GKSS-87/E/10] p 48 N88-17163
- RADAR SCANNING**
Future research directions in the quantitative radar remote sensing of land and oceanic surface features p 39 A88-27841
- RADAR SCATTERING**
Sea return at C and Ku bands p 31 A88-22947
Remote sensing of wave patterns with oceanographic implications p 31 A88-23545
Interpretation of Seasat radar-altimeter data over sea ice using near-simultaneous SAR imagery p 31 A88-23547
SAR imaging of volume scatterers p 60 A88-28681
The use of a helicopter mounted ranging scatterometer for estimation of extinction and scattering properties of forest canopies-II: Experimental results for high-density aspen p 11 A88-28683
- RADAR SIGNATURES**
Radar descriptors for the classification of terrain features [AD-A188145] p 63 N88-18983
- RADIANCE**
Calculations of ocean-atmosphere radiance on the basis of remote sensing p 37 A88-27204
Atmospheric effect on spectral signature - Measurements p 58 A88-27822
An improved method for detecting clear sky and cloudy radiances from AVHRR data p 69 A88-29284
Exact Rayleigh scattering calculations for use with the Nimbus-7 Coastal Zone Color Scanner p 41 A88-30415
The influence of yellow substances on remote sensing of sea water constituents from space. Volume 1: Summary [ESA-CR(P)-2443-VOL-1] p 43 N88-15292
The influence of yellow substances on remote sensing of sea water constituents from space. Volume 2: Appendices [ESA-CR(P)-2443-VOL-2] p 43 N88-15293
Monte Carlo method calculation of spectral brightness coefficient of vegetation cover as function of illumination conditions p 14 N88-16113
Remote sensing of atmospheric optical thickness and sea-water attenuation when submerged: Wavelength selection and anticipated errors [AD-A187609] p 49 N88-19262
- RADIANT FLUX DENSITY**
The role of anisotropy in the long range reconnaissance of the albedo of land surfaces p 62 N88-16169
- RADIATION ABSORPTION**
Remote sensing of atmospheric optical thickness and sea-water attenuation when submerged: Wavelength selection and anticipated errors [AD-A187609] p 49 N88-19262
- RADIATION DISTRIBUTION**
The role of anisotropy in the long range reconnaissance of the albedo of land surfaces p 62 N88-16169
- RADIATIVE HEAT TRANSFER**
The ocean heat budget [AD-A186130] p 44 N88-15346
- RADIATIVE TRANSFER**
A canopy reflectance model based on an analytical solution to the multiple scattering equation p 7 A88-25447
Downward longwave irradiance at the ocean surface from satellite data - Methodology and in situ validation p 38 A88-27493
Estimation of atmospheric liquid-water amount by Nimbus 7 SMMR data - A new method and its application to the western North-Pacific region p 69 A88-30731
Thematic mapper research in the earth sciences: Small scale patches of suspended matter and phytoplankton in the Elbe River Estuary, German Bight and Tidal Flats [NASA-CR-182378] p 45 N88-16180
Application of satellite data in variational analysis for global cyclonic systems [NASA-CR-182468] p 62 N88-17152
- RADIO ALTIMETERS**
Radar altimeter data quality flagging p 39 A88-27837
Swath altimetry of oceans and terrain p 39 A88-27838
- RADIO PHYSICS**
Methods for processing radio-physical measurement data in studies of the environment --- Russian book p 19 A88-29427
- RADIOMETERS**
Mapping NOAA-AVHRR imagery using equal-area radial projections p 10 A88-28015
Sea surface current estimates off central California as derived from enhanced AVHRR (Advanced Very High Resolution Radiometer) infrared images [AD-A186867] p 47 N88-17155
- General determination of Earth surface type and cloud amount using multispectral AVHRR data [NOAA-TR-NESDIS-39] p 72 N88-18997
Remote sensing of atmospheric optical thickness and sea-water attenuation when submerged: Wavelength selection and anticipated errors [AD-A187609] p 49 N88-19262
- RADIOMETRIC CORRECTION**
Radiometric correction of C-band imagery for topographic effects in regions of moderate relief p 59 A88-28680
Preliminary assessment of radiometric accuracies for MOS-1 sensors p 39 A88-29276
- RADIOMETRIC RESOLUTION**
Estimation of evapotranspiration in the Sahelian zone by use of Meteosat and NOAA AVHRR data p 9 A88-27818
Recent data quality and earth science results from the Landsat thematic mapper p 58 A88-27824
Preliminary assessment of radiometric accuracies for MOS-1 sensors p 39 A88-29276
- RAIN**
Characteristics of extreme rainfall events in northwestern Peru during the 1982-1983 El Nino period p 52 A88-25730
Analysis of algorithms for the retrieval of rain-rate profiles from a spaceborne dual-wavelength radar p 69 A88-28679
Design of the primary pre-TRMM and TRMM ground truth site [NASA-CR-182609] p 53 N88-19865
- RAIN FORESTS**
Structure and growth of the mixing layer over the Amazonian rain forest p 8 A88-27252
Shuttle imaging radar A analysis of land use in Amazonia p 12 A88-29282
Mapping of the mangroves of the Guanabarra Bay through the utilization of remote sensing techniques [INPE-3942-TDL/229] p 16 N88-19804
- RANGE FINDING**
On differential scale changes and the satellite Doppler system z-shift p 21 A88-25850
The effects of atmospheric and thermohaline variability on the validation of the GEOSAT altimeter oceanographic signal between Scotland and Iceland [AD-A189324] p 50 N88-19882
- RANGELANDS**
Aerial and ground spectral characteristics of rangeland plant communities in Nevada p 3 A88-21353
Surface anisotropy and hemispheric reflectance for a semiarid ecosystem p 3 A88-21354
Suitability of spectral indices for evaluating vegetation characteristics on arid rangelands p 3 A88-21355
Near-real-time video systems for rangeland assessment p 4 A88-21360
Satellite remote sensing of Australian rangelands p 4 A88-21361
Detection of yearly cover change with Landsat MSS on pastoral landscapes in central Australia p 4 A88-21362
The use of spectral and spatial variability to monitor cover change on inert landscapes p 4 A88-21363
Spectral assessment of indicators of range degradation in the Botswana hardveld environment p 5 A88-21365
Canopy reflectance of seven rangeland plant species with variable leaf pubescence p 5 A88-23764
- RATES (PER TIME)**
Analysis of algorithms for the retrieval of rain-rate profiles from a spaceborne dual-wavelength radar p 69 A88-28679
- RAYLEIGH SCATTERING**
Exact Rayleigh scattering calculations for use with the Nimbus-7 Coastal Zone Color Scanner p 41 A88-30415
- REAL TIME OPERATION**
A smart, mapping, charting and geodesy control generator, phase 1 [AD-A188184] p 23 N88-18055
- RECEIVERS**
Remote sensing of atmospheric crosswinds by utilizing speckle-turbulence interaction and optical heterodyne detection [AD-A187580] p 71 N88-18052
- REFLECTANCE**
Exploring the relationships between leaf nitrogen content, biomass and the near-infrared/red reflectance ratio p 12 A88-29288
Estimation of wheat canopy resistance using combined remotely sensed spectral reflectance and thermal observations p 13 A88-30448
The anisotropy of reflected solar radiation over several types of land surface p 62 N88-16171
- Statistics of two-dimensional structure elements of mountainous ranges (mosaic model) for calculating three-dimensional reflection functions [DFVLR-FB-87-33] p 29 N88-17099
Improved canopy reflectance modeling and scene inference through improved understanding of scene pattern [NASA-CR-182488] p 15 N88-18049
The angular reflectance signature of the canopy hot spot in the optical regime [DE88-005385] p 15 N88-18991
- REGRESSION ANALYSIS**
The use of regression analysis to determine sea surface temperatures from Cosmos-1151 measurements of IR radiation p 41 A88-30085
Detection of soil erosion with Thematic Mapper (TM) satellite data within Pinyon-Juniper woodlands [NASA-CR-182476] p 15 N88-17103
- RELIEF MAPS**
Comparison of submarine relief features on a radar satellite image and on a Skylab satellite photograph p 40 A88-29279
Study of relief of ore regions using space images (on the example of Eastern Yakutia) p 28 N88-16111
Photogrammetric principles for combining remote sounding and three-dimensional mapping p 61 N88-16135
- REMOTE SENSING**
Hierarchical segmentation using a composite criterion for remotely sensed imagery p 54 A88-20841
The development and state of the art of remote sensing p 64 A88-20903
Remote sensing applications - An outlook for the future p 64 A88-20904
Measuring ocean waves from space p 30 A88-20942
American Society for Photogrammetry and Remote Sensing and ACSM, Annual Convention, Baltimore, MD, Mar. 29-Apr. 3, 1987, Technical Papers. Volume 1 - Remote sensing p 64 A88-21001
Remote sensing of Chesapeake Bay water quality required for healthy oyster beds p 30 A88-21003
Comparison of Landsat MSS pixel array sizes for estimating water quality variables in small lakes p 50 A88-21004
Monitoring North Carolina's nutrient-sensitive reservoirs using Landsat TM digital data p 50 A88-21006
Remote sensing of aquatic macrophyte distribution in selected South Carolina reservoirs p 51 A88-21007
A remote sensing based methodology for quantifying the spatial and functional relationships amongst industrial land uses delineated around the port of Baltimore p 17 A88-21012
An evaluation of the use of TM digital data for updating the land cover component of the SCS 1987 multisource inventory of New Jersey --- soil conservation service p 1 A88-21013
Interrelationships between spatial resolution and per-pixel classifiers for extracting information classes. I - The urban environment. II - The natural environment p 17 A88-21014
Multispectral video survey of a Northern Ontario forest p 1 A88-21015
Mid-infrared (1.45 to 2.0 microns) video - A potential aid in wildfire mop-up operations p 1 A88-21016
Multi-stage remote sensing - A tool for Minnesota natural resources management p 64 A88-21018
The use of remote sensing in developing and validating a ground hydrology/vegetation model for GCM3 --- general circulation models p 51 A88-21021
Extended abstract modelling interactions between the terrestrial biosphere and the global atmosphere p 65 A88-21022
Implementation of the Land Analysis System on a workstation p 54 A88-21026
Estimating forest productivity in southern Illinois using Landsat Thematic Mapper data and geographic information system analysis techniques p 2 A88-21028
Principal component analysis of aerial video imagery p 54 A88-21030
Characterization of vegetation with combined Thematic Mapper (TM) and Shuttle Imaging Radar (SIR-B) image data p 2 A88-21032
Radar flood inundation mapping of upper Benue Trough, Nigeria p 2 A88-21035
Application of data from the U.S. Geological Survey's side-looking airborne radar program p 25 A88-21036
Image based SAR product simulation for analysis p 55 A88-21037
A time-lapse analysis of the Mississippi Delta using Landsat MSS Band 4 (IR2) photographic imagery p 51 A88-21039

American Society for Photogrammetry and Remote Sensing and ACSM, Annual Convention, Baltimore, MD, Mar. 29-Apr. 3, 1987, Technical Papers. Volume 2 - Photogrammetry p 2 A88-21046
Computer-assisted color generation for thematic mapping p 55 A88-21048
American Society for Photogrammetry and Remote Sensing and ACSM, Annual Convention, Baltimore, MD, Mar. 29-Apr. 3, 1987, Technical Papers. Volume 3 - Surveying p 20 A88-21054
American Society for Photogrammetry and Remote Sensing and ACSM, Annual Convention, Baltimore, MD, Mar. 29-Apr. 3, 1987, Technical Papers. Volume 6 - Image data processing p 55 A88-21062
Refining image segmentation by polygon skeletonization p 56 A88-21068
Application of frequency filtering in remotely sensed imagery p 57 A88-21072
Landsat remote sensing imagery analysis program p 57 A88-21075
Introduction to the physics and techniques of remote sensing --- Book p 65 A88-21168
Remote sensing science applications in arid environments p 3 A88-21351
Aerial and ground spectral characteristics of rangeland plant communities in Nevada p 3 A88-21353
Suitability of spectral indices for evaluating vegetation characteristics on arid rangelands p 3 A88-21355
Satellite remote sensing of drought conditions p 3 A88-21357
Aircraft and satellite remote sensing of desert soils and landscapes p 3 A88-21358
Satellite remote sensing of Australian rangelands p 4 A88-21361
Detection of yearly cover change with Landsat MSS on pastoral landscapes in central Australia p 4 A88-21362
The use of spectral and spatial variability to monitor cover change on inert landscapes p 4 A88-21363
Reflectance modeling of semiarid woodlands p 4 A88-21364
Spectral assessment of indicators of range degradation in the Botswana hardveld environment p 5 A88-21365
Modelling radar backscatter from vegetation p 5 A88-21501
The Earth-Observation Preparatory Programme p 66 A88-22724
Remote sensing of wave patterns with oceanographic implications p 31 A88-23545
Multiband-scatterometer data analysis of forests p 5 A88-23548
Integrating sphere transmissometer for field measurement of leaf transmittance p 6 A88-23766
Single-source three-dimensional imaging system for remote sensing p 66 A88-23772
An application of divergence measurement using transformed video data p 6 A88-24510
Using remotely sensed data for census surveys and population estimation in developing countries - Examples from Nigeria p 18 A88-24511
Remote sensing of forest cover distribution in the Phu Wiang watershed area of Khon Kaen Province, Northeast of Thailand p 6 A88-24514
Effect of ice-grain size distribution on the thermal emission of snow cover p 52 A88-24662
Asian Conference on Remote Sensing, 7th, Seoul, Republic of Korea, Oct. 23-28, 1986, Proceedings p 66 A88-24818
Spectral changes in conifers subjected to air pollution and water stress: Experimental studies p 6 A88-24932
The application of perceptual color spaces to the display of remotely sensed imagery p 58 A88-24935
A transformation for ordering multispectral data in terms of image quality with implications for noise removal p 58 A88-24937
Differences in vegetation indices for simulated Landsat-5 MSS and TM, NOAA-9 AVHRR, and SPOT-1 sensor systems p 7 A88-25446
Characteristics of the subsurface radar sounding of natural objects p 26 A88-25551
Remote sensing of water vapor convergence, deep convection, and precipitation over the tropical Pacific Ocean during the 1982-1983 El Nino p 33 A88-25728
Remote sensing methods and instrumentation for obtaining data on earth resources and the environment p 66 A88-26050
Observations of ocean and sea bottom relief from space p 35 A88-26099
Sea ice and sea-surface temperatures in the Strait of Fram according to NOAA-AVHRR data p 35 A88-26131
The legal problems of the commercialization of satellite remote sensing p 35 A88-26149

Polarized and non-polarized leaf reflectances of *Coleus blumei* p 7 A88-26624
The onset of spring melt in first-year ice regions of the Arctic as determined from scanning multichannel microwave radiometer data for 1979 and 1980 p 37 A88-27016
Calculations of ocean-atmosphere radiance on the basis of remote sensing p 37 A88-27204
Choosing conditions for the remote sensing of ocean features in the visible spectrum, with the effect of coastal zone taken into account p 37 A88-27209
The efficiency of polarization measurements in passive remote sensing of the ocean in the visible spectrum p 38 A88-27210
A method for synthesizing optimal space systems for earth surveying p 67 A88-27214
The relationships between orbit parameters and the geometry of the trajectory for remote sensing satellites p 67 A88-27215
Complex remote monitoring of lakes --- Russian book p 52 A88-27741
Remote sensing from space: Proceedings of Symposium 3, Workshop V, and Topical Meeting A2 of the Twenty-sixth COSPAR Plenary Meeting, Toulouse, France, June 30-July 11, 1986 p 67 A88-27801
Relations between canopy reflectance, photosynthesis and transpiration - Links between optics, biophysics and canopy architecture p 8 A88-27802
Remote sensing surveys design in regional agricultural inventories p 8 A88-27804
Spectral and botanical classification of grasslands - Auxois example p 8 A88-27805
Estimation of biophysical properties of forest canopies using C-band microwave data p 9 A88-27809
Importance of a remote measurement of spectral thermal infrared emissivities - Presentation and validation of such a determination p 67 A88-27813
Remote sensing of soil moisture p 52 A88-27815
Analyzing long-term changes in vegetation with geographic information system and remotely sensed data p 10 A88-27820
Comprehensive studies of the dynamics of geosystems with the use of remote sensing techniques p 10 A88-27821
Atmospheric effect on spectral signature - Measurements p 58 A88-27822
Proposed uses of ERS-1 p 68 A88-27833
Speckle in SAR images - An evaluation of filtering techniques p 59 A88-27834
Characterizing forest stands with multi-incidence angle and multi-polarized SAR data p 10 A88-27836
Swath altimetry of oceans and terrain p 39 A88-27838
Detection of oil films by active and passive microwave sensors p 39 A88-27840
Extraction of spectral hemispherical reflectance (albedo) of surfaces from nadir and directional reflectance data p 59 A88-28009
Measurement of canopy interception of solar radiation by stands of trees in sparsely wooded savanna p 10 A88-28010
Determining the rate of forest conversion in Mato Grosso, Brazil, using Landsat MSS and AVHRR data p 10 A88-28011
Evaluation of several classification schemes for mapping forest cover types in Michigan p 10 A88-28012
Principles of field spectroscopy p 68 A88-28013
Identification and measurement of the areal extent of settlements from Landsat - An exploration into the Nigerian case p 19 A88-28014
Mapping NOAA-AVHRR imagery using equal-area radial projections p 10 A88-28015
Terrestrial imaging spectroscopy p 69 A88-28266
Use of airborne imaging spectrometer data to map minerals associated with hydrothermally altered rocks in the Northern Grapevine Mountains, Nevada, and California p 26 A88-28267
Discrimination of hydrothermal alteration mineral assemblages at Virginia City, Nevada, using the airborne imaging spectrometer p 27 A88-28268
Comparison of techniques for discriminating hydrothermal alteration minerals with Airborne Imaging Spectrometer data p 27 A88-28269
Remote sensing of forest canopy and leaf biochemical contents p 11 A88-28270
Comparison of in situ and airborne spectral measurements of the blue shift associated with forest decline p 11 A88-28271
Preliminary assessment of airborne imaging spectrometer and airborne thematic mapper data acquired for forest decline areas in the Federal Republic of Germany p 11 A88-28272
Exploration of crustal/mantle material for the earth and moon using reflectance spectroscopy p 27 A88-28273

The use of space technology for the remote sensing of earth resources and mapping p 69 A88-28447
Thematic mapper and SPOT integration with a geographic information system p 59 A88-28602
Remote sensing and geographic information system techniques for aquatic resource evaluation p 19 A88-28603
Microwave remote sensing of ice in Lake Melville and the Labrador Sea p 39 A88-28850
Shuttle imaging radar A analysis of land use in Amazonia p 12 A88-29282
The acquisition of SPOT-1 HRV imagery over southern Britain and northern France, May 1986-May 1987 p 60 A88-29286
Methods for processing radio-physical measurement data in studies of the environment --- Russian book p 19 A88-29427
An integrated approach for automated cover-type mapping of large inaccessible areas in Alaska p 60 A88-29491
Detection and identification of Arctic landforms - An assessment of remotely sensed data p 40 A88-29492
Information content of spectral signatures and textures and structures for remote sensing of the earth p 60 A88-29499
The use of the optical classification of ocean waters to estimate correlations between the concentrations of variable components with reference to the development of remote-sensing methods p 41 A88-30078
Relationship between brightness temperature in the RF range and the radiative dryness index p 69 A88-30082
Estimation of the accuracy of determining atmospheric temperature profiles from microwave remote sensing at frequencies of 117-118.5 GHz p 41 A88-30084
Current status and problems of satellite investigations of the ocean (Review of non-Soviet publications) p 41 A88-30089
Calculation of canopy bidirectional reflectance using the Monte Carlo method p 13 A88-30439
Estimation of wheat canopy resistance using combined remotely sensed spectral reflectance and thermal observations p 13 A88-30448
Remote sensing of the sea surface p 42 A88-30662
Applications of microwaves to remote sensing p 69 A88-30670
Microwave vegetation index - A new long-term global data set for biospheric studies p 14 A88-32658
Simulation of solar zenith angle effect on global vegetation index (GVI) data p 14 A88-32660
Vegetative and optical characteristics of four-row crop canopies p 14 A88-32661
Radiometric leaf area index p 14 A88-32662
Evaluation of middle and thermal infrared radiance in indices used to estimate GLAI p 14 A88-32663
Crop canopy spectral reflectance p 14 A88-32664
An integrated camera and radiometer for aerial monitoring of vegetation p 14 A88-32666
Review of the potential of satellite remote sensing for marine flood protection p 43 A88-15280
[IOS-237] p 43 A88-15280
From pattern to process: The strategy of the Earth Observing System: Volume 2: EOS Science Steering Committee report [NASA-TM-89702] p 70 A88-15283
SAR (Synthetic Aperture Radar). Earth observing system. Volume 2F: Instrument panel report [NASA-TM-89701] p 70 A88-15284
The influence of yellow substances on remote sensing of sea water constituents from space. Volume 1: Summary p 43 A88-15292
[ESA-CR(P)-2443-VOL-1] p 43 A88-15292
The influence of yellow substances on remote sensing of sea water constituents from space. Volume 2: Appendices p 43 A88-15293
[ESA-CR(P)-2443-VOL-2] p 43 A88-15293
Multistep component analysis of correlations p 61 A88-16115
Commercial applications and scientific research requirements for thermal-infrared observations of terrestrial surfaces p 70 A88-16179
[NASA-TM-89704] p 70 A88-16179
Ocean Colour Workshop --- conference [ESA-SP-1083] p 45 A88-16292
Overview of ESA's activities in ocean colour remote sensing p 45 A88-16294
Remote sensing of ocean colour for studies of biological productivity and biochemical cycles p 45 A88-16296
Technical aspects of future ocean colour remote sensing p 46 A88-16298
Status and prospects of the Joint Research Committee (JRC) work on the application of ocean colour monitoring from space p 46 A88-16299
Canadian activities and goals in remote sensing of ocean colour and fluorescence from space p 46 A88-16300

- Federal Republic of Germany's interests, activities and goals in remote sensing of ocean colour/fluorescence from space p 46 N88-16302
- Italian activities in ocean colour remote sensing p 46 N88-16304
- National Remote Sensing Program (NRSP) of the Netherlands p 46 N88-16305
- The use of chlorophyll fluorescence measurements from space for separating constituents of sea water p 47 N88-16307
- The influence of yellow substances on remote sensing of sea-water constituents from space p 47 N88-16308
- Construction of airborne radars for remote sensing [PB88-113063] p 71 N88-16916
- Report of the Workshop on Space Systems Possibilities for a Global Energy and Water Cycle Experiment [WCP-137] p 53 N88-17147
- Space-based remote sensing of the Earth: A report to the Congress [NASA-TM-89709] p 72 N88-18046
- Remote sensing of atmospheric crosswinds by utilizing speckle-turbulence interaction and optical heterodyne detection [AD-A187580] p 71 N88-18052
- Evaluation of a temperature remote sensing technique [AD-A187885] p 71 N88-18053
- Coordination: Southeast continental shelf studies [DE88-003680] p 49 N88-18110
- Multisource context classification methods in remote sensing p 63 N88-18985
- General determination of Earth surface type and cloud amount using multispectral AVHRR data [NOAA-TR-NESDIS-39] p 72 N88-18997
- Report of the participation in the International Training Course: Remote Sensing in Village Forestry [INPE-4476-NTE/278] p 16 N88-19802
- Mapping of the mangroves of the Guanabara Bay through the utilization of remote sensing techniques [INPE-3942-TDL/229] p 16 N88-19804
- Research in remote sensing of vegetation [NASA-CR-182663] p 16 N88-19817
- National Severe Storms Laboratory, fiscal year 1987 [PB88-140108] p 72 N88-19863
- Photographic filters [INPE-4448-RPE/558] p 64 N88-20124
- REMOTE SENSORS**
- Near-real-time video systems for rangeland assessment p 4 A88-21360
- Autonomous control of image sensor for the optimal acquisition of ground information for dynamic analysis p 65 A88-21660
- Preliminary assessment of radiometric accuracies for MOS-1 sensors p 39 A88-29276
- Selecting the spatial resolution of satellite sensors required for global monitoring of land transformations p 20 A88-32659
- HIRIS (High-Resolution Imaging Spectrometer: Science opportunities for the 1990s. Earth observing system. Volume 2C: Instrument panel report [NASA-TM-89703] p 70 N88-15282
- SAR (Synthetic Aperture Radar). Earth observing system. Volume 2F: Instrument panel report [NASA-TM-89701] p 70 N88-15284
- Technical aspects of future ocean colour remote sensing p 46 N88-16298
- Developments in ocean colour research in the United Kingdom p 46 N88-16306
- Sea surface current estimates off central California as derived from enhanced AVHRR (Advanced Very High Resolution Radiometer) infrared images [AD-A186867] p 47 N88-17155
- Remote sensing of atmospheric optical thickness and sea-water attenuation when submerged: Wavelength selection and anticipated errors [AD-A187609] p 49 N88-19262
- Airborne electromagnetic sounding of sea ice thickness and sub-ice bathymetry [AD-A188939] p 50 N88-19879
- RESEARCH AND DEVELOPMENT**
- A proposed semi-supervised two stage classification technique p 56 A88-21063
- RESEARCH MANAGEMENT**
- WOCE Core Project 2 Planning Meeting: The Southern Ocean [WCP-138] p 44 N88-15348
- RESERVOIRS**
- Monitoring North Carolina's nutrient-sensitive reservoirs using Landsat TM digital data p 50 A88-21006
- Remote sensing of aquatic macrophyte distribution in selected South Carolina reservoirs p 51 A88-21007
- RESOURCES MANAGEMENT**
- Monitoring North Carolina's nutrient-sensitive reservoirs using Landsat TM digital data p 50 A88-21006
- Multispectral video survey of a Northern Ontario forest p 1 A88-21015
- Multi-stage remote sensing - A tool for Minnesota natural resources management p 64 A88-21018
- Geographic information systems for resource management: A compendium --- Book p 5 A88-23253
- Detection of soil erosion with Thematic Mapper (TM) satellite data within Pinyon-Juniper woodlands [NASA-CR-182476] p 15 N88-17103
- REVISIONS**
- Model-based building verification in aerial photographs [AD-A186010] p 20 N88-15278
- RHEOLOGY**
- Mantle rheology and satellite signatures from present-day glacial forcings p 21 A88-25225
- RIVER BASINS**
- Fluvial perturbation in the western Amazon basin - Regulation by long-term sub-Andean tectonics p 24 A88-20878
- Preliminary study of the characterization of the riverine forests of the Garonne using Landsat MSS and TM data p 9 A88-27811
- ROADS**
- Automated road network extraction from Landsat TM imagery p 18 A88-21044
- ROCKS**
- Nature and origin of mineral coatings on volcanic rocks of the Black Mountain, Stonewall Mountain, and Kane Springs Wash volcanic centers, Southern Nevada [NASA-CR-181437] p 29 N88-17140
- S**
- SALINITY**
- Landsat imagery for mapping saline soils and wet lands in north-west India p 12 A88-29278
- Physical properties of summer sea ice in the Fram Strait, June-July 1984 [AD-A186937] p 53 N88-17156
- SALTS**
- Size distributions of sea-source aerosol particles - A physical explanation of observed nearshore versus open-sea differences p 33 A88-25289
- SATELLITE ALTIMETRY**
- Interpretation of Seasat radar-altimeter data over sea ice using near-simultaneous SAR imagery p 31 A88-23547
- Potential applications of digital image analysis systems for displaying satellite altimetry data p 31 A88-23762
- Geosat altimeter observations of Kelvin waves and the 1986-87 El Nino p 32 A88-24582
- Swath altimetry of oceans and terrain p 39 A88-27838
- Gravity field mapping from satellite altimetry, sea-gravimetry and bathymetry in the Eastern Mediterranean p 42 A88-30836
- Thermal expansion of a rig --- oceanographic platform for satellite altimetry p 42 A88-32508
- An efficient algorithm for computing the crossovers in satellite altimetry [NASA-CR-182389] p 43 N88-15286
- On estimating the basin-scale ocean circulation from satellite altimetry. Part 1: Straightforward spherical harmonic expansion [NASA-CR-182387] p 44 N88-15352
- The effects of atmospheric and thermohaline variability on the validation of the GEOSAT altimeter oceanographic signal between Scotland and Iceland [AD-A189324] p 50 N88-19882
- SATELLITE IMAGERY**
- Hierarchical segmentation using a composite criterion for remotely sensed imagery p 54 A88-20841
- Operational revision of national topographic maps in Canada using Landsat images p 54 A88-20901
- Detection of subsurface geologic structures in the Tharthar area of central Iraq using Landsat images p 24 A88-20902
- Remote sensing applications - An outlook for the future p 64 A88-20904
- Development of multirate estuarine water quality models using Landsat 2 and 4 MSS data p 50 A88-21002
- Comparison of Landsat MSS pixel array sizes for estimating water quality variables in small lakes p 50 A88-21004
- Observations of surface and atmospheric features from passive microwave satellite measurements p 64 A88-21019
- Validating regional differences in modelled satellite microwave signatures p 1 A88-21020
- A time-lapse analysis of the Mississippi Delta using Landsat MSS Band 4 (IR2) photographic imagery p 51 A88-21039
- Evaluation of Thematic Mapper data for mapping tidal wetlands in South Carolina p 2 A88-21040
- Large-scale hurricane hazard mapping along the coastal plain of Honduras using Landsat data p 17 A88-21041
- Spectral enhancements of Landsat MSS and TM imagery applied to ground water investigations in Kenya p 51 A88-21042
- Automated road network extraction from Landsat TM imagery p 18 A88-21044
- A satellite image mosaic of Illinois p 55 A88-21047
- Comparison of the gridded finite element and the polynomial interpolations for geometric rectification and mosaicking of Landsat data p 55 A88-21049
- Detecting subpixel woody features using simulated multispectral and panchromatic SPOT imagery p 3 A88-21065
- A semi-automated training sample selector for multispectral land cover classification p 56 A88-21066
- A comparison of the hierarchical cluster and homogeneous training field detection methods in classifying urban landcovers from TM data p 56 A88-21067
- Landsat remote sensing imagery analysis program p 57 A88-21075
- Satellite observed seasonal and inter-annual variation of vegetation over the Kalahari, the Great Victoria Desert, and the Great Sandy Desert - 1979-1984 p 3 A88-21356
- Satellite remote sensing of Australian rangelands p 4 A88-21361
- Detection of yearly cover change with Landsat MSS on pastoral landscapes in central Australia p 4 A88-21362
- Satellite maps of Antarctic total ozone [AIAA PAPER 88-0210] p 30 A88-22154
- Contribution of SPOT images to the geological mapping of arid countries - Example of the Yemen Arab Republic p 25 A88-22616
- Preliminary SPOT results in Lorraine related to permanent grasslands p 5 A88-22617
- Assessment of SIR-B for topographic mapping p 57 A88-23761
- Quantification of biomass of the marsh grass Spartina alterniflora Loisel using Landsat Thematic Mapper imagery p 6 A88-23765
- Landsat classification of the barren hydrotelluric areas of Lake Yli-Kitka, north-eastern Finland p 51 A88-24198
- A snapshot of the Labrador current inferred from ice-floe movement in NOAA satellite imagery p 32 A88-24456
- The baroclinic circulation in Hudson Strait p 32 A88-24457
- The application of perceptual color spaces to the display of remotely sensed imagery p 58 A88-24935
- Registration of images with geometric distortions p 58 A88-24936
- A transformation for ordering multispectral data in terms of image quality with implications for noise removal p 58 A88-24937
- Satellite-derived color-temperature relationship in the Alboran Sea p 33 A88-25445
- Differences in vegetation indices for simulated Landsat-5 MSS and TM, NOAA-9 AVHRR, and SPOT-1 sensor systems p 7 A88-25446
- Geostrophical evolution of the Southern Alps - Lineaments trends detected on Landsat images p 26 A88-25448
- SPOT 1 - Earth observing satellite p 66 A88-26166
- Operational interpretation of AVHRR vegetation indices for world crop information p 7 A88-26335
- Assessment of thematic mapper imagery for forestry applications under Lake States conditions p 7 A88-26336
- Satellite observations of a western boundary current in the Bay of Bengal p 36 A88-27010
- Satellite passive microwave studies of the Sea of Okhotsk ice cover and its relation to oceanic processes, 1978-1982 p 36 A88-27014
- Multiple dipole eddies in the Alaska Coastal Current detected with Landsat thematic mapper data p 36 A88-27015
- The onset of spring melt in first-year ice regions of the Arctic as determined from scanning multichannel microwave radiometer data for 1979 and 1980 p 37 A88-27016
- Investigating the northern Caspian Sea ice regime from meteorological-satellite data p 37 A88-27202
- Computer-aided mapping of Antarctic Sea ice using along-the-course radiometric measurements aboard the Cosmos-1500 satellite p 38 A88-27213
- Monitoring of global vegetation dynamics for assessment of primary productivity using NOAA advanced very high resolution radiometer p 9 A88-27808
- Comprehensive studies of the dynamics of geosystems with the use of remote sensing techniques p 10 A88-27821
- Recent data quality and earth science results from the Landsat thematic mapper p 58 A88-27824

- Digital stereo processing of satellite image data
p 58 A88-27825
- Quantitative use of satellite SAR imagery of sea ice
p 39 A88-27839
- Extraction of spectral hemispherical reflectance (albedo) of surfaces from nadir and directional reflectance data
p 59 A88-28009
- Measurement of canopy interception of solar radiation by stands of trees in sparsely wooded savanna
p 10 A88-28010
- Determining the rate of forest conversion in Mato Grosso, Brazil, using Landsat MSS and AVHRR data
p 10 A88-28011
- Identification and measurement of the areal extent of settlements from Landsat - An exploration into the Nigerian case
p 19 A88-28014
- Mapping NOAA-AVHRR imagery using equal-area radial projections
p 10 A88-28015
- Thematic mapper and SPOT integration with a geographic information system
p 59 A88-28602
- The potential for automated mapping from Geocoded digital image data
p 59 A88-28604
- Evaluation of the stereoscopic accuracy of the SPOT satellite
p 59 A88-28605
- Land-cover monitoring with SPOT for landfill investigations
p 19 A88-28606
- Landsat imagery for mapping saline soils and wet lands in north-west India
p 12 A88-29278
- Comparison of submarine relief features on a radar satellite image and on a Skylab satellite photograph
p 40 A88-29279
- Forecasting patterns of soil erosion in arid lands from Landsat MSS data
p 12 A88-29280
- Comparison of Landsat MSS and SIR-A data for geological applications in Pakistan
p 27 A88-29281
- Atmospheric correction of thermal infrared images
p 40 A88-29283
- An improved method for detecting clear sky and cloudy radiances from AVHRR data
p 69 A88-29284
- The acquisition of SPOT-1 HRV imagery over southern Britain and northern France, May 1986-May 1987
p 60 A88-29286
- Relating Nimbus-7 37 GHz data to global land-surface evaporation, primary productivity and the atmospheric CO₂ concentration
p 60 A88-29287
- Multitemporal Landsat multispectral scanner and Thematic Mapper data of the Hubbard Glacier region, southeast Alaska
p 52 A88-29493
- Current status and problems of satellite investigations of the ocean (Review of non-Soviet publications)
p 41 A88-30089
- Exact Rayleigh scattering calculations for use with the Nimbus-7 Coastal Zone Color Scanner
p 41 A88-30415
- Identification and spectral characteristics of hydrothermal alteration on Landsat TM imagery of north Chile
p 27 A88-31125
- Large area crop classification in New South Wales, Australia, using Landsat data
p 14 A88-32665
- Review of the potential of satellite remote sensing for marine flood protection
p 43 A88-15280
- Space photographs of the Onega-Ladoga isthmus and prediction of useful minerals
p 28 A88-16108
- French activities in ocean colour observations
p 46 A88-16303
- Earthnet's experience with Seasat SAR image processing
p 62 A88-16760
- Detection of soil erosion with Thematic Mapper (TM) satellite data within Pinyon-Juniper woodlands
p 15 A88-17103
- Nature and origin of mineral coatings on volcanic rocks of the Black Mountain, Stonewall Mountain, and Kane Springs Wash volcanic centers, Southern Nevada
p 29 A88-17140
- Meteorological Information Extraction Center (MIEC) processing --- Meteosat imagery
p 71 A88-17143
- Application of satellite data in variational analysis for global cyclonic systems
p 62 A88-17152
- Character of five selected LANDSAT lineaments in southwestern Pennsylvania: Report of investigations, 1987
p 30 A88-18988
- Mesoscale monitoring of the soil freeze/thaw boundary from orbital microwave radiometry
p 17 A88-19855
- SATELLITE INSTRUMENTS**
- Estimates of primary productivity over the Thar Desert based upon Nimbus-7 37 GHz data - 1979-1985
p 11 A88-28016
- Estimating surface soil moisture from satellite microwave measurements and a satellite derived vegetation index
p 13 A88-30446

SATELLITE NETWORKS

- Method for joint adjustment of satellite and surface geodetic networks
p 22 A88-16105
- The orientation of global satellite networks
p 63 A88-18996

SATELLITE OBSERVATION

- Land cover change detection with Landsat MSS and TM data in the Kitchener-Waterloo area, Canada
p 18 A88-21071
- Satellite remote sensing of drought conditions
p 3 A88-21357
- Aircraft and satellite remote sensing of desert soils and landscapes
p 3 A88-21358
- Preliminary SPOT results in Lorraine related to permanent grasslands
p 5 A88-22617
- Interpretation of satellite imagery of a rapidly deepening cyclone
p 57 A88-23502
- On the accuracy of marine gravity measurements
p 21 A88-25224
- Mantle rheology and satellite signatures from present-day glacial forcings
p 21 A88-25225
- Observations of ocean and sea bottom relief from space
p 35 A88-26099
- SPOT 1 - Earth observing satellite
p 66 A88-26166
- Shelf water entrainment by Gulf Stream warm-core rings
p 36 A88-27013
- Comparison of total ozone amounts derived from satellite and ground-based measurements
p 66 A88-27027
- An investigation of small-offset fracture zone geoid waveforms
p 22 A88-27465
- Downward longwave irradiance at the ocean surface from satellite data - Methodology and in situ validation
p 38 A88-27493
- The Natal pulse - An extreme transient on the Agulhas Current
p 38 A88-27494
- The first ISLSCP field experiment (FIFE) --- International Satellite Land Surface Climatology Project
p 67 A88-27497
- Remote sensing from space; Proceedings of Symposium 3, Workshop V, and Topical Meeting A2 of the Twenty-sixth COSPAR Plenary Meeting, Toulouse, France, June 30-July 11, 1986
p 67 A88-27801
- Problems related to the determination of land surface parameters and fluxes over heterogeneous media from satellite data
p 19 A88-27803
- Remote sensing surveys design in regional agricultural inventories
p 8 A88-27804
- Determination of vegetated fraction of surface from satellite measurements
p 8 A88-27807
- Monitoring of global vegetation dynamics for assessment of primary productivity using NOAA advanced very high resolution radiometer
p 9 A88-27808
- Satellite observation of atmosphere and surface interaction parameters
p 38 A88-27812
- A global survey of surface climate parameters from satellite observations - Preliminary results over Africa
p 67 A88-27814
- Monitoring hydroclimatic characteristics using satellite observations from West Africa
p 52 A88-27816
- Evaluating North American net primary productivity with satellite observations
p 9 A88-27819
- Preliminary assessment of radiometric accuracies for MOS-1 sensors
p 39 A88-29276
- Principal component analysis of satellite passive microwave data over sea ice
p 41 A88-30199
- Review of the potential of satellite remote sensing for marine flood protection
p 43 A88-15280
- The influence of yellow substances on remote sensing of sea water constituents from space. Volume 1: Summary
p 43 A88-15292
- [ESA-CR(P)-2443-VOL-1]
p 43 A88-15292
- The influence of yellow substances on remote sensing of sea water constituents from space. Volume 2: Appendices
p 43 A88-15293
- [ESA-CR(P)-2443-VOL-2]
p 43 A88-15293
- The use of chlorophyll fluorescence measurements from space for separating constituents of sea water. Volume 1: Summary
p 43 A88-15294
- [ESA-CR(P)-2444-VOL-1]
p 43 A88-15294
- The use of chlorophyll fluorescence measurements from space for separating constituents of sea water. Volume 2: Appendices
p 44 A88-15295
- [ESA-CR(P)-2444-VOL-2]
p 44 A88-15295
- Satellite monitoring of earthquake precursor effects in magnetosphere
p 28 A88-16103
- Commercial applications and scientific research requirements for thermal-infrared observations of terrestrial surfaces
p 70 A88-16179
- [NASA-TM-89704]
p 70 A88-16179
- Proceedings of an ESA-NASA Workshop on a Joint Solid Earth Program
p 23 A88-19844
- [NASA-CR-182642]
p 23 A88-19844
- Spaceborne magnetometry
p 24 A88-19846

- Terrestrial gravity data and comparisons with satellite data
p 24 A88-19848

SATELLITE ORBITS

- The relationships between orbit parameters and the geometry of the trajectory for remote sensing satellites
p 67 A88-27215
- Identical-route satellite orbits for long-term periodic global survey of the earth, not dependent on solar illumination
p 67 A88-27216

SATELLITE SOUNDING

- A sequential estimation approach to cloud-clearing for satellite temperature sounding
p 66 A88-23511
- A method for the estimate of broadband directional surface albedo from a geostationary satellite
p 22 A88-27299
- The use of direct readout, high resolution TOVS data in short and medium range weather predictions
p 68 A88-27844
- Scatterometer wind speed bias induced by the large-scale component of the wave field
p 40 A88-29325
- Methods for processing radio-physical measurement data in studies of the environment --- Russian book
p 19 A88-29427
- Detection of internal waves using data from satellite microwave radiometry and the research ship Academician Alexander Nesmeianov
p 41 A88-30083
- The use of regression analysis to determine sea surface temperatures from Cosmos-1151 measurements of IR radiation
p 41 A88-30085
- Limiting accuracy of scatterometer determination of wind speed over ocean from satellite
p 44 A88-16107

SATELLITE TRACKING

- On differential scale changes and the satellite Doppler system z-shift
p 21 A88-25850

SATELLITE-BORNE INSTRUMENTS

- Wind-fetch dependence of Seasat scatterometer measurements
p 31 A88-23546
- Integrating sphere transmissometer for field measurement of leaf transmittance
p 6 A88-23766
- Source of the Australasian tektite strewn field - A possible off-shore impact site
p 42 A88-31793
- Selecting the spatial resolution of satellite sensors required for global monitoring of land transformations
p 20 A88-32659
- HIRIS (High-Resolution Imaging Spectrometer: Science opportunities for the 1990s. Earth observing system. Volume 2C: Instrument panel report
p 70 A88-15282
- [NASA-TM-89703]
p 70 A88-15282
- LANDSAT thematic mapper radiometric calibration study
p 61 A88-15287
- [NASA-CR-182410]
p 61 A88-15287
- Spaceborne gravity gradiometry characterizing the data type
p 24 A88-19847

SATELLITE-BORNE PHOTOGRAPHY

- Enigma of a thermal anomaly - A TM/AVHRR study of the volcanic Arabian highlands
p 25 A88-21045
- The Earth-Observation Preparatory Programme
p 66 A88-22724
- Techniques of geomorphological mapping on the basis of space photographs
p 26 A88-26708
- Interpretation of the visible manifestations of sea water dynamics from space imagers of the Caspian Sea
p 37 A88-27201
- A study to produce 1:100,000 scale LFC color photomap --- Large Format Camera
p 68 A88-27826
- The use of Meteor-Priroda space photographs for the compilation of small-scale and medium-scale tectonic and geological maps
p 27 A88-30079
- Karst and erosion topography on space photographs (With reference to the Ustiurt plateau)
p 60 A88-30080
- Investigation of the foci of powerful earthquakes and seismically hazardous areas on space photographs for the Baikal-Aldan region
p 27 A88-30081
- Adaptive computer-aided system for crop inventory according to space photographs
p 13 A88-30087
- Investigations on the application of space photographs (Spacelab metric camera) for routine inventories of extensively managed forest areas
p 15 A88-17098
- [DFVLR-FB-87-22]
p 15 A88-17098
- Oceanographic features of the east and southeast Indian Ocean for June 1983
p 47 A88-17158
- [AD-A186948]
p 47 A88-17158
- SATELLITE-BORNE RADAR**
- Measuring ocean waves from space
p 30 A88-20942
- Geometric accuracy testing of orbital radar imagery
p 57 A88-23760
- Remote sensing from space; Proceedings of Symposium 3, Workshop V, and Topical Meeting A2 of the Twenty-sixth COSPAR Plenary Meeting, Toulouse, France, June 30-July 11, 1986
p 67 A88-27801
- Simulation of bit-quantization influence on SAR images
p 59 A88-27831

- Design concept of the SAR installed on ERS-1 p 68 A88-27832
- Future research directions in the quantitative radar remote sensing of land and oceanic surface features p 39 A88-27841
- Analysis of algorithms for the retrieval of rain-rate profiles from a spaceborne dual-wavelength radar p 69 A88-28679
- SCALE (RATIO)**
- A study to produce 1:100,000 scale LFC color photomap --- Large Format Camera p 68 A88-27826
- SCANNERS**
- ISTP SBIR phase 1 Full-Sky Scanner: A feasibility study [NASA-CR-180749] p 71 N88-17964
- SCATTER PROPAGATION**
- Active and passive remote sensing of ice [AD-A186685] p 47 N88-17162
- SCATTERING COEFFICIENTS**
- Active and passive remote sensing of ice [AD-A186685] p 47 N88-17162
- SCATTEROMETERS**
- Wind-fetch dependence of Seasat scatterometer measurements p 31 A88-23546
- Multiband-scatterometer data analysis of forests p 5 A88-23548
- The DUT airborne scatterometer p 5 A88-23549
- Measurements of the backscatter and attenuation properties of forest stands at X-, C- and L-band p 7 A88-25444
- The use of a helicopter mounted ranging scatterometer for estimation of extinction and backscattering properties of forest canopies-I: Experimental approach and calibration p 11 A88-28682
- The use of a helicopter mounted ranging scatterometer for estimation of extinction and scattering properties of forest canopies-II: Experimental results for high-density aspen p 11 A88-28683
- Scatterometer wind speed bias induced by the large-scale component of the wave field p 40 A88-29325
- SCENE ANALYSIS**
- Problems related to the determination of land surface parameters and fluxes over heterogeneous media from satellite data p 19 A88-27803
- Thematic mapper research in the earth sciences: Small scale patches of suspended matter and phytoplankton in the Elbe River Estuary, German Bight and Tidal Flats [NASA-CR-182378] p 45 N88-16180
- General determination of Earth surface type and cloud amount using multispectral AVHRR data [NOAA-TR-NESDIS-39] p 72 N88-18997
- SEA GRASSES**
- Five New South Wales barrier lagoons: Their macrobenthic fauna and seagrass communities p 49 N88-19059
- SEA ICE**
- Interpretation of Seasat radar-altimeter data over sea ice using near-simultaneous SAR imagery p 31 A88-23547
- Observation of sea-ice dynamics using synthetic aperture radar images: Automated analysis p 32 A88-24934
- Sea ice and sea-surface temperatures in the Strait of Fram according to NOAA-AVHRR data p 35 A88-26131
- Satellite passive microwave studies of the Sea of Okhotsk ice cover and its relation to oceanic processes, 1978-1982 p 36 A88-27014
- The onset of spring melt in first-year ice regions of the Arctic as determined from scanning multichannel microwave radiometer data for 1979 and 1980 p 37 A88-27016
- Investigating the northern Caspian Sea ice regime from meteorological-satellite data p 37 A88-27202
- Computer-aided mapping of Antarctic Sea ice using along-the-course radiometric measurements aboard the Cosmos-1500 satellite p 38 A88-27213
- Quantitative use of satellite SAR imagery of sea ice p 39 A88-27839
- Microwave remote sensing of ice in Lake Melville and the Labrador Sea p 39 A88-28850
- Ice floe collisions and their relation to ice deformation in the Bering Sea during February 1983 p 40 A88-29324
- Principal component analysis of satellite passive microwave data over sea ice p 41 A88-30199
- Ice breakup - Observations of the acoustic signal p 41 A88-30200
- Physical properties of summer sea ice in the Fram Strait, June-July 1984 [AD-A186937] p 53 N88-17156
- Active and passive remote sensing of ice [AD-A186685] p 47 N88-17162
- NASA Oceanic Processes Program [NASA-TM-4025] p 48 N88-18109
- Airborne electromagnetic sounding of sea ice thickness and sub-ice bathymetry [AD-A188939] p 50 N88-19879
- SEA LEVEL**
- Geosat altimeter observations of Kelvin waves and the 1986-87 El Nino p 32 A88-24582
- SEA ROUGHNESS**
- An approximate model for the microwave brightness temperature of the sea p 31 A88-23544
- SEA SURFACE TEMPERATURE**
- North Atlantic thermohaline circulation during the past 20,000 years linked to high-latitude surface temperature p 30 A88-20978
- Relationships between monthly precipitation and SST variations in the tropical Pacific region p 65 A88-21382
- The western equatorial Pacific Ocean circulation study p 30 A88-22911
- Satellite-derived color-temperature relationship in the Alboran Sea p 33 A88-25445
- El Nino events and their relation to the Southern Oscillation - 1925-1986 p 33 A88-25726
- Sea surface temperature, low-level moisture, and convection in the tropical Pacific, 1982-1985 p 34 A88-25729
- An investigation of the El Nino-Southern Oscillation Cycle with statistical models. I - Predictor field characteristics. II - Model results p 34 A88-25731
- Remote forcing of sea surface temperature in the El Nino region p 34 A88-25732
- The role of synoptic scale processes in the transfer of sea surface temperature anomalies p 35 A88-26065
- Sea ice and sea-surface temperatures in the Strait of Fram according to NOAA-AVHRR data p 35 A88-26131
- The relationship between the temporal variability of ocean temperature and the meridional shifts of the intertropical convergence zone p 37 A88-27203
- Atmospheric correction of thermal infrared images p 40 A88-29283
- A model of the tropical Pacific sea surface temperature climatology p 40 A88-29323
- The use of regression analysis to determine sea surface temperatures from Cosmos-1151 measurements of IR radiation p 41 A88-30085
- Emissivity of pure and sea waters for the model sea surface in the infrared window regions p 42 A88-30445
- NASA Oceanic Processes Program [NASA-TM-4025] p 48 N88-18109
- Spatial-temporal variability of North Pacific sea surface temperature anomaly patterns p 49 N88-19058
- SEA WATER**
- On the problem of evolution of oceanic water composition in the Phanerozoic p 35 A88-26676
- Satellite observations of a western boundary current in the Bay of Bengal p 36 A88-27010
- Coastal upwelling and eddy development off Nova Scotia p 36 A88-27011
- Multiple dipole eddies in the Alaska Coastal Current detected with Landsat thematic mapper data p 36 A88-27015
- Interpretation of the visible manifestations of sea water dynamics from space imagers of the Caspian Sea p 37 A88-27201
- The use of the optical classification of ocean waters to estimate correlations between the concentrations of variable components with reference to the development of remote-sensing methods p 41 A88-30078
- Emissivity of pure and sea waters for the model sea surface in the infrared window regions p 42 A88-30445
- The influence of yellow substances on remote sensing of sea water constituents from space. Volume 1: Summary [ESA-CR(P)-2443-VOL-1] p 43 N88-15292
- The influence of yellow substances on remote sensing of sea water constituents from space. Volume 2: Appendices [ESA-CR(P)-2443-VOL-2] p 43 N88-15293
- The use of chlorophyll fluorescence measurements from space for separating constituents of sea water. Volume 1: Summary [ESA-CR(P)-2444-VOL-1] p 43 N88-15294
- The use of chlorophyll fluorescence measurements from space for separating constituents of sea water. Volume 2: Appendices [ESA-CR(P)-2444-VOL-2] p 44 N88-15295
- The use of chlorophyll fluorescence measurements from space for separating constituents of sea water p 47 N88-16307
- The influence of yellow substances on remote sensing of sea-water constituents from space p 47 N88-16308
- Sea surface current estimates off central California as derived from enhanced AVHRR (Advanced Very High Resolution Radiometer) infrared images [AD-A186867] p 47 N88-17155
- Remote sensing of atmospheric optical thickness and sea-water attenuation when submerged: Wavelength selection and anticipated errors [AD-A187609] p 49 N88-19262
- SEASAT SATELLITES**
- Wind-fetch dependence of Seasat scatterometer measurements p 31 A88-23546
- Interpretation of Seasat radar-altimeter data over sea ice using near-simultaneous SAR imagery p 31 A88-23547
- Geometric accuracy testing of orbital radar imagery p 57 A88-23760
- Digitized global land-sea map and access software p 35 A88-26346
- Radar altimeter data quality flagging p 39 A88-27837
- Scatterometer wind speed bias induced by the large-scale component of the wave field p 40 A88-29325
- Measurement of global oceanic winds from Seasat-SMMR and its comparison with Seasat-SASS and ALT derived winds p 40 A88-29766
- Earthnet's experience with Seasat SAR image processing p 62 N88-16760
- SECULAR VARIATIONS**
- North Atlantic thermohaline circulation during the past 20,000 years linked to high-latitude surface temperature p 30 A88-20978
- SEDIMENTS**
- North Atlantic thermohaline circulation during the past 20,000 years linked to high-latitude surface temperature p 30 A88-20978
- Geological evolution and analysis of confirmed or suspected gas hydrate localities. Volume 10: Basin analysis, formation and stability of gas hydrates of the Aleutian Trench and the Bering Sea [DE88-001008] p 29 N88-18048
- SEGMENTS**
- Hierarchical segmentation using a composite criterion for remotely sensed imagery p 54 A88-20841
- Refining image segmentation by polygon skeletonization p 56 A88-21068
- SEISMIC WAVES**
- Materials of the World Data Center B. Deep Seismic Sounding (DSS): Pacific data p 48 N88-17167
- SEISMOLOGY**
- Investigation of the foci of powerful earthquakes and seismically hazardous areas on space photographs for the Baikal-Aldan region p 27 A88-30081
- Use of space photographs for paleoseismogeological studies (on the example of Mongolian Altay) p 28 N88-16110
- SENSORS**
- ISTP SBIR phase 1 Full-Sky Scanner: A feasibility study [NASA-CR-180749] p 71 N88-17964
- SHALLOW WATER**
- Nearshore wave transformation study of sites near Port Canaveral Inlet, Florida [AD-A186965] p 47 N88-17159
- SHUTTLE IMAGING RADAR**
- Definition of forest stand characteristics based on multi-incidence angle SIR-B data p 2 A88-21031
- Characterization of vegetation with combined Thematic Mapper (TM) and Shuttle Imaging Radar (SIR-B) image data p 2 A88-21032
- Assessment of SIR-B for topographic mapping p 57 A88-23761
- A study on the utilization of SIR-A data for population estimation in the eastern part of Spain p 18 A88-24512
- Talemzane - Algerian impact crater detected on SIR-A orbital imaging radar p 25 A88-25217
- Geological and vegetational applications of Shuttle Imaging Radar-B, Mineral County, Nevada p 26 A88-26337
- Characterizing forest stands with multi-incidence angle and multi-polarized SAR data p 10 A88-27836
- Comparison of Landsat MSS and SIR-A data for geological applications in Pakistan p 27 A88-29281
- Shuttle imaging radar A analysis of land use in Amazonia p 12 A88-29282
- SIDE-LOOKING RADAR**
- Geologic applications of side-looking airborne radar images in the Appalachian Valley and Ridge Province p 24 A88-21034
- Application of data from the U.S. Geological Survey's side-looking airborne radar program p 25 A88-21036
- Methods and accuracy of operational digital image mapping with aircraft SAR p 55 A88-21059
- Geometric accuracy testing of orbital radar imagery p 57 A88-23760

- Synthetic aperture radar imagery of range traveling ocean waves p 32 A88-24933
Construction of airborne radars for remote sensing [PB88-113063] p 71 N88-16916
- SIGNAL ANALYSIS**
Ice breakup - Observations of the acoustic signal p 41 A88-30200
- SIGNAL MEASUREMENT**
The effects of atmospheric and thermohaline variability on the validation of the GEOSAT altimeter oceanographic signal between Scotland and Iceland [AD-A189324] p 50 N88-19882
- SIGNAL REFLECTION**
Correlation characteristics of images of the earth surface obtained with a synthetic-aperture radar p 66 A88-21784
- SIGNAL TO NOISE RATIOS**
A transformation for ordering multispectral data in terms of image quality with implications for noise removal p 58 A88-24937
- SIGNATURES**
The angular reflectance signature of the canopy hot spot in the optical regime [DE88-005385] p 15 N88-18991
- SIMULATION**
Gradiometer mission spectral analysis and simulation studies: Past and future p 24 N88-19851
- SITE SELECTION**
Land-cover monitoring with SPOT for landfill investigations p 19 A88-28606
- SITES**
Crustal Dynamics Project: Catalogue of site information [NASA-RP-1198] p 23 N88-19037
- SKY**
ISTP SBIR phase 1 Full-Sky Scanner: A feasibility study [NASA-CR-180749] p 71 N88-17964
- SNOW**
Active and passive remote sensing of ice [AD-A186635] p 47 N88-17162
- SNOW COVER**
Effect of ice-grain size distribution on the thermal emission of snow cover p 52 A88-24662
- SOIL EROSION**
An evaluation of the use of TM digital data for updating the land cover component of the SCS 1987 multiresource inventory of New Jersey --- soil conservation service p 1 A88-21013
Forecasting patterns of soil erosion in arid lands from Landsat MSS data p 12 A88-29280
Karst and erosion topography on space photographs (With reference to the Ustiurt plateau) p 60 A88-30080
- SOIL MAPPING**
Results of testing digital image measurements and enhancements on the remote work processing facility p 56 A88-21064
Spectral characteristics of selected soils and vegetation in northern Nevada and their discrimination using band ratio techniques p 3 A88-21352
Aircraft and satellite remote sensing of desert soils and landscapes p 3 A88-21358
Comparative study of temperature data from NOAA7-AVHRR and WMO - An interpretation through the use of a soil-vegetation model p 8 A88-27806
Landsat imagery for mapping saline soils and wet lands in north-west India p 12 A88-29278
The Earthnet Heat Capacity Mapping Mission (HCMM) data-processing system at Lannion (France) p 62 N88-16761
- SOIL MOISTURE**
Validating regional differences in modelled satellite microwave signatures p 1 A88-21020
Geological and vegetational applications of Shuttle Imaging Radar-B, Mineral County, Nevada p 26 A88-26337
Remote sensing of soil moisture p 52 A88-27815
Relating Nimbus-7 37 GHz data to global land-surface evaporation, primary productivity and the atmospheric CO2 concentration p 60 A88-29287
Estimating surface soil moisture from satellite microwave measurements and a satellite derived vegetation index p 13 A88-30446
Applications of microwaves to remote sensing p 69 A88-30670
- SOIL SCIENCE**
Landsat imagery for mapping saline soils and wet lands in north-west India p 12 A88-29278
The unsteady ground heat flow at the contact surface between a glacier run and the subsoil p 53 N88-16147
- SOILS**
Size distributions of sea-source aerosol particles - A physical explanation of observed nearshore versus open-sea differences p 33 A88-25289

- The emissivity of the vegetation-soil system p 8 A88-27208
- Detection of soil erosion with Thematic Mapper (TM) satellite data within Pinyon-Juniper woodlands [NASA-CR-182476] p 15 N88-17103
- SOLAR POSITION**
Simulation of solar zenith angle effect on global vegetation index (GVI) data p 14 A88-32660
- SOLAR RADIATION**
A canopy reflectance model based on an analytical solution to the multiple scattering equation p 7 A88-25447
Measurement of canopy interception of solar radiation by stands of trees in sparsely wooded savanna p 10 A88-28010
The anisotropy of reflected solar radiation over several types of land surface p 62 N88-16171
- SOLID STATE DEVICES**
Remote sensing of soil moisture p 52 A88-27815
- SOLID SUSPENSIONS**
The influence of yellow substances on remote sensing of sea-water constituents from space p 47 N88-16308
- SOUNDING**
Materials of the World Data Center B. Deep Seismic Sounding (DSS): Pacific data p 48 N88-17167
Airborne electromagnetic sounding of sea ice thickness and sub-ice bathymetry [AD-A188939] p 50 N88-19879
- SOUTHERN OSCILLATION**
El Nino events and their relation to the Southern Oscillation - 1925-1986 p 33 A88-25726
Longitudinal variations in tropical tropopause properties in relation to tropical convection and El Nino-Southern Oscillation events p 33 A88-25727
An investigation of the El Nino-Southern Oscillation Cycle with statistical models. I - Predictor field characteristics. II - Model results p 34 A88-25731
On the evolution of the southern oscillation p 36 A88-26923
- SPACE BASED RADAR**
Simulation of spaceborne SAR imagery from airborne SAR data p 58 A88-27830
- SPACE COMMERCIALIZATION**
The legal problems of the commercialization of satellite remote sensing p 35 A88-26149
Space-based remote sensing of the Earth: A report to the Congress [NASA-TM-89709] p 72 N88-18046
- SPACE LAW**
The legal problems of the commercialization of satellite remote sensing p 35 A88-26149
- SPACE SHUTTLE PAYLOADS**
Geographical position plotting by photo interpreters from Space Shuttle Large Format Camera photography p 65 A88-21050
- SPACE-TIME FUNCTIONS**
Spatial-temporal variability of North Pacific sea surface temperature anomaly patterns p 49 N88-19058
- SPACEBORNE PHOTOGRAPHY**
Geographical position plotting by photo interpreters from Space Shuttle Large Format Camera photography p 65 A88-21050
Parallax bar heighting accuracy of large format camera photography p 65 A88-21051
Comparison of submarine relief features on a radar satellite image and on a Skylab satellite photograph p 40 A88-29279
Space applications in geography p 22 N88-16104
Use of space photographs for geomorphological studies in southwestern Tajikistan p 28 N88-16109
Academic course Space Methods for Studying Modern Landscapes of Continents p 72 N88-16133
Photogrammetric principles for combining remote sounding and three-dimensional mapping p 61 N88-16135
- SPACECRAFT TRAJECTORIES**
The relationships between orbit parameters and the geometry of the trajectory for remote sensing satellites p 67 A88-27215
- SPACELAB PAYLOADS**
Investigations on the application of space photographs (Spacelab metric camera) for routine inventories of extensively managed forest areas [DFVLR-FB-87-22] p 15 N88-17098
- SPATIAL DISTRIBUTION**
The use of chlorophyll fluorescence measurements from space for separating constituents of sea water. Volume 1: Summary [ESA-CR(P)-2444-VOL-1] p 43 N88-15294
The use of chlorophyll fluorescence measurements from space for separating constituents of sea water. Volume 2: Appendices [ESA-CR(P)-2444-VOL-2] p 44 N88-15295

SPATIAL RESOLUTION

- Interrelationships between spatial resolution and per-pixel classifiers for extracting information classes. I - The urban environment. II - The natural environment p 17 A88-21014
Selecting the spatial resolution of satellite sensors required for global monitoring of land transformations p 20 A88-32659
HIRIS (High-Resolution Imaging Spectrometer: Science opportunities for the 1990s. Earth observing system. Volume 2C: Instrument panel report [NASA-TM-89703] p 70 N88-15282
- SPECIES DIFFUSION**
Remote sensing of aquatic macrophyte distribution in selected South Carolina reservoirs p 51 A88-21007
- SPECKLE PATTERNS**
Speckle in SAR images - An evaluation of filtering techniques p 59 A88-27834
- SPECTRA**
Estimation of sea surface wave spectra using acoustic tomography [AD-A187837] p 49 N88-19057
- SPECTRAL CORRELATION**
Multistep component analysis of correlations p 61 N88-16115
- SPECTRAL RECONNAISSANCE**
The role of anisotropy in the long range reconnaissance of the albedo of land surfaces p 62 N88-16169
- SPECTRAL REFLECTANCE**
Spectral characteristics of selected soils and vegetation in northern Nevada and their discrimination using band ratio techniques p 3 A88-21352
Aerial and ground spectral characteristics of rangeland plant communities in Nevada p 3 A88-21353
Surface anisotropy and hemispheric reflectance for a semiarid ecosystem p 3 A88-21354
The use of spectral and spatial variability to monitor cover change on inert landscapes p 4 A88-21363
Reflectance modeling of semiarid woodlands p 4 A88-21364
Spectral assessment of indicators of range degradation in the Botswana hardveld environment p 5 A88-21365
Canopy reflectance of seven rangeland plant species with variable leaf pubescence p 5 A88-23764
Remote sensing of forest cover distribution in the Phu Wiang watershed area of Khon Kaen Province, Northeast of Thailand p 6 A88-24514
Spectral changes in conifers subjected to air pollution and water stress: Experimental studies p 6 A88-24932
A canopy reflectance model based on an analytical solution to the multiple scattering equation p 7 A88-25447
Polarized and non-polarized leaf reflectances of *Coleus blumei* p 7 A88-26624
Relations between canopy reflectance, photosynthesis and transpiration - Links between optics, biophysics and canopy architecture p 8 A88-27802
Spectral and botanical classification of grasslands - Auxois example p 8 A88-27805
Simulations of the Meteosat visible sensor response to changing boundary conditions p 67 A88-27823
Extraction of spectral hemispherical reflectance (albedo) of surfaces from nadir and directional reflectance data p 59 A88-28009
Comparison of in situ and airborne spectral measurements of the blue shift associated with forest decline p 11 A88-28271
Calculation of canopy bidirectional reflectance using the Monte Carlo method p 13 A88-30439
Crop canopy spectral reflectance p 14 A88-32664
Monte Carlo method calculation of spectral brightness coefficient of vegetation cover as function of illumination conditions p 14 N88-16113
Research in remote sensing of vegetation [NASA-CR-182663] p 16 N88-19817
- SPECTRAL RESOLUTION**
HIRIS (High-Resolution Imaging Spectrometer: Science opportunities for the 1990s. Earth observing system. Volume 2C: Instrument panel report [NASA-TM-89703] p 70 N88-15282
- SPECTRAL SIGNATURES**
Atmospheric effect on spectral signature - Measurements p 58 A88-27822
Comparison of techniques for discriminating hydrothermal alteration minerals with Airborne Imaging Spectrometer data p 27 A88-28269
Information content of spectral signatures and textures and structures for remote sensing of the earth p 60 A88-29499
- SPECTROMETERS**
Evaluation of a temperature remote sensing technique [AD-A187885] p 71 N88-18053

SPECTRORADIOMETERS

- Canopy reflectance of seven rangeland plant species with variable leaf pubescence p 5 A88-23764
Principles of field spectroscopy p 68 A88-28013

SPECTROSCOPY

- Principles of field spectroscopy p 68 A88-28013

SPECTRUM ANALYSIS

- Nature and origin of mineral coatings on volcanic rocks of the Black Mountain, Stonewall Mountain, and Kane Springs Wash volcanic centers, Southern Nevada [NASA-CR-181437] p 29 N88-17140
Gradiometer mission spectral analysis and simulation studies: Past and future p 24 N88-19851

SPIN

- ISTP SBIR phase 1 Full-Sky Scanner: A feasibility study [NASA-CR-180749] p 71 N88-17964

SPLINE FUNCTIONS

- Registration of images with geometric distortions p 58 A88-24936

SPOT (FRENCH SATELLITE)

- Contribution of SPOT images to the geological mapping of arid countries - Example of the Yemen Arab Republic p 25 A88-22616
Preliminary SPOT results in Lorraine related to permanent grasslands p 5 A88-22617
SPOT 1 - Earth observing satellite p 66 A88-26166
Evaluation of the stereoscopic accuracy of the SPOT satellite p 59 A88-28605
Land-cover monitoring with SPOT for landfill investigations p 19 A88-28606

SPRAY CHARACTERISTICS

- Spray droplet generation, transport, and evaporation in a wind wave tunnel during the humidity exchange over the sea experiments in the simulation tunnel p 38 A88-27492

SPRAYERS

- Spray droplet generation, transport, and evaporation in a wind wave tunnel during the humidity exchange over the sea experiments in the simulation tunnel p 38 A88-27492

SPRING (SEASON)

- The onset of spring melt in first-year ice regions of the Arctic as determined from scanning multichannel microwave radiometer data for 1979 and 1980 p 37 A88-27016

STATISTICAL ANALYSIS

- An investigation of the El Nino-Southern Oscillation Cycle with statistical models. I - Predictor field characteristics. II - Model results p 34 A88-25731
Statistical model of interaction of electromagnetic waves with natural objects being sensed p 70 N88-16112
Statistics of two-dimensional structure elements of mountainous ranges (mosaic model) for calculating three-dimensional reflection functions [DFVLR-FB-87-33] p 29 N88-17099

STATISTICAL DISTRIBUTIONS

- Five New South Wales barrier lagoons: Their macrobenthic fauna and seagrass communities p 49 N88-19059
Design of the primary pre-TRMM and TRMM ground truth site [NASA-CR-182609] p 53 N88-19865

STEERABLE ANTENNAS

- Definition of forest stand characteristics based on multi-incidence angle SIR-B data p 2 A88-21031

STEREOPHOTOGRAPHY

- Difficulties and recommendations for obtaining very large scale 70 mm aerial photography for rangeland monitoring p 1 A88-21017
Automated photointerpretation - A stereoscopic workstation p 54 A88-21027
Digital stereo processing of satellite image data p 58 A88-27825
Evaluation of the stereoscopic accuracy of the SPOT satellite p 59 A88-28605

STEREOSCOPY

- Parallax bar heighting accuracy of large format camera photography p 65 A88-21051
Single-source three-dimensional imaging system for remote sensing p 66 A88-23772

STORMS

- National Severe Storms Laboratory, fiscal year 1987 [PB88-140108] p 72 N88-19863

STRAITS

- The baroclinic circulation in Hudson Strait p 32 A88-24457

STRATEGIC MATERIALS

- International role of US geoscience [NASA-CR-182407] p 28 N88-16281

STRATIGRAPHY

- North Atlantic thermohaline circulation during the past 20,000 years linked to high-latitude surface temperature p 30 A88-20978

- Geological evolution and analysis of confirmed or suspected gas hydrate localities. Volume 10: Basin analysis, formation and stability of gas hydrates of the Aleutian Trench and the Bering Sea [DE88-001008] p 29 N88-18048

STRUCTURAL BASINS

- On estimating the basin-scale ocean circulation from satellite altimetry. Part 1: Straightforward spherical harmonic expansion [NASA-CR-182387] p 44 N88-15352

STRUCTURAL PROPERTIES (GEOLOGY)

- Geostrucural evolution of the Southern Alps - Lineaments trends detected on Landsat images p 26 A88-25448
Statistics of two-dimensional structure elements of mountainous ranges (mosaic model) for calculating three-dimensional reflection functions [DFVLR-FB-87-33] p 29 N88-17099
Character of five selected LANDSAT lineaments in southwestern Pennsylvania: Report of investigations, 1987 [PB88-133517] p 30 N88-18988

SUBARCTIC REGIONS

- North Pacific Ocean. Central Pacific Transition Zone, R/V Thomas G. Thompson: 25 March - 3 May 1968. STD data report [AD-A186570] p 47 N88-17160

SUDDEN STORM COMMENCEMENTS

- National Severe Storms Laboratory, fiscal year 1987 [PB88-140108] p 72 N88-19863

SUGAR CANE

- Report on phase 1 of the project estimate development of a model for yield estimation of sugar cane based on LANDSAT and agromet data [INPE-4466-RPE/560] p 16 N88-19807

SUMMER

- Physical properties of summer sea ice in the Fram Strait, June-July 1984 [AD-A186937] p 53 N88-17156

SUPERHIGH FREQUENCIES

- Sea return at C and Ku bands p 31 A88-22947
X-band features of canopy cover - An up to date summary of active and passive measurements p 10 A88-27835
Investigation of the quantitative determination of two dimensional sea surface wave spectra from shipborne radar measurements [GKSS-87/E/10] p 48 N88-17163

SURFACE DISTORTION

- Registration of images with geometric distortions p 58 A88-24936

SURFACE PROPERTIES

- The use of remote sensing in developing and validating a ground hydrology/vegetation model for GCM3 - general circulation models p 51 A88-21021
Information content of spectral signatures and textures and structures for remote sensing of the earth p 60 A88-29499
Airborne elect-omagnetic sounding of sea ice thickness and sub-ice bathymetry [AD-A186939] p 50 N88-19879

SURFACE TEMPERATURE

- The emissivity of the vegetation-soil system p 8 A88-27208
Comparative study of temperature data from NOAA7-AVHRR and WMO - An interpretation through the use of a soil-vegetation model p 8 A88-27806
Satellite observation of atmosphere and surface interaction parameters p 38 A88-27812
Importance of a remote measurement of spectral thermal infrared emissivities - Presentation and validation of such a determination p 67 A88-27813
Sea surface current estimates off central California as derived from enhanced AVHRR (Advanced Very High Resolution Radiometer) infrared images [AD-A186867] p 47 N88-17155

SURFACE WATER

- Evaluation of X-band SAR imagery for mapping open surface water in the northeastern United States p 51 A88-21038

SURFACE WAVES

- Investigation of the quantitative determination of two dimensional sea surface wave spectra from shipborne radar measurements [GKSS-87/E/10] p 48 N88-17163
Estimation of sea surface wave spectra using acoustic tomography [AD-A187837] p 49 N88-19057

SURVEILLANCE

- Automatic knowledge acquisition for aerial image interpretation [AD-A188616] p 63 N88-19810

SURVEYS

- Surveying with GPS in Australia p 71 N88-18986

SUSPENDING (MIXING)

- Thematic mapper research in the earth sciences: Small scale patches of suspended matter and phytoplankton in the Elbe River Estuary, German Bight and Tidal Flats [NASA-CR-182378] p 45 N88-16180

SWATH WIDTH

- Swath altimetry of oceans and terrain p 39 A88-27838

SWITZERLAND

- Research in Switzerland on ocean and inland-water colour monitoring p 46 N88-16301

SYNCHRONOUS SATELLITES

- A method for the estimate of broadband directional surface albedo from a geostationary satellite p 22 A88-27299

SYNOPTIC MEASUREMENT

- The role of synoptic scale processes in the transfer of sea surface temperature anomalies p 35 A88-26065

SYNTHETIC APERTURE RADAR

- Definition of forest stand characteristics based on multi-incidence angle SIR-B data p 2 A88-21031
Parametric analysis of synthetic aperture radar data for characterization of deciduous forest stands p 2 A88-21033
Image based SAR product simulation for analysis p 55 A88-21037
Evaluation of X-band SAR imagery for mapping open surface water in the northeastern United States p 51 A88-21038
Correlation characteristics of images of the earth surface obtained with a synthetic-aperture radar p 66 A88-21784

- Remote sensing of wave patterns with oceanographic implications p 31 A88-23545
Interpretation of Seasat radar-altimeter data over sea ice using near-simultaneous SAR imagery p 31 A88-23547

- Assessment of SIR-B for topographic mapping p 57 A88-23761

- Application of predictive compression methods to synthetic aperture radar imagery I p 57 A88-23768

- A study on the utilization of SIR-A data for population estimation in the eastern part of Spain p 18 A88-24512

- Synthetic aperture radar imagery of range traveling ocean waves p 32 A88-24933

- Observation of sea-ice dynamics using synthetic aperture radar images: Automated analysis p 32 A88-24934

- Geological and vegetational applications of Shuttle Imaging Radar-B, Mineral County, Nevada p 26 A88-26337

- Simulation of spaceborne SAR imagery from airborne SAR data p 58 A88-27830

- Simulation of bit-quantization influence on SAR images p 59 A88-27831

- Design concept of the SAR installed on ERS-1 p 68 A88-27832

- Speckle in SAR images - An evaluation of filtering techniques p 59 A88-27834

- Characterizing forest stands with multi-incidence angle and multi-polarized SAR data p 10 A88-27836

- Quantitative use of satellite SAR imagery of sea ice p 39 A88-27839

- Future research directions in the quantitative radar remote sensing of land and oceanic surface features p 39 A88-27841

- Radiometric correction of C-band imagery for topographic effects in regions of moderate relief p 59 A88-28680

- SAR imaging of volume scatterers p 60 A88-28681

- Microwave remote sensing of ice in Lake Melville and the Labrador Sea p 39 A88-28850

- Texture study of Synthetic Aperture Radar (SAR) images of ocean surfaces [AD-A186021] p 42 N88-15101

- SAR (Synthetic Aperture Radar). Earth observing system. Volume 2F: Instrument panel report [NASA-TM-89701] p 70 N88-15284

- Earthnet's experience with Seasat SAR image processing p 62 N88-16760

SYSTEMS ANALYSIS

- Estimating forest productivity in southern Illinois using Landsat Thematic Mapper data and geographic information system analysis techniques p 2 A88-21028

SYSTEMS ENGINEERING

- A method for synthesizing optimal space systems for earth surveying p 67 A88-27214

- Design concept of the SAR installed on ERS-1 p 68 A88-27832

- SAR (Synthetic Aperture Radar). Earth observing system. Volume 2F: Instrument panel report [NASA-TM-89701] p 70 N88-15284

SYSTEMS INTEGRATION

- Thematic mapper and SPOT integration with a geographic information system p 59 A88-28602

T

TECHNOLOGICAL FORECASTING

- Remote sensing applications - An outlook for the future p 64 A88-20904

TECHNOLOGY ASSESSMENT

- The development and state of the art of remote sensing p 64 A88-20903

TECHNOLOGY UTILIZATION

- Comparison of Landsat MSS and SIR-A data for geological applications in Pakistan p 27 A88-29281

TECTONICS

- Fluvial perturbation in the western Amazon basin - Regulation by long-term sub-Andean tectonics p 24 A88-20878

- The use of Meteor-Priroda space photographs for the compilation of small-scale and medium-scale tectonic and geological maps p 27 A88-30079

- Thematic mapper study of Alaskan ophiolites [NASA-CR-182554] p 30 A88-18984

TEKTITES

- Source of the Australasian tektite strewn field - A possible off-shore impact site p 42 A88-31793

TEMPERATURE DISTRIBUTION

- Surface temperature variations of the world ocean in the Eocene p 32 A88-24655

- Comparative study of temperature data from NOAA7-AVHRR and WMO - An interpretation through the use of a soil-vegetation model p 8 A88-27806

TEMPERATURE MEASUREMENT

- Estimation of the accuracy of determining atmospheric temperature profiles from microwave remote sensing at frequencies of 117-118.5 GHz p 41 A88-30084

- The use of regression analysis to determine sea surface temperatures from Cosmos-1151 measurements of IR radiation p 41 A88-30085

TEMPERATURE MEASURING INSTRUMENTS

- Evaluation of a temperature remote sensing technique [AD-A187885] p 71 A88-18053

TEMPERATURE SENSORS

- Evaluation of a temperature remote sensing technique [AD-A187885] p 71 A88-18053

TEMPORAL RESOLUTION

- Multitemporal Landsat multispectral scanner and Thematic Mapper data of the Hubbard Glacier region, southeast Alaska p 52 A88-29493

TERMS

- Radar descriptors for the classification of terrain features [AD-A188145] p 63 A88-18983

TERRAIN

- Academic course Space Methods for Studying Modern Landscapes of Continents p 72 A88-16133

- The digital landmass simulation production overview [AD-A187978] p 62 A88-18978

- Three-dimensional image generation from an aerial photograph [AD-A188039] p 63 A88-18979

- Radar descriptors for the classification of terrain features [AD-A188145] p 63 A88-18983

- A digital terrain system for microcomputers [INPE-4170-PRE/1067] p 63 A88-18987

TERRAIN ANALYSIS

- Implementation of the Land Analysis System on a workstation p 54 A88-21026

- American Society for Photogrammetry and Remote Sensing and ACSM, Annual Convention, Baltimore, MD, Mar. 29-Apr. 3, 1987, Technical Papers. Volume 4 - Cartography p 21 A88-21058

- An automated system for terrain database construction p 18 A88-21060

- Digital terrain analysis employing X-Y-Z point vectors as input data p 55 A88-21061

- The downward continuation of aerial gravimetric data without density hypothesis p 21 A88-26347

- Determination of vegetated fraction of surface from satellite measurements p 8 A88-27807

- Problems in geologic and geomorphic interpretation and geometric modeling of radar images using a digital terrain model p 26 A88-28024

- Statistics of two-dimensional structure elements of mountainous ranges (mosaic model) for calculating three-dimensional reflection functions [DFVLR-FB-87-33] p 29 A88-17099

TEXTURES

- Information content of spectral signatures and textures and structures for remote sensing of the earth p 60 A88-29499

- Texture study of Synthetic Aperture Radar (SAR) images of ocean surfaces [AD-A186021] p 42 A88-15101

- Textural features for image classification in remote sensing [INPE-4169-PRE/1066] p 62 A88-16181

THEMATIC MAPPERS (LANDSAT)

- An evaluation of the use of TM digital data for updating the land cover component of the SCS 1987 multiresource inventory of New Jersey --- soil conservation service p 1 A88-21013

- Geobotanical detection of linear features in the Silver Mine area of southeastern Missouri p 25 A88-21043

- Automated road network extraction from Landsat TM imagery p 18 A88-21044

- Engima of a thermal anomaly - A TM/AVHRR study of the volcanic Arabian highlands p 25 A88-21045

- Assessment of thematic mapper imagery for forestry applications under Lake States conditions p 7 A88-26336

- Preliminary study of the characterization of the riverine forests of the Garonne using Landsat MSS and TM data p 9 A88-27811

- Recent data quality and earth science results from the Landsat thematic mapper p 58 A88-27824

- Determining the rate of forest conversion in Mato Grosso, Brazil, using Landsat MSS and AVHRR data p 10 A88-28011

- Use of airborne imaging spectrometer data to map minerals associated with hydrothermally altered rocks in the Northern Grapevine Mountains, Nevada, and California p 26 A88-28267

- Preliminary assessment of airborne imaging spectrometer and airborne thematic mapper data acquired for forest decline areas in the Federal Republic of Germany p 11 A88-28272

- Thematic mapper and SPOT integration with a geographic information system p 59 A88-28602

- Multitemporal Landsat multispectral scanner and Thematic Mapper data of the Hubbard Glacier region, southeast Alaska p 52 A88-29493

- Assessing forest damage in high-elevation coniferous forests in Vermont and New Hampshire using Thematic Mapper data p 13 A88-30440

- LANDSAT thematic mapper radiometric calibration study [NASA-CR-182410] p 61 A88-15287

- Thematic mapper research in the earth sciences: Small scale patches of suspended matter and phytoplankton in the Elbe River Estuary, German Bight and Tidal Flats [NASA-CR-182378] p 45 A88-16180

- Evaluation of the flooding areas of the Sao Goncalo Canal through LANDSAT 5 thematic mapper images [INPE-4118-PRE/1039] p 53 A88-16185

- Detection of soil erosion with Thematic Mapper (TM) satellite data within Pinyon-Juniper woodlands [NASA-CR-182476] p 15 A88-17103

- Operational revision of national topographic maps in Canada using Landsat images p 54 A88-20901

- Estimating forest productivity in southern Illinois using Landsat Thematic Mapper data and geographic information system analysis techniques p 2 A88-21028

- Characterization of vegetation with combined Thematic Mapper (TM) and Shuttle Imaging Radar (SIR-B) image data p 2 A88-21032

- Radar flood inundation mapping of upper Benue Trough, Nigeria p 2 A88-21035

- Evaluation of Thematic Mapper data for mapping tidal wetlands in South Carolina p 2 A88-21040

- Large-scale hurricane hazard mapping along the coastal plain of Honduras using Landsat data p 17 A88-21041

- Spectral enhancements of Landsat MSS and TM imagery applied to ground water investigations in Kenya p 51 A88-21042

- A satellite image mosaic of Illinois p 55 A88-21047

- Computer-assisted color generation for thematic mapping p 55 A88-21048

- A comparison of the hierarchical cluster and homogeneous training field detection methods in classifying urban landcovers from TM data p 56 A88-21067

- Land cover change detection with Landsat MSS and TM data in the Kitchener-Waterloo area, Canada p 18 A88-21071

- Land cover change detection using a GIS-guided, feature-based classification of Landsat thematic mapper data --- Geographic Information System p 18 A88-21073

- Contribution of SPOT images to the geological mapping of arid countries - Example of the Yemen Arab Republic p 25 A88-22616

- Quantification of biomass of the marsh grass *Spartina alterniflora* Loisel using Landsat Thematic Mapper imagery p 6 A88-23765

- Landsat classification of the barren hydrolittoral areas of Lake Yli-Kitka, north-eastern Finland p 51 A88-24198

- Spectral changes in conifers subjected to air pollution and water stress: Experimental studies p 6 A88-24932

- Techniques of geomorphological mapping on the basis of space photographs p 26 A88-26708

- Multiple dipole eddies in the Alaska Coastal Current detected with Landsat thematic mapper data p 36 A88-27015

- A new strategy for vegetation mapping with the aid of Landsat MSS data p 9 A88-27810

- Evaluation of several classification schemes for mapping forest cover types in Michigan p 10 A88-28012

- Discrimination of hydrothermal alteration mineral assemblages at Virginia City, Nevada, using the airborne imaging spectrometer p 27 A88-28268

- The potential for automated mapping from Geocoded digital image data p 59 A88-28604

- Identification and spectral characteristics of hydrothermal alteration on Landsat TM imagery of north Chile p 27 A88-31125

- Vegetative and optical characteristics of four-row crop canopies p 14 A88-32661

- Use of space photographs for geomorphological studies in southwestern Tajikistan p 28 A88-16109

- Thematic mapper research in the earth sciences: Small scale patches of suspended matter and phytoplankton in the Elbe River Estuary, German Bight and Tidal Flats [NASA-CR-182378] p 45 A88-16180

- Design and implementation of a data base system for Digital Land Mass System (DLMS) data [FEL-IR-1987-19] p 71 A88-17101

- Thematic mapper study of Alaskan ophiolites [NASA-CR-182554] p 30 A88-18984

- Terrestrial gravity data and comparisons with satellite data p 24 A88-19848

- Effect of ice-grain size distribution on the thermal emission of snow cover p 52 A88-24662

- Thermal expansion of a rig --- oceanographic platform for satellite altimetry p 42 A88-32508

- Processing and analysis of large volumes of satellite-derived thermal infrared data --- for physical oceanographic studies p 36 A88-27012

- Atmospheric correction of thermal infrared images p 40 A88-29283

- Importance of a remote measurement of spectral thermal infrared emissivities - Presentation and validation of such a determination p 67 A88-27813

- Commercial applications and scientific research requirements for thermal-infrared observations of terrestrial surfaces [NASA-TM-89704] p 70 A88-16179

- Use of the thermodynamic evaporation formula of Hoffmann in energy balance models for flowing water p 52 A88-16143

- Geological evolution and analysis of confirmed or suspected gas hydrate localities. Volume 10: Basin analysis, formation and stability of gas hydrates of the Aleutian Trench and the Bering Sea [DE88-001008] p 29 A88-18048

- Airborne electromagnetic sounding of sea ice thickness and sub-ice bathymetry [AD-A188939] p 50 A88-19879

- Three-dimensional transient electromagnetic modeling for exploration geophysics p 29 A88-18047

- Evaluation of Thematic Mapper data for mapping tidal wetlands in South Carolina p 2 A88-21040

- Measuring crown cover in interior Alaska vegetation types p 12 A88-29495

- Assessing forest damage in high-elevation coniferous forests in Vermont and New Hampshire using Thematic Mapper data p 13 A88-30440

- Application of the Global Positioning System (GPS) time receivers to the fundamental station Wettzell p 71 A88-18995

- The use of direct readout, high resolution TOVS data in short and medium range weather predictions p 68 A88-27844

TITANIUM

The space metal: All about titanium --- Russian book
p 25 A88-24781

TOMOGRAPHY

Estimation of sea surface wave spectra using acoustic tomography
[AD-A187837] p 49 N88-19057

TOPOGRAPHY

Operational revision of national topographic maps in Canada using Landsat images p 54 A88-20901
Assessment of SIR-B for topographic mapping p 57 A88-23761

Observations of ocean and sea bottom relief from space p 35 A88-26099
Radiometric correction of C-band imagery for topographic effects in regions of moderate relief p 59 A88-28680

Laser system for automating topographic terrain survey p 70 N88-16136
NASA Oceanic Processes Program [NASA-TM-4025] p 48 N88-18109

Automatic knowledge acquisition for aerial image interpretation [AD-A188616] p 63 N88-19810
Airborne electromagnetic sounding of sea ice thickness and sub-ice bathymetry [AD-A188939] p 50 N88-19879

TRAINING ANALYSIS

Report of the participation in the International Training Course: Remote Sensing in Village Forestry [INPE-4476-NTE/278] p 16 N88-19802

TRAJECTORY OPTIMIZATION

Identical-route satellite orbits for long-term periodic global survey of the earth, not dependent on solar illumination p 67 A88-27216

TRANSMISSOMETERS

Integrating sphere transmissometer for field measurement of leaf transmittance p 6 A88-23766

TRANSMITTANCE

Integrating sphere transmissometer for field measurement of leaf transmittance p 6 A88-23766

TRANSPARATION

Relations between canopy reflectance, photosynthesis and transpiration - Links between optics, biophysics and canopy architecture p 8 A88-27802
Relating seasonal patterns of the AVHRR vegetation index to simulated photosynthesis and transpiration of forests in different climates p 13 A88-30447

TRAVELING WAVES

Synthetic aperture radar imagery of range traveling ocean waves p 32 A88-24933

TREES (PLANTS)

Effects of fire on composition, biomass, and nutrients in oak scrub vegetation on John F. Kennedy Space Center, Florida [NASA-TM-100305] p 15 N88-16182

TRIANGULATION

Optimization of photogrammetric image adjustment [SER-C-323] p 22 N88-15289

TROPICAL METEOROLOGY

Relationships between monthly precipitation and SST variations in the tropical Pacific region p 65 A88-21382
Simultaneity of response of Atlantic Ocean tropical cyclones and Indian monsoons p 34 A88-25736

A model of the tropical Pacific sea surface temperature climatology p 40 A88-28323

TROPICAL REGIONS

Longitudinal variations in tropical tropopause properties in relation to tropical convection and El Nino-Southern Oscillation events p 33 A88-25727
Sea surface temperature, low-level moisture, and convection in the tropical Pacific, 1982-1985 p 34 A88-25729

Geosat crossover analysis in the tropical Pacific. Part 1: Constrained sinusoidal crossover adjustment [NASA-CR-182391] p 43 N88-15285
Mapping of the mangroves of the Guanabarra Bay through the utilization of remote sensing techniques [INPE-3942-TDL/229] p 16 N88-19804

TROPOPAUSE

Longitudinal variations in tropical tropopause properties in relation to tropical convection and El Nino-Southern Oscillation events p 33 A88-25727

TROPOSPHERE

Size distributions of sea-source aerosol particles - A physical explanation of observed nearshore versus open-sea differences p 33 A88-25289
Sea surface temperature, low-level moisture, and convection in the tropical Pacific, 1982-1985 p 34 A88-25729

TURBULENCE

Remote sensing of atmospheric crosswinds by utilizing speckle-turbulence interaction and optical heterodyne detection [AD-A187580] p 71 N88-18052

TURBULENT MIXING

Structure and growth of the mixing layer over the Amazonian rain forest p 8 A88-27252

U**U.S.S.R.**

Geochemistry of continental volcanism --- Russian book p 27 A88-29431

U.S.S.R. SPACE PROGRAM

The use of space technology for the remote sensing of earth resources and mapping p 69 A88-28447

UK SPACE PROGRAM

Developments in ocean colour research in the United Kingdom p 46 N88-16306

UNDERGROUND STRUCTURES

Characteristics of the subsurface radar sounding of natural objects p 26 A88-25551

UNDERWATER OPTICS

The use of the optical classification of ocean waters to estimate correlations between the concentrations of variable components with reference to the development of remote-sensing methods p 41 A88-30078

UNITED NATIONS

System-wide medium-term environment programme for the period 1990-1995: Strategies of the United Nations system for the environment [UNEP/GC/SS.I/2] p 20 N88-19826

UNITED STATES

International role of US geoscience [NASA-CR-182407] p 28 N88-16281

UPWELLING WATER

Coastal upwelling and eddy development off Nova Scotia p 36 A88-27011
Blocking of the Benguela Current by a single anticyclone - Analysis of satellite and ship data p 41 A88-30077

V**VECTORS (MATHEMATICS)**

Digital terrain analysis employing X-Y-Z point vectors as input data p 55 A88-21061

VEGETATION

Characterization of vegetation with combined Thematic Mapper (TM) and Shuttle Imaging Radar (SIR-B) image data p 2 A88-21032
Spectral characteristics of selected soils and vegetation in northern Nevada and their discrimination using band ratio techniques p 3 A88-21352

Surface anisotropy and hemispheric reflectance for a semiarid ecosystem p 3 A88-21354
Suitability of spectral indices for evaluating vegetation characteristics on arid rangelands p 3 A88-21355

Satellite observed seasonal and inter-annual variation of vegetation over the Kalahari, the Great Victoria Desert, and the Great Sandy Desert - 1979-1984 p 3 A88-21356

Discriminating semiarid vegetation using airborne imaging spectrometer data - A preliminary assessment p 4 A88-21359
The DUT airborne scatterometer p 5 A88-23549

Operational interpretation of AVHRR vegetation indices for world crop information p 7 A88-26335
The emissivity of the vegetation-soil system p 8 A88-27208

A new strategy for vegetation mapping with the aid of Landsat MSS data p 9 A88-27810
Analyzing long-term changes in vegetation with geographic information system and remotely sensed data p 10 A88-27820

Intermediate-scale vegetation mapping of Innoko National Wildlife Refuge, Alaska using Landsat MSS digital data p 12 A88-29494
Selecting the spatial resolution of satellite sensors required for global monitoring of land transformations p 20 A88-32659

An integrated camera and radiometer for aerial monitoring of vegetation p 14 A88-32666
Effects of fire on composition, biomass, and nutrients in oak scrub vegetation on John F. Kennedy Space Center, Florida [NASA-TM-100305] p 15 N88-16182

Research in remote sensing of vegetation [NASA-CR-182663] p 16 N88-19817
Mesoscale monitoring of the soil freeze/thaw boundary from orbital microwave radiometry [NASA-CR-182659] p 17 N88-19855

VEGETATION GROWTH

Detecting subpixel woody features using simulated multispectral and panchromatic SPOT imagery p 3 A88-21065
Aircraft MSS data registration and vegetation classification for wetland change detection p 12 A88-29277

Relative sensitivity of Normalized Difference Vegetation Index (NDVI) and Microwave Polarization Difference Index (MPDI) for vegetation and desertification monitoring p 13 A88-30444

VEGETATIVE INDEX

Validating regional differences in modelled satellite microwave signatures p 1 A88-21020
The use of remote sensing in developing and validating a ground hydrology/vegetation model for GCM3 --- general circulation models p 51 A88-21021

Geobotanical detection of linear features in the Silver Mine area of southeastern Missouri p 25 A88-21043
Suitability of spectral indices for evaluating vegetation characteristics on arid rangelands p 3 A88-21355

Differences in vegetation indices for simulated Landsat-5 MSS and TM, NOAA-9 AVHRR, and SPOT-1 sensor systems p 7 A88-25446
Relations between canopy reflectance, photosynthesis and transpiration - Links between optics, biophysics and canopy architecture p 8 A88-27802

Determination of vegetated fraction of surface from satellite measurements p 8 A88-27807
Monitoring of global vegetation dynamics for assessment of primary productivity using NOAA advanced very high resolution radiometer p 9 A88-27808

A global survey of surface climate parameters from satellite observations - Preliminary results over Africa p 67 A88-27814
Evaluating North American net primary productivity with satellite observations p 9 A88-27819

Mapping NOAA-AVHRR imagery using equal-area radial projections p 10 A88-28015
Relative sensitivity of Normalized Difference Vegetation Index (NDVI) and Microwave Polarization Difference Index (MPDI) for vegetation and desertification monitoring p 13 A88-30444

Estimating surface soil moisture from satellite microwave measurements and a satellite derived vegetation index p 13 A88-30446
Relating seasonal patterns of the AVHRR vegetation index to simulated photosynthesis and transpiration of forests in different climates p 13 A88-30447

Estimation of wheat canopy resistance using combined remotely sensed spectral reflectance and thermal observations p 13 A88-30448
Microwave vegetation index - A new long-term global data set for biospheric studies p 14 A88-32658

Simulation of solar zenith angle effect on global vegetation index (GVI) data p 14 A88-32660

VERTICAL DISTRIBUTION

The use of direct readout, high resolution TOVS data in short and medium range weather predictions p 68 A88-27844

VERY LONG BASE INTERFEROMETRY

Crustal dynamics project data analysis, 1987. Volume 1: Fixed station VLBI geodetic results, 1979-1986 [NASA-TM-100682] p 23 N88-16279
Crustal dynamics project data analysis, 1987. Volume 2: Mobile VLBI geodetic results, 1982-1986 [NASA-TM-100689-VOL-2] p 23 N88-16280

VIDEO DATA

Multispectral video survey of a Northern Ontario forest p 1 A88-21015
Mid-infrared (1.45 to 2.0 microns) video - A potential aid in wildfire mop-up operations p 1 A88-21016

Principal component analysis of aerial video imagery p 54 A88-21030
Near-real-time video systems for rangeland assessment p 4 A88-21360

An application of divergence measurement using transformed video data p 6 A88-24510

VIDEO EQUIPMENT

Near-real-time video systems for rangeland assessment p 4 A88-21360

VISIBLE SPECTRUM

Choosing conditions for the remote sensing of ocean features in the visible spectrum, with the effect of coastal zone taken into account p 37 A88-27209
The efficiency of polarization measurements in passive remote sensing of the ocean in the visible spectrum p 38 A88-27210

The acquisition of SPOT-1 HRV imagery over southern Britain and northern France, May 1986-May 1987 p 60 A88-29286

VISUAL OBSERVATION

Observations of ocean and sea bottom relief from space p 35 A88-26099

VOLCANOES

Engima of a thermal anomaly - A TM/AVHRR study of the volcanic Arabian highlands p 25 A88-21045

VOLCANOLOGY

Geochemistry of continental volcanism --- Russian book p 27 A88-29431

VORTICES

Coastal upwelling and eddy development off Nova Scotia p 36 A88-27011

- Multiple dipole eddies in the Alaska Coastal Current detected with Landsat thematic mapper data p 36 A88-27015
- Blocking of the Benguela Current by a single anticyclone - Analysis of satellite and ship data p 41 A88-30077

W

WASTE DISPOSAL

- Land-cover monitoring with SPOT for landfill investigations p 19 A88-28606

WATER CIRCULATION

- The baroclinic circulation in Hudson Strait p 32 A88-24457
- Surface temperature variations of the world ocean in the Eocene p 32 A88-24655
- Coastal upwelling and eddy development off Nova Scotia p 36 A88-27011
- Interpretation of the visible manifestations of sea water dynamics from space imagers of the Caspian Sea p 37 A88-27201
- Blocking of the Benguela Current by a single anticyclone - Analysis of satellite and ship data p 41 A88-30077

WATER COLOR

- Satellite-derived color-temperature relationship in the Alboran Sea p 33 A88-25445
- The influence of yellow substances on remote sensing of sea water constituents from space. Volume 1: Summary [ESA-CR(P)-2443-VOL-1] p 43 A88-15292
- The influence of yellow substances on remote sensing of sea water constituents from space. Volume 2: Appendices [ESA-CR(P)-2443-VOL-2] p 43 A88-15293
- Ocean Colour Workshop --- conference [ESA-SP-1083] p 45 A88-16292
- Europe's position concerning ocean colour activities p 45 A88-16293
- Overview of ESA's activities in ocean colour remote sensing p 45 A88-16294
- Update of NASA's ocean colour activities p 45 A88-16295
- Remote sensing of ocean colour for studies of biological productivity and biochemical cycles p 45 A88-16296
- Ocean colour applications in ocean dynamics and coastal processes p 45 A88-16297
- Technical aspects of future ocean colour remote sensing p 46 A88-16298
- Federal Republic of Germany's interests, activities and goals in remote sensing of ocean colour/fluorescence from space p 46 A88-16302
- French activities in ocean colour observations p 46 A88-16303
- Italian activities in ocean colour remote sensing p 46 A88-16304
- National Remote Sensing Program (NRSP) of the Netherlands p 46 A88-16305
- Developments in ocean colour research in the United Kingdom p 46 A88-16306

WATER CURRENTS

- Use of the thermodynamic evaporation formula of Hoffmann in energy balance models for flowing water p 52 A88-16143

WATER DEPTH

- Landsat classification of the barren hydrolittoral areas of Lake Yli-Kitka, north-eastern Finland p 51 A88-24198

WATER EROSION

- A time-lapse analysis of the Mississippi Delta using Landsat MSS Band 4 (IR2) photographic imagery p 51 A88-21039

WATER POLLUTION

- A multi-frequency-multi-nadir-angle pushbroom-radiometer for oil spill detection and mapping (On the surface of the sea) [MBB-UR-952-87] p 31 A88-23988

WATER QUALITY

- Development of multivariate estuarine water quality models using Landsat 2 and 4 MSS data p 50 A88-21002
- Remote sensing of Chesapeake Bay water quality required for healthy oyster beds p 30 A88-21003
- Comparison of Landsat MSS pixel array sizes for estimating water quality variables in small lakes p 50 A88-21004

WATER RESOURCES

- Remote sensing and geographic information system techniques for aquatic resource evaluation p 19 A88-28603

WATER VAPOR

- Remote sensing of water vapor convergence, deep convection, and precipitation over the tropical Pacific Ocean during the 1982-1983 El Nino p 33 A88-25728

WATER WAVES

- Measuring ocean waves from space p 30 A88-20942

- Synthetic aperture radar imagery of range traveling ocean waves p 32 A88-24933

- Variations in the intensity of emitted and scattered microwave radiation of the sea surface sensed at grazing angles in a field of surface manifestations of internal waves p 37 A88-27205

- Detection of internal waves using data from satellite microwave radiometry and the research ship Academician Alexander Nesmeianov p 41 A88-30083

- Nearshore wave transformation study of sites near Port Canaveral Inlet, Florida [AD-A186965] p 47 A88-17159

- Investigation of the quantitative determination of two dimensional sea surface wave spectra from shipborne radar measurements [GKSS-87/E/10] p 48 A88-17163

WAVE ATTENUATION

- Measurements of the backscatter and attenuation properties of forest stands at X-, C- and L-band p 7 A88-25444

WAVE INTERACTION

- Parametric analysis of synthetic aperture radar data for characterization of deciduous forest stands p 2 A88-21033

WAVE SCATTERING

- Remote sensing of wave patterns with oceanographic implications p 31 A88-23545

WEATHER

- North Pacific Ocean. Central Pacific Transition Zone, R/V Thomas G. Thompson: 25 March - 3 May 1968. STD data report [AD-A186570] p 47 A88-17160
- Continental shelf processes affecting the oceanography of the South Atlantic Bight [DE88-004102] p 48 A88-17166
- Proceedings of the Forest-Atmosphere Interaction Workshop [CONF-8510250] p 17 A88-19824

WEATHER FORECASTING

- Remote sensing from space: Proceedings of Symposium 3, Workshop V, and Topical Meeting A2 of the Twenty-sixth COSPAR Plenary Meeting, Toulouse, France, June 30-July 11, 1986 p 67 A88-27801
- The use of direct readout, high resolution TOVS data in short and medium range weather predictions p 68 A88-27844
- Assessment of the use of satellite derived winds in monsoon forecasting using a general circulation model p 68 A88-27846
- National Severe Storms Laboratory, fiscal year 1987 [PB88-140108] p 72 A88-19863

WEIGHTING FUNCTIONS

- Five-diagonal weighting scheme for geoidal profiles [AD-A188033] p 23 A88-18054

WEST GERMANY

- Observations of Earth tides by the German Geodetic Research Institute, division 1, in the period 1979-1985 at the Berchtesgaden and Wetzell stations [SER-B-280] p 22 A88-15291
- Federal Republic of Germany's interests, activities and goals in remote sensing of ocean colour/fluorescence from space p 46 A88-16302

WETLANDS

- Evaluation of Thematic Mapper data for mapping tidal wetlands in South Carolina p 2 A88-21040
- Correlation between aircraft MSS and lidar remotely sensed data on a forested wetland p 6 A88-24513
- Aircraft MSS data registration and vegetation classification for wetland change detection p 12 A88-29277
- Landsat imagery for mapping saline soils and wet lands in north-west India p 12 A88-29278

WHEAT

- Estimation of wheat canopy resistance using combined remotely sensed spectral reflectance and thermal observations p 13 A88-30448

WILDLIFE

- The use of digital Landsat data for wildlife management on the Warm Springs Indian Reservation of Oregon p 2 A88-21029

WIND (METEOROLOGY)

- Remote sensing of atmospheric crosswinds by utilizing speckle-turbulence interaction and optical heterodyne detection [AD-A187580] p 71 A88-18052

WIND DIRECTION

- Remote sensing of atmospheric crosswinds by utilizing speckle-turbulence interaction and optical heterodyne detection [AD-A187580] p 71 A88-18052

WIND EFFECTS

- Mesoscale coastal ocean dynamics p 49 A88-19060

WIND MEASUREMENT

- Wind-fetch dependence of Seasat scatterometer measurements p 31 A88-23546

WIND PROFILES

- Assessment of the use of satellite derived winds in monsoon forecasting using a general circulation model p 68 A88-27846
- Measurement of global oceanic winds from Seasat-SMMR and its comparison with Seasat-SASS and ALT derived winds p 40 A88-29766
- Vertical sounding of the air layer close to a glacier on Mount Vernagferner in the Oetzal Alps, Tyrol (experiment LUZIVER 1983) p 44 A88-16152

WIND TUNNEL TESTS

- Spray droplet generation, transport, and evaporation in a wind wave tunnel during the humidity exchange over the sea experiments in the simulation tunnel p 38 A88-27492

WIND VELOCITY

- Measuring ocean waves from space p 30 A88-20942
- Gas exchange on Mono Lake and Crowley Lake, California p 52 A88-25735
- Measurement of global oceanic winds from Seasat-SMMR and its comparison with Seasat-SASS and ALT derived winds p 40 A88-29766

WIND VELOCITY MEASUREMENT

- Scatterometer wind speed bias induced by the large-scale component of the wave field p 40 A88-29325
- Limiting accuracy of scatterometer determination of wind speed over ocean from satellite p 44 A88-16107
- Vertical sounding of the air layer close to a glacier on Mount Vernagferner in the Oetzal Alps, Tyrol (experiment LUZIVER 1983) p 44 A88-16152

WINTER

- The ice thickness distribution across the Atlantic sector of the Antarctic Ocean in midwinter p 34 A88-25734

WOOD

- Detecting subpixel woody features using simulated multispectral and panchromatic SPOT imagery p 3 A88-21065

WORKSTATIONS

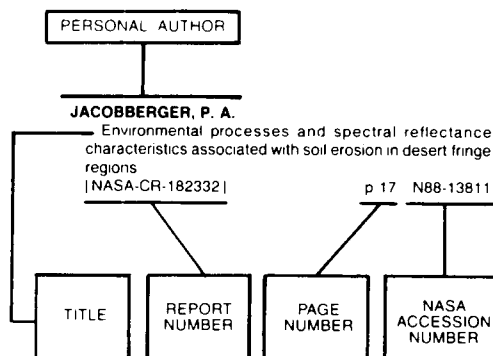
- Development of a 32-bit UNIX-based ELAS workstation p 54 A88-21025
- Implementation of the Land Analysis System on a workstation p 54 A88-21026

Z

ZENITH

- Simulation of solar zenith angle effect on global vegetation index (GVI) data p 14 A88-32660

Typical Personal Author Index Listing



Listings in this index are arranged alphabetically by personal author. The title of the document provides the user with a brief description of the subject matter. The report number helps to indicate the type of document listed (e.g., NASA report, translation, NASA contractor report). The page and accession numbers are located beneath and to the right of the title. Under any one author's name the accession numbers are arranged in sequence with the AIAA accession numbers appearing first.

A

- ABER, JOHN D.**
Remote sensing of forest canopy and leaf biochemical contents p 11 A88-28270
- ACHTEMEIER, G. L.**
Application of satellite data in variational analysis for global cyclonic systems [NASA-CR-182468] p 62 N88-17152
- ACKLEY, STEPHEN F.**
The ice thickness distribution across the Atlantic sector of the Antarctic Ocean in midwinter p 34 A88-25734
- ADENIYI, PETER O.**
Using remotely sensed data for census surveys and population estimation in developing countries - Examples from Nigeria p 18 A88-24511
- AHLNAS, KRISTINA**
Multiple dipole eddies in the Alaska Coastal Current detected with Landsat thematic mapper data p 36 A88-27015
- AHMAD, D.**
Remote sensing of forest cover distribution in the Phu Wiang watershed area of Khon Kaen Province, Northeast of Thailand p 6 A88-24514
- AHMAD, SURAIYA P.**
Surface anisotropy and hemispheric reflectance for a semiarid ecosystem p 3 A88-21354
- AIROLA, TEUVO M.**
An evaluation of the use of TM digital data for updating the land cover component of the SCS 1987 multisource inventory of New Jersey p 1 A88-21013
- AITKEN, DOUGLAS S.**
Computer-assisted color generation for thematic mapping p 55 A88-21048
- ALFULTIS, MICHAEL A.**
Satellite passive microwave studies of the Sea of Okhotsk ice cover and its relation to oceanic processes, 1978-1982 p 36 A88-27014
- ALI, ABDALLA ELSADIG**
Geometric accuracy testing of orbital radar imagery p 57 A88-23760
- ALI, JAWED**
Comparison of Landsat MSS and SIR-A data for geological applications in Pakistan p 27 A88-29281

- ALISHOUSE, JOHN C.**
Observations of surface and atmospheric features from passive microwave satellite measurements p 64 A88-21019
- ALIZAI, S. A. K.**
Comparison of Landsat MSS and SIR-A data for geological applications in Pakistan p 27 A88-29281
- ALLAM, R. J.**
The use of direct readout, high resolution TOVS data in short and medium range weather predictions p 68 A88-27844
- ALLAN, T. D.**
Review of the potential of satellite remote sensing for marine flood protection [IOS-237] p 43 N88-15280
- ALPERS, W.**
Detection of oil films by active and passive microwave sensors p 39 A88-27840
- ALPERS, WERNER**
Comparison of submarine relief features on a radar satellite image and on a Skylab satellite photograph p 40 A88-29279
- AMANN, V.**
The influence of yellow substances on remote sensing of sea water constituents from space. Volume 1: Summary [ESA-CR(P)-2443-VOL-1] p 43 N88-15292
The influence of yellow substances on remote sensing of sea water constituents from space. Volume 2: Appendices [ESA-CR(P)-2443-VOL-2] p 43 N88-15293
The use of chlorophyll fluorescence measurements from space for separating constituents of sea water. Volume 1: Summary [ESA-CR(P)-2444-VOL-1] p 43 N88-15294
The use of chlorophyll fluorescence measurements from space for separating constituents of sea water. Volume 2: Appendices [ESA-CR(P)-2444-VOL-2] p 44 N88-15295
- AMMER, ULRICH**
Preliminary assessment of airborne imaging spectrometer and airborne thematic mapper data acquired for forest decline areas in the Federal Republic of Germany p 11 A88-28272
- ANDERSON, MARK R.**
The onset of spring melt in first-year ice regions of the Arctic as determined from scanning multichannel microwave radiometer data for 1979 and 1980 p 37 A88-27016
- ANDRE, C. G.**
Enigma of a thermal anomaly - A TM/AVHRR study of the volcanic Arabian highlands p 25 A88-21045
- ANDREAE, M. O.**
Biomass-burning emissions and associated haze layers over Amazonia p 18 A88-27265
- ANDREEV, G. G.**
Remote sensing surveys design in regional agricultural inventories p 8 A88-27804
- ANGELL, JAMES K.**
Comparison of total ozone amounts derived from satellite and ground-based measurements p 66 A88-27027
- ANTON, IA. A.**
The emissivity of the vegetation-soil system p 8 A88-27208
- ANTONINETTI, MASSIMO**
Geostrucutural evolution of the Southern Alps - Lineaments trends detected on Landsat images p 26 A88-25448
- ANTONOVA, I. B.**
Space photographs of the Onega-Ladoga isthmus and prediction of useful minerals p 28 N88-16108
- ARABELOS, D.**
Gravity field mapping from satellite altimetry, sea-gravimetry and bathymetry in the Eastern Mediterranean p 42 A88-30836
- ARAI, KOHEI**
Preliminary assessment of radiometric accuracies for MOS-1 sensors p 39 A88-29276
- ARDANUY, PHILIP E.**
Remote sensing of water vapor convergence, deep convection, and precipitation over the tropical Pacific Ocean during the 1982-1983 El Nino p 33 A88-25728
- ARKANI-HAMED, JAFAR**
Remanent magnetization of the oceanic upper mantle p 37 A88-27036
- ARMAND, NEON ALEKSANDROVICH**
Methods for processing radio-physical measurement data in studies of the environment p 19 A88-29427
- ARNONE, ROBERT A.**
Satellite-derived color-temperature relationship in the Alboran Sea p 33 A88-25445
- ARTZ, R.**
Meteorological and aerosol measurements from the NOAA WP-3D aircraft during WATOX-86, January 4-9, 1986 [PB88-120860] p 20 N88-18079
- ASMUS, V. V.**
Adaptive computer-aided system for crop inventory according to space photographs p 13 A88-30087
- ASRAR, G.**
The first ISLSCP field experiment (FIFE) p 67 A88-27497
- ASSAD, E.**
Estimation of evapotranspiration in the Sahelian zone by use of Meteosat and NOAA AVHRR data p 9 A88-27818
- ASTLE, W. L.**
Monitoring of global vegetation dynamics for assessment of primary productivity using NOAA advanced very high resolution radiometer p 9 A88-27808
- ATKINSON, L. P.**
Continental shelf processes affecting the oceanography of the South Atlantic Bight [DE88-004102] p 48 N88-17166
- AUSTIN, R. W.**
Remote sensing of atmospheric optical thickness and sea-water attenuation when submerged: Wavelength selection and anticipated errors [AD-A187609] p 49 N88-19262

B

- BADHWAR, GAUTAM D.**
Estimation of biophysical properties of forest canopies using C-band microwave data p 9 A88-27809
The use of a helicopter mounted ranging scatterometer for estimation of extinction and backscattering properties of forest canopies-I: Experimental approach and calibration p 11 A88-28682
The use of a helicopter mounted ranging scatterometer for estimation of extinction and scattering properties of forest canopies-II: Experimental results for high-density aspen p 11 A88-28683
- BAGHERI, SIMA**
Groundwater identification using digitally enhanced NHAP p 51 A88-21011
- BAGROVA, Z. A.**
Space photographs of the Onega-Ladoga isthmus and prediction of useful minerals p 28 N88-16108
- BAKER, MICHAEL C. W.**
Identification and spectral characteristics of hydrothermal alteration on Landsat TM imagery of north Chile p 27 A88-31125
- BAKER, T. F.**
Review of the potential of satellite remote sensing for marine flood protection [IOS-237] p 43 N88-15280
- BAKOS, GEORGE Y. B.**
Detection of subsurface geologic structures in the Tharthar area of central Iraq using Landsat images p 24 A88-20902
- BALANDIN, V. A.**
Study of relief of ore regions using space images (on the example of Eastern Yakutia) p 28 N88-16111
- BALLINGER, M. Y.**
User's guide to a data base of current environmental monitoring projects in the US-Canadian transboundary region [DE88-002476] p 20 N88-17119

BALMINO, G.

Gradiometer mission spectral analysis and simulation studies: Past and future p 24 N88-19851

BARKER, JOHN L.

Recent data quality and earth science results from the Landsat thematic mapper p 58 A88-27824

BARNABA, EUGENIA M.

Land-cover monitoring with SPOT for landfill investigations p 19 A88-28606

BARNETT, TIM P.

An investigation of the El Nino-Southern Oscillation Cycle with statistical models. I - Predictor field characteristics. II - Model results p 34 A88-25731

BATISTA, GETULIO TEIXEIRA

Report on phase 1 of the project estimate development of a model for yield estimation of sugar cane based on LANDSAT and agromet data [INPE-4466-RPE/560] p 16 N88-19807

BEAL, ROBERT C.

Measuring ocean waves from space p 30 A88-20942

BECKER, F.

Problems related to the determination of land surface parameters and fluxes over heterogeneous media from satellite data p 19 A88-27803
Importance of a remote measurement of spectral thermal infrared emissivities - Presentation and validation of such a determination p 67 A88-27813

BECKER, FRANCOIS

Relative sensitivity of Normalized Difference Vegetation Index (NDVI) and Microwave Polarization Difference Index (MPDI) for vegetation and desertification monitoring p 13 A88-30444

BECKER, PAUL

Ice floe collisions and their relation to ice deformation in the Bering Sea during February 1983 p 40 A88-29324

BECKERING, A.

Status and prospects of the Joint Research Committee (JRC) work on the application of ocean colour monitoring from space p 46 N88-16299

BEGNI, G.

Evaluation of the stereoscopic accuracy of the SPOT satellite p 59 A88-28605

BEIER, NORBERT

Use of the thermodynamic evaporation formula of Hoffmann in energy balance models for flowing water p 52 N88-16143

BENDER, STEPHEN O.

Large-scale hurricane hazard mapping along the coastal plain of Honduras using Landsat data p 17 A88-21041

BENNETT, BRIAN S.

Computer-assisted color generation for thematic mapping p 55 A88-21048

BENNETT, ROBERT M.

An autoCAD-based mapping system for encoded stereoplotters p 60 A88-29490

BERGEN, WILLIAM R.

Application of frequency filtering in remotely sensed imagery p 57 A88-21072

BERMAN, MARK

A transformation for ordering multispectral data in terms of image quality with implications for noise removal p 58 A88-24937

BERRY, JOSEPH K.

Computer-assisted map analysis - A set of primitive operators for a flexible approach p 17 A88-21023

BETTINSON, M. D.

User's guide to a data base of current environmental monitoring projects in the US-Canadian transboundary region [DE88-002476] p 20 N88-17119

BHARGAVA, G. P.

Landsat imagery for mapping saline soils and wet lands in north-west India p 12 A88-29278

BIRD, JOHN M.

Thematic mapper study of Alaskan ophiolites [NASA-CR-182554] p 30 N88-18984

BIRKMAYER, W.

A multi-frequency-multi-nadir-angle pushbroom-radiometer for oil spill detection and mapping (On the surface of the sea) [MBB-UR-952-87] p 31 A88-23988

BISHOP, MICHAEL P.

Geobotanical detection of linear features in the Silver Mine area of southeastern Missouri p 25 A88-21043

BLAHA, GEORGES

Five-diagonal weighting scheme for geoidal profiles [AD-A188033] p 23 N88-18054

BLIUM, N. S.

Surface temperature variations of the world ocean in the Eocene p 32 A88-24655

BLODGET, H. W.

Engima of a thermal anomaly - A TM/AVHRR study of the volcanic Arabian highlands p 25 A88-21045

BOATMAN, J.

Size distributions of sea-source aerosol particles - A physical explanation of observed nearshore versus open-sea differences p 33 A88-25269

BONN, F.

Radiometric correction of C-band imagery for topographic effects in regions of moderate relief p 59 A88-28680

BONNEFOY, R. F.

The Earth-Observation Preparatory Programme p 66 A88-22724

BORENGASSER, M. X.

Geological and vegetational applications of Shuttle Imaging Radar-B, Mineral County, Nevada p 26 A88-26337

BOROVIKOV, A. M.

Investigation of the foci of powerful earthquakes and seismically hazardous areas on space photographs for the Baikal-Aldan region p 27 A88-30081

BOUCHER, C.

Geodetic application of the Global Positioning System p 21 A88-24269

BOW, SING T.

Autonomous control of image sensor for the optimal acquisition of ground information for dynamic analysis p 65 A88-21660

BOYLE, EDWARD A.

North Atlantic thermohaline circulation during the past 20,000 years linked to high-latitude surface temperature p 30 A88-20978

BRACEWELL, RONALD N.

Observation of sea-ice dynamics using synthetic aperture radar images: Automated analysis p 32 A88-24934

BRAUN, G.

A multi-frequency-multi-nadir-angle pushbroom-radiometer for oil spill detection and mapping (On the surface of the sea) [MBB-UR-952-87] p 31 A88-23988

BREIDO, M. D.

The use of successive clustering to analyze multispectral imagery p 61 A88-30086

BRIDGMAN, H.

Meteorological and aerosol measurements from the NOAA WP-3D aircraft during WATOX-86, January 4-9, 1986 [PB88-120860] p 20 N88-18079

BROCK, ROBERT

Results of testing digital image measurements and enhancements on the remote work processing facility p 56 A88-21064

BROCKMANN, C.

Thematic mapper research in the earth sciences: Small scale patches of suspended matter and phytoplankton in the Elbe River Estuary, German Bight and Tidal Flats [NASA-CR-182378] p 45 N88-16180

BROECKER, WALLACE S.

Gas exchange on Mono Lake and Crowley Lake, California p 52 A88-25735

BRON, J. C.

Design and implementation of a data base system for Digital Land Mass System (DLMS) data [FEL-IR-1987-19] p 71 N88-17101

BROOKS, REBECCA M.

Nearshore wave transformation study of sites near Port Canaveral Inlet, Florida [AD-A186965] p 47 N88-17159

BROWELL, E. V.

Biomass-burning emissions and associated haze layers over Amazonia p 18 A88-27265

BROWELL, EDWARD

Structure and growth of the mixing layer over the Amazonian rain forest p 8 A88-27252

BROWN, JAMES W.

Exact Rayleigh scattering calculations for use with the Nimbus-7 Coastal Zone Color Scanner p 41 A88-30415

BROWN, OTIS

Processing and analysis of large volumes of satellite-derived thermal infrared data p 36 A88-27012

BROWN, WILLIE A.

Nearshore wave transformation study of sites near Port Canaveral Inlet, Florida [AD-A186965] p 47 N88-17159

BROWNING, K. A.

Interpretation of satellite imagery of a rapidly deepening cyclone p 57 A88-23502

BRUNFELDT, DAVID R.

The use of a helicopter mounted ranging scatterometer for estimation of extinction and backscattering properties of forest canopies-I: Experimental approach and calibration p 11 A88-28682

BRYANT, N. A.

An automated system for terrain database construction p 18 A88-21060

BUCHHEIM, MARTIN P.

A semi-automated training sample selector for multispectral land cover classification p 56 A88-21066

BUELL, RUEDIGER H.

Statistics of two-dimensional structure elements of mountainous ranges (mosaic model) for calculating three-dimensional reflection functions [DFVLR-FB-87-33] p 29 N88-17099

BURGE, R. E.

SAR imaging of volume scatterers p 60 A88-28681

BURKE, W. R.

Meteorological Information Extraction Center (MIEC) processing [ESA-STR-224] p 71 N88-17143

BURLESHIN, M. I.

Karst and erosion topography on space photographs (With reference to the Ustiurt plateau) p 60 A88-30080

C**CADEAU, F.**

Multispectral video survey of a Northern Ontario forest p 1 A88-21015

CAMILLO, PETER

A canopy reflectance model based on an analytical solution to the multiple scattering equation p 7 A88-25447

CANE, MARK A.

A model of the tropical Pacific sea surface temperature climatology p 40 A88-29323

CAPPA, C.

Sea return at C and Ku bands p 31 A88-22947

CARD, DON H.

Remote sensing of forest canopy and leaf biochemical contents p 11 A88-28270

CARY, ERNESTINE

Determination of fraction of surface from satellite measurements p 8 A88-27807

CASANOVA, H.

Preliminary study of the characterization of the riverine forests of the Garonne using Landsat MSS and TM data p 9 A88-27811

CATHEY, LECONTE

Single-source three-dimensional imaging system for remote sensing p 66 A88-23772

CAVALERI, L.

Thermal expansion of a rig p 42 A88-32508

CHAHINE, MOUSTAFA T.

Satellite observation of atmosphere and surface interaction parameters p 38 A88-27812

CHALLENGER, P. G.

Review of the potential of satellite remote sensing for marine flood protection [IOS-237] p 43 N88-15280

CHANG, ALFRED

Estimating surface soil moisture from satellite microwave measurements and a satellite derived vegetation index p 13 A88-30446

CHANTARAPANICH, ALAI

Remote sensing of forest cover distribution in the Phu Wiang watershed area of Khon Kaen Province, Northeast of Thailand p 6 A88-24514

CHAPMAN, E. G.

User's guide to a data base of current environmental monitoring projects in the US-Canadian transboundary region [DE88-002476] p 20 N88-17119

CHEN, C. F.

Application of frequency filtering in remotely sensed imagery p 57 A88-21072

CHEN, DAVIDSON T.

Remote sensing of wave patterns with oceanographic implications p 31 A88-23545

CHENEY, ROBERT E.

Geosat altimeter observations of Kelvin waves and the 1986-87 El Nino p 32 A88-24582

CHENG, THOMAS D.

Development of a 32-bit UNIX-based ELAS workstation p 54 A88-21025

CHERNIAWSKY, JOSEF

The baroclinic circulation in Hudson Strait p 32 A88-24457

CHESHIRE, H. M.

Monitoring North Carolina's nutrient-sensitive reservoirs using Landsat TM digital data p 50 A88-21006

CHEWINGS, V. H.

Forecasting patterns of soil erosion in arid lands from Landsat MSS data p 12 A88-29280

CHIKISHEV, A. G.

Karst and erosion topography on space photographs (With reference to the Ustiurt plateau) p 60 A88-30080

D

- CHOROWICZ, JEAN**
Problems in geologic and geomorphic interpretation and geometric modeling of radar images using a digital terrain model p 26 A88-28024
- CHOU, SHU-SHIEN**
Airborne measurements of surface layer turbulence over the ocean during cold air outbreaks p 35 A88-26911
- CHOUDHURY, B. J.**
Satellite observed seasonal and inter-annual variation of vegetation over the Kalahari, the Great Victoria Desert, and the Great Sandy Desert - 1979-1984 p 3 A88-21356
Estimates of primary productivity over the Thar Desert based upon Nimbus-7 37 GHz data - 1979-1985 p 11 A88-28016
Relating Nimbus-7 37 GHz data to global land-surface evaporation, primary productivity and the atmospheric CO₂ concentration p 60 A88-29287
- CHOUDHURY, BHASKAR J.**
Satellite remote sensing of drought conditions p 3 A88-21357
Relative sensitivity of Normalized Difference Vegetation Index (NDVI) and Microwave Polarization Difference Index (MPDI) for vegetation and desertification monitoring p 13 A88-30444
Microwave vegetation index - A new long-term global data set for biospheric studies p 14 A88-32658
- CHRISTENSEN, E. J.**
Aircraft MSS data registration and vegetation classification for wetland change detection p 12 A88-29277
- CHRISTMANN, P.**
Contribution of SPOT images to the geological mapping of arid countries - Example of the Yemen Arab Republic p 25 A88-22616
- CHRISTOU, NIKOLAOS**
Potential applications of digital image analysis systems for displaying satellite altimetry data p 31 A88-23762
- CHUKHLANTSEV, A. A.**
Use of microwave radiometry for measuring the biometric characteristics of vegetation cover p 7 A88-27207
- CIESNIK, M.**
Geological evolution and analysis of confirmed or suspected gas hydrate localities. Volume 10: Basin analysis, formation and stability of gas hydrates of the Aleutian Trench and the Bering Sea [DE88-001008] p 29 N88-18048
- CINI, R.**
Sea return at C and Ku bands p 31 A88-22947
- CLARKE, KEITH C.**
Refining image segmentation by polygon skeletonization p 56 A88-21068
- COLEMAN, LELAND G.**
Three-dimensional image generation from an aerial photograph [AD-A188039] p 63 N88-18979
- CONNORS, K. F.**
Aircraft and satellite remote sensing of desert soils and landscapes p 3 A88-21358
- COOK, ELIZABETH A.**
Estimating forest productivity in southern Illinois using Landsat Thematic Mapper data and geographic information system analysis techniques p 2 A88-21028
- COOPER, CHARLES M.**
Comparison of Landsat MSS pixel array sizes for estimating water quality variables in small lakes p 50 A88-21004
- CORNILLON, PETER**
Processing and analysis of large volumes of satellite-derived thermal infrared data p 36 A88-27012
- CRAIG, MAURICE D.**
A transformation for ordering multispectral data in terms of image quality with implications for noise removal p 58 A88-24937
- CROUCH, JANICE L.**
The ARSUP database and its access through the CMCIRS catalog - Making available to the public digital maps from the ARSUP process p 60 A88-29496
- CUDDAPAH, PRABHAKARA**
Remote sensing of water vapor convergence, deep convection, and precipitation over the tropical Pacific Ocean during the 1982-1983 El Nino p 33 A88-25728
- CURIOTTO, S.**
Thermal expansion of a rig p 42 A88-32508
- CURRAN, P. J.**
Radiometric leaf area index p 14 A88-32662
- CUSHNIE, JANIS**
The acquisition of SPOT-1 HRV imagery over southern Britain and northern France, May 1986-May 1987 p 60 A88-29286
- CWICK, GARY J.**
Geobotanical detection of linear features in the Silver Mine area of southeastern Missouri p 25 A88-21043
- D'SOUZA, GILES**
Mapping NOAA-AVHRR imagery using equal-area radial projections p 10 A88-28015
- DAHLBERG, RICHARD E.**
A satellite image mosaic of Illinois p 55 A88-21047
- DAIDA, JASON M.**
Observation of sea-ice dynamics using synthetic aperture radar images: Automated analysis p 32 A88-24934
- DAMINOVA, T.**
Observations of ocean and sea bottom relief from space p 35 A88-26099
- DASCH, W.**
Hydrographic and current measurements in the North-East Atlantic Ocean. Data report on F.S. Meteor cruises 69/5 and 69/6, October to November 1984 [REPT-166] p 48 N88-17164
- DAUGHTRY, C. S. T.**
Differences in vegetation indices for simulated Landsat-5 MSS and TM, NOAA-9 AVHRR, and SPOT-1 sensor systems p 7 A88-25446
Polarized and non-polarized leaf reflectances of Coleus blumei p 7 A88-26624
- DAVIS, A. W.**
Reflectance modeling of semiarid woodlands p 4 A88-21364
- DAVIS, BRUCE A.**
Remote sensing of aquatic macrophyte distribution in selected South Carolina reservoirs p 51 A88-21007
- DAVIS, M. R.**
Mid-infrared (1.45 to 2.0 microns) video - A potential aid in wildfire mop-up operations p 1 A88-21016
- DAWBIN, KEN W.**
Large area crop classification in New South Wales, Australia, using Landsat data p 14 A88-32665
- DAY, R. L.**
Aircraft and satellite remote sensing of desert soils and landscapes p 3 A88-21358
- DE GAUJAC, A. C.**
Evaluation of the stereoscopic accuracy of the SPOT satellite p 59 A88-28605
- DEABREUSA, LEONARDO D.**
Crop forecasting in Brazil: A short history of productivity models [INPE-4150-PRE/1056] p 16 N88-19801
- DEALMEIDA, FAUSTO C.**
Crop forecasting in Brazil: A short history of productivity models [INPE-4150-PRE/1056] p 16 N88-19801
- DEAN, KENNEDON G.**
Detection and identification of Arctic landforms - An assessment of remotely sensed data p 40 A88-29492
- DEANE, JACQUELINE M.**
Modelling radar backscatter from vegetation p 5 A88-21501
- DEAVER, GREG H.**
Remote sensing applications by consulting engineers - Three case histories p 24 A88-21009
- DEDIEU, G.**
A global survey of surface climate parameters from satellite observations - Preliminary results over Africa p 67 A88-27814
- DEERING, D.**
Techniques of ground-truth measurements of desert-scrub structure p 9 A88-27817
- DEERING, DONALD W.**
Surface anisotropy and hemispheric reflectance for a semiarid ecosystem p 3 A88-21354
- DEFFERDING, J.**
User's guide to a data base of current environmental monitoring projects in the US-Canadian transboundary region [DE88-002476] p 20 N88-17119
- DEMEDEIROS, JOSE SIMEAO**
Report of the participation in the International Training Course: Remote Sensing in Village Forestry [INPE-4476-NTE/278] p 16 N88-19802
- DERENYI, EUGENE**
Potential applications of digital image analysis systems for displaying satellite altimetry data p 31 A88-23762
- DESCHAMPS, P. Y.**
A global survey of surface climate parameters from satellite observations - Preliminary results over Africa p 67 A88-27814
- DESER, CLARA**
El Nino events and their relation to the Southern Oscillation - 1925-1986 p 33 A88-25726
- DESYATYKH, YU. M.**
Laser system for automating topographic terrain survey p 70 N88-16136
- DEUTSCH, MORRIS**
Spectral enhancements of Landsat MSS and TM imagery applied to ground water investigations in Kenya p 51 A88-21042
- DEWITT, D. P.**
Integrating sphere transmissometer for field measurement of leaf transmittance p 6 A88-23766
- DEY, M. M.**
Remote sensing of forest cover distribution in the Phu Wiang watershed area of Khon Kaen Province, Northeast of Thailand p 6 A88-24514
- DIAS, LUIZ ALBERT VIEIRA**
A digital terrain system for microcomputers [INPE-4170-PRE/1067] p 63 N88-18987
- DIASVELASCO, FLAVIO ROBERTO**
A variant of the ISODATA algorithm for application to agricultural targets [INPE-4436-PRE/1235] p 17 N88-20023
- DICKEY, T. D.**
On the parameterization of irradiance for open ocean photoprocesses p 34 A88-25737
- DIEBEL-LANGOHR, D.**
The influence of yellow substances on remote sensing of sea water constituents from space. Volume 1: Summary [ESA-CR(P)-2443-VOL-1] p 43 N88-15292
The influence of yellow substances on remote sensing of sea water constituents from space. Volume 2: Appendices [ESA-CR(P)-2443-VOL-2] p 43 N88-15293
- DIGBY-ARGUS, SUSAN A.**
Microwave remote sensing of ice in Lake Melville and the Labrador Sea p 39 A88-28850
- DINER, D. J.**
Extraction of spectral hemispherical reflectance (albedo) of surfaces from nadir and directional reflectance data p 59 A88-28009
- DMITRIEV, V. V.**
Effect of ice-grain size distribution on the thermal emission of snow cover p 52 A88-24662
- DOBSON, M. CRAIG**
Mesoscale monitoring of the soil freeze/thaw boundary from orbital microwave radiometry [NASA-CR-182659] p 17 N88-19855
- DOERFFER, R.**
The influence of yellow substances on remote sensing of sea water constituents from space. Volume 1: Summary [ESA-CR(P)-2443-VOL-1] p 43 N88-15292
The influence of yellow substances on remote sensing of sea water constituents from space. Volume 2: Appendices [ESA-CR(P)-2443-VOL-2] p 43 N88-15293
The use of chlorophyll fluorescence measurements from space for separating constituents of sea water. Volume 1: Summary [ESA-CR(P)-2444-VOL-1] p 43 N88-15294
The use of chlorophyll fluorescence measurements from space for separating constituents of sea water. Volume 2: Appendices [ESA-CR(P)-2444-VOL-2] p 44 N88-15295
Thematic mapper research in the earth sciences: Small scale patches of suspended matter and phytoplankton in the Elbe River Estuary, German Bight and Tidal Flats [NASA-CR-182378] p 45 N88-16180
- DOERFFER, ROLAND**
Comparison of submarine relief features on a radar satellite image and on a Skylab satellite photograph p 40 A88-29279
- DOMIK, G.**
Image based SAR product simulation for analysis p 55 A88-21037
Methods and accuracy of operational digital image mapping with aircraft SAR p 55 A88-21059
- DOUGLAS, BRUCE C.**
Geosat altimeter observations of Kelvin waves and the 1986-87 El Nino p 32 A88-24582
- DU, LI-JEN**
Texture study of Synthetic Aperture Radar (SAR) images of ocean surfaces [AD-A186021] p 42 N88-15101
- DUCHOSSOIS, G.**
Proposed uses of ERS-1 p 68 A88-27833
Europe's position concerning ocean colour activities p 45 N88-16293
- DURAND, J. M.**
Speckle in SAR images - An evaluation of filtering techniques p 59 A88-27834
- DURAND, PHILIPPE**
Problems in geologic and geomorphic interpretation and geometric modeling of radar images using a digital terrain model p 26 A88-28024
- DVORIANINOV, G. S.**
The relationship between the temporal variability of ocean temperature and the meridional shifts of the intertropical convergence zone p 37 A88-27203
- DYE, DENNIS G.**
Evaluating North American net primary productivity with satellite observations p 9 A88-27819

DYER, K. R.

- Review of the potential of satellite remote sensing for marine flood protection
[IOS-237] p 43 N88-15280

DZHEMARDIAN, I. A.

- Remote sensing surveys design in regional agricultural inventories p 8 A88-27804

E

ECK, T.

- Techniques of ground-truth measurements of desert-scrub structure p 9 A88-27817

ECKELS, ROD

- Surveying with GPS in Australia p 71 N88-18986

EIDEL, THOMAS FRANK

- The ARSUP database and its access through the CMCIRS catalog - Making available to the public digital maps from the ARSUP process p 60 A88-29496

EL'MAN, R. I.

- The use of successive clustering to analyze multispectral imagery p 61 A88-30086

ELACHI, CHARLES

- Introduction to the physics and techniques of remote sensing p 65 A88-21168

ENSLIN, WILLIAM R.

- Land cover change detection using a GIS-guided, feature-based classification of Landsat thematic mapper data p 18 A88-21073

ENTIN, Z. E.

- Variations in the intensity of emitted and scattered microwave radiation of the sea surface sensed at grazing angles in a field of surface manifestations of internal waves p 37 A88-27205

ERNST, JOHN ALBERT

- Spatial-temporal variability of North Pacific sea surface temperature anomaly patterns p 49 N88-19058

ERTHAL, GUARACI JOSE

- A digital terrain system for microcomputers [INPE-4170-PRE/1067] p 63 N88-18987

ESCHER-VETTER, HEIDI

- Energy balance and discharge of an Alpine glacier, illustrated by Mount Vernagtferner in the Oetzal Alps, Tyrol p 53 N88-16145

ESCOBAR, D. E.

- Mid-infrared (1.45 to 2.0 microns) video - A potential aid in wildfire mop-up operations p 1 A88-21016
Near-real-time video systems for rangeland assessment p 4 A88-21360

ESTES, JOHN E.

- Requirements and principles for the implementation and construction of large-scale geographic information systems p 19 A88-28684

ETKIN, V. S.

- Effect of ice-grain size distribution on the thermal emission of snow cover p 52 A88-24662

EVANS, DAVID L.

- Shelf water entrainment by Gulf Stream warm-core rings p 36 A88-27013

EVANS, JOHN C.

- Large area crop classification in New South Wales, Australia, using Landsat data p 14 A88-32665

EVANS, ROBERT

- Processing and analysis of large volumes of satellite-derived thermal infrared data p 36 A88-27012

EVANS, ROBERT H.

- Exact Rayleigh scattering calculations for use with the Nimbus-7 Coastal Zone Color Scanner p 41 A88-30415

EVERITT, J. H.

- Mid-infrared (1.45 to 2.0 microns) video - A potential aid in wildfire mop-up operations p 1 A88-21016
Near-real-time video systems for rangeland assessment p 4 A88-21360
Canopy reflectance of seven rangeland plant species with variable leaf pubescence p 5 A88-23764

EYRE, J. R.

- A sequential estimation approach to cloud-clearing for satellite temperature sounding p 66 A88-23511

EZKOV, V. V.

- Remote sensing surveys design in regional agricultural inventories p 8 A88-27804

F

FANG, CHUNG-MING

- Sea surface current estimates off central California as derived from enhanced AVHRR (Advanced Very High Resolution Radiometer) infrared images [AD-A186867] p 47 N88-17155

FARMER, D. M.

- Ice breakup - Observations of the acoustic signal p 41 A88-30200

FEDOROV, A. S.

- Laser system for automating topographic terrain survey p 70 N88-16136

FELDMAN, SANDRA C.

- Comparison of techniques for discriminating hydrothermal alteration minerals with Airborne Imaging Spectrometer data p 27 A88-28269

FELGUEIRAS, CARLOS ALBERTO

- A digital terrain system for microcomputers [INPE-4170-PRE/1067] p 63 N88-18987

FELLOUS, J.-L.

- French activities in ocean colour observations p 46 N88-16303

FERLET, ROGER

- SPOT 1 - Earth observing satellite p 66 A88-26166

FERRARO, RALPH R.

- Observations of surface and atmospheric features from passive microwave satellite measurements p 64 A88-21019

FERRETTI, STEPHEN B.

- A time-lapse analysis of the Mississippi Delta using Landsat MSS Band 4 (IR2) photographic imagery p 51 A88-21039

FILY, M.

- Quantitative use of satellite SAR imagery of sea ice p 39 A88-27839

FINE, RANA

- The western equatorial Pacific Ocean circulation study p 30 A88-22911

FINKE, M.

- Hydrographic and current measurements in the North-East Atlantic Ocean. Data report on F.S. Meteor cruises 69/5 and 69/6, October to November 1984 [REPT-166] p 48 N88-17164

FINLEY, P.

- Geological evolution and analysis of confirmed or suspected gas hydrate localities. Volume 9: Formation and stability of gas hydrates of the Middle America Trench [DE88-001007] p 29 N88-18050

FIRING, ERIC

- The western equatorial Pacific Ocean circulation study p 30 A88-22911

FISCELLA, B.

- Sea return at C and Ku bands p 31 A88-22947

FISCHER, J.

- The influence of yellow substances on remote sensing of sea water constituents from space. Volume 1: Summary [ESA-CR(P)-2443-VOL-1] p 43 N88-15292

- The influence of yellow substances on remote sensing of sea water constituents from space. Volume 2: Appendices [ESA-CR(P)-2443-VOL-2] p 43 N88-15293

- The use of chlorophyll fluorescence measurements from space for separating constituents of sea water. Volume 1: Summary [ESA-CR(P)-2444-VOL-1] p 43 N88-15294

- The use of chlorophyll fluorescence measurements from space for separating constituents of sea water. Volume 2: Appendices [ESA-CR(P)-2444-VOL-2] p 44 N88-15295

- Thematic mapper research in the earth sciences: Small scale patches of suspended matter and phytoplankton in the Elbe River Estuary, German Bight and Tidal Flats [NASA-CR-182378] p 45 N88-16180

FITZJARRALD, DAVID

- Structure and growth of the mixing layer over the Amazonian rain forest p 8 A88-27252

FLATHER, R. A.

- Review of the potential of satellite remote sensing for marine flood protection [IOS-237] p 43 N88-15280

FLEMING, MICHAEL D.

- An integrated approach for automated cover-type mapping of large inaccessible areas in Alaska p 60 A88-29491

FOOTE, H. P.

- LANDSAT thematic mapper radiometric calibration study [NASA-CR-182410] p 61 N88-15287

FORAN, B. D.

- Detection of yearly cover change with Landsat MSS on pastoral landscapes in central Australia p 4 A88-21362

- The use of spectral and spatial variability to monitor cover change on inert landscapes p 4 A88-21363

FORSELL, T.

- Construction of airborne radars for remote sensing [PB88-113063] p 71 N88-16916

FORSTREUTER, WOLF

- Investigations on the application of space photographs (Spacelab metric camera) for routine inventories of extensively managed forest areas [DFVLR-FB-87-22] p 15 N88-17098

FOSCHI, PATRICIA G.

- Detecting subpixel woody features using simulated multispectral and panchromatic SPOT imagery p 3 A88-21065

FRANCHETEAU, J.

- Evolution of the Juan Fernandez microplate during the last three million years p 25 A88-25045

FRANKLIN, JANET

- Improved canopy reflectance modeling and scene inference through improved understanding of scene pattern [NASA-CR-182488] p 15 N88-18049

FRASSETTO, R.

- Italian activities in ocean colour remote sensing p 46 N88-16304

FRAYSSE, G.

- Status and prospects of the Joint Research Committee (JRC) work on the application of ocean colour monitoring from space p 46 N88-16299

FREDERICKS, WILLIAM J.

- North Pacific Ocean. Central Pacific Transition Zone, R/V Thomas G. Thompson: 25 March - 3 May 1968. STD data report [AD-A186570] p 47 N88-17160

FRETEAUD, J. P.

- Estimation of evapotranspiration in the Sahelian zone by use of Meteosat and NOAA AVHRR data p 9 A88-27818

FRETZ, R. K.

- An automated system for terrain database construction p 18 A88-21060

FREW, RONALD L.

- Remote sensing applications by consulting engineers - Three case histories p 24 A88-21009

FROUIN, ROBERT

- Downward longwave irradiance at the ocean surface from satellite data - Methodology and in situ validation p 38 A88-27493

FUNG, TUNG

- Land cover change detection with Landsat MSS and TM data in the Kitchener-Waterloo area, Canada p 18 A88-21071

FUSCO, L.

- The Earthnet Heat Capacity Mapping Mission (HCMM) data-processing system at Lannion (France) p 62 N88-16761

G

GAGE, K. S.

- Longitudinal variations in tropical tropopause properties in relation to tropical convection and El Nino-Southern Oscillation events p 33 A88-25727

GALLIDEPARATESI, S.

- Status and prospects of the Joint Research Committee (JRC) work on the application of ocean colour monitoring from space p 46 N88-16299

GALLO, K. P.

- Differences in vegetation indices for simulated Landsat-5 MSS and TM, NOAA-9 AVHRR, and SPOT-1 sensor systems p 7 A88-25446

GARDNER, T. W.

- Aircraft and satellite remote sensing of desert soils and landscapes p 3 A88-21358

GARFIELD, NEWELL, III

- Shelf water entrainment by Gulf Stream warm-core rings p 36 A88-27013

GARSTANG, M.

- Biomass-burning emissions and associated haze layers over Amazonia p 18 A88-27265

GARSTANG, MICHAEL

- Structure and growth of the mixing layer over the Amazonian rain forest p 8 A88-27252
Design of the primary pre-TRMM and TRMM ground truth site [NASA-CR-182609] p 53 N88-19865

GASPERINI, PAOLO

- Mantle rheology and satellite signatures from present-day glacial forcings p 21 A88-25225

GAUTIER, CATHERINE

- Downward longwave irradiance at the ocean surface from satellite data - Methodology and in situ validation p 38 A88-27493

GEARHART, S. A.

- Evaluation of a temperature remote sensing technique [AD-A187885] p 71 N88-18053

GELLER, MARVIN A.

- Looking at the earth from space p 69 A88-29235

GEORGE, THOMAS H.

- Multiple dipole eddies in the Alaska Coastal Current detected with Landsat thematic mapper data p 36 A88-27015

GEREKE, WALDEMAR

The unsteady ground heat flow at the contact surface between a glacier run and the subsoil p 53 N88-16147

GERSHENZON, V. E.

Variations in the intensity of emitted and scattered microwave radiation of the sea surface sensed at grazing angles in a field of surface manifestations of internal waves p 37 A88-27205

GERSTL, S. A. W.

The angular reflectance signature of the canopy hot spot in the optical regime [DE88-005385] p 15 N88-18991

GIBBONS, D. E.

LANDSAT thematic mapper radiometric calibration study [NASA-CR-182410] p 61 N88-15287

GIBBS, PHILIP JOHN

Five New South Wales barrier lagoons: Their macrobenthic fauna and seagrass communities p 49 N88-19059

GIGORD, P.

Evaluation of the stereoscopic accuracy of the SPOT satellite p 59 A88-28605

GILES, CHRISTOPHER

Results of testing digital image measurements and enhancements on the remote work processing facility p 56 A88-21064

GILLESPIE, D. D.

Characterizing forest stands with multi-incidence angle and multi-polarized SAR data p 10 A88-27836

GILMAN, CRAIG

Processing and analysis of large volumes of satellite-derived thermal infrared data p 36 A88-27012

GIMONET, B. J.

Speckle in SAR images - An evaluation of filtering techniques p 59 A88-27834

GIRARD, C. M.

Spectral and botanical classification of grasslands - Auxois example p 8 A88-27805

GIRARD, COLETTE M.

Preliminary SPOT results in Lorraine related to permanent grasslands p 5 A88-22617

GLANTZ, C. S.

User's guide to a data base of current environmental monitoring projects in the US-Canadian transboundary region [DE88-002476] p 20 N88-17119

GLAZMAN, R. E.

Scatterometer wind speed bias induced by the large-scale component of the wave field p 40 A88-29325

GLAZMAN, ROMAN E.

Wind-fetch dependence of Seasat scatterometer measurements p 31 A88-23546

GLUSHKO, YE. V.

Academic course Space Methods for Studying Modern Landscapes of Continents p 72 N88-16133

GODFREY, STUART

The western equatorial Pacific Ocean circulation study p 30 A88-22911

GOETZ, ALEXANDER F. H.

Terrestrial imaging spectroscopy p 69 A88-28266

GOLDBERG, MORRIS

Hierarchical segmentation using a composite criterion for remotely sensed imagery p 54 A88-20841

GOLDBERG, R. A.

Characteristics of extreme rainfall events in northwestern Peru during the 1982-1983 El Nino period p 52 A88-25730

GOLDHIRSH, JULIUS

Analysis of algorithms for the retrieval of rain-rate profiles from a spaceborne dual-wavelength radar p 69 A88-28679

GOLOV, V. S.

Laser system for automating topographic terrain survey p 70 N88-16136

GOLUS, ROBERT E.

Estimating surface soil moisture from satellite microwave measurements and a satellite derived vegetation index p 13 A88-30446

GONZALES, G.

Preliminary study of the characterization of the riverine forests of the Garonne using Landsat MSS and TM data p 9 A88-27811

GOODENOUGH, DAVID G.

Thematic mapper and SPOT integration with a geographic information system p 59 A88-28602

GORBUSHINA, E. A.

Multistep component analysis of correlations p 61 N88-16115

GORDON, DANIEL K.

The use of automated computer vision techniques for the recognition of features on radar imagery p 56 A88-21069

GORDON, HOWARD R.

Exact Rayleigh scattering calculations for use with the Nimbus-7 Coastal Zone Color Scanner p 41 A88-30415

GORIAINOV, I. N.

Features of hydrological anomalies in connection with the search for deep-water polymetallic sulfides p 32 A88-24654

GOSHTASBY, ARDESHIR

Registration of images with geometric distortions p 58 A88-24936

GOW, ANTHONY J.

Physical properties of summer sea ice in the Fram Strait, June-July 1984 [AD-A186937] p 53 N88-17156

GOWARD, S. N.

Remote sensing from space; Proceedings of Symposium 3, Workshop V, and Topical Meeting A2 of the Twenty-sixth COSPAR Plenary Meeting, Toulouse, France, June 30-July 11, 1986 p 67 A88-27801

GOWARD, SAMUEL N.

Evaluating North American net primary productivity with satellite observations p 9 A88-27819

Commercial applications and scientific research requirements for thermal-infrared observations of terrestrial surfaces [NASA-TM-89704] p 70 N88-16179

GOWER, J. F. R.

Canadian activities and goals in remote sensing of ocean colour and fluorescence from space p 46 N88-16300

GRAETZ, R. D.

Satellite remote sensing of Australian rangelands p 4 A88-21361

GRAHAM, NICHOLAS E.

An investigation of the El Nino-Southern Oscillation Cycle with statistical models. I - Predictor field characteristics. II - Model results p 34 A88-25731

GRAHAM, ROBIN LAMBERT

Estimating forest productivity in southern Illinois using Landsat Thematic Mapper data and geographic information system analysis techniques p 2 A88-21028

GRAMBERG, I. S.

Features of hydrological anomalies in connection with the search for deep-water polymetallic sulfides p 32 A88-24654

GRANT, LOIS

Polarized and non-polarized leaf reflectances of Coleus blumei p 7 A88-26624

GRASSL, H.

The influence of yellow substances on remote sensing of sea water constituents from space. Volume 1: Summary [ESA-CR(P)-2443-VOL-1] p 43 N88-15292

The influence of yellow substances on remote sensing of sea water constituents from space. Volume 2: Appendices [ESA-CR(P)-2443-VOL-2] p 43 N88-15293

The use of chlorophyll fluorescence measurements from space for separating constituents of sea water. Volume 1: Summary [ESA-CR(P)-2444-VOL-1] p 43 N88-15294

The use of chlorophyll fluorescence measurements from space for separating constituents of sea water. Volume 2: Appendices [ESA-CR(P)-2444-VOL-2] p 44 N88-15295

Thematic mapper research in the earth sciences: Small scale patches of suspended matter and phytoplankton in the Elbe River Estuary, German Bight and Tidal Flats [NASA-CR-182378] p 45 N88-16180

The use of chlorophyll fluorescence measurements from space for separating constituents of sea water p 47 N88-16307

The influence of yellow substances on remote sensing of sea-water constituents from space p 47 N88-16308

GRECO, STEVE

Structure and growth of the mixing layer over the Amazonian rain forest p 8 A88-27252

GREELEY, RONALD

Talamzane - Algerian impact crater detected on SIR-A orbital imaging radar p 25 A88-25217

GREEN, ANDREW A.

A transformation for ordering multispectral data in terms of image quality with implications for noise removal p 58 A88-24937

GREGORY, G. L.

Biomass-burning emissions and associated haze layers over Amazonia p 18 A88-27265

GRIFFIN, DAVID A.

Mesoscale coastal ocean dynamics p 49 N88-19060

GRIFFITHS, H. D.

Swath altimetry of oceans and terrain p 39 A88-27838

GRIGORIAN, S. V.

Geochemistry of continental volcanism p 27 A88-29431

GRIN, A. M.

Space applications in geography p 22 N88-16104

GRISHIN, G. A.

Current status and problems of satellite investigations of the ocean (Review of non-Soviet publications) p 41 A88-30089

GRODY, NORMAN C.

Observations of surface and atmospheric features from passive microwave satellite measurements p 64 A88-21019

GROMOV, V. K.

Variations in the intensity of emitted and scattered microwave radiation of the sea surface sensed at grazing angles in a field of surface manifestations of internal waves p 37 A88-27205

GROSS, M. F.

Quantification of biomass of the marsh grass *Spartina alterniflora* Loisel using Landsat Thematic Mapper imagery p 6 A88-23765

GROVES, J. E.

Landsat determined geographic change p 27 A88-29489

GRUBER, ARNOLD

General determination of Earth surface type and cloud amount using multispectral AVHRR data [NOAA-TR-NESDIS-39] p 72 N88-18997

GUENTHER, K.

The use of chlorophyll fluorescence measurements from space for separating constituents of sea water. Volume 1: Summary [ESA-CR(P)-2444-VOL-1] p 43 N88-15294

The use of chlorophyll fluorescence measurements from space for separating constituents of sea water. Volume 2: Appendices [ESA-CR(P)-2444-VOL-2] p 44 N88-15295

GUIGNARD, J. P.

Earthnet's experience with Seasat SAR image processing p 62 N88-16760

GUIGNARD, J.-P.

Proposed uses of ERS-1 p 68 A88-27833

GUISSARD, A.

An approximate model for the microwave brightness temperature of the sea p 31 A88-23544

GUNTER, L.

Size distributions of sea-source aerosol particles - A physical explanation of observed nearshore versus open-sea differences p 33 A88-25289

GUSTAFSON, GLEN C.

Geographical position plotting by photo interpreters from Space Shuttle Large Format Camera photography p 65 A88-21050

GUYENNE, T. D.

Ocean Colour Workshop [ESA-SP-1083] p 45 N88-16292

Proceedings of an ESA-NASA Workshop on a Joint Solid Earth Program [NASA-CR-182642] p 23 N88-19844

GUYMER, T. H.

Review of the potential of satellite remote sensing for marine flood protection [IOS-237] p 43 N88-15280

GWYN, Q. H. J.

Radiometric correction of C-band imagery for topographic effects in regions of moderate relief p 59 A88-28680

H**HAAPANEN, J.**

Construction of airborne radars for remote sensing [PB88-113063] p 71 N88-16916

HAARDT, H.

The use of chlorophyll fluorescence measurements from space for separating constituents of sea water. Volume 1: Summary [ESA-CR(P)-2444-VOL-1] p 43 N88-15294

The use of chlorophyll fluorescence measurements from space for separating constituents of sea water. Volume 2: Appendices [ESA-CR(P)-2444-VOL-2] p 44 N88-15295

HAERTEL, VITOR

Textural features for image classification in remote sensing [INPE-4169-PRE/1066] p 62 N88-16181

HALBERT, RICHARD V.

The digital landmass simulation production overview [AD-A187978] p 62 N88-18978

HALL, F. G.

The first ISLSCP field experiment (FIFE) p 67 A88-27497

HALL, T. J.

SAR imaging of volume scatterers p 60 A88-28681

HALLIKAINEN, M.

Construction of airborne radars for remote sensing
[PB88-113063] p 71 N88-16916

HALSTEAD, P.

An integrated camera and radiometer for aerial
monitoring of vegetation p 14 A88-32666

HAMILTON, L. J.

Oceanographic features of the east and southeast Indian
Ocean for June 1983
[AD-A186348] p 47 N88-17158

HANDLER, PAUL

Simultaneity of response of Atlantic Ocean tropical
cyclones and Indian monsoons p 34 A88-25736

HARDISKY, M. A.

Quantification of biomass of the marsh grass *Spartina*
alterniflora Loisel using Landsat Thematic Mapper
imagery p 6 A88-23765

HARJES, MARK

A smart, mapping, charting and geodesy control
generator, phase 1
[AD-A188184] p 23 N88-18055

HARRISS, R. C.

Biomass-burning emissions and associated haze layers
over Amazonia p 18 A88-27265

HARTMANN, CARLOS

Evaluation of the flooding areas of the Sao Goncalo
Canal through LANDSAT 5 thematic mapper images
[INPE-4118-PRE/1039] p 53 N88-16185

HARVEY, WILSON A.

Automatic knowledge acquisition for aerial image
interpretation
[AD-A188616] p 63 N88-19810

HASKINS, ROBERT D.

Satellite observation of atmosphere and surface
interaction parameters p 38 A88-27812

HASLER, A. F.

Remote sensing from space; Proceedings of Symposium
3, Workshop V, and Topical Meeting A2 of the Twenty-sixth
COSPAR Plenary Meeting, Toulouse, France, June 30-July
11, 1986 p 67 A88-27801

HATFIELD, J. L.

Vegetative and optical characteristics of four-row crop
canopies p 14 A88-32661

HAWKINS, DAVE

The potential for automated mapping from Geocoded
digital image data p 59 A88-28604

HAWKINS, ROBERT K.

Microwave remote sensing of ice in Lake Melville and
the Labrador Sea p 39 A88-28850

HENDERSON, FLOYD M.

Evaluation of X-band SAR imagery for mapping open
surface water in the northeastern United States
p 51 A88-21038

HENLEY, J. PONDER

Spectral characteristics of selected soils and vegetation
in northern Nevada and their discrimination using band
ratio techniques p 3 A88-21352

HENNINGS, I.

The influence of yellow substances on remote sensing
of sea water constituents from space. Volume 1:
Summary
[ESA-CR(P)-2443-VOL-1] p 43 N88-15292

The influence of yellow substances on remote sensing
of sea water constituents from space. Volume 2:
Appendices
[ESA-CR(P)-2443-VOL-2] p 43 N88-15293

The use of chlorophyll fluorescence measurements from
space for separating constituents of sea water. Volume
1: Summary
[ESA-CR(P)-2444-VOL-1] p 43 N88-15294

The use of chlorophyll fluorescence measurements from
space for separating constituents of sea water. Volume
2: Appendices
[ESA-CR(P)-2444-VOL-2] p 44 N88-15295

HENNINGS, INGO

Comparison of submarine relief features on a radar
satellite image and on a Skylab satellite photograph
p 40 A88-29279

HENRY, B. M.

Status and prospects of the Joint Research Committee
(JRC) work on the application of ocean colour monitoring
from space p 46 N88-16299

HERRMANN, KARIN

Preliminary assessment of airborne imaging
spectrometer and airborne thematic mapper data acquired
for forest decline areas in the Federal Republic of
Germany p 11 A88-28272

HEYDT, HOWARD L.

Spectral enhancements of Landsat MSS and TM
imagery applied to ground water investigations in Kenya
p 51 A88-21042

HIELKEMA, J. U.

Monitoring of global vegetation dynamics for
assessment of primary productivity using NOAA advanced
very high resolution radiometer p 9 A88-27808

HIGASHI, M.

A study to produce 1:100,000 scale LFC color
photomap p 68 A88-27826

HILL, G. F.

Biomass-burning emissions and associated haze layers
over Amazonia p 18 A88-27265

HILL, J. W.

The ocean heat budget
[AD-A186130] p 44 N88-15346

HINKLE, C. ROSS

Effects of fire on composition, biomass, and nutrients
in oak scrub vegetation on John F. Kennedy Space Center,
Florida
[NASA-TM-100305] p 15 N88-16182

HINSE, MARIO

Radiometric correction of C-band imagery for
topographic effects in regions of moderate relief
p 59 A88-28680

HODGSON, MICHAEL E.

Interrelationships between spatial resolution and
per-pixel classifiers for extracting information classes. I -
The urban environment. II - The natural environment
p 17 A88-21014

Correlation between aircraft MSS and lidar remotely
sensed data on a forested wetland p 6 A88-24513

HOEKMAN, D. H.

Measurements of the backscatter and attenuation
properties of forest stands at X-, C- and L-band
p 7 A88-25444

HOEKMAN, DIRK H.

Multiband-scatterometer data analysis of forests
p 5 A88-23548

HOFFER, R. M.

Definition of forest stand characteristics based on
multi-incidence angle SIR-B data p 2 A88-21031

Characterizing forest stands with multi-incidence angle
and multi-polarized SAR data p 10 A88-27836

HOLLADAY, J. S.

Airborne electromagnetic sounding of sea ice thickness
and sub-ice bathymetry
[AD-A188939] p 50 N88-19879

HOLLIGAN, P. M.

Remote sensing of ocean colour for studies of biological
productivity and biochemical cycles p 45 N88-16296

Developments in ocean colour research in the United
Kingdom p 46 N88-16306

HOLMES, J. F.

Remote sensing of atmospheric crosswinds by utilizing
speckle-turbulence interaction and optical heterodyne
detection
[AD-A187580] p 71 N88-18052

HOPE, A. S.

Estimation of wheat canopy resistance using combined
remotely sensed spectral reflectance and thermal
observations p 13 A88-30448

HOPKINS, PAUL F.

Assessment of thematic mapper imagery for forestry
applications under Lake States conditions
p 7 A88-26336

HORDON, ROBERT M.

Groundwater identification using digitally enhanced
NHAP p 51 A88-21011

HORNING, NED

Determining the rate of forest conversion in Mato
Grosso, Brazil, using Landsat MSS and AVHRR data
p 10 A88-28011

HORVATH, H.

Size distributions of sea-source aerosol particles - A
physical explanation of observed nearshore versus
open-sea differences p 33 A88-25289

HOSHIZAKI, T.

Comparison of in situ and airborne spectral
measurements of the blue shift associated with forest
decline p 11 A88-28271

HOWARTH, P. J.

Automated road network extraction from Landsat TM
imagery p 18 A88-21044

HOWE, ROBERT C.

Geobotanical detection of linear features in the Silver
Mine area of southeastern Missouri p 25 A88-21043

HSU, LIANG C.

Nature and origin of mineral coatings on volcanic rocks
of the Black Mountain, Stonewall Mountain, and Kane
Springs Wash volcanic centers, Southern Nevada
[NASA-CR-181437] p 29 N88-17140

HUDSON, RICK D.

Multiyear sea ice floe distribution in the Canadian Arctic
Ocean p 35 A88-25738

HUDSON, W. D.

Evaluation of several classification schemes for mapping
forest cover types in Michigan p 10 A88-28012

HUETE, A. R.

Suitability of spectral indices for evaluating vegetation
characteristics on arid rangelands p 3 A88-21355

HUNT, D. M.

An integrated camera and radiometer for aerial
monitoring of vegetation p 14 A88-32666

HUNT, J. J.

Proceedings of an ESA-NASA Workshop on a Joint Solid
Earth Program
[NASA-CR-182642] p 23 N88-19844

HUTHNANCE, J. M.

Review of the potential of satellite remote sensing for
marine flood protection
[IOS-237] p 43 N88-15280

HUTSPILLER, AMY

Discrimination of hydrothermal alteration mineral
assemblages at Virginia City, Nevada, using the airborne
imaging spectrometer p 27 A88-28268

HYYPYAE, J.

Construction of airborne radars for remote sensing
[PB88-113063] p 71 N88-16916

I

IL'IN, A. L.

Correlation characteristics of images of the earth surface
obtained with a synthetic-aperture radar p 66 A88-21784

INGRAM, ARLYNN

Land-cover monitoring with SPOT for landfill
investigations p 19 A88-28606

INKSTER, JOHN

Geographical position plotting by photo interpreters from
Space Shuttle Large Format Camera photography
p 65 A88-21050

IP, J.

Scatterometer wind speed bias induced by the
large-scale component of the wave field p 40 A88-29325

ISAACSON, DENNIS L.

Research in remote sensing of vegetation
[NASA-CR-182663] p 16 N88-19817

ISHIZAWA, Y.

Design concept of the SAR installed on ERS-1
p 68 A88-27832

ISIORHO, SOLOMON A.

Radar flood inundation mapping of upper Benue Trough,
Nigeria p 2 A88-21035

ISLAM, K. R.

Remote sensing of forest cover distribution in the Phu
Wiang watershed area of Khon Kaen Province, Northeast
of Thailand p 6 A88-24514

ITTEKOT, V.

The influence of yellow substances on remote sensing
of sea water constituents from space. Volume 1:
Summary
[ESA-CR(P)-2443-VOL-1] p 43 N88-15292

The influence of yellow substances on remote sensing
of sea water constituents from space. Volume 2:
Appendices
[ESA-CR(P)-2443-VOL-2] p 43 N88-15293

IVERSON, LOUIS R.

Estimating forest productivity in southern Illinois using
Landsat Thematic Mapper data and geographic
information system analysis techniques p 2 A88-21028

Analyzing long-term changes in vegetation with
geographic information system and remotely sensed
data p 10 A88-27820

J

JACKSON, R. D.

Suitability of spectral indices for evaluating vegetation
characteristics on arid rangelands p 3 A88-21355

JACOB, D. J.

Biomass-burning emissions and associated haze layers
over Amazonia p 18 A88-27265

JAIN, ANIL

Land cover change detection using a GIS-guided,
feature-based classification of Landsat thematic mapper
data p 18 A88-21073

JAMES, I. D.

Review of the potential of satellite remote sensing for
marine flood protection
[IOS-237] p 43 N88-15280

JANTUNEN, H.

Landsat classification of the barren hydrolittoral areas
of Lake Yli-Kitka, north-eastern Finland p 51 A88-24198

JAQUET, J.-M.

Research in Switzerland on ocean and inland-water
colour monitoring p 46 N88-16301

JEKELI, CHRISTOPHER

The downward continuation of aerial gravimetric data
without density hypothesis p 21 A88-26347

- JENSEN, J. R.**
Aircraft MSS data registration and vegetation classification for wetland change detection p 12 A88-29277
- JENSEN, JOHN R.**
Remote sensing of aquatic macrophyte distribution in selected South Carolina reservoirs p 51 A88-21007
Interrelationships between spatial resolution and per-pixel classifiers for extracting information classes. I - The urban environment. II - The natural environment p 17 A88-21014
Evaluation of Thematic Mapper data for mapping tidal wetlands in South Carolina p 2 A88-21040
Correlation between aircraft MSS and lidar remotely sensed data on a forested wetland p 6 A88-24513
- JOHNSON, HERBERT**
Results of testing digital image measurements and enhancements on the remote work processing facility p 56 A88-21064
- JOHNSON, L. F.**
An automated system for terrain database construction p 18 A88-21060
- JOHNSTONE, WILLIAM**
The potential for automated mapping from Geocoded digital image data p 59 A88-28604
- JONES, EDWIN R.**
Single-source three-dimensional imaging system for remote sensing p 66 A88-23772
- JONES, JOHN EDWIN**
Application of data from the U.S. Geological Survey's side-looking airborne radar program p 25 A88-21036
- JOSHI, P. C.**
Assessment of the use of satellite derived winds in monsoon forecasting using a general circulation model p 68 A88-27846
- JURY, MARK**
Marine boundary layer modification across the edge of the Agulhas Current p 38 A88-27495
- JUSTICE, C. O.**
Selecting the spatial resolution of satellite sensors required for global monitoring of land transformations p 20 A88-32659

K

- KACZYNSKI, R.**
Comprehensive studies of the dynamics of geosystems with the use of remote sensing techniques p 10 A88-27821
- KALLIOLA, RISTO J.**
Fluvial perturbation in the western Amazon basin - Regulation by long-term sub-Andean tectonics p 24 A88-20878
- KARASEV, A. B.**
Choosing conditions for the remote sensing of ocean features in the visible spectrum, with the effect of coastal zone taken into account p 37 A88-27209
Adaptive computer-aided system for crop inventory according to space photographs p 13 A88-30087
- KAUFMAN, YORAM J.**
Atmospheric effect on spectral signature - Measurements p 58 A88-27822
- KAZ'MIN, A. S.**
Blocking of the Benguela Current by a single anticyclone - Analysis of satellite and ship data p 41 A88-30077
- KECHKEMETI, L.**
Adaptive computer-aided system for crop inventory according to space photographs p 13 A88-30087
- KEIGWIN, LLOYD**
North Atlantic thermohaline circulation during the past 20,000 years linked to high-latitude surface temperature p 30 A88-20978
- KERGOMARD, CL.**
Sea ice and sea-surface temperatures in the Strait of Fram according to NOAA-AVHRR data p 35 A88-26131
- KERR, Y. H.**
A global survey of surface climate parameters from satellite observations - Preliminary results over Africa p 67 A88-27814
Estimation of evapotranspiration in the Sahelian zone by use of Meteosat and NOAA AVHRR data p 9 A88-27818
- KEYDEL, W.**
Detection of oil films by active and passive microwave sensors p 39 A88-27840
- KHALSA, SIRI JODHA SINGH**
Sea surface temperature, low-level moisture, and convection in the tropical Pacific, 1982-1985 p 34 A88-25729
- KHORRAM, S.**
Monitoring North Carolina's nutrient-sensitive reservoirs using Landsat TM digital data p 50 A88-21006

- KHORRAM, SIAMAK**
Development of multivariate estuarine water quality models using Landsat 2 and 4 MSS data p 50 A88-21002
- KHOTIN, M. M.**
Method for joint adjustment of satellite and surface geodetic networks p 22 A88-16105
- KHRISTOFOROV, G. N.**
Limiting accuracy of scatterometer determination of wind speed over ocean from satellite p 44 A88-16107
- KIEFER, RALPH W.**
Automated photointerpretation - A stereoscopic workstation p 54 A88-21027
- KIENKO, IU. P.**
The use of space technology for the remote sensing of earth resources and mapping p 69 A88-28447
- KIEVIT, J.**
Design and implementation of a data base system for Digital Land Mass System (DLMS) data [FEL-IR-1987-19] p 71 A88-17101
- KIMES, D. S.**
Extraction of spectral hemispherical reflectance (albedo) of surfaces from nadir and directional reflectance data p 59 A88-28009
- KIMURA, H.**
Simulation of spaceborne SAR imagery from airborne SAR data p 58 A88-27830
- KING, D.**
Multispectral video survey of a Northern Ontario forest p 1 A88-21015
- KINN, GERALD**
Results of testing digital image measurements and enhancements on the remote work processing facility p 56 A88-21064
- KISHTWAL, C. M.**
Assessment of the use of satellite derived winds in monsoon forecasting using a general circulation model p 68 A88-27846
- KLEINER, E. F.**
Geological and vegetational applications of Shuttle Imaging Radar-B, Mineral County, Nevada p 26 A88-26337
- KLEMAS, V.**
Quantification of biomass of the marsh grass *Spartina alterniflora* Loisel using Landsat Thematic Mapper imagery p 6 A88-23765
- KLENITSKIY, B. M.**
Method for joint adjustment of satellite and surface geodetic networks p 22 A88-16105
- KLIEFORTH, H.**
Geological and vegetational applications of Shuttle Imaging Radar-B, Mineral County, Nevada p 26 A88-26337
- KLIORIN, N. I.**
Effect of ice-grain size distribution on the thermal emission of snow cover p 52 A88-24662
- KOBER, WOODY**
A smart, mapping, charting and geodesy control generator, phase 1 [AD-A188184] p 23 A88-18055
- KODAIRA, N.**
Simulation of spaceborne SAR imagery from airborne SAR data p 58 A88-27830
Design concept of the SAR installed on ERS-1 p 68 A88-27832
- KOEPKE, PETER**
The role of anisotropy in the long range reconnaissance of the albedo of land surfaces p 62 A88-16169
- KOMAI, J.**
Design concept of the SAR installed on ERS-1 p 68 A88-27832
- KONDRANIN, T. V.**
The efficiency of polarization measurements in passive remote sensing of the ocean in the visible spectrum p 38 A88-27210
- KONDRAT'EV, K. IA.**
Complex remote monitoring of lakes p 52 A88-27741
- KONECNY, GOTTFRIED**
The development and state of the art of remote sensing p 64 A88-20903
- KONG, JIN A.**
Active and passive remote sensing of ice [AD-A186685] p 47 A88-17162
- KOROLEV, S. N.**
The use of regression analysis to determine sea surface temperatures from Cosmos-1151 measurements of IR radiation p 41 A88-30085
- KORSUNOV, G. V.**
Correlation characteristics of images of the earth surface obtained with a synthetic-aperture radar p 66 A88-21784
- KOSKE, P.**
The use of chlorophyll fluorescence measurements from space for separating constituents of sea water. Volume 1: Summary [ESA-CR(P)-2444-VOL-1] p 43 A88-15294

- The use of chlorophyll fluorescence measurements from space for separating constituents of sea water. Volume 2: Appendices [ESA-CR(P)-2444-VOL-2] p 44 A88-15295
- KOTLIAR, I. B.**
Estimation of the accuracy of determining atmospheric temperature profiles from microwave remote sensing at frequencies of 117-118.5 GHz p 41 A88-30084
- KOTTSOV, V. A.**
Multistep component analysis of correlations p 61 A88-16115
- KOVACS, AUSTIN**
Airborne electromagnetic sounding of sea ice thickness and sub-ice bathymetry [AD-A188939] p 50 A88-19879
- KOVALENOK, V.**
Observations of ocean and sea bottom relief from space p 35 A88-26099
- KOVALEVICH, V. M.**
On the problem of evolution of oceanic water composition in the Phanerozoic p 35 A88-26676
- KOVER, ALLAN N.**
Application of data from the U.S. Geological Survey's side-looking airborne radar program p 25 A88-21036
- KRABILL, WILLIAM**
Correlation between aircraft MSS and lidar remotely sensed data on a forested wetland p 6 A88-24513
Estimating forest biomass and volume using airborne laser data p 13 A88-30441
- KRAMBER, WILLIAM**
An application of divergence measurement using transformed video data p 6 A88-24510
- KRAMBER, WILLIAM J.**
Principal component analysis of aerial video imagery p 54 A88-21030
- KRAPIVIN, VLADIMIR FEDOROVICH**
Methods for processing radio-physical measurement data in studies of the environment p 19 A88-29427
- KRASNOZHON, G. F.**
Investigating the northern Caspian Sea ice regime from meteorological-satellite data p 37 A88-27202
- KRASON, J.**
Geological evolution and analysis of confirmed or suspected gas hydrate localities. Volume 10: Basin analysis, formation and stability of gas hydrates of the Aleutian Trench and the Bering Sea [DE88-001008] p 29 A88-18048
Geological evolution and analysis of confirmed or suspected gas hydrate localities. Volume 9: Formation and stability of gas hydrates of the Middle America Trench [DE88-001007] p 29 A88-18050
- KRAVTSOVA, V. I.**
Interpretation of the visible manifestations of sea water dynamics from space imagers of the Caspian Sea p 37 A88-27201
- KRIEBEL, K. T.**
An improved method for detecting clear sky and cloudy radiances from AVHRR data p 69 A88-29284
- KRONFELD, U.**
The use of chlorophyll fluorescence measurements from space for separating constituents of sea water. Volume 1: Summary [ESA-CR(P)-2444-VOL-1] p 43 A88-15294
The use of chlorophyll fluorescence measurements from space for separating constituents of sea water. Volume 2: Appendices [ESA-CR(P)-2444-VOL-2] p 44 A88-15295
- KROTKOV, N. A.**
The efficiency of polarization measurements in passive remote sensing of the ocean in the visible spectrum p 38 A88-27210
- KRUEGER, ARLIN J.**
Satellite maps of Antarctic total ozone [AIAA PAPER 88-0210] p 30 A88-22154
- KRUSE, FRED A.**
Use of airborne imaging spectrometer data to map minerals associated with hydrothermally altered rocks in the Northern Grapevine Mountains, Nevada, and California p 26 A88-28267
- KUHN, WILLIAM R.**
Mesoscale monitoring of the soil freeze/thaw boundary from orbital microwave radiometry [NASA-CR-182659] p 17 A88-19855
- KUMAR, MAHENDRA**
Crop canopy spectral reflectance p 14 A88-32664
- KWONG, HELENANN H.**
Characterization of vegetation with combined Thematic Mapper (TM) and Shuttle Imaging Radar (SIR-B) image data p 2 A88-21032
- KYLE, H. LEE**
Remote sensing of water vapor convergence, deep convection, and precipitation over the tropical Pacific Ocean during the 1982-1983 El Nino p 33 A88-25728

L

- LACY, RICHARD B.**
Evaluation of Thematic Mapper data for mapping tidal wetlands in South Carolina p 2 A88-21040
- LADSTAEETER, PETER**
The aerophotogrammetric determination of Earth surface deformations [SER-C-321] p 28 N88-15288
- LAGOS, PABLO**
Remote forcing of sea surface temperature in the El Nino region p 34 A88-25732
- LAGOUARDE, J. P.**
Estimation of evapotranspiration in the Sahelian zone by use of Meteosat and NOAA AVHRR data p 9 A88-27818
- LAMPARELLI, R. A. C.**
Evaluation of the flooding areas of the Sao Goncalo Canal through LANDSAT 5 thematic mapper images [INPE-4118-PRE/1039] p 53 N88-16185
- LAMPINEN, J.**
Landsat classification of the barren hydrolittoral areas of Lake Yli-Kitka, north-eastern Finland p 51 A88-24198
- LANGE, MANFRED A.**
The ice thickness distribution across the Atlantic sector of the Antarctic Ocean in midwinter p 34 A88-25734
- LAPORTE, DANIEL**
Commercial applications and scientific research requirements for thermal-infrared observations of terrestrial surfaces [NASA-TM-89704] p 70 N88-16179
- LAPOTIN, P. J.**
Remote sensing of soil moisture p 52 A88-27815
- LARSON, FREDERIC R.**
Measuring crown cover in interior Alaska vegetation types p 12 A88-29495
- LAXON, S. W.**
Radar altimeter data quality flagging p 39 A88-27837
- LAZAREV, A.**
Observations of ocean and sea bottom relief from space p 35 A88-26099
- LEBERL, F.**
Image based SAR product simulation for analysis p 55 A88-21037
- LEBERL, F. W.**
Methods and accuracy of operational digital image mapping with aircraft SAR p 55 A88-21059
- LEBERL, FRANZ**
A smart, mapping, charting and geodesy control generator, phase 1 [AD-A188184] p 23 N88-18055
- LEBLOND, PAUL H.**
The baroclinic circulation in Hudson Strait p 32 A88-24457
- LEDREW, ELLSWORTH**
Land cover change detection with Landsat MSS and TM data in the Kitchener-Waterloo area, Canada p 18 A88-21071
- LEDWELL, JAMES R.**
Gas exchange on Mono Lake and Crowley Lake, California p 52 A88-25735
- LEE, CHIN-HWA**
Model-based building verification in aerial photographs [AD-A186010] p 20 N88-15278
- LEE, HSI-JIAN**
Model-based building verification in aerial photographs [AD-A186010] p 20 N88-15278
- LEE, TONG**
Multisource context classification methods in remote sensing p 63 N88-18985
- LEFAUCONNIER, CLAUDE**
Spray droplet generation, transport, and evaporation in a wind wave tunnel during the humidity exchange over the sea experiments in the simulation tunnel p 38 A88-27492
- LEGECKIS, RICHARD**
Satellite observations of a western boundary current in the Bay of Bengal p 36 A88-27010
- LEHMAN, DAVID J.**
Simultaneous determination of astronomic position and azimuth from observations of zenith distances and horizontal directions p 20 A88-21055
- LENTZ, STEVEN J.**
A heat budget for the northern California shelf during CODE 2 p 34 A88-25733
- LEVENTUEV, V. P.**
The use of the optical classification of ocean waters to estimate correlations between the concentrations of variable components with reference to the development of remote-sensing methods p 41 A88-30078
- LEVIN, I. M.**
Calculations of ocean-atmosphere radiance on the basis of remote sensing p 37 A88-27204
- LI, DEREN**
Theory and research on the disjunction of cross passage errors and systematic image errors in photogrammetric point determination [SER-C-324] p 61 N88-15290
- LI, ZHIRONG**
Atmospheric correction of thermal infrared images p 40 A88-29283
- LILLESAND, THOMAS**
Comparison of the gridded finite element and the polynomial interpolations for geometric rectification and mosaicking of Landsat data p 55 A88-21049
- LILLESAND, THOMAS M.**
A semi-automated training sample selector for multispectral land cover classification p 56 A88-21066
- LINDSTROM, ERIC**
Assessment of thematic mapper imagery for forestry applications under Lake States conditions p 7 A88-26336
- LIONELLO, P.**
Thermal expansion of a rig p 42 A88-32508
- LIU, GUOSHENG**
Estimation of atmospheric liquid-water amount by Nimbus 7 SMMR data - A new method and its application to the western North-Pacific region p 69 A88-30731
- LIUBOMIROVA, K. S.**
Investigating the northern Caspian Sea ice regime from meteorological-satellite data p 37 A88-27202
- LLOYD, DANIEL**
Mapping NOAA-AVHRR imagery using equal-area radial projections p 10 A88-28015
- LO, C. P.**
Parallax bar heighting accuracy of large format camera photography p 65 A88-21051
- LOGAN, T. L.**
An automated system for terrain database construction p 18 A88-21060
- LOMBARDINI, P. P.**
Sea return at C and Ku bands p 31 A88-22947
- LOOMER, SCOTT A.**
Landsat remote sensing imagery analysis program p 57 A88-21075
- LOZANO-GARCIA, D. F.**
Definition of forest stand characteristics based on multi-incidence angle SIR-B data p 2 A88-21031
- Characterizing forest stands with multi-incidence angle and multi-polarized SAR data p 10 A88-27836**
- LOZIVYEV, V. P.**
Use of space photographs for geomorphological studies in southwestern Tajikistan p 28 N88-16109
- LUKAS, ROGER**
The western equatorial Pacific Ocean circulation study p 30 A88-22911
- LULLA, KAMLESH**
Principal component analysis of aerial video imagery p 54 A88-21030
- LUMAN, DONALD E.**
A satellite image mosaic of Illinois p 55 A88-21047
- LUTHER, TERRY**
The use of digital Landsat data for wildlife management on the Warm Springs Indian Reservation of Oregon p 2 A88-21029
- LUTJEHARMS, J. R. E.**
The Natal pulse - An extreme transient on the Agulhas Current p 38 A88-27494
- M**
- MA, C.**
Crustal dynamics project data analysis, 1987. Volume 1: Fixed station VLBI geodetic results, 1979-1986 [NASA-TM-100682] p 23 N88-16279
- Crustal dynamics project data analysis, 1987. Volume 2: Mobile VLBI geodetic results, 1982-1986 [NASA-TM-100689-VOL-2] p 23 N88-16280**
- MACKEY, H. E., JR.**
Aircraft MSS data registration and vegetation classification for wetland change detection p 12 A88-29277
- MACKEY, HALKARD E., JR.**
Correlation between aircraft MSS and lidar remotely sensed data on a forested wetland p 6 A88-24513
- MACLEAN, ANN L.**
Assessment of thematic mapper imagery for forestry applications under Lake States conditions p 7 A88-26336
- MALAN, O. G.**
A new strategy for vegetation mapping with the aid of Landsat MSS data p 9 A88-27810
- MARACCI, G.**
Status and prospects of the Joint Research Committee (JRC) work on the application of ocean colour monitoring from space p 46 N88-16299
- MARKON, CARL J.**
Intermediate-scale vegetation mapping of Innoko National Wildlife Refuge, Alaska using Landsat MSS digital data p 12 A88-29494
- MAROV, M. N.**
Correlation characteristics of images of the earth surface obtained with a synthetic-aperture radar p 66 A88-21784
- MARSH, J. G.**
Source of the Australasian tektite strewn field - A possible off-shore impact site p 42 A88-31793
- MARSHAK, A. L.**
Calculation of canopy bidirectional reflectance using the Monte Carlo method p 13 A88-30439
- Monte Carlo method calculation of spectral brightness coefficient of vegetation cover as function of illumination conditions p 14 N88-16113**
- MARTIN, CHARLES L.**
Structure and growth of the mixing layer over the Amazonian rain forest p 8 A88-27252
- MARTIN, SEELYE**
Satellite passive microwave studies of the Sea of Okhotsk ice cover and its relation to oceanic processes, 1978-1982 p 36 A88-27014
- Ice floe collisions and their relation to ice deformation in the Bering Sea during February 1983 p 40 A88-29324**
- MARTUCCI, L. M.**
LANDSAT thematic mapper radiometric calibration study [NASA-CR-182410] p 61 N88-15287
- MASELLI, ARTHUR V.**
Automated photointerpretation - A stereoscopic workstation p 54 A88-21027
- MASUDA, K.**
Emissivity of pure and sea waters for the model sea surface in the infrared window regions p 42 A88-30445
- MASUOKA, P. M.**
Enigma of a thermal anomaly - A TM/AVHRR study of the volcanic Arabian highlands p 25 A88-21045
- MATHESON, WILMA**
Spectral assessment of indicators of range degradation in the Botswana hardveld environment p 5 A88-21365
- MATSON, PAMELA A.**
Remote sensing of forest canopy and leaf biochemical contents p 11 A88-28270
- MAUSEL, PAUL**
An application of divergence measurement using transformed video data p 6 A88-24510
- MCADOO, D. C.**
NASA's geodynamics program p 24 N88-19845
- MCCONNELL, ROSS M.**
Matching of dissimilar radar images using Marr-Hildreth zero crossings p 56 A88-21070
- MCCULLOCH, THOMAS M.**
Computer-assisted color generation for thematic mapping p 55 A88-21048
- MCDONNELL, M. J.**
Atmospheric correction of thermal infrared images p 40 A88-29283
- MCHONE, JOHN F.**
Talemzane - Algerian impact crater detected on SIR-A orbital imaging radar p 25 A88-25217
- MCKEOWN, DAVID M., JR.**
Automatic knowledge acquisition for aerial image interpretation [AD-A188616] p 63 N88-19810
- MCKIM, H. L.**
Remote sensing of soil moisture p 52 A88-27815
- MCLAURIN, A. PORTER**
Single-source three-dimensional imaging system for remote sensing p 66 A88-23772
- MCLELLAN, JIM**
GPS survey techniques for deformation analysis p 21 A88-21057
- MEERKOEETTER, RALF**
The anisotropy of reflected solar radiation over several types of land surface p 62 N88-16171
- MELIA, J.**
A study on the utilization of SIR-A data for population estimation in the eastern part of Spain p 18 A88-24512
- MENON, SUDHAKAR**
Requirements and principles for the implementation and construction of large-scale geographic information systems p 19 A88-28684
- MENZEL, D. W.**
Coordination: Southeast continental shelf studies [DE88-003680] p 49 N88-18110

- MERCER, B.**
Methods and accuracy of operational digital image mapping with aircraft SAR p 55 A88-21059
- MESTAYER, PATRICE**
Spray droplet generation, transport, and evaporation in a wind wave tunnel during the humidity exchange over the sea experiments in the simulation tunnel p 38 A88-27492
- MICHAELSEN, JOEL**
An investigation of the El Nino-Southern Oscillation Cycle with statistical models. I - Predictor field characteristics. II - Model results p 34 A88-25731
- MIDDLETON, ELIZABETH M.**
Surface anisotropy and hemispheric reflectance for a semiarid ecosystem p 3 A88-21354
- MILLER, ALVIN J.**
Comparison of total ozone amounts derived from satellite and ground-based measurements p 66 A88-27027
- MILLER, D. A.**
Aircraft and satellite remote sensing of desert soils and landscapes p 3 A88-21358
- MILLER, J. R.**
Comparison of in situ and airborne spectral measurements of the blue shift associated with forest decline p 11 A88-28271
- MILLER, JAMES H.**
Estimation of sea surface wave spectra using acoustic tomography [AD-A187837] p 49 N88-19057
- MILLER, LAURY**
Geosat altimeter observations of Kelvin waves and the 1986-87 El Nino p 32 A88-24582
- MILOVANOV, V. I.**
A method for synthesizing optimal space systems for earth surveying p 67 A88-27214
- MILTON, E. J.**
Principles of field spectroscopy p 68 A88-28013
- MINNETT, P. J.**
The effects of atmospheric and thermohaline variability on the validation of the GEOSAT altimeter oceanographic signal between Scotland and Iceland [AD-A189324] p 50 N88-19882
- MIRCHINK, I. M.**
Features of hydrological anomalies in connection with the search for deep-water polymetallic sulfides p 32 A88-24654
- MIROVSKII, V. G.**
Effect of ice-grain size distribution on the thermal emission of snow cover p 52 A88-24662
- MITCHELL, TODD P.**
Remote forcing of sea surface temperature in the El Nino region p 34 A88-25732
- MITNIK, L. M.**
Detection of internal waves using data from satellite microwave radiometry and the research ship Academician Alexander Nesmejanov p 41 A88-30083
- MKRTCHIAN, FERDINAND ANUSHAVANOVICH**
Methods for processing radio-physical measurement data in studies of the environment p 19 A88-29427
- MOEBS, N. N.**
Character of five selected LANDSAT lineaments in southwestern Pennsylvania: Report of investigations, 1987 [PB88-133517] p 30 N88-18988
- MOHNEN, VOLKER A.**
Proceedings of the Forest-Atmosphere Interaction Workshop [CONF-8510250] p 17 N88-19824
- MONK, G. A.**
Interpretation of satellite imagery of a rapidly deepening cyclone p 57 A88-23502
- MORCRETE, JEAN-JACQUES**
Downward longwave irradiance at the ocean surface from satellite data - Methodology and in situ validation p 38 A88-27493
- MOREL, A.**
Remote sensing of ocean colour for studies of biological productivity and biochemical cycles p 45 N88-16296
French activities in ocean colour observations p 46 N88-16303
- MORELLI, THOMAS D.**
A remote sensing based methodology for quantifying the spatial and functional relationships amongst industrial land uses delineated around the port of Baltimore p 17 A88-21012
- MORIMOTO, S.**
Design concept of the SAR installed on ERS-1 p 68 A88-27832
- MORRISSEY, LESLIE A.**
Detection and identification of Arctic landforms - An assessment of remotely sensed data p 40 A88-29492
- MOSES, HARRY**
Proceedings of the Forest-Atmosphere Interaction Workshop [CONF-8510250] p 17 N88-19824
- MOTOMURA, N.**
Simulation of spaceborne SAR imagery from airborne SAR data p 58 A88-27830
- MUELLER, T. J.**
Hydrographic and current measurements in the North-East Atlantic Ocean. Data report on F.S. Meteor cruises 69/5 and 69/6, October to November 1984 [REPT-166] p 48 N88-17164
Analysis of low frequency current fluctuations in the North-East Atlantic Ocean [REPT-170] p 48 N88-17165
- MUNIER, P.**
Evaluation of the stereoscopic accuracy of the SPOT satellite p 59 A88-28605
- MURPHY, R. E.**
The first ISLSCP field experiment (FIFE) p 67 A88-27497
- MUSIN, O. R.**
Photogrammetric principles for combining remote sounding and three-dimensional mapping p 61 N88-16135
- MUSTARD, JOHN F.**
Exploration of crustal/mantle material for the earth and moon using reflectance spectroscopy p 27 A88-28273

N

- NARAYANAN, M. S.**
Assessment of the use of satellite derived winds in monsoon forecasting using a general circulation model p 68 A88-27846
- NASRETDINOV, K. K.**
Method for joint adjustment of satellite and surface geodetic networks p 22 N88-16105
- NELSON, ROSS**
Determining the rate of forest conversion in Mato Grosso, Brazil, using Landsat MSS and AVHRR data p 10 A88-28011
Estimating forest biomass and volume using airborne laser data p 13 A88-30441
- NEMANI, RAMAKRISHNA R.**
Relating seasonal patterns of the AVHRR vegetation index to simulated photosynthesis and transpiration of forests in different climates p 13 A88-30447
- NERRY, F.**
Importance of a remote measurement of spectral thermal infrared emissivities - Presentation and validation of such a determination p 67 A88-27813
- NESTERENKO, O. P.**
A method for synthesizing optimal space systems for earth surveying p 67 A88-27214
- NETO, GILBERTO CAMARA**
A digital terrain system for microcomputers [INPE-4170-PRE/1067] p 63 N88-18987
- NEWMAN, GREGORY ALEX**
Three-dimensional transient electromagnetic modeling for exploration geophysics p 29 N88-18047
- NEY, B. I.**
Comprehensive studies of the dynamics of geosystems with the use of remote sensing techniques p 10 A88-27821
- NIKITIN, P. A.**
Computer-aided mapping of Antarctic Sea ice using along-the-course radiometric measurements aboard the Cosmos-1500 satellite p 38 A88-27213
- NIKOLAEV, S. D.**
Surface temperature variations of the world ocean in the Eocene p 32 A88-24655
- NIKOLAEV, V. I.**
Surface temperature variations of the world ocean in the Eocene p 32 A88-24655
- NITHACK, J.**
Remote sensing from space; Proceedings of Symposium 3, Workshop V, and Topical Meeting A2 of the Twenty-sixth COSPAR Plenary Meeting, Toulouse, France, June 30-July 11, 1986 p 67 A88-27801
- NIWA, S.**
Design concept of the SAR installed on ERS-1 p 68 A88-27832
- NIXON, P. R.**
Mid-infrared (1.45 to 2.0 microns) video - A potential aid in wildfire mop-up operations p 1 A88-21016
Near-real-time video systems for rangeland assessment p 4 A88-21360
- NIXON, PAUL R.**
Principal component analysis of aerial video imagery p 54 A88-21030
- NOLL, CAREY E.**
Crustal Dynamics Project: Catalogue of site information [NASA-RP-1198] p 23 N88-19037

- NOVAK, B. L.**
Estimation of the accuracy of determining atmospheric temperature profiles from microwave remote sensing at frequencies of 117-118.5 GHz p 41 A88-30084
- NOVAKOVSKIY, B. A.**
Photogrammetric principles for combining remote sounding and three-dimensional mapping p 61 N88-16135
- NUMAN, NAZAR M. S.**
Detection of subsurface geologic structures in the Tharthar area of central Iraq using Landsat images p 24 A88-20902
- NYKJAER, L.**
Status and prospects of the Joint Research Committee (JRC) work on the application of ocean colour monitoring from space p 46 N88-16299

O

- O'CALLAGHAN, JOHN F.**
The application of perceptual color spaces to the display of remotely sensed imagery p 58 A88-24935
- O'HEAR, JAMES**
Geographical position plotting by photo interpreters from Space Shuttle Large Format Camera photography p 65 A88-21050
- O'NEILL, BRIDGET**
Simultaneity of response of Atlantic Ocean tropical cyclones and Indian monsoons p 34 A88-25736
- OETTL, H.**
Future research directions in the quantitative radar remote sensing of land and oceanic surface features p 39 A88-27841
- OJO, O.**
Monitoring hydroclimatic characteristics using satellite observations from West Africa p 52 A88-27816
- OLESON, LYNDON R.**
Implementation of the Land Analysis System on a workstation p 54 A88-21026
- OLIVEIRA, AMAURI P.**
Structure and growth of the mixing layer over the Amazonian rain forest p 8 A88-27252
- OLMSTED, C.**
Landsat determined geographic change p 27 A88-29489
- OLORUNFEMI, J. FUNSO**
Identification and measurement of the areal extent of settlements from Landsat - An exploration into the Nigerian case p 19 A88-28014
- ONUFRIUK, T. P.**
The use of Meteor-Priroda space photographs for the compilation of small-scale and medium-scale tectonic and geological maps p 27 A88-30079
- OTTERMANN, J.**
Techniques of ground-truth measurements of desert-scrub structure p 9 A88-27817
- OUCHI, KAZUO**
Synthetic aperture radar imagery of range traveling ocean waves p 32 A88-24933
- OVSIANNIKOV, A. E.**
Features of hydrological anomalies in connection with the search for deep-water polymetallic sulfides p 32 A88-24654
- OWE, MANFRED**
Validating regional differences in modelled satellite microwave signatures p 1 A88-21020
Estimating surface soil moisture from satellite microwave measurements and a satellite derived vegetation index p 13 A88-30446

P

- PAIVA, JOAO ARGEMIRO C.**
A digital terrain system for microcomputers [INPE-4170-PRE/1067] p 63 N88-18987
- PALEY, HELEN N.**
Preliminary assessment of airborne imaging spectrometer and airborne thematic mapper data acquired for forest decline areas in the Federal Republic of Germany p 11 A88-28272
- PALOSCIA, S.**
X-band features of canopy cover - An up to date summary of active and passive measurements p 10 A88-27835
- PAMPALONI, P.**
X-band features of canopy cover - An up to date summary of active and passive measurements p 10 A88-27835
- PANDEY, PREM C.**
Measurement of global oceanic winds from Seasat-SMMR and its comparison with Seasat-SASS and ALT derived winds p 40 A88-29766
- PANGBURN, T.**
Remote sensing of soil moisture p 52 A88-27815

PANTANI, L.

Italian activities in ocean colour remote sensing
p 46 N88-16304

PANTIUKHOV, S. V.

Choosing conditions for the remote sensing of ocean features in the visible spectrum, with the effect of coastal zone taken into account
p 37 A88-27209

PARAMONOV, A. G.

Laser system for automating topographic terrain survey
p 70 N88-16136

PARIS, JACK F.

Characterization of vegetation with combined Thematic Mapper (TM) and Shuttle Imaging Radar (SIR-B) image data
p 2 A88-21032

PASCUCCI, RICHARD F.

An expert system for the computer-assisted analysis of radar imagery
p 55 A88-21053

PATRIAT, PH.

Evolution of the Juan Fernandez microplate during the last three million years
p 25 A88-25045

PEARSON, RONNIE W.

Development of a 32-bit UNIX-based ELAS workstation
p 54 A88-21025

PECH, R. P.

Reflectance modeling of semiarid woodlands
p 4 A88-21364

PELKEY, PATRICK D.

Development of multivariate estuarine water quality models using Landsat 2 and 4 MSS data
p 50 A88-21002

PELLINEN, L. P.

New possibilities for using gravity data in developing geodetic coordinate systems
p 23 N88-16116

PERBOS, J. R.

Speckle in SAR images - An evaluation of filtering techniques
p 59 A88-27834

PETERSEN, G. W.

Aircraft and satellite remote sensing of desert soils and landscapes
p 3 A88-21358

PETERSON, DAVID L.

Remote sensing of forest canopy and leaf biochemical contents
p 11 A88-28270

PETERSON, F. F.

Geological and vegetational applications of Shuttle Imaging Radar-B, Mineral County, Nevada
p 26 A88-26337

PETERSON, INGRID

A snapshot of the Labrador current inferred from ice-floe movement in NOAA satellite imagery
p 32 A88-24456

PETRIE, BRIAN

Coastal upwelling and eddy development off Nova Scotia
p 36 A88-27011

PETROV, A. F.

Investigation of the foci of powerful earthquakes and seismically hazardous areas on space photographs for the Baikal-Aldan region
p 27 A88-30081

PETZOLD, T. J.

Remote sensing of atmospheric optical thickness and sea-water attenuation when submerged: Wavelength selection and anticipated errors
[AD-A187609]
p 49 N88-19262

PFEIFFER, B.

The Earth-Observation Preparatory Programme
p 66 A88-22724

PHILIPSON, WARREN R.

Operational interpretation of AVHRR vegetation indices for world crop information
p 7 A88-26335
Land-cover monitoring with SPOT for landfill investigations
p 19 A88-28606

PHILLIPS, O. M.

Remote sensing of the sea surface
p 42 A88-30662

PICKUP, G.

The use of spectral and spatial variability to monitor cover change on inert landscapes
p 4 A88-21363
Forecasting patterns of soil erosion in arid lands from Landsat MSS data
p 12 A88-29280

PIETERS, CARLE M.

Exploration of crustal/mantle material for the earth and moon using reflectance spectroscopy
p 27 A88-28273

PIHOS, G. G.

Scatterometer wind speed bias induced by the large-scale component of the wave field
p 40 A88-29325

PIKE, T. K.

Simulation of bit-quantization influence on SAR images
p 59 A88-27831

PINKER, R. T.

Simulations of the Meteosat visible sensor response to changing boundary conditions
p 67 A88-27823

PINTY, B.

A method for the estimate of broadband directional surface albedo from a geostationary satellite
p 22 A88-27299

PIRES, IVAN DEOLIVEIRA

Mapping of the mangroves of the Guanabarra Bay through the utilization of remote sensing techniques
[INPE-3942-TDL/229]
p 16 N88-19804

PITERBARG, L. I.

The role of synoptic scale processes in the transfer of sea surface temperature anomalies
p 35 A88-26065

PITERI, S.

Accuracy of mapping by panoramic photography
p 60 A88-29479

A comparison between panoramic photography and conventional aerial photography in terms of mapping accuracy
p 61 A88-32167

PITTS, DAVID E.

Estimation of biophysical properties of forest canopies using C-band microwave data
p 9 A88-27809

The use of a helicopter mounted ranging scatterometer for estimation of extinction and backscattering properties of forest canopies-I: Experimental approach and calibration
p 11 A88-28682

The use of a helicopter mounted ranging scatterometer for estimation of extinction and scattering properties of forest canopies-II: Experimental results for high-density aspen
p 11 A88-28683

PLANET, WALTER G.

Comparison of total ozone amounts derived from satellite and ground-based measurements
p 66 A88-27027

PLUMMER, S. E.

Exploring the relationships between leaf nitrogen content, biomass and the near-infrared/red reflectance ratio
p 12 A88-29288

PONZONI, FLAVIO JORGE

Report of the participation in the International Training Course: Remote Sensing in Village Forestry
[INPE-4476-NTE/278]
p 16 N88-19802

PORTER, TODD

GPS survey techniques for deformation analysis
p 21 A88-21057

POTAPOV, A. N.

The use of successive clustering to analyze multispectral imagery
p 61 A88-30086

PRICE, CURTIS V.

Spectral changes in conifers subjected to air pollution and water stress: Experimental studies
p 6 A88-24932

PRICE, KEVIN PAUL

Detection of soil erosion with Thematic Mapper (TM) satellite data within Pinyon-Juniper woodlands
[NASA-CR-182476]
p 15 N88-17103

PRINCE, S. D.

Monitoring of global vegetation dynamics for assessment of primary productivity using NOAA advanced very high resolution radiometer
p 9 A88-27808

Measurement of canopy interception of solar radiation by stands of trees in sparsely wooded savanna
p 10 A88-28010

An integrated camera and radiometer for aerial monitoring of vegetation
p 14 A88-32666

PRUSOV, A. V.

The relationship between the temporal variability of ocean temperature and the meridional shifts of the intertropical convergence zone
p 37 A88-27203

PUTNAM, EVELYN S.

Commercial applications and scientific research requirements for thermal-infrared observations of terrestrial surfaces
[NASA-TM-89704]
p 70 N88-16179

R

RABERANTO, P.

A global survey of surface climate parameters from satellite observations - Preliminary results over Africa
p 67 A88-27814

RADOMYSLSKAIA, T. M.

Calculations of ocean-atmosphere radiance on the basis of remote sensing
p 37 A88-27204

RAFFY, M.

Problems related to the determination of land surface parameters and fluxes over heterogeneous media from satellite data
p 19 A88-27803

RAITALA, J.

Landsat classification of the barren hydrolittoral areas of Lake Yli-Kitka, north-eastern Finland
p 51 A88-24198

RAMAN, SETHU

The Genesis of Atlantic Lows Experiment - The planetary-boundary-layer subprogram of GALE
p 42 A88-31111

RAMANANTSIZEHENA, P.

Importance of a remote measurement of spectral thermal infrared emissivities - Presentation and validation of such a determination
p 67 A88-27813

RAMM, N. S.

The relationships between orbit parameters and the geometry of the trajectory for remote sensing satellites
p 67 A88-27215

RAMOND, D.

A method for the estimate of broadband directional surface albedo from a geostationary satellite
p 22 A88-27299

RAMSEY, E. W.

Aircraft MSS data registration and vegetation classification for wetland change detection
p 12 A88-29277

RAND, ROBERT S.

Autocorrelation of control points on 11-band multispectral imagery
[AD-A188185]
p 62 N88-18056

RAPLEY, C. G.

Radar altimeter data quality flagging
p 39 A88-27837

Swath altimetry of oceans and terrain

p 39 A88-27838

RAPP, R. H.

Terrestrial gravity data and comparisons with satellite data
p 24 N88-19848

RASANEN, MATTI E.

Fluvial perturbation in the western Amazon basin - Regulation by long-term sub-Andean tectonics
p 24 A88-20878

RAST, M.

Overview of ESA's activities in ocean colour remote sensing
p 45 N88-16294

Technical aspects of future ocean colour remote sensing
p 46 N88-16298

REDFIELD, ALICE E.

Remote sensing applications by consulting engineers - Three case histories
p 24 A88-21009

REED, KENNETH L.

Computer-assisted map analysis - A set of primitive operators for a flexible approach
p 17 A88-21023

REID, G. C.

Longitudinal variations in tropical tropopause properties in relation to tropical convection and El Nino-Southern Oscillation events
p 33 A88-25727

REISNYDER, WILLIAM E.

Proceedings of the Forest-Atmosphere Interaction Workshop
[CONF-8510250]
p 17 N88-19824

REMILLARD, M. MADDEN

Remote sensing and geographic information system techniques for aquatic resource evaluation
p 19 A88-28603

REUTER, DENNIS

Satellite observation of atmosphere and surface interaction parameters
p 38 A88-27812

REUTER, R.

The influence of yellow substances on remote sensing of sea water constituents from space. Volume 1: Summary
[ESA-CR(P)-2443-VOL-1]
p 43 N88-15292

The influence of yellow substances on remote sensing of sea water constituents from space. Volume 2: Appendices
[ESA-CR(P)-2443-VOL-2]
p 43 N88-15293

REUTOV, E. A.

Relationship between brightness temperature in the RF range and the radiative dryness index
p 69 A88-30082

REYNA, E.

Estimation of biophysical properties of forest canopies using C-band microwave data
p 9 A88-27809

REYNA, EDDIE

The use of a helicopter mounted ranging scatterometer for estimation of extinction and backscattering properties of forest canopies-I: Experimental approach and calibration
p 11 A88-28682

The use of a helicopter mounted ranging scatterometer for estimation of extinction and scattering properties of forest canopies-II: Experimental results for high-density aspen
p 11 A88-28683

REYNOLDS, M.

Overview of ESA's activities in ocean colour remote sensing
p 45 N88-16294

RICHARDSON, A. J.

Canopy reflectance of seven rangeland plant species with variable leaf pubescence
p 5 A88-23764

RICHARDSON, ARTHUR J.

Principal component analysis of aerial video imagery
p 54 A88-21030

RICKETS, J. N.

The use of direct readout, high resolution TOVS data in short and medium range weather predictions
p 68 A88-27844

RIES, J. C.

Digitized global land-sea map and access software
p 35 A88-26346

- RIGTERINK, PAUL V.**
Remote sensing of Chesapeake Bay water quality required for healthy oyster beds p 30 A88-21003
- RINGROSE, S.**
Techniques of ground-truth measurements of desert-scrub structure p 9 A88-27817
- RINGROSE, SUSAN**
Spectral assessment of indicators of range degradation in the Botswana hardveld environment p 5 A88-21365
- RIORDAN, ALLEN J.**
The Genesis of Atlantic Lows Experiment - The planetary-boundary-layer subprogram of GALE p 42 A88-31111
- RIPPLE, WILLIAM J.**
The use of digital Landsat data for wildlife management on the Warm Springs Indian Reservation of Oregon p 2 A88-21029
Geographic information systems for resource management: A compendium p 5 A88-23253
Research in remote sensing of vegetation [NASA-CR-182663] p 16 N88-19817
- RISSE, PAUL G.**
Analyzing long-term changes in vegetation with geographic information system and remotely sensed data p 10 A88-27820
- RITCHIE, JERRY C.**
Comparison of Landsat MSS pixel array sizes for estimating water quality variables in small lakes p 50 A88-21004
- ROBERTS, H. R.**
The Natal pulse - An extreme transient on the Agulhas Current p 38 A88-27494
- ROBERTSON, PHILIP K.**
The application of perceptual color spaces to the display of remotely sensed imagery p 58 A88-24935
- ROBINSON, B. F.**
Integrating sphere transmissometer for field measurement of leaf transmittance p 6 A88-23766
- ROBINSON, I. S.**
Ocean colour applications in ocean dynamics and coastal processes p 45 N88-16297
Developments in ocean colour research in the United Kingdom p 46 N88-16306
- ROCK, B. N.**
Comparison of in situ and airborne spectral measurements of the blue shift associated with forest decline p 11 A88-28271
- ROCK, BARRETT**
Preliminary assessment of airborne imaging spectrometer and airborne thematic mapper data acquired for forest decline areas in the Federal Republic of Germany p 11 A88-28272
- ROCK, BARRETT N.**
Assessing forest damage in high-elevation coniferous forests in Vermont and New Hampshire using Thematic Mapper data p 13 A88-30440
- RODEN, GUNNAR I.**
North Pacific Ocean. Central Pacific Transition Zone, R/V Thomas G. Thompson: 25 March - 3 May 1968. STD data report [AD-A186570] p 47 N88-17160
- RODRIQUES, JOSE EDUARDO**
Photographic filters [INPE-4448-RPE/558] p 64 N88-20124
- RODRIGUEZ, V.**
Evaluation of the stereoscopic accuracy of the SPOT satellite p 59 A88-28605
- ROGERS, JAMES A.**
An autoCAD-based mapping system for encoded stereoplotters p 60 A88-29490
- ROGERS, JERRY D.**
Absolute infrared intensities for F-113 and F-114 and an assessment of their greenhouse warming potential relative to other chlorofluorocarbons p 19 A88-31103
- ROHDE, FREDERICK W.**
Radar descriptors for the classification of terrain features [AD-A188145] p 63 N88-18983
- ROLPH, G.**
Meteorological and aerosol measurements from the NOAA WP-3D aircraft during WATOX-86, January 4-9, 1986 [PB88-120860] p 20 N88-18079
- ROSA, R.**
Evaluation of the flooding areas of the Sao Goncalo Canal through LANDSAT 5 thematic mapper images [INPE-4118-PRE/1039] p 53 N88-16185
- ROSENZWEIG, CYNTHIA**
The use of remote sensing in developing and validating a ground hydrology/vegetation model for GCM3 p 51 A88-21021
Determination of vegetated fraction of surface from satellite measurements p 8 A88-27807
- ROSS, I. K.**
The emissivity of the vegetation-soil system p 8 A88-27208
Calculation of canopy bidirectional reflectance using the Monte Carlo method p 13 A88-30439
- ROSS, YU. K.**
Monte Carlo method calculation of spectral brightness coefficient of vegetation cover as function of illumination conditions p 14 N88-16113
- ROST, ANDREW A.**
Digital terrain analysis employing X-Y-Z point vectors as input data p 55 A88-21061
- ROTHROCK, D. A.**
Quantitative use of satellite SAR imagery of sea ice p 39 A88-27839
Principal component analysis of satellite passive microwave data over sea ice p 41 A88-30199
- ROYER, THOMAS C.**
Multiple dipole eddies in the Alaska Coastal Current detected with Landsat thematic mapper data p 36 A88-27015
- RUDANT, JEAN-PAUL**
Problems in geologic and geomorphic interpretation and geometric modeling of radar images using a digital terrain model p 26 A88-28024
- RUDORFF, BERNARDO FRIEDRICH THEODOR**
Report on phase 1 of the project estimate development of a model for yield estimation of sugar cane based on LANDSAT and agromet data [INPE-4466-RPE/560] p 16 N88-19807
- RUFF, IRWIN**
General determination of Earth surface type and cloud amount using multispectral AVHRR data [NOAA-TR-NESDIS-39] p 72 N88-18997
- RUNNING, STEVEN W.**
Relating seasonal patterns of the AVHRR vegetation index to simulated photosynthesis and transpiration of forests in different climates p 13 A88-30447
- RYAN, J. W.**
Crustal dynamics project data analysis, 1987. Volume 1: Fixed station VLBI geodetic results, 1979-1986 [NASA-TM-100682] p 23 N88-16279
Crustal dynamics project data analysis, 1987. Volume 2: Mobile VLBI geodetic results, 1982-1986 [NASA-TM-100689-VOL-2] p 23 N88-16280
- RYNSKAIA, A. K.**
The relationships between orbit parameters and the geometry of the trajectory for remote sensing satellites p 67 A88-27215
Identical-route satellite orbits for long-term periodic global survey of the earth, not dependent on solar illumination p 67 A88-27216
- RZYMANEK, JERZY**
The legal problems of the commercialization of satellite remote sensing p 35 A88-26149
- S**
- SABADINI, ROBERTO**
Mantle rheology and satellite signatures from present-day glacial forcings p 21 A88-25225
- SACHSE, G. W.**
Biomass-burning emissions and associated haze layers over Amazonia p 18 A88-27265
- SAIDOV, M. S.**
Use of space photographs for geomorphological studies in southwestern Tajikistan p 28 N88-16109
- SALO, JUKKA S.**
Fluvial perturbation in the western Amazon basin - Regulation by long-term sub-Andean tectonics p 24 A88-20878
- SALOMONSON, VINCENT V.**
Recent data quality and earth science results from the Landsat thematic mapper p 58 A88-27824
Future research directions in the quantitative radar remote sensing of land and oceanic surface features p 39 A88-27841
- SALZER, D.**
A multi-frequency-multi-nadir-angle pushbroom-radiometer for oil spill detection and mapping (On the surface of the sea) [MBB-UR-952-87] p 31 A88-23988
- SAMADANI, RAMIN**
Observation of sea-ice dynamics using synthetic aperture radar images: Automated analysis p 32 A88-24934
- SAMES, G. P.**
Character of five selected LANDSAT lineaments in southwestern Pennsylvania: Report of investigations, 1987 [PB88-133517] p 30 N88-18988
- SANO, E. E.**
Evaluation of the flooding areas of the Sao Goncalo Canal through LANDSAT 5 thematic mapper images [INPE-4118-PRE/1039] p 53 N88-16185
- SANTANNABINS, LEONARDO**
A variant of the ISODATA algorithm for application to agricultural targets [INPE-4436-PRE/1235] p 17 N88-20023
- SANTOSDEALMEIDA, WAGNER**
Photographic filters [INPE-4448-RPE/558] p 64 N88-20124
- SATTERWHITE, MELVIN B.**
Spectral characteristics of selected soils and vegetation in northern Nevada and their discrimination using band ratio techniques p 3 A88-21352
- SAUNDERS, R. W.**
An improved method for detecting clear sky and cloudy radiances from AVHRR data p 69 A88-29284
- SAZANOV, N. V.**
Remote sensing surveys design in regional agricultural inventories p 8 A88-27804
- SCANVIC, J. Y.**
Contribution of SPOT images to the geological mapping of arid countries - Example of the Yemen Arab Republic p 25 A88-22616
- SCARPACE, FRANK L.**
Automated photointerpretation - A stereoscopic workstation p 54 A88-21027
A proposed semi-supervised two stage classification technique p 56 A88-21063
Application of frequency filtering in remotely sensed imagery p 57 A88-21072
- SCHANDA, ERWIN**
Applications of microwaves to remote sensing p 69 A88-30670
- SCHLITTENHARDT, P.**
Status and prospects of the Joint Research Committee (JRC) work on the application of ocean colour monitoring from space p 46 N88-16299
- SCHLUETER, WOLFGANG**
Application of the Global Positioning System (GPS) time receivers to the fundamental station Wettzell p 71 N88-18995
- SCHMALZER, PAUL A.**
Effects of fire on composition, biomass, and nutrients in oak scrub vegetation on John F. Kennedy Space Center, Florida [NASA-TM-100305] p 15 N88-16182
- SCHMITZ-HUEBSCH, HARALD**
Observations of Earth tides by the German Geodetic Research Institute, division 1, in the period 1979-1985 at the Berchtesgaden and Wettzell stations [SER-B-280] p 22 N88-15291
- SCHNELL, R.**
Meteorological and aerosol measurements from the NOAA WP-3D aircraft during WATOX-86, January 4-9, 1986 [PB88-120860] p 20 N88-18079
- SCHNETZLER, C. C.**
Source of the Australasian tektite strewn field - A possible off-shore impact site p 42 A88-31793
- SCHRUMPF, BARRY J.**
Research in remote sensing of vegetation [NASA-CR-182663] p 16 N88-19817
- SCHURINK, M. R.**
Design and implementation of a data base system for Digital Land Mass System (DLMS) data [FEL-IR-1987-19] p 71 N88-17101
- SCHUTZ, B. E.**
Digitized global land-sea map and access software p 35 A88-26346
- SCOFIELD, R. A.**
Characteristics of extreme rainfall events in northwestern Peru during the 1982-1983 El Niño period p 52 A88-25730
- SEAGER, RICHARD**
A model of the tropical Pacific sea surface temperature climatology p 40 A88-29323
- SEGUIN, B.**
Estimation of evapotranspiration in the Sahelian zone by use of Meteosat and NOAA AVHRR data p 9 A88-27818
- SELLERS, P. J.**
The first ISLSCP field experiment (FIFE) p 67 A88-27497
Relations between canopy reflectance, photosynthesis and transpiration - Links between optics, biophysics and canopy architecture p 8 A88-27802
Extraction of spectral hemispherical reflectance (albedo) of surfaces from nadir and directional reflectance data p 59 A88-28009
- SELLERS, PERS J.**
Extended abstract modelling interactions between the terrestrial biosphere and the global atmosphere p 65 A88-21022
- SEMENTOV, S. S.**
Variations in the intensity of emitted and scattered microwave radiation of the sea surface sensed at grazing angles in a field of surface manifestations of internal waves p 37 A88-27205

SEMOVSKII, S. V.

The role of synoptic scale processes in the transfer of sea surface temperature anomalies p 35 A88-26065

SERAFINI, Y. V.

Comparative study of temperature data from NOAA7-AVHRR and WMO - An interpretation through the use of a soil-vegetation model p 8 A88-27806

SERBENYUK, S. N.

Photogrammetric principles for combining remote sounding and three-dimensional mapping p 61 N88-16135

SHARMA, O. P.

Assessment of the use of satellite derived winds in monsoon forecasting using a general circulation model p 68 A88-27846

SHARMA, R. C.

Landsat imagery for mapping saline soils and wet lands in north-west India p 12 A88-29278

SHATALOV, A. V.

The use of successive clustering to analyze multispectral imagery p 61 A88-30086

SHAW, PETER R.

An investigation of small-offset fracture zone geoid waveforms p 22 A88-27465

SHEA, DENNIS J.

On the evolution of the southern oscillation p 36 A88-26923

SHERES, DAVID

Remote sensing of wave patterns with oceanographic implications p 31 A88-23545

SHIFRIN, K. S.

Calculations of ocean-atmosphere radiance on the basis of remote sensing p 37 A88-27204

SHIMABUKURO, YOSIO EDEMIR

Textural features for image classification in remote sensing [INPE-4169-PRE/1066] p 62 N88-16181

SHOKUROV, M. V.

The relationship between the temporal variability of ocean temperature and the meridional shifts of the intertropical convergence zone p 37 A88-27203

SHUM, C. K.

Digitized global land-sea map and access software p 35 A88-26346

SHUTKO, A. M.

Use of microwave radiometry for measuring the biometric characteristics of vegetation cover p 7 A88-27207
Relationship between brightness temperature in the RF range and the radiative dryness index p 69 A88-30082

SIEGEL, DAVID A.

On the parameterization of irradiance for open ocean photoprocesses p 34 A88-25737

SIEVERING, H.

Size distributions of sea-source aerosol particles - A physical explanation of observed nearshore versus open-sea differences p 33 A88-25289

SIMARD, R.

Digital stereo processing of satellite image data p 58 A88-27825

SIMONETT, DAVID

Improved canopy reflectance modeling and scene inference through improved understanding of scene pattern [NASA-CR-182488] p 15 N88-18049

SINGH, KESHAVA P.

Microwave remote sensing of ice in Lake Melville and the Labrador Sea p 39 A88-28850

SINGH, S. M.

Simulation of solar zenith angle effect on global vegetation index (GVI) data p 14 A88-32660

SLACK, R. B.

Remote sensing and geographic information system techniques for aquatic resource evaluation p 19 A88-28603

SLADE, DAVID H.

Proceedings of the Forest-Atmosphere Interaction Workshop [CONF-8510250] p 17 N88-19824

SLADKOPEVTSEV, S. A.

Techniques of geomorphological mapping on the basis of space photographs p 26 A88-26708

SLASHCHEV, V. G.

Choosing conditions for the remote sensing of ocean features in the visible spectrum, with the effect of coastal zone taken into account p 37 A88-27209

SMITH, MARTHA P.

Observation of sea-ice dynamics using synthetic aperture radar images: Automated analysis p 32 A88-24934

SMITH, TERENCE R.

Requirements and principles for the implementation and construction of large-scale geographic information systems p 19 A88-28684

SMOLOV, V. YE.

Limiting accuracy of scatterometer determination of wind speed over ocean from satellite p 44 N88-16107

SNOEIJ, PAUL

The DUT airborne scatterometer p 5 A88-23549

SOBIESKI, P.

An approximate model for the microwave brightness temperature of the sea p 31 A88-23544

SOBRINO, J. A.

A study on the utilization of SIR-A data for population estimation in the eastern part of Spain p 18 A88-24512

SOELLNER, R.

Information content of spectral signatures and textures and structures for remote sensing of the earth p 60 A88-29499

SOLER, TOMAS

On differential scale changes and the satellite Doppler system z-shift p 21 A88-25850

SOLTAU, GERHARD

The orientation of global satellite networks p 63 N88-18996

SONNABEND, D.

Spaceborne gravity gradiometry characterizing the data type p 24 N88-19847

SOUTHWORTH, C. SCOTT

Geologic applications of side-looking airborne radar images in the Appalachian Valley and Ridge Province p 24 A88-21034

SPANNER, MICHAEL

Remote sensing of forest canopy and leaf biochemical contents p 11 A88-28270

SPATZ, DAVID

Nature and origin of mineral coatings on volcanic rocks of the Black Mountain, Stonewall Mountain, and Kane Springs Wash volcanic centers, Southern Nevada [NASA-CR-181437] p 29 N88-17140

SPIERING, BRUCE A.

Development of a 32-bit UNIX-based ELAS workstation p 54 A88-21025

SPIRIDONOV, IU. G.

Computer-aided mapping of Antarctic Sea ice using along-the-course radiometric measurements aboard the Cosmos-1500 satellite p 38 A88-27213

SPITZER, D.

Ocean colour applications in ocean dynamics and coastal processes p 45 N88-16297
National Remote Sensing Program (NRSP) of the Netherlands p 46 N88-16305

SPITZY, A.

The influence of yellow substances on remote sensing of sea water constituents from space. Volume 1: Summary [ESA-CR(P)-2443-VOL-1] p 43 N88-15292
The influence of yellow substances on remote sensing of sea water constituents from space. Volume 2: Appendices [ESA-CR(P)-2443-VOL-2] p 43 N88-15293

STAFFORD, DAVID R.

Operational revision of national topographic maps in Canada using Landsat images p 54 A88-20901

STAR, JEFFREY L.

Requirements and principles for the implementation and construction of large-scale geographic information systems p 19 A88-28684

STEINER, ELLEN J.

Sea surface temperature, low-level moisture, and convection in the tropical Pacific, 1982-1985 p 34 A88-25729

STEPHENS, ROBERT D.

Absolute infrared intensities for F-113 and F-114 and an assessment of their greenhouse warming potential relative to other chlorofluorocarbons p 19 A88-31103

STOESSEL, M.

Thematic mapper research in the earth sciences: Small scale patches of suspended matter and phytoplankton in the Elbe River Estuary, German Bight and Tidal Flats [NASA-CR-182378] p 45 N88-16180

STOHR, CHRISTOPHER J.

A satellite image mosaic of Illinois p 55 A88-21047

STOLL, M. P.

Importance of a remote measurement of spectral thermal infrared emissivities - Presentation and validation of such a determination p 67 A88-27813

STONE, THOMAS A.

Determining the rate of forest conversion in Mato Grosso, Brazil, using Landsat MSS and AVHRR data p 10 A88-28011

Shuttle imaging radar A analysis of land use in Amazonia p 12 A88-29282

STRAMMA, LOTHAR

Processing and analysis of large volumes of satellite-derived thermal infrared data p 36 A88-27012

STREBEL, D. E.

The first ISLSCP field experiment (FIFE) p 67 A88-27497

STRINGER, W. J.

Landsat determined geographic change p 27 A88-29489

STROM, A. L.

Use of space photographs for paleoseismogeological studies (on the example of Mongolian Altay) p 28 N88-16110

STUNDER, B.

Meteorological and aerosol measurements from the NOAA WP-3D aircraft during WATOX-86, January 4-9, 1986 [PB88-120860] p 20 N88-18079

STURM, B.

Status and prospects of the Joint Research Committee (JRC) work on the application of ocean colour monitoring from space p 46 N88-16299

SUETIN, V. S.

The use of regression analysis to determine sea surface temperatures from Cosmos-1151 measurements of IR radiation p 41 A88-30085

SUGIMURA, T.

A study to produce 1:100,000 scale LFC color photomap p 68 A88-27826

SUSSKIND, JOEL

Satellite observation of atmosphere and surface interaction parameters p 38 A88-27812

SUTYRIN, G. G.

Blocking of the Benguela Current by a single anticyclone - Analysis of satellite and ship data p 41 A88-30077

SWANBERG, NANCY

Remote sensing of forest canopy and leaf biochemical contents p 11 A88-28270

SWANN, RICHARD

The potential for automated mapping from Geocoded digital image data p 59 A88-28604

SWART, PETER J. F.

The DUT airborne scatterometer p 5 A88-23549

SWITZER, PAUL

A transformation for ordering multispectral data in terms of image quality with implications for noise removal p 58 A88-24937

T**TAI, CHANG-KOU**

Geosat crossover analysis in the tropical Pacific. Part 1: Constrained sinusoidal crossover adjustment [NASA-CR-182391] p 43 N88-15285

An efficient algorithm for computing the crossovers in satellite altimetry [NASA-CR-182389] p 43 N88-15286

On estimating the basin-scale ocean circulation from satellite altimetry. Part 1: Straightforward spherical harmonic expansion [NASA-CR-182387] p 44 N88-15352

TAKASHIMA, T.

Emissivity of pure and sea waters for the model sea surface in the infrared window regions p 42 A88-30445

TAKAYAMA, Y.

Emissivity of pure and sea waters for the model sea surface in the infrared window regions p 42 A88-30445

TAKEDA, TAKAO

Estimation of atmospheric liquid-water amount by Nimbus 7 SMMR data - A new method and its application to the western North-Pacific region p 69 A88-30731

TAKET, N. D.

SAR imaging of volume scatterers p 60 A88-28681

TALBOT, R. W.

Biomass-burning emissions and associated haze layers over Amazonia p 18 A88-27265

TALBOT, STEPHEN S.

Intermediate-scale vegetation mapping of Innoko National Wildlife Refuge, Alaska using Landsat MSS digital data p 12 A88-29494

TANAKA, S.

A study to produce 1:100,000 scale LFC color photomap p 68 A88-27826

TAPLEY, B. D.

Digitized global land-sea map and access software p 35 A88-26346

TARAKANCHIKOV, V. V.

Interpretation of the visible manifestations of sea water dynamics from space imagers of the Caspian Sea p 37 A88-27201

TARANIK, JAMES V.

Comparison of techniques for discriminating hydrothermal alteration minerals with Airborne Imaging Spectrometer data p 27 A88-28269

- Commercial applications and scientific research requirements for thermal-infrared observations of terrestrial surfaces [NASA-TM-89704] p 70 N88-16179
- Nature and origin of mineral coatings on volcanic rocks of the Black Mountain, Stonewall Mountain, and Kane Springs Wash volcanic centers, Southern Nevada [NASA-CR-181437] p 29 N88-17140
- TARPLEY, J. D.**
Observations of surface and atmospheric features from passive microwave satellite measurements p 64 A88-21019
- TASSAN, S.**
Status and prospects of the Joint Research Committee (JRC) work on the application of ocean colour monitoring from space p 46 N88-16299
- TAYLOR, P. T.**
Spaceborne magnetometry p 24 N88-19846
- TENG, WILLIAM L.**
Operational interpretation of AVHRR vegetation indices for world crop information p 7 A88-26335
- THOMAS, DONALD R.**
Principal component analysis of satellite passive microwave data over sea ice p 41 A88-30199
- THOMAS, M. E.**
Evaluation of a temperature remote sensing technique [AD-A187885] p 71 N88-18053
- THOMAS, RANDALL W.**
Discriminating semiarid vegetation using airborne imaging spectrometer data - A preliminary assessment p 4 A88-21359
- THOMPSON, EDWARD F.**
Nearshore wave transformation study of sites near Port Canaveral Inlet, Florida [AD-A186965] p 47 N88-17159
- THORMODSGARD, JUNE M.**
Comparison of the gridded finite element and the polynomial interpolations for geometric rectification and mosaicking of Landsat data p 55 A88-21049
- THORNDIKE, ALAN S.**
Principal component analysis of satellite passive microwave data over sea ice p 41 A88-30199
- TIMCHENKO, A. I.**
Characteristics of the subsurface radar sounding of natural objects p 26 A88-25551
- TISNADO, G. M.**
Characteristics of extreme rainfall events in northwestern Peru during the 1982-1983 El Nino period p 52 A88-25730
- TOIKKA, M.**
Construction of airborne radars for remote sensing [PB88-113063] p 71 N88-16916
- TON, JEZCHING**
Land cover change detection using a GIS-guided, feature-based classification of Landsat thematic mapper data p 18 A88-21073
- TONELLI, JOHN**
Estimating forest biomass and volume using airborne laser data p 13 A88-30441
- TOOMEY, DANIEL A.**
A proposed semi-supervised two stage classification technique p 56 A88-21063
- TOPLISS, BRENDA J.**
Coastal upwelling and eddy development off Nova Scotia p 36 A88-27011
- TORRES, A. L.**
Biomass-burning emissions and associated haze layers over Amazonia p 18 A88-27265
- TOWNSHEND, J. R. G.**
Selecting the spatial resolution of satellite sensors required for global monitoring of land transformations p 20 A88-32659
- TRAPEZNIKOVA, N. B.**
Computer-aided mapping of Antarctic Sea ice using along-the-course radiometric measurements aboard the Cosmos-1500 satellite p 38 A88-27213
- TRENBERTH, KEVIN E.**
On the evolution of the southern oscillation p 36 A88-26923
- TRINDER, J. C.**
Assessment of SIR-B for topographic mapping p 57 A88-23761
- TRIVERO, P.**
Sea return at C and Ku bands p 31 A88-22947
- TSCHERNING, C. C.**
Gravity field mapping from satellite altimetry, sea-gravimetry and bathymetry in the Eastern Mediterranean p 42 A88-30836
- TUCKER, C. J.**
Satellite observed seasonal and inter-annual variation of vegetation over the Kalahari, the Great Victoria Desert, and the Great Sandy Desert - 1979-1984 p 3 A88-21356
- TUCKER, COMPTON J.**
Satellite remote sensing of drought conditions p 3 A88-21357
- TUCKER, WALTER B., III**
Physical properties of summer sea ice in the Fram Strait, June-July 1984 [AD-A186937] p 53 N88-17156
- TUELLER, PAUL T.**
Remote sensing science applications in arid environments p 3 A88-21351
Aerial and ground spectral characteristics of rangeland plant communities in Nevada p 3 A88-21353
- TULINOV, V. F.**
Remote sensing methods and instrumentation for obtaining data on earth resources and the environment p 66 A88-26050
- TURNER, ANTHONY M.**
Operational revision of national topographic maps in Canada using Landsat images p 54 A88-20901
- TURNER, J.**
The use of direct readout, high resolution TOVS data in short and medium range weather predictions p 68 A88-27844
- U**
- UDWARI, JOSEPH J.**
Remote sensing applications by consulting engineers - Three case histories p 24 A88-21009
- ULABY, FAWWAZ T.**
The use of a helicopter mounted ranging scatterometer for estimation of extinction and backscattering properties of forest canopies-I: Experimental approach and calibration p 11 A88-28682
Mesoscale monitoring of the soil freeze/thaw boundary from orbital microwave radiometry [NASA-CR-182659] p 17 N88-19855
- ULANDER, LARS M. H.**
Interpretation of Seasat radar-altimeter data over sea ice using near-simultaneous SAR imagery p 31 A88-23547
- UNGAR, S. G.**
Remote sensing from space; Proceedings of Symposium 3, Workshop V, and Topical Meeting A2 of the Twenty-sixth COSPAR Plenary Meeting, Toulouse, France, June 30-July 11, 1986 p 67 A88-27801
- UPADHYAY, H. C.**
Assessment of the use of satellite derived winds in monsoon forecasting using a general circulation model p 68 A88-27846
- USTIN, SUSAN L.**
Discriminating semiarid vegetation using airborne imaging spectrometer data - A preliminary assessment p 4 A88-21359
- V**
- V.D.PIEPEN, H.**
The influence of yellow substances on remote sensing of sea water constituents from space. Volume 1: Summary [ESA-CR(P)-2443-VOL-1] p 43 N88-15292
The influence of yellow substances on remote sensing of sea water constituents from space. Volume 2: Appendices [ESA-CR(P)-2443-VOL-2] p 43 N88-15293
The use of chlorophyll fluorescence measurements from space for separating constituents of sea water. Volume 1: Summary [ESA-CR(P)-2444-VOL-1] p 43 N88-15294
The use of chlorophyll fluorescence measurements from space for separating constituents of sea water. Volume 2: Appendices [ESA-CR(P)-2444-VOL-2] p 44 N88-15295
- VADAS, V.**
Adaptive computer-aided system for crop inventory according to space photographs p 13 A88-30087
- VALENZUELA, GASPARD R.**
Remote sensing of wave patterns with oceanographic implications p 31 A88-23545
- VALLEAU, NICHOLAS C.**
Airborne electromagnetic sounding of sea ice thickness and sub-ice bathymetry [AD-A188939] p 50 N88-19879
- VAN GELDER, BOUDEWIJN H. W.**
On differential scale changes and the satellite Doppler system z-shift p 21 A88-25850
- VANDERBILT, V. C.**
Integrating sphere transmissometer for leaf measurement of leaf transmittance p 6 A88-23766
Polarized and non-polarized leaf reflectances of *Coleus blumei* p 7 A88-26624
- VANDERPIEPEN, H.**
Federal Republic of Germany's interests, activities and goals in remote sensing of ocean colour/fluorescence from space p 46 N88-16302
- VANE, GREGG**
Terrestrial imaging spectroscopy p 69 A88-28266
- VASIL'EV, L. N.**
Comprehensive studies of the dynamics of geosystems with the use of remote sensing techniques p 10 A88-27821
- VASIL'KOV, A. P.**
The efficiency of polarization measurements in passive remote sensing of the ocean in the visible spectrum p 38 A88-27210
- VENSLAVSKII, V. B.**
Variations in the intensity of emitted and scattered microwave radiation of the sea surface sensed at grazing angles in a field of surface manifestations of internal waves p 37 A88-27205
- VERSTAPPEN, HERMAN TH.**
Remote sensing applications - An outlook for the future p 64 A88-20904
- VESECKY, JOHN F.**
Observation of sea-ice dynamics using synthetic aperture radar images: Automated analysis p 32 A88-24934
- VILLMANN, CH.**
Observations of ocean and sea bottom relief from space p 35 A88-26099
- VLCEK, J.**
Multispectral video survey of a Northern Ontario forest p 1 A88-21015
- VOGEL, JOANNE**
An evaluation of the use of TM digital data for updating the land cover component of the SCS 1987 multiresource inventory of New Jersey p 1 A88-21013
- VOGELMANN, JAMES E.**
Assessing forest damage in high-elevation coniferous forests in Vermont and New Hampshire using Thematic Mapper data p 13 A88-30440
- VOLKOV, A. M.**
Remote sensing methods and instrumentation for obtaining data on earth resources and the environment p 66 A88-26050
- VREELAND, P.**
Geological and vegetational applications of Shuttle Imaging Radar-B, Mineral County, Nevada p 26 A88-26337
- W**
- WADDELL, S. R.**
Ice breakup - Observations of the acoustic signal p 41 A88-30200
- WADHAMS, PETER**
The ice thickness distribution across the Atlantic sector of the Antarctic Ocean in midwinter p 34 A88-25734
- WALKER, KIM-MARIE**
Multitemporal Landsat multispectral scanner and Thematic Mapper data of the Hubbard Glacier region, southeast Alaska p 52 A88-29493
- WALKER, NAN**
Marine boundary layer modification across the edge of the Agulhas Current p 38 A88-27495
- WALLACE, JOHN M.**
El Nino events and their relation to the Southern Oscillation - 1925-1986 p 33 A88-25726
Remote forcing of sea surface temperature in the El Nino region p 34 A88-25732
- WALSH, J. E.**
Remote sensing of soil moisture p 52 A88-27815
- WALTER, L. S.**
Source of the Australasian tektite strewn field - A possible off-shore impact site p 42 A88-31793
- WANG, J. F.**
Automated road network extraction from Landsat TM imagery p 18 A88-21044
- WANJURA, D. F.**
Vegetative and optical characteristics of four-row crop canopies p 14 A88-32661
- WANNINKHOF, RIK**
Gas exchange on Mono Lake and Crowley Lake, California p 52 A88-25735
- WARDLEY, N. W.**
Radiometric leaf area index p 14 A88-32662
- WARREN, ALDEN**
A satellite image mosaic of Illinois p 55 A88-21047
- WASOWSKI, RONALD J.**
A time-lapse analysis of the Mississippi Delta using Landsat MSS Band 4 (IR2) photographic imagery p 51 A88-21039
- WATTS, ANTHONY B.**
On the accuracy of marine gravity measurements p 21 A88-25224
- WATTS, P. D.**
A sequential estimation approach to cloud-clearing for satellite temperature sounding p 66 A88-23511

WEARE, BRYAN C.

- Relationships between monthly precipitation and SST variations in the tropical Pacific region p 65 A88-21382

WEBER, MARKUS

- Vertical sounding of the air layer close to a glacier on Mount Vernagferner in the Oetzal Alps, Tyrol (experiment LUZIVER 1983) p 44 N88-16152

WEEKS, WILFORD F.

- Physical properties of summer sea ice in the Fram Strait, June-July 1984 [AD-A186937] p 53 N88-17156

WELCH, R.

- Remote sensing and geographic information system techniques for aquatic resource evaluation p 19 A88-28603

WELLMAN, D.

- Size distributions of sea-source aerosol particles - A physical explanation of observed nearshore versus open-sea differences p 33 A88-25289

WERNES, SUSAN A. S.

- Application of predictive compression methods to synthetic aperture radar imagery I p 57 A88-23768

WERTH, LEE F.

- Difficulties and recommendations for obtaining very large scale 70 mm aerial photography for rangeland monitoring p 1 A88-21017

WESSEL, PAL

- On the accuracy of marine gravity measurements p 21 A88-25224

WESSMAN, CAROL

- Remote sensing of forest canopy and leaf biochemical contents p 11 A88-28270

WESTFALL, R. H.

- A new strategy for vegetation mapping with the aid of Landsat MSS data p 9 A88-27810

WESTFIELD, LEE M.

- Multi-stage remote sensing - A tool for Minnesota natural resources management p 64 A88-21018

WESTMAN, WALTER E.

- Spectral changes in conifers subjected to air pollution and water stress: Experimental studies p 6 A88-24932

- Aboveground biomass, surface area, and production relations of red fir (*Abies magnifica*) and white fir (*A. concolor*) p 12 A88-28705

WESTWELL-ROPER, ANDREW

- The potential for automated mapping from Geocoded digital image data p 59 A88-28604

WHEELER, DOUGLAS J.

- A comparison of the hierarchical cluster and homogeneous training field detection methods in classifying urban landcovers from TM data p 56 A88-21067

WIESNET, DONALD R.

- Large-scale hurricane hazard mapping along the coastal plain of Honduras using Landsat data p 17 A88-21041

WILLIAMS, VICKI L.

- Land-cover monitoring with SPOT for landfill investigations p 19 A88-28606

WILLIAMSON, H. D.

- Evaluation of middle and thermal infrared radiance in indices used to estimate GLAI p 14 A88-32663

WILLIS, P.

- Geodetic application of the Global Positioning System p 21 A88-24289

WILLSON, P. J.

- An integrated camera and radiometer for aerial monitoring of vegetation p 14 A88-32666

WILSON, RICHARD O.

- Aerial and ground spectral characteristics of rangeland plant communities in Nevada p 3 A88-21353

WINTERBERGER, KENNETH C.

- Measuring crown cover in interior Alaska vegetation types p 12 A88-29495

WISE, P. J.

- Assessment of SIR-B for topographic mapping p 57 A88-23761

WITTSTOCK, R.-R.

- Hydrographic and current measurements in the North-East Atlantic Ocean. Data report on F.S. Meteor cruises 69/5 and 69/6, October to November 1984 [REPT-166] p 48 N88-17164

WOLF, P. L.

- Quantification of biomass of the marsh grass *Spartina alterniflora* Loisel using Landsat Thematic Mapper imagery p 6 A88-23765

WOLFRAMM, A. P.

- Simulation of bit-quantization influence on SAR images p 59 A88-27831

WOODWELL, GEORGE M.

- Shuttle imaging radar A analysis of land use in Amazonia p 12 A88-29282

WOODWORTH, P. L.

- Review of the potential of satellite remote sensing for marine flood protection [IOS-237] p 43 N88-15280

WORRELL, KURT J.

- Application of frequency filtering in remotely sensed imagery p 57 A88-21072

WRIGHT, DANIEL G.

- Coastal upwelling and eddy development off Nova Scotia p 36 A88-27011

WU, SHIH-TSENG

- Parametric analysis of synthetic aperture radar data for characterization of deciduous forest stands p 2 A88-21033

WUKELIC, G. E.

- LANDSAT thematic mapper radiometric calibration study [NASA-CR-182410] p 61 N88-15287

Y**YAZDANI, ROSTAM**

- Potential applications of digital image analysis systems for displaying satellite altimetry data p 31 A88-23762

YEGOROV, V. V.

- Statistical model of interaction of electromagnetic waves with natural objects being sensed p 70 N88-16112

YEH, EUENG-NAN

- Airborne measurements of surface layer turbulence over the ocean during cold air outbreaks p 35 A88-26911

YELLES-CHAUOUCHE, A.

- Evolution of the Juan Fernandez microplate during the last three million years p 25 A88-25045

YODER, J. A.

- Update of NASA's ocean colour activities p 45 N88-16295

YOSHIMURA, M.

- A study to produce 1:100,000 scale LFC color photomap p 68 A88-27826

YOUNG, M. V.

- Interpretation of satellite imagery of a rapidly deepening cyclone p 57 A88-23502

YUAN, X.

- Multispectral video survey of a Northern Ontario forest p 1 A88-21015

YUEN, DAVID A.

- Mantle rheology and satellite signatures from present-day glacial forcings p 21 A88-25225

Z**ZAPEVALOV, A. S.**

- Limiting accuracy of scatterometer determination of wind speed over ocean from satellite p 44 N88-16107

ZAYTSEV, YU. I.

- Satellite monitoring of earthquake precursor effects in magnetosphere p 28 N88-16103

ZEBIAK, STEPHEN E.

- A model of the tropical Pacific sea surface temperature climatology p 40 A88-29323

ZENONE, CHESTER

- Multitemporal Landsat multispectral scanner and Thematic Mapper data of the Hubbard Glacier region, southeast Alaska p 52 A88-29493

ZHANG, JINYUN

- Hierarchical segmentation using a composite criterion for remotely sensed imagery p 54 A88-20841

ZIEMER, F.

- Investigation of the quantitative determination of two dimensional sea surface wave spectra from shipborne radar measurements [GKSS-87/E/10] p 48 N88-17163

ZILIOLI, EUGENIO

- Geostructural evolution of the Southern Alps - Lineaments trends detected on Landsat images p 26 A88-25448

ZINNDORF, STEPHAN

- Optimization of photogrammetric image adjustment [SER-C-323] p 22 N88-15289

ZUBKOV, LEONID BORISOVICH

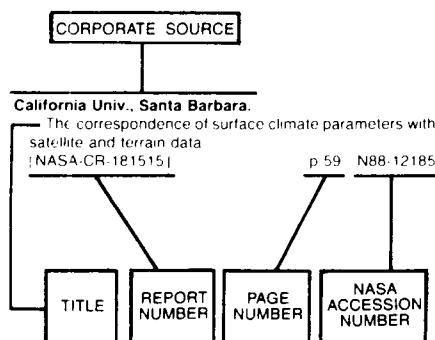
- The space metal: All about titanium p 25 A88-24781

CORPORATE SOURCE INDEX

EARTH RESOURCES / A Continuing Bibliography (Issue 58)

AUGUST 1988

Typical Corporate Source Index Listing



Listings in this index are arranged alphabetically by corporate source. The title of the document is used to provide a brief description of the subject matter. The page number and the accession number are included in each entry to assist the user in locating the abstract in the abstract section. If applicable, a report number is also included as an aid in identifying the document.

A

- Academy of Sciences (USSR), Moscow.**
Materials of the World Data Center B. Deep Seismic Sounding (DSS): Pacific data p 48 N88-17167
- Alaska Univ., Fairbanks.**
Multiple dipole eddies in the Alaska Coastal Current detected with Landsat thematic mapper data p 36 A88-27015
Detection and identification of Arctic landforms - An assessment of remotely sensed data p 40 A88-29492
- Applied Microwave Corp., Lawrence, Kans.**
The use of a helicopter mounted ranging scatterometer for estimation of extinction and backscattering properties of forest canopies-I: Experimental approach and calibration p 11 A88-28682
- Arizona State Univ., Tempe.**
Taleznane - Algerian impact crater detected on SIR-A orbital imaging radar p 25 A88-25217
- Army Cold Regions Research and Engineering Lab., Hanover, N.H.**
Physical properties of summer sea ice in the Fram Strait, June-July 1984 [AD-A186937] p 53 N88-17156
Airborne electromagnetic sounding of sea ice thickness and sub-ice bathymetry [AD-A188939] p 50 N88-19879
- Army Engineer Topographic Labs., Fort Belvoir, Va.**
Autocorrelation of control points on 11-band multispectral imagery [AD-A188185] p 62 N88-18056
Radar descriptors for the classification of terrain features [AD-A188145] p 63 N88-18983

B

- Bionetics Corp., Cocoa Beach, Fla.**
Effects of fire on composition, biomass, and nutrients in oak scrub vegetation on John F. Kennedy Space Center, Florida [NASA-TM-100305] p 15 N88-16182
- Bologna Univ. (Italy).**
Mantle rheology and satellite signatures from present-day glacial forcings p 21 A88-25225
- Brown Univ., Providence, R. I.**
Exploration of crustal/mantle material for the earth and moon using reflectance spectroscopy p 27 A88-28273
- Bureau Gravimetrique International, Toulouse (France).**
Gradiometer mission spectral analysis and simulation studies: Past and future p 24 A88-19851
- Bureau of Mines, Pittsburgh, Pa.**
Character of five selected LANDSAT lineaments in southwestern Pennsylvania: Report of investigations, 1987 [PB88-133517] p 30 N88-18988

C

- California Univ., Berkeley.**
Discriminating semiarid vegetation using airborne imaging spectrometer data - A preliminary assessment p 4 A88-21359
Spectral changes in conifers subjected to air pollution and water stress: Experimental studies p 6 A88-24932
- California Univ., Davis.**
Discriminating semiarid vegetation using airborne imaging spectrometer data - A preliminary assessment p 4 A88-21359
- California Univ., Los Angeles.**
Aboveground biomass, surface area, and production relations of red fir (*Abies magnifica*) and white fir (*A. concolor*) p 12 A88-28705
- California Univ., Santa Barbara.**
Requirements and principles for the implementation and construction of large-scale geographic information systems p 19 A88-28684
Improved canopy reflectance modeling and scene inference through improved understanding of scene pattern [NASA-CR-182488] p 15 N88-18049
- Carnegie-Mellon Univ., Pittsburgh, Pa.**
Automatic knowledge acquisition for aerial image interpretation [AD-A188616] p 63 N88-19810
- Centre National d'Etudes Spatiales, Paris (France).**
French activities in ocean colour observations p 46 N88-16303
- Coastal Engineering Research Center, Vicksburg, Miss.**
Nearshore wave transformation study of sites near Port Canaveral Inlet, Florida [AD-A186965] p 47 N88-17159
- Colorado Univ., Boulder.**
Correlation between aircraft MSS and lidar remotely sensed data on a forested wetland p 6 A88-24513
Terrestrial imaging spectroscopy p 69 A88-28266
Meteorological and aerosol measurements from the NOAA WP-3D aircraft during WATOX-86, January 4-9, 1986 [PB88-120860] p 20 N88-18079
- Columbia Univ., New York, N.Y.**
A model of the tropical Pacific sea surface temperature climatology p 40 A88-29323
- Consiglio Nazionale delle Ricerche, Venice (Italy).**
Italian activities in ocean colour remote sensing p 46 N88-16304
- Cornell Univ., Ithaca, N.Y.**
Thematic mapper study of Alaskan ophiolites [NASA-CR-182554] p 30 N88-18984

D

- Defense Mapping Agency Aerospace Center, St. Louis, Mo.**
The digital landmass simulation production overview [AD-A187978] p 62 N88-18978
- Delaware Univ., Newark.**
Quantification of biomass of the marsh grass *Spartina alterniflora* Loisel using Landsat Thematic Mapper imagery p 6 A88-23765
- Department of Energy, Washington, D. C.**
Proceedings of the Forest-Atmosphere Interaction Workshop [CONF-8510250] p 17 N88-19824
- Deutsche Forschungs- und Versuchsanstalt fuer Luft- und Raumfahrt, Freiburg (West Germany).**
Investigations on the application of space photographs (Spacelab metric camera) for routine inventories of extensively managed forest areas [DFVLR-FB-87-22] p 15 N88-17098
- Deutsche Forschungs- und Versuchsanstalt fuer Luft- und Raumfahrt, Oberpfaffenhofen (West Germany).**
Federal Republic of Germany's interests, activities and goals in remote sensing of ocean colour/fluorescence from space p 46 N88-16302
Statistics of two-dimensional structure elements of mountainous ranges (mosaic model) for calculating three-dimensional reflection functions [DFVLR-FB-87-33] p 29 N88-17099
- Deutsche Forschungs- und Versuchsanstalt fuer Luft- und Raumfahrt, Wesseling (West Germany).**
Remote sensing from space: Proceedings of Symposium 3, Workshop V, and Topical Meeting A2 of the Twenty-sixth COSPAR Plenary Meeting, Toulouse, France, June 30-July 11, 1986 p 67 A88-27801
Future research directions in the quantitative radar remote sensing of land and oceanic surface features p 39 A88-27841
- Deutsche Geodatische Kommission, Munich (West Germany).**
The aerophotogrammetric determination of Earth surface deformations [SER-C-321] p 28 N88-15288
Optimization of photogrammetric image adjustment [SER-C-323] p 22 N88-15289
Theory and research on the disjunction of cross passage errors and systematic image errors in photogrammetric point determination [SER-C-324] p 61 N88-15290
Observations of Earth tides by the German Geodetic Research Institute, division 1, in the period 1979-1985 at the Berchtesgaden and Wettzell stations [SER-B-280] p 22 N88-15291
- Du Pont de Nemours (E. I.) and Co., Alken, S.C.**
Correlation between aircraft MSS and lidar remotely sensed data on a forested wetland p 6 A88-24513

E

- Ecole Nationale Supérieure de Physique, Strasbourg (France).**
Importance of a remote measurement of spectral thermal infrared emissivities - Presentation and validation of such a determination p 67 A88-27813
- European Space Agency, Paris (France).**
Ocean Colour Workshop [ESA-SP-1083] p 45 N88-16292
Europe's position concerning ocean colour activities p 45 N88-16293
Proceedings of an ESA-NASA Workshop on a Joint Solid Earth Program [NASA-SP-182642] p 23 N88-19844
- European Space Agency, ESRIN, Frascati (Italy).**
The Earthnet Heat Capacity Mapping Mission (HCMM) data-processing system at Lannion (France) p 62 N88-16761
- European Space Agency, European Space Operations Center, Darmstadt (West Germany).**
Meteorological Information Extraction Center (MIEC) processing [ESA-STR-224] p 71 N88-17143

SOURCE

European Space Agency. European Space Research and Technology Center, ESTEC, Noordwijk (Netherlands).

- Overview of ESA's activities in ocean colour remote sensing p 45 N88-16294
- Technical aspects of future ocean colour remote sensing p 46 N88-16298
- Earthnet's experience with Seasat SAR image processing p 62 N88-16760

G**Geneva Univ. (Switzerland).**

- Research in Switzerland on ocean and inland-water colour monitoring p 46 N88-16301

Geosplorers International, Inc., Denver, Colo.

- Geological evolution and analysis of confirmed or suspected gas hydrate localities. Volume 10: Basin analysis, formation and stability of gas hydrates of the Aleutian Trench and the Bering Sea p 29 N88-18048
- Geological evolution and analysis of confirmed or suspected gas hydrate localities. Volume 9: Formation and stability of gas hydrates of the Middle America Trench [DE88-001007] p 29 N88-18050

Geological Survey, Trenton, N.J.

- Spectral changes in conifers subjected to air pollution and water stress: Experimental studies p 6 A88-24932

GKSS-Forschungszentrum Geesthacht (West Germany).

- The influence of yellow substances on remote sensing of sea water constituents from space. Volume 1: Summary [ESA-CR(P)-2443-VOL-1] p 43 N88-15292
- The influence of yellow substances on remote sensing of sea water constituents from space. Volume 2: Appendices [ESA-CR(P)-2443-VOL-2] p 43 N88-15293
- The use of chlorophyll fluorescence measurements from space for separating constituents of sea water. Volume 1: Summary [ESA-CR(P)-2444-VOL-1] p 43 N88-15294
- The use of chlorophyll fluorescence measurements from space for separating constituents of sea water. Volume 2: Appendices [ESA-CR(P)-2444-VOL-2] p 44 N88-15295
- Thematic mapper research in the earth sciences: Small scale patches of suspended matter and phytoplankton in the Elbe River Estuary, German Bight and Tidal Flats [NASA-CR-182378] p 45 N88-16180
- The use of chlorophyll fluorescence measurements from space for separating constituents of sea water p 47 N88-16307
- The influence of yellow substances on remote sensing of sea-water constituents from space p 47 N88-16308
- Investigation of the quantitative determination of two dimensional sea surface wave spectra from shipborne radar measurements [GKSS-87/E/10] p 48 N88-17163

H**Harvard Univ., Cambridge, Mass.**

- Biomass-burning emissions and associated haze layers over Amazonia p 18 A88-27265

Helsinki Univ. of Technology, Espoo (Finland).

- Construction of airborne radars for remote sensing [PB88-113063] p 71 N88-16916

Hunter Coll., New York.

- Refining image segmentation by polygon skeletonization p 56 A88-21068

I**Illinois Natural History Survey, Champaign.**

- Estimating forest productivity in southern Illinois using Landsat Thematic Mapper data and geographic information system analysis techniques p 2 A88-21028

Illinois State Water Survey, Champaign.

- Application of satellite data in variational analysis for global cyclonic systems [NASA-CR-182468] p 62 N88-17152

Institut fuer Angewandte Geodasie, Frankfurt am Main (West Germany).

- Reports on cartography and geodesy. Series 1, report 98 [ISSN-0469-4236] p 23 N88-18993
- Application of the Global Positioning System (GPS) time receivers to the fundamental station Wettzell p 71 N88-18995

The orientation of global satellite networks

p 63 N88-18996

Institute of Ocean Sciences, Sidney (British Columbia).

- Canadian activities and goals in remote sensing of ocean colour and fluorescence from space p 46 N88-16300

Institute of Oceanographic Sciences, Birkenhead (England).

- Review of the potential of satellite remote sensing for marine flood protection [IOS-237] p 43 N88-15280

Instituto de Pesquisas Espaciais, Sao Jose dos Campos (Brazil).

- Textural features for image classification in remote sensing [INPE-4169-PRE/1066] p 62 N88-16181
- Evaluation of the flooding areas of the Sao Goncalo Canal through LANDSAT 5 thematic mapper images [INPE-4118-PRE/1039] p 53 N88-16185
- A digital terrain system for microcomputers [INPE-4170-PRE/1067] p 63 N88-18987
- Crop forecasting in Brazil: A short history of productivity models [INPE-4150-PRE/1056] p 16 N88-19801
- Report of the participation in the International Training Course: Remote Sensing in Village Forestry [INPE-4476-NTE/278] p 16 N88-19802
- Mapping of the mangroves of the Guanabarra Bay through the utilization of remote sensing techniques [INPE-3942-TDL/229] p 16 N88-19804
- Report on phase 1 of the project estimate development of a model for yield estimation of sugar cane based on LANDSAT and agromet data [INPE-4466-RPE/560] p 16 N88-19807
- A variant of the ISODATA algorithm for application to agricultural targets [INPE-4436-PRE/1235] p 17 N88-20023
- Photographic filters [INPE-4448-RPE/558] p 64 N88-20124
- International Council of Scientific Unions, Rome (Italy).**
- WOCE Core Project 2 Planning Meeting: The Southern Ocean [WCP-138] p 44 N88-15348
- International Paper Co., Tuxedo Park, N.Y.**
- Estimating forest biomass and volume using airborne laser data p 13 A88-30441
- Ithaco, Inc., Ithaca, N.Y.**
- ISTP SBIR phase 1 Full-Sky Scanner: A feasibility study [NASA-CR-180749] p 71 N88-17964

J**Jet Propulsion Lab., California Inst. of Tech., Pasadena.**

- Characterization of vegetation with combined Thematic Mapper (TM) and Shuttle Imaging Radar (SIR-B) image data p 2 A88-21032
- An automated system for terrain database construction p 18 A88-21060
- Introduction to the physics and techniques of remote sensing p 65 A88-21168
- Wind-fetch dependence of Seasat scatterometer measurements p 31 A88-23546
- Landsat classification of the barren hydroclittoral areas of Lake Yli-Kitka, north-eastern Finland p 51 A88-24198
- Satellite observation of atmosphere and surface interaction parameters p 38 A88-27812
- Extraction of spectral hemispherical reflectance (albedo) of surfaces from nadir and directional reflectance data p 59 A88-28009
- Terrestrial imaging spectroscopy p 69 A88-28266
- Comparison of in situ and airborne spectral measurements of the blue shift associated with forest decline p 11 A88-28271
- Preliminary assessment of airborne imaging spectrometer and airborne thematic mapper data acquired for forest decline areas in the Federal Republic of Germany p 11 A88-28272
- Scatterometer wind speed bias induced by the large-scale component of the wave field p 40 A88-29325
- Measurement of global oceanic winds from Seasat-SMMR and its comparison with Seasat-SASS and ALT derived winds p 40 A88-29766
- Assessing forest damage in high-elevation coniferous forests in Vermont and New Hampshire using Thematic Mapper data p 13 A88-30440
- Spaceborne gravity gradiometry characterizing the data type p 24 N88-19847
- Johns Hopkins Univ., Laurel, Md.**
- Analysis of algorithms for the retrieval of rain-rate profiles from a spaceborne dual-wavelength radar p 69 A88-28679

- Evaluation of a temperature remote sensing technique [AD-A187885] p 71 N88-18053

Joint Publications Research Service, Arlington, Va.

- Satellite monitoring of earthquake precursor effects in magnetosphere p 28 N88-16103
- Space applications in geography p 22 N88-16104
- Method for joint adjustment of satellite and surface geodetic networks p 22 N88-16105
- Limiting accuracy of scatterometer determination of wind speed over ocean from satellite p 44 N88-16107
- Space photographs of the Onega-Ladoga isthmus and prediction of useful minerals p 28 N88-16108
- Use of space photographs for geomorphological studies in southwestern Tajikistan p 28 N88-16109
- Use of space photographs for paleoseismogeological studies (on the example of Mongolian Altay) p 28 N88-16110
- Study of relief of ore regions using space images (on the example of Eastern Yakutia) p 28 N88-16111
- Statistical model of interaction of electromagnetic waves with natural objects being sensed p 70 N88-16112
- Monte Carlo method calculation of spectral brightness coefficient of vegetation cover as function of illumination conditions p 14 N88-16113
- Multistep component analysis of correlations p 61 N88-16115
- New possibilities for using gravity data in developing geodetic coordinate systems p 23 N88-16116
- Academic course Space Methods for Studying Modern Landscapes of Continents p 72 N88-16133
- Photogrammetric principles for combining remote sounding and three-dimensional mapping p 61 N88-16135
- Laser system for automating topographic terrain survey p 70 N88-16136
- Joint Research Centre of the European Communities, Ispra (Italy).**
- Status and prospects of the Joint Research Committee (JRC) work on the application of ocean colour monitoring from space p 46 N88-16299

K**Kansas State Univ., Manhattan.**

- The first ISLSCP field experiment (FIFE) p 67 A88-27497

Kiel Univ. (West Germany).

- Hydrographic and current measurements in the North-East Atlantic Ocean. Data report on F.S. Meteor cruises 69/5 and 69/6, October to November 1984 [REPT-166] p 48 N88-17164
- Analysis of low frequency current fluctuations in the North-East Atlantic Ocean [REPT-170] p 48 N88-17165

L**Lamont-Doherty Geological Inst., Palisades, N.Y.**

- A model of the tropical Pacific sea surface temperature climatology p 40 A88-29323

Lebanon Valley Coll., Annville, Pa.

- Quantification of biomass of the marsh grass *Spartina alterniflora* Loisel using Landsat Thematic Mapper imagery p 6 A88-23765

Lockheed Engineering and Management Services Co., Inc., Houston, Tex.

- Estimation of biophysical properties of forest canopies using C-band microwave data p 9 A88-27809
- The use of a helicopter mounted ranging scatterometer for estimation of extinction and backscattering properties of forest canopies-I: Experimental approach and calibration p 11 A88-28682
- The use of a helicopter mounted ranging scatterometer for estimation of extinction and scattering properties of forest canopies-II: Experimental results for high-density aspen p 11 A88-28683

Los Alamos National Lab., N. Mex.

- The angular reflectance signature of the canopy hot spot in the optical regime [DE88-005385] p 15 N88-18991

Ludwig-Maximilians-Universitaet, Munich (West Germany).

- Preliminary assessment of airborne imaging spectrometer and airborne thematic mapper data acquired for forest decline areas in the Federal Republic of Germany p 11 A88-28272
- Use of the thermodynamic evaporation formula of Hoffmann in energy balance models for flowing water p 52 N88-16143
- Energy balance and discharge of an Alpine glacier, illustrated by Mount Vernagferner in the Oetzal Alps, Tyrol p 53 N88-16145

- The unsteady ground heat flow at the contact surface between a glacier run and the subsoil p 53 N88-16147
- Vertical sounding of the air layer close to a glacier on Mount Vernagferner in the Oetzal Alps, Tyrol (experiment LUZIVER 1983) p 44 N88-16152
- The role of anisotropy in the long range reconnaissance of the albedo of land surfaces p 62 N88-16169
- The anisotropy of reflected solar radiation over several types of land surface p 62 N88-16171

M

- Marine Biological Association of the United Kingdom, Plymouth (England).**
- Remote sensing of ocean colour for studies of biological productivity and biochemical cycles p 45 N88-16296
- Marine Biological Lab., Woods Hole, Mass.**
- Determining the rate of forest conversion in Mato Grosso, Brazil, using Landsat MSS and AVHRR data p 10 A88-28011
- Shuttle imaging radar A analysis of land use in Amazonia p 12 A88-29282
- Maryland Univ., College Park.**
- The first ISLSCP field experiment (FIFE) p 67 A88-27497
- Remote sensing from space; Proceedings of Symposium 3, Workshop V, and Topical Meeting A2 of the Twenty-sixth COSPAR Plenary Meeting, Toulouse, France, June 30-July 11, 1986 p 67 A88-27801
- Relations between canopy reflectance, photosynthesis and transpiration - Links between optics, biophysics and canopy architecture p 8 A88-27802
- Evaluating North American net primary productivity with satellite observations p 9 A88-27819
- Extraction of spectral hemispherical reflectance (albedo) of surfaces from nadir and directional reflectance data p 59 A88-28009
- Selecting the spatial resolution of satellite sensors required for global monitoring of land transformations p 20 A88-32659
- Commercial applications and scientific research requirements for thermal-infrared observations of terrestrial surfaces [NASA-TM-89704] p 70 N88-16179
- Spatial-temporal variability of North Pacific sea surface temperature anomaly patterns p 49 N88-19058
- Massachusetts Inst. of Tech., Cambridge.**
- Active and passive remote sensing of ice [AD-A186685] p 47 N88-17162
- Max-Planck-Inst. fuer Chemie, Mainz (West Germany).**
- Biomass-burning emissions and associated haze layers over Amazonia p 18 A88-27265
- Miami Univ., Coral Gables, Fla.**
- Exact Rayleigh scattering calculations for use with the Nimbus-7 Coastal Zone Color Scanner p 41 A88-30415
- Miami Univ., Fla.**
- Exact Rayleigh scattering calculations for use with the Nimbus-7 Coastal Zone Color Scanner p 41 A88-30415
- Michigan State Univ., East Lansing.**
- Land cover change detection using a GIS-guided, feature-based classification of Landsat thematic mapper data p 18 A88-21073
- Evaluation of several classification schemes for mapping forest cover types in Michigan p 10 A88-28012
- Michigan Univ., Ann Arbor.**
- The use of a helicopter mounted ranging scatterometer for estimation of extinction and backscattering properties of forest canopies-I: Experimental approach and calibration p 11 A88-28682
- Mesoscale monitoring of the soil freeze/thaw boundary from orbital microwave radiometry [NASA-CR-182659] p 17 N88-19855
- Ministry of Transport and Waterways, The Hague (Netherlands).**
- National Remote Sensing Program (NRSP) of the Netherlands p 46 N88-16305
- Minnesota Univ., Minneapolis.**
- Mantle rheology and satellite signatures from present-day glacial forcings p 21 A88-25225
- Montana Univ., Missoula.**
- Relating seasonal patterns of the AVHRR vegetation index to simulated photosynthesis and transpiration of forests in different climates p 13 A88-30447

N

- National Academy of Sciences - National Research Council, Washington, D. C.**
- International role of US geoscience [NASA-CR-182407] p 28 N88-16281

- Critical issues in NASA information systems [NASA-CR-182380] p 72 N88-16577
- National Aeronautics and Space Administration, Washington, D.C.**
- The first ISLSCP field experiment (FIFE) p 67 A88-27497
- Commercial applications and scientific research requirements for thermal-infrared observations of terrestrial surfaces [NASA-TM-89704] p 70 N88-16179
- Update of NASA's ocean colour activities p 45 N88-16295
- Space-based remote sensing of the Earth: A report to the Congress [NASA-TM-89709] p 72 N88-18046
- NASA Oceanic Processes Program [NASA-TM-4025] p 48 N88-18109
- NASA's geodynamics program p 24 N88-19845
- National Aeronautics and Space Administration. Ames Research Center, Moffett Field, Calif.**
- Spectral changes in conifers subjected to air pollution and water stress: Experimental studies p 6 A88-24932
- Polarized and non-polarized leaf reflectances of *Coleus blumei* p 7 A88-26624
- Remote sensing of forest canopy and leaf biochemical contents p 11 A88-28270
- Aboveground biomass, surface area, and production relations of red fir (*Abies magnifica*) and white fir (*A. concolor*) p 12 A88-28705
- National Aeronautics and Space Administration. Earth Resources Lab., Bay St. Louis, Miss.**
- Development of a 32-bit UNIX-based ELAS workstation p 54 A88-21025
- Parametric analysis of synthetic aperture radar data for characterization of deciduous forest stands p 2 A88-21033
- National Aeronautics and Space Administration. Goddard Inst. for Space Studies, New York, N.Y.**
- Remote sensing from space; Proceedings of Symposium 3, Workshop V, and Topical Meeting A2 of the Twenty-sixth COSPAR Plenary Meeting, Toulouse, France, June 30-July 11, 1986 p 67 A88-27801
- Determination of vegetated fraction of surface from satellite measurements p 8 A88-27807
- National Aeronautics and Space Administration. Goddard Space Flight Center, Greenbelt, Md.**
- Validating regional differences in modelled satellite microwave signatures p 1 A88-21020
- Engima of a thermal anomaly - A TM/AVHRR study of the volcanic Arabian highlands p 25 A88-21045
- Surface anisotropy and hemispheric reflectance for a semiarid ecosystem p 3 A88-21354
- Satellite observed seasonal and inter-annual variation of vegetation over the Kalahari, the Great Victoria Desert, and the Great Sandy Desert - 1979-1984 p 3 A88-21356
- Satellite remote sensing of drought conditions p 3 A88-21357
- Satellite maps of Antarctic total ozone [AIAA PAPER 88-0210] p 30 A88-22154
- A canopy reflectance model based on an analytical solution to the multiple scattering equation p 7 A88-25447
- Remote sensing of water vapor convergence, deep convection, and precipitation over the tropical Pacific Ocean during the 1982-1983 El Nino p 33 A88-25728
- Characteristics of extreme rainfall events in northwestern Peru during the 1982-1983 El Nino period p 52 A88-25730
- Airborne measurements of surface layer turbulence over the ocean during cold air outbreaks p 35 A88-26911
- The first ISLSCP field experiment (FIFE) p 67 A88-27497
- Remote sensing from space; Proceedings of Symposium 3, Workshop V, and Topical Meeting A2 of the Twenty-sixth COSPAR Plenary Meeting, Toulouse, France, June 30-July 11, 1986 p 67 A88-27801
- Problems related to the determination of land surface parameters and fluxes over heterogeneous media from satellite data p 19 A88-27803
- Satellite observation of atmosphere and surface interaction parameters p 38 A88-27812
- Importance of a remote measurement of spectral thermal infrared emissivities - Presentation and validation of such a determination p 67 A88-27813
- Techniques of ground-truth measurements of desert-scrub structure p 9 A88-27817
- Evaluating North American net primary productivity with satellite observations p 9 A88-27819
- Atmospheric effect on spectral signature - Measurements p 58 A88-27822
- Recent data quality and earth science results from the Landsat thematic mapper p 58 A88-27824

- Future research directions in the quantitative radar remote sensing of land and oceanic surface features p 39 A88-27841
- Extraction of spectral hemispherical reflectance (albedo) of surfaces from nadir and directional reflectance data p 59 A88-28009
- Determining the rate of forest conversion in Mato Grosso, Brazil, using Landsat MSS and AVHRR data p 10 A88-28011
- Estimates of primary productivity over the Thar Desert based upon Nimbus-7 37 GHz data - 1979-1985 p 11 A88-28016
- Looking at the earth from space p 69 A88-29235
- Relating Nimbus-7 37 GHz data to global land-surface evaporation, primary productivity and the atmospheric CO2 concentration p 60 A88-29287
- Estimating forest biomass and volume using airborne laser data p 13 A88-30441
- Relative sensitivity of Normalized Difference Vegetation Index (NDVI) and Microwave Polarization Difference Index (MPDI) for vegetation and desertification monitoring p 13 A88-30444
- Estimating surface soil moisture from satellite microwave measurements and a satellite derived vegetation index p 13 A88-30446
- Source of the Australasian tektite strewn field - A possible off-shore impact site p 42 A88-31793
- Microwave vegetation index - A new long-term global data set for biospheric studies p 14 A88-32658
- HIRIS (High-Resolution Imaging Spectrometer): Science opportunities for the 1990s. Earth observing system. Volume 2C: Instrument panel report [NASA-TM-89703] p 70 N88-15282
- From pattern to process: The strategy of the Earth Observing System: Volume 2: EOS Science Steering Committee report [NASA-TM-89702] p 70 N88-15283
- SAR (Synthetic Aperture Radar). Earth observing system. Volume 2F: Instrument panel report [NASA-TM-89701] p 70 N88-15284
- Crustal dynamics project data analysis, 1987. Volume 1: Fixed station VLBI geodetic results, 1979-1986 [NASA-TM-100689-VOL-1] p 23 N88-16279
- Crustal dynamics project data analysis, 1987. Volume 2: Mobile VLBI geodetic results, 1982-1986 [NASA-TM-100689-VOL-2] p 23 N88-16280
- Crustal Dynamics Project: Catalogue of site information [NASA-RP-1198] p 23 N88-19037
- Spaceborne magnetometry p 24 N88-19846
- National Aeronautics and Space Administration. Lyndon B. Johnson Space Center, Houston, Tex.**
- Estimation of biophysical properties of forest canopies using C-band microwave data p 9 A88-27809
- The use of a helicopter mounted ranging scatterometer for estimation of extinction and backscattering properties of forest canopies-I: Experimental approach and calibration p 11 A88-28682
- The use of a helicopter mounted ranging scatterometer for estimation of extinction and scattering properties of forest canopies-II: Experimental results for high-density aspen p 11 A88-28683
- National Aeronautics and Space Administration. Langley Research Center, Hampton, Va.**
- Structure and growth of the mixing layer over the Amazonian rain forest p 8 A88-27252
- Biomass-burning emissions and associated haze layers over Amazonia p 18 A88-27265
- National Aeronautics and Space Administration. Wallops Flight Center, Wallops Island, Va.**
- Correlation between aircraft MSS and lidar remotely sensed data on a forested wetland p 6 A88-24513
- Biomass-burning emissions and associated haze layers over Amazonia p 18 A88-27265
- Estimating forest biomass and volume using airborne laser data p 13 A88-30441
- National Environmental Satellite Service, Washington, D. C.**
- Comparison of total ozone amounts derived from satellite and ground-based measurements p 66 A88-27027
- National Oceanic and Atmospheric Administration, Boulder, Colo.**
- Comparison of total ozone amounts derived from satellite and ground-based measurements p 66 A88-27027
- National Oceanic and Atmospheric Administration, Silver Spring, Md.**
- Meteorological and aerosol measurements from the NOAA WP-3D aircraft during WATOX-86, January 4-9, 1986 [PB88-120860] p 20 N88-18079

National Oceanic and Atmospheric Administration, Washington, D. C.

Characteristics of extreme rainfall events in northwestern Peru during the 1982-1983 El Nino period p 52 A88-25730

Space-based remote sensing of the Earth: A report to the Congress [NASA-TM-89709] p 72 N88-18046

General determination of Earth surface type and cloud amount using multispectral AVHRR data [NOAA-TR-NESDIS-39] p 72 N88-18997

National Severe Storms Lab., Norman, Okla.

National Severe Storms Laboratory, fiscal year 1987 [PB88-140108] p 72 N88-19863

National Weather Service, Silver Spring, Md.

Comparison of total ozone amounts derived from satellite and ground-based measurements p 66 A88-27027

Naval Postgraduate School, Monterey, Calif.

Model-based building verification in aerial photographs [AD-A186010] p 20 N88-15278

Sea surface current estimates off central California as derived from enhanced AVHRR (Advanced Very High Resolution Radiometer) infrared images [AD-A186867] p 47 N88-17155

Three-dimensional image generation from an aerial photograph [AD-A188039] p 63 N88-18979

Naval Research Lab., Washington, D.C.

Texture study of Synthetic Aperture Radar (SAR) images of ocean surfaces [AD-A186021] p 42 N88-15101

Nevada Univ., Reno.

Geological and vegetational applications of Shuttle Imaging Radar-B, Mineral County, Nevada p 26 A88-26337

Discrimination of hydrothermal alteration mineral assemblages at Virginia City, Nevada, using the airborne imaging spectrometer p 27 A88-28268

Comparison of techniques for discriminating hydrothermal alteration minerals with Airborne Imaging Spectrometer data p 27 A88-28269

Nature and origin of mineral coatings on volcanic rocks of the Black Mountain, Stonewall Mountain, and Kane Springs Wash volcanic centers, Southern Nevada [NASA-CR-181437] p 29 N88-17140

New Hampshire Univ., Durham.

Comparison of in situ and airborne spectral measurements of the blue shift associated with forest decline p 11 A88-28271

Preliminary assessment of airborne imaging spectrometer and airborne thematic mapper data acquired for forest decline areas in the Federal Republic of Germany p 11 A88-28272

New South Wales Univ., Kensington (Australia).

Multisource context classification methods in remote sensing p 63 N88-18985

Surveying with GPS in Australia p 71 N88-18986

New South Wales Univ., Sydney (Australia).

Five New South Wales barrier lagoons: Their macrobenthic fauna and seagrass communities p 49 N88-19059

Mesoscale coastal ocean dynamics p 49 N88-19060

Nova Univ., Dania, Fla.

Five-diagonal weighting scheme for geoidal profiles [AD-A188033] p 23 N88-18054

O**Oak Ridge National Lab., Tenn.**

Estimating forest productivity in southern Illinois using Landsat Thematic Mapper data and geographic information system analysis techniques p 2 A88-21028

Ohio State Univ., Columbus.

Terrestrial gravity data and comparisons with satellite data p 24 N88-19848

Old Dominion Univ., Norfolk, Va.

Continental shelf processes affecting the oceanography of the South Atlantic Bight [DE88-004102] p 48 N88-17166

Oregon Graduate Center for Study and Research, Beaverton.

Remote sensing of atmospheric crosswinds by utilizing speckle-turbulence interaction and optical heterodyne detection [AD-A187580] p 71 N88-18052

Oregon State Univ., Corvallis.

Research in remote sensing of vegetation [NASA-CR-182663] p 16 N88-19817

Oulu Univ. (Finland).

Landsat classification of the barren hydrolittoral areas of Lake Yli-Kittka, north-eastern Finland p 51 A88-24198

P**Pacific Northwest Labs., Richland, Wash.**

LANDSAT thematic mapper radiometric calibration study [NASA-CR-182410] p 61 N88-15287

User's guide to a data base of current environmental monitoring projects in the US-Canadian transboundary region [DE88-002476] p 20 N88-17119

Paris VI Univ. (France).

Quantitative use of satellite SAR imagery of sea ice p 39 A88-27839

Pennsylvania State Univ., University Park.

Aircraft and satellite remote sensing of desert soils and landscapes p 3 A88-21358

Physics and Electronics Lab. TNO, The Hague (Netherlands).

Design and implementation of a data base system for Digital Land Mass System (DLMS) data [FEL-IR-1987-19] p 71 N88-17101

Purdue Univ., West Lafayette, Ind.

Integrating sphere transmissometer for field measurement of leaf transmittance p 6 A88-23766

Polarized and non-polarized leaf reflectances of *Coleus blumei* p 7 A88-26624

Characterizing forest stands with multi-incidence angle and multi-polarized SAR data p 10 A88-27836

R**Research and Data Systems, Inc., Lanham, Md.**

Remote sensing of water vapor convergence, deep convection, and precipitation over the tropical Pacific Ocean during the 1982-1983 El Nino p 33 A88-25728

Royal Australian Navy Research Lab., Edgelycliff.

The ocean heat budget [AD-A186130] p 44 N88-15346

Oceanographic features of the east and southeast Indian Ocean for June 1983 [AD-A186948] p 47 N88-17158

Rutgers Univ., New Brunswick, N. J.

Determination of vegetated fraction of surface from satellite measurements p 8 A88-27807

S**SACLANT ASW Research Center, La Spezia (Italy).**

The effects of atmospheric and thermohaline variability on the validation of the GEOSAT altimeter oceanographic signal between Scotland and Iceland [AD-A189324] p 50 N88-19882

San Diego State Univ., Calif.

Estimation of wheat canopy resistance using combined remotely sensed spectral reflectance and thermal observations p 13 A88-30448

Sao Paulo Univ. (Brazil).

Structure and growth of the mixing layer over the Amazonian rain forest p 8 A88-27252

Science Applications Research, Lanham, Md.

Engima of a thermal anomaly - A TM/AVHRR study of the volcanic Arabian highlands p 25 A88-21045

Surface anisotropy and hemispheric reflectance for a semiarid ecosystem p 3 A88-21354

The first ISLSCP field experiment (FIFE) p 67 A88-27497

Techniques of ground-truth measurements of desert-scrub structure p 9 A88-27817

Determining the rate of forest conversion in Mato Grosso, Brazil, using Landsat MSS and AVHRR data p 10 A88-28011

Estimating surface soil moisture from satellite microwave measurements and a satellite derived vegetation index p 13 A88-30446

Scranton Univ., Pa.

Quantification of biomass of the marsh grass *Spartina alterniflora* Loisel using Landsat Thematic Mapper imagery p 6 A88-23765

Scripps Institution of Oceanography, La Jolla, Calif.

The onset of spring melt in first-year ice regions of the Arctic as determined from scanning multichannel microwave radiometer data for 1979 and 1980 p 37 A88-27016

Geosat crossover analysis in the tropical Pacific. Part 1: Constrained sinusoidal crossover adjustment [NASA-CR-182391] p 43 N88-15285

An efficient algorithm for computing the crossovers in satellite altimetry [NASA-CR-182389] p 43 N88-15286

On estimating the basin-scale ocean circulation from satellite altimetry. Part 1: Straightforward spherical harmonic expansion [NASA-CR-182387] p 44 N88-15352

Remote sensing of atmospheric optical thickness and sea-water attenuation when submerged: Wavelength selection and anticipated errors [AD-A187609] p 49 N88-19262

Simpson Weather Associates, Inc., Charlottesville, Va.

Structure and growth of the mixing layer over the Amazonian rain forest p 8 A88-27252

Skidaway Inst. of Oceanography, Savannah, Ga.

Coordination: Southeast continental shelf studies [DE88-003680] p 49 N88-18110

Smithsonian Institution, Washington, D. C.

Engima of a thermal anomaly - A TM/AVHRR study of the volcanic Arabian highlands p 25 A88-21045

South Carolina Univ., Columbia.

Correlation between aircraft MSS and lidar remotely sensed data on a forested wetland p 6 A88-24513

Southampton Univ. (England).

Ocean colour applications in ocean dynamics and coastal processes p 45 N88-16297

Developments in ocean colour research in the United Kingdom p 46 N88-16306

Stanford Univ., Calif.

Observation of sea-ice dynamics using synthetic aperture radar images: Automated analysis p 32 A88-24934

State Univ. of New York, Albany.

Structure and growth of the mixing layer over the Amazonian rain forest p 8 A88-27252

Proceedings of the Forest-Atmosphere Interaction Workshop [CONF-8510250] p 17 N88-19824

Strasbourg Univ. (France).

Problems related to the determination of land surface parameters and fluxes over heterogeneous media from satellite data p 19 A88-27803

T**Technion - Israel Inst. of Tech., Haifa.**

Atmospheric effect on spectral signature - Measurements p 58 A88-27822

TGS Technology, Inc., Moffett Field, Calif.

Remote sensing of forest canopy and leaf biochemical contents p 11 A88-28270

Aboveground biomass, surface area, and production relations of red fir (*Abies magnifica*) and white fir (*A. concolor*) p 12 A88-28705

Detection and identification of Arctic landforms - An assessment of remotely sensed data p 40 A88-29492

U**United Nations Environment Program, Nairobi (Kenya).**

System-wide medium-term environment programme for the period 1990-1995: Strategies of the United Nations system for the environment [UNEP/GCSS.1/2] p 20 N88-19826

Utah Univ., Salt Lake City.

Detection of soil erosion with Thematic Mapper (TM) satellite data within Pinyon-Juniper woodlands [NASA-CR-182476] p 15 N88-17103

Three-dimensional transient electromagnetic modeling for exploration geophysics p 29 N88-18047

V**Vexcell Corp., Boulder, Colo.**

Image based SAR product simulation for analysis p 55 A88-21037

Matching of dissimilar radar images using Marr-Hildreth zero crossings p 56 A88-21070

A smart, mapping, charting and geodesy control generator, phase 1 [AD-A188184] p 23 N88-18055

Virginia Univ., Charlottesville.

Structure and growth of the mixing layer over the Amazonian rain forest p 8 A88-27252

Biomass-burning emissions and associated haze layers over Amazonia p 18 A88-27265

Design of the primary pre-TRMM and TRMM ground truth site [NASA-CR-182609] p 53 N88-19865

W**Washington Univ., Seattle.**

Satellite passive microwave studies of the Sea of Okhotsk ice cover and its relation to oceanic processes, 1978-1982 p 36 A88-27014

Quantitative use of satellite SAR imagery of sea ice p 39 A88-27839

CORPORATE SOURCE

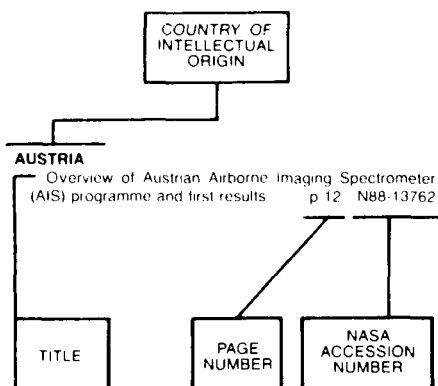
York Univ., Toronto (Ontario).

North Pacific Ocean. Central Pacific Transition Zone,
R/V Thomas G. Thompson: 25 March - 3 May 1968. STD
data report p 47 N88-17160
[AD-A186570]
Wisconsin Univ., Madison.
Remote sensing of forest canopy and leaf biochemical
contents p 11 A88-28270
Woods Hole Oceanographic Institution, Mass.
Shuttle imaging radar A analysis of land use in
Amazonia p 12 A88-29282
Estimation of sea surface wave spectra using acoustic
tomography p 49 N88-19057
[AD-A187837]
World Climate Programme, Geneva (Switzerland).
WOCE Core Project 2 Planning Meeting: The Southern
Ocean p 44 N88-15348
[WCP-138]
Report of the Workshop on Space Systems Possibilities
for a Global Energy and Water Cycle Experiment
[WCP-137] p 53 N88-17147

Y

Yale Univ., New Haven, Conn.
Proceedings of the Forest-Atmosphere Interaction
Workshop p 17 N88-19824
[CONF-8510250]
York Univ., Toronto (Ontario).
Comparison of in situ and airborne spectral
measurements of the blue shift associated with forest
decline p 11 A88-28271

Typical Foreign Technology Index Listing



Listings in this index are arranged alphabetically by country of intellectual origin. The title of the document is used to provide a brief description of the subject matter. The page number and the accession number are included in each entry to assist the user in locating the citation in the abstract section. If applicable, a report number is also included as an aid in identifying the document.

A

AUSTRALIA

- Satellite remote sensing of Australian rangelands p 4 A88-21361
- Detection of yearly cover change with Landsat MSS on pastoral landscapes in central Australia p 4 A88-21362
- The use of spectral and spatial variability to monitor cover change on inert landscapes p 4 A88-21363
- Reflectance modeling of semiarid woodlands p 4 A88-21364
- The western equatorial Pacific Ocean circulation study p 30 A88-22911
- Assessment of SIR-B for topographic mapping p 57 A88-23761
- The application of perceptual color spaces to the display of remotely sensed imagery p 58 A88-24935
- A transformation for ordering multispectral data in terms of image quality with implications for noise removal p 58 A88-24937
- Forecasting patterns of soil erosion in arid lands from Landsat MSS data p 12 A88-29280
- Evaluation of middle and thermal infrared radiance in indices used to estimate GLAI p 14 A88-32663
- Large area crop classification in New South Wales, Australia, using Landsat data p 14 A88-32665
- The ocean heat budget [AD-A186130] p 44 A88-15346
- Oceanographic features of the east and southeast Indian Ocean for June 1983 [AD-A186948] p 47 A88-17158
- Multisource context classification methods in remote sensing p 63 A88-18985
- Surveying with GPS in Australia p 71 A88-18986
- Five New South Wales barrier lagoons: Their macrobenthic fauna and seagrass communities p 49 A88-19059
- Mesoscale coastal ocean dynamics p 49 A88-19060

B

BELGIUM

- An approximate model for the microwave brightness temperature of the sea p 31 A88-23544

BOTSWANA

- Spectral assessment of indicators of range degradation in the Botswana hardveld environment p 5 A88-21365

BRAZIL

- Textural features for image classification in remote sensing [INPE-4169-PRE/1066] p 62 A88-16181
- Evaluation of the flooding areas of the Sao Goncalo Canal through LANDSAT 5 thematic mapper images [INPE-4118-PRE/1039] p 53 A88-16185
- A digital terrain system for microcomputers [INPE-4170-PRE/1067] p 63 A88-18987
- Crop forecasting in Brazil: A short history of productivity models [INPE-4150-PRE/1056] p 16 A88-19801
- Report of the participation in the International Training Course: Remote Sensing in Village Forestry [INPE-4476-NTE/276] p 16 A88-19802
- Mapping of the mangroves of the Guanabarra Bay through the utilization of remote sensing techniques [INPE-3942-TDL/228] p 16 A88-19804
- Report on phase 1 of the project estimate development of a model for yield estimation of sugar cane based on LANDSAT and agromet data [INPE-4466-RPE/560] p 16 A88-19807
- A variant of the ISODATA algorithm for application to agricultural targets [INPE-4436-PRE/1235] p 17 A88-20023
- Photographic filters [INPE-4448-RPE/558] p 64 A88-20124

C

CANADA

- Hierarchical segmentation using a composite criterion for remotely sensed imagery p 54 A88-20841
- Operational revision of national topographic maps in Canada using Landsat images p 54 A88-20901
- Multispectral videx survey of a Northern Ontario forest p 1 A88-21015
- Automated road network extraction from Landsat TM imagery p 18 A88-21044
- GPS survey techniques for deformation analysis p 21 A88-21057
- Land cover change detection with Landsat MSS and TM data in the Kitchener-Waterloo area, Canada p 18 A88-21071
- Potential applications of digital image analysis systems for displaying satellite altimetry data p 31 A88-23762
- A snapshot of the Labrador current inferred from ice-floe movement in NOAA satellite imagery p 32 A88-24456
- The baroclinic circulation in Hudson Strait p 32 A88-24457
- Multiyear sea ice floe distribution in the Canadian Arctic Ocean p 35 A88-25738
- Coastal upwelling and eddy development off Nova Scotia p 36 A88-27011
- Remanent magnetization of the oceanic upper mantle p 37 A88-27036
- Digital stereo processing of satellite image data p 58 A88-27825
- Thematic mapper and SPOT integration with a geographic information system p 59 A88-28602
- The potential for automated mapping from Geocoded digital image data p 59 A88-28604
- Radiometric correction of C-band imagery for topographic effects in regions of moderate relief p 59 A88-28680
- Microwave remote sensing of ice in Lake Melville and the Labrador Sea p 39 A88-28850
- Ice breakup - Observations of the acoustic signal p 41 A88-30200
- Canadian activities and goals in remote sensing of ocean colour and fluorescence from space p 46 A88-16300

E

ESTONIA

- Observations of ocean and sea bottom relief from space p 35 A88-26099
- The emissivity of the vegetation-soil system p 8 A88-27208
- Calculation of canopy bidirectional reflectance using the Monte Carlo method p 13 A88-30439

F

FINLAND

- Fluvial perturbation in the western Amazon basin - Regulation by long-term sub-Andean tectonics p 24 A88-20878
- Construction of airborne radars for remote sensing [PB88-113063] p 71 A88-16916

FRANCE

- Contribution of SPOT images to the geological mapping of arid countries - Example of the Yemen Arab Republic p 25 A88-22616
- Preliminary SPOT results in Lorraine related to permanent grasslands p 5 A88-22617
- Geodetic application of the Global Positioning System p 21 A88-24289
- Evolution of the Juan Fernandez microplate during the last three million years p 25 A88-25045
- Sea ice and sea-surface temperatures in the Strait of Fram according to NOAA-AVHRR data p 35 A88-26131
- SPOT 1 - Earth observing satellite p 66 A88-26166
- A method for the estimate of broadband directional surface albedo from a geostationary satellite p 22 A88-27299
- Spray droplet generation, transport, and evaporation in a wind wave tunnel during the humidity exchange over the sea experiments in the simulation tunnel p 38 A88-27492
- Spectral and botanical classification of grasslands - Auxois example p 8 A88-27805
- Comparative study of temperature data from NOAA7-AVHRR and WMO - An interpretation through the use of a soil-vegetation model p 8 A88-27806
- Preliminary study of the characterization of the riverine forests of the Garonne using Landsat MSS and TM data p 9 A88-27811
- A global survey of surface climate parameters from satellite observations - Preliminary results over Africa p 67 A88-27814
- Estimation of evapotranspiration in the Sahelian zone by use of Meteosat and NOAA AVHRR data p 9 A88-27818
- Speckle in SAR images - An evaluation of filtering techniques p 59 A88-27834
- Quantitative use of satellite SAR imagery of sea ice p 39 A88-27839
- Problems in geologic and geomorphic interpretation and geometric modeling of radar images using a digital terrain model p 26 A88-28024
- Evaluation of the stereoscopic accuracy of the SPOT satellite p 59 A88-28605
- Ocean Colour Workshop [ESA-SP-1083] p 45 A88-16292
- Europe's position concerning ocean colour activities p 45 A88-16293
- Technical aspects of future ocean colour remote sensing p 46 A88-16298
- French activities in ocean colour observations p 46 A88-16303
- Proceedings of an ESA-NASA Workshop on a Joint Solid Earth Program [NASA-CR-182642] p 23 A88-19844
- Gradiometer mission spectral analysis and simulation studies: Past and future p 24 A88-19851

G

GERMANY DEMOCRATIC REPUBLIC

Information content of spectral signatures and textures and structures for remote sensing of the earth p 60 A88-29499

GERMANY, FEDERAL REPUBLIC OF

The development and state of the art of remote sensing p 64 A88-20903

A multi-frequency-multi-nadir-angle pushbroom-radiometer for oil spill detection and mapping (On the surface of the sea) p 31 A88-23988

Biomass-burning emissions and associated haze layers over Amazonia p 18 A88-27265

Simulation of bit-quantization influence on SAR images p 59 A88-27831

Detection of oil films by active and passive microwave sensors p 39 A88-27840

Preliminary assessment of airborne imaging spectrometer and airborne thematic mapper data acquired for forest decline areas in the Federal Republic of Germany p 11 A88-28272

Comparison of submarine relief features on a radar satellite image and on a Skylab satellite photograph p 40 A88-29279

The aerophotogrammetric determination of Earth surface deformations p 28 A88-15288

Optimization of photogrammetric image adjustment [SER-C-323] p 22 A88-15289

Theory and research on the disjunction of cross passage errors and systematic image errors in photogrammetric point determination p 61 A88-15290

Observations of Earth tides by the German Geodetic Research Institute, division 1, in the period 1979-1985 at the Berchtesgaden and Wettzell stations [SER-B-280] p 22 A88-15291

The influence of yellow substances on remote sensing of sea water constituents from space. Volume 1: Summary p 43 A88-15292

The influence of yellow substances on remote sensing of sea water constituents from space. Volume 2: Appendices p 43 A88-15293

[ESA-CR(P)-2443-VOL-2] p 43 A88-15293

The use of chlorophyll fluorescence measurements from space for separating constituents of sea water. Volume 1: Summary p 43 A88-15294

The use of chlorophyll fluorescence measurements from space for separating constituents of sea water. Volume 2: Appendices p 44 A88-15295

Use of the thermodynamic evaporation formula of Hoffmann in energy balance models for flowing water p 52 A88-16143

Energy balance and discharge of an Alpine glacier, illustrated by Mount Vernagferner in the Oetzal Alps, Tyrol p 53 A88-16145

The unsteady ground heat flow at the contact surface between a glacier run and the subsoil p 53 A88-16147

Vertical sounding of the air layer close to a glacier on Mount Vernagferner in the Oetzal Alps, Tyrol (experiment LUZIVER 1983) p 44 A88-16152

The role of anisotropy in the long range reconnaissance of the albedo of land surfaces p 62 A88-16169

The anisotropy of reflected solar radiation over several types of land surface p 62 A88-16171

Thematic mapper research in the earth sciences: Small scale patches of suspended matter and phytoplankton in the Elbe River Estuary, German Bight and Tidal Flats [NASA-CR-182378] p 45 A88-16180

Federal Republic of Germany's interests, activities and goals in remote sensing of ocean colour/fluorescence from space p 46 A88-16302

The use of chlorophyll fluorescence measurements from space for separating constituents of sea water p 47 A88-16307

The influence of yellow substances on remote sensing of sea-water constituents from space p 47 A88-16308

Investigations on the application of space photographs (Spacelab metric camera) for routine inventories of extensively managed forest areas p 15 A88-17098

Statistics of two-dimensional structure elements of mountainous ranges (mosaic model) for calculating three-dimensional reflection functions [DFVLR-FB-87-33] p 29 A88-17099

Meteorological Information Extraction Center (MIEC) processing [ESA-STR-224] p 71 A88-17143

Investigation of the quantitative determination of two dimensional sea surface wave spectra from shipborne radar measurements [GKSS-87/E/10] p 48 A88-17163

Hydrographic and current measurements in the North-East Atlantic Ocean. Data report on F.S. Meteor cruises 69/5 and 69/6, October to November 1984 [REPT-166] p 48 A88-17164

Analysis of low frequency current fluctuations in the North-East Atlantic Ocean [REPT-170] p 48 A88-17165

Reports on cartography and geodesy. Series 1, report 98 [ISSN-0469-4236] p 23 A88-18993

Application of the Global Positioning System (GPS) time receivers to the fundamental station Wettzell p 71 A88-18995

The orientation of global satellite networks p 63 A88-18996

GREECE

Accuracy of mapping by panoramic photography p 60 A88-29479

Gravity field mapping from satellite altimetry, sea-gravimetry and bathymetry in the Eastern Mediterranean p 42 A88-30836

A comparison between panoramic photography and conventional aerial photography in terms of mapping accuracy p 61 A88-32167

I

INDIA

Assessment of the use of satellite derived winds in monsoon forecasting using a general circulation model p 68 A88-27846

Landsat imagery for mapping saline soils and wet lands in north-west India p 12 A88-29278

INTERNATIONAL ORGANIZATION

The Earth-Observation Preparatory Programme p 66 A88-22724

Monitoring of global vegetation dynamics for assessment of primary productivity using NOAA advanced very high resolution radiometer p 9 A88-27808

Proposed uses of ERS-1 p 68 A88-27833

IRAQ

Detection of subsurface geologic structures in the Tharthar area of central Iraq using Landsat images p 24 A88-20902

ITALY

Sea return at C and Ku bands p 31 A88-22947

Mantle rheology and satellite signatures from present-day glacial forcings p 21 A88-25225

Geostrophical evolution of the Southern Alps - Lineaments trends detected on Landsat images p 26 A88-25448

X-band features of canopy cover - An up to date summary of active and passive measurements p 10 A88-27835

Status and prospects of the Joint Research Committee (JRC) work on the application of ocean colour monitoring from space p 46 A88-16299

Italian activities in ocean colour remote sensing p 46 A88-16304

The Earthnet Heat Capacity Mapping Mission (HCMM) data-processing system at Lannion (France) p 62 A88-16761

The effects of atmospheric and thermohaline variability on the validation of the GEOSAT altimeter oceanographic signal between Scotland and Iceland [AD-A189324] p 50 A88-19882

J

JAPAN

Asian Conference on Remote Sensing, 7th, Seoul, Republic of Korea, Oct. 23-28, 1986, Proceedings p 66 A88-24818

A study to produce 1:100,000 scale LFC color photomap p 68 A88-27826

Simulation of spaceborne SAR imagery from airborne SAR data p 58 A88-27830

Design concept of the SAR installed on ERS-1 p 68 A88-27832

Preliminary assessment of radiometric accuracies for MOS-1 sensors p 39 A88-29276

Emissivity of pure and sea waters for the model sea surface in the infrared window regions p 42 A88-30445

Estimation of atmospheric liquid-water amount by Nimbus 7 SMMR data - A new method and its application to the western North-Pacific region p 69 A88-30731

K

KENYA

System-wide medium-term environment programme for the period 1990-1995: Strategies of the United Nations system for the environment [UNEP/GCSS.1/2] p 20 A88-19826

N

NETHERLANDS

Remote sensing applications - An outlook for the future p 64 A88-20904

Multiband-scatterometer data analysis of forests p 5 A88-23548

The DUT airborne scatterometer p 5 A88-23549

Measurements of the backscatter and attenuation properties of forest stands at X-, C- and L-band p 7 A88-25444

Overview of ESA's activities in ocean colour remote sensing p 45 A88-16294

National Remote Sensing Program (NRSP) of the Netherlands p 46 A88-16305

Earthnet's experience with Seasat SAR image processing p 62 A88-16760

Design and implementation of a data base system for Digital Land Mass System (DLMS) data [FEL-IR-1987-19] p 71 A88-17101

NEW ZEALAND

Atmospheric correction of thermal infrared images p 40 A88-29283

NIGERIA

Using remotely sensed data for census surveys and population estimation in developing countries - Examples from Nigeria p 18 A88-24511

Monitoring hydroclimatic characteristics using satellite observations from West Africa p 52 A88-27816

Identification and measurement of the areal extent of settlements from Landsat - An exploration into the Nigerian case p 19 A88-28014

O

OTHER

Remote sensing of forest cover distribution in the Phu Wiang watershed area of Khon Kaen Province, Northeast of Thailand p 6 A88-24514

P

PAKISTAN

Comparison of Landsat MSS and SIR-A data for geological applications in Pakistan p 27 A88-29281

POLAND

The legal problems of the commercialization of satellite remote sensing p 35 A88-26149

S

SOMALIA

Geometric accuracy testing of orbital radar imagery p 57 A88-23760

SOUTH AFRICA, REPUBLIC OF

The Natal pulse - An extreme transient on the Agulhas Current p 38 A88-27494

Marine boundary layer modification across the edge of the Agulhas Current p 38 A88-27495

A new strategy for vegetation mapping with the aid of Landsat MSS data p 9 A88-27810

SPAIN

A study on the utilization of SIR-A data for population estimation in the eastern part of Spain p 18 A88-24512

SWEDEN

Interpretation of Seasat radar-altimeter data over sea ice using near-simultaneous SAR imagery p 31 A88-23547

SWITZERLAND

Applications of microwaves to remote sensing p 69 A88-30670

WOCE Core Project 2 Planning Meeting: The Southern Ocean [WCP-138] p 44 A88-15348

Research in Switzerland on ocean and inland-water colour monitoring p 46 A88-16301

Report of the Workshop on Space Systems Possibilities for a Global Energy and Water Cycle Experiment [WCP-137] p 53 A88-17147

U

U.S.S.R.

Correlation characteristics of images of the earth surface obtained with a synthetic-aperture radar

p 66 A88-21784

Features of hydrological anomalies in connection with the search for deep-water polymetallic sulfides

p 32 A88-24654

Surface temperature variations of the world ocean in the Eocene

p 32 A88-24655

Effect of ice-grain size distribution on the thermal emission of snow cover

p 52 A88-24662

The space metal: All about titanium

p 25 A88-24781

Characteristics of the subsurface radar sounding of natural objects

p 26 A88-25551

Remote sensing methods and instrumentation for obtaining data on earth resources and the environment

p 66 A88-26050

The role of synoptic scale processes in the transfer of sea surface temperature anomalies

p 35 A88-26065

On the problem of evolution of oceanic water composition in the Phanerozoic

p 35 A88-26676

Techniques of geomorphological mapping on the basis of space photographs

p 26 A88-26708

Interpretation of the visible manifestations of sea water dynamics from space imagers of the Caspian Sea

p 37 A88-27201

Investigating the northern Caspian Sea ice regime from meteorological-satellite data

p 37 A88-27202

The relationship between the temporal variability of ocean temperature and the meridional shifts of the intertropical convergence zone

p 37 A88-27203

Calculations of ocean-atmosphere radiance on the basis of remote sensing

p 37 A88-27204

Variations in the intensity of emitted and scattered microwave radiation of the sea surface sensed at grazing angles in a field of surface manifestations of internal waves

p 37 A88-27205

Use of microwave radiometry for measuring the biometric characteristics of vegetation cover

p 7 A88-27207

Choosing conditions for the remote sensing of ocean features in the visible spectrum, with the effect of coastal zone taken into account

p 37 A88-27209

The efficiency of polarization measurements in passive remote sensing of the ocean in the visible spectrum

p 38 A88-27210

Computer-aided mapping of Antarctic Sea ice using along-the-course radiometric measurements aboard the Cosmos-1500 satellite

p 38 A88-27213

A method for synthesizing optimal space systems for earth surveying

p 67 A88-27214

The relationships between orbit parameters and the geometry of the trajectory for remote sensing satellites

p 67 A88-27215

Identical-route satellite orbits for long-term periodic global survey of the earth, not dependent on solar illumination

p 67 A88-27216

Complex remote monitoring of lakes

p 52 A88-27741

Remote sensing surveys design in regional agricultural inventories

p 8 A88-27804

Comprehensive studies of the dynamics of geosystems with the use of remote sensing techniques

p 10 A88-27821

The use of space technology for the remote sensing of earth resources and mapping

p 69 A88-28447

Methods for processing radio-physical measurement data in studies of the environment

p 19 A88-29427

Geochemistry of continental volcanism

p 27 A88-29431

Blocking of the Benguela Current by a single anticyclone - Analysis of satellite and ship data

p 41 A88-30077

The use of the optical classification of ocean waters to estimate correlations between the concentrations of variable components with reference to the development of remote-sensing methods

p 41 A88-30078

The use of Meteor-Priroda space photographs for the compilation of small-scale and medium-scale tectonic and geological maps

p 27 A88-30079

Karst and erosion topography on space photographs (With reference to the Ustiut plateau)

p 60 A88-30080

Investigation of the foci of powerful earthquakes and seismically hazardous areas on space photographs for the Baikal-Aldan region

p 27 A88-30081

Relationship between brightness temperature in the RF range and the radiative dryness index

p 69 A88-30082

Detection of internal waves using data from satellite microwave radiometry and the research ship Academician Alexander Nesmeianov

p 41 A88-30083

Estimation of the accuracy of determining atmospheric temperature profiles from microwave remote sensing at frequencies of 117-118.5 Ghz

p 41 A88-30084

The use of regression analysis to determine sea surface temperatures from Cosmos-1151 measurements of IR radiation

p 41 A88-30085

The use of successive clustering to analyze multispectral imagery

p 61 A88-30086

Adaptive computer-aided system for crop inventory according to space photographs

p 13 A88-30087

Current status and problems of satellite investigations of the ocean (Review of non-Soviet publications)

p 41 A88-30089

Satellite monitoring of earthquake precursor effects in magnetosphere

p 28 A88-16103

Space applications in geography

p 22 A88-16104

Method for joint adjustment of satellite and surface geodetic networks

p 22 A88-16105

Limiting accuracy of scatterometer determination of wind speed over ocean from satellite

p 44 A88-16107

Space photographs of the Onega-Ladoga isthmus and prediction of useful minerals

p 28 A88-16108

Use of space photographs for geomorphological studies in southwestern Tajikistan

p 28 A88-16109

Use of space photographs for paleoseismogeological studies (on the example of Mongolian Altay)

p 28 A88-16110

Study of relief of one regions using space images (on the example of Eastern Yakutia)

p 28 A88-16111

Statistical model of interaction of electromagnetic waves with natural objects being sensed

p 70 A88-16112

Monte Carlo method calculation of spectral brightness coefficient of vegetation cover as function of illumination conditions

p 14 A88-16113

Multistep component analysis of correlations

p 61 A88-16115

New possibilities for using gravity data in developing geodetic coordinate systems

p 23 A88-16116

Academic course Space Methods for Studying Modern Landscapes of Continents

p 72 A88-16133

Photogrammetric principles for combining remote sounding and three-dimensional mapping

p 61 A88-16135

Laser system for automating topographic terrain survey

p 70 A88-16136

Materials of the World Data Center B. Deep Seismic Sounding (DSS): Pacific data

p 48 A88-17167

UNITED KINGDOM

Detecting subpixel woody features using simulated multispectral and panchromatic SPOT imagery

p 3 A88-21065

Modelling radar backscatter from vegetation

p 5 A88-21501

Interpretation of satellite imagery of a rapidly deepening cyclone

p 57 A88-23502

A sequential estimation approach to cloud-clearing for satellite temperature sounding

p 66 A88-23511

Synthetic aperture radar imagery of range traveling ocean waves

p 32 A88-24933

The ice thickness distribution across the Atlantic sector of the Antarctic Ocean in midwinter

p 34 A88-25734

Radar altimeter data: quality flagging

p 39 A88-27837

Swath altimetry of oceans and terrain

p 39 A88-27838

The use of direct readout, high resolution TOVS data in short and medium range weather predictions

p 68 A88-27844

Measurement of canopy interception of solar radiation by stands of trees in sparsely wooded savanna

p 10 A88-28010

Principles of field spectroscopy

p 68 A88-28013

Mapping NOAA-AVHRR imagery using equal-area radial projections

p 10 A88-28015

SAR imaging of volume scatterers

p 60 A88-28681

An improved method for detecting clear sky and cloudy radiances from AVHRR data

p 69 A88-29284

The acquisition of SPOT-1 HRV imagery over southern Britain and northern France, May 1986-May 1987

p 60 A88-29286

Exploring the relationships between leaf nitrogen content, biomass and the near-infrared/red reflectance ratio

p 12 A88-29288

Identification and spectral characteristics of hydrothermal alteration on Landsat TM imagery of north Chile

p 27 A88-31125

Selecting the spatial resolution of satellite sensors required for global monitoring of land transformations

p 20 A88-32659

Simulation of solar zenith angle effect on global vegetation index (GVI) data

p 14 A88-32660

Radiometric leaf area index

p 14 A88-32662

Crop canopy spectral reflectance

p 14 A88-32664

An integrated camera and radiometer for aerial monitoring of vegetation

p 14 A88-32666

Review of the potential of satellite remote sensing for marine flood protection

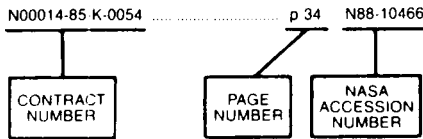
[IOS-237] p 43 A88-15280

CONTRACT NUMBER INDEX

EARTH RESOURCES / A Continuing Bibliography (Issue 58)

AUGUST 1988

Typical Contract Number Index Listing



Listings in this index are arranged alphanumerically by contract number. Under each contract number, the accession numbers denoting documents that have been produced as a result of research done under the contract are arranged in ascending order with the AIAA accession numbers appearing first. The accession number denotes the number by which the citation is identified in the abstract section. Preceding the accession number is the page number on which the citation may be found.

CNR-PSN-86,060	p 21	A88-25225
DAAL03-86-K-0022	p 71	N88-18052
DACA72-86-C-0008	p 23	N88-18055
DE-AC05-84OR-21400	p 10	A88-28011
DE-AC06-76RL-01830	p 61	N88-15287
	p 20	N88-17119
DE-AC09-76SR-00001	p 6	A88-24513
	p 12	A88-29277
DE-AC21-84MC-21181	p 29	N88-18048
	p 29	N88-18050
DE-FG05-85ER-60348	p 48	N88-17166
DE-FG09-86ER-60450	p 49	N88-18110
DMA800-85-C-0033	p 56	A88-21064
EEC-ST2J-39-DK(EDB)	p 42	A88-30836
EPA-SR-1301-NAEX	p 19	A88-28603
ESA-RFQ-3-5060/84-NL-MD	p 47	N88-16308
ESA-5285/82	p 31	A88-23544
ESA-5952/84-NL-MD	p 43	N88-15294
	p 44	N88-15295
ESA-5953/84-NL-MD	p 43	N88-15292
	p 43	N88-15293
ESA-6001/84/NL/BI	p 39	A88-27838
ESA-6153/85/NL/MS	p 59	A88-27834
ESA-6617/85/F/FL(SC)	p 31	A88-23547
F19628-86-K-0006	p 23	N88-18054
F33615-84-K-1520	p 63	N88-19810
JPL-956428	p 25	A88-25217
JPL-956952	p 10	A88-27836
JPL-957363	p 56	A88-21070
JPL-957549	p 55	A88-21037
MIPR-HM0050-6-357	p 20	N88-15278
NAGW-1045	p 36	A88-27014
NAGW-273	p 41	A88-30415
NAGW-28	p 27	A88-28273
NAGW-363	p 37	A88-27016
NAGW-374	p 6	A88-23765
NAGW-419	p 32	A88-24934
NAGW-455	p 19	A88-28684
NAGW-667	p 52	A88-25735
NAGW-700	p 36	A88-27014
NAGW-738	p 27	A88-28273
NAGW-808	p 43	N88-15285
	p 43	N88-15286
	p 44	N88-15352
NAGW-916	p 40	A88-29323
NAGW-924	p 16	N88-19817
NAGW-952	p 13	A88-30447
NAGW-95	p 15	N88-17103
NAG1-028	p 37	A88-27016
NAG2-36	p 37	A88-27016
NAG5-269	p 7	A88-26624
NAG5-399	p 20	A88-32659
NAG5-492	p 8	A88-27802
NAG5-770	p 21	A88-25225
NAG5-852	p 17	N88-19855
NAG5-870	p 53	N88-19865
NAG8-059	p 62	N88-17152
NASA ORDER L-61130-C	p 26	A88-26337
NASW-4048	p 27	A88-28273
NASW-4050	p 27	A88-28268
NASW-4066	p 27	A88-31125
NASW-4124	p 72	N88-16577
NAS5-28762	p 36	A88-27015
NAS5-28739	p 30	N88-18984
NAS5-28765	p 29	N88-17140
NAS5-28781	p 2	A88-21028
NAS5-28798	p 41	A88-30415
NAS5-29276	p 71	N88-17964
NAS7-918	p 4	A88-21359
	p 10	A88-27836
NAS9-14016	p 6	A88-23766
NAVY TASK NR-083-012	p 40	A88-29324
NA84-AA-D-00009	p 28	N88-16281
NCA2-IR-390-402	p 12	A88-28705
NCA2-138	p 13	A88-30447
NCA2-27	p 13	A88-30447
NCC5-26	p 9	A88-27819
NCC5-29	p 40	A88-29323
NERC-F60/G6/12	p 20	A88-32659
	p 14	A88-32660
NERC-GR3/5046	p 14	A88-32663
NGL-23-004-083	p 18	A88-21073
	p 10	A88-28012
NGT-05-010-804	p 15	N88-18049
NOAA-NA-80AAD00120	p 50	A88-21002
NOAA-NA-85AADAC132	p 34	A88-25731
NOAA-NA-85AADSG033	p 6	A88-23765
NR PROJECT 083-012	p 36	A88-27014
NSERC-A-0766	p 18	A88-21044
NSERC-A-2037	p 37	A88-27036
NSF ATM-83-11812	p 42	A88-31111
NSF ATM-83-18853	p 33	A88-25726
	p 34	A88-25732
NSF ATM-84-07137	p 18	A88-27265
NSF ATM-85-13713	p 34	A88-25731
NSF ATM-86-12570	p 40	A88-29323
NSF DAR-80-17836	p 6	A88-23765
NSF DPP-82-17265	p 37	A88-27016
NSF DPP-85-12728	p 34	A88-25734
NSF DPP-86-17176	p 41	A88-30199
NSF EAR-85-11200	p 21	A88-25225
NSF OCE-84-17769	p 34	A88-25733
NSF OCE-85-10828	p 36	A88-27012
NSF OCE-86-14512	p 22	A88-27465
NSG-7415	p 25	A88-25217
N00014-67-A-0103	p 47	N88-17160
N00014-78-C-0556	p 49	N88-19262
N00014-80-C-0440	p 38	A88-27493
N00014-81-C-0062	p 36	A88-27012
N00014-81-K-0095	p 41	A88-30199
N00014-83-K-0258	p 47	N88-17162
N00014-84-C-0111	p 36	A88-27014
	p 40	A88-29324
	p 47	N88-17160
N00014-84-K-0080	p 42	A88-30662
N00014-84-K-0620	p 42	A88-31111
N00014-85-C-0140	p 38	A88-27493
N00014-87-K-0017	p 49	N88-19057
N00039-87-C-5301	p 69	A88-28679
	p 71	N88-18053
W-7405-ENG-36	p 15	N88-18991

CONTRACT

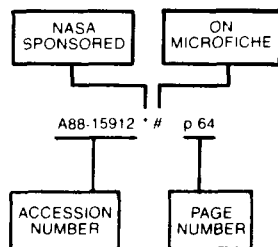
RANRL-TM-3/87	p 47	N88-17158	#
RANRL-TN-3/87	p 44	N88-15346	#
REPT-166	p 48	N88-17164	#
REPT-16	p 16	N88-19817	* #
REPT-170	p 48	N88-17165	#
REPT-87-B-0480	p 23	N88-16279	* #
REPT-88-B-0042	p 23	N88-16280	* #
REPT-88B9999	p 23	N88-19037	* #
REPT-93226	p 71	N88-17964	* #
S-171	p 71	N88-16916	#
SACLANTCEN-SR-128	p 50	N88-19882	#
SER-B-280	p 22	N88-15291	
SER-C-321	p 28	N88-15288	
SER-C-323	p 22	N88-15289	
SER-C-324	p 61	N88-15290	
SIO-REF-87-18	p 49	N88-19262	#
TR-87-12	p 48	N88-17166	#
UNEP/GCSSL/2	p 20	N88-19826	#
USAETL-R-109	p 63	N88-18983	#
WCP-137	p 53	N88-17147	#
WCP-138	p 44	N88-15348	#
WHOI-87-31	p 49	N88-19057	#
WMO/TD-180	p 53	N88-17147	#
WMO/TD-181	p 44	N88-15348	#

ACCESSION NUMBER INDEX

EARTH RESOURCES / A Continuing Bibliography (Issue 58)

AUGUST 1988

Typical Accession Number Index Listing



Listings in this index are arranged alphanumerically by accession number. The page number listed to the right indicates the page on which the citation is located. An asterisk (*) indicates that the item is a NASA report. A pound sign (#) indicates that the item is available on microfiche.

A88-20841	p 54	A88-21053	p 55	A88-23549	p 5	A88-27203	p 37	A88-28606	p 19
A88-20878	p 24	A88-21054	p 20	A88-23760	p 57	A88-27204	p 37	A88-28679 *	p 69
A88-20901	p 54	A88-21055	p 20	A88-23761	p 57	A88-27205	p 37	A88-28680	p 59
A88-20902	p 24	A88-21057	p 21	A88-23762	p 31	A88-27207	p 7	A88-28681	p 60
A88-20903	p 64	A88-21058	p 21	A88-23764	p 5	A88-27208	p 8	A88-28682 *	p 11
A88-20904	p 64	A88-21059	p 55	A88-23765 *	p 6	A88-27209	p 37	A88-28683 *	p 11
A88-20942	# p 30	A88-21060 *	p 18	A88-23766 *	p 6	A88-27210	p 38	A88-28684 *	p 19
A88-20978	p 30	A88-21061	p 55	A88-23768	p 57	A88-27213	p 38	A88-28705 *	p 12
A88-21001	p 64	A88-21062	p 55	A88-23772	p 66	A88-27214	p 67	A88-28850	p 39
A88-21002	p 50	A88-21063	p 56	A88-23988	# p 31	A88-27215	p 67	A88-29235 *	p 69
A88-21003	p 30	A88-21064	p 56	A88-24198 *	p 51	A88-27216	p 67	A88-29276	p 39
A88-21004	p 50	A88-21065	p 3	A88-24289	p 21	A88-27252 *	p 8	A88-29277	p 12
A88-21006	p 50	A88-21066	p 56	A88-24456	p 32	A88-27265 *	p 18	A88-29278	p 12
A88-21007	p 51	A88-21067	p 56	A88-24457	p 32	A88-27299	p 22	A88-29279	p 40
A88-21009	p 24	A88-21068 *	p 56	A88-24510	p 6	A88-27465	p 22	A88-29280	p 12
A88-21011	p 51	A88-21069	p 56	A88-24511	p 18	A88-27492	p 38	A88-29281	p 27
A88-21012	p 17	A88-21070 *	p 56	A88-24512	p 18	A88-27493	p 38	A88-29282 *	p 12
A88-21013	p 1	A88-21071	p 18	A88-24513 *	p 6	A88-27494	p 38	A88-29283	p 40
A88-21014	p 17	A88-21072	p 57	A88-24514	p 6	A88-27495	p 38	A88-29284	p 69
A88-21015	p 1	A88-21073 *	p 18	A88-24582	p 32	A88-27497 *	p 67	A88-29286	p 60
A88-21016	p 1	A88-21075	p 57	A88-24654	p 32	A88-27741	p 52	A88-29287 *	p 60
A88-21017	p 1	A88-21168 *	p 65	A88-24655	p 32	A88-27801 *	p 67	A88-29288	p 12
A88-21018	p 64	A88-21351	p 3	A88-24662	p 52	A88-27802 *	p 8	A88-29323 *	p 40
A88-21019	p 64	A88-21352	p 3	A88-24781	p 25	A88-27803 *	p 19	A88-29324	p 40
A88-21020 *	p 1	A88-21353	p 3	A88-24818	p 66	A88-27804	p 8	A88-29325 *	p 40
A88-21021	p 51	A88-21354 *	p 3	A88-24932 *	p 6	A88-27805	p 8	A88-29427	p 19
A88-21022	p 65	A88-21355	p 3	A88-24933	p 32	A88-27806	p 8	A88-29431	p 27
A88-21023	p 17	A88-21356 *	p 3	A88-24934 *	p 32	A88-27807 *	p 8	A88-29479	p 60
A88-21025 *	p 54	A88-21357 *	p 3	A88-24935	p 58	A88-27808	p 9	A88-29489	p 27
A88-21026	p 54	A88-21358 *	p 3	A88-24936	p 58	A88-27809 *	p 9	A88-29490	p 60
A88-21027	p 54	A88-21359 *	p 4	A88-24937	p 58	A88-27810	p 9	A88-29491	p 60
A88-21028 *	p 2	A88-21360	p 4	A88-25045	p 25	A88-27811	p 9	A88-29492 *	p 40
A88-21029	p 2	A88-21361	p 4	A88-25217 *	# p 25	A88-27812 *	p 38	A88-29493	p 52
A88-21030	p 54	A88-21362	p 4	A88-25224	p 21	A88-27813 *	p 67	A88-29494	p 12
A88-21031	p 2	A88-21363	p 4	A88-25225 *	p 21	A88-27814	p 67	A88-29495	p 12
A88-21032 *	p 2	A88-21364	p 4	A88-25289	p 33	A88-27815	p 52	A88-29496	p 60
A88-21033 *	p 2	A88-21365	p 5	A88-25444	p 7	A88-27816	p 52	A88-29499	p 60
A88-21034	p 24	A88-21382	p 65	A88-25445	p 33	A88-27817 *	p 9	A88-29766 *	p 40
A88-21035	p 2	A88-21365	p 5	A88-25446	p 7	A88-27818	p 9	A88-30077	p 41
A88-21036	p 25	A88-21501	p 5	A88-25447 *	p 7	A88-27819 *	p 9	A88-30078	p 41
A88-21037 *	p 55	A88-21660	p 65	A88-25448	p 26	A88-27820	p 10	A88-30079	p 27
A88-21038	p 51	A88-21784	p 66	A88-25551	p 26	A88-27821	p 10	A88-30080	p 60
A88-21039	p 51	A88-22154 *	# p 30	A88-25726	p 33	A88-27822 *	p 58	A88-30081	p 27
A88-21040	p 2	A88-22616	p 25	A88-25727 *	# p 33	A88-27823	p 67	A88-30082	p 69
A88-21041	p 17	A88-22617	p 5	A88-25728 *	p 33	A88-27824 *	p 58	A88-30083	p 41
A88-21042	p 51	A88-22724	# p 66	A88-25729	p 34	A88-27825	p 58	A88-30084	p 41
A88-21043	p 25	A88-22911	p 30	A88-25730 *	p 52	A88-27826	p 68	A88-30085	p 41
A88-21044	p 18	A88-22947	p 31	A88-25731	p 34	A88-27830	p 58	A88-30086	p 61
A88-21045 *	p 25	A88-23253	p 5	A88-25732	p 34	A88-27831	p 59	A88-30087	p 13
A88-21046	p 2	A88-23502	# p 57	A88-25733	p 34	A88-27832	p 68	A88-30089	p 41
A88-21047	p 55	A88-23511	# p 66	A88-25734	p 34	A88-27833	p 68	A88-30199	p 41
A88-21048	p 55	A88-23544	p 31	A88-25735 *	p 52	A88-27834	p 59	A88-30200	p 41
A88-21049	p 55	A88-23545	p 31	A88-25736	p 34	A88-27835	p 10	A88-30415 *	p 41
A88-21050	p 65	A88-23546 *	p 31	A88-25737	p 34	A88-27836 *	p 10	A88-30439	p 13
A88-21051	p 65	A88-23547	p 31	A88-25738	p 35	A88-27837	p 39	A88-30440 *	p 13
		A88-23548	p 5	A88-25850	p 21	A88-27838	p 39	A88-30441 *	p 13
				A88-26050	p 66	A88-27839	p 39	A88-30444 *	p 13
				A88-26065	p 35	A88-27840	p 39	A88-30445	p 42
				A88-26099	p 35	A88-27841 *	p 39	A88-30446 *	p 13
				A88-26131	p 35	A88-27844	p 68	A88-30447 *	p 13
				A88-26149	p 35	A88-27846	p 68	A88-30448 *	p 13
				A88-26166	p 66	A88-28009 *	p 59	A88-30662	p 42
				A88-26335	p 7	A88-28010	p 10	A88-30670	# p 69
				A88-26336	p 7	A88-28011 *	p 10	A88-30731	p 69
				A88-26337 *	p 26	A88-28012 *	p 10	A88-30836	p 42
				A88-26346	p 35	A88-28013	p 68	A88-31103	p 19
				A88-26347	p 21	A88-28014	p 19	A88-31111	p 42
				A88-26624 *	p 7	A88-28015	p 10	A88-31125 *	p 27
				A88-26676	p 35	A88-28016 *	p 11	A88-31793 *	# p 42
				A88-26708	p 26	A88-28024	p 26	A88-32167	p 61
				A88-26911 *	# p 35	A88-28266 *	p 69	A88-32508	p 42
				A88-26923	p 36	A88-28267	p 26	A88-32658 *	p 14
				A88-27010	# p 36	A88-28268 *	# p 27	A88-32659 *	p 20
				A88-27011	p 36	A88-28269 *	p 27	A88-32660	p 14
				A88-27012	p 36	A88-28270 *	# p 11	A88-32661	p 14
				A88-27013	p 36	A88-28271 *	p 11	A88-32662	p 14
				A88-27014 *	p 36	A88-28272 *	p 11	A88-32663	p 14
				A88-27015 *	p 36	A88-28273 *	p 11	A88-32664	p 14
				A88-27016 *	p 37	A88-28447	p 69	A88-32665	p 14
				A88-27027 *	# p 66	A88-28602	p 59	A88-32666	p 14
				A88-27036	p 37	A88-28603	p 19		
				A88-27201	p 37	A88-28604	p 59	N88-15101	# p 42
				A88-27202	p 37	A88-28605	p 59	N88-15278	# p 20

ACCESSION

N88-15280

N88-15280	#	p 43	N88-18054	#	p 23
N88-15282	* #	p 70	N88-18055	#	p 23
N88-15283	* #	p 70	N88-18056	#	p 62
N88-15284	* #	p 70	N88-18079	#	p 20
N88-15285	* #	p 43	N88-18109	* #	p 48
N88-15286	* #	p 43	N88-18110	#	p 49
N88-15287	* #	p 61	N88-18978	#	p 62
N88-15288		p 28	N88-18979	#	p 63
N88-15289		p 22	N88-18983	#	p 63
N88-15290		p 61	N88-18984	* #	p 30
N88-15291		p 22	N88-18985		p 63
N88-15292	#	p 43	N88-18986		p 71
N88-15293	#	p 43	N88-18987	#	p 63
N88-15294	#	p 43	N88-18988	#	p 30
N88-15295	#	p 44	N88-18991	#	p 15
N88-15346	#	p 44	N88-18993	#	p 23
N88-15348	#	p 44	N88-18995	#	p 71
N88-15352	* #	p 44	N88-18996	#	p 63
N88-16103	#	p 28	N88-18997	#	p 72
N88-16104	#	p 22	N88-19037	* #	p 23
N88-16105	#	p 22	N88-19057	#	p 49
N88-16107	#	p 44	N88-19058		p 49
N88-16108	#	p 28	N88-19059		p 49
N88-16109	#	p 28	N88-19060		p 49
N88-16110	#	p 28	N88-19262	#	p 49
N88-16111	#	p 28	N88-19801	#	p 16
N88-16112	#	p 70	N88-19802	#	p 16
N88-16113	#	p 14	N88-19804	#	p 16
N88-16115	#	p 61	N88-19807	#	p 16
N88-16116	#	p 23	N88-19810	#	p 63
N88-16133	#	p 72	N88-19817	* #	p 16
N88-16135	#	p 61	N88-19824	#	p 17
N88-16136	#	p 70	N88-19826	#	p 20
N88-16143	#	p 52	N88-19844	* #	p 23
N88-16145	#	p 53	N88-19845	* #	p 24
N88-16147	#	p 53	N88-19846	* #	p 24
N88-16152	#	p 44	N88-19847	* #	p 24
N88-16169	#	p 62	N88-19848	* #	p 24
N88-16171	#	p 62	N88-19851	* #	p 24
N88-16179	* #	p 70	N88-19855	* #	p 17
N88-16180	* #	p 45	N88-19863	#	p 72
N88-16181	#	p 62	N88-19865	* #	p 53
N88-16182	* #	p 15	N88-19879	#	p 50
N88-16185	#	p 53	N88-19882	#	p 50
N88-16279	* #	p 23	N88-20023	#	p 17
N88-16280	* #	p 23	N88-20124	#	p 64
N88-16281	* #	p 28			
N88-16292	#	p 45			
N88-16293	#	p 45			
N88-16294	#	p 45			
N88-16295	* #	p 45			
N88-16296	#	p 45			
N88-16297	#	p 45			
N88-16298	#	p 46			
N88-16299	#	p 46			
N88-16300	#	p 46			
N88-16301	#	p 46			
N88-16302	#	p 46			
N88-16303	#	p 46			
N88-16304	#	p 46			
N88-16305	#	p 46			
N88-16306	#	p 46			
N88-16307	#	p 47			
N88-16308	#	p 47			
N88-16577	* #	p 72			
N88-16760	#	p 62			
N88-16761	#	p 62			
N88-16916	#	p 71			
N88-17098	#	p 15			
N88-17099	#	p 29			
N88-17101	#	p 71			
N88-17103	* #	p 15			
N88-17119	#	p 20			
N88-17140	* #	p 29			
N88-17143	#	p 71			
N88-17147	#	p 53			
N88-17152	* #	p 62			
N88-17155	#	p 47			
N88-17156	#	p 53			
N88-17158	#	p 47			
N88-17159	#	p 47			
N88-17160	#	p 47			
N88-17162	#	p 47			
N88-17163		p 48			
N88-17164	#	p 48			
N88-17165	#	p 48			
N88-17166	#	p 48			
N88-17167	#	p 48			
N88-17964	* #	p 71			
N88-18046	* #	p 72			
N88-18047	#	p 29			
N88-18048	#	p 29			
N88-18049	* #	p 15			
N88-18050	#	p 29			
N88-18052	#	p 71			
N88-18053	#	p 71			

AVAILABILITY OF CITED PUBLICATIONS

IAA ENTRIES (A88-10000 Series)

Publications announced in *IAA* are available from the AIAA Technical Information Service as follows: Paper copies of accessions are available at \$10.00 per document (up to 50 pages), additional pages \$0.25 each. Microfiche⁽¹⁾ of documents announced in *IAA* are available at the rate of \$4.00 per microfiche on demand. Standing order microfiche are available at the rate of \$1.45 per microfiche for *IAA* source documents and \$1.75 per microfiche for AIAA meeting papers.

Minimum air-mail postage to foreign countries is \$2.50. All foreign orders are shipped on payment of pro-forma invoices.

All inquiries and requests should be addressed to: Technical Information Service, American Institute of Aeronautics and Astronautics, 555 West 57th Street, New York, NY 10019. Please refer to the accession number when requesting publications.

STAR ENTRIES (N88-10000 Series)

One or more sources from which a document announced in *STAR* is available to the public is ordinarily given on the last line of the citation. The most commonly indicated sources and their acronyms or abbreviations are listed below. If the publication is available from a source other than those listed, the publisher and his address will be displayed on the availability line or in combination with the corporate source line.

Avail: NTIS. Sold by the National Technical Information Service. Prices for hard copy (HC) and microfiche (MF) are indicated by a price code preceded by the letters HC or MF in the *STAR* citation. Current values for the price codes are given in the tables on NTIS PRICE SCHEDULES.

Documents on microfiche are designated by a pound sign (#) following the accession number. The pound sign is used without regard to the source or quality of the microfiche.

Initially distributed microfiche under the NTIS SRIM (Selected Research in Microfiche) is available at greatly reduced unit prices. For this service and for information concerning subscription to NASA printed reports, consult the NTIS Subscription Section, Springfield, Va. 22161.

NOTE ON ORDERING DOCUMENTS: When ordering NASA publications (those followed by the * symbol), use the N accession number. NASA patent applications (only the specifications are offered) should be ordered by the US-Patent-Appl-SN number. Non-NASA publications (no asterisk) should be ordered by the AD, PB, or other *report number* shown on the last line of the citation, not by the N accession number. It is also advisable to cite the title and other bibliographic identification.

Avail: SOD (or GPO). Sold by the Superintendent of Documents, U.S. Government Printing Office, in hard copy. The current price and order number are given following the availability line. (NTIS will fill microfiche requests, as indicated above, for those documents identified by a # symbol.)

(1) A microfiche is a transparent sheet of film, 105 by 148 mm in size containing as many as 60 to 98 pages of information reduced to micro images (not to exceed 26.1 reduction).

- Avail: BLL (formerly NLL): British Library Lending Division, Boston Spa, Wetherby, Yorkshire, England. Photocopies available from this organization at the price shown. (If none is given, inquiry should be addressed to the BLL.)
- Avail: DOE Depository Libraries. Organizations in U.S. cities and abroad that maintain collections of Department of Energy reports, usually in microfiche form, are listed in *Energy Research Abstracts*. Services available from the DOE and its depositories are described in a booklet, *DOE Technical Information Center - Its Functions and Services* (TID-4660), which may be obtained without charge from the DOE Technical Information Center.
- Avail: ESDU. Pricing information on specific data, computer programs, and details on ESDU topic categories can be obtained from ESDU International Ltd. Requesters in North America should use the Virginia address while all other requesters should use the London address, both of which are on the page titled ADDRESSES OF ORGANIZATIONS.
- Avail: Fachinformationszentrum, Karlsruhe. Sold by the Fachinformationszentrum Energie, Physik, Mathematik GMBH, Eggenstein Leopoldshafen, Federal Republic of Germany, at the price shown in deutschmarks (DM).
- Avail: HMSO. Publications of Her Majesty's Stationery Office are sold in the U.S. by Pendragon House, Inc. (PHI), Redwood City, California. The U.S. price (including a service and mailing charge) is given, or a conversion table may be obtained from PHI.
- Avail: NASA Public Document Rooms. Documents so indicated may be examined at or purchased from the National Aeronautics and Space Administration, Public Documents Room (Room 126), 600 Independence Ave., S.W., Washington, D.C. 20546, or public document rooms located at each of the NASA research centers, the NASA Space Technology Laboratories, and the NASA Pasadena Office at the Jet Propulsion Laboratory.
- Avail: Univ. Microfilms. Documents so indicated are dissertations selected from *Dissertation Abstracts* and are sold by University Microfilms as xerographic copy (HC) and microfilm. All requests should cite the author and the Order Number as they appear in the citation.
- Avail: US Patent and Trademark Office. Sold by Commissioner of Patents and Trademarks, U.S. Patent and Trademark Office, at the standard price of \$1.50 each, postage free. (See discussion of NASA patents and patent applications below.)
- Avail: (US Sales Only). These foreign documents are available to users within the United States from the National Technical Information Service (NTIS). They are available to users outside the United States through the International Nuclear Information Service (INIS) representative in their country, or by applying directly to the issuing organization.
- Avail: USGS. Originals of many reports from the U.S. Geological Survey, which may contain color illustrations, or otherwise may not have the quality of illustrations preserved in the microfiche or facsimile reproduction, may be examined by the public at the libraries of the USGS field offices whose addresses are listed in this Introduction. The libraries may be queried concerning the availability of specific documents and the possible utilization of local copying services, such as color reproduction.
- Avail: Issuing Activity, or Corporate Author, or no indication of availability. Inquiries as to the availability of these documents should be addressed to the organization shown in the citation as the corporate author of the document.

PUBLIC COLLECTIONS OF NASA DOCUMENTS

DOMESTIC: NASA and NASA-sponsored documents and a large number of aerospace publications are available to the public for reference purposes at the library maintained by the American Institute of Aeronautics and Astronautics, Technical Information Service, 555 West 57th Street, 12th Floor, New York, New York 10019.

EUROPEAN: An extensive collection of NASA and NASA-sponsored publications is maintained by the British Library Lending Division, Boston Spa, Wetherby, Yorkshire, England for public access. The British Library Lending Division also has available many of the non-NASA publications cited in *STAR*. European requesters may purchase facsimile copy or microfiche of NASA and NASA-sponsored documents, those identified by both the symbols # and * from ESA - Information Retrieval Service European Space Agency, 8-10 rue Mario-Nikis, 75738 CEDEX 15, France.

FEDERAL DEPOSITORY LIBRARY PROGRAM

In order to provide the general public with greater access to U.S. Government publications, Congress established the Federal Depository Library Program under the Government Printing Office (GPO), with 50 regional depositories responsible for permanent retention of material, inter-library loan, and reference services. At least one copy of nearly every NASA and NASA-sponsored publication, either in printed or microfiche format, is received and retained by the 50 regional depositories. A list of the regional GPO libraries, arranged alphabetically by state, appears on the inside back cover. These libraries are *not* sales outlets. A local library can contact a Regional Depository to help locate specific reports, or direct contact may be made by an individual.

STANDING ORDER SUBSCRIPTIONS

NASA SP-7041 and its supplements are available from the National Technical Information Service (NTIS) on standing order subscription as PB 88-903800 at the price of \$15.50 domestic and \$31.00 foreign. Standing order subscriptions do not terminate at the end of a year, as do regular subscriptions, but continue indefinitely unless specifically terminated by the subscriber.

ADDRESSES OF ORGANIZATIONS

American Institute of Aeronautics and
Astronautics
Technical Information Service
555 West 57th Street, 12th Floor
New York, New York 10019

British Library Lending Division,
Boston Spa, Wetherby, Yorkshire,
England

Commissioner of Patents and
Trademarks
U.S. Patent and Trademark Office
Washington, D.C. 20231

Department of Energy
Technical Information Center
P.O. Box 62
Oak Ridge, Tennessee 37830

ESA-Information Retrieval Service
ESRIN
Via Galileo Galilei
00044 Frascati (Rome) Italy

ESDU International, Ltd.
1495 Chain Bridge Road
McLean, Virginia 22101

ESDU International, Ltd.
251-259 Regent Street
London, W1R 7AD, England

Fachinformationszentrum Energie, Physik,
Mathematik GMBH
7514 Eggenstein Leopoldshafen
Federal Republic of Germany

Her Majesty's Stationery Office
P.O. Box 569, S.E. 1
London, England

NASA Scientific and Technical Information
Facility
P.O. Box 8757
B.W.I. Airport, Maryland 21240

National Aeronautics and Space
Administration
Scientific and Technical Information
Division (NTT-1)
Washington, D.C. 20546

National Technical Information Service
5285 Port Royal Road
Springfield, Virginia 22161

Pendragon House, Inc.
899 Broadway Avenue
Redwood City, California 94063

Superintendent of Documents
U.S. Government Printing Office
Washington, D.C. 20402

University Microfilms
A Xerox Company
300 North Zeeb Road
Ann Arbor, Michigan 48106

University Microfilms, Ltd.
Tylers Green
London, England

U.S. Geological Survey Library
National Center - MS 950
12201 Sunrise Valley Drive
Reston, Virginia 22092

U.S. Geological Survey Library
2255 North Gemini Drive
Flagstaff, Arizona 86001

U.S. Geological Survey
345 Middlefield Road
Menlo Park, California 94025

U.S. Geological Survey Library
Box 25046
Denver Federal Center, MS914
Denver, Colorado 80225

NTIS PRICE SCHEDULES

(Effective January 1, 1988)

Schedule A STANDARD PRICE DOCUMENTS AND MICROFICHE

PRICE CODE	NORTH AMERICAN PRICE	FOREIGN PRICE
A01	\$ 6.95	\$13.90
A02	9.95	19.90
A03	12.95	25.90
A04-A05	14.95	29.90
A06-A09	19.95	39.90
A10-A13	25.95	51.90
A14-A17	32.95	65.90
A18-A21	38.95	77.90
A22-A25	44.95	89.90
A99	*	*
NO1	49.50	89.90
NO2	48.00	80.00

Schedule E EXCEPTION PRICE DOCUMENTS AND MICROFICHE

PRICE CODE	NORTH AMERICAN PRICE	FOREIGN PRICE
E01	\$ 8.50	17.00
E02	11.00	22.00
E03	12.00	24.00
E04	14.50	29.00
E05	16.50	33.00
E06	19.00	38.00
E07	21.50	43.00
E08	24.00	48.00
E09	26.50	53.00
E10	29.00	58.00
E11	31.50	63.00
E12	34.00	68.00
E13	36.50	73.00
E14	39.50	79.00
E15	43.00	86.00
E16	47.00	94.00
E17	51.00	102.00
E18	55.00	110.00
E19	61.00	122.00
E20	71.00	142.00
E99	*	*

* Contact NTIS for price quote.

IMPORTANT NOTICE

NTIS Shipping and Handling Charges

U.S., Canada, Mexico -- ADD \$3.00 per TOTAL ORDER

All Other Countries -- ADD \$4.00 per TOTAL ORDER

Exceptions -- Does NOT apply to:

ORDERS REQUESTING NTIS RUSH HANDLING
ORDERS FOR SUBSCRIPTION OR STANDING ORDER PRODUCTS ONLY

NOTE: Each additional delivery address on an order
requires a separate shipping and handling charge.

1. Report No. NASA SP-7041 (58)	2. Government Accession No.	3. Recipient's Catalog No.	
4. Title and Subtitle EARTH RESOURCES A Continuing Bibliography with Indexes (Issue 58)		5. Report Date August, 1988	
		6. Performing Organization Code	
7. Author(s)		8. Performing Organization Report No.	
		10. Work Unit No.	
9. Performing Organization Name and Address National Aeronautics and Space Administration Washington, DC 20546		11. Contract or Grant No.	
		13. Type of Report and Period Covered	
12. Sponsoring Agency Name and Address		14. Sponsoring Agency Code	
15. Supplementary Notes			
16. Abstract <p>This bibliography lists 500 reports, articles and other documents introduced into the NASA scientific and technical information system between April 1 and June 30, 1988. Emphasis is placed on the use of remote sensing and geophysical instrumentation in spacecraft and aircraft to survey and inventory natural resources and urban areas. Subject matter is grouped according to agriculture and forestry, environmental changes and cultural resources, geodesy and cartography, geology and mineral resources, hydrology and water management, data processing and distribution systems, instrumentation and sensors, and economic analysis.</p>			
17. Key Words (Suggested by Author(s)) Bibliographies Earth Resources Remote Sensors		18. Distribution Statement Unclassified - Unlimited	
19. Security Classif. (of this report) Unclassified	20. Security Classif. (of this page) Unclassified	21. No. of Pages 140	22. Price * A07/HC

*For sale by the National Technical Information Service, Springfield, Virginia 22161